Lipophilically Functionalized Analogs of Muraymycin Nucleoside Antibiotics

Dissertation

zur Erlangung des Grades

des Doktors der Naturwissenschaften

der Naturwissenschaftlich-Technischen Fakultät

der Universität des Saarlandes

von

Simone Kerstin Rosinus, M. Sc.

Saarbrücken

2025

Tag des Kolloquiums:	05.08.2025
Dekan:	Prof. Dr.-Ing. Dirk Bähre
Berichterstatter:	Prof. Dr. Christian Ducho
	Prof. Dr. Johann Jauch
Akad. Mitglied:	Dr. Josef Zapp
Vorsitz:	Prof. Dr. Gregor Jung

Die vorliegende Arbeit wurde im Zeitraum von September 2020 bis Februar 2025 im Fachbereich Pharmazie der Universität des Saarlandes im Arbeitskreis von Prof. Dr. Christian Ducho angefertigt.

Erstgutachter: Prof. Dr. Christian Ducho

Zweitgutachter: Prof. Dr. Johann Jauch

My philosophy is that worrying means you suffer twice.

~ Newt Scamander

Abstract

The central focus of this PhD study was the synthesis and biological evaluation of simplified muraymycin derivatives as part of a structure-activity relationship (SAR) study. The focus was particularly on the structure of the central amino acid and the influence of the attached lipophilic side chain on the antibiotic activity. In addition, the urea-dipeptide motif in the muraymycin backbone was simplified. Further insights into the relevance and impact of the lipophilic side chain were obtained by a set of truncated muraymycin derivatives.

The conducted SAR study revealed a couple of very potent compounds, which might serve as lead structures for future projects. Furthermore, the relevance of the lipophilic side chain was re-evaluated. Additionally, a highly efficient synthetic route, which significantly facilitates an easy and fast synthesis of new derivatives, was established.

Zusammenfassung

Ziel dieser Dissertation war die Synthese und die biologische Evaluierung vereinfachter Muraymycin-Derivate im Rahmen einer Struktur-Aktivitäts-Beziehungs-Studie (SAR-Studie). Dabei wurde sich besonders auf die Struktur der zentralen Aminosäure, sowie auf den Einfluss der daran gebundenen lipophilien Seitenkette auf die antibiotische Aktivität, fokussiert. Außerdem wurde eine Vereinfachung der Teilstruktur des Harnstoff-Dipeptids im Muraymycin-Rückgrat angestrebt. Anhand einer Serie verkürzter Muraymycin-Derivate konnten zusätzliche Einblicke in die Bedeutung und Wirkung der lipophilen Seitenkette erhalten werden.

Die durchgeführte SAR-Studie offenbarte einige hochpotente Verbindungen, die für zukünftige Projekte als Leitstrukturen dienen können. Darüber hinaus konnte die Bedeutung der lipophilen Seitenkette im Muraymycin-Rückgrat neu bewertet werden. Zusätzlich wurde eine sehr effiziente Syntheseroute entwickelt, welche die Herstellung neuer Derivate signifikant beschleunigt und vereinfacht.

Abbreviations and Symbols

$[\alpha]_{20}^{D}$	specific rotation [°]
Ac	acetyl
Alloc	allyloxycarbonyl
AllocCl	allyl chloroformate
aq.	aqueous
ATP	adenosine triphosphate
ATR	attenuated total reflection
Bn	benzyl
Boc	*tert*-butyloxycarbonyl
Bu	butyl
Cbz	benzyloxycarbonyl
cf.	confer
calcd.	calculated
CoA	coenzyme A
COSY	correlation spectroscopy (NMR)
δ	chemical shift [ppm] (NMR)
D	doublet (NMR) or day(s)
DCC	dicyclohexylcarbodiimde
DCM	dichloromethane
DFT	discrete *Fourier* transform
DIPEA	*N*,*N*-diisopropylethylamine
DMAP	4-dimethylformamide
DMF	*N*,*N*-dimethylformamide
DMSO	dimethyl sulfoxide
DNA	deoxyribonucleic acid
dTMP	deoxythymidine monophosphate
dTTP	deoxythymidine triphosphate

dUMP	deoxyuridine monophosphate
e.g.	for example (lat. *exempli gratia*)
EDC • HCl	*N*-(3-dimethylaminopropyl)-*N*'-ethylcarbodiimide hydrochloride
EEDQ	*N*-ethoxycarbonyl-2-ethoxy-1,2-dihydroquinoline
eq.	equivalents
ESI	electrospray ionisation (MS)
Et	ethyl
et al.	and others (lat. *et alii*)
EtOAc	ethyl acetate
Fmoc	9-Fluorenylmethyloxycarbonyl
FT	*Fourier* transform
Glc	glucose
Glc*N*Ac	*N*-acetyl glucosamine
GPT	UDP-N-acetylglucosamine: dolichyl phosphate *N*-acetylglucosamine-1-phosphate transferase or Glc*N*Ac-1-P-transferase (human transferase)
h	hours
HMBC	heteronuclear multiple bon coherence (NMR)
HOBt	1-hydroxybenzotriazole
HPLC	high performance liquid chromatography
HR	high resolution
HRMS	high resolution mass spectrometry
HSQC	heteronuclear single quantum coherence (NMR)
Hz	Hertz
IBX	2-iodoxybenzoic acid
IC_{50}	half maximal inhibitory concentration
IR	infrared (spectroscopy)
J	scarlar coupling constant [Hz] (NMR)
KHMDS	potassium bis(trimethylsilyl)amide

λ_{max}	wavelength [nm] (UV)
LB	Luria-Bertain/Lysogenyl Broth
LC-MS	liquid chromatography-mass spectrometry
lat.	Latin
M	molar
m	multiplet
max.	maximum
Me	methyl
MeCN	acetonitrile
MeOH	methanol
MIC	minimum inhibitory concentration
min	minute(s)
MRSA	methicillin-restistant *Staphylococcus aureus*
MS	mass spectrometry
Mur	muraminic acid or muraymycin
Mur*N*Ac	*N*-acetyl muraminic acid
$\tilde{\upsilon}$	wave number [cm^{-1}] (IR)
n.d.	not determined
NaHMDS	sodium bis(trimethylsilyl)amide
NMR	nuclear magnetic resonance
Pbf	2,2,4,6,7-pentamethyldihydrobenzofuren-5-sulfonyl
PEP	phosphoenolpyruvate
Ph	phenyl
PMB	*p*-methoxybenzyl
POM	pivaloyloxymethyl
PPh_3	triphenylphosphine
ppm	part per million
pTsOH	*para*-toluene sulfonic acid

PyBOP	benzotriazole-1-oxytripyrrolidinophosphonium hexafluorophosphate
quant.	quantitative
rt	room temperature
R_f	retardation factor (TLC)
RNA	ribonucleic acid
s	singlet
SAR	structure-activity relationship
t	triplet
T_3P	propane phosphonic acid anhydride
t_R	retention time (HPLC)
TBDMS	*tert*-butyldimethylsilyl
TBDMS-Cl	*tert*-butyldimethylsilyl chloride
TEMPO	2,2,6,6-tetramethylpiperidinyloxyl
TLC	thin layer chromatography
TFA	trifluoroacetic acid
THF	tetrahydrofuran
UDP	uridine diphosphate
UMP	uridine monophosphate
UTP	uridine triphosphate
UV	ultraviolet (spectroscopy)

Abbreviations of Amino Acids

amino acid	single letter code	triple letter code
alanine	A	Ala
arginine	R	Arg
asparagine	N	Asn
aspartic acid	D	Asp
cysteine	C	Cys
glutamic acid	E	Glu
glutamine	Q	Gln
histidine	H	His
isoleucine	I	Ile
leucine	L	Leu
lysine	K	Lys
methionine	M	Met
ornithine	O	Orn
phenylalanine	F	Phe
proline	P	Pro
serine	S	Ser
threonine	T	Thr
tryptophane	W	Try
tyrosine	Y	Tyr
valine	V	Val

Contents

1 Introduction

Since the early 20th century, antibiotics have had a profound impact on public health and revolutionized the treatment of bacterial infections. Today, they are used within a broad spectrum of applications, including the treatment of bacterial infections or as prophylaxis against secondary infections in cancer therapy.[1–3] Since antibiotics are indispensable in modern medicine, the continuous emergence of resistances is especially alarming and requires continuing research, including the development of efficient antibiotics.

When S. A. Waksman defined the word 'antibiotic' (Greek ἀντί = against; βίος = life) in 1941, their activity against bacteria but also the development of resistances were already known.[4–6] Today, various families of drugs are addressed with the term 'antibiotic'. The first of which was the famous 'penicillin', discovered by chance: In 1928, Scottish bacteriologist Sir A. Fleming discovered an inhibitory activity of penicillium fungi against *Staphylococci*, leading to the suggestion of an antibacterial substance which he named penicillin.[7] The active agent itself however, was isolated and characterized a few years later by E. Chain and H. W. Florey. In their studies, they were not only able to demonstrate its antibacterial activity, but their investigations on the compound also lead them to suggest penicillin as a potential new chemotherapeutic agent.[8] A few years earlier, a different class of substances was introduced as antibiotics, the sulfonamides. The first representative was the sulfonamide precursor Prontosil, which was also the first commercially available antibacterial drug.[9,10]

Since then, a variety of antibacterial compounds have been discovered and introduced during the 'golden age' (approximately 1940-1960). Prominent representatives are the polyketide tetracycline,[11] the aminoglycoside streptomycin[12,13] or the glycopeptide vancomycin.[14,15] During this time, the semi- and full-synthetic approaches were the main path of discovery besides isolation and testing of natural compounds. Furthermore, the *Waksman* platform, a digital screening platform for antibiotic-producing organisms, has promoted research and development in the field.[3,16–18]

Today, the efficacy of antibiotics can be classified as bacteriostatic (inhibition of bacterial growth) or bactericidal (killing bacteria). Although, this categorization is challenging when transferred from laboratory conditions to the clinical setting, it can still be used as an orientation in the antibacterial drug research.[19]

After the period of strong development of antibiotics during the 'golden age', a significant decline can be observed from the 1960s until today.[20–23] Many of the antibiotics, which were discovered after 1960, were synthetic modifications of known substances, such as ampicillin derived from penicillin or telithromycin from erythromycin.[16,21,22]

The situation is particularly threatening because the development of resistance in bacteria is steadily advancing, compared to the very slow progress in antibiotic research. This ultimately leads to established drugs becoming less effective. In this context, it is important to classify the two kind of resistance: intrinsic (natural) resistance, an innate ability of an organism due to evolution, and acquired resistance, which was developed as a result of external factors.[24]

For each class of known antibacterial substances, one or more resistant bacterial strains have been discovered in predominantly short periods of time (cf. **Fig. 1**).[20–22] Thus making the bacterial resistance only a matter of time and not of possibility. As some of the mentioned substances in **Fig. 1** are synthetically produced while the others are natural products, it is evident that the origin of the compound has no influence on resistance development.[17,25,26]

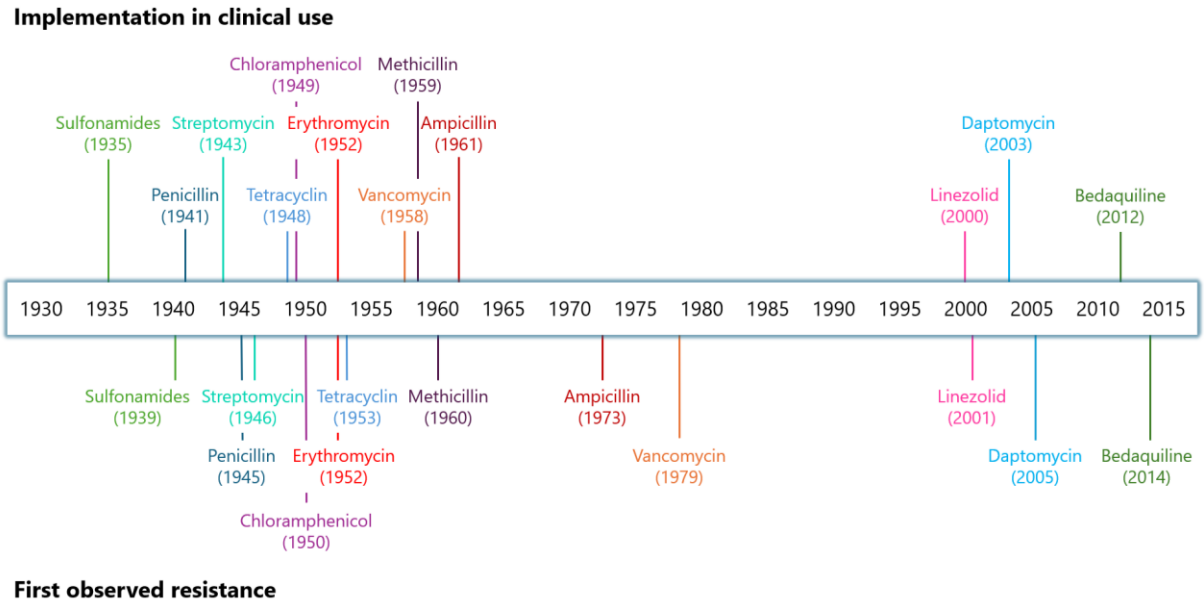

Fig. 1: Timeline of the introduction of antibiotics in clinical use versus the first observed resistance. (design based on: E. A. Clatworthy *et al. Nat. Chem. Biol.* **2007**, *3*, 541-548.)[2,11,20,27–30]

Although the development of resistance is an evolutionary process that bacteria undergo anyway, the wrong use of antibiotics has further promoted it.[2,25–27] Two of the main supporters are the misuse in human medicine and industrial farming. In both

cases, the medicinal compounds reach the environment primarily via excretions. Additionally, wastewater from pharmaceutical manufacturing also contributes significantly to the environmental contamination. This high selection pressure provokes bacteria to continuously develop more resistances.[31–34]

Two well-known pathogens are *Clostridioides difficile* (old: *Clostridium difficile*)[25] and *Staphylococcus aureus*. Those are called hospital bugs and can be partially treated with some of the mentioned antibiotics. Unfortunately, new types of *Clostridioides difficile* (*C. difficile*) have been found, which show resistances against well-used drugs. This is an issue because the main symptom of a *C. difficile* infection is severe diarrhea, which can lead to dehydration (exsiccosis) and, in some cases, to death.[25,35,36] The mortality rate among this infections raised to approximately 10% compared from 1999 to 2012 in the US.[37] In 2019, *C. difficile* was classified as an 'urgent threat' according to the Centers of Disease Control and Prevention (CDC) in the US.[38,39]

For other nosocomial infections, there are also strains, which developed resistances against the last back-up antibiotics today. A very prominent example are the so called 'ESKAPE' pathogens, a collection of drug-resistant bacterial strains, which cause severe infections but cannot be fought with the known antibacterial substances (vancomycin-resistant *Enterococci*, methicillin-resistant *Staphylococcus aureus*, *Klebsiella pneumoniae*, *Acinetobacter baumannii, Pseudomonas aeruginosa, Enterobacter* spp.).[27,40] A strain which must be pointed out here, is the methicillin-resistant *Staphylococcus aureus* (MRSA). According to the report from the CDC in 2019, MRSA is classified as a 'serious threat'.[38,39] The world health organization (WHO) identified it as "one of the leading causes of health-care-associated and community-acquired infections worldwide" (WHO Bacterial Priority Pathogens List 2024: Bacterial Pathogens of Public Health, to Guide Research, Development, and Strategies to Prevent and Control Antimicrobial Resistance, **2024**, p. 13).[41] The Annual Epidemiological Report for 2023, published by the European Centre for Disease Prevention and Control (ECDC), reported that 18.5% of the reported invasive *S. aureus* isolates were resistant against at least one of the antimicrobial groups including fluoroquinolones or rifampicin.[42] MRSA even shows vancomycin-resistance and is referred to as VRSA since.[17,25,43,44]

Bacteria have different mechanisms of resistance.[45] They can inactivate a compound using enzymes that degrade or modify its molecular structure. This primarily involves the hydrolysis of functional groups, thus leading to its inefficiency, or the transfer of different chemical groups onto the compound. The latter results in reduced or no

binding compatibility between the compound and its target. Besides the structure of the antibiotic substance, the active side of the target can also be altered, which ultimately leads to the same result. Two possible scenarios are mutations in the gene encoding the protein target or the enzymatic alteration of the binding side. Another possibility is the replacement of the target enzyme with a novel protein, which has the same function, but cannot be inhibited by applied antibiotics, thus making it ineffective. In addition, it is possible for some bacteria to shield the target enzyme via a protection protein, so that the interaction of the antibacterial substance with the target is impeded. Bacteria possess not only intercellular resistance mechanisms. Sometimes the structure of the cell membrane changes in a way that the influx of various compounds, such as antibiotics, is reduced. In addition to influx, the efflux system can also influence the effectiveness of an antibiotic drug. It can reduce the concentration of the antibiotic compound inside the cell to an extent, so that it is no longer effective.[23,26,46]

As the existing classes of antibiotics act on different targets, it is equally essential to explore new targets alongside the development of new compounds.[47,48] **Fig. 2** illustrates some of the known targets. There is the cell wall biosynthesis (**a**), which is for example addressed by the β-lactam antibiotics and glycopeptides like vancomycin. Others interfere with the protein biosynthesis (**b**), the DNA and RNA replication (**c**) or the folate metabolism (**d**).[17,47]

Overall, there is a number of new compound classes, which show very promising activities, and which address both new and old targets (cf. chapter 2). The protein MraY, which is involved in the biosynthesis of the cell wall will be discussed in more detail below. In addition, the class of muraymycins, a type of nucleoside natural product, will be investigated.

Various strategies have been proposed in order to revive the research-intensive period of the 'golden age'. One of these is to address new targets (cf. **Fig. 2**),[49] another to use drug combinations to prolong their efficiency and effect.[50] Also, the use of established platforms, such as the *Waksman* platform,[16] or the combination of new and old platforms can also open new perspectives in the search for potential drugs or targets.[18] Overall, interdisciplinary research is the key to develop new lead structures and active substances against multi-resistant bacteria.

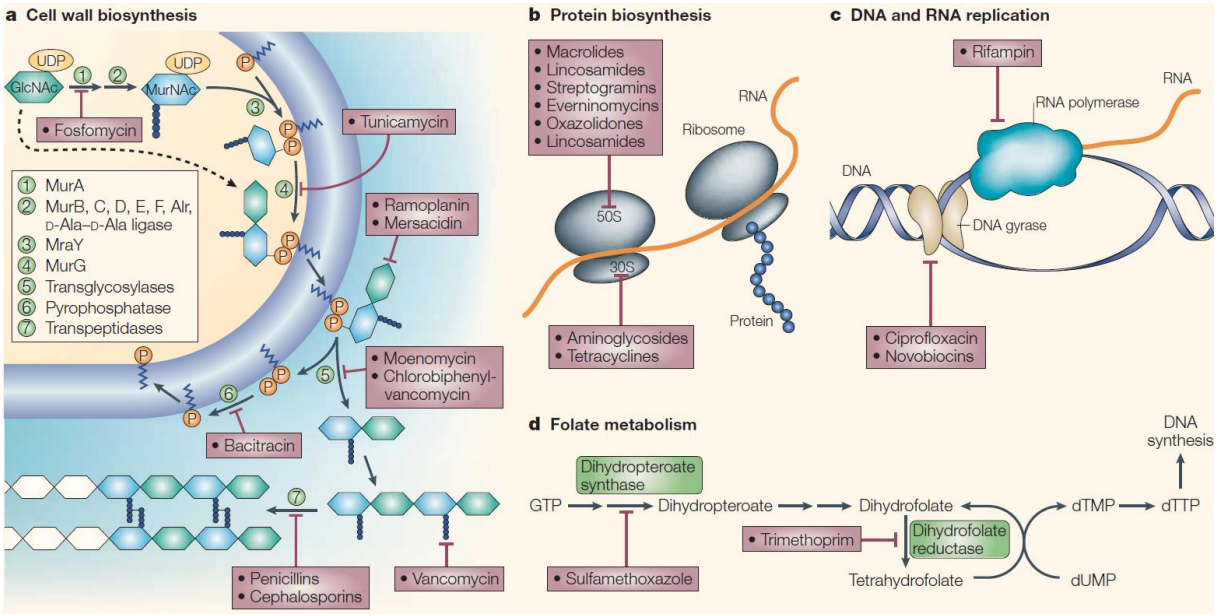

Fig. 2: Potential targets for antibiotics today and the future (from: C. Walsh, *Nat. Rev. Microbiol.* **2003**, *1*, 65-70).[17]

This thesis contributes to these goals. The main focus of the presented study was the identification and characterization of potential new antibacterial lead compounds, based on the results gained from structure-activity relationship (SAR) studies. These lead structures could serve as the foundation for the development of new drugs, which may be applicable for *in vivo* use in the future.

2 State of Knowledge

This chapter focuses on the aforementioned topics of new antibiotic targets, potential new antibiotics, and the current state of research on their development.

2.1 Potential new targets

The four potential new targets (cf. **Fig. 2**) mentioned in chapter 1 are the protein biosynthesis, the DNA and RNA replication or the folate metabolism. The target we are mostly interested in, is the cell wall biosynthesis.[17,47] For the survival of all types of bacterial organisms, an intact cell wall is essential. This barrier protects the inner part of the cell, stabilizes its structure, regulates osmotic pressure, and is involved in the release of cellular products.[51–53] Fortunately, since the bacterial cell-wall biosynthesis consists of many steps involving different enzymes, there are many possible targets within the synthetic cycle.[54,55]

2.1.1 Cell wall of Gram-positive and Gram-negative bacteria

The main difference between the bacterial cell wall of Gram-positive and Gram-negative bacteria is the cell envelope structure.[56,57] The label Gram-'positive' or -'negative' refers to the ability of a bacterium to absorb crystal violet into the cell. This classification procedure was developed 140 years ago by H. C. Gram and is still used today. However, the strict division into two classes is an old point of view, as classes which are referred to as Gram-variable are also known today.[58,59]

The cell wall of Gram-negative bacteria consists mainly of three layers: the outer membrane, the peptidoglycan cell wall and the cytoplasmic membrane. The peptidoglycan usually consists of a single layer with a thickness of only 3-6 nm. Gram-positive bacteria, on the other hand, lack the outer membrane. To compensate for this deficiency, these organisms have a much thicker peptidoglycan layer (10-20 nm). It consists mainly of stacked peptidoglycan layers interspersed with anionic polymers (= teichoic acids and capsular polysaccharides). The latter are generally made up of glycerol phosphate, glucosyl phosphate or ribitol phosphate.[56,57,60] The resistance of Gram-negative bacteria (e.g. *E. coli*, *P. aeruginosa*) to the penetration of different substances can be attributed to the presence of the outer membrane. This significant difference contributes to the fact that Gram-negative bacteria are more resistant to antimicrobial compounds compared to Gram-positive bacteria.[52]

2.1.2 Peptidoglycan biosynthesis

The diverse and complex structures of bacterial cell walls all contain peptidoglycan, with the exception of mycoplasma and scrub typhus agent *Orientia (Rickettsia) tsutsugamaushi*.[53,61–63] The term murein (*lat.*: murus = wall) used for peptidoglycan reflects the significant role of the polypeptide. As already mentioned, it contributes greatly to the survival of the organisms and is therefore a promising target for new antibacterial compounds.[55]

Peptidoglycan consists mainly of linear glycan chains, which alternate between Glc*N*Ac and Mur*N*Ac sugar moieties and are connected to each other by β-linkages (1→4). They are terminated by a 1,6-anydroMur*N*Ac residue.[53] The chains are connected to each other by short peptides, which are linked to the Mur*N*Ac molecules by their carboxylic groups. These short peptides vary in structure depending on the organism. In most cases, they consist of an L-Ala-γ-D-Glu-DA-D-Ala-D-Ala sequence. The term DA refers to L-lysine for Gram-positive and to *meso*-2,6-diaminopimelic acid for Gram-negative bacteria.[51,53,64] The second D-Ala moiety is only present in freshly forming peptidoglycan and is gone in the mature polypeptide.[51,51] The short peptide chains are cross linked by one or more amino acids by the carboxyl group of D-Ala (position 4 in the peptide) and DA (cf. **Fig. 3**).[53,60,64]

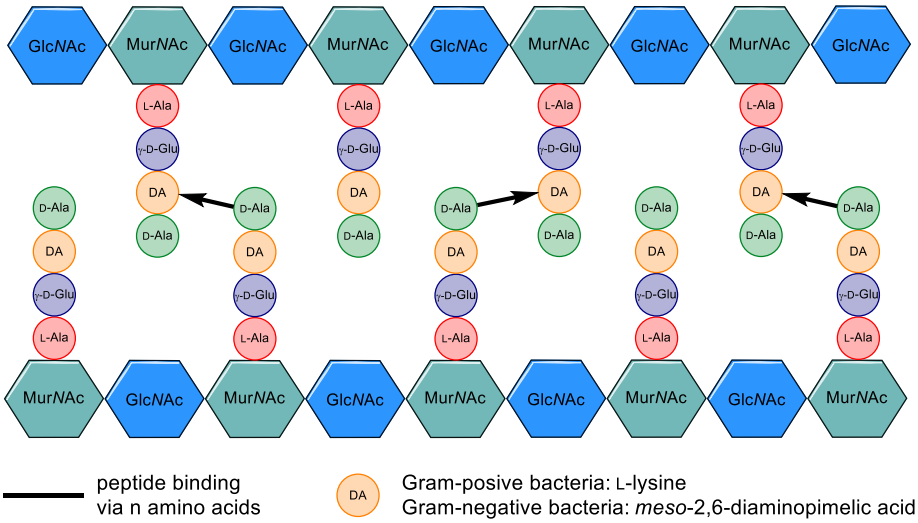

Fig. 3: Schematic structure of peptidoglycan: glycan chains consisting of Glc*N*Ac and Mur*N*Ac crosslinked with short peptides over multiple amino acids (n = 1, 2, 3, etc.).[51,53,65]

The biosynthetic pathway of peptidoglycan consists of approximately twenty different steps, which involve a variety of different enzymes. They can be divided into three main stages: (**1**) synthesis of the required sugar units and formation of UDP-Mur*N*Ac pentapeptide in the cytoplasm, (**2**) attachment of the precursor to a lipid carrier,

conversion to a disaccharide and transfer of this intermediate across the membrane to the periplasm (cf. **Fig. 4**), (**3**) polymerization of the monomer to form the peptidoglycan (not illustrated).[60,64–68]

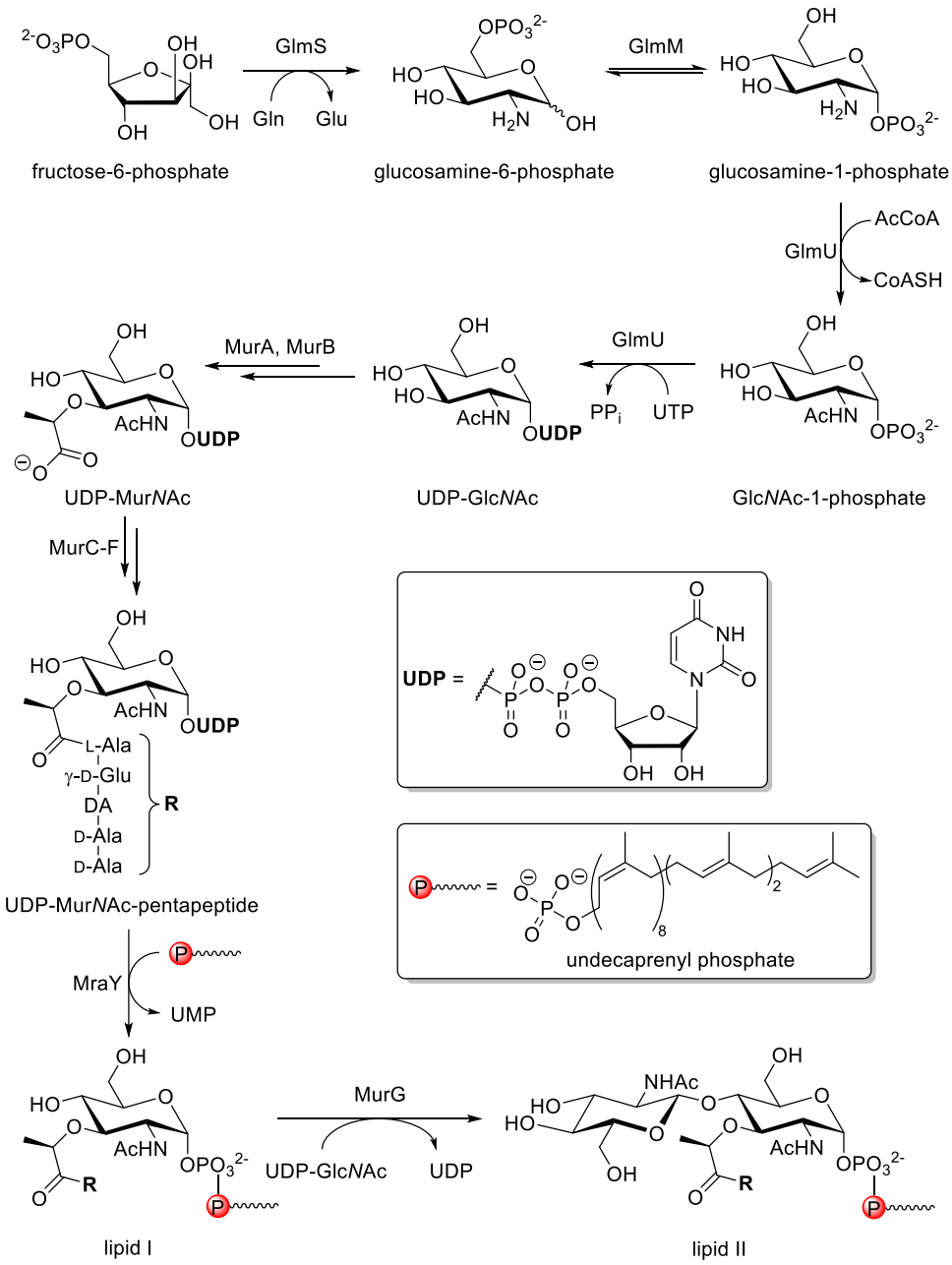

Fig. 4: Biosynthesis of lipid II starting with fructose-6-phosphate. (DA: L-Lys or *meso*-2,6-diaminopimelic acid).[64,66,67]

In the first step of the biosynthesis, fructose-6-phosphate is converted into glucosamine-6-phosphate catalyzed by the amidotransferase GlmS. The enzyme uses the amide moiety of glutamine as ammonia source.[64,67] In the second step, the mutase GlmM catalyzes the intermolecular transfer of the phosphate moiety onto the 1-position.[64,67] The mechanism of the interconversion is described as a 'ping-pong bi-bi

mechanism' with Glc*N*Ac-1,6-diphosphate as intermediate.[64,67,69] The bifunctional enzyme GlmU acts as both acetyltransferase and uridyltransferase forming the product UDP-Glc*N*Ac.[64,67] The reactions take place in two different, functionally independent domains of the enzyme.[70,71] First, the acetyltransfer from AcCoA onto the glucosamine-1-phosphate leading to Glc*N*Ac-1-phosphate and CoASH takes place in the *C*-terminal domain. Then, GlmU catalyzes the uridyltransfer, from UDP onto the Glc*N*Ac-1-phosphate with Mg^{2+} as cofactor, releasing the UDP-Glc*N*Ac and pyrophosphate. This catalysis takes place in the *N*-terminal domain. Although the order of the latter two transfers is strictly followed in most cases, there are some known exceptions where the order is reversed.[64,67] Nevertheless, in both cases UDP-Glc*N*Ac is the main product of the sequence.

The complex conversion of UDP-Glc*N*Ac into UDP-Mur*N*Ac is catalyzed by the transferase MurA and reductase MurB. In the first step, MurA transfers an enolpyruvate of phosphoenolpyruvate (PEP) onto the 3'-OH moiety of UDP-Glc*N*Ac resulting in inorganic phosphate and UDP-Glc*N*Ac-enolpyruvate. Then, MurB catalyzes the reduction of the intermediate, releasing UDP-Mur*N*Ac in two half-reactions activated by various cations. In this context, a difference was observed between Gram-positive and Gram-negative bacteria, which applies to the *murA* gene. While Gram-negative bacteria have only one copy of this gene, Gram-positive bacteria have two. It is speculated that this might be due to gene duplication. In addition, the MurB protein shows structural differences in several bacterial strains and is therefore classified as type I or type II.[64,67]

In the next steps, the strands that later connect the GlcNAc-MurNAc sugar chains (cf. **Fig. 3**) are introduced. The so-called Mur ligases (MurC-F) are responsible for the incorporation of a peptide strain (cf. **Fig. 4**) into the UDP-MurNAc. Each Mur ligase adds a different amino acid under the usage of ATP and Mg^{2+} or Mn^{2+}: L-Ala (MurC), γ-D-Glu (MurD), L-Lys (Gram-pos.) or meso-2,6-diaminopimelic acid (Gram-neg.) (MurE) and the D-Ala-D-Ala dipeptide (MurF).[64,67]

The next step is the first membrane-involved step. The integral membrane protein MraY catalyzes the transfer of the UDP-Mur*N*Ac-pentapeptide onto the undecaprenyl phosphate (C_{55}-P), yielding undecaprenyl-pyrophosphoryl-Mur*N*Ac-pentapeptide (lipid I) and UMP. Subsequently, the transferase MurG catalyzes the formation of lipid II by transferring a UDP-Glc*N*Ac moiety onto lipid I. After transfer to the outside of the membrane by the flippase MurJ,[72] lipid II is used to form peptidoglycan.[64] The

polymerization of lipid II building blocks and the formation of cross-linkages, catalyzed by transpeptidases, are not relevant for the topic presented here and are therefore not described in detail.[64]

Some known antibiotics and potential drug-candidates already show promising inhibition of the enzymes involved in the peptidoglycan biosynthesis.[55,65,73] One of these is the translocase MraY, a promising new antibacterial target that will be discussed in more detail in the following section.

2.1.3 Translocase I (MraY)

The integral membrane protein MraY belongs to a subfamily of the polyprenyl-phosphate *N*-acetyl hexosamine 1-phosphate transferases (PNPT) and plays a key role in the peptidoglycan synthesis (cf. **Fig. 4**).[74] As mentioned before, it catalyzes the formation of lipid I from UDP-MurNAc pentapeptide and undecaprenyl phosphate (cf. **Fig. 5**).[64,75–79]

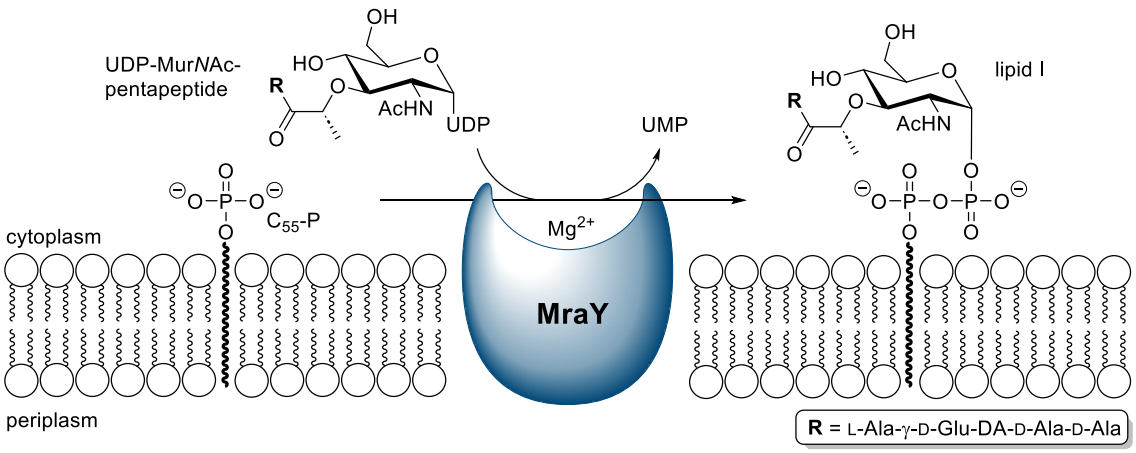

Fig. 5: Schematic synthesis of lipid I catalyzed by MraY in die peptidoglycan synthesis.

Based on overexpression experiments, Matsuhashi and co-workers proposed in 1991 that the *mraY* gene encodes the enzyme MraY.[80] This gene played an important role in a knockout experiment by Boyle and Donachie. They were able to observe that the absence of the *mraY* gene led to lysis and inevitable death of the bacterial cells. This emphasizes the relevance of the protein for the bacterial survival and makes it a very promising target for new antibiotics.[81]

Although the protein was first identified in the 1960s, the first topology model was not established until almost forty years later by Bouhss *et al.*[78,82] They proposed a two-dimensional model with ten transmembrane segments, five cytoplasmic domains and

six periplasmic domains including the *N*- and *C*-terminal ends.[82] Bouhss and co-workers were also the first to isolate and characterize MraY from *Bacillus subtilis*. This was an important step towards a better understanding of the enzyme and its mode of action.[83] In 2011, Bernhard and co-workers presented a cell-free expression method for translocase I.[84]

In 2013, Chung *et al.* published the first crystal structure of $MraY_{AA}$ (*Aquifex aeolicus*) thus making a major contribution to research. Initially, they postulated that the enzyme appears to have a dimeric crystal structure with a hydrophobic cleft in its center. Furthermore, their observations confirmed and even extended the topology model by Bouhss *et al.* An additional interfacial helix (IH), a periplasmic β hairpin (PB) and a periplasmic helix (PH), ten transmembrane helices (TM1-TM10) and five cytoplasmic loops (loop A-E) were identified. The crystal structure confirmed that the *N*- and *C*-termini are located in the periplasm. Transmembrane helix TM9 shows a special confirmation, as it is divided into two helical fragments (TM9a and TM9b), with TM9b showing a significant curvature in the center of the membrane. As a result, TM9b extends into the lipid membrane, away from the rest of the structure.[74]

The active site of the enzyme was hypothesized to be around the inner leaflet membrane region of TM8, resulting from a cleft formed by the transmembrane helices TM3, TM4, TM8 and TM9b surrounding TM5. In additional studies, a number of essential amino acids were identified, that have a major influence on the enzyme activity. Most of them were localized in the described clef, which led to the assumption that this region represents the active center of the enzyme.[74,76] This proposition was further supported by mutational mapping studies. From the amino acids in the cleft, at least four (Asp^{117}, Asp^{118}, Asp^{265}, and His^{324}) were identified to be highly important for the activity of the integral membrane protein.[74]

In previous studies, two of these residues (Asp^{117} and Asp^{118}) were presumed coordination sites for cofactor Mg^{2+}.[85] Chung *et al.* refuted this assumption in anomalous scattering studies and identified Asp^{265} as a direct interaction site with the cation. Furthermore, their studies supported the previous theory, that Asp^{117} (Asp^{98} in $MraY_{B.\ subtilis}$) is the binding site for the phosphate group of the undecaprenyl phosphate.[74,76]

In addition, a possible binding site for a sugar motif in loop E was also identified. This region was recognized as the so-called HHH-motif, a specific conserved sequence

within the PNPT superfamily. Eventually, a binding site for lipid C_{55}-P was also identified as an inverted U-shape groove on the surface of the dimeric enzyme.[74]

In 1969, shortly after its identification, the first catalytic mechanism of MraY was described by Heydanek *et al.* As illustrated in **Fig. 6**, they assumed a two-stage mechanism in which a phosphor-Mur*N*Ac-pentapeptide enzyme complex is formed as an intermediate in the first step, after elimination of uridine monophosphate (UMP). In the second step, undecaprenyl phosphate attacks the phosphate of the covalent intermediate, resulting in the formation of lipid I and regeneration of the enzyme. Back then, it was already postulated that Mg^{2+} is an essential cofactor for the enzyme. Furthermore, the reverse reaction has also been demonstrated, confirming that the catalyzed reaction is an equilibrium.[75–78,86]

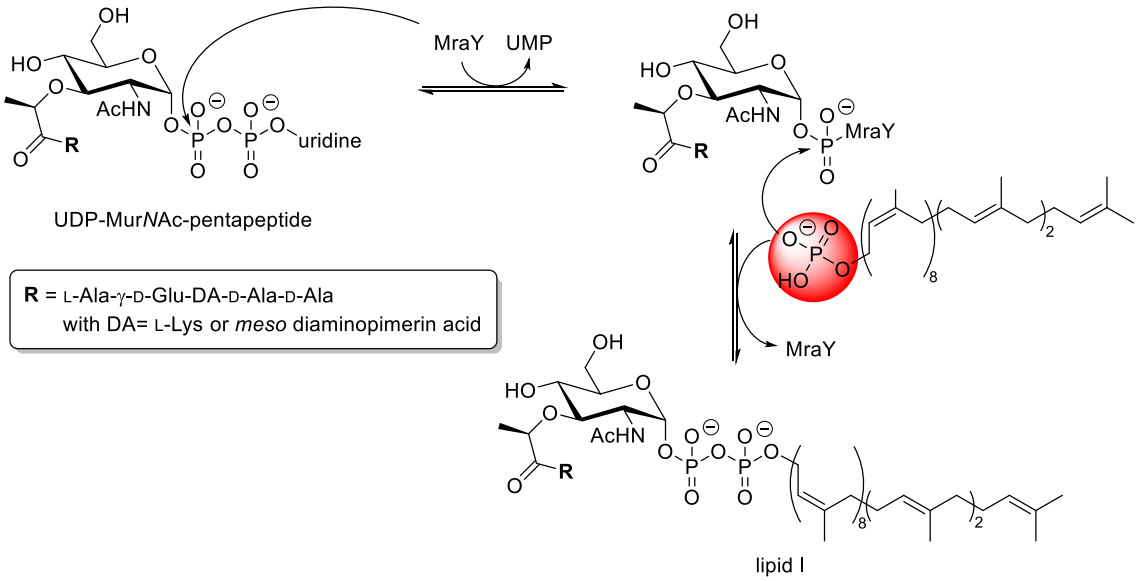

Fig. 6: Two-step catalytic mechanism of MraY proposed by Heydanek *et al.*[76–78,86]

Bouhss and co-workers postulated a one-step mechanism for translocase I. According to their investigations, Asp^{98} is involved in the catalytic reaction of MraY, where it is responsible for the deprotonation of the phosphonate of C_{55}-P (cf. **Fig. 7**). This enables a nucleophilic attack of the phosphonate towards the UDP-Mur*N*Ac pentapeptide, resulting in the formation of lipid I and UMP. This mechanism was supported by the crystal structure published by Chung *et al.* They confirmed that Asp^{98} ($MraY_{\textit{B. subtilis}}$) is the binding site of the phosphonate in C_{55}-P. In addition, the presence of Mg^{2+} in the active center of the enzyme in close proximity to the essential aspartate residue emphasizes the high possibility of a one-step mechanism.[74–76]

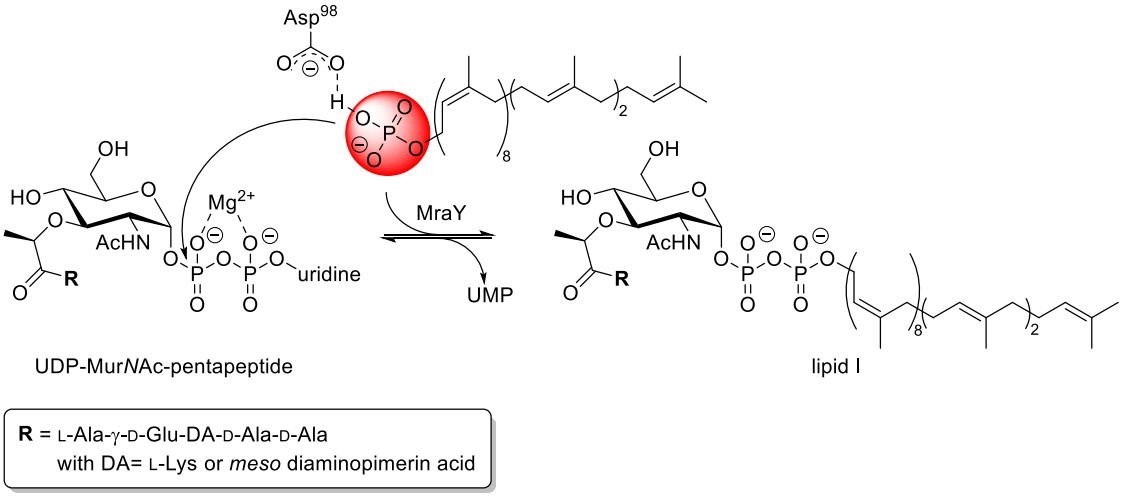

Fig. 7: One-step catalytic mechanism of MraY proposed by Bouhss *et al.*[75,76]

In general, different types of MraY inhibitors are known today. The most prominent can be divided into three categories: the lipopeptide amphomycin, the peptide inhibitor protein E from ϕX174 and different classes of natural nucleoside antibiotics.[87,88]

Since different classes of natural inhibitors of the protein MraY have been identified and investigated, the nucleoside-containing substances have attracted particular attention from researchers.[88–91] Some prominent examples are the tunicamycins,[92–96] mureidomycins,[96–100] liposidomycins,[96,101–104] capuramycin[105,106] and caprazamycins[107–109] (structures not included). Another class which will be investigated further in this thesis are the muraymycins (cf. section 2.2).[110,111] In addition, different synthetic analogs were produced as well, allowing more insights into the mode of action and the properties/characteristics of the enzyme.[104,112–116]

Another important step in regard of drug development was taken in 2016, when the first crystal structure complex of $MraY_{AA}$ with inhibitor muraymycin **D2** was published. The results of the study surprisingly revealed that the inhibitor did not show any interaction with the cofactor Mg^{2+} nor with the three residues important for the activity.[117] In addition, other crystal structures of MraY in complex with different members of the nucleoside inhibitors were presented.[118,119] Based on their results, Mashalidis *et al.* developed a map of the enzyme in 2019, marking important interaction 'hot spots' with different inhibitors, even featuring the Mg^{2+}-ion binding site.[119] This model could be useful for the development of new compounds in the future.

2.2 Potential new antibiotics: muraymycins

This section focuses on the aforementioned class of muraymycin nucleoside antibiotics. The discovery and structural features of the natural products as well as synthetic and semi-synthetic approaches are discussed. Furthermore, different synthetic strategies for muraymycin analogs are described. Finally, a SAR study containing all received data at the time of planning this thesis, is presented.

2.2.1 Natural products

The muraymycins were isolated from a *Streptomyces sp.* organism in 2002 by McDonald *et al.* At that time, they discovered nineteen different agents and were able to characterize their structures using NMR-spectroscopy and FT-mass spectrometry.[111] In 2018, the list was expanded to include the derivatives **B8**, **B9** and **C6** (cf. **Fig. 8**).[120]

The backbone of the natural products consists of a uridine glycine-modified motif, connected to the central amino acid, an L-Leu or 3-hydroxy-L-Leu, by an aminopropyl linker. The left site of the core structure is a urea dipeptide consisting of the cyclic arginine analog L-epicapreomycidine (Epic) and L-Val. In many cases, various lipophilic side chains with different head groups are linked to the central amino acid, 3-hydroxy-L-Leu, via an ester bond. Usually, the uridine structure features an *O*-glycosylic linked amino ribose (Arib) unit at its 5'-position, where $\mathbf{R^3}$ is a methoxy or hydroxy group or hydrogen. The only exceptions are **A5** and **C5**, which are suspected to be hydrolysis products. Muraymycin **C6** is also very special as it carries a *N*Ac-amino ribose unit instead of Arib. The natural derivatives are divided into four different series: **A**-**D**, based on their structural similarities. All compounds of the **A** series have lipophilic chains with different lengths and a hydroxy-guanidino or guanidino (only **A3**) head group. The lipophilic chains of the **B** series muraymycins are alkyl chains with different lengths and differently branched head groups. The **C** series has still a 3-hydroxy-L-Leu moiety in the backbone but no lipophilic side chain while the **D** series contains L-Leu as the central amino acid.[111,120]

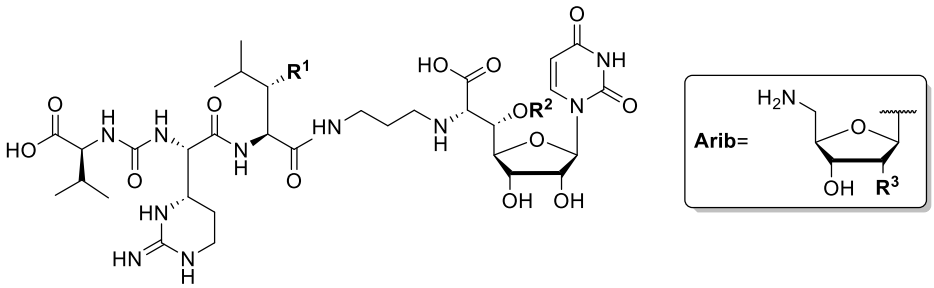

	R¹	R²	R³		R¹	R²	R³
A1	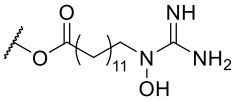	**Arib**	OCH₃	**A4**	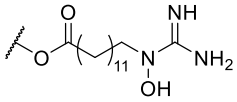	**Arib**	OH
A2	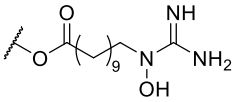	**Arib**	OCH₃	**A5**	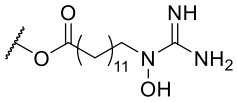	H	
A3	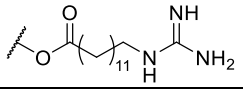	**Arib**	OCH₃				
B1	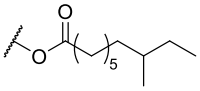	**Arib**	OCH₃	**B6**	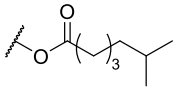	**Arib**	OCH₃
B2	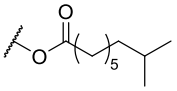	**Arib**	OCH₃	**B7**	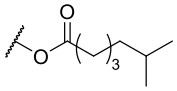	**Arib**	OH
B3	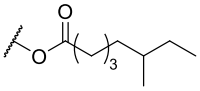	**Arib**	OCH₃	**B8**	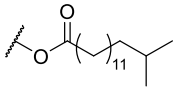	**Arib**	OCH₃
B4	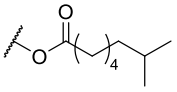	**Arib**	OCH₃	**B9**	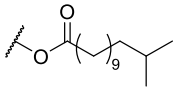	**Arib**	OCH₃
B5	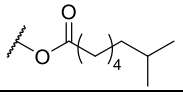	**Arib**	OH				
C1	OH	**Arib**	OCH₃	**C4**	OH	H	
C2	OH	**Arib**	OH	**C6**	OH	*N*Ac-**Arib**	OCH₃
C3	OH	**Arib**	H				
D1	H	**Arib**	OCH₃	**D3**	H	**Arib**	H
D2	H	**Arib**	OH				

Fig. 8: Structures of the isolated naturally occurring muraymycins.[111,120]

Since their discovery, five of the natural muraymycins (**A1**, **A5**, **B6**, **C2** and **C3**) showed strong inhibitory effect on the formation of lipid II and thus the peptidoglycan at low concentrations (0.027 µg/mL). Muraymycin **A1** is considered one of the most potent representatives of the natural products with a strong inhibition of the enzyme MraY

($IC_{50}(MraY_{S.\ aureus})$ = 27 ± 3 pM) and antibacterial activity against both Gram-positive ($MIC_{Staph.}$ = 2 to 16 µg/mL and $MIC_{Enterococcus}$ = 16 to >64 µg/mL) and Gram-negative strains (MIC = 8 to >64 µg/mL).[111] Furthermore, the compound showed strong activity against *E. coli* strains with higher membrane permeability (MIC <0.03 µg/mL) and against an efflux deficient strain (MIC = 2 µg/mL). The later discovered muraymycin **B8** showed a stronger inhibition of the desired enzyme ($IC_{50}(MraY_{S.\ aureus})$ = 4.0 ± 0.7 pM). It also excelled muraymycin **A1** in terms of antibacterial activity against *S. aureus* (MIC = 2 µg/mL) and showed comparable activity against the efflux-deficient *E. coli* strain (MIC = 4 µg/mL). Although compounds of the **C** and **D** series showed activity against the target MraY, their antibacterial activity was considerably lower than that of the derivatives already mentioned.[111,120,121] These observations led to the strong assumption that the lipophilic side chain plays an important role in cellular uptake, but less so in the interaction with the target itself.[120,121] This hypothesis was supported by uptake experiments published by Ries *et al.* Their results even showed that the unusual structure of the fatty acid chains in the **A** series are beneficial for cellular uptake.[122]

The publication of the co-crystal structures of various inhibitors with $MraY_{AA}$ revealed that the conformation of the binding pocket changes and adapts depending on the substance. This flexibility could also explain why many natural compounds, some of which are structurally very diverse, address the enzyme.[117,119,121] Due to this conformational flexibility of MraY, it is very challenging to predict interactions of new muraymycin derivatives with the target.

In order to obtain an initial overview on the potential toxicity of muraymycins, the modes of interaction between muraymycin **D2** and MraY and muraymycin **D2** and the very similar human transferases GPT were compared. This study suggest that the natural compound cannot be a potent inhibitor of GPT.[123] Furthermore, it was hypothesized that compounds which could interact with the uridine-adjacent site of MraY may be better suited to selectively target MraY over GPT.[124] For many new and potent muraymycin derivatives (cf. sections 2.2.3, 2.2.4), this interaction and thus the mentioned selectivity does not apply. Additional studies must therefore be carried out to eliminate toxicity for use in humans or animals.

In recent years, different approaches have been developed to obtain synthetic muraymycins and new derivatives. These are discussed in the following sections.

2.2.2 Semi-synthetic muraymycins

In 2002, Lin and co-workers published the semi-synthesis of sixteen muraymycin derivatives (structures not included). They used the natural muraymycin **C1** as their starting point and carried out selective reactions on the primary and secondary amino functions. In particular, lipophilic residues were integrated into the structure, as earlier studies suggested a strong impact of this structural feature on the biological activity.[110,120,121] The results of their SAR study revealed that the substitution of the secondary amine at the 6'-position was tolerated and yielded more or less active substances. In addition, a correlation between the introduced lipophilic moiety and the inhibitory activity was observed. Two of the compounds even exhibit comparable activities to muraymycin **C1**. However, the additional substitution of the secondary amine of the amino ribose moiety eliminates any activity on the target MraY or MurG.[110]

2.2.3 Synthetic muraymycins and their simplified analogs

The first series of fully synthetic muraymycin analogs by Yamashita *et al*. was produced almost parallel to the semi-synthetic derivatives. They chose a tripartite synthetic approach, which enabled them to replace the middle amino acid easily. The synthesis of muraymycin analog **9a** is illustrated as an example for the entire series in **Fig. 9**. The fully protected uridine aldehyde **1** was synthesized over four steps starting from uridine. In an aldol reaction an isomeric mixture of **3a** and **3b** (2:1) was isolated. After separation of the isomers, both were used separately in the following synthesis. The nucleosyl amino acid building blocks **4a** and **4b** were linked to the corresponding middle building blocks **5** by reductive amination. These compounds showed various alternatives for $\mathbf{R^2}$ and $\mathbf{R^3}$, including alkyl moieties and hydroxy groups. In the final steps, the resulting intermediates **6a** and **6b** were Cbz-deprotected and in case of compound **7a** subsequently linked to urea dipeptide **8**. For the latter, the authors chose to replace the Epic in the urea dipeptide structure with Arg due to simplification. Their synthetic approach led to a variety of protected muraymycin analogs. Some of these compounds showed antimicrobial and inhibitory activity against the target MraY.[125]

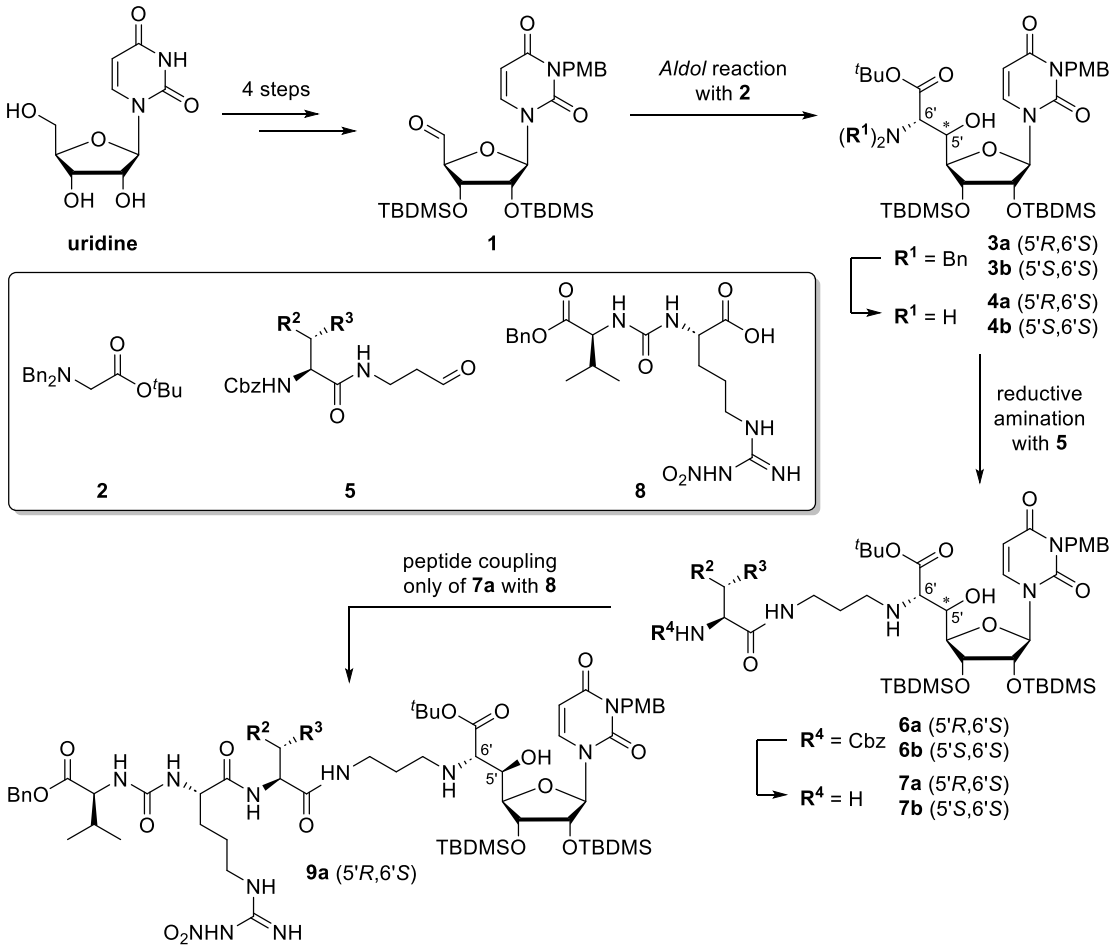

Fig. 9: Synthesis of simplified muraymycin analogs by Yamashita *et al.*[125]

The first total synthesis of a naturally occurring muraymycin was achieved by Tanino *et al.* in 2010. They presented the successful synthesis of muraymycin **D2** and its epimer using an Ugi four component approach (cf. **Fig. 10**, compound **14**).[126,127]

The required urea dipeptide **10** was synthesized in twelve steps, and the preparation of nucleosyl amino acid **13** was based on the former published synthesis of caprazol, the core structure of caprazamycin (figures not included).[127–130] The four reactants urea dipeptide **10**, 2,4-dimethoxy-benzylamine **11**, the corresponding aldehyde (isovaleraldehyde) **12** and nucleosyl amino acid **13** were linked in an *Ugi* reaction. After global deprotection the diastereomers **14a** (*S*-epimer, muraymycin **D2**) and **14b** (*R*-epimer, *epi*-**D2**) were separated by HPLC.[127]

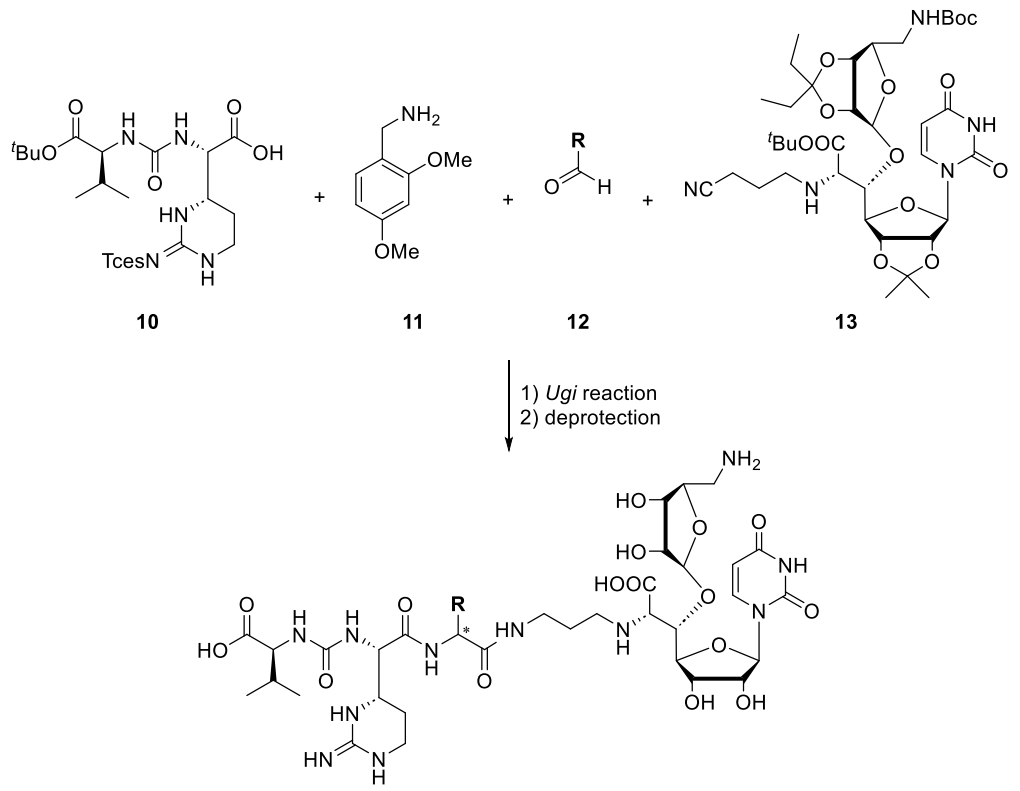

compound	R	MIC [µg/mL]	
		***S*-epimer**	***R*-epimer**
14: **D2**		>64	>64
15	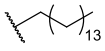	2-4	0.25-4
16	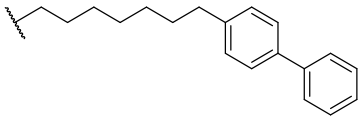	4-16	4-16
17	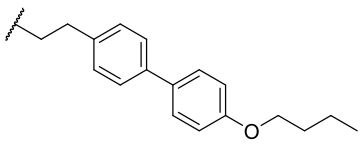	16-64	4-64
18	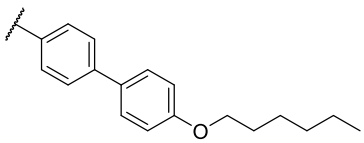	4-8	4-16

Fig. 10: Structures of muraymycin **D2** and *epi*-**D2** (**14**) and lipophillically functionalized derivatives, achieved using an *Ugi* four component reaction by Tanino *et al.*[127,131]

As implied in **Fig. 10**, Tanino *et al.* used the same approach to synthesize muraymycin analogs **15**-**18** and the corresponding epimers.[126,131,132] The synthesis of these analogs was based on the idea to establish an initial SAR study focusing on the role of the lipophilic side chain.[120–122] Muraymycin **D2** and its epimer showed inhibition of the

target enzyme MraY in the micromolar range (IC_{50}(**D2**) = 0.01 µM, IC_{50}(*epi*-**D2**) = 0.09 µM), but almost no antibacterial activity (MIC >64 µg/mL). The structural comparison of the compounds (**Fig. 10**) indicated that the presence of a side chain of any type improves antibacterial activity. This is consistent with the previous hypothesis regarding the strong activities of the natural muraymycins of series **A** and **B** (cf. section 2.2.1). The best activities were observed for compound **15** (and its epimer), with a non-functionalized *n*-alkyl side chain in the center of the structure. All derivatives with a more or less rigid lipophilic unit showed weaker bacterial activity, suggesting that a certain degree of flexibility may play an important role (cf. **Fig. 10**).[126,131,132]

Tanino *et al.* also presented a set of analogs with various urea dipeptide moieties. Here, they primarily replaced Epic with different, but structurally similar amino acids (structures not included). These variations had little impact on antibacterial activity. So, this structural motif showed great potential for the design of new muraymycin derivatives. In addition, masking the terminal carboxylic moiety of Val reduced the antibacterial activity only insignificantly.[126,132,133] All of these SAR studies emphasize the importance of the lipophilic side chain for the biological activity, especially for cell penetration. This leads to the assumption that the simplification of the muraymycin backbone is possible to a certain extent if this particular structural motive is considered in the design.[126,131–133]

In 2014, Takeoka *et al.* published a SAR-study on a series of muraymycin derivatives (structures not included), some of which inhibit Gram-negative *Pseudomonas aeruginosa* strains at concentrations of 4-8 µg/mL. Compared to muraymycin **D2**, these compounds were further structurally simplified, containing only the nucleosyl amino acid and the amino ribose unit at the 5'-position, including the propyl linker (cf. **Fig. 8**). They all featured a combination of lipophilic side chains with terminal guanidine units and *n*-alkyl fatty acid chains. The latter being a prominent structural motif in the muraymycin **A**-series (cf. **Fig. 8**). The study revealed that the lipophilic side chain and the guanidino functionality are decisive for the activity against *Pseudomonas*.[126,133]

In 2016, Kurosu and co-workers succeeded in the stereo controlled synthesis of muraymycin **D2**. They also synthesized two amide derivatives of the natural product (structures not included). All compounds showed strong enzyme inhibitory activities against the bacterial phosphotransferases MurX and WecA (IC_{50} = 0.096-0.69 µM) and strong growth inhibitory activity against the pathogen *Mycobacterium tuberculosis* (MIC_{50} = 1.56-6.25 µg/mL).[134]

All derivatives presented above still contain the amino ribose unit at the 5'-position. This moiety addresses a specific uridine-adjacent pocket and thus has a strong interaction with the target, which contributes to the activity.[91,117,119] However, the incorporation of this structural motif is synthetically very complex and not very attractive with regard to new derivatives. Therefore, Ducho and his team developed a stereo-controlled tripartite approach for the synthesis of simplified muraymycin analogs.[135,136] They based their concept on the natural muraymycin **A5**, a congener of **A1**, which lacks the amino ribose unit but still has a strong inhibitory effect (cf. section 2.2.1).[111] Three building blocks were designed for the synthesis of 5'-deoxy muraymycin **C4** derivative **28** (cf. **Fig. 11**). These are the urea dipeptide **27**, aldehyde **24** and nucleosyl amino acid **23**.[68,135,137] The syntheses of these building blocks were established by M. Büschleb, O. Ries and A. Spork.[135,138–140]

The synthesis of **28** starts with the preparation of compound **19** over three steps. Therefore, uridine was protected as a *tris tert*-butyl dimethyl silyl ether (TBDMS), followed by selective deprotection of the hydroxy group at the 5'-position.[137,140,141] The primary alcohol was oxidized to aldehyde **19**, which subsequently underwent a *Horner-Wadsworth-Emmons* reaction with phosphonate **20**, leading selectively to nucleosyl amino acid **21**. The controlled formation of the stereocenter at the 6'-position is a key step in this route. It was accomplished by highly selective asymmetric hydrogenation with the chiral rhodium catalyst (*S*,*S*)-Me-DUPHOS-Rh. The same reaction was also performed with (*R*,*R*)-Me-DUPHOS-Rh leading to the epimer of **22** (structure not included), thus revealing that a variation at this position is possible for future projects. In order to perform a reductive amination with aldehyde **24**, Cbz-protected amine **22** was converted into free amine **23** under mild hydrogenolytic conditions.[137,140] Aldehyde **24** was synthesized following the protocol of O. Ries and Laïb *et al.* (structure not included).[135,139,142,143] After another mild deprotection of the Cbz group, free amine **26** was linked to urea dipeptide **27** via peptide coupling. The synthesis of compound **27** was established by M. Büschleb.[135,138] After global deprotection 5'-deoxy muraymycin **C4** derivative **28** was achieved as a double TFA-salt.[135]

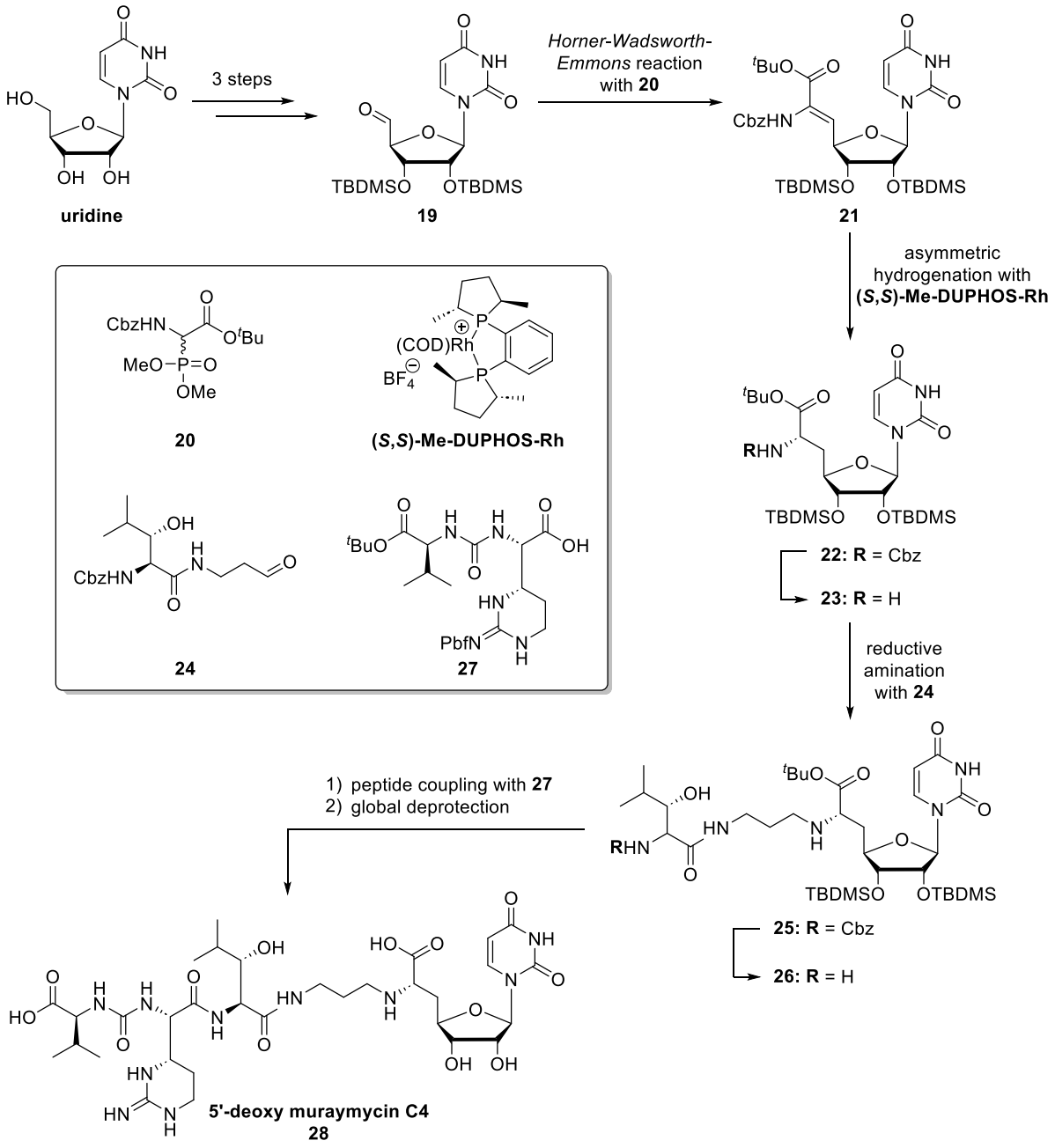

Fig. 11: Tripartite approach of the 5'-deoxy muraymycin **C4** analog **28** by Spork *et al.*[135]

As expected, muraymycin analog **28** had a lower inhibitory effect on $MraY_{S.\ aureus}$ than the most similar natural counterpart muraymycin **C1** (IC_{50}(**28**) = 95 ± 19 nM, IC_{50}(**C1**) = 0.016 ± 0.002 nM), demonstrating once again the importance of the amino ribose moiety for the interaction with the target. Compared to the natural products, the decrease in activity is significant. However, muraymycin derivative **28** still exhibited detectable activity. Although the simplified structure had no lipophilic side chain, which is still one of the main criteria for antibacterial activity, moderate to weak growth inhibition was observed for *E. coli* ($MIC_{E.\ coli\ DH5\alpha}$ = 15 µg/mL, $MIC_{E.\ coli\ \Delta tolC}$ = 50 µg/mL).

Furthermore, compound **28** showed no degradation *in vitro* (human plasma, metabolic stability) and no cytotoxicity.[121,135]

The simplified synthesis in combination with the generally promising biological data make the tripartite approach and muraymycin analog **28** itself a good starting point for new muraymycin derivatives. For example, the same approach was used to synthesize a series of muraymycin epimers for SAR study purposes. Here, Epic was replaced with Lys in the urea dipeptide structure and the configurations at the 6'-position and the leucine moiety were varied. Some of the compounds even lacked the hydroxy group at the central amino acid (structures not included).[144]

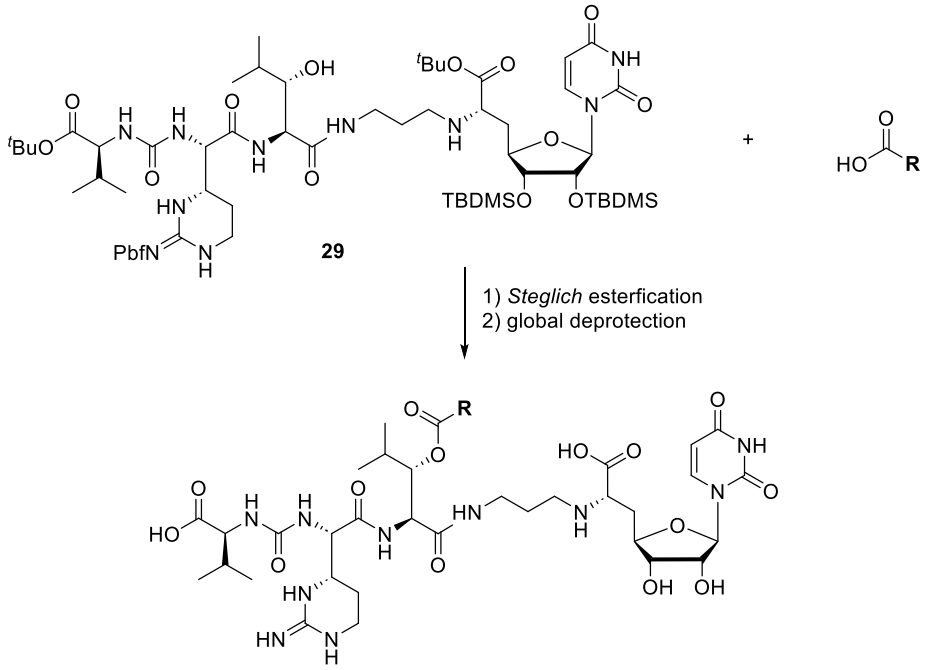

compound	R	IC_{50} [nM][a] MraY	IC_{50} [µg/mL] *E. coli* ΔtolC	bacterial growth MIC [µg/mL] *S. aureus* Newman	MRSA
30	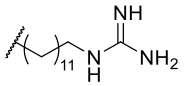	4.0 ± 0.7	<1	11.4[b]	24[b]
31	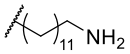	4.5 ± 0.3	<1	40	>100
32		5.8 ± 0.5	<1	10	5.5[b]
33		82 ± 12	<1	>100	n.d.

[a] crude membrane preparation; [b] preliminary result; n.d. not determined yet

Fig. 12: Structures of various *O*-acetylated muraymycin derivatives by M. Wirth.[145]

Furthermore, M. Wirth also used the route described above to synthesize globally protected muraymycin analog **29**. In addition, he introduced various fatty acid chains with different head groups into the backbone via *Steglich* esterification. The head groups included guanidinyl residues, amino groups and alkyl substituents (cf. **Fig. 12**) All derivatives are acylated at the central amino acid, corresponding to the natural structures (cf. section 2.2.1, **Fig. 8**). The derivatives with long lipophilic side chains (**30**-**32**) showed strong inhibition of the target enzyme in the nanomolar range (IC_{50}(MraY) ≈ 5 nM). Furthermore, these compounds showed strong inhibition of the bacterial growth of *E. coli* Δ*tolC*, but most importantly, promising data against *S. aureus* and clinically relevant MRSA. The most promising compound is derivative **32**, where an C_{13}-alkyl chain ($COC_{12}H_{25}$) was introduced into the backbone.[145] The results confirm previously published data by Tanino *et al.*, who also found an increase in antibacterial activity in the presence of long alkyl side chains in the muraymycin structure (cf. **Fig. 10**). Compound **32** even exceeds the most active natural products and is therefore a very promising lead structure.[131,132]

The field of muraymycin research was expanded by studies on solid-phase synthesis of the peptide building block, a prodrug approach and muraymycin conjugates by K. Leyerer, D. Wiegmann and C. Rohrbacher.[146–150]

2.2.4 Overview: SAR studies on muraymycins

The biological data obtained from various muraymycin derivatives provided many insights into the relevance of certain features of the molecular skeleton and gave a first impression of the extent to which variations are tolerated. The summarized results are illustrated in **Fig. 13**.

First, it was demonstrated, that an intact muraymycin structure is beneficial for the inhibition of the desired target MraY.[146,147] SAR studies focusing on the nucleobase structure revealed that uridine is accepted best and that minor variations can lead to nearly complete loss of inhibitory activity.[151,152] Replacing Epic with similar amino acids (Arg, Orn or Met) had little impact on the antibacterial activity, when other moieties like a lipophilic side chain and an amino ribose unit feature in the backbone.[126,132,133] In addition, masking of the terminal carboxylic moiety of Val or truncating this position is tolerated.[126,132,133,146] Since this structural motif is not relevant for this thesis, it is not highlighted in **Fig. 13**. However, substitution of Epic with Lys in the urea dipeptide structure resulted in reduced MraY-inhibition (100-fold decrease compared to Epic). In

addition, a complete loss of antibacterial activity was observed for some Lys-containing derivatives. In this context, it has to be mentioned that this Lys-containing derivatives lack the important additional features (lipophilic side chain, amino ribose unit). It can therefore be assumed that these moieties might compensate for the replacement in the urea motif. Nevertheless, the reduced synthetic effort combined with the still detectable micromolar inhibitory activities make this simplification highly useful for SAR study purposes.[144,146,147,149]

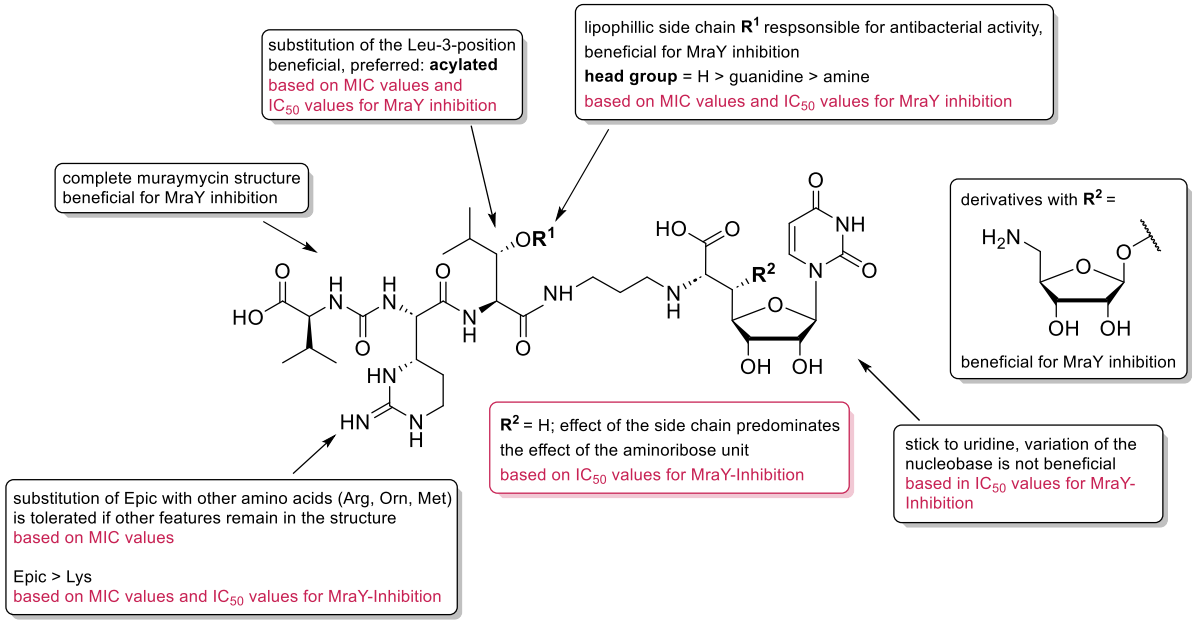

Fig. 13: Summarized results of the muraymycin SAR studies.[121,126,132,133,144–147,149,151,152]

Ducho and co-workers observed that introducing Leu instead of 3-hydroxy-Leu as central amino acid resulted in a loss of affinity towards the target.[121] An Ala-scan revealed that a substitution of this position lead to the most significant activity loss.[146,147] While not directly relevant for this thesis, it was observed that the configuration of the leucine moiety (α-position) has only weak influence on the inhibition activity (not illustrated in **Fig. 13**).[144]

The biological data of some natural compounds revealed that derivatives lacking a lipophilic side chain but still featuring the hydroxy moiety at the 3-Leu position exhibit inhibitory activity within the same range as the compounds featuring a lipophilic side chain (cf. section 2.2.1). Compounds lacking also the hydroxy group, showed reduced affinity towards MraY, although the activity is still in the sub-nanomolar range. However, the acylated compounds showed significantly higher antibacterial activity.

Additional results revealed that the absence of the amino ribose unit at the 5'-positon is tolerated although it leads to affinity loss at the target.[121] It can be speculated that in the data of the natural products, the effect of the amino ribose unit covered the comparable minor effects of other structural features. This hypothesis partially corresponds to the aforementioned results by Tanino *et al.*, who substituted Epic with other amino acids in a muraymycin scaffold featuring a lipophilic side chain and an amino ribose unit.[126,132] With the compounds of M. Wirth (cf. section 2.2.3, **Fig. 12**) it was discovered, that the presence of a side chain predominates the effect of the amino ribose unit.[145] A rather surprising result, because the amino ribose unit has a well-known strong interaction with the target.[91,117,119] Overall, the presence of an amino ribose unit strongly affects the target affinity (100-1000-fold) but has less impact on the antibacterial activity.[111,120,121,145] Thus, leading to the assumption that it can be removed from the structure design of new derivatives. In summary, this indicates that preserving a lipophilic side chain could allow the substitution of Epic and the amino ribose unit.

Since entering the cell is necessary to reach the target enzyme MraY in the cytoplasm, the strong antibacterial activities of the derivatives **30**-**32** can be attributed to the improved cell penetration. These results are consistent with the hypothesis that the fatty acid motif contributes to cellular uptake.[121,126,131–133] Furthermore, comparison of the structures **30**-**32** with each other shows that the absence of a head group on the lipophilic moiety gives the best antibacterial activities. This also matches with the fact that muraymycin **B8**, with a lipophilic alkyl chain is the most potent derivative to date. However, the additional presence of the amino ribose unit in **B8** must be considered when comparing the data.

The comparison of the IC_{50} values of the four muraymycin analogs in **Fig. 12** (cf. section 2.2.3) leads to the hypothesis that, contrary to previous assumptions, the lipophilic side chain also influences the interaction between the target and the inhibitor. The acetylated compound **33** is ten times less active in terms of MraY inhibition than the other derivatives with a long side chain. The inclusion of the lipophilic moiety in the hydrophobic cleft of MraY could be a 'new' target interaction that improves the affinity of the corresponding compound.[145]

In this work, the *O*-acetylated structures introduced by M. Wirth are further investigated.

3 Aims and Scope of this Thesis

3.1 General considerations

The primary aim of this thesis was the synthesis of novel muraymycin derivatives, with a special focus on modifying the central amino acid within the scaffold. **Fig. 14** illustrates a simplified muraymycin derivative designed and synthesized by M. Wirth, which features 3-hydroxy-Leu as central amino acid. Since muraymycin analog **32** was identified as the most potent simplified candidate overall (cf. section 2.2.3, **Fig. 12**), it was chosen as the lead structure for this work.[145] A successful structural simplification of the central amino acid would enhance the synthetic efficiency for new derivatives in the future. In particular, this would render the time-consuming synthesis of the 3-hydroxy-Leu unnecessary, which is present in the natural products and many synthetic derivatives.[135,139,142]

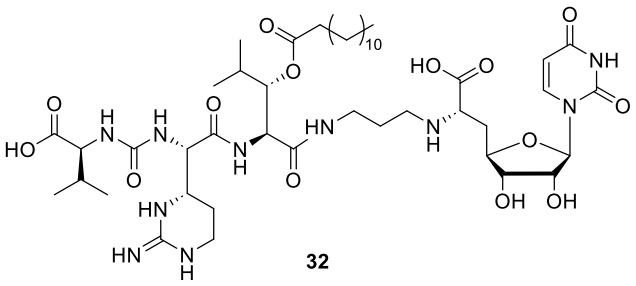

Fig. 14: Lead structure **32** with 3-hydroxy-Leu as central amino acid.[145]

Furthermore, the effect of the structure of the lipophilic side chain on the biological activity should also be investigated. For this purpose, an additional series of truncated muraymycin analogs was designed. In order to test the limits of structural simplification, it was planned to replace the cyclic amino acid L-epicapreomycidine in the urea dipeptide structure.

Overall, as part of a SAR study, a new lead structure should be identified, with a more simplified backbone compared to compound **32**. Also, the synthetic optimization achieved in this thesis is expected to be a significant advantage for future projects.

All muraymycin derivatives should be synthesized via a tripartite approach. This method was successfully introduced in the dissertation of M. Wirth and further developed in the preceding master thesis.[145,153] Thereby, the muraymycin scaffold is divided into three building blocks: a urea dipeptide, a central amino acid with lipophilic

side chain and nucleosyl amino acid **35**. **Fig. 15** illustrates the retrosynthesis of target compound **T1** as an example.

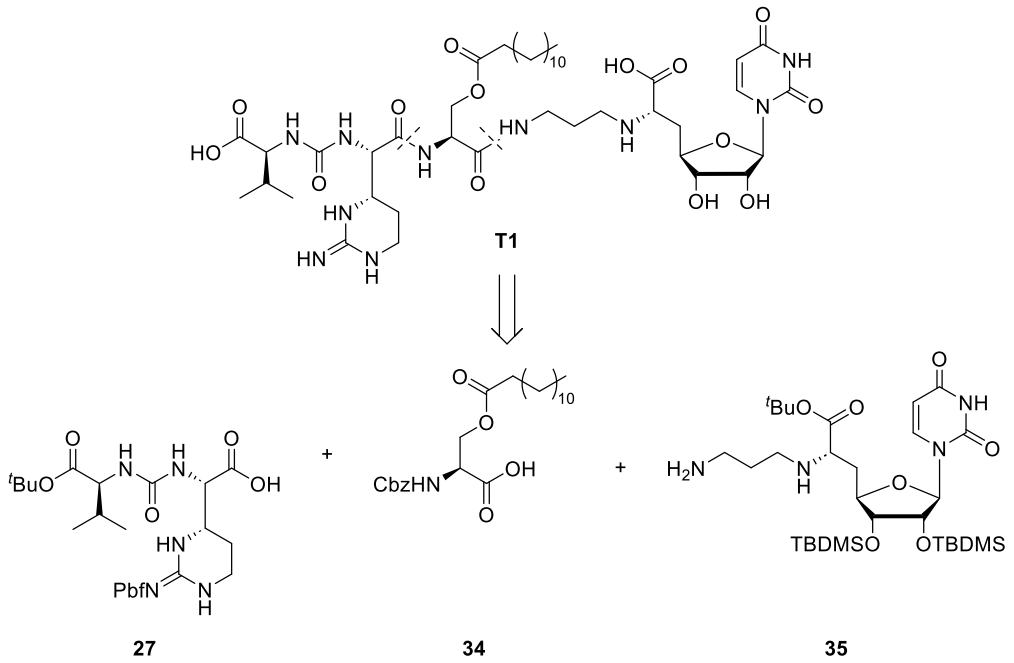

Fig. 15: Retrosynthesis of the tripartite approach exemplified for target compound **T1**.[153]

In the final stage, the corresponding building blocks are connected by peptide coupling. First, nucleosyl amino acid **35** is linked to any central amino acid. After cleavage of the *N*-Cbz group, the corresponding urea dipeptide is then introduced in a second peptide coupling. Due to issues arising from side product formation during established peptide coupling procedures with 1-hydroxybenzotriazole (HOBt) and benzotriazol-1-yloxytripyrrolidinophosphonium hexafluorophosphate (PyBOP),[146] an optimization of the coupling conditions is also part of this thesis.

3.2 Retrosynthesis

3.2.1 Retrosynthetic approach of the muraymycin derivatives with *n*-alkyl side chains

The first intended simplification of the muraymycin scaffold was the replacement of the central amino acid. The natural products (cf. section 2.2.1, **Fig. 8**) as well as the reference structure **32** (cf. **Fig. 14**) feature 3-hydroxy-Leu in their scaffold.[111,120,145] In order to simplify the synthesis, commercially available amino acids are the most convenient alternative. To maintain the common mode of connection via an ester motif, the proteinogenic amino acids L-serine, L-*allo*-threonine and L-threonine were the obvious choices. In the case of serine, the 3'''-position would lack the stereocenter.

All derivatives known to date are (3'''*S*)-configured. So, a series of Ser containing analogs might provide additional information about the significance of a stereocenter at this position. For a simplified scaffold with the natural (*S*)-configuration, the *allo*-form of L-threonine was selected as central amino acid. To elucidate the importance of the configuration, L-threonine was also included into a new derivative.

Another point of interest in this thesis is the degree of steric hindrance at the position adjacent to the ester group. All naturally occurring muraymycins contain an *iso*-propyl group in this moiety. As the natural congeners of the **C**-series may be hydrolysis products of the **A** and **B**-series compounds (cf. section 2.2.1, **Fig. 8**), the stability of the ester bond in biological media and the factors influencing it are of great interest. The comparison of the *allo*-Thr and Thr containing derivatives (methyl group) with the natural products (*iso*-propyl group) may provide insights into this particular issue. The structure of the lipophilic side chain remained a *n*-alkyl chain in all newly designed derivatives to enable a direct comparison with the model compound **32**.

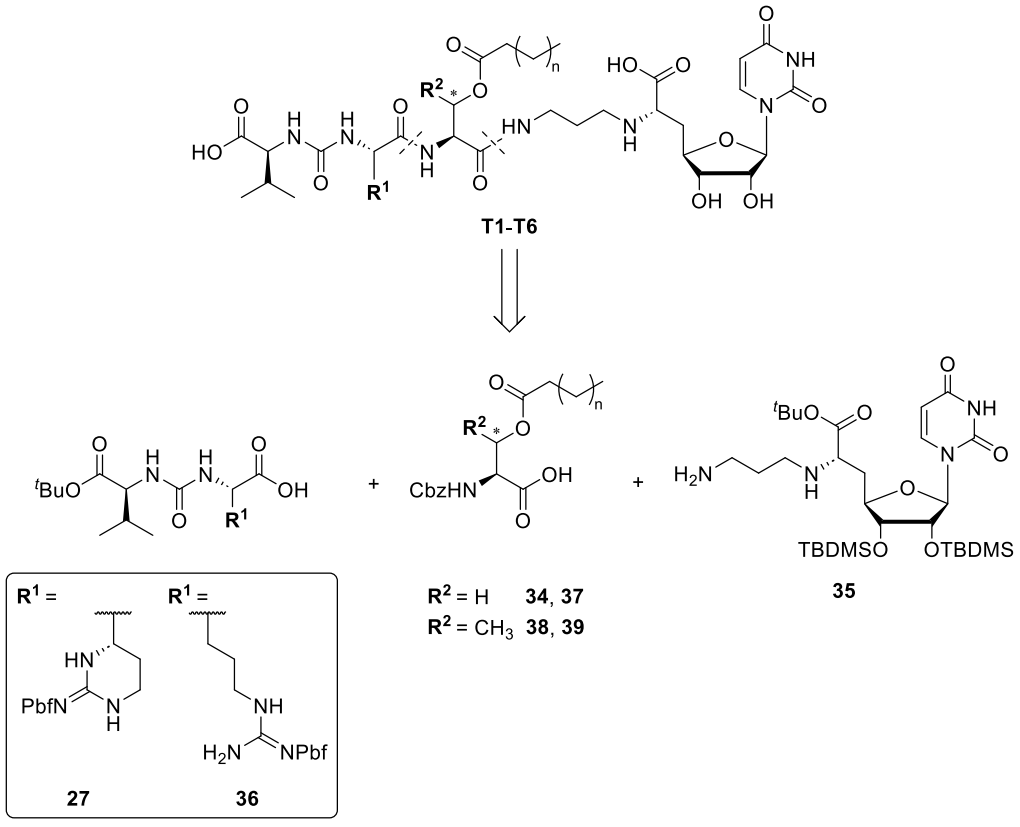

Fig. 16: Schematic tripartite approach for the new muraymycin derivatives with *n*-alkyl chains.[153]

As illustrated in **Fig. 16**, the desired derivatives were retrosynthetically divided into urea dipeptide **27** or **36**, various central building blocks and nucleosyl amino acid **35**. In the previously used tripartite approach, the central building block was not acylated and the

lipophilic side chains were introduced into the globally protected muraymycin scaffold. In this context, M. Wirth observed the formation of a side product during the peptide coupling with a Lys-containing urea dipeptide. Here, the free alcohol moiety partially underwent the peptide coupling instead of the primary amine, leading to a regioisomeric side product (structure not included).[145] So, it can be assumed that the designed acylated central amino acid(s) cannot undergo to this side reaction.

All naturally occurring muraymycins contain Epic in their scaffold (cf. section 2.2.1, **Fig. 8**) The first simplification of the urea dipeptide was performed by K. Leyerer and C. Rohrbacher, who synthesized a significant number of analogs in which Leu replaced Epic. These modifications led to a loss in activity.[146,147,149] In order to reduce the synthetic effort, but maintain the antibacterial activity, a set of derivatives was designed where the "cyclic Arg" amino acid Epic is replaced by commercially available Arg. They show greater similarity to the natural products, since both have a guanidinyl moiety and not only a primary amine like Leu. This could be the key to future simplification strategies of the urea dipeptide. To render the SAR as precisely as possible and therefore to gradually change various features in the scaffold, some derivatives with Epic were also designed.

The synthesis of Epic-containing urea dipeptide **27** was described by M. Büschleb, while C. Schütz introduced the synthesis of Arg-containing compound **36**.[135,138,142,154] Since **27** was available in the research group, the retrosynthesis is not presented here. However, it should be noted that it consists of fifteen more or less challenging synthetic steps. In comparison, urea dipeptide **36** can be synthesized in two steps (cf. **Fig. 17**), starting from L-valine *tert*-butyl ester. The amine is first converted into the corresponding isocyanate **40**, which then reacts with H-Arg(Pbf)-OH to urea dipeptide **36** in a second step.[154]

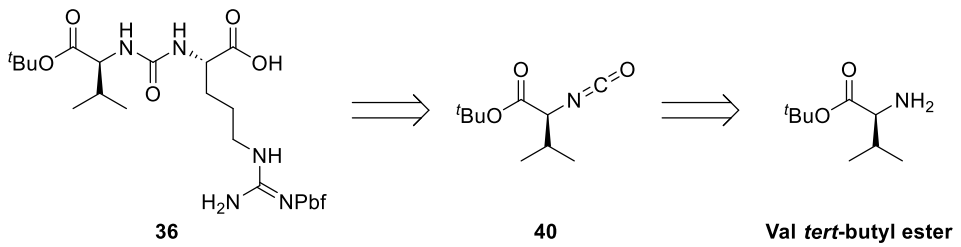

Fig. 17: Retrosynthesis of Arg-containing urea dipeptide **36**.[154]

All central building blocks can be synthesized following the protocol of the previous master thesis (cf. **Fig. 18**).[153] Herein, the carboxylic acid moiety of the corresponding amino acid is protected as a *tert*-butyl ester before the lipophilic side chains can be introduced by *Steglich* esterification. Subsequently, the carboxylic acid function is restored again. With the exchange of the central amino acid, the designed muraymycin derivatives exhibit reduced lipophilicity compared to the previous congeners. It can be hypothesized that this will lead to decreased activity, since lipophilicity was found to be beneficial for the cellular penetration.[121,126,131–133] In order to investigate whether an enlargement of the lipophilic side chain by three CH_2-groups (mirroring the *iso*-propyl group-atoms) could cover and counteract this loss, target compound **T2** was designed. The required central amino acid **37** can be synthesized using the same method as the other central building blocks, with the only difference being the use of hexadecanoic acid in the *Steglich* esterification.

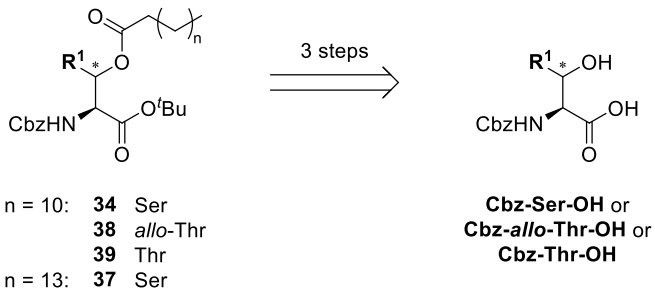

Fig. 18: Retrosynthesis of central building blocks **34**, **37**-**39**.[153]

Nucleosyl amino acid **35** (cf. **Fig. 19**) can be obtained by the well-established synthetic protocol of A. Spork.[135,137,140,144,155] The desired building block can be synthesized over eight steps starting from uridine. The synthesis includes an IBX oxidation, a *Horner-Wadsworth-Emmons* reaction, asymmetric hydrogenation and a reductive amination. During the reductive amination, *N*-Cbz-amino propionaldehyde **41** is treated with amine **23**. The propyl-linker aldehyde **41** can be obtained over two steps starting with 1-amino-3,3-diethoxypropane.[140,146] For the *Horner-Wadsworth-Emmons* reaction, the required phosphonate **20** can be synthesized according to the well-established synthesis of A. Spork starting from glyoxylic acid monohydrate.[137,140] For this work, the first step of this routine was already accomplished by S. Lauterbach and the compound was kindly provided for this work.

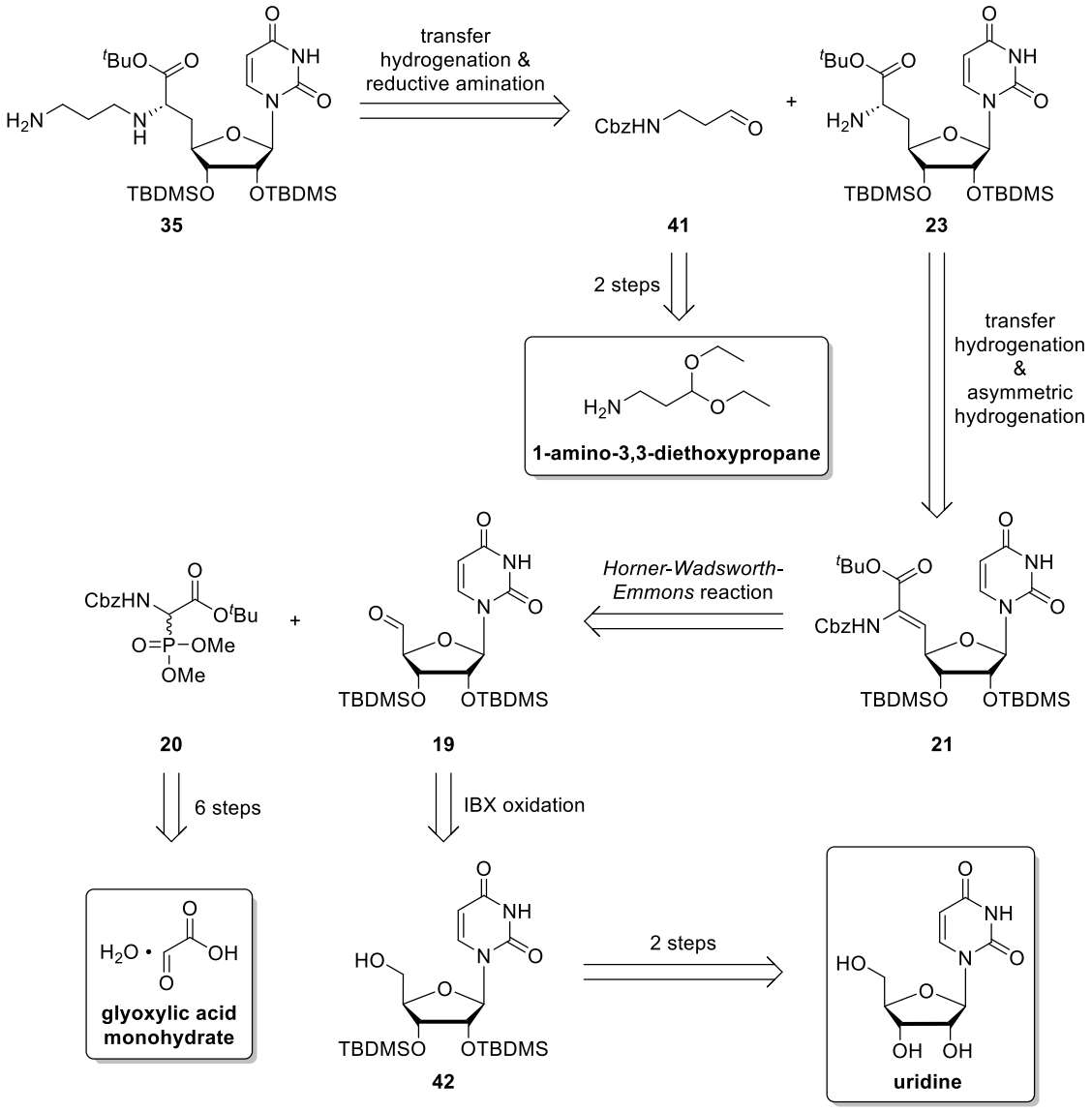

Fig. 19: Retrosynthesis of nucleosyl amino acid **35**.[137,140,146]

3.2.2 Retrosynthetic approach of the muraymycin derivatives with special side chains

In order to further investigate the fatty acid chain as an aspect of the SAR study, two additional compounds with special side chains were designed. Muraymycin analog **T7** features the shortest possible side chain, an acetyl group, while derivative **T8** has the identical side chain ($CO^{iso}C_{15}H_{31}$) as the most active natural muraymycin **B8** (cf. section 2.2.1, **Fig. 8**).[120] The retrosynthetic pathway for the required compounds (cf. **Fig. 20**) will be limited to central building block **44**, as **27** and **35** have already been described in section 3.2 and serine-based central building block **43** was available from the preceding master thesis.[153]

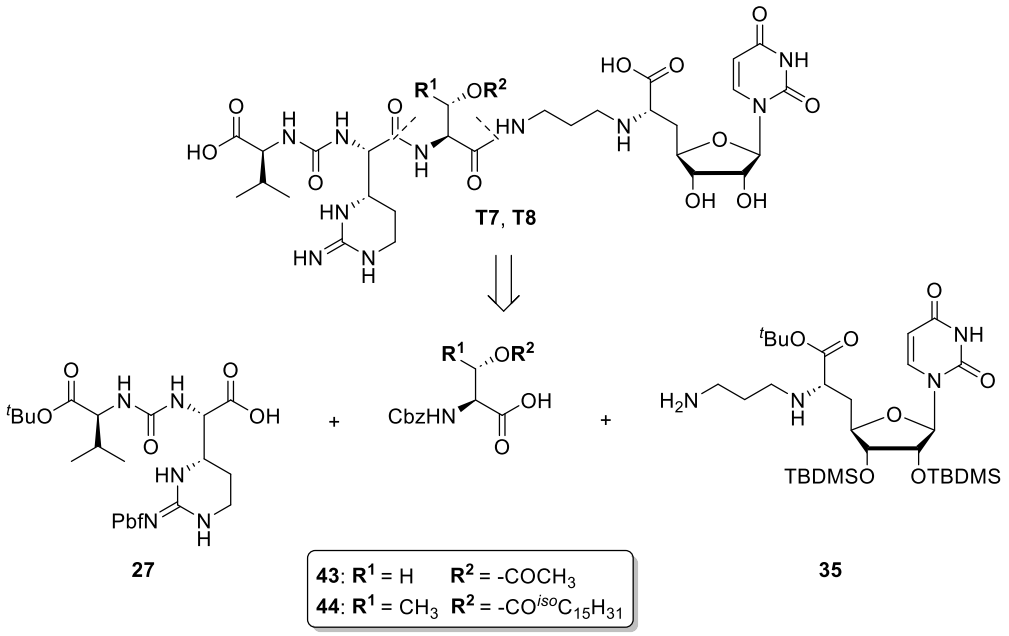

Fig. 20: Schematic tripartite approach for the acetylated muraymycin derivative **T7** and the muraymycin **B8** analog **T8**.[153]

Similar to the other central building blocks (cf. section 3.2.1, **Fig. 18**), derivative **44** can be synthesized in three steps. However, the carboxylic acid of the branched lipophilic side chain has to be prepared first. For this purpose, the strategy of Richardson and Williams is pursued.[156] They describe the synthesis of various branched long chains including the needed 14-methylpentadecaonic acid **45**. Using a combination of the *Chugaev* reaction and oxidative cleavage, different chain lengths of branched lipophilic side chains can be obtained. In the planned synthesis, **45** should be prepared in four steps from 15-methylhexadecanol (cf. **Fig. 21**).

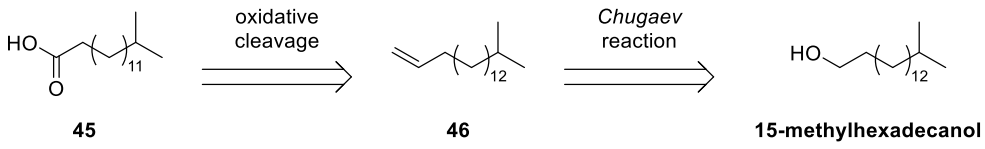

Fig. 21: Retrosynthesis of the branched fatty acid **45**.[156]

Muraymycin derivative **T9** was designed to investigate how the target tolerates a more rigid lipophilic side chain. For this purpose, the unsaturated fatty acid **47** should be incorporated into the muraymycin scaffold. A *Z*-double bond was chosen to induce maximal rigidity with minimal change to the side chain. The designed lipophilic side chain **47** has a *Z*-double bond at the 6-position. It can be obtained using a protocol of Wube *et al.* describing a synthesis to achieve isomerically pure *Z*-configured aliphatic side chains via a *Wittig* reaction.[157] In this particular case, the length of C_{13} should be retained so that it can be directly compared with the analogs carrying *n*-alkyl chains.

Overall, carboxylic acid **47** can be synthesized from the commercially available reagents 6-bromohexanoic acid and *n*-heptanal (cf. **Fig. 22**) in two steps.

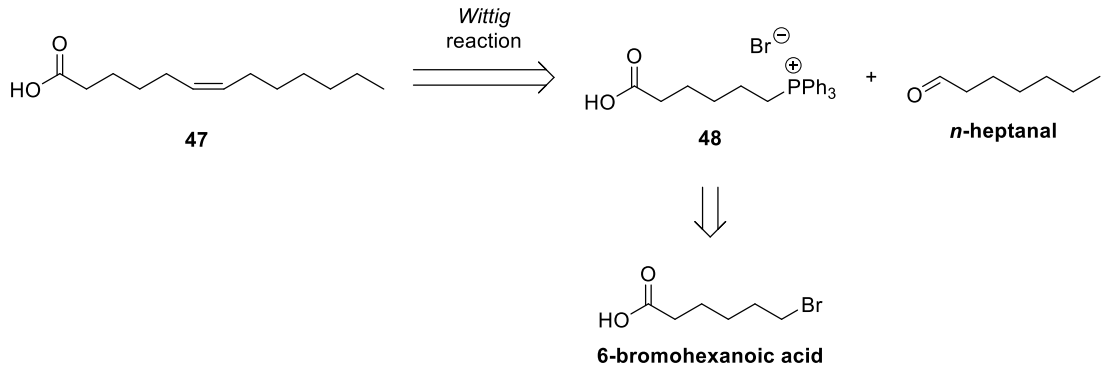

Fig. 22: Retrosynthesis of the unsaturated fatty acid **47**.[157]

Since the new fatty acid chain includes a *Z*-isomeric double bond, the already described tripartite approach cannot be used. Therefore, the globally protected acetyl analog **50** is synthesized, which can then be selectively deprotected at the central amino acid. The required acetylated amino acid **51** can be synthesized in a similar way to the corresponding Ser derivative from the preceding master thesis. For this purpose, Cbz-*allo*-Thr-OH is converted into building block **51** in a single step with acetic anhydride and pyridine (not displayed).[153,158] After the selective cleavage of the acetyl moiety, the unsaturated lipophilic side chain **47** can be introduced by *Steglich* esterification. A protocol by *Glen Research* describes a very promising method of deprotecting the acetyl group under mild conditions.[159] The desired compound **T9** can be obtained after global deprotection (cf. **Fig. 23**).

The approach described in **Fig. 23** harbors the potential for an alternative approach for future projects. It would ease the introduction of various lipophilic side chains into the muraymycin scaffold. Therefore each new muraymycin would not have to be synthesized following the tripartite approach, in which the central amino acid with the desired lipophilic side has to be synthesized for each new derivative individually.

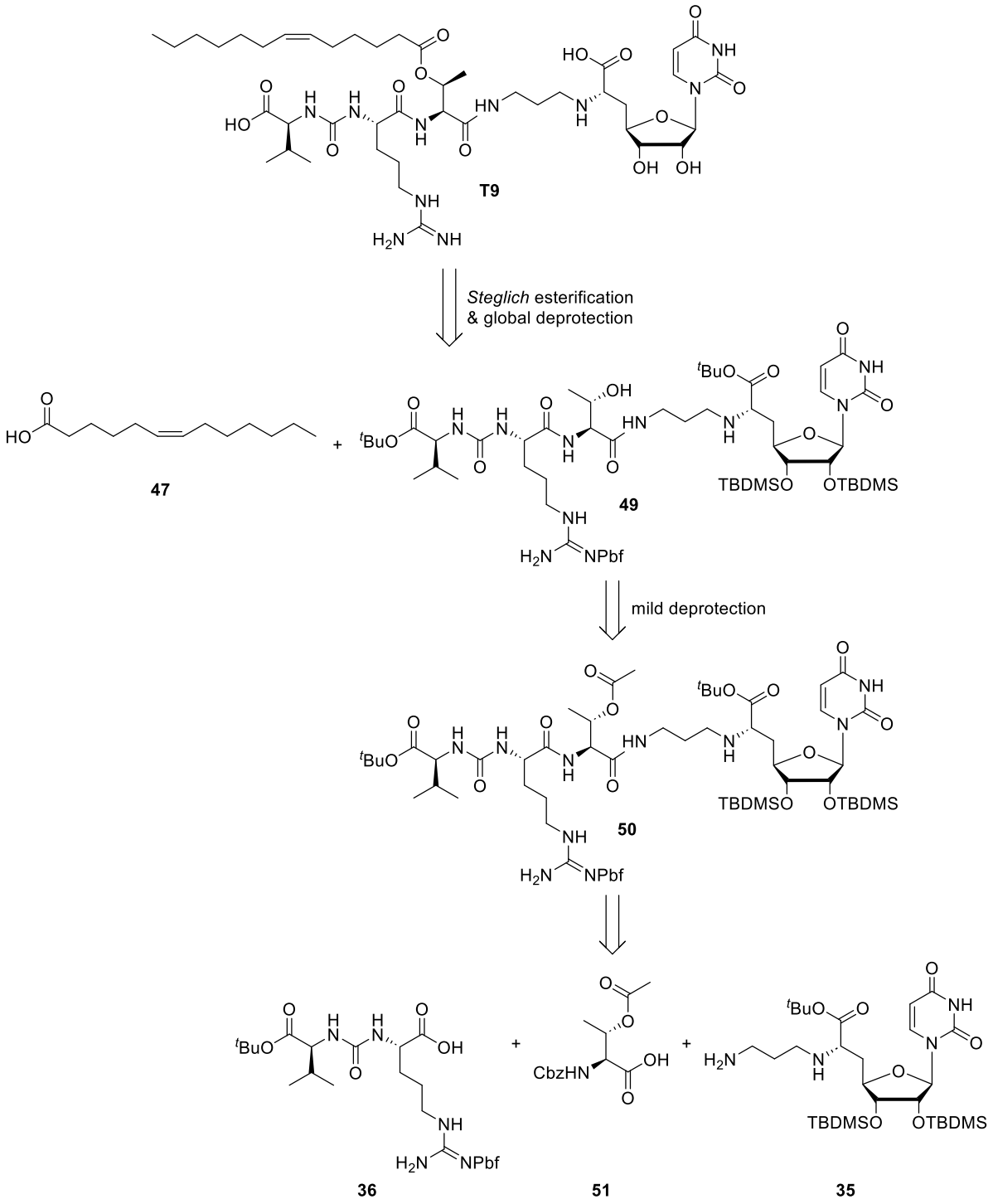

Fig. 23: Retrosynthesis of muraymycin derivative **T9** with an unsaturated lipophilic side chain.[153,158,159]

3.2.3 Retrosynthetic approach of the truncated muraymycin derivatives

In order to determine the role of the urea dipeptide moiety and to evaluate whether the absence of this particular structural motif can be compensated by a lipophilic side chain, a series of truncated muraymycin analogs was designed. The impact of the lipophilic side chain may be overshadowed by the urea dipeptide, as the latter is

essential for target interaction and bacterial activity. **Fig. 24** shows the three designed compounds, all of which can be synthesized starting from compound **52**.

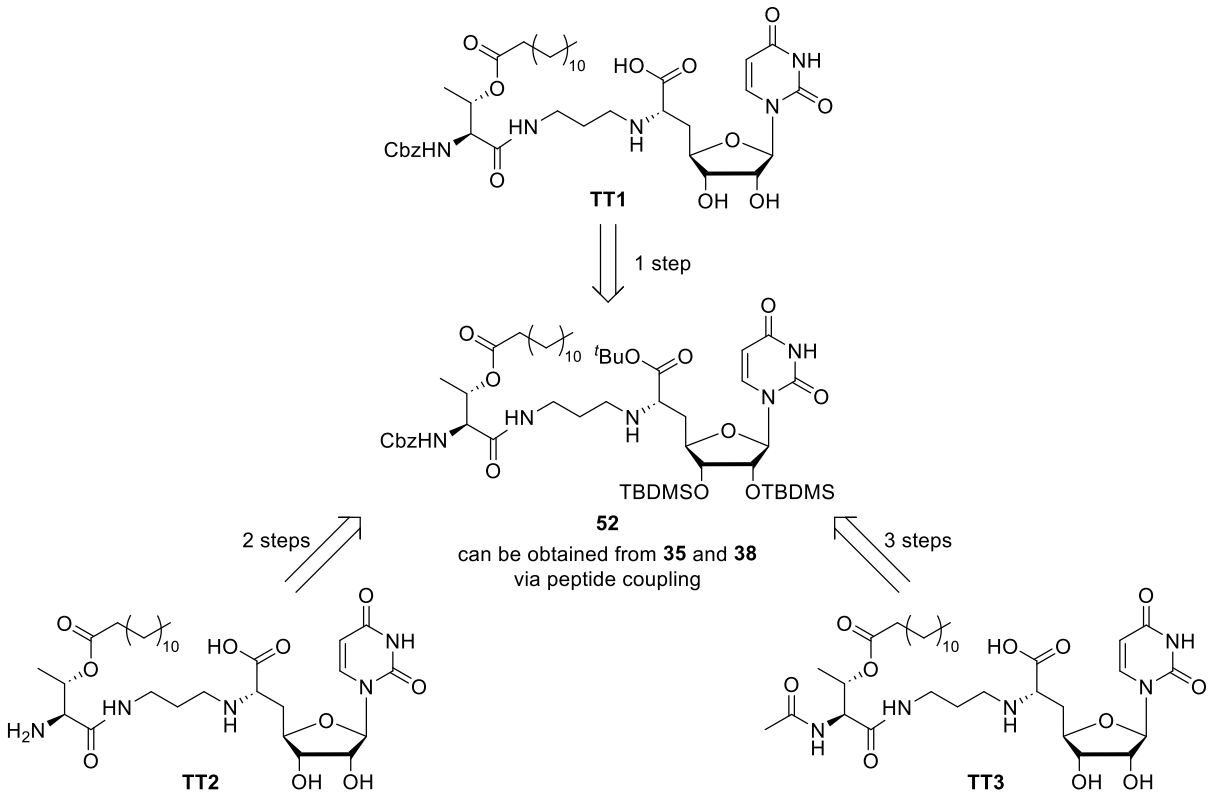

Fig. 24: Retrosynthesis of the truncated derivatives **TT1**-**TT3** starting from intermediate **52**.

The first truncated derivative **TT1** contains a Cbz-protecting group, which is very bulky and would have a different mode of interaction due to its aromatic character. Target compound **TT1** can be obtained after global deprotection of derivative **52**, which is an intermediate in the synthesis of the desired compounds **T4** and **T5**. Secondly, the free amine **TT2** is the smallest possible truncated analog. Due to its polar character, it is believed to interact less efficiently with the target and was specifically designed as a negative control. It can be obtained after Cbz-deprotection during the synthesis of derivatives **T4** and **T5** and subsequent global deprotection. For compound **TT3**, the amine is converted into the smallest possible amide, which carries an acetyl group. This modification mirrors the interaction at this specific position in the original backbone (cf. section 2.2.1, **Fig. 8**), while applying the least possible impact on the overall interaction. The amide is believed to interact with the target in the same manner as in the intact muraymycin scaffold. Hence, any negative effects associated with the free amine in compound **TT2** is eliminated. Compound **TT3** can be synthesized via Cbz-deprotection of compound **52** followed by a peptide coupling with acetic acid and subsequent global deprotection.

3.3 Summary: planned derivatives for SAR study

Overall, nine full-length muraymycin derivatives were designed (cf. **Fig. 25**). The structure-activity relationship study based on these derivatives will provide detailed insights into the role and effect of the lipophilic side chain and the requirements for the central amino acid. Furthermore, it will be revealed if replacing Epic with Arg would be tolerated by the target and how or whether this exchange would affect antibacterial activity.

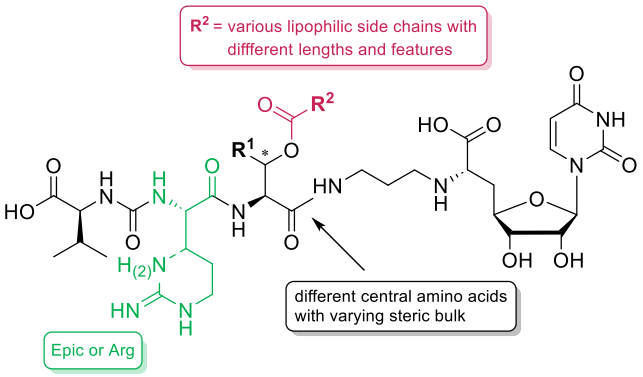

Fig. 25: Overview of the planned modifications within the nine target structures **T1**-**T9**.

The SAR study will be extended by the truncated derivatives **TT1**-**TT3** shown in **Fig. 26**. These will provide further knowledge of the role and effect of the lipophilic side chain in an isolated fashion. This is valuable because in many SAR studies, the loss of activity due to the absence of the side chain is difficult to quantify, since the rather strong interaction of the dipeptide often compensates for this effect. Therefore, more aspects could be covered for this particular structural feature. Furthermore, the designed residues for **R**^{1} will interact differently with the target site. This can also provide insights into which structural motifs are compatible or tolerated at this position.

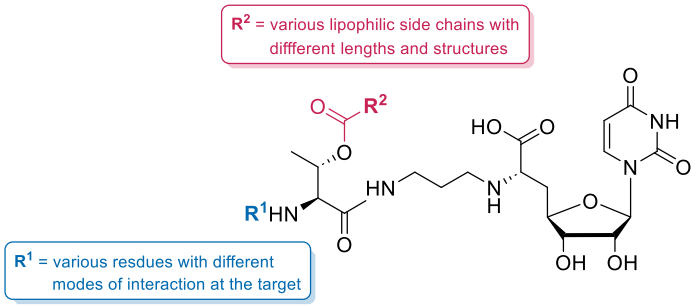

Fig. 26: Overview of the planned truncated muraymycins **TT1**-**TT3**.

4 Results and Discussion

4.1 Synthesis of nucleosyl amino acid derivative 35

The scaffold of all planned derivatives contains the 6'-deoxy nucleosyl amino acid **35**, which can be synthesized according to the protocol of A. Spork.[137,140]

In order to selectively modify the primary alcohol moiety of uridine, the 2'- and 3'-hydroxy groups must be protected. A specific protection of the secondary alcohols is not possible and can only be achieved via a two-step reaction sequence. So, uridine was first treated with *tert*-butyl dimethyl silyl chloride (TBDMSCl) under basic conditions for 3 days at room temperature. The intermediate **53** was isolated by silica gel column chromatography with a good yield of 82%. The selective deprotection of the 5'-hydroxy group was achieved with acidic treatment of **53** at 0 °C. These reaction conditions and the continuous observation by TLC help to prevent the deprotection of the secondary alcohols at the 2'- and 3'-positions. After 5.5 hours, a new polar component appeared on the TLC sheet, which can be assumed to be a double-deprotected uridine derivative. The reaction was therefore ended at incomplete conversion. The free alcohol **42** was isolated by silica gel column chromatography with a very good yield of 94% (cf. **Fig. 27**).

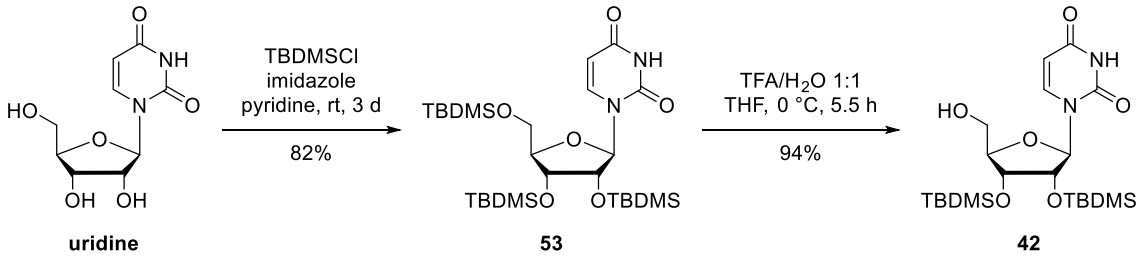

Fig. 27: Synthesis of uridine derivative **42** over two steps starting with uridine.

In order to perform the subsequent *Horner-Wadsworth-Emmons* reaction,[160–162] alcohol **42** had to be oxidized to the corresponding aldehyde. The latter then reacts with phosphonate **20** to provide alkene **21**.

The *tert*-butyl ester phosphonate **20** was synthesized via a well-established five-step reaction sequence, whereby only the last three steps were performed during this work.[137,140,163,164] Methyl ester **54** was kindly provided by S. Lauterbach and was used for the following reactions. First, compound **54** was refluxed in dry toluene. Then, phosphorus trichloride was added dropwise at this temperature to activate the methyl ester. After 4 hours, trimethyl phosphite was added for the formation of methyl

phosphonate **55** in a *Michaelis-Arbuzov*-like reaction.[140] After workup, the desired intermediate **55** was isolated with a solid yield of 80%. The transesterification to *tert*-butyl ester **20** was performed in two steps.[140] The alkaline hydrolysis of methyl ester **55** was carried out at 12 °C over 18 minutes, resulting in free acid **56** with an excellent yield of 99%. The formation of *tert*-butyl ester **20** was performed in dry *tert*-butanol using the alcohol simultaneously as reagent and solvent. *N*-ethoxycarbonyl-2-ethoxy-1,2-dihydroquino-line (EEDQ) was used as an activator of carboxylic acid **56**. To facilitate the ester formation, molecular sieve (3 and 4 Å) was added, which absorbed the accruing water from the reaction mixture. After 17 hours, the molecular sieve was filtered off using celite® and *tert*-butyl ester **20** was isolated after purification by silica gel column chromatography with a good yield of 74%. The sequence yielded phosphonate **20** in three steps with an overall yield of 59% (cf. **Fig. 28**).

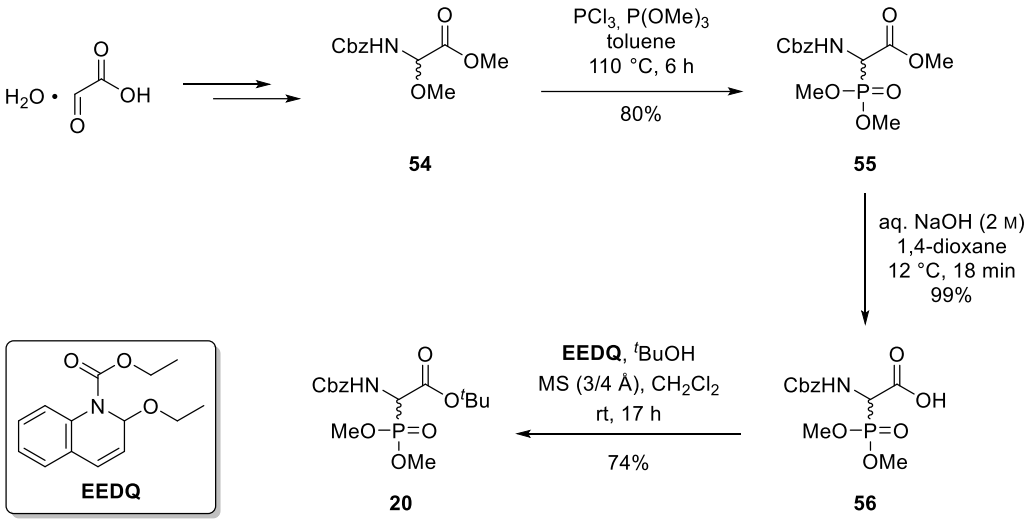

Fig. 28: Synthesis of *tert*-butyl ester phosphonate **20** over five steps starting with glyoxylic acid monohydrate (compound **54** kindly provided by S. Lauterbach).

Alcohol **42** was turned into the corresponding aldehyde **19** with 2-iodoxybenzoic acid (IBX).[137,140,146,165] The reaction was performed in refluxing dry acetonitrile over 1.5 hours. Then, the reaction mixture was cooled down to 0 °C to precipitate remaining IBX and formed 2-iodobenzoic acid, which were filtered off. The hydrolysis-sensitive aldehyde **19** was verified using ^{1}H NMR and its purity (~70%) was determined. In another attempt, **19** was synthesized with commercially available IBX (stabilized with benzoic acid and isophthalic acid). The reaction was carried out in the same way as described above. In order to remove the remaining stabilizer, the crude product was purified by silica gel column chromatography with ethyl ether and dichloromethane as eluents. After removal of the solvent, aldehyde **19** was obtained with a yield of 79%

(calcd. form ^{1}H NMR). However, a small amount of stabilizers remained in the product, which turned out to be not harmful for the subsequent *Horner-Wadsworth-Emmons* reaction. Although aldehyde **19** had previously been described as an unstable compound,[140] it was possible to purify it by silica gel column chromatography. To verify whether decomposition or side reactions could have taken place, the NMR data of the purified and a non-purified batch were compared and found to be identical. Since the batch, which underwent column chromatographic purification was also used in a *Horner-Wadsworth-Emmons* reaction, this definitely proves that the aldehyde is rather stable under the chosen conditions. This means that purification can be attempted if necessary.

The subsequent *Horner-Wadsworth-Emmons* reaction required special reaction conditions to ensure the formation of the desired *Z*-isomer.[137,140,160] Initially, phosphonate **20** was stirred with the strong base potassium bis(trimethylsilyl)amide (KHMDS, 0.5 M in toluene) for 15 minutes at room temperature. In order to ensure the formation of the *Z*-isomer (cf. **Fig. 29**), aldehyde **19** was added dropwise at -82 °C over a period of 45 minutes. The reaction mixture was stirred overnight, during which it was allowed to warm up to room temperature. Then, methanol was added to end the reaction by deactivation of the remaining base, phosphonate carbanion and aldehyde. Purification by silica gel column chromatography yielded the isomerically pure *Z*-isomer **21** in 69% yield. Its purity was confirmed by comparison of the ^{1}H NMR data with previously published results.[137,140,166]

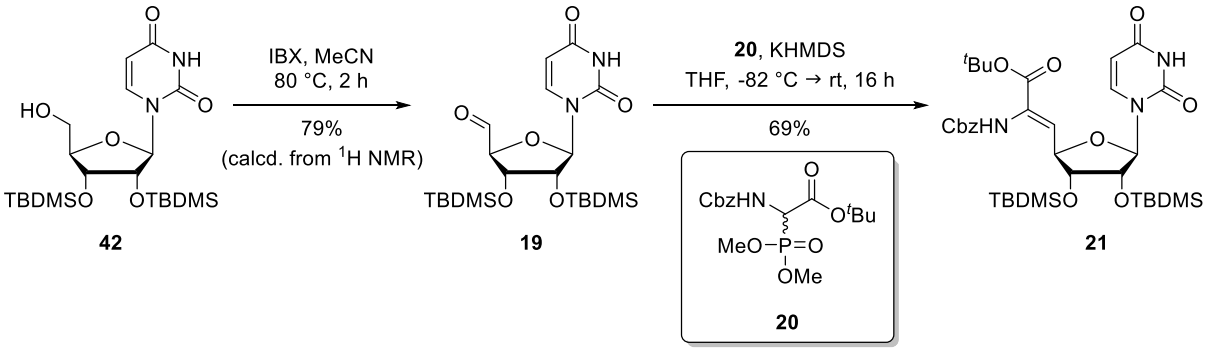

Fig. 29: Synthesis of uridine derivative **21** via IBX oxidation and *Horner-Wadsworth-Emmons* reaction with phosphonate **20**.

The *Z*-didehydro amino acid **21** was stereoselective turned into the (6'*S*)-isomer **22** by asymmetric hydrogenation.[136,137,140] This reaction was carried out in dry methanol under hydrogen atmosphere (1 bar). The used rhodium catalyst (+)-1,2-bis-[(2*S*,5*S*)-2,5-dimethylphospholano]bezene(cyclooctadiene)rhodium(I)-tetrafluoroborat ((*S*,*S*)-

Me-DUPHOS-Rh) was developed and published by Burk.[167] The configuration of the chiral phosphine ligand in this catalyst determines the resulting confirmation of the developing steric center.[168,169] The reaction was handled with great care, as the catalyst is air and moisture sensitive. Therefore, the solution of nucleosyl amino acid **21** in dry methanol was degassed repeatedly, before the orange catalyst (*S*,*S*)-Me-DUPHOS-Rh was added. Then, hydrogen (1 bar) was bubbled through the solution once a day for 5 days. During this time, the color of the reaction mixture turned darker, showing degradation of the catalyst. The progress of the reaction was monitored by ^{1}H NMR spectra until the reaction was finished. Complete conversion of compound **21** into **22** is crucial for the following reaction sequence because both compounds cannot be separated by silica gel column chromatography due to their almost identical structure and behavior on silica gel. The desired compound **22** was obtained in 91% yield after purification (cf. **Fig. 30**).

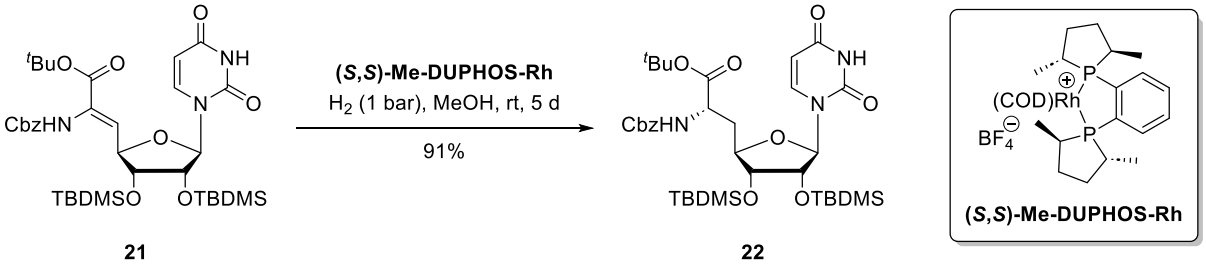

Fig. 30: Asymmetric hydrogenation of uridine derivative **21** with catalyst (*S*,*S*)-Me-DUPHOS-Rh.

Nucleosyl amino acid **22** is connected to any central building block via propyl linker **41**. The applied synthesis for this derivative, which is illustrated in **Fig. 31**, was synthesized according to the protocol of A. Spork.[137,140] First, 3,3-diethoxypropane-1-amine was treated with benzyl chloroformate under basic conditions at 0 °C. The mixture was stirred for 18 hours. During this time, the mixture warmed up to room temperature to give carbamate **57**. The substance was isolated after silica gel column chromatograph with a good yield of 88%. Since propyl linker **41** is connected to nucleosyl amino acid **23** via reductive amination, an aldehyde moiety is required, which can undergo the reaction. Treatment of carbamate **57** with aqueous acidic conditions for 105 minutes at room temperature led to the formation of the desired aldehyde **41**. Silica gel column chromatography yielded propyl linker **41** with 88%. The short synthesis sequence gave linker **41** in 77% yield over two steps.

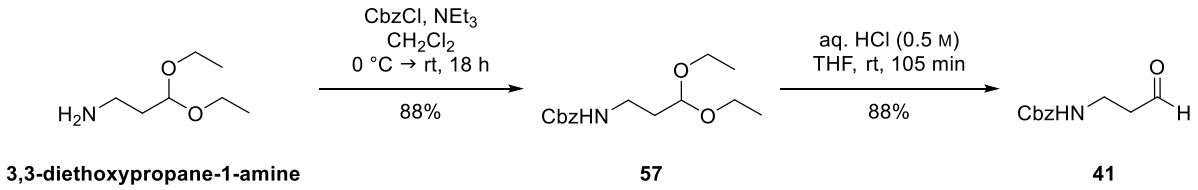

Fig. 31: Synthesis of *N*-Cbz-3-aminopropanal **41** over two steps starting from 3,3-diethoxypropane-1-amine.

The free amine **23** required for the reductive amination can be easily obtained by mild deprotection of nucleosyl amino acid **22**.[146] For this purpose, **22** is dissolved in dry *iso*-propanol and then 1,4-cyclohexadiene and palladium black are added. The reaction was previously executed in dry methanol, but D. Wiegmann discovered a potential side reaction, taking place with the former solvent. He observed a cyclization between the freed amine at the 6'-position and the 3-amide due to the formation of formaldehyde from methanol.[148] This side reaction could be excluded when the solvent was switched to *iso*-propanol. It was observed that the deprotection is induced by heat supply, which was often given by hand warmth. Here, a water bath of 40 °C was used. The catalyst agglomerates during the reaction, which indicates its progress and finally complete conversion. In addition, the progress was monitored by TLC. After one hour, the palladium black was filtered off using a syringe filter. After removal of the solvent, the free amine **23** was isolated 98% yield. For the following reaction, both reagents needed to be completely water- and solvent-free. Therefore, both were dried in high vacuum for a longer period of time. The reductive amination is carried out over several days. First, the amine **23** and aldehyde **41** were diluted in dry tetrahydrofuran and stirred for 24 hours at room temperature. During this time, the corresponding imine formed, releasing water as a side product. Molecular sieve (4 Å) was used to adsorb the water and thus prevent the reverse reaction. The formation of the imide cannot be observed by TLC nor LC-MS due to its instability. Therefore, a period of 24 hours is provided to give the imine enough time to form. Then, sodium triacetoxyborohydride and Amberlyst-15^{TM} were added to the suspension. The latter is an ion exchange resin, providing hydrogen cations. The reducing agent was dried for 5 days in vacuum before usage, as it degrades to acetic acid over time, which would interfere with the wanted reduction. The reaction was stirred for 3 days at room temperature and monitored by TLC until no reaction progress could be detected. The reaction mixture was filtered over celite® to remove the molecular sieve. Nucleosyl amino acid **58** was obtained in 84% yield after silica gel column chromatography. During the reaction time of 4 days,

the molecular sieve is usually pulverized. It can therefore be assumed that the re-released water could have interfered with the reduction step by splitting the imide into amine **23** and aldehyde **41**. This might be the reason for incomplete conversion.

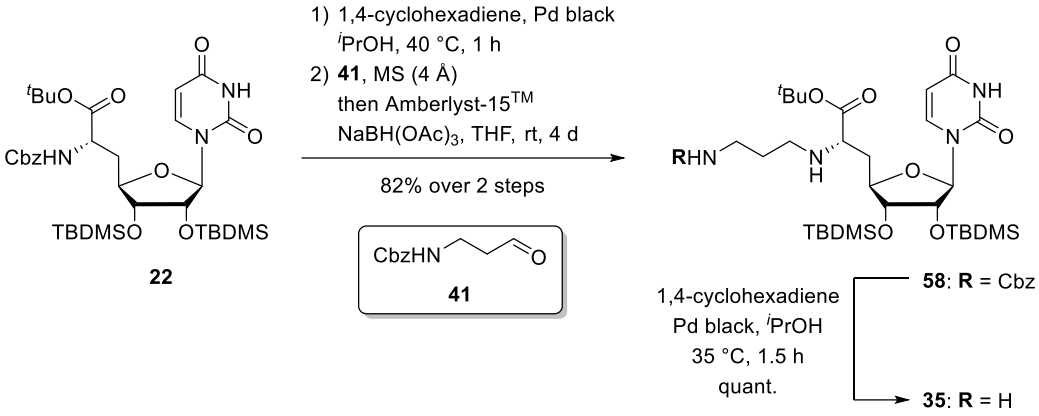

Fig. 32: Synthesis of nucleosyl amino acid **35** via Cbz-deprotections and reductive amination.

Nucleosyl amino acid **58** had to be Cbz-deprotected for the subsequent peptide coupling. The well-established method described above was used again for this purpose.[148] Thus, 1,4-cyclohexadiene and palladium black were added to a solution of **58** in dry *iso*-propanol. The reaction mixture was stirred at 35 °C for 1.5 hours. As previously mentioned, the reaction is initiated by heat, which was again provided by a water bath. While an exact temperature is not required, the temperature should not exceed 40 °C to prevent side reactions. After 1.5 hours, the catalyst agglomerated, indicating the end of the reaction, which was also confirmed by TLC and LC-MS. The reaction mixture was filtered through a syringe filter, which was washed multiple times with methanol. After solvent removal, the compound **35** was obtained quantitatively (cf. **Fig. 32**).

4.2 Synthesis of the L-serine-containing muraymycin derivatives

4.2.1 Synthesis of Ser-based central building blocks 34 and 37 with *n*-alkyl chains

The synthesis of the central building block **34** was first presented in the preceding master thesis. The compounds **60** and **61** (cf. **Fig. 33**) were synthesized for the afore-mentioned work and were used in this thesis. Consequently, the syntheses of these two compounds is not discussed in detail here, but reference is made to the earlier master thesis.[153]

The commonly used method for introducing a lipophilic side chain via *Steglich* esterification (cf. **Fig. 33**) was applied to conjugate hexadecanoic acid to the protected

Cbz-Ser-O^{t}Bu **60**.[153] This particular alkyl chain, which is extended by three CH_2 units compared to **61** and **34**, was introduced to evaluate whether lengthening the side chain by an equivalent number of carbon and hydrogen atoms could compensate for the omission of the *iso*-propyl group (cf. section 2.2.1, **Fig. 8**)[111,120] on the central building block. Additionally, the study aimed to investigate how this modification might affect the interaction with the target and the compound's absorption into bacterial cells.

For the introduction of the hexadecanoyl side chain ($COC_{15}H_{31}$), the corresponding hexadecanoic acid, the primary alcohol **60** and catalyst 4-dimethylamino-pyridine (DMAP) were dissolved in dry tetrahydrofuran. Then, 1-ethyl-3-(3-dimethylamino-propyl)carbodiimide hydrochloride (EDC • HCl) was added as an activator and the reaction mixture was stirred for 6 hours at room temperature. During this time, the poorly soluble hydrochloride gradually dissolved, and an insoluble white solid formed throughout the synthesis. This precipitated solid is most likely EDU, the urea derivative of EDC. The reaction was monitored using TLC and was ended by the addition of hydrochloric acid (0.5 M). Compound **62** was obtained after purification by silica gel column chromatography, resulting in a high yield of 94% (cf. **Fig. 33**). Each of the *tert*-butyl esters, **61** and **62**, was treated with aqueous trifluoroacetic acid (80%) to release the corresponding carboxylic acids. For both compounds, the reaction time of 2.5 hours was sufficient (based on TLC monitoring). In each case, the solvent was diluted with water and removed by lyophilization, resulting in the isolation of Cbz-Ser($COC_{12}H_{25}$)-OH **34** and Cbz-Ser($COC_{15}H_{31}$)-OH **37** as white solids in 98% and 82% yield, respectively. The reaction sequence gave **34** in 57% and **37** in 47% yield over three steps. The introduction of the *tert*-butyl ester was the yield-limiting step. It was observed that during the reaction, a double functionalized derivative, in which an additional *tert*-butyl ether is introduced at the alcohol moiety (cf. **Fig. 33**, compound **60SP**), was formed. This side reaction was the primary factor contributing to the reduced yield.[153]

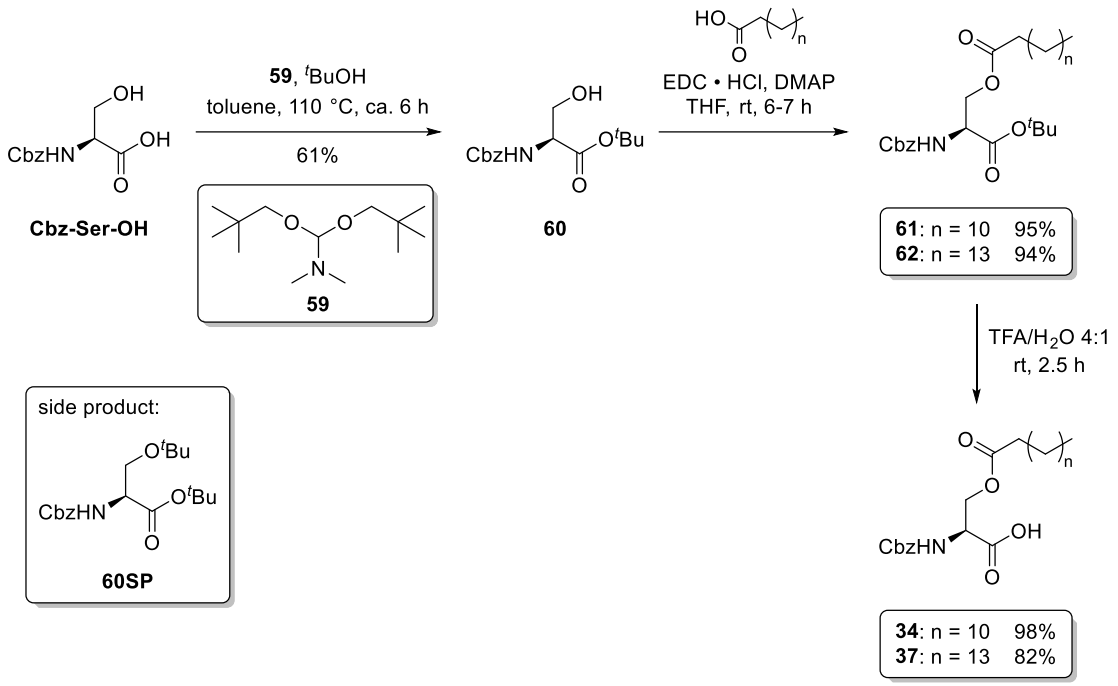

Fig. 33: Synthesis of Ser-based derivatives **34** and **37** starting with Cbz-Ser-OH (syntheses of **60** and **61** from preceding master thesis).[153]

4.2.2 Synthesis of target compound T1: Val-Epic-Ser($COC_{12}H_{25}$)-NuAA

All building blocks required for the desired derivatives could now be combined. As described in chapter 3, the initial step is the peptide coupling of nucleosyl amino acid **35** with any central building block.

For this purpose, the reaction between L-serine derivative **34** and **35** was carried out under already established conditions (**Fig. 34**).[146,153] First, 1-hydroxybenzotriazole (HOBt), benzotriazol-1-yloxytripyrrolidinophosphonium hexafluorophosphate (PyBOP) and *N*,*N*-diisopropylethylamine (DIPEA) were added to a solution of compound **34** in dry tetrahydrofuran to activate the acid. The mixture was stirred for 30 minutes at room temperature to form the HOBt active ester. Then, nucleosyl amino acid **35** was added dropwise to the cooled reaction mixture. After 1 hour at this temperature, the reaction mixture was stirred for 24 hours at room temperature. The progress of the reaction was monitored by TLC and LC-MS and was considered complete after 25 hours. The solvent was removed under reduced pressure and a yellowish resin was obtained after silica gel column chromatography.

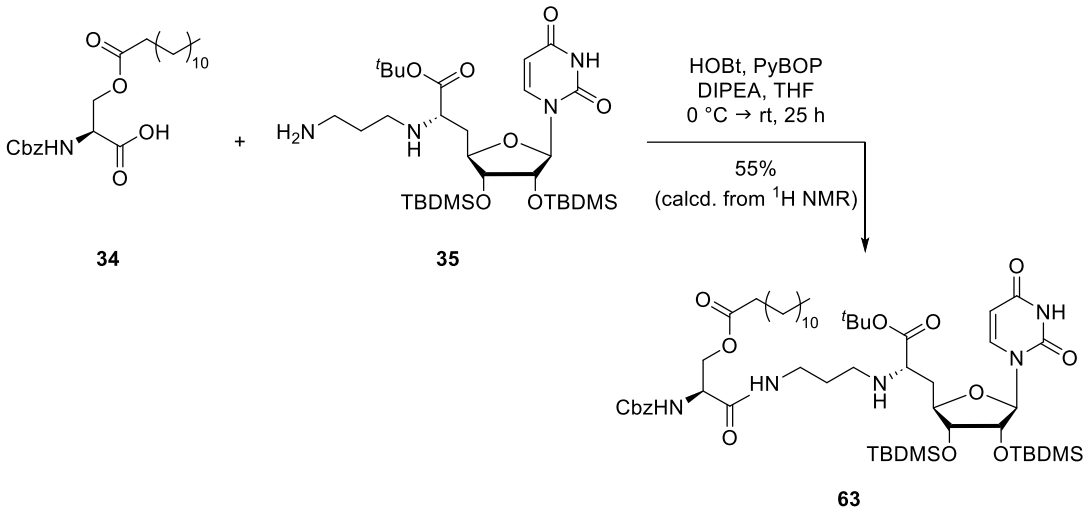

Fig. 34: Synthesis of **63** via peptide coupling of Ser-based derivative **34** and nucleosyl amino acid **35**.

The NMR analysis of the coupling product **63** revealed the presence of phosphine oxide **64** (**Fig. 35**), which is a known by-product of the peptide coupling with PyBOP described above. It is suggested that the lipophilic side chain eases the elution of **64** due to its lipophilic nature and intermolecular nonpolar interactions. The yield of compound **63** was calculated from the ^{1}H NMR spectrum to be 55%. Since **64** does not interfere with the subsequent reactions, compound **63** was used without further purification.

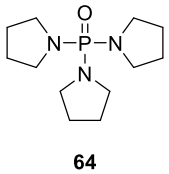

Fig. 35: Known by-product phosphine oxide **64** of the employed peptide coupling.

Prior to the second peptide coupling, the Cbz-protection group was cleaved. Therefore, 1,4-cyclohexadiene and palladium-black were added to the solution of compound **63** in dry *iso*-propanol. Furthermore, trifluoroacetic acid was added as a 10% solution in dry *iso*-propanol to the reaction mixture. In contrast to the previously described conditions, the addition of trifluoroacetic acid was essential at this point. It was necessary to prevent the possible intramolecular nucleophilic attack of the emerging primary amine on the carbonyl group via a five-member transition state, which would result in the migration of the side chain. In order to avoid partial deprotection of the *tert*-butyl ester or the TBDMS groups, only two equivalents of trifluoroacetic acid were used for the reaction. Two equivalents were required to inactivate the emerging primary amine as well as the existing secondary amine. Otherwise, the secondary amine

would partially consume the acid, thereby reducing the amount of acid available to 'deactivate' the emerging amine.[148,153] In contrast to the previously described protocol, the reaction was carried out at room temperature to reduce the risk of the described intramolecular rearrangement. The palladium black agglomerated after one hour, indicating the end of the reaction. However, TLC monitoring showed that his was not the case. So, 1,4-clycohexadiene (9.1 eq.) and palladium black (four spatula tips) were added again. The end of the reaction was finally determined by TLC and LC-MS. The suspension was filtered through a syringe filter, which was washed multiple times with methanol resulting in bis-TFA salt **65**. The compound was identified by LC-MS (m/z = 926.55 $[M+H]^+$) and comparison with the NMR data of the master thesis preceding this work.[153] The gained bis-TFA salt **65** was used without further purification in the subsequent peptide coupling with urea dipeptide **27**. As illustrated in **Fig. 36**, the second peptide coupling was carried out again with HOBt, PyBOP and DIPEA under the previously described conditions. Two additional equivalents of DIPEA were used to scavenge the accruing trifluoroacetic acid. The reaction progress was monitored using TLC and LC-MS, showing the desired product (m/z = 766.87 $[M+2H]^{2+}$). Based on these data, the reaction was ended after 5.5 hours, and the solvent was removed under reduced pressure. The crude compound underwent global deprotection in aqueous trifluoroacetic acid (80%) at room temperature. Over time, the initially colorless reaction mixture turned greenish blue. The color change results from the cleavage of the Pbf group and is a first hint of the progress of the global deprotection. After 25 hours, the reaction was ended by the addition of water (**Fig. 36**). The resulting residue was dissolved in a mixture of water, acetonitrile and trifluoroacetic acid, and subsequently purified by HPLC. Due to the presence of by-product **64**, the HPLC purification of target compound **T1** was carried out three times. Since **64** was not detectable by UV absorbance, it complicates the purification. Two different columns were used for the purification. First, a column with a stationary reverse-phase (RP-C_{18}) was used. The conditions corresponded to the protocol of M. Wirth, in which the interaction between the lipophilic residues could interact with the fatty acid chain of the derivative. Unfortunately, the by-product **64** could not be fully separated from the compound. It was assumed that the lipophilic side chain of target compound **T1** might 'drag along' the by-product **64**. Therefore, a phenyl hexyl stationary phase was considered. It was anticipated that interactions between the phenyl residues and the nucleobase in the product scaffold in addition to the interactions between the lipophilic

side chain and the hexyl residues, could facilitate the separation of the two compounds. This hypothesis was partially confirmed, as nearly the entire by-product could be separated. However, the remaining phosphine oxide **64** could not be fully separated even after the third attempt. Thus, the muraymycin derivative **T1** was obtained as a bis-TFA salt with 2.5% yield over three steps (calcd. from the ^{1}H NMR spectrum). A negligible amount of PyBOP by-product **64** (<0.6%) remained in the product. Reviewing the preceding work of M. Wirth, **64** was also found in small amounts in his final compounds after purification by HPLC.[145]

The low yield of Ser-containing target compound **T1** can be attributed to the multiple HPLC purification steps and the sterically complex second peptide coupling caused by the bulky reactants. In order to assess the effect of the by-product **64** on the biological evaluation, the phosphine oxide was purchased and tested in the same way as each muraymycin derivative. Fortunately, first biological data suggest that phosphine oxide **64** does not significantly affect MraY inhibition or bacterial growth in the assays.

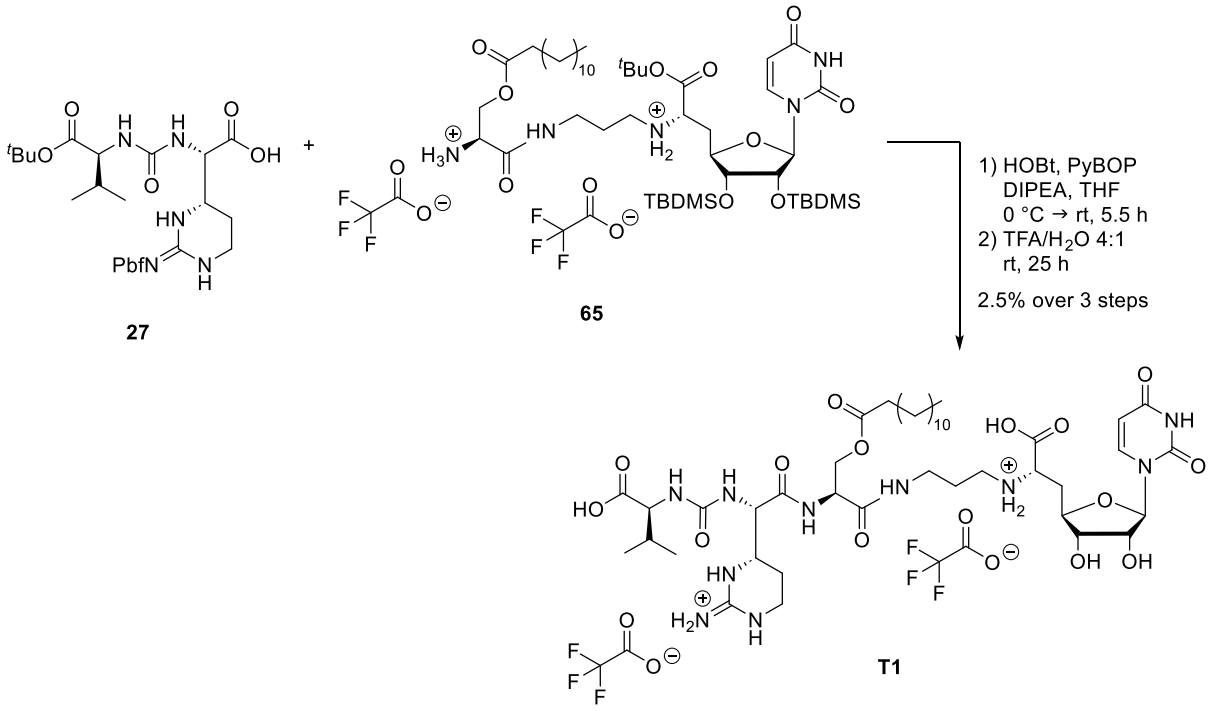

Fig. 36: Synthesis of muraymycin derivative **T1** via peptide coupling and global deprotection.

The connectivity of the tridecanoyl side chain to the backbone at the desired position was confirmed by the HMBC NMR spectrum. The cross-peaks between the protons at the 3'''-H or 2^{iv}-H position and the carbonyl carbon atom C-1^{iv} (cf. **Fig. 37**) provide strong evidence for the expected linkage.

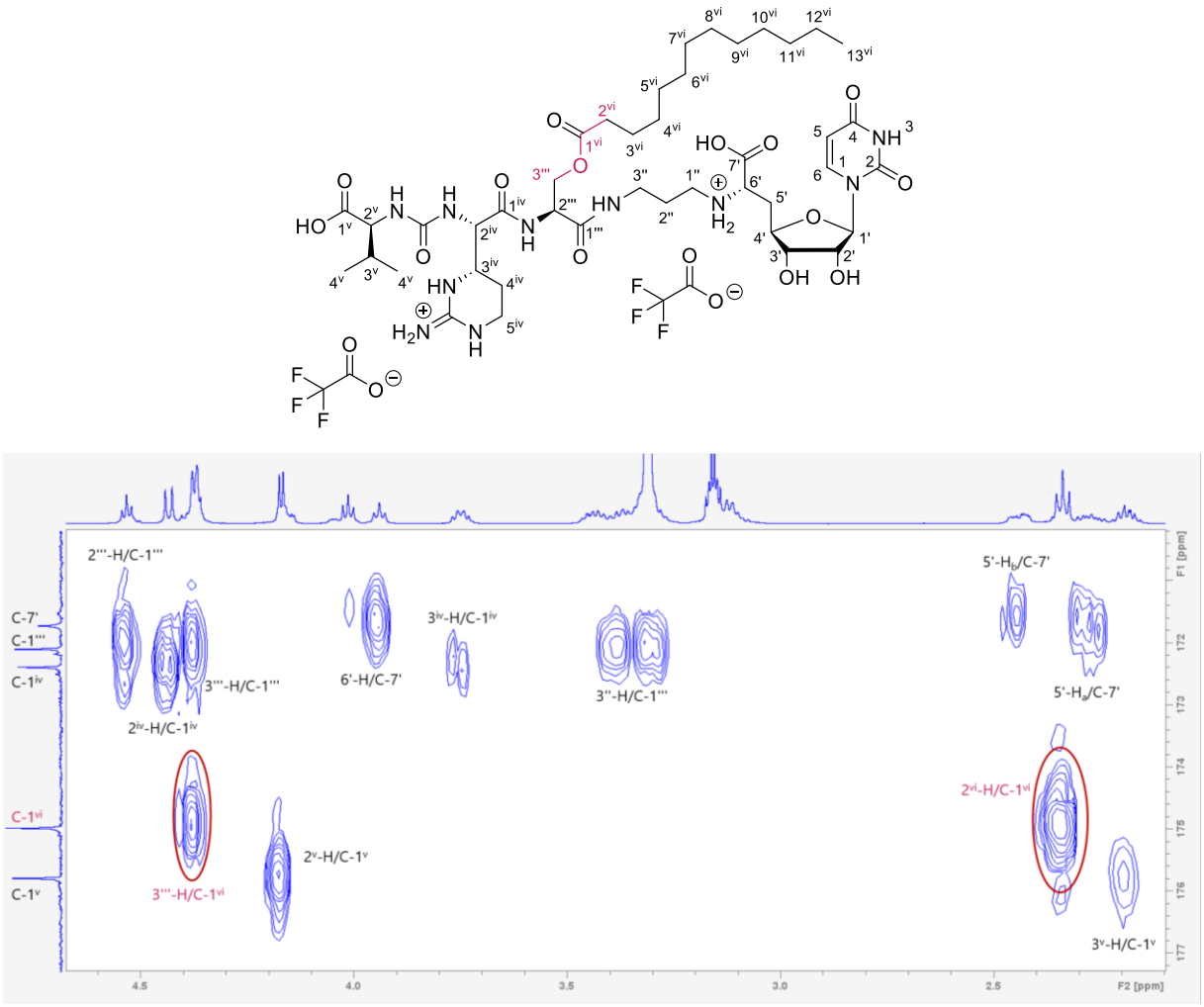

Fig. 37: Excerpt of the HMBC NMR spectrum, proving the connectivity of the lipophilic side chain to the backbone of muraymycin derivative **T1**.

4.2.3 Synthesis of target compound T2: Val-Epic-Ser($COC_{15}H_{31}$)-NuAA

Muraymycin derivative **T2** was synthesized following the same reaction sequence described in section 4.2.2. The central building block **37** now contains a hexadecanoyl side chain instead of the tridecanoyl side chain. The extension of the side chain was performed to gain further insights into the effect of the *iso*-propyl group at the central building block. A comparison of target compounds **T1** and **T2** could provide answers as to whether the longer side chains compensates for the omission of the *iso*-propyl group at the 3'''-position.

The first peptide coupling was carried out under established conditions with HOBt, PyBOP and DIPEA in dry tetrahydrofuran.[146,153] Once again, the order of addition of the reagents and the temperature range were important. After 25 hours, the reaction was ended, and the solvent was removed under reduced pressure. Purification by silica

gel column chromatography yielded 59% of derivative **66**, which contained no PyBOP by-product **64** (**Fig. 38**).

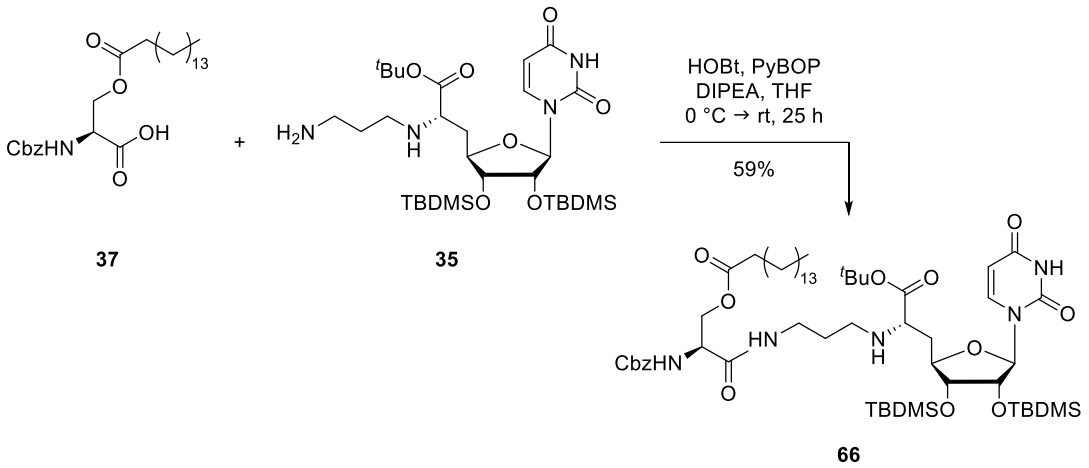

Fig. 38: Synthesis of compound **66** via peptide coupling of Ser-based derivative **37** and nucleosyl amino acid **35**.

The cleavage of the Cbz-protecting group was carried out under the established conditions, using 1,4-cycloheaxdiene and palladium black in dry *iso*-propanol.[148,153] To avoid the nucleophilic attack of the formed primary amine, trifluoroacetic acid was added to achieve the bis-TFA salt **67**. Furthermore, the reaction was carried out at room temperature to avoid the aforementioned rearrangement. After 3.5 hours, the reaction was ended, and the mixture was filtered through a syringe filter to obtain derivative **67**. The compound was identified by LC-MS (m/z = 968.56 $[M+H]^+$) and used without further purification.

The peptide coupling between urea dipeptide **27** and bis-TFA salt **67** was carried out with HOBt, PyBOP and DIPEA.[146,153] The reaction time was extended to 29 hours to ensure complete conversion. After solvent removal, the globally protected derivative was purified by HPLC. Based on the chromatograms from the LC-MS analysis, an additional purification step was carried out at this stage. These showed a complete separation between the desired coupling product and the PyBOP by-product **64**, a separation that was no longer detectable after global deprotection. This suggested that purification prior to global deprotection offered a high probability of obtaining a clean compound. Both the LC-MS method and a phenyl-hexyl column were used for the HPLC purification. The globally protected muraymycin derivative was identified by LC-MS (m/z = 787.71 $[M+2H]^{2+}$).

The subsequent global deprotection was carried out in aqueous trifluoroacetic acid (80%) (cf. **Fig. 39**). The reaction, which turned turquois over time, was ended after 28 hours by adding water. The solvent was removed by lyophilization. The green residue was then dissolved in a mixture of water, acetonitrile and trifluoroacetic acid, followed by purification via HPLC. Target compound **T2** was obtained with an overall yield of 5.9% over three steps. The additional purification step proved to be effective, as no by-product impurity **64** was detected in the NMR nor LC-MS spectra of **T2**.

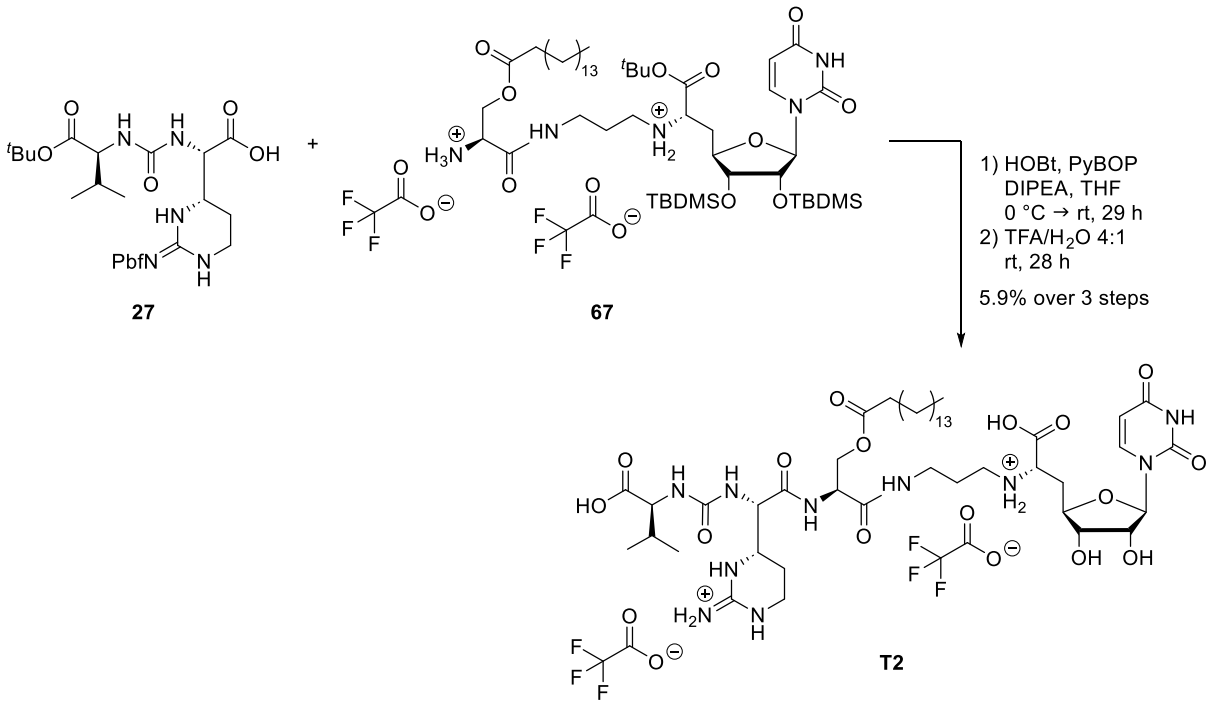

Fig. 39: Synthesis of muraymycin derivative **T2** via peptide coupling and global deprotection.

The low yield can be primarily attributed to the second peptide coupling. During the reaction, bis-TFA salt **67** turns into a free amine, which, in addition to the desired peptide coupling, also enables the intramolecular migration of the lipophilic side chain described above. Additionally, the peptide coupling between the two sterically hindered coupling partners is an additional kinetic difficulty. Furthermore, HPLC purification revealed a fraction in which the side chain had been cleaved (LC-MS: m/z = 743.23 $[M+H]^+$), which further reduced the yield of compound **T2**. This cleavage most likely occurred during the global deprotection or the subsequent dilution with water prior to the lyophilization. The connectivity of the lipophilic side chain was again confirmed by the HMBC NMR spectrum of the compound, which showed the expected cross peaks between 3'''-H or 2^{vi}-H and the carbonyl carbon atom C-1^{vi} (cf. **Fig. 40**).

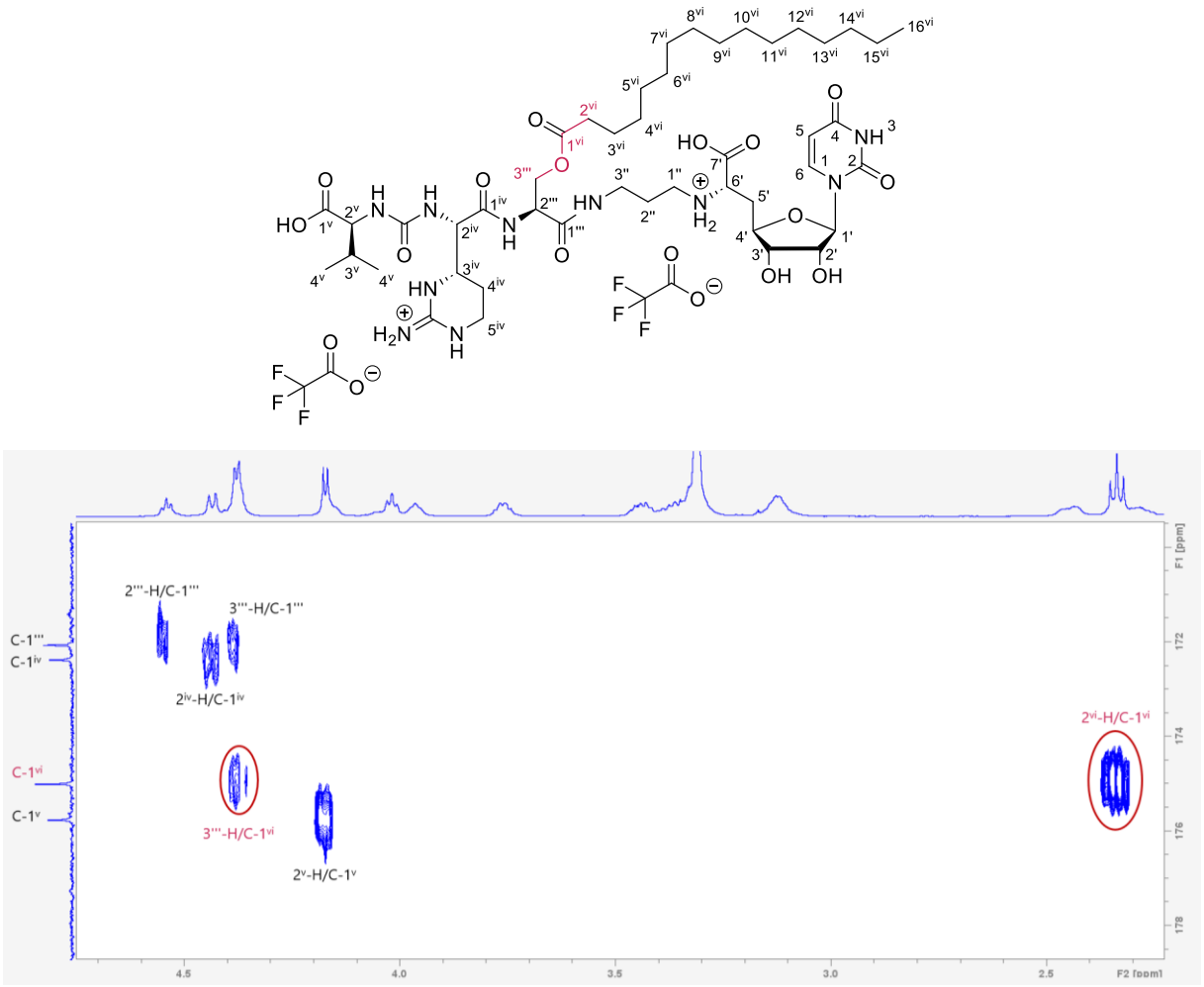

Fig. 40: Excerpt of the HMBC NMR spectrum, proving the connectivity of the lipophilic side chain to the backbone of muraymycin derivative **T2**.

4.2.4 Synthesis of target compound T7: Val-Epic-Ser(COCH$_3$)-NuAA

In order to investigate the functional significance of the fatty acid chain, the acetylated muraymycin derivative **T7** was synthesized. This approach aimed to elucidate the role of the fatty acid modification. The synthetic strategy for this compound was the same as for target compounds **T1** and **T2**. So, the building blocks **35** and **43** were initially connected via the already established peptide coupling using HOBt, PyBOP and DIPEA (cf. **Fig. 41**).[146,153] Amine **35** was added dropwise to a cooled solution of Cbz-Ser(COCH$_3$)-OH **43**, HOBt, PyBOP and DIPEA. The reaction was monitored by TLC and LC-MS. After 19 hours, the reaction was ended by removing the solvent. After the purification by silica gel column chromatography, the already known PyBOP by-product **64** (cf. section 4.2.2, **Fig. 35**) and the TFA-DIPEA salt were identified in the NMR spectra. Since chromatotron purification allows a narrower solvent gradient, it was tested as a method for separating the impurities from derivative **68**. This attempt

resulted in the removal of the DIPEA salt, but not of by-product **64**. Since the latter does not affect the subsequent Cbz-deprotection and would be generated again during the upcoming peptide coupling, **68** was used as a crude product. It was assumed that the side product could be completely removed as HPLC purification, which proved effective for **T2**, was planned prior to the global deprotection (cf. section 4.2.3). The yield of approximately 46% for the first peptide coupling was calculated from the ^{1}H NMR spectrum.

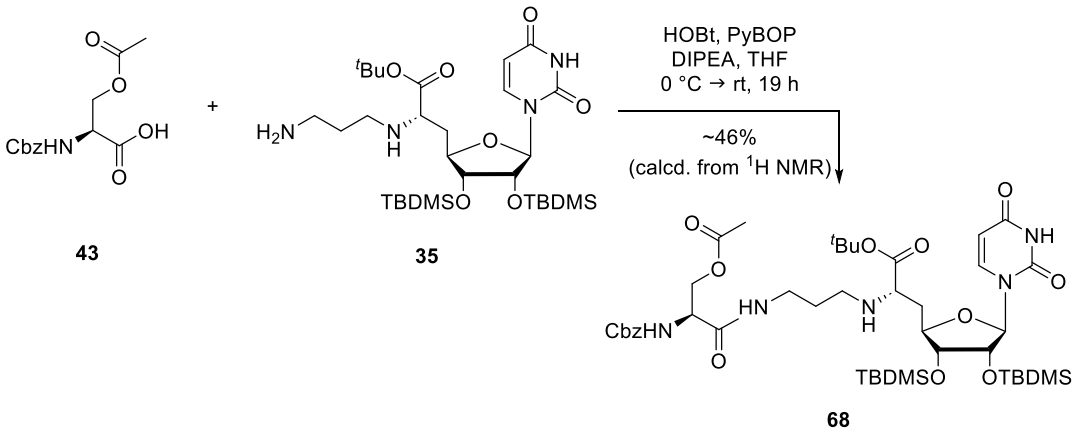

Fig. 41: Synthesis of derivative **68** via peptide coupling with HOBt, PyBOP and DIPEA.

The Cbz group was cleaved under the well-known conditions with 1,4-cyclohexadiene and palladium black in dry *iso*-propanol.[146,148] During the reaction, palladium black flocculated, indicating the progress of the reaction. To prevent the intramolecular nucleophilic attack of the primary amine, trifluoroacetic acid was added to form the bis-TFA salt **69**.[148,153] The reaction was monitored by LC-MS and was determined to be complete after 3.5 hours. The crude compound was used in the subsequent reaction after workup. The peptide coupling was carried out in dry tetrahydrofuran using PyBOP, HOBt and DIPEA as described above.[146,153] After 23 hours, no further reaction progress was observed with TLC and the reaction was ended by removing the solvent. As planned, the globally protected derivative was purified by HPLC and identified by LC-MS (m/z = 689.75 $[M+2H]^{2+}$).

The resulting colorless solid was dissolved in aqueous trifluoroacetic acid (80%) and stirred for 25 hours. During this time, the reaction mixture turned blue, indicating cleavage of the Pbf-protecting group. LC-MS monitoring revealed that the acetyl group was partially cleaved during the global deprotection. Since the amount of the desired product remaining could only be estimated, a purification by HPLC was pursued. Unfortunately, only insufficient amounts were obtained after work-up and HPLC

purification. So, muraymycin derivative **T7** could not be biologically evaluated. It can be assumed that the dilution of the reaction mixture with water at room temperature prior to the lyophilization also supported the cleavage of the acetyl group. The dilution of the acid with water caused an exothermic reaction. These conditions facilitate the hydrolysis of the acetyl group. Overall, the reaction conditions in addition to the dilution led to the cleavage of the acetyl group. The isolation of the cleaved muraymycin derivative was not further pursued. As biological studies of different target compounds revealed that changing the central amino acid is beneficial (cf. sections 4.3, 4.6), the synthesis of muraymycin derivative **T7** was not repeated. Instead, the structurally similar compound with *allo*-Thr as the central amino acid was synthesized (cf. section 4.5.2).

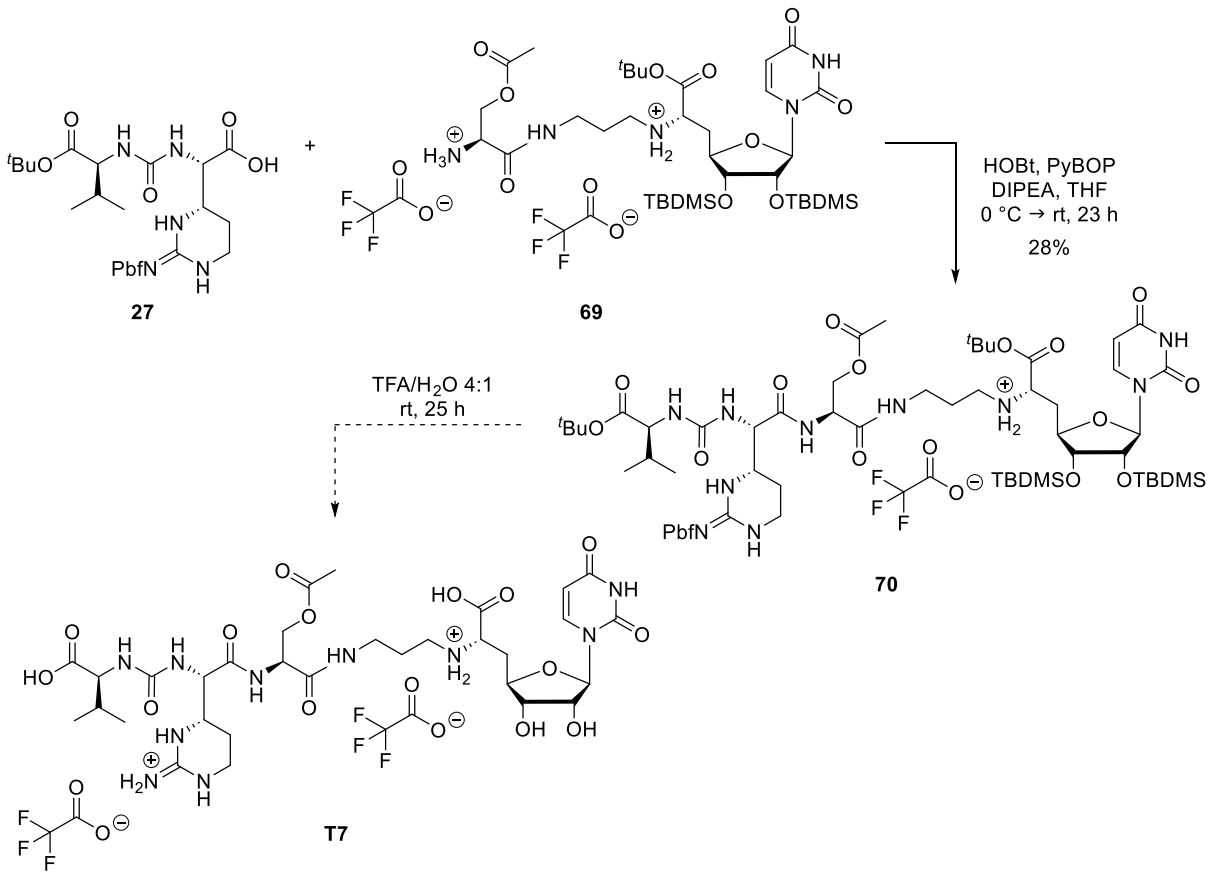

Fig. 42: Attempted synthesis of derivative **T7** via peptide coupling and global deprotection.

4.2.5 Synthesis of target compound T3: Val-Arg-Ser($COC_{12}H_{25}$)-NuAA

All naturally occurring muraymycins feature the cyclic pendant of L-arginine, referred to as L-epicapreomycidine.[111,120] Since the synthesis of the corresponding urea dipeptide **27** is complicated and some steps have limited reproducibility, the approach of replacing Epic with Arg in the backbone was pursued. This strategy aims to provide

new insights into the role and importance of the unnatural amino acid Epic in the muraymycin structure. Ultimately, this could facilitate the synthesis of new derivatives, if the replacement of the amino acid leads to comparable results in biological testing. Hence, target compound **T3** was designed and synthesized.

First, urea dipeptide **36** was synthesized over two steps starting with L-valine *tert*-butyl ester hydrochloride (H-Val-O^{t}Bu • HCl) according to the protocol of C. Schütz.[154] For the preparation of isocyanate **40**, the hydrochloride was dissolved in a mixture of dichloromethane and aqueous saturated sodium bicarbonate solution and cooled to 0°C. At this temperature, triphosgene was added under vigorous stirring. After 25 minutes, the reaction was ended, and the mixture was worked up. The reaction yielded isocyanate **40** with 96%, which could be used without further purification. The product was identified by NMR, which showed no dimer formation, in contrast to the results observed by C. Schütz.[154] In order to form the urea dipeptide **36**, compound **40** was dissolved in tetrahydrofuran. Then, H-Arg(Pbf)-OH in dimethylformamide was added to the solution. Full conversion was observed (TLC monitoring) after 19 hours. After work-up, the crude product was purified by silica gel column chromatography, yielding **36** in 74%. Altogether, Arg-containing urea dipeptide **36** was obtained in 71% yield over two steps (cf. **Fig. 43**).

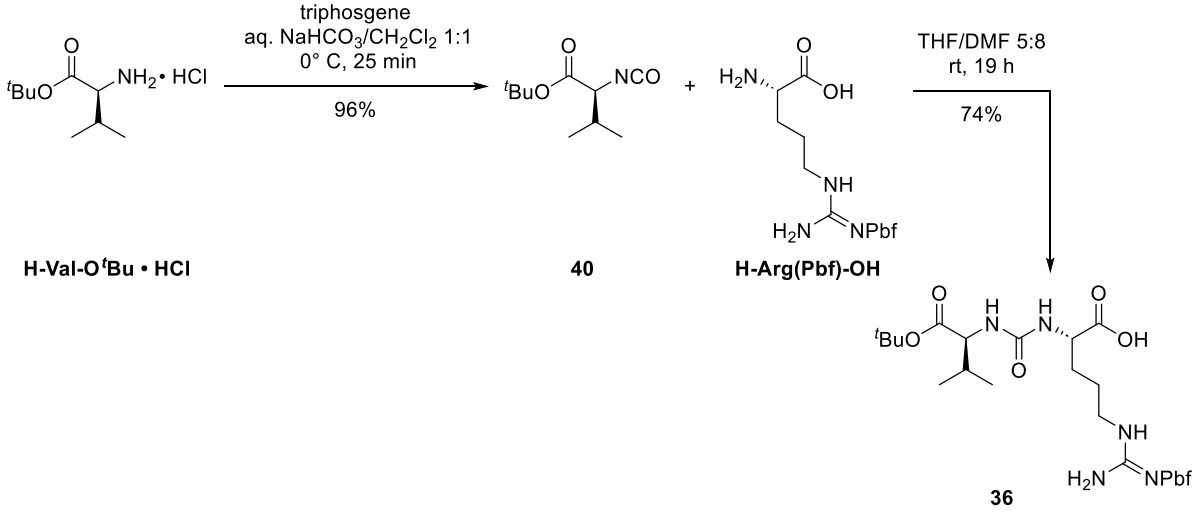

Fig. 43: Synthesis of Arg-containing urea dipeptide **36** starting with H-Val-O^{t}Bu • HCl.

Since the coupling by-product **64** (cf. section 4.2.1, **Fig. 35**) complicates the purification of all desired derivatives, alternative coupling agents were urgently required. C. Schütz tried other coupling conditions in dummy reactions. But none of those gave an enantiopure coupling product.[154] In this thesis, propane phosphonic acid anhydride

(T_3P, cf. **Fig. 44**) turned out to be a very promising candidate.[170,171] The great advantage of this coupling agent is its slow degradation in water. So, the resulting decomposition product as well as remaining T_3P can already be separated during extraction.

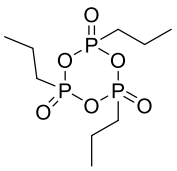

Fig. 44: Peptide coupling agent propane phosphonic acid anhydride (T_3P).

To evaluate the suitability of T_3P for the specific peptide couplings in the muraymycin synthesis, a model experiment was performed. Here, conditions most similar to the final circumstances were tested. So, amine **71** and urea dipeptide **36** were selected for the dummy reaction.

Compound **71** was synthesized from building block **62** by cleavage of the Cbz group under the well-established conditions. One equivalent of trifluoroacetic acid was added to prevent the intramolecular nucleophilic attack of the free amine.[146,148,153] Mono-TFA salt **71** was obtained with a very good yield of 95% (cf. **Fig. 45**).

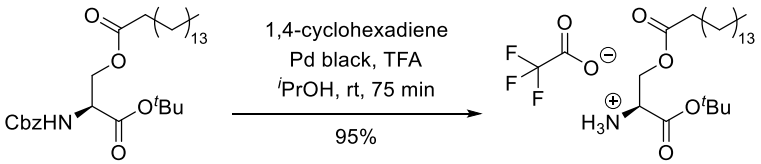

Fig. 45: Cleavage of the Cbz-protecting group of the Ser-based building block **62**.

In the model experiments, particular attention was paid to the enantiopurity and the yield (cf. **Fig. 46**). For the first approach urea dipeptide **36**, compound **71** and DIPEA were dissolved in dry ethyl acetate at 0 °C. After 15 minutes, T_3P (50% solution in ethyl acetate) was added.[170] The activator for the carboxylic acid was used without further additives. Based on TLC, the reaction was ended after 30 minutes. The reaction mixture was diluted with ethyl acetate and the organic phase was washed with water and saturated aqueous sodium chloride solution. After purification by silica gel column chromatography, derivative **72** was obtained as a colorless solid with a yield of 93%. Analysis of the ^1H and ^{13}C NMR spectra confirmed the enantiopurity of the product.

The reaction was repeated with the same reactants under the already established conditions with PyBOP and HOBt in order to enable a direct comparison.[146] Now,

carboxylic acid **36** was dissolved in dry tetrahydrofuran together with activator PyBOP and additive HOBt. DIPEA was added and the reaction mixture was stirred for 30 minutes at 0 °C to form the activated acid. Then, serine derivative **71** in dry tetrahydrofuran was added dropwise at 0 °C. The reaction was stirred for another hour at 0 °C and was then allowed to warm up to room temperature. Based on TLC, the reaction was ended after 20 hours. The crude product could not be purified by silica gel column chromatography. Examination of the ^{1}H and ^{13}C NMR spectra revealed a mixture of the desired coupling product **72** (80%) and PyBOP by-product **64** (20%). However, the NMR spectra also confirmed that no epimerization had taken place. Based on these results, T_3P was selected as a promising agent for the upcoming peptide couplings. It should be mentioned that the reagent was used only in the second peptide coupling. In the first peptide coupling, where nucleosyl amino acid **35** is linked to the central building block, its usage led to undefinable side products and very low yields of the desired coupling product. As discussed below, hexafluorophosphate azabenzotriazole tetramethyl uronium (HATU) or EDC • HCl proved to be the better choice for this reaction (cf. section 4.4.2, **Fig. 50**).

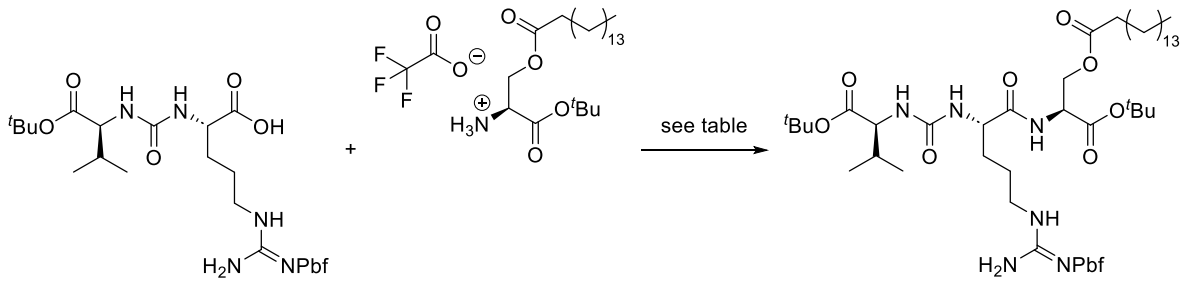

36 **71** **72**

approach	activator	additive	conditions	yield	epimerization
1	T_3P	-	DIPEA EtOAc, 0 °C, 30 min	93%	none
2	PyBOP	HOBt	DIPEA THF, 0 °C → rt, 23 h	39%*	none

* calcd. from ^{1}H NMR spectrum

Fig. 46: Different approaches of the peptide coupling of urea dipeptide **36** and compound **71**.

The new coupling approach was initially used for the peptide coupling of urea dipeptide **36** with bis-TFA salt **65** (cf. **Fig. 47**). Therefore, **36**, **65** and DIPEA were dissolved in dry ethyl acetate. The resulting reaction mixture was cooled to 0 °C and was stirred for 15 minutes. Then, T_3P (50% solution in ethyl acetate) was added and the

reaction mixture continued stirring. Based on TLC, the reaction was ended after 30 minutes, and the mixture was extracted as described above. Although no by-products from the new coupling agent could be identified, the resulting crude product required HPLC purification, as reactant **65** contained PyBOP by-product **64** from the previous peptide coupling (cf. section 4.2.2). The globally protected muraymycin derivative was only identified by LC-MS (m/z = 1534.44 $[M+H]^+$, 767.57 $[M+2H]^{2+}$) due to the complexity of the NMR data. The global deprotection was carried out at room temperature in aqueous trifluoroacetic acid (80%). LC-MS monitoring indicated complete conversion after 24 hours, at which point the reaction mixture was diluted with water at 0 °C, lyophilized and purified by HPLC. The dilution was carried out at low temperature to prevent the former observed cleavage of the side chain moiety (cf. section 4.2.4). The purified muraymycin derivative **T3** was gained as a bis-TFA salt with a yield of 3.8% over two steps. The low yield can be explained by product loss during the global deprotection. LC-MS analysis showed the muraymycin derivative without the lipophilic side chain as a side product, indicating that even cooling the reaction during dilution was insufficient to prevent the cleavage. Since enough material was isolated for biological testing, no further attempts were made to repeat the synthesis.

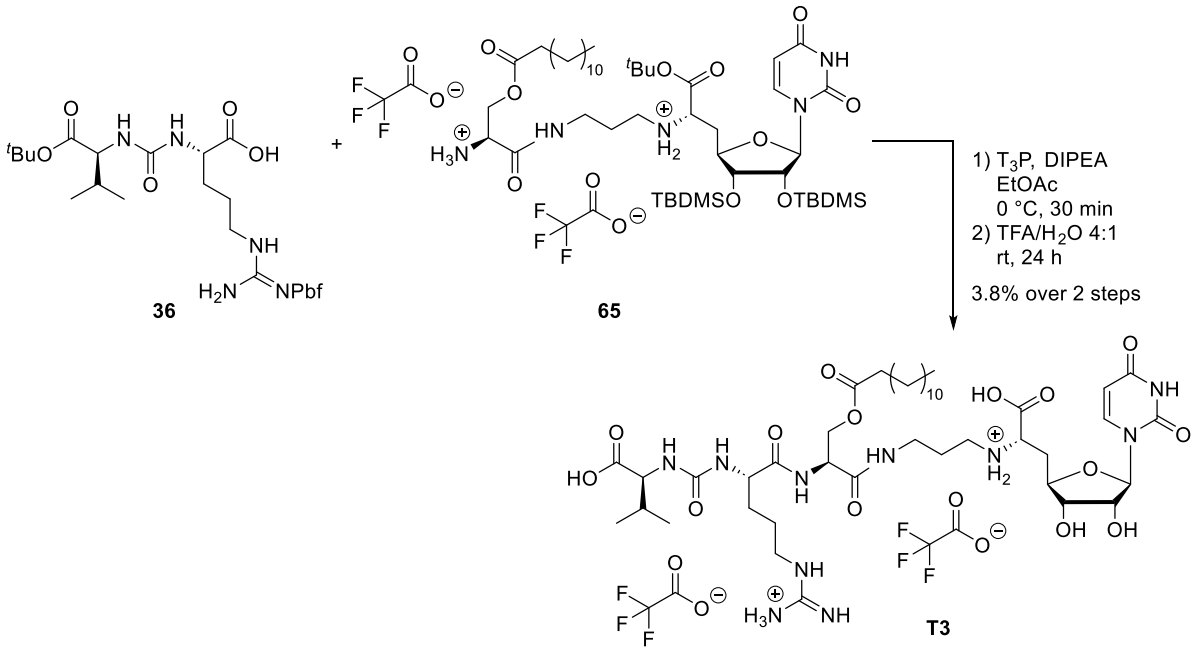

Fig. 47: Synthesis of target compound **T3** via peptide coupling and global deprotection.

The connectivity of the side chain to the backbone of muraymycin derivative **T3** was proven with the HMBC NMR spectrum. As illustrated in **Fig. 48**, it clearly shows the

cross-peaks between 3'''-H or 2^{vi}-H with the carbonyl carbon atom C-1^{vi}, thus confirming the structure of **T3**.

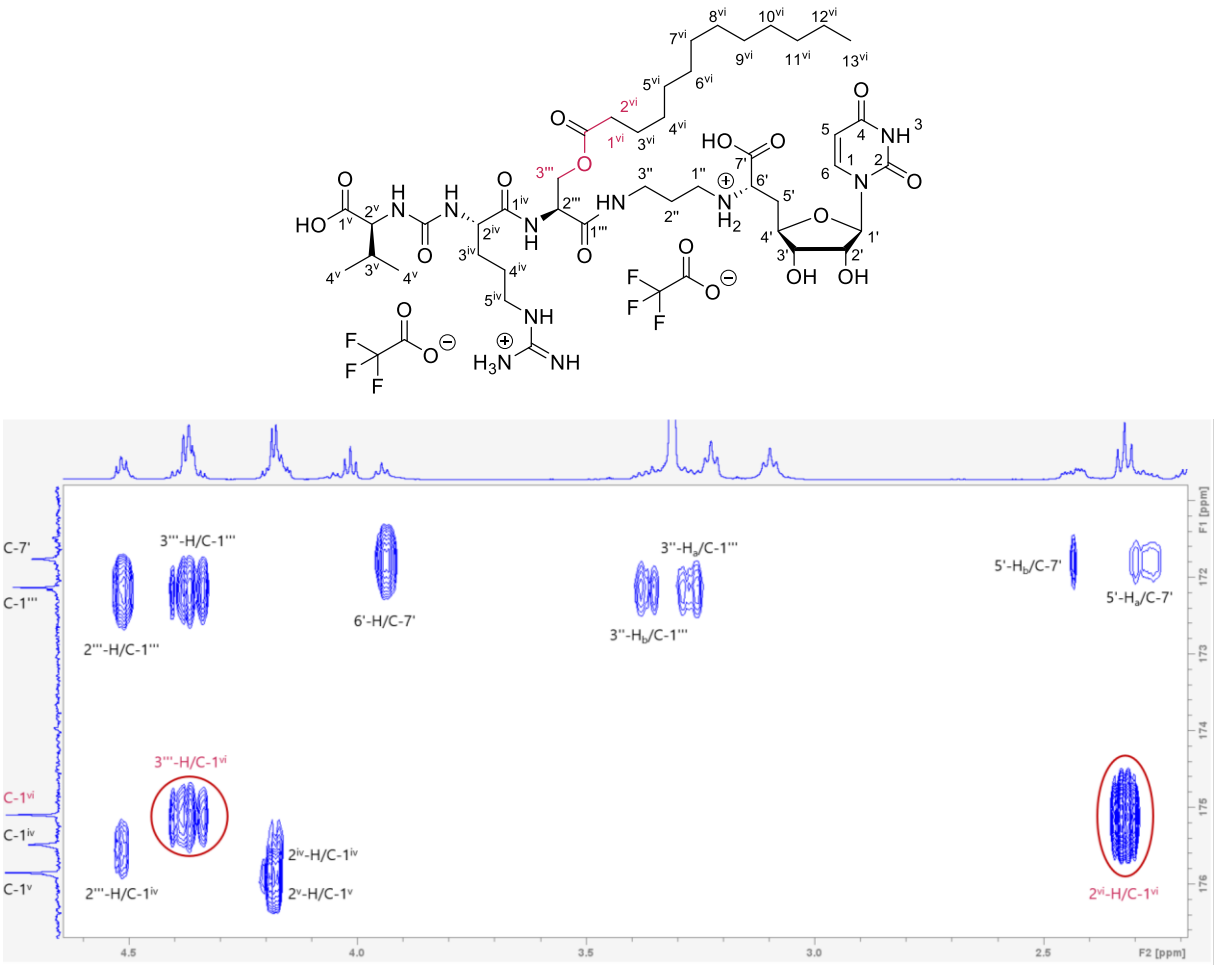

Fig. 48: Excerpt of the HMBC NMR spectrum, proving the connectivity of the lipophilic side chain to the backbone of muraymycin derivative **T3**.

4.3 Biological evaluation of the Ser muraymycin derivatives

The first set of new, simplified muraymycin derivatives with L-serine as the central amino acid was biologically evaluated. Their ability to inhibit the enzyme MraY (crude membrane)[96,121,172–174] and their antibacterial activity (growth inhibition) against multiple bacterial strains were tested (cf. **Table 1**). Therefore, two strains of the Gram-negative bacteria *E. coli* (efflux-deficient strain Δ*tolC* and DH5α) and two Gram-positive bacterial strains (*S. aureus* Newman and *C. difficile*) were investigated.[120,121,135,144,174] Finally, stability tests were also conducted on selected derivatives in *E. coli* Δ*tolC* cell lysate, Luria-Bertain-Medium (LB-medium), and human plasma (cf. section 4.9) to provide more detailed insights into their stability profiles.

Table 1: Biological data of the new Ser muraymycin derivatives **T1**-**T3** (references: **28** and **32**).[121,145]

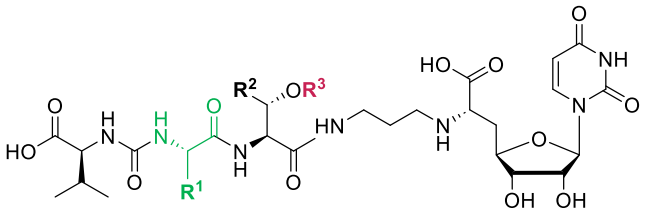

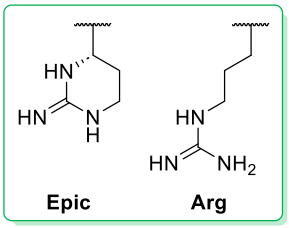

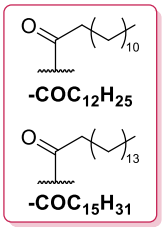

compound	MraY IC_{50} [nM][a]	bacterial growth			
		IC_{50} [µg/mL]		MIC [µg/mL]	
		E. coli Δ*tolC*	*E. coli* DH5α	*S. aureus* Newman	*C. difficile*
L-serine					
T1: Val-Epic-Ser($COC_{12}H_{25}$)-NuAA	3.4 ± 0.2[b]	1.6	>100	>32	>32
T2: Val-Epic-Ser($COC_{15}H_{31}$)-NuAA	3.1 ± 0.3	5.5	>100	>32	8-16
T3: Val-Arg-Ser($COC_{12}H_{25}$)-NuAA	5.2 ± 0.4	6.6	>100	>32	>32
3-hydroxy-L-leucine					
28: Val-Epic-3-hydroxy-Leu-NuAA	95 ± 19	50	15	>50	n.d.
32: Val-Epic-3-hydroxy-Leu($COC_{12}H_{25}$)-NuAA	5.8 ± 0.5	0.5	>100	10	2.5

[a] crude membrane preparation; [b] preliminary result; n.d. not determined yet

The comparison of reference compound **32** with the new derivatives confirmed that replacing 3-hydroxy-Leu with Ser did not affect the inhibition of the enzyme MraY (cf. **Table 1**). This demonstrates that the simplification of the central amino acid is well tolerated by the target enzyme and also implies that the influence of the *iso*-propyl group on the interaction with the target enzyme is less significant. Furthermore, all compounds in **Table 1** containing a lipophilic side chain show stronger MraY inhibition than 5'-deoxy **C4** muraymycin analog **28**, which lacks this moiety. This supports the hypothesis that the lipophilic side chain not only facilitates the penetration of the cell membrane but is also beneficial for target affinity. In addition, the substitution of Epic with Arg in the urea dipeptide moiety (**T3**) had no effect on the enzymatic inhibition.

Hence, the replacement can be considered for the design of new derivatives, thereby essentially simplifying the synthetic procedure.

The set of new muraymycin derivatives showed strong antibacterial activity against the efflux-deficient strain *E. coli* Δ*tolC*. Compared to **32**, the compounds were less active, but ~10 times more active than **28**. This trend correlates with the proportion of lipophilic residues in the compounds. The reference compound **32** contains the *iso*-propyl group and the lipophilic side chain, while the Ser-derivatives only have a lipophilic side chain. The muraymycin analog **28**, on the other hand, lacks the lipophilic side chain, containing only the *iso*-propyl group. This pattern further supports the idea that the lipophilic side chain benefits the compound's ability to cross the membrane by increasing its overall lipophilicity.

Moreover, no inhibition of *E. coli* DH5α or *S. aureus* Newman was observed for the new derivatives. However, derivative **T2** exhibited activity against several *C. difficile* strains. Since the only difference between **T1** and **T2** is the length of their side chains ($COC_{12}H_{25}$ vs. $COC_{15}H_{31}$), it can be speculated that even a small increase in lipophilicity of **T2** could presumably enhance the cellular uptake and, ultimately, its antibacterial activity. Compound **32**, which contains the shorter lipophilic side chain like **T1** but also the *iso*-propyl group, shows activity against *C. difficile*. Comparing **T2** with **32**, it can be hypothesized that the longer lipophilic side chain of compound **T2** might be able to partially compensate for the loss of the *iso*-propyl group's contribution to lipophilicity. In summary, it can be suggested that the longer side chain of **T2** primarily contributes to cellular uptake, while having a negligible impact on target interaction.

Additionally, the stabilities of the three new synthetic compounds were evaluated in *E. coli* Δ*tolC* cell lysate (period: 150 min for **T1**, **T2** and **T3**) and in Luria-Bertain-Medium (period: 150 min and 24 h for **T1** and **T2**). The precise half-lives of **T1**, **T2** and **T3** could not be determined as all compounds either reached a plateau during the experiment (remaining compound [%] as a function of time; cf. chapter 9), or the reproduction of results proved to be especially challenging. Overall, these data require further investigation.

4.4 Synthesis of the *allo*-L-threonine- and L-threonine-containing muraymycin derivatives with *n*-alkyl side chain $COC_{12}H_{25}$

To gain further insights into whether a change of the central amino acid would affect the antibacterial activity L-*allo*-threonine was chosen. This choice allows a direct comparison with the former muraymycin derivatives, since it possesses the same stereochemistry at the β-carbon atom as 3-hydroxy-L-leucine (cf. section 2.2.1, **Fig. 8**). In addition, another derivative with L-threonine was designed and synthesized to investigate the impact of the configuration at this particular steric center (cf. section 4.4.3).

4.4.1 Synthesis of *allo*-Thr- and Thr-based central building blocks with *n*-alkyl chain $COC_{12}H_{25}$

The new central building blocks based on *allo*-Thr and Thr each feature a tridecanoyl side chain. So, the resulting muraymycin derivatives can be directly compared with reference compound **32**, and the target compounds **T1** and **T3**.

The reaction sequence for both compounds was based on the already established route for the Ser-based derivatives (cf. section 4.2.1). In order to modify the alcohol moieties, the carboxylic functions were protected by converting them into the corresponding *tert*-butyl esters. This was initially attempted under the same conditions as described in section 4.2.1, using *N*,*N*-dimethylformamiddineopentyl acetal **59**. However, no conversion was observed after 19 hours. Therefore, *tert*-butyl 2,2,2-trichloroacetimidate **73** was employed to obtain the desired compounds. This reagent had previously been used by Shabani *et al.* to convert Cbz-Thr-OH into its corresponding *tert*-butyl ester.[175]

For the conversion of the two Cbz-protected isomers, the corresponding amino acid was dissolved in dry tetrahydrofuran. Then, *tert*-butyl 2,2,2-trichloroacetimidate **73** in dry tetrahydrofuran was added dropwise at room temperature. In both reactions, only 1.2 equivalents of the *tert*-butyl reagent were used to minimize the formation of the corresponding *tert*-butyl ether. Both reactions were monitored by TLC, and in both cases, some unreacted amino acid remained after 18 hours (*allo*-Thr) and 21 hours (Thr), respectively. Therefore, 0.5 equivalents of the *tert*-butyl reagent were added again in each case to ensure complete conversion. In both cases, the TLC revealed *tert*-butyl ether side product after 22 hours (*allo*-Thr) and 24 hours (Thr), and the reactions

were thus ended by removing the solvent under reduced pressure. Each *tert*-butyl ester (**76** and **77**) was purified by silica gel column chromatography, yielding 55% (*allo*-Thr) and 52% (Thr), respectively (cf. **Fig. 49**). In the reaction with *allo*-Thr, the double-substituted derivative **74SP** was isolated in a negligible yield of 9%.

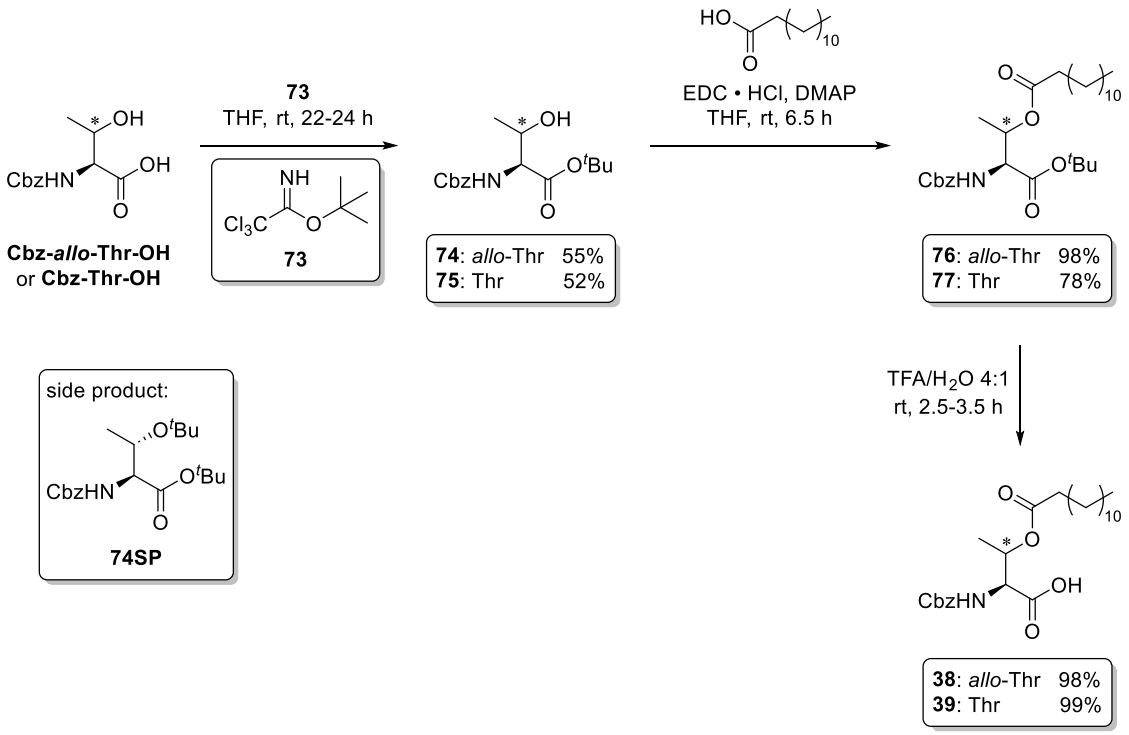

Fig. 49: Synthesis of the central building blocks based on *allo*-Thr (**38**) and Thr (**39**).

The subsequent *Steglich* esterifications were carried out following the synthetic route for the Ser-based derivative **61**.[153] The tridecanoyl side chain ($COC_{12}H_{25}$) was introduced by diluting the corresponding protected amino acid in dry tetrahydrofuran, followed by adding tridecanoic acid, DMAP and EDC • HCl. The reactions were both ended by adding aqueous hydrochloride solution (0.5 M) after 6.5 hours based on TLC monitoring. As already described above (cf. section 4.2.1), the poorly soluble hydrochloride dissolved over time and an insoluble white solid (EDU) precipitated, indicating the progress of the reaction. The *tert*-butyl esters **76** and **77** were isolated by silica gel column chromatography with yields of 98% (*allo*-Thr) and 78% (Thr). The 20% yield loss for compound **77** could be attributed to the different reaction kinetics due to the varied steric conditions.

Both *tert*-butyl esters **76** and **77** were stirred in aqueous trifluoroacetic acid (80%) to rerelease the corresponding carboxylic acids. After 2.5 hours (*allo*-Thr) and 3.5 hours (Thr), the solution was diluted with water and the solvent was removed by

lyophilization. No further purification of the new central building blocks **38** and **39** was necessary, and they were isolated in very good yields of 98% and 99%, respectively.

Cbz-*allo*-Thr($COC_{12}H_{25}$)-OH **38** was obtained in 53%, and Cbz-Thr($COC_{12}H_{25}$)-OH **39** in 40% yield, via the three-step reaction sequence. In both cases, the yield-limiting step was the introduction of the *tert*-butyl ester.[153]

4.4.2 Synthesis of target compounds T4: Val-Epic-*allo*-Thr($COC_{12}H_{25}$)-NuAA and T5: Val-Arg-*allo*-Thr($COC_{12}H_{25}$)-NuAA

In order to avoid double purification by HPLC, and because the use of T_3P in the first peptide coupling led to a mixture of undefinable side products and very low yields of the desired coupling product (cf. section 4.2.5), EDC • HCl/HOBt and HATU were tested as potential coupling agents. The great advantage of both coupling agents is the water solubility of their side and decomposition products accruing during the corresponding reaction.

The protocol of K. Leyerer was employed for the synthesis with EDC • HCl/HOBt.[146] First, amino acid **38** was dissolved in dry tetrahydrofuran and DIPEA (1.0 eq.), EDC • HCl and HOBt were added. The reaction mixture was stirred for 1 hour at room temperature before it was cooled to 0 °C. During this time, the active ester of **38** was expected to form. Amine **35** in dry tetrahydrofuran was added dropwise at this temperature. The reaction was monitored by TLC and thus ended after 23 hours. During this time, the reaction mixture warmed to room temperature. It was diluted with ethyl acetate and then washed with aqueous saturated sodium carbonate solution. The title compound was obtained in 44% yield after silica gel column chromatography.

In a not displayed attempt, a second equivalent DIPEA, which supposedly should scavenge the emerging water during the synthesis, was added during the formation of the active ester. The outcome of this approach was the elimination of the central amino acid and a subsequent addition of the lipophilic side chain to the primary amine of the nucleosyl amino acid **35**. It was assumed that the fatty acid ester was cleaved under the basic nucleophilic conditions caused by restudies of water in the implemented batch of DIPEA or tetrahydrofuran. The free fatty acid could form the reactive ester with the activation reagent and was subsequently attacked by the primary amine **35**. Based on these observations, the second equivalent of the base was added just before the addition of the amine in order to avoid possible preceding side reactions. This

precaution was implemented for each peptide coupling performed from this point on, regardless of the coupling agent.

For the reaction with HATU, one equivalent of DIPEA was added to a solution of *allo*-Thr derivative **38** in dry dichloromethane. The clear solution was stirred for 30 minutes at room temperature, to ensure a complete deprotonation of the carboxylic acid. To obtain the activated species of **38**, HATU was added, and the mixture was stirred again for 30 minutes. Then, the second equivalent of DIPEA was added, the solution was cooled to 0 °C and the nucleosyl amino acid **35** in dry dichloromethane was added dropwise (cf. **Fig. 50**). The reaction mixture was stirred for 15 hours, during which time it was allowed to warm to room temperature. The reaction was ended by addition of aqueous ammonium chloride solution (1 M). After extraction, the crude product was purified by silica gel column chromatography, yielding a mixed fraction (unknown impurities) and a pure fraction (45%) of derivative **52**.

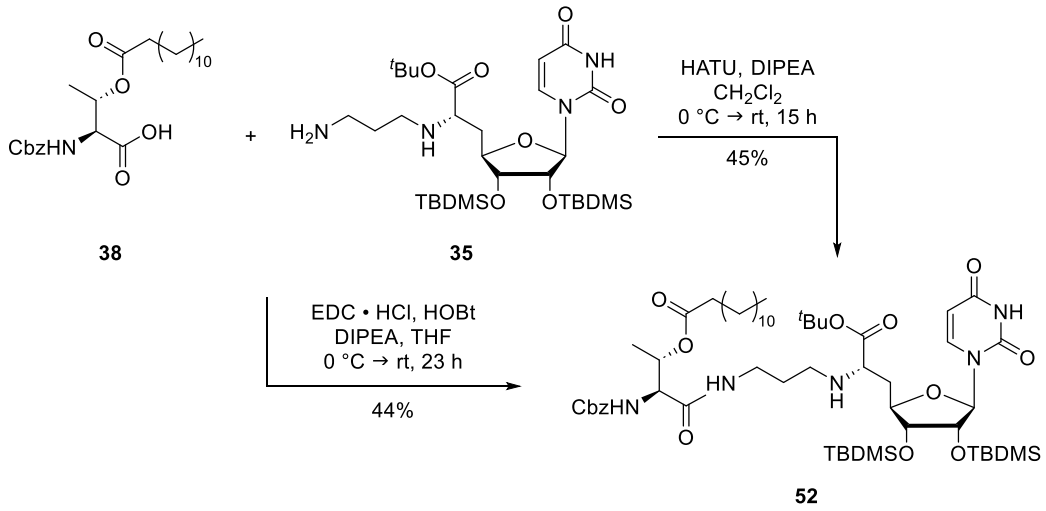

Fig. 50: Two alternatives for the synthesis of derivative **52** via peptide coupling.

Overall, both synthetic routs were effective for obtaining compound **52** with nearly the same yield. It can be assumed that the coupling between nucleosyl amino acid **35** and any other central building block would behave in a similar way, since the central building blocks bear a close structural resemblance to one another.

The pure fraction of the second attempt was used to synthesize target compound **T4** (cf. **Fig. 51**). First the Cbz group was cleaved under the well-known conditions with 1,4-cyclohexadiene and palladium black in dry *iso*-propanol. Here, trifluoroacetic acid was added again, to maintain the core structure (cf. section 4.2.2).[148,153] The following peptide coupling was performed with the approved method using T_3P and DIPEA. Here

3.5 equivalents of the *Hünig*'s base were used in the approach: to scavenge the accruing water and the two equivalents trifluoroacetic acid, and for the deprotonation of the urea dipeptide **27**. First **27**, bis-TFA salt **78** and DIPEA were stirred in dry ethyl acetate at 0 °C. After 15 minutes, T_3P (50% in ethyl acetate) was added to the mixture. The reaction progress was monitored by LC-MS. After 1 h, T_3P (0.75 eq.) were added again to achieve a complete transformation. The reaction was ended after additional 30 minutes by adding ethyl acetate, followed by extraction with water and saturated aqueous sodium chloride solution. The global protected derivative was only verified by LC-MS (m/z = 1546.32 $[M+H]^+$) due to the complexity of the NMR data and was used without further purification.

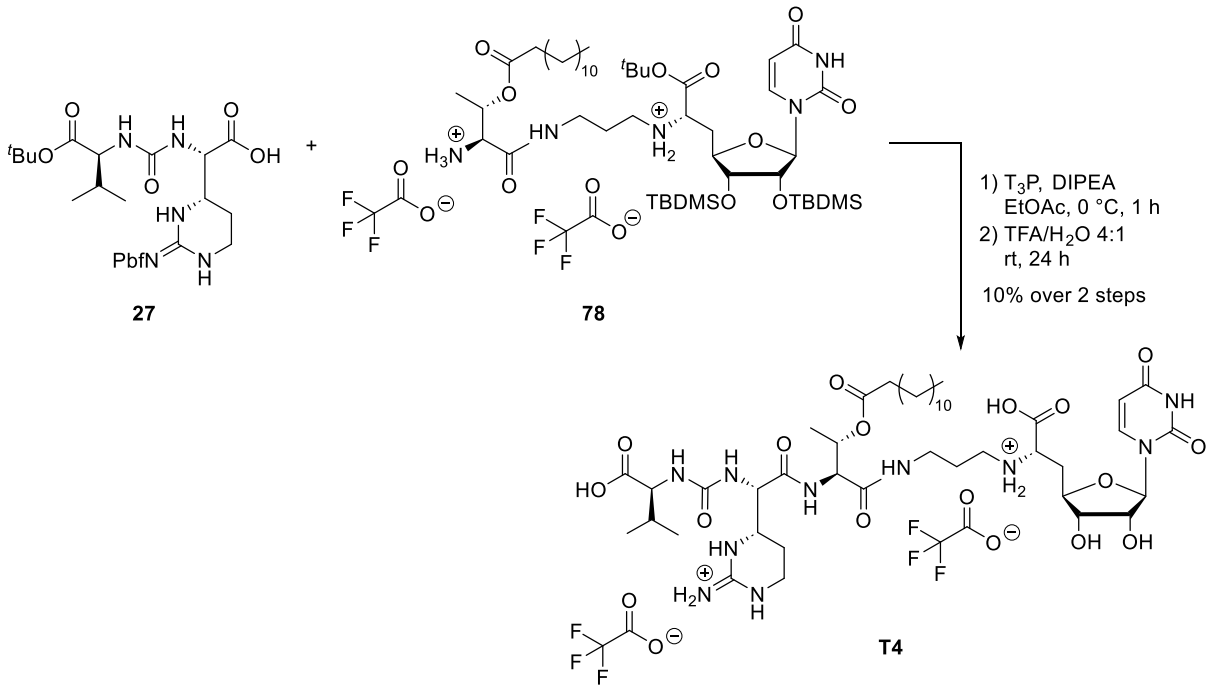

Fig. 51: Synthesis of target compound **T4** via peptide coupling and global deprotection.

The residue was dissolved in aqueous trifluoroacetic acid (80%) and was stirred at room temperature. The reaction progress was monitored by LC-MS. Based on these analyses the reaction was ended after 24 hours. The mixture was diluted with water at 0° C and subsequently freeze-dried. After lyophilization, the LC-MS chromatogram also showed the decomposed product, which lacked the lipophilic side chain. It was again assumed that the addition of water, although performed slowly and at low temperature, led to the cleavage of the lipophilic side chain. Since a truncated muraymycin derivative (globally deprotected **78** or a structure with identical mass) was also detected, two scenarios can be assumed. On the one hand, the migration of the side chain could have occurred during the peptide coupling via an intramolecular five-member transition

state, leading to the formation of the non-reactive amide. On the other hand, it could also mean that reactant **78** was not completely converted during the peptide coupling. No final result was achieved based on the LC-MS data, as both components have the same molecular weight. Unfortunately, the amount isolated by HPLC was too small for NMR analysis to make a definitive statement.

The muraymycin derivative **T4** was isolated after purification by HPLC with 10% yield over two steps. The final step of the global deprotection, specifically the dilution of the reaction mixture, is likely to be the yield lowering step. The HMBC NMR spectrum in **Fig. 52** illustrates the interaction of the protons 3'''-H and 2^{vi}-H with the carboxylic carbon atom C-1^{vi}, proving the connection of the lipophilic side chain to the backbone at the desired position.

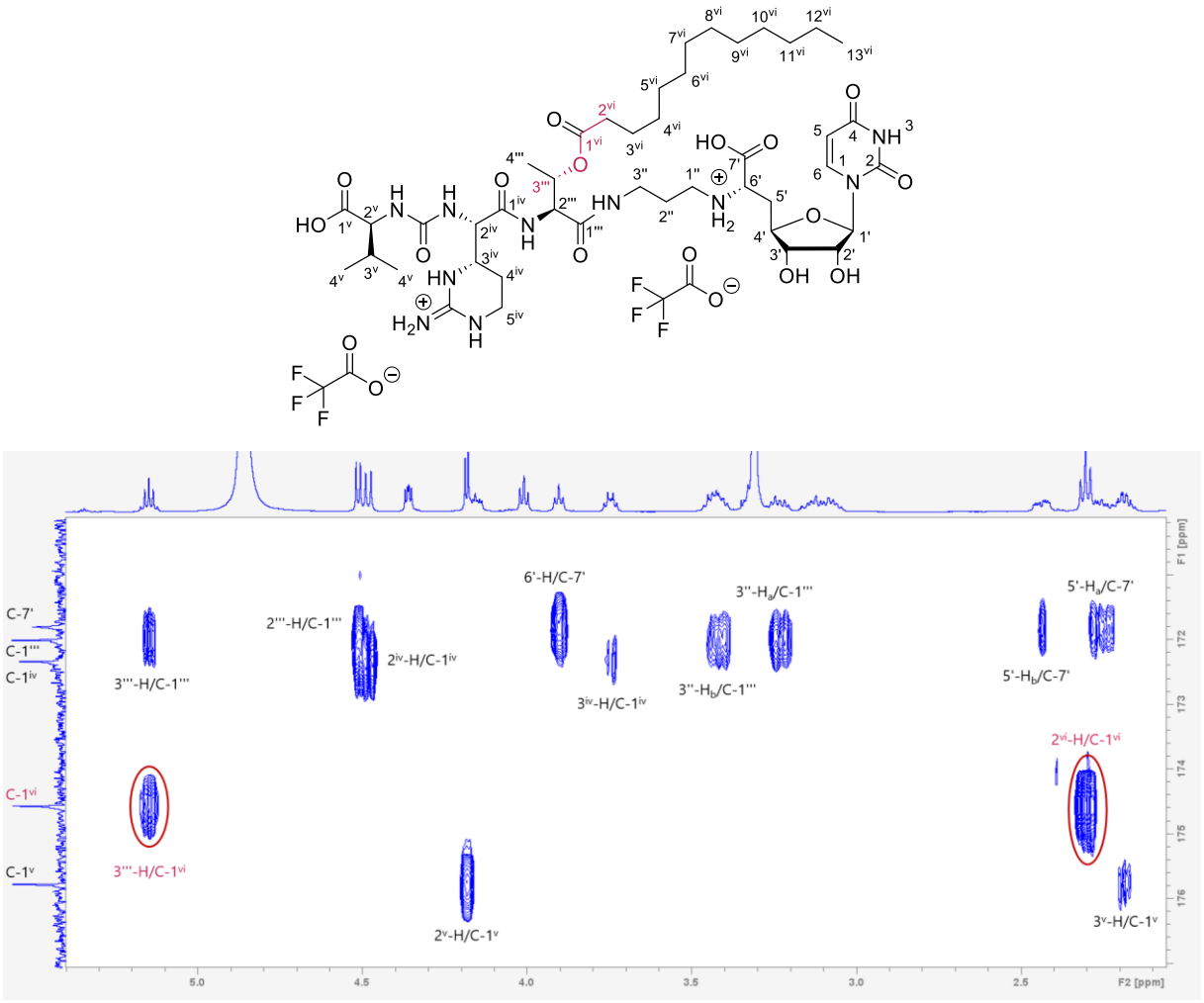

Fig. 52: Excerpt of the HMBC NMR spectrum, proving the connectivity of the lipophilic side chain to the backbone of muraymycin derivative **T4**.

The isolated amount of the Cbz-protected coupling product **52** from the EDC • HCl approach (**cf. Fig 50**) was used to synthesize the Arg-containing derivative **T5** (cf. **Fig. 53**).

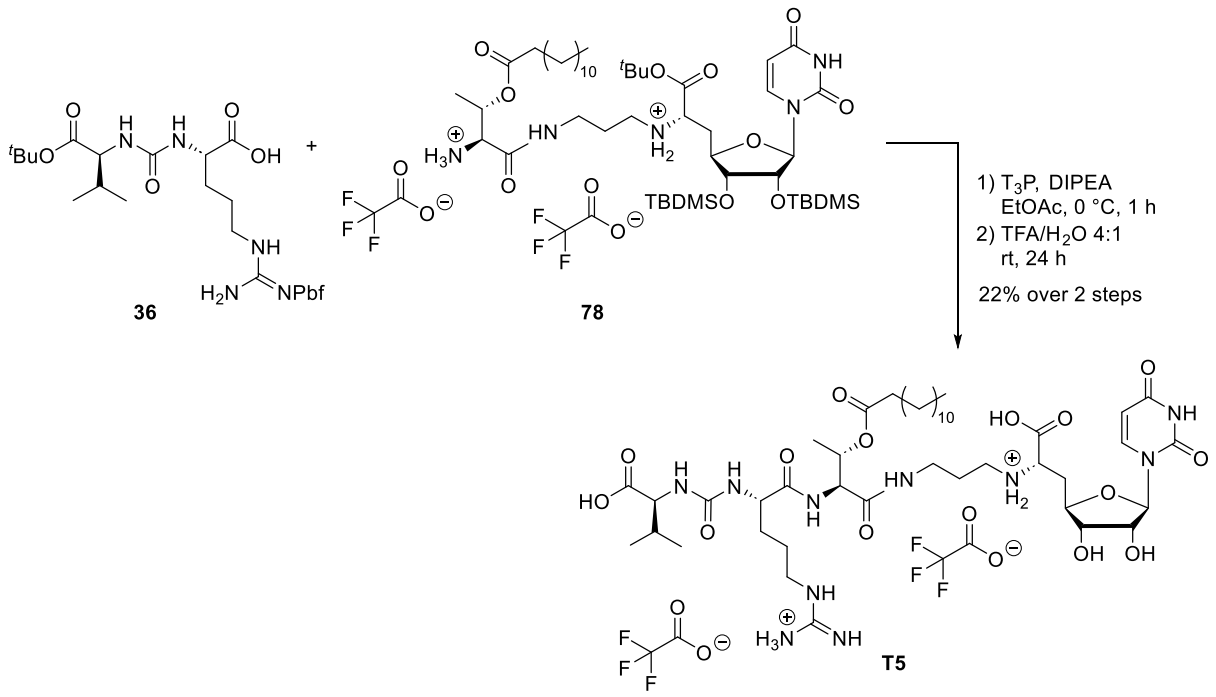

Fig. 53: Synthesis of target compound **T5** via peptide coupling and global deprotection.

First, the Cbz group of derivative **52** was cleaved as previously described.[146,148,153] The subsequent peptide coupling was carried out with T_3P as coupling agent and DIPEA (3.5 eq.). These equivalents were required to scavenge the emerging water and trifluoroacetic acid, and to deprotonate urea dipeptide **36**. So, compound **36**, bis-TFA salt **78** and DIPEA were diluted in dry ethyl acetate. Then T_3P (50% in ethyl acetate) was added to the cooled reaction mixture. The reaction progress was monitored by TLC and LC-MS. Based on these analyses, the reaction was ended after 1 hour by adding ethyl acetate. The organic layer was washed with water and aqueous saturated sodium chloride solution. The intermediate was not purified further and was only identified by LC-MS (m/z = 1548.80 $[M+H]^+$). The residue was dissolved in aqueous trifluoroacetic acid (80%) and was stirred for 24 hours at room temperature. This time, the solvent was removed under reduced pressure first before redissolving the residue in water at 0 °C, to avoid possible side reactions. After lyophilization, muraymycin derivative **T5** was purified by HPLC and obtained with a yield of 22% over two steps. The connectivity of the lipophilic side chain to the backbone was proven with the HMBC NMR spectrum (cf. **Fig. 56**). In addition, no derivative lacking the lipophilic side chain was identified nor isolated. Therefore, removing the acidic solvent prior to the addition of water

appeared to be a promising approach to avoid the potential cleavage of the lipophilic side chain.

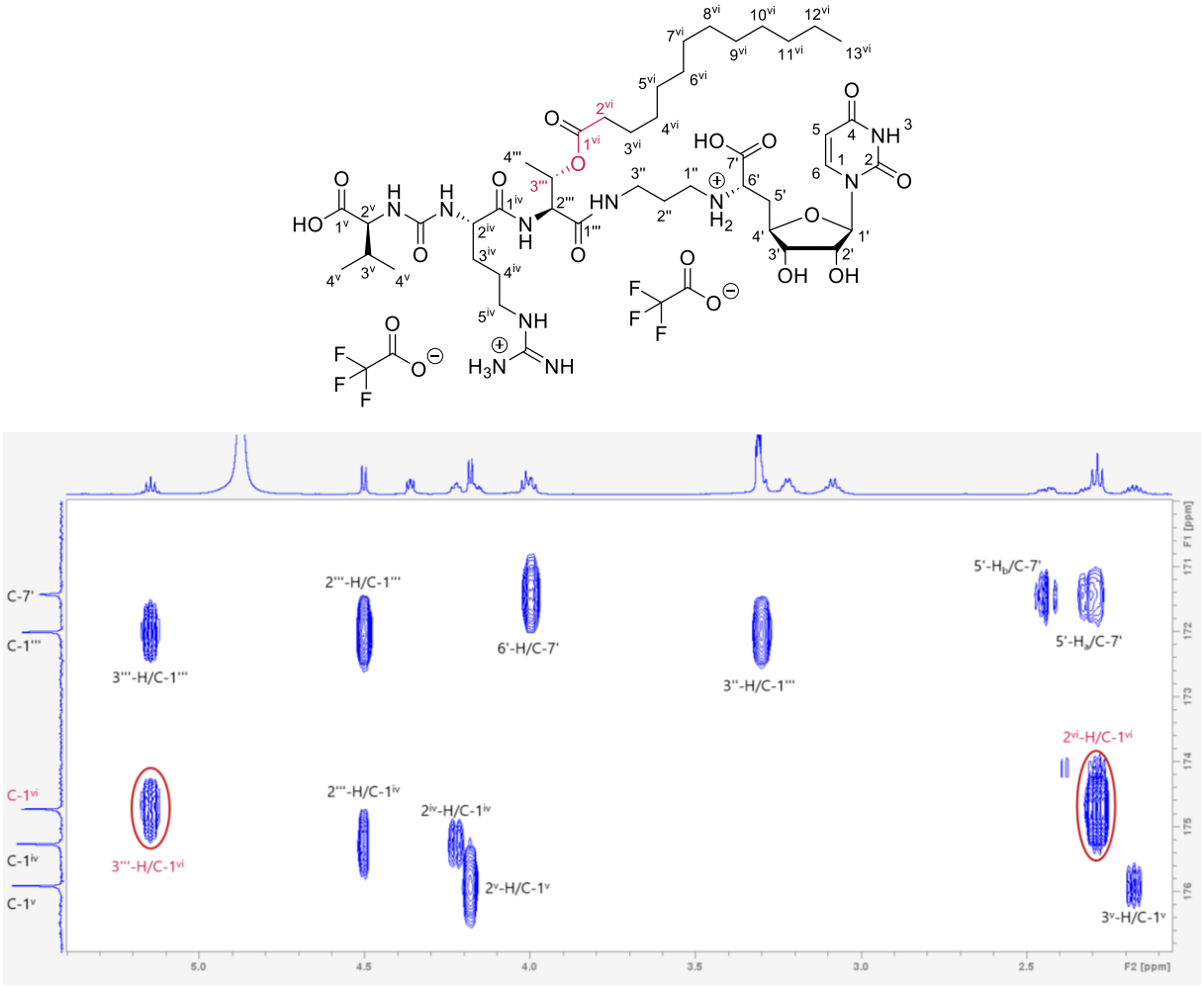

Fig. 54: Excerpt of the HMBC NMR spectrum, proving the connectivity of the lipophilic side chain to the backbone of muraymycin derivative **T5**.

4.4.3 Synthesis of target compound T6: Val-Arg-Thr($COC_{12}H_{25}$)-NuAA

The relevance of the steric center at the 3-position of the central amino acid had never been examined in detail prior to this work. To gain further insights regarding biological and antibacterial activities, derivative **T6** was designed and synthesized.

First, Thr-based building block **39** was connected to nucleosyl amino acid **35** in a peptide coupling using EDC • HCl and HOBt. The reaction was carried out as described in section 4.4.2, based on the protocol of K. Leyerer.[146] It was monitored by TLC and was ended after 16 hours. After purification by silica gel column chromatography, the NMR revealed two components. To rule out the presence of the isomer, a high temperature NMR was carried out, which lead to the conclusion that the second component was a different, unknown species. Due to the similar behavior of the desired

product and the impurity on silica gel, HPLC purification was performed, yielding the desired coupling **79** in 44% as a mono-TFA salt (cf. **Fig. 55**). The unknown species was not further identified.

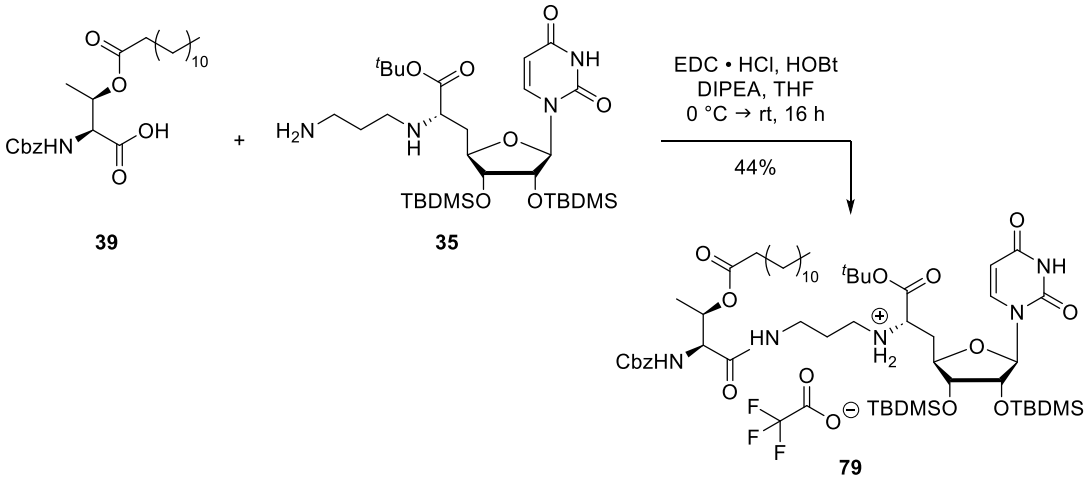

Fig. 55: Synthesis of derivative **79** via peptide coupling with EDC • HCl, HOBt and DIPEA.

Bis-TFA salt **80** was obtained from compound **79** via the already described mild hydrogenolysis using 1,4-cyclohexadiene, palladium black and trifluoroacetic acid in dry *iso*-propanol (cf. section 4.2.2).[146,148,153] The subsequent peptide coupling was accomplished with the coupling agent HATU in dry dichloromethane (cf. **Fig. 56**). The switching of the coupling agent was mainly due to the observed storage instability of T_3P over a longer period of time. So, urea dipeptide **36** and 1 equivalent of DIPEA were dissolved in dry dichloromethane. After 10 minutes, HATU was added, and the reaction mixture was stirred for 30 minutes at room temperature. Then the reaction mixture was cooled to 0 °C and 2.5 equivalents of the *Hünig*'s base were added. Bis-TFA salt **80** in dry dichloromethane was added dropwise. The reaction was monitored by LC-MS and showed no complete transformation after 18 hours. Therefore, another equivalent of HATU was added. Altogether, the reaction stirred for 42 hours and was ended by removing of the solvent. The residue was dissolved in ethyl acetate and was washed with water. The aqueous layer was extracted with ethyl acetate and the solvent was removed under reduced pressure. The coupling product was identified by LC-MS (m/z = 1549.78 $[M+H]^+$). The molecular masses of the reactants **36** and **80** were also detected in the chromatogram, suggesting that complete transformation was not achieved. It could be assumed that a rearrangement of **80** with migration of the side chain occurred when the nucleophilic amine was released (cf. section 4.4.2). This rearranged derivative is unable to undergo a peptide coupling, which explains the

remaining urea dipeptide **36**, which could not couple. Furthermore, the observed presence of the bis-TFA salt of the attempted product is based solely on the mass data. Unfortunately, compound **80** and its rearranged derivative share the same molecular weight and therefore have identical masse spectra. Thus, a definitive distinction is not possible at this stage and can only be assumed.

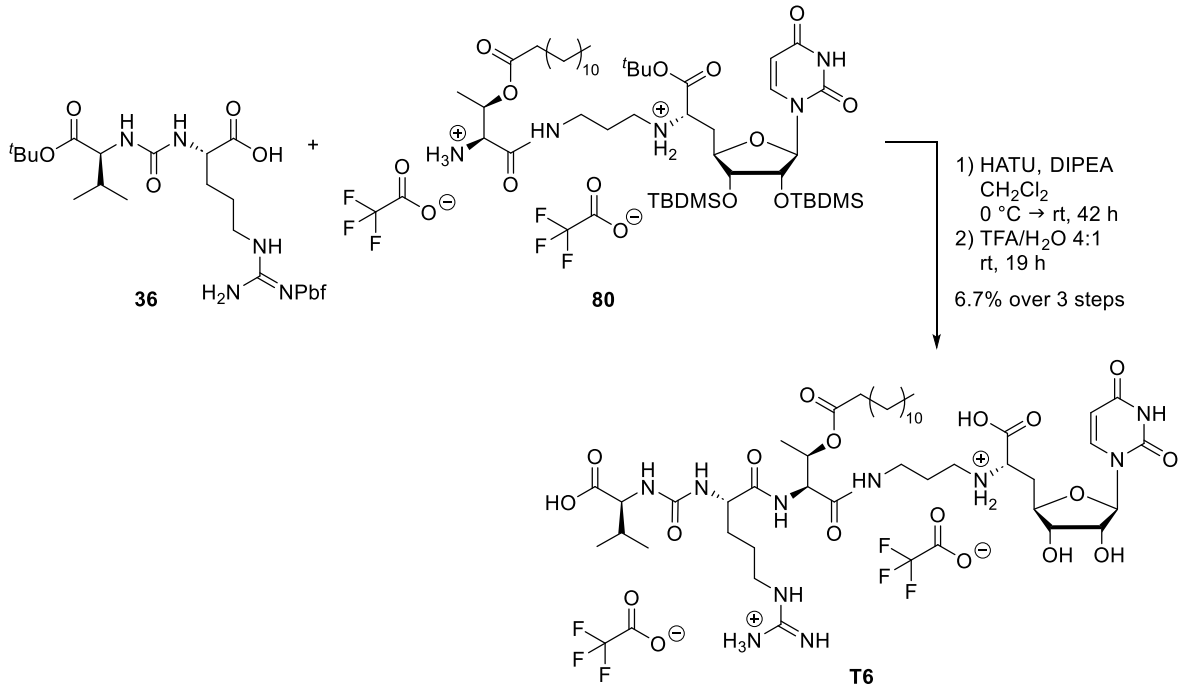

Fig. 56: Synthesis of target compound **T6** via peptide coupling and global deprotection.

The crude product was dissolved in aqueous trifluoroacetic acid (80%) and was stirred for 19 hours at room temperature. Then, the solvent was removed under reduced pressure and the residue was dissolved in water at 0 °C. After purification by HPLC, target compound **T6** was isolated with 6.7% yield as bis-TFA salt over three steps. The peptide coupling is assumed to be the yield-limiting step, as the intramolecular rearrangement of compound **80** may contribute to an incomplete conversion. To prove the connectivity of the lipophilic side chain, the HMBC NMR spectrum of the derivative was employed again. In this particular case, the varied stereochemistry of the central amino acid led to a loss of the signal between proton 3'''-H and the carbonyl carbon atom C-1^{vi}. Since the cross-peak between 2^{vi}-H and C-1^{vi} were visible, the missing signal would confirm the desired connectivity. Selective stimulation of the relevant part of the HMBC NMR spectrum revealed the missing cross peak, providing evidence of the connectivity and thus the structure of muraymycin derivative **T6**.

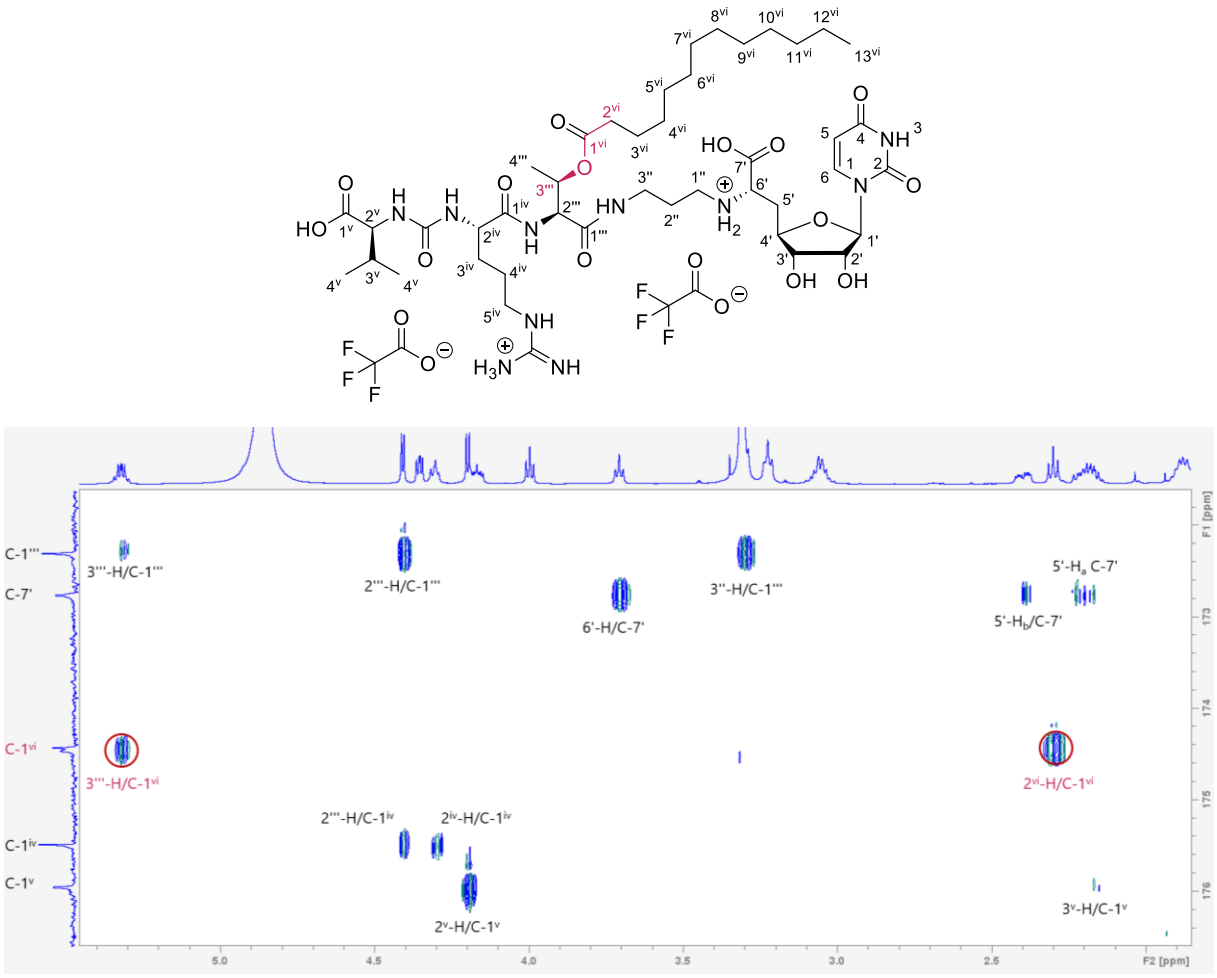

Fig. 57: Excerpt of the HMBC NMR spectrum, proving the connectivity of the lipophilic side chain to the backbone of muraymycin derivative **T6**.

4.5 Synthesis of the *allo*-L-threonine-containing muraymycin derivatives with special side chains

This section will focus on the introduction of different lipophilic side chains into the muraymycin core structure, with the goal of investigating the effects of these modifications on the compound's overall properties. The design choices for the fatty acid chain should enhance the understanding of the role and significance of this key structural unit for the compound's biological activity.

4.5.1 Synthesis of target compound T8: Val-Epic-*allo*-Thr(CO^{iso}C$_{15}$H$_{31}$)-NuAA

The design for the first special fatty moiety was inspired by the natural product muraymycin **B8**, which remains the most active natural derivative to date. With the incorporation of its branched C$_{16}$-alkyl chain (CO^{iso}C$_{15}$H$_{31}$; cf. section 2.2.1, **Fig. 8**, **B8**) into a simplified backbone, we wanted to investigate the contribution of the lipophilic

side chain to the overall biological activity of the compound. The gained data may elucidate why certain natural compounds feature these specific side chains.[120] In order to apply the established synthesis of the central amino building block, it is necessary to synthesize the corresponding acids for the lipophilic side chains first.

4.5.1.1 Synthesis of 14-methylpentadecanoic acid 45

In 2013, Richardson and Williams published a synthetic approach of different *n*-alkyl carboxylic acids with an *iso*-propyl head group. The synthesis begins with the ring opening of exaltolide followed by selective reduction of the resulting tertiary alcohol to give 15-methylhexadecan-1-ol (synthesis not shown).[156] However, the first two steps were omitted in this study, and the synthesis for the desired acid **45** started directly with 15-methylhexadecan-1-ol, which was commercially available (cf. **Fig. 58**). The first two steps involve a *Chugaev* reaction sequence. Therefore, the primary alcohol was diluted with dry tetrahydrofuran, and sodium hydride (60% in mineral oil) was added to the clear solution. To achieve complete deprotonation, the mixture was stirred for 1 hour before carbon disulfide in dry tetrahydrofuran was added. Then, the yellowish-silver reaction mixture was stirred for another hour at room temperature. Methyl iodide in dry tetrahydrofuran was added to complete the formation of the xanthate **81**. Due to the toxicity of the reactants, no reaction monitoring was performed. However, to ensure the best possible yield, the reaction was stirred for additional 5 hours. It was ended by adding saturated ammonium chloride solution. After extraction, xanthate **81** was isolated by silica gel column chromatography with a good yield of 81%. The second step of the *Chugaev* reaction sequence is the thermally induced intramolecular elimination resulting in the formation of terminal alkene **46**. To initiate this reaction, **81** was heated slowly over a *Bunsen* burner flame, producing white smoke. In a previous attempt, heating with a heat gun proved insufficient, so a *Bunsen* burner was employed instead. After cooling, the apparatus was rinsed with petroleum ether. Following extraction and removal of the solvent, alkene **46** was purified by silica gel column chromatography and isolated with 73% yield. The final step of the published synthetic sequence is a one pot oxidative cleavage using potassium permanganate ($KMnO_4$) and acetic acid (cf. **Fig. 58**).[156] To carry out this reaction, alkene **46**, $KMnO_4$, acetic acid and phase transfer catalyst tetrabutylammonium bromide ($^nBu_4NBr$) were dissolved in a mixture of dichloromethane and water. The violet reaction mixture was refluxed for 40 hours. After cooling, aqueous hydrogen

chloride solution (5 M) was added to the brown suspension to dissolve the resulting manganese dioxide. The layers were separated, and the aqueous layer was extracted with ethyl acetate. The crude product was purified by silica gel column chromatography resulting in a grease-like colorless substance. At this point, based on NMR data, it was assumed that pure compound **45** had been obtained. Since **45** is not UV-active, LC-MS analysis was limited to the mass trace. The mass spectrum revealed the presence of a second species (m/z = 241.22 [M(**45**)-14]). From the observed mass, it was inferred that this species is the acid truncated by a single CH_2 group. Such a compound would be indistinguishable from the desired product in the NMR spectrum, because integration of the alkyl signals in the ^1H NMR spectrum was found to be not precise enough. In addition, the second species would not have been detected by TLC monitoring. Its mobility on silica gel would be very similar to that of the desired product, as a difference of only one CH_2 group is insufficient to cause a visible difference in the elution behavior.

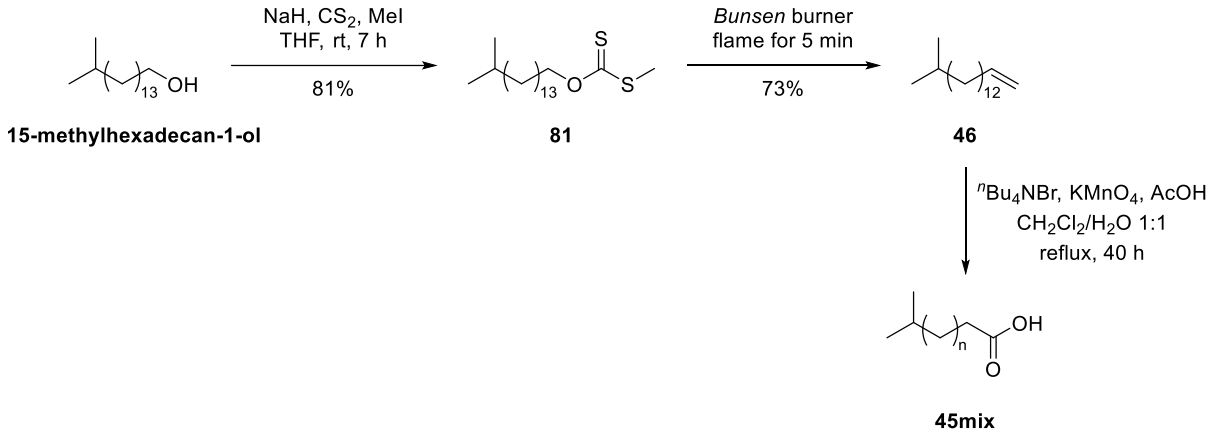

Fig. 58: First synthetic approach of 14-methylpentadecanoic acid **45mix** via *Chugaev* reaction and oxidation with $KMnO_4$.

During the synthesis of the required central building block with compound mixture **45mix**, the presence of a truncated acid missing a single CH_2 group could not only be confirmed, but the existence of even shorter side chains was also observed. High-resolution mass spectrometry data confirmed the presence of the decomposition components. **Fig. 59** illustrates the *Steglich* esterification of Cbz-*allo*-Thr-O^{t}Bu **74**, along with the corresponding HRMS spectra, including the UV trace and mass spectrum of the product mixture.

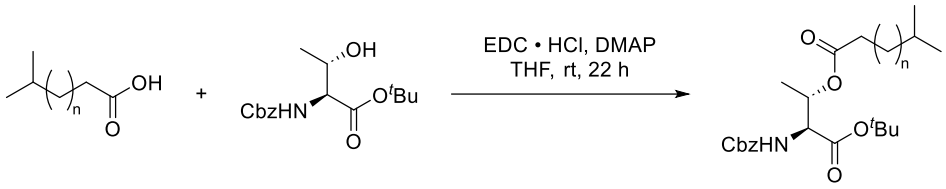

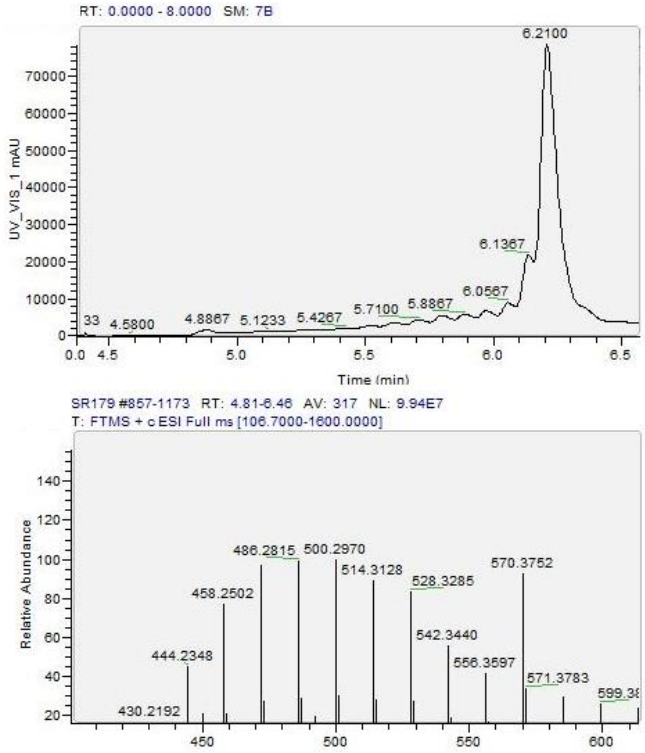

compound	m/z	
	calcd.	found
n = 11	570.3766 $[M+Na]^+$	570.3752
n = 10	556.3609 $[M-CH_2+Na]^+$	556.3597
n = 9	542.3453 $[M-2CH_2+Na]^+$	542.3440
n = 8	528.3296 $[M-3CH_2+Na]^+$	528.3284
n = 7	514.3140 $[M-4CH_2+Na]^+$	514.3128
n = 6	500.2983 $[M-5CH_2+Na]^+$	500.2970
n = 5	486.2827 $[M-6CH_2+Na]^+$	486.2815
n = 4	472.2670 $[M-7CH_2+Na]^+$	472.2659
n = 3	458.2514 $[M-8CH_2+Na]^+$	458.2502
n = 2	444.2357 $[M-9CH_2+Na]^+$	444.2347

Fig. 59: Proof of the decomposition of the branched lipophilic side chain **45mix** by HRMS of compound-mixture **82mix** (top: excerpt of UV-trace (256 nm), bottom: excerpt of mass spectrum).

Since the different components of the product mixture **82mix** are also distinguishable in the UV trace (cf. **Fig. 59**), it can be assumed that the mass spectrum does not result from iron fragmentation during the measurement process. Since alkene **46** appeared to be pure in the corresponding mass spectra and was employed in other subsequent research without any trace of side chain fragmentation, the preceding *Chugaev* reaction sequence cannot be the origin of the mixture of different side chains. It is much more likely that the $KMnO_4$-promoted oxidative cleavage of the terminal double bond led to the formation of side products, a consequence of the overoxidation frequently observed in this reaction.[176,177] However, the mixture of compounds **82mix** was used in subsequent reactions without any separation attempts, as it was assumed that a separation using HPLC would be possible at a later stage. Ultimately, it was used to obtain new muraymycin derivative **T8** (cf. section 4.5.1.3).

In order to avoid the side product formation of the $KMnO_4$ oxidation step and to obtain pure compound **45**, an alternative synthesis was explored. It was accomplished as shown in **Fig. 60** by performing the dihydroxylation and the oxidative cleave in two separate steps. As a milder dihydroxylation, the known asymmetric *Sharpless* dihydroxylation was employed.[160,178,179] Although the exact configuration is not important in this synthesis sequence, the *Sharpless* method proved to be the most reliable, and high-yielding alternative at this stage. All attempted two-step epoxidation-hydrolysis sequences were found to be less efficient. The diol was then converted into the corresponding carboxylic acid by an oxidation sequence including a *Pinnick* oxidation.

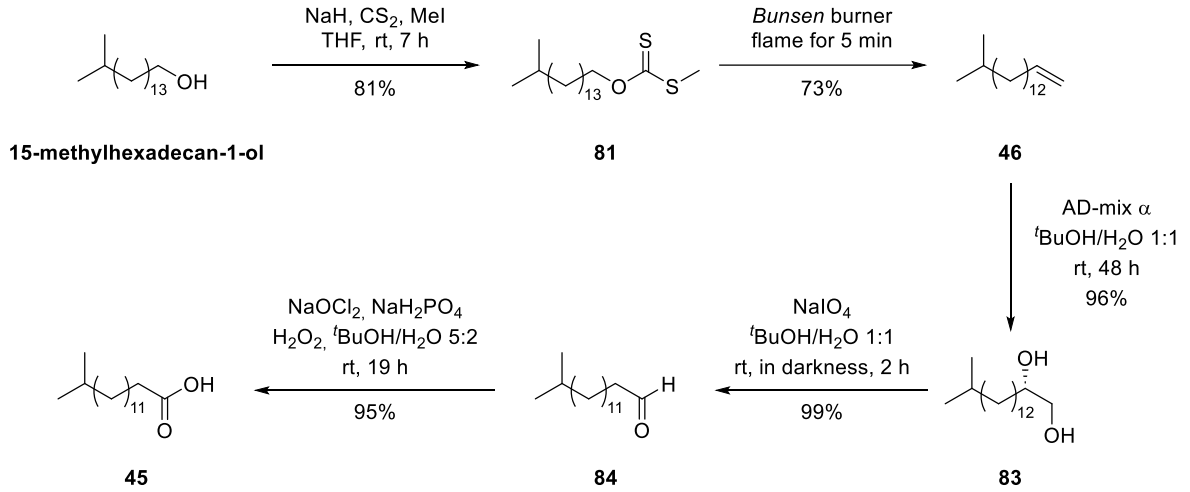

Fig. 60: Second synthetic approach of 14-methylpentadecanoic acid **45** via *Sharpless* asymmetric dihydroxylation and oxidation sequence.

Since the synthesis of the terminal alkene **46**, based on the protocol from Richardson and Williams, was successful, it was also applied to the new approach.[156] For the *Sharpless* dihydroxylation, **46** was suspended in a 1:1 mixture of *tert*-butanol and water before AD-mix α was added. AD-mix α was used in this case because it was readily available. It would have made no difference to use AD-mix β, as the stereo information is removed again in the next step, when the resulting diol is cleaved. The reaction mixture was stirred vigorously at room temperature for 48 hours. *Tert*-butanol was removed under reduced pressure and the residue was dissolved in water. Diol **83** was isolated after extraction and stirring with sodium sulfate with a very good yield of 96%. The oxidative cleavage was performed with sodium periodate in a *Malaprade* reaction. For this purpose, diol **83** in *tert*-butanol and sodium periodate in water were mixed. The reaction was stirred for 2 hours at room temperature in the absence of light to

avoid possible radical side reactions. The reaction was monitored with TLC and was terminated after 2 hours. *Tert*-butanol was removed under reduced pressure and the remaining aqueous layer was extracted with diethyl ether. Aldehyde **84** was isolated without further purification with a yield of 99%. The final step of the sequence was a *Pinnick* oxidation with sodium chlorite as oxidative agent and sodium dihydrogen phosphate to adjust the pH value.[146,180,181] The mixture of sodium chlorite and sodium hydrogen phosphate was added dropwise to the aldehyde in *tert*-butanol, resulting in a green colored reaction mixture. Finally, hydrogen peroxide (33% in water) was added to intercept the accruing sodium hypochlorite. The reaction was monitored by TLC and was ended after 19 hours by removing the *tert*-butanol under reduced pressure. The aqueous layer was extracted with *n*-hexane. After removing the solvent, the wanted carboxylic acid **45** was isolated without further purification with a yield of 95%. The resulting substance was a white powder. In the first attempt (cf. **Fig. 58**), the product had a greasy consistency, which can be considered to be an additional indication of the impurity of derivative **45mix**. The purity of the new product was confirmed by NMR and HRMS, which showed no hints of any shortened derivatives. Overall, the pure branched lipophilic side chain **45** was achieved in 53% yield over five steps.

Compared to the route presented by Richardson and Williams, the new reaction sequence requires two additional steps. However, since a clean product can be obtained via this route and no purification was required for the latter three steps, it is a convincing alternative. To ensure the purity of the final product, lipophilic side chain **45** was used to synthesize the corresponding *allo*-Thr-based derivative **44** (cf. section 4.5.1.2).

4.5.1.2 Synthesis of the central building blocks 44 and 85 with branched lipophilic side chain $CO^{iso}C_{15}H_{31}$

Before exchanging the central amino acid to *allo*-Thr, it was planned to synthesize the muraymycin **B8** analog with Ser as the central amino acid. The previously described reaction sequence to obtain the central building block was employed to synthesize the required building block **86** (cf. **Fig. 61**).

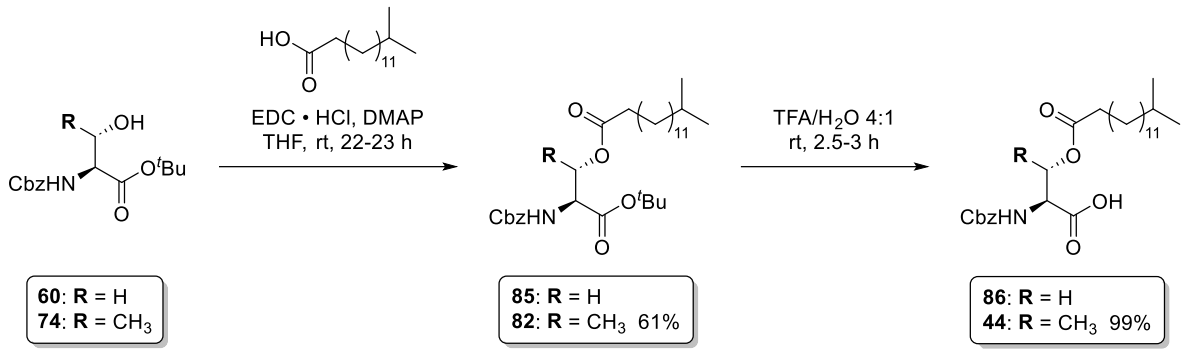

Fig. 61: Synthesis of Ser-based derivative **86** and *allo*-Thr-based derivative **44** via *Steglich* esterification and cleavage of the *tert*-butyl ester.

The *Steglich* esterification was carried out in dry tetrahydrofuran at room temperature with EDC • HCl and DMAP.[145,153] Carboxylic acid **45mix**, which contained impurities with shorter side chains (cf. section 4.5.1.1, **Fig. 58**), was used for the reaction. After 22 h, the reaction was terminated by adding aqueous hydrochloride solution (5 M). After extraction and purification by silica gel column chromatography, *tert*-butyl ester **85mix** containing impurities with different side chain lengths, was isolated. The intermediate was dissolved in aqueous trifluoroacetic acid (80%) to cleave the *tert*-butyl ester. After 2.5 hours, water was added, and the suspension was lyophilized to obtain Ser-based derivative **86**. The HRMS data of **86** revealed the previously described derivatives, which showed a successively shortening of CH_2 groups in the side chain (spectrum not shown). Although **86** was a mixture of different compounds, it was intended to be used for the synthesis of a new muraymycin derivative. A later planned HPLC purification was regarded as a possibility to finally separate the derivatives with shortened side chains and to obtain the required compound in a pure form. However, since the muraymycin Ser-series was not pursued further, the *Steglich* esterification and subsequent ester cleavage were not repeated for the central building block. Therefore, there is no data on the corresponding pure compounds.

The *allo*-Thr-based building block **44** was synthesized twice. In the initial attempt, the same derivatization as described for **86** was observed, which was expected, considering that the compound mixture **45mix** was employed. However, in the second attempt, pure compound **45** was used, leading to the successful formation of the pure derivatives **82** and **44**. Thus, the intermediates of this second reaction sequence can be characterized, including the determination of yields. The *Steglich* esterification and subsequent ester cleavage were both carried out as previously described (cf. section 4.2.1). Overall, building block **44** was achieved with a 33% yield over three steps with

the formation of the *tert*-butyl ester being the yield-limiting step. Furthermore, it was observed that the *Steglich* esterification in this case resulted in lower yields compared to the other building blocks. It can be assumed that the different shape and size of the corresponding acid could kinetically hamper the formation of the active ester or the nucleophilic attack. The required extension of the reaction time for both *tert*-butyl esters **82** and **85** supports this assumption.

For the subsequent peptide coupling, the batch of Cbz-*allo*-Thr-OH **44** containing different chain lengths was used, based on the assumption that the desired coupling product could be eventually purified using HPLC. The pure substance was synthesized primarily to demonstrate the advantage of the new route for the branched lipophilic side chain **45**, which can be applied in the design and development of future muraymycin derivatives.

4.5.1.3 Endgame for target compound T8: Val-Epic-*allo*-Thr($CO^{iso}C_{15}H_{31}$)-NuAA

The synthesis of the muraymycin **B8** analog required the conjugation of the three building blocks via peptide coupling. First, **44mix** was coupled with amine **35** using EDC • HCl and HOBt, as described in section 4.4.3. The reaction illustrated in **Fig. 62**, was monitored by TLC and was ended after 16 hours.

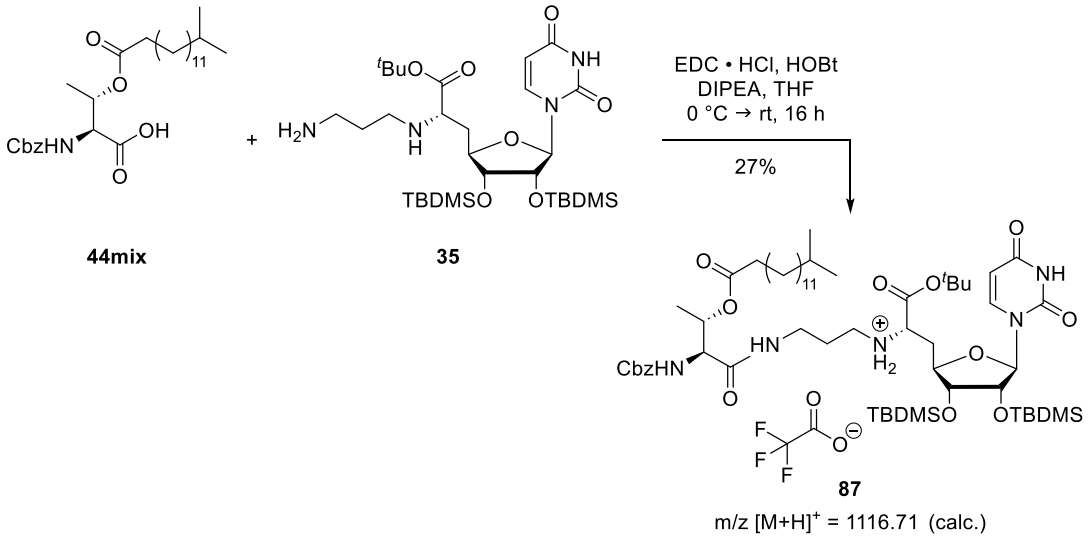

Fig. 62: Synthesis of derivative **87** via peptide coupling with EDC • HCl, HOBt and DIPEA.

It was assumed that compound **87** could be purified during the work-up. Silica gel column chromatography was used to separate probably remaining reactants and side products from the desired compound. The analysis of the HRMS data (cf. **Fig. 63**) after this purification demonstrated that the previously recommended HPLC purification was

required to separate the derivatives with different chain lengths (cf. section 4.5.1.2). Since the compounds only differ in their chain length and behave almost identical on silica gel, this result was expected. The UV-trace of the LC-MS chromatograms showed promising separation of the individual components, so the HPLC purification method was designed based on the solvent gradient used during the measurement. The pure product was isolated with a yield of 27% (relative to amine **35**). The compound missing a single CH_2 group was isolated with 3.8%. The shorter derivatives could not be isolated due to their low amounts.

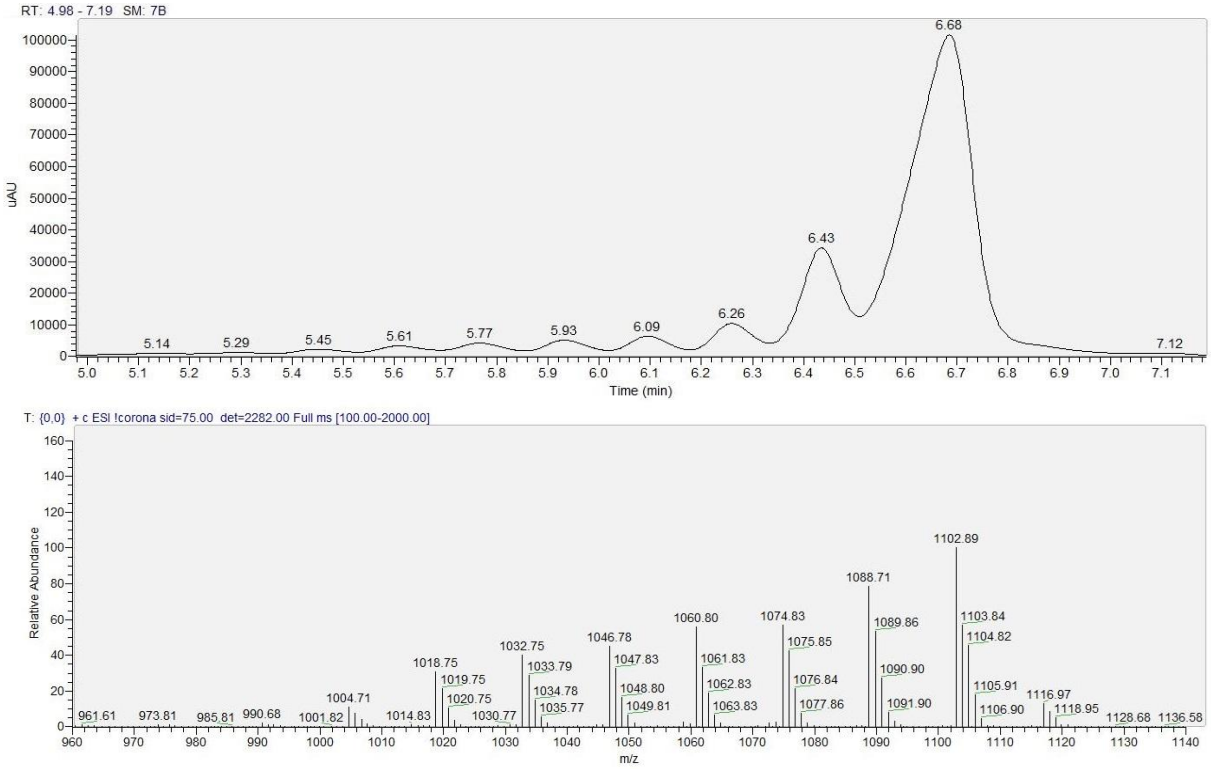

Fig. 63: UV trace (λ = 256 nm, top) and mass trace (bottom) of the LC-MS analysis of crude product **87** showing the gradually shorter lipophilic side chains (desired compound: m/z = 1116.97 [M+H$^+$]).

For the endgame, mono-TFA salt **87** was Cbz-deprotected under the well-known conditions with 1,4-cyclohexadiene, palladium black and trifluoroacetic acid (cf. **Fig 64**).[146,148,153] The resulting bis-TFA salt **88** and urea dipeptide **27** were coupled using HATU and DIPEA following the protocol described above (cf. section 4.4.3). LC-MS monitoring after 18 hours revealed the presence of the two reactants **27** and **88**. Therefore, 1.1 equivalents of HATU were added, and the reaction was continued at room temperature. After a total of 42 hours, both reactants were still detectable in the mass. Thus it was hypothesized that an intramolecular rearrangement occurred in **88**, preventing the peptide coupling. This phenomenon has been previously observed, for example during the synthesis of target compound **T6** (cf. section 4.4.3). Thus, the

reaction was ended, and the desired coupling product was verified by LC-MS (m/z = 1549.78 $[M+H]^+$). For the global deprotection, the crude product was dissolved in aqueous trifluoroacetic acid (80%) and was stirred for 35 hours at room temperature. The extended reaction time was needed for a complete deprotection, which was monitored by LC-MS. The solvent was removed under reduced pressure, water was added under ice cooling and the greenish reaction mixture was freeze-dried. The muraymycin **B8** analog **T8** was isolated as a bis-TFA salt after purification by HPLC in a yield of 9.8% over three steps. The low yield can be attributed to the second peptide coupling, during which **88** most likely underwent an intramolecular rearrangement with migration of the side chain. Unfortunately, this side reaction cannot be avoided during the peptide coupling once the primary amine is no longer protected as a TFA salt.

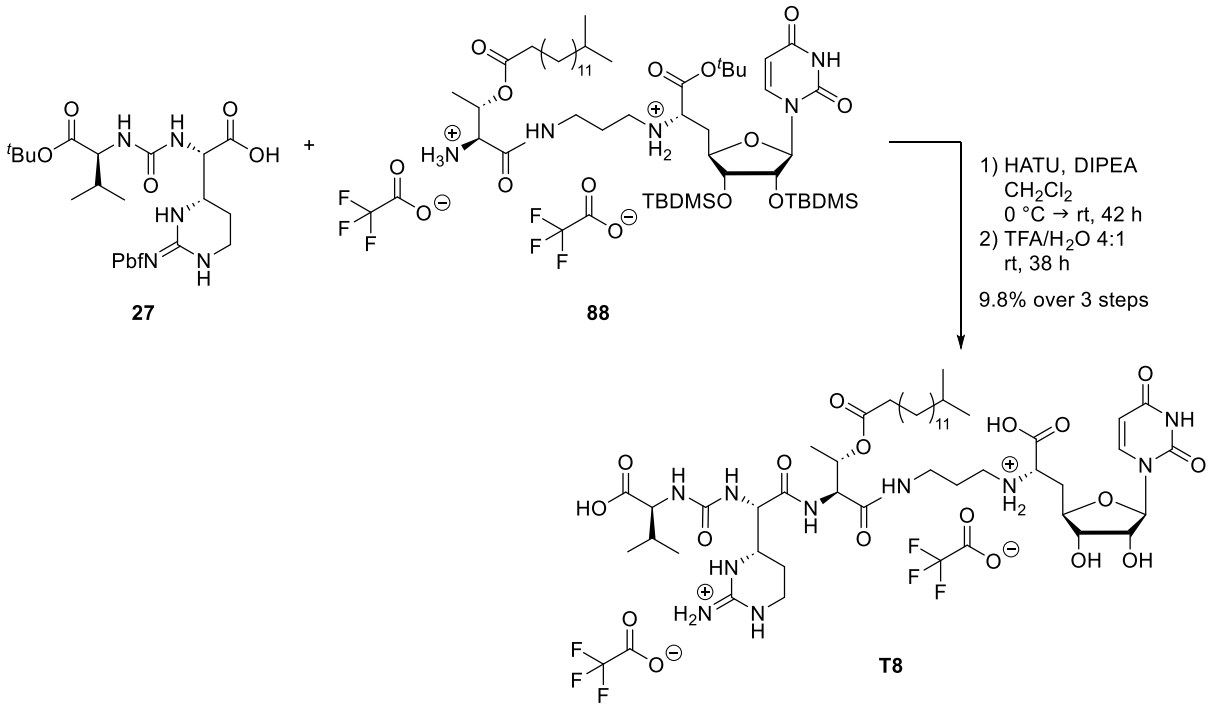

Fig. 64: Synthesis of target compound **T8** via peptide coupling and global deprotection.

Compound **T8** was characterized by HRMS and NMR, whereby the connectivity of the lipophilic side chain to the backbone was proven again using the HMBC NMR spectrum (cf. **Fig. 65**). Here, the cross peaks between 3'''-H or 2^{vi}-H and carbonyl carbon atom C-1^{vi} verify the connectivity of the side chain to the backbone and thus the structure of **T8**.

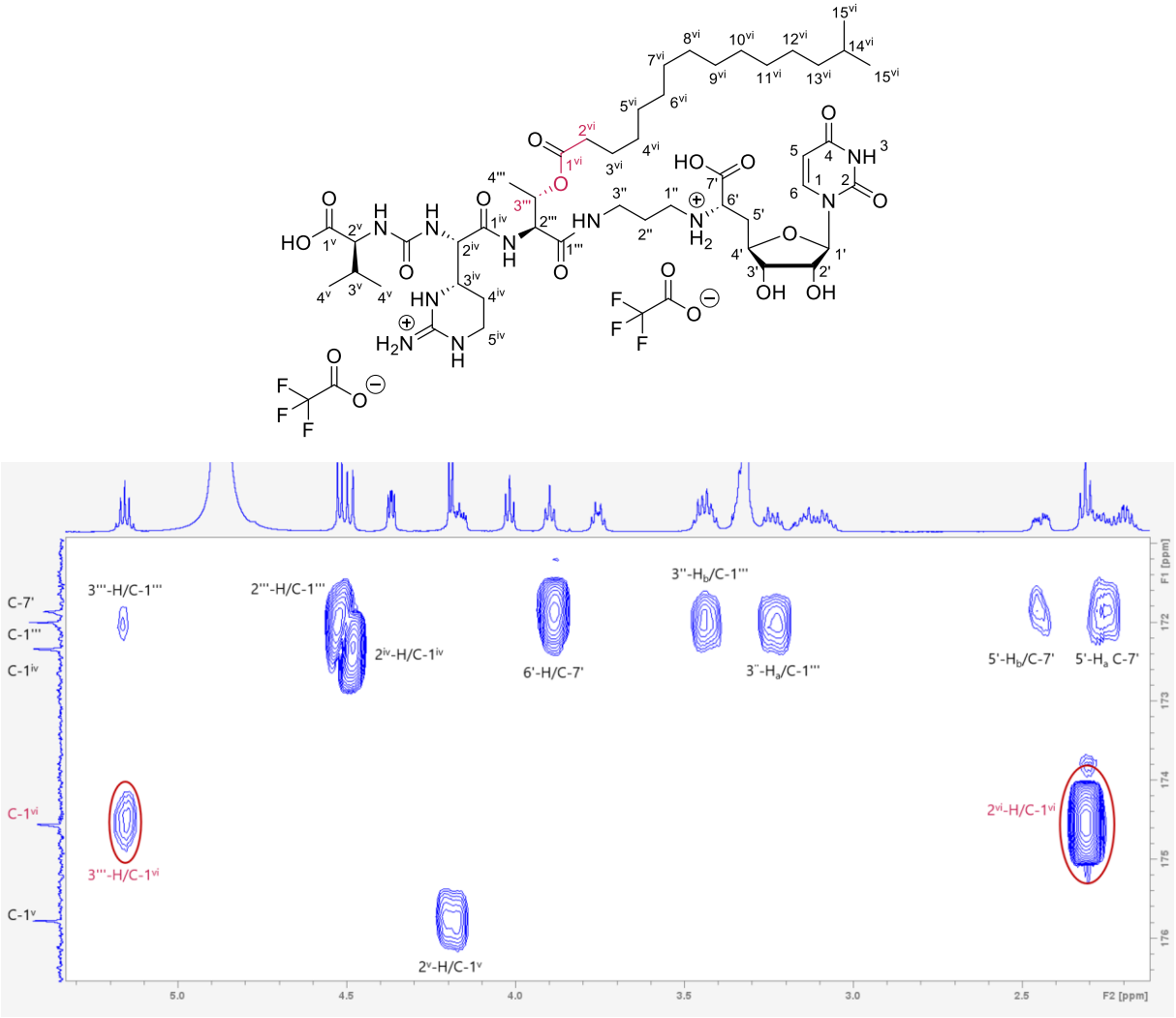

Fig. 65: Excerpt of the HMBC NMR spectrum, proving the connectivity of the branched lipophilic side chain to the backbone of muraymycin derivative **T8**.

4.5.2 Synthesis of target compound *a*T-T7: Val-Epic-*allo*-Thr($COCH_3$)-NuAA

To assess the role of the lipophilic side chain in a structure-activity relationship study, the Ser-containing reference derivative **T7**, with the shortest possible side chain ($COCH_3$), was designed and its synthesis was attempted. As already described, the isolation of compound **T7** was not successful (cf. section 4.2.4). However, before repeating the synthesis, the biological data of the *allo*-Thr-containing derivatives revealed that exchanging the central amino acid was beneficial (cf. sections 4.3, 4.6). Hence, the synthesis of **T7** was not repeated and instead, an *allo*-Thr-containing analog of derivative **T7** was designed and synthesized. This derivative contained acetylated *allo*-Thr **51** as central amino acid. In contrast to the other central building blocks, **51** could be obtained from Cbz-*allo*-Thr-OH in just one step. The reaction was carried out according to the protocol of Previero *et al.*, which had been successfully applied in the

preceding master thesis to synthesize the corresponding Ser-based building block.[153,158] As described in the literature, acetic anhydride was stirred in pyridine for 15 minutes to form the highly active 1-acetyl-1-pyridinium ion.[182] The solution was cooled to 0 °C, then the nucleophile was added, and the reaction was stirred for one hour at this temperature. The reaction was ended by adding water, followed by extraction with ethyl acetate. The solvent was removed under reduced pressure, ensuring that the water bath temperature did not exceed 25 °C. This was necessary because it had previously been found that at higher temperatures, even small traces of water could lead to an acid-catalyzed cleavage of the acetyl group, leading eventually to its removal from the molecule and the recovery of the reactant.[153] Building block **51** was obtained after purification by silica gel chromatography in a good yield of 84% (cf. **Fig. 66**).

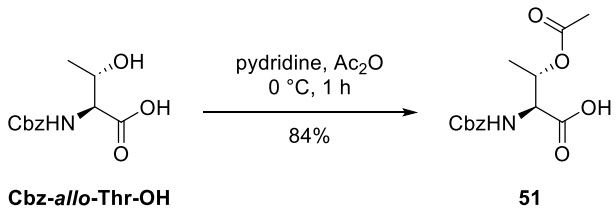

Cbz-*allo*-Thr-OH **51**

Fig. 66: Synthesis of acetylated *allo*-Thr-based compound **51** with pyridine and acetic anhydride.

The subsequent peptide coupling between central building block **51** and nucleosyl amino acid **35** was performed using HATU and DIPEA according to the described procedure. First, amino acid derivative **51** and one equivalent of DIPEA were dissolved in dry dichloromethane and were stirred for 10 minutes at room temperature. To form the active ester, HATU was added to the reaction mixture. After 30 minutes, the suspension was cooled to 0 °C and the second equivalent of DIPEA was added. Amine **35** in dichloromethane was added dropwise at this temperature. The reaction was stirred for 14 hours during which time it warmed up to room temperature. Based on TLC, the reaction was ended by adding water slowly at 0 °C. These conditions were chosen in order to avoid the cleavage of the acetyl ester. The aqueous layer was extracted with dichloromethane. The solvent was removed under reduced pressure, again using only a 25 °C water bath. The crude product was purified by silica gel column chromatography yielding 66% of the coupling product **89** (cf. **Fig. 67**). The improved yield of the peptide coupling is most likely due to the significantly lower steric demand of the central building block **51**. The formation of the active ester and the subsequent

nucleophilic attack are thus kinetically simplified compared to the previous peptide couplings.

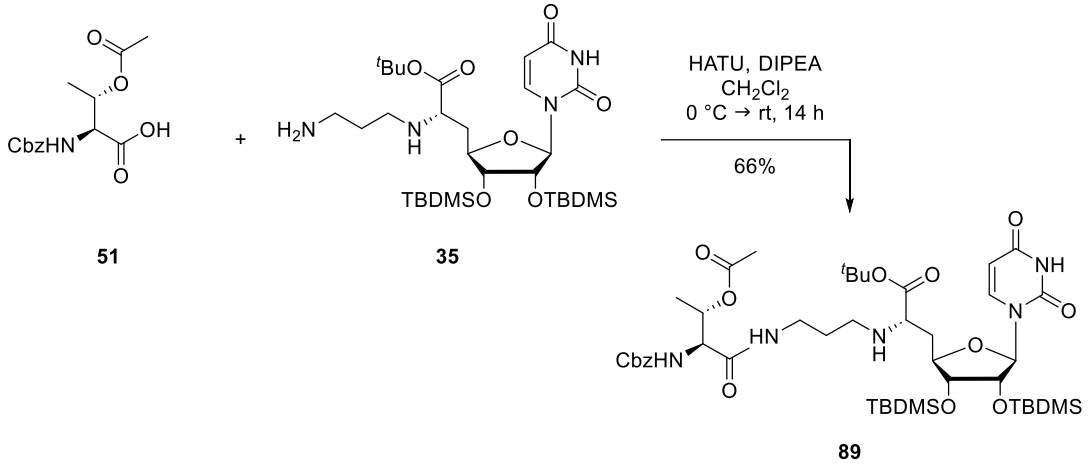

Fig. 67: Synthesis of derivative **89** via peptide coupling with HATU and DIPEA.

The required Cbz-deprotection of compound **89** was performed under the well-established conditions using 1,4-cyclohexadiene, palladium black and trifluoroacetic acid.[146,148,153] Bis-TFA salt **90** was synthesized twice. In both attempts, the Cbz group was completely cleaved. However in one approach the five-member intramolecular rearrangement took place, resulting in the formation of side product **90SP** (cf. **Fig. 68**). Based on ^{1}H NMR calculations, it was found that 72% of the desired product **90** and 22% of the rearranged product **90SP** were formed during the reaction.

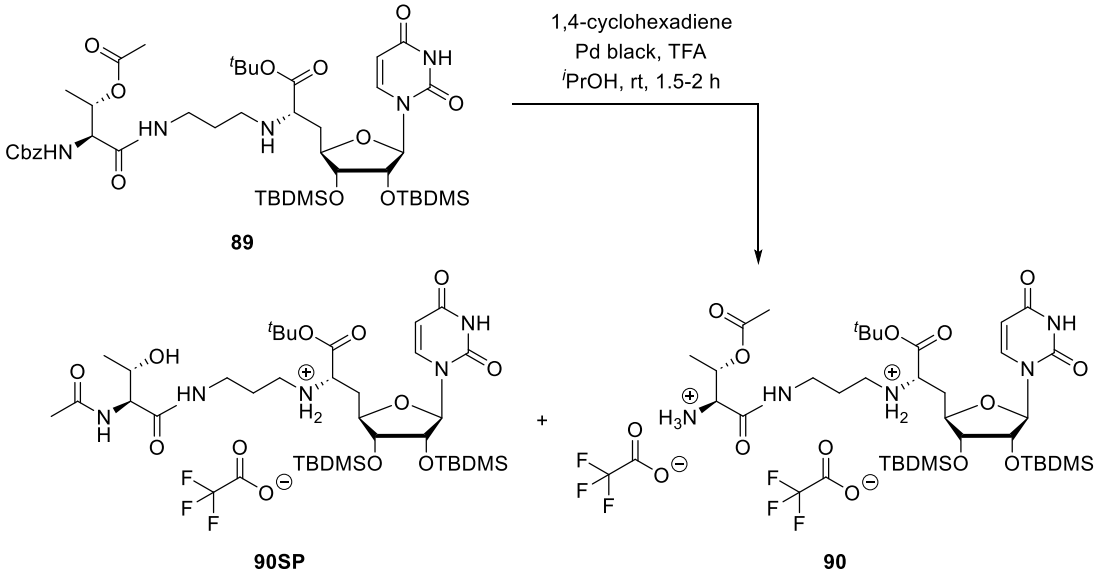

Fig. 68: Main product **90** and rearrangement product **90SP** formed during the Cbz-deprotection of **89**.

In the second approach, additional 0.3 equivalents of trifluoroacetic acid were added to ensure the protonation of the amino group and thereby counteract the

rearrangement. Here, no side product **90SP** was found in the NMR, supporting the idea of the addition of more than 2 equivalents of the trifluoroacetic acid. Although the NMR analysis of bis-TFA salt **90** mainly showed the product, small traces of undefinable impurities were also detected. It was assumed that these originated from the reagents employed, e.g. the palladium black. The product mixture was nevertheless used for the reaction described below. It was assumed that the side product **90SP** would not participate in the peptide coupling and that the subsequent HPLC purification would effectively separate all side products.

Since the intramolecular rearrangement was already observed during the synthesis of **T8** (cf. section 4.5.1.3), it was assumed that it would also occur during the peptide coupling, which is shown in **Fig. 69**. It was also expected that the significantly lower steric hindrance of derivative **90** compared to compound **88** (with lipophilic side chain $CO^{iso}C_{15}H_{31}$) would contribute to a faster and facilitated acetyl migration.

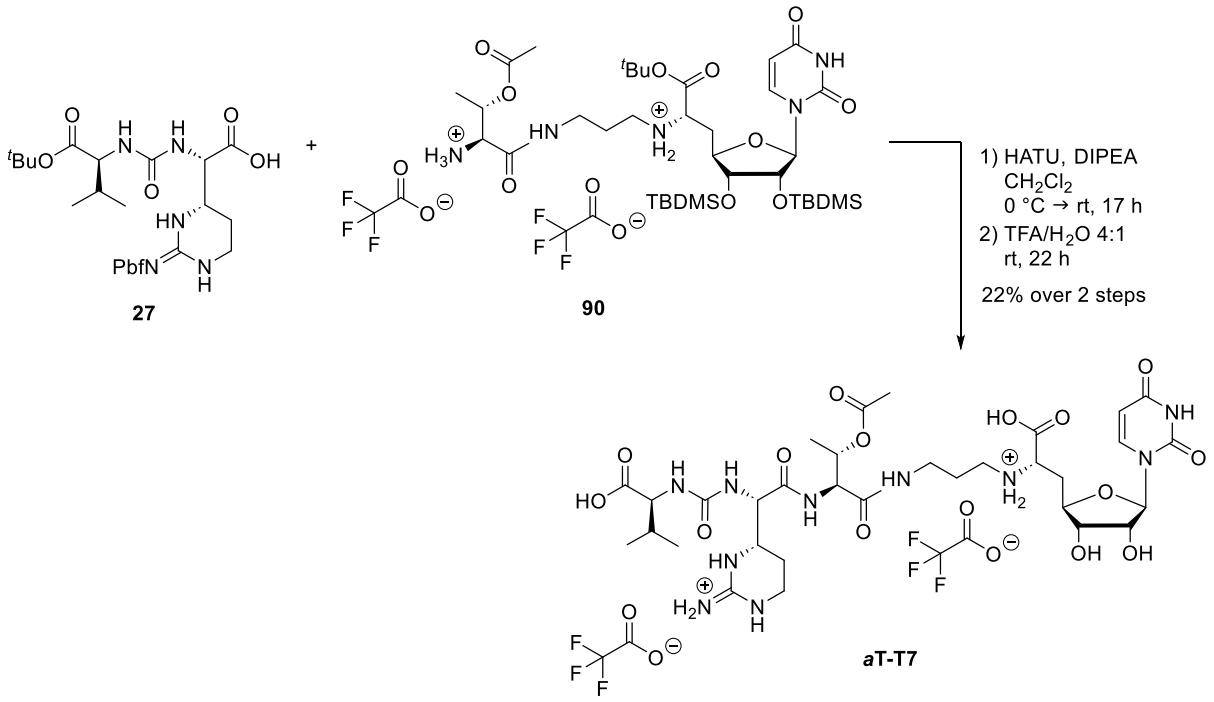

Fig. 69: Synthesis of target compound ***a*T-T7** via peptide coupling and global deprotection.

The peptide coupling was performed using HATU and DIPEA as described above, with the required equivalents of the base added at the appropriate stages. Specifically, one equivalent of DIPEA was used for the deprotection of urea dipeptide **27**, and the remaining equivalents were added before the addition of bis-TFA salt **90**. To minimize possible side reactions, like the intramolecular attack, the reaction was stirred at 0 °C for as long as possible. It warmed to room temperature overnight. Monitoring of the

reaction by TLC and LC-MS revealed a finished reaction after 17 hours, with side product **90SP** still present in the LC-MS chromatogram. After extraction, the global protected muraymycin derivative was only identified by LC-MS (m/z = 1392.16 $[M+H]^+$) and was subsequently dissolved in aqueous trifluoroacetic acid (80%). The deprotection was monitored by LC-MS and was terminated after 22 hours. To protect the acetyl moiety from cleavage, the trifluoroacetic caid was removed in high vacuum before water was added in order to lyophilize the residue. Muraymycin derivative ***a*T-T7** (*a*T for *allo*-Thr) was isolated by HPLC in 22% yield over two steps (cf. **Fig. 69**). Despite the inevitable side reaction, the yield for the reaction sequence is the best compared to any other. This is almost certainly due to the reduced steric hindrance of the side-chain-containing building block **90**.

The HMBC NMR spectrum in **Fig. 75** shows the cross peaks between the 3'''-H or 2^{iv}-H and the carbonyl carbon atom C-1^{iv}, proving the desired connectivity of the side chain to the backbone in muraymycin derivative ***a*T-T7**.

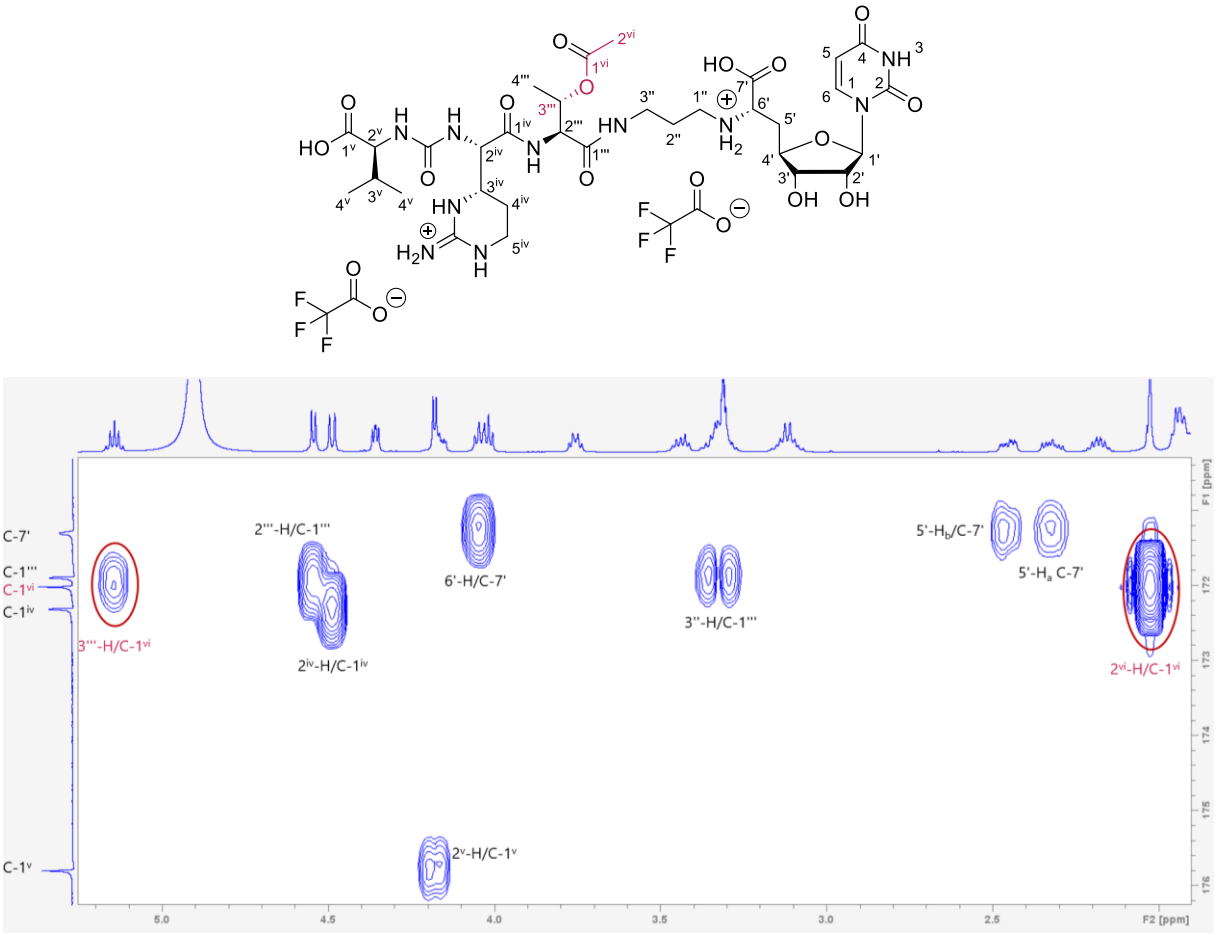

Fig. 70: Excerpt of the HMBC NMR spectrum, proving the connectivity of the acetyl side chain to the backbone of muraymycin derivative ***a*T-T7**.

Despite the challenges described above, particularly the intramolecular rearrangement, the synthesis of derivative ***a*T-T7** is a very promising, alternative approach for an easier production of new muraymycin derivatives with diverse side chains. It benefits from the improved yields of the peptide couplings using the acetylated central building block. The acetyl group could then be selectively deprotected and any lipophilic residue could be introduced into the muraymycin scaffold prior to the global deprotection. This approach will be further explored in the following section.

4.5.3 Synthesis of target compound T9: Val-Arg-*allo*-Thr($COC_{12}H_{23}$)-NuAA

At the time of this thesis, no muraymycin derivative containing an unsaturated lipophilic side chain was known, nor was the impact of this type of fatty acid moiety. It was hypothesized that an *E*-symmetric double bond would have less or no effect on the biological or intramolecular activity. A compound with a *Z*-symmetric side chain, however, would lead to a partial rigidity of the side chain, possibly influencing the biological properties of the compound. Therefore, the required lipophilic side chain **47** was synthesized following the *Wittig* reaction sequence by Wube *et al.* (cf. **Fig. 71**).[157]

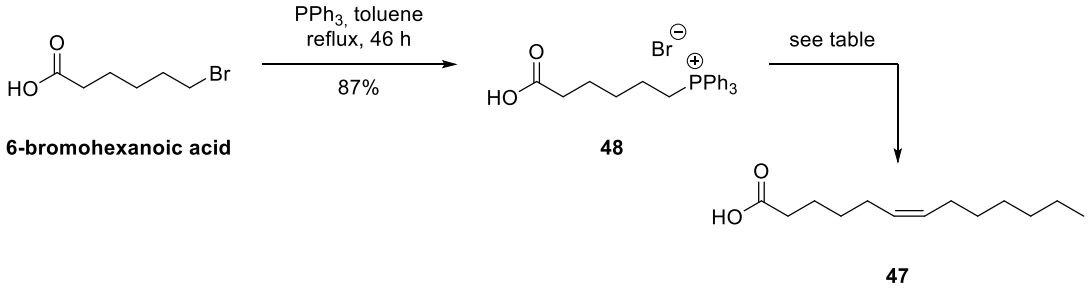

attempt	reagents, solvent	temperature, time	yield (*Z*/*E*)
1	*n*-heptanal, NaHMDS, THF	rt, 5 h	55% (85:15)
2		-82 °C, 5 h	-
3		-82 °C → rt, 18 h	51% (94:6)

Fig. 71: Synthesis of (*Z*)-tridec-6-enoic acid **47** via *Wittig* reaction.

First, the *Wittig* reagent was synthesized from 6-bromo-hexanoic acid and triphenyl-phosphine (PPh_3). The carboxylic acid and PPh_3 were dissolved in dry toluene, and the resulting clear solution was refluxed for 46 hours. During this time, a second phase emerged. The reaction mixture was cooled to room temperature and the solvent was removed under reduced pressure. The residue was resuspended in fresh toluene and was heated to reflux again. The suspension was filtered while hot, whereby the product

remained in the filter. The isolated colorless solid was dried under vacuum. The solid was used without further purification as the NMR and HRMS data indicated its sufficient purity (>98%).

The synthesis of the desired stereoisomer **47** turned out to be more challenging than expected. The ylide formed during the reaction can be classified as a destabilized ylide, as it lacks electron withdrawing groups next to the deprotonated carbon atom.[160] As commonly known, this would lead mainly to the formation of the *Z*-isomer. Also the absence of a lithium salt favors the formation of a cis-double bond.[183,184] In the literature, the *Wittig* reaction in this particular case was performed at room temperature.[157] Thus, the conditions were adopted in the first approach (cf. **Fig. 71**). To form the ylide, phosphonium salt **48** was dissolved in dry tetrahydrofuran and sodium bis(trimethylsilyl)amide (NaHMDS, 1 M solution in THF) was added dropwise to the resulting suspension. The suspension turned orange and was stirred for 2 hours at room temperature. During this time, a white solid, presumably sodium bromide, precipitated. Then, *n*-heptanal in dry tetrahydrofuran was added dropwise to the reaction mixture, which became yellowish and murky. The reaction was ended after 3 hours by the addition of water, which turned the reaction mixture into a clear solution. After extraction with diethyl ether, the aqueous layer was acidified with hydrogen chloride to a pH value of ~2 to protonate the desired product. After multiple extractions, the solvent was removed, and the crude product was purified by silica gel column chromatography, resulting in 55% yield of a mixture of *Z*/*E*-isomers (85:15).

In order to improve the isomer ratio, the reaction temperature was lowered to -82 °C (cooling bath consisting of liquid nitrogen and acetone). Under these conditions, the thermodynamically controlled isomer (*E*-isomer) should be formed in even lower quantities. The temperature range was adapted from the protocol of the *Horner-Wadsworth-Emmons* reaction (cf. section 4.1). In the second attempt, the reaction was repeated as described before, at the new temperature. Unfortunately, no conversion took place at this low temperature. Therefore, in a subsequent experiment, a temperature gradient, similar to that used in the *Horner-Wadsworth-Emmons* reaction for the nucleosyl amino acid **21** (cf. section 4.1), was applied. This time, the aldehyde was added dropwise at -82 °C. The reaction was then stirred for 16 hours, during which it warmed up to room temperature. After extraction and purification by silica gel column chromatography, side chain **47** was isolated with 51% yield in a *Z*/*E* ratio of 94:6. In addition, a high-temperature NMR was performed to confirm the presence of

both isomers and to exclude the possibility of rotameric isomers. Since this ratio was sufficiently high, no further optimization was carried out. In order to improve the isomer ratio, it might be beneficial to determine the specific temperature at which the reaction begins. Then, the reaction could be repeated at this precise temperature and potentially the isomerically pure product **47** could be obtained.

The configuration of the double bond was determined using the coupling constants in the ^{1}H NMR. The coupling constant for vinylic *trans* protons tend to be larger than for vinylic *cis* protons.[185–187] In the given example, the coupling constant of 10.8 Hz indicates a *cis* double bond,[187] hence confirming the tendency, that the *Z*-isomer would be preferentially formed in this kind of *Wittig* reaction. It was not possible to determine the coupling constants for the other isomer due to the chemical shift causing an overlap of signals for the required protons (cf. **Fig. 72b**). In order to investigate the conformation further, a NOESY NMR spectrum was recorded (cf. **Fig. 72a**).

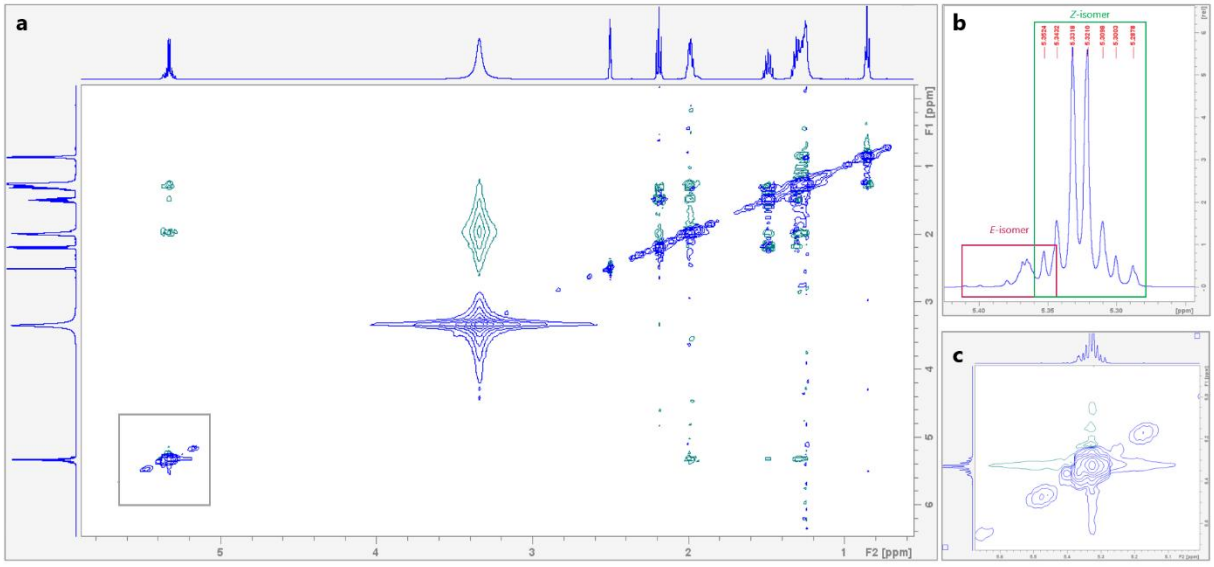

Fig. 72: NOESY NMR spectrum of unsaturated lipophilic side chain **47** (**a**) with a section of the region of the double bond protons (**b**) and required cross-peak (**c**).

It was expected that the protons of the *Z*-configurated double bond would interact spatially with each other, while in the *E*-configuration this interaction would not be detectable. **Fig. 72** illustrates the NOESY NMR spectrum (**a**), the relevant signal of the resembling double bonds (**b**) and the corresponding section of the NOESY NMR spectrum (**c**). The double bond protons of the *E*-isomer are overlapping with the signals of the *Z*-isomer. Since the signals of the double bond protons overlap with each other (cf. **Fig. 72b**), the required cross peak, proving the isomerization (turquoise cross peaks,

cf. **Fig. 72c**) is located under the diagonal cross peak (dark blue). However, the signal is still detectable underneath, and its extensions are also visible (cf. **Fig. 72c**). Furthermore, the cross-peak proofing the *Z*-isomeric double bond can be assigned to the bigger signals in **b**. This is a very strong indication of the presence of the *Z*-isomer as the main compound. Furthermore, there is evidence in literature based on DFT calculations that supports the general accepted stereoselectivity in *Wittig* reactions, meaning that under lithium-salt-free conditions with a destabilized ylid, the *Z*-alkene is formed preferentially over a puckered transition state.[184]

Since the unsaturated carbon species of the new lipophilic side chain would most likely not tolerate the established Cbz-deprotection conditions, an alternative synthetic approach was required. So, the aforementioned concept, on the basis of the reaction sequence for the acetylated muraymycin derivative (cf. section 4.5.2), was applied.

In this particular case, it was decided to incorporate the acetyl group in the central amino acid moiety and to explore the selective cleavage of this ester. This decision was based on the observations of M. Wirth, who was able to identify a regioisomeric side product that formed during the second peptide coupling with the simplified Lys-containing urea dipeptide. Since the formation of the side product was only possible because the free secondary alcohol in the central amino acid could act as a nucleophile, this problem was avoided by the presence of an acetyl ester at this position.[145]

Before working directly on the muraymycin scaffold, two test reactions were performed to investigate whether the unsaturated side chain could withstand the conditions of the *Steglich* esterification and global deprotection. The *Steglich* esterification was carried out using the Ser-containing derivative **60** and carboxylic acid **47** (cf. **Fig. 73**).[145,153] Both reactants were dissolved in dry tetrahydrofuran before DMAP and EDC • HCl were added. The reaction was stirred for 4 hours at room temperature. During this time it was monitored by TLC. The reaction was ended by the addition of hydrochloric acid (10%). Compound **91** was isolated with 94% yield after extraction and purification by silica gel column chromatography. The analysis of the ^{1}H NMR spectrum confirmed the formation of the functionalized Ser derivative **91**. Particular attention was paid to the isomer ratio of the side chain. It was found that it was still 94:6 (*Z*/*E*), the same as for reactant **47**. This demonstrates that the unsaturated side chain maintained its structure and that no rearrangement or isomerization occurred during the *Steglich* esterification.

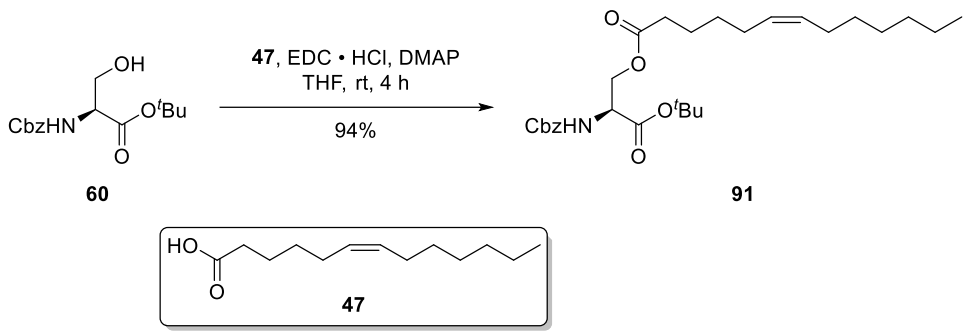

Fig. 73: Test reaction of Cbz-Ser-O^{t}Bu **60** with (*Z*)-tridec-6-enoic acid **47** via *Steglich* esterification.

To investigate the stability of the double bond during the global deprotection, side chain **47** was stirred in aqueous trifluoroacetic acid (80%) for 24 hours. After work-up and lyophilization, the resulting substance was analyzed by high-temperature NMR, which confirmed the unchanged structure of compound **47**. Furthermore, no variation in the isomeric ratio could be observed. Based on these results, it was most likely that **47** would undergo the upcoming *Steglich* esterification and will retain its structure during the global deprotection.

Another test reaction was carried out in order to test the selective deprotection of the acetyl ester. Therefore, the mild acetyl-deprotection conditions recommended by *Glen Research* for base-sensitive oligonucleotides were evaluated.[159] As shown in **Fig. 74**, the deprotection was performed with potassium carbonate in dry methanol at room temperature. The reaction was monitored by TLC and LC-MS. After 40 minutes, Cbz-Ser-O^{t}Bu **60** was fully converted, and the reaction was ended by the addition of water. After extraction and purification by silica gel column chromatography, **60** was isolated with a yield of 50%. Despite the moderate yield, the method was still chosen for the selective deprotection of the global protected muraymycin derivative. It was assumed that any side reaction that might have occurred in this experiment would not recur in the reaction with a larger, more complex and therefore more sterically hindered derivative.

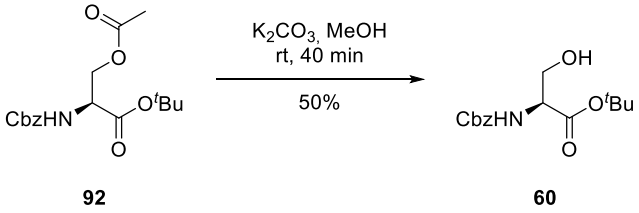

Fig. 74: Mild deprotection conditions by *Glen Research* tested on Cbz-Ser($COCH_3$)-O^{t}Bu **92**.

Based on the promising results from the test reactions, the synthesis of a new muraymycin derivative was pursued; and in this context, the proposed new synthetic pathway investigated.

The design of the new muraymycin derivative featured Arg-containing urea dipeptide **36**, as this simplified alternative has been shown to be well tolerated and as previously discussed, facilitates the synthesis immensely. The peptide coupling between **36** and **90** was performed with HATU and DIPEA in dry dichloromethane as described above. In this approach, the batch of bis-TFA salt **90** without side product (intramolecular rearrangement) was used (cf. section 4.5.2). Based on the monitoring with TLC and LC-MS, the reaction was terminated after 16 hours. The reaction mixture was diluted with water and was extracted multiple times. Purification by silica gel column chromatography yielded the globally protected derivative **50** with approximately 68% yield (cf. **Fig. 75**). The yield was estimated from the ^{1}H NMR, where the DIPEA • TFA salt was identified as a minor impurity and a second, unknown species. The LC-MS data confirmed the successful achievement of product **50** and that no reactant (**36** or **90**) remained in the isolated compound.

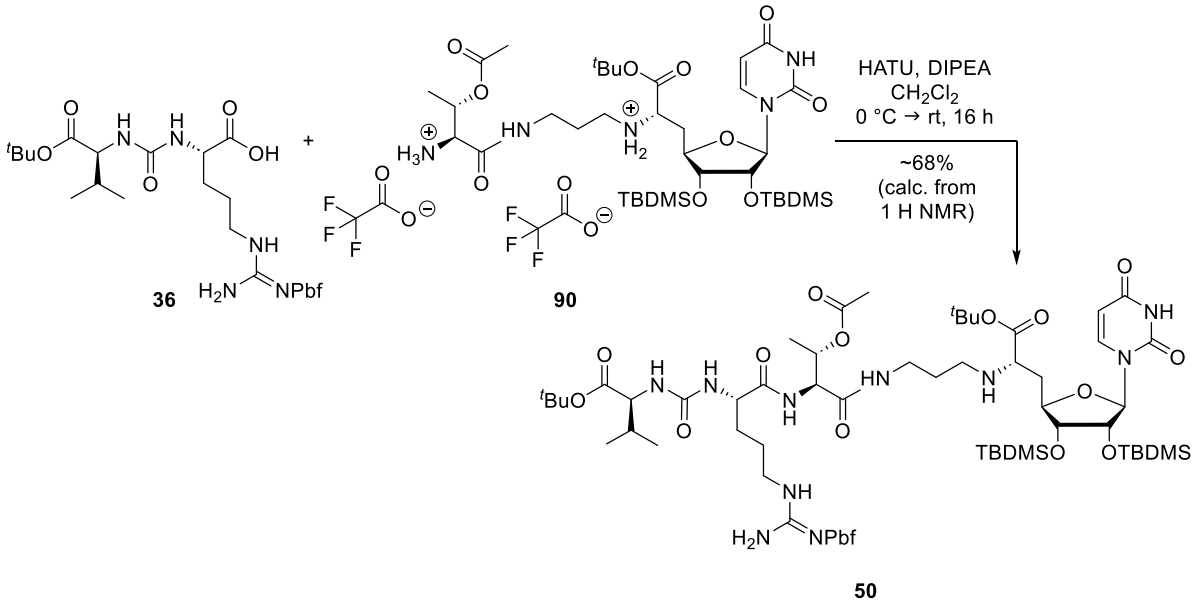

Fig. 75: Synthesis of globally protected muraymycin **50** via peptide coupling.

The selective deprotection of globally protected muraymycin derivative **50** was performed under the postulated mild conditions by *Glen Research*.[159] Therefore, **50** was diluted in dry methanol and sodium carbonate was added to the clear solution. The reaction mixture was stirred for a total of 5.5 hours at room temperature. During this time, samples were taken at various intervals and analyzed by LC-MS to investigate

the reaction progress. As both components are almost identical, the difference in the retention time was insignificant. Nevertheless, the gradual formation of the desired product **49** could be observed (cf. **Fig. 76**). During the reaction, 0.2 equivalents of potassium carbonate were added to the reaction after 30, 105 and 270 minutes to support the formation of the product. The reaction was ended after 5.5 hours by removing the solvent in high vacuum. The residue was dissolved in water and was extracted multiple times with diethyl ether. The product was obtained after removal of the solvent as a colorless powder. Due to the complexity of the NMR spectra, **49** was only identified using HRMS (m/z = 1351.7434 $[M+H]^+$) and its purity was estimated based on the UV-trace of the LC-MS. Based on these data, **49** was obtained in approximately 95% yield. This reaction turned out to be very suitable for the selective deprotection of complex structures such as a globally protected muraymycin. Different than in the test reaction, no side reactions nor yield loss were observed. With the successful implementation of this key step, the new synthesis strategy can be established for further projects.

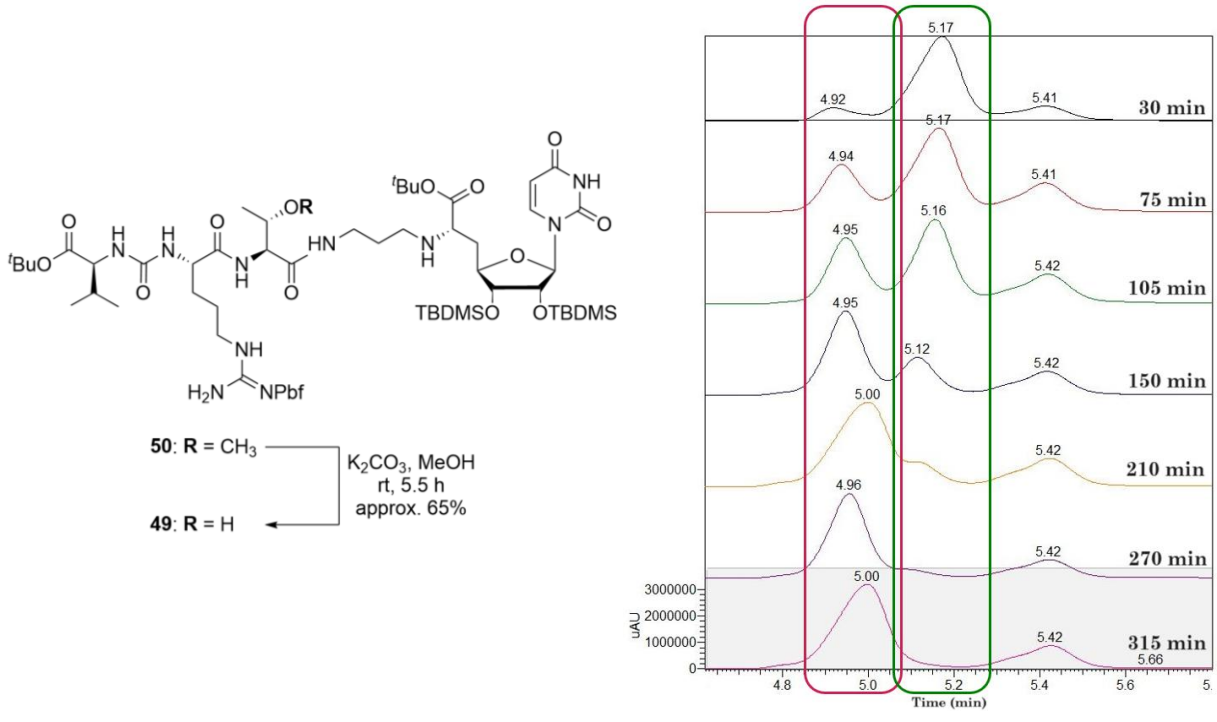

Fig. 76: LC-MS monitoring of the selective cleavage of the acetyl group of derivative **50** (red: product **49** with retention time at ~5 min, green: reactant **50** with retention time at ~5.2 min).

For the subsequent *Steglich* esterification, the well-established conditions were employed.[145,153] Alcohol **49**, side chain **47** and DMAP were diluted in dry tetrahydrofuran. Then, EDC • HCl was added to the clear solution. The reaction

progress was monitored by LC-MS but could also be observed as the hardly soluble carbodiimide gradually dissolved and subsequently a non-soluble white solid (urea form of EDC) precipitated over time. After 5.5 hours, the reaction was ended by the addition of hydrogen chloride solution (0.5 M). The globally protected intermediate was identified by LC-MS (m/z = 1546.75 $[M+H]^+$). For the global deprotection, the residue was dissolved in aqueous trifluoroacetic acid (80%) at 0 °C. The resulting clear solution was stirred at room temperature for 23 hours and the progress was monitored by LC-MS. Then, the red solution was concentrated in high vacuum. The residue was dissolved in water at 0 °C and was freeze-dried. After purification by HPLC, the desired muraymycin derivative **T9** was isolated as a colorless solid with 19% yield over two steps (cf. **Fig. 77**).

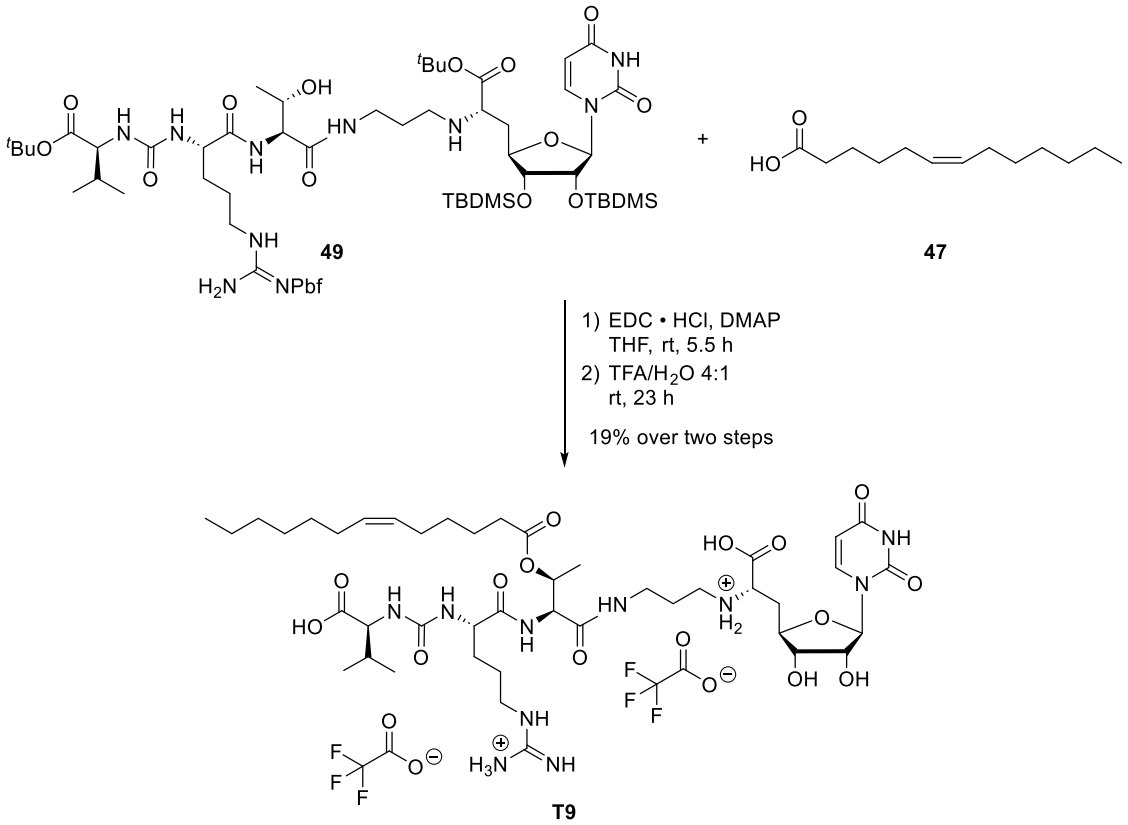

Fig. 77: Synthesis of target compound **T9** via *Steglich* esterification and global deprotection.

The position of the lipophilic side chain at the muraymycin scaffold was proven again by the HMBC NMR spectrum. The cross peaks between 3'''-H or 2^{vi}-H and carbonyl carbon atom C-1^{vi} showed the desired connectivity (cf. **Fig. 78**). Furthermore, the configuration of the double bond was also determined by the coupling constants in the ^{1}H NMR. The ^3J coupling constant was 11.4 Hz for the vicinal protons 6^{vi}-H/7^{vi}-H.

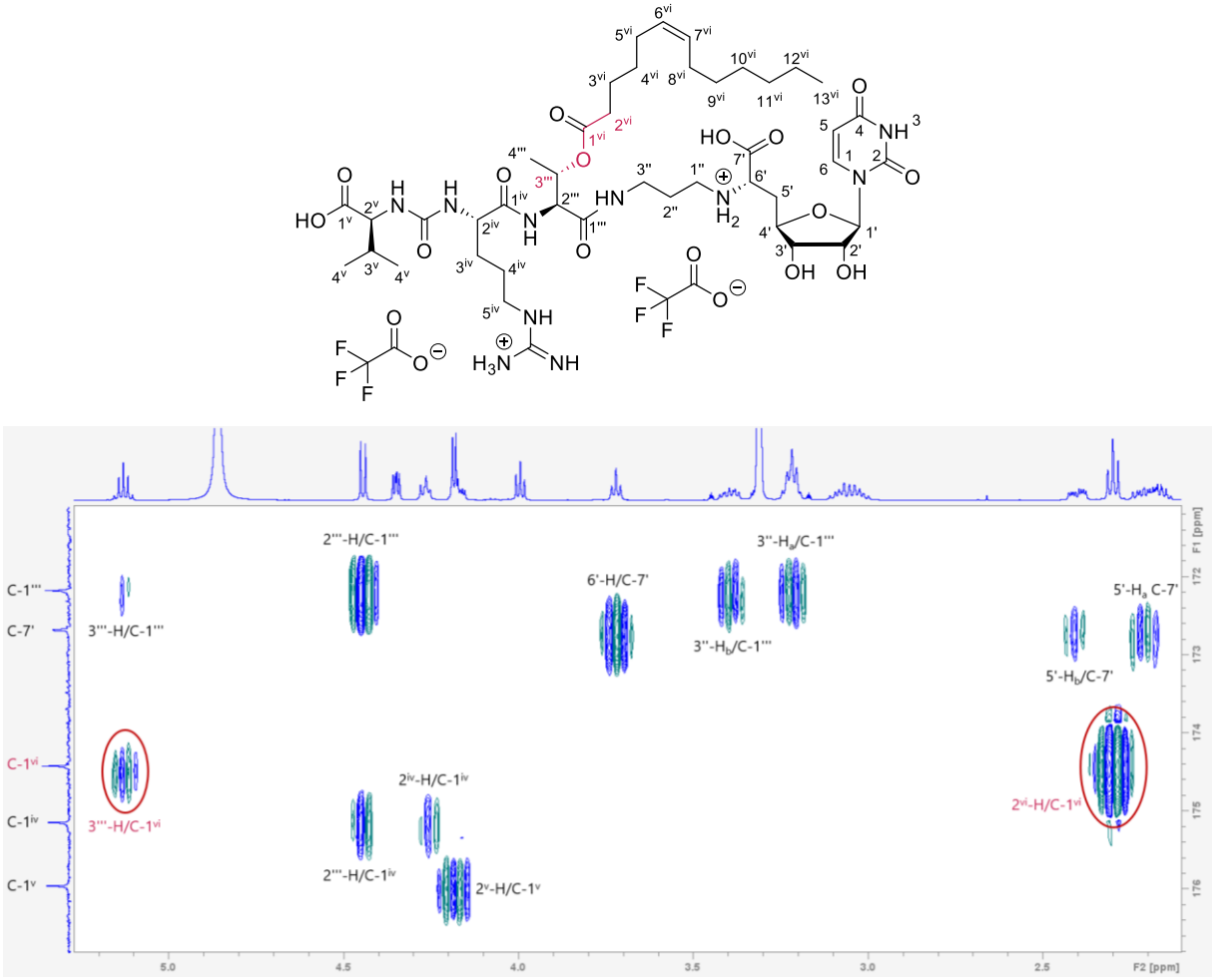

Fig. 78: Excerpt of the HMBC spectrum, proving the connectivity of the unsaturated lipophilic side chain to the backbone of muraymycin derivative **T9**.

4.6 Biological evaluation of the *allo*-Thr and Thr muraymycin derivatives

Overall, the six newly synthesized muraymycin derivatives, which contain either *allo*-Thr or Thr (compound **T6**) as central amino acid, were biologically evaluated (cf. **Table 2**).[96,120,121,135,144,172–174] Again, the two strains of the Gram-negative bacteria *E. coli* (Δ*tolC* and DH5α) and two Gram-positive bacterial strains (*S. aureus* Newman and *C. difficile*) were investigated. In addition, the stability tests mentioned in section 4.3 were conducted on selected derivatives as well.

The structural change of the central amino acid to Thr was planned to examine the impact of steric hindrance and the stereochemistry of the position adjacent to the ester. In this context, it was observed that reduced activity of the Ser derivatives (cf. section 4.3) might be associated with the excessive simplification of the central amino acid.

Furthermore, the structure of the lipophilic side chain and its impact were also of particular interest in this SAR study.

Based on the previous evaluation of the structures of the natural products and the molecules by M. Wirth, it was not possible to define the role of the *iso*-propyl group within the muraymycin scaffold. It was assumed that its presence supports the penetration of the bacterial cell wall or that it could counteract degradation or hydrolysis of the ester moiety (cf. section 3.2.1). As already mentioned, the biological data of the Ser-containing compounds revealed that the *iso*-propyl group had no impact on the interaction with the target MraY (cf. section 4.3).

The following table illustrates the biological data of the new derivatives, with muraymycin **B8**, simplified muraymycin analogs **28** and **32** listed as references. Based on the data of the compounds **T4** and **T5**, it is reconfirmed that changing the urea dipeptide structure by replacing Epic with Arg has no effect on the interaction with the target. Furthermore, it is revealed that the stereochemistry at the 3-position of the central amino acid does not affect the inhibition of MraY (**T6**). Moreover, a close relation of the compounds inhibitory properties to the structure and size of the lipophilic side chain is immediately apparent. The derivative with the smallest possible side chain (***a*T-T7**) shows the least inhibition of MraY even compared to side chain lacking compound **28**. This particular loss in activity could be attributed to the additional absence of the *iso*-propyl group, which K. Leyerer demonstrated to have a beneficial effect on the inhibitory activity.[146,147] This might indicate that neither the methyl group nor the acetyl group could compensate for the effect of the *iso*-propyl group. However, an alternative, less likely explanation could be that the introduction of the acetyl ester might prevent an alternate interaction with the binding pocket, in which the free hydroxy group of compound **28** might normally participate. This would mean that a side chain that is too short is even less efficient than a free alcohol moiety. Overall, the acetyl ester might be too short to contribute to the target interaction in the same way as the longer lipophilic side chains. The target interaction of compound **T9**, which contains a rigidity-inducing double bond at the center of the lipophilic side chain, is significantly reduced. This loss in activity may primarily be due to the steric requirement and missing flexibility of the incorporated side chain since the replacement of Epic appears to have a negligible impact (**T4** and **T5**).

Table 2: Biological data of the new *allo*-Thr and Thr muraymycin derivatives. (references: **B8**, **28** and **32**).[120,121,145]

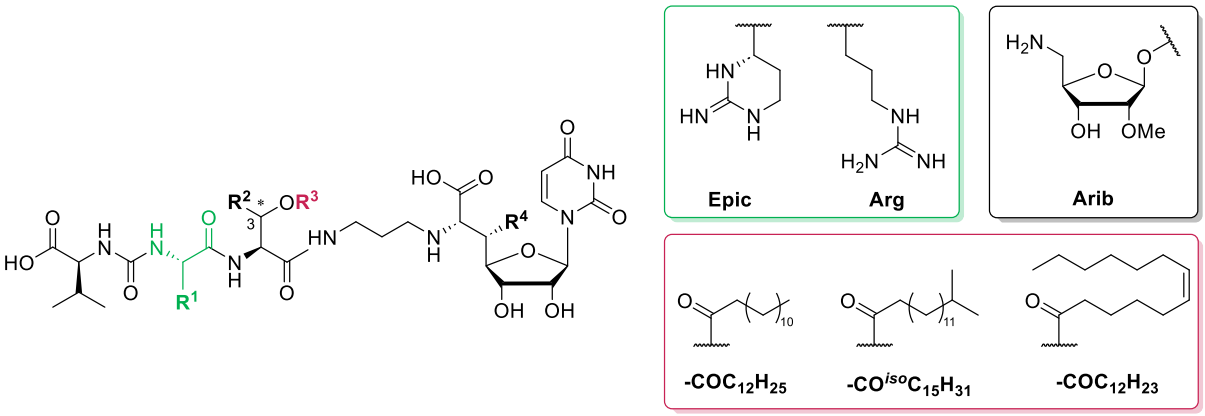

compound	MraY IC_{50} [nM][a]	bacterial growth			
		IC_{50} [µg/mL]		MIC [µg/mL]	
		E. coli Δ*tolC*	*E. coli* DH5α	*S. aureus* Newman	*C. difficile*
L-*allo*-threonine					
T4: Val-Epic-*allo*-Thr($COC_{12}H_{25}$)-NuAA	1.1 ± 0.1	<0.5	2.5-5	>32	2-4
T5: Val-Arg-*allo*-Thr($COC_{12}H_{25}$)-NuAA	2.2 ± 0.5	<1.3	2.5-5	>32	16-32
***a*T-T7**: Val-Epic-*allo*-Thr($COCH_3$)-NuAA	455 ± 79	>20[b]	>20[b]	>32	>32
T8: Val-Epic-*allo*-Thr($CO^{iso}C_{15}H_{31}$)-NuAA	1.8 ± 0.3	<0.1	>100	8-16	1-2
T9: Val-Arg-*allo*-Thr($COC_{12}H_{23}$)-NuAA	132 ± 43[b]	<0.3[b]	0.6-13	>32	>32
L-threonine					
T6: Val-Arg-Thr($COC_{12}H_{25}$)-NuAA	1.9 ± 0.9	<0.1	>100	>32	>32
references: 3-hydroxy-L-leucine					
B8: Val-Arg-3-hydroxy-Leu($CO^{iso}C_{15}H_{31}$)-NuAA+Arib	4.0 ± 0.7 pM	n.d.	n.d.	4-8	4-8
28: Val-Epic-3-hydroxy-Leu-NuAA	95 ± 19	50	15	>50	n.d.
32: Val-Epic-3-hydroxy-Leu($COC_{12}H_{25}$)-NuAA	5.8 ± 0.5	0.5	>100	10	2.5

[a] crude membrane preparation; [b] preliminary result; n.d. not determined yet

The muraymycin derivative **T8** features an *n*-alkyl side chain with an *iso*-propyl head group, similar to the natural product muraymycin **B8**. Compared to the compounds with simple *n*-alkyl side chains (**T4** and **T5**), the head group does not significantly influence the interaction with the target. Instead, the loss of the amino ribose unit is likely the primary cause for the reduced activity of **T8** compared to muraymycin **B8**.

However, the omission of the amino ribose unit remains a reasonable modification, as derivatives without this structural motif still exhibit strong activity (cf. **Table 2**).

Compared to the IC_{50} values of the Ser derivatives discussed in section 4.3 (IC_{50}(MraY) ≈ 3-6 nM), the *allo*-Thr (**T4**, **T5**, **T8**) or Thr (**T6**) derivatives exhibit target affinities within the same nanomolar range. Overall, the IC_{50} data reveal that a long lipophilic side chain is beneficial for the inhibition of the target. Furthermore, the replacement of the synthetically challenging urea dipeptide is tolerated. Short lipophilic side chains or those that affect the side chain's rigidity, lead to loss of target affinity. Head groups, on the other hand, are apparently tolerated. This is consistent with the data for the natural compounds and synthetic derivatives of M. Wirth (cf. section 2.2.3, **Fig. 12**).[111,120,121,145]

The potencies against the efflux-deficient strain *E. coli* Δ*tolC* were ~10 times better (bacterial growth: IC_{50} ≈ <0.1-1.3 µg/mL) than for the Ser-containing derivatives (bacterial growth: IC_{50} ≈ 1.6-6.6 µg/mL) and comparable to reference compound **32**. The only exception is acetylated compound ***a*T-T7**, where the absence of a longer lipophilic side chain is most likely the cause for the lower inhibition.

Three of the new derivatives showed unexpected strong inhibition of the *E. coli* DH5α strain (bacterial growth: IC_{50} ≈ 0.6-13 µg/mL). They surpass the most potent natural compounds (cf. section 2.2.1) and reference compound **32**. These data reconfirm once again that the replacement of Epic by Arg had no impact on the bacterial growth inhibition (**T4** vs **T5**). Furthermore, compound **T9**, with the double bond containing lipophilic side chain also inhibits the bacterial growth of DH5α. The only other active compound was 5'-deoxy muraymycin **C4** analog **28**, which most striking difference is the lacking lipophilic side chain. The compounds **T6** and **T8** showed comparable potencies towards *E. coli* Δ*tolC* like **T4** and **T5** but were inactive against DH5α. Their structures only differ in the stereochemistry of the central amino acid (**T5** vs. **T6**) or in the structure of the lipophilic side chain (**T4** vs. **T8**) when compared to the DH5α-active compounds. Therefore, it can only be speculated that these slight modifications in the molecular structure might favor conformations that exhibit less affinity to the *E. coli* efflux pumps.

Among all the new compounds of this series, only compound **T8** showed notable antibacterial activity against the *S. aureus* Newman stain (MIC = 8-16 µg/mL). Important trends are revealed by structural comparison with reference compound **32** (MIC = 10 µg/mL) and the best in-class natural compound muraymycin **B8** (MIC = 4-8 µg/mL).

The synthetic compounds **T8** and **32** both lack the amino ribose unit. However, *allo*-Thr-containing compound **T8** features the same lipophilic side chain as muraymycin **B8** but differs in the central amino acid. On the other hand, reference compound **32** contains the same central amino acid as muraymycin **B8** but has only a simple *n*-alkyl side chain. Since the target affinity of the two simplified compounds (**T8** and **32**) is similar, it can be suggested that the structure of the lipophilic side chain plays an essential role regarding the antibacterial activity of **T8** against the *S. aureus* Newman strain. In this context, it can be speculated that this particular side chain compensates for the loss of the *iso*-propyl group at the 3-position of the central amino acid. Again, the relatively small structural adjustments could lead to a different conformation of the molecule, influencing its cell penetration ability and/or its affinity towards the efflux systems. Overall, it was shown that the adjustments made in compound **T8** compared to the natural compound muraymycin **B8** still preserve strong activity against *S. aureus*.

The biological data regarding *C. difficile* revealed strong to moderate activities for the six new compounds. Here, two different strains were tested: a test strain, which is less clinically relevant (*C. difficile* CD630 (RT012)) and a clinically relevant one from a strain collection (*C. difficile* R20291 (RT027)). The target compounds **T4**, **T5** and **T8** showed comparable results to the references muraymycin **B8** and **32**, where it should be noted that the latter was solely tested against the clinically relevant strain. Here, simplified compound **T8** showed the best inhibition, even exceeding the overall most potent muraymycin **B8**. Since the structures of the active compounds differ gradually, it can be summarized that the omission of the amino ribose unit as well as the simplification of the central amino acid are tolerated. A requirement for activity seems to be the presence of a sufficient long lipophilic side chain. Here, only *n*-alkyl fatty acid chains, with or without an *iso*-propyl head group, maintain the activity. In addition, it was observed that preserving an *n*-alkyl chain while simplifying the urea dipeptide, reduces antibiotic activity (cf. compound **T5**). Thus, the Epic-containing urea dipeptide appears to be favored for the activity against *C. difficile*.

In addition, the stabilities in *E. coli* Δ*tolC* cell lysate were evaluated for **T4** and **T5**. Unfortunately, it was not possible to determine the exact half-lives of the derivatives. These data were difficult to interpret in multiple attempts (cf. chapter 9). The potential ability of the muraymycin derivatives to form micelles during the assay might be the reason for these inconsistent results. The data revealed a significant increase in concentration for compound **T4** over time, suggesting that the potential micelles

slowly dissolve throughout the assay. It is also possible that dilution propagate errors caused by the micelle formation complicated the execution of the assay. In another attempt, Tween was added in the assay to evaluate the stability of **T4** to prevent possible micelle formation (cf. chapter 9). Based on these results, it can be cautiously assumed that the compound is stable in *E. coli* Δ*tolC* lysate. This is also the case for the tests of compound **T5**, which imply stability over 150 min, although minor inconsistencies of the data were noticed. Since the stability evaluation is very challenging and needs to be refined for these compounds first, no other derivatives were tested to save material. The same applies for the stability tests in Luria-Bertain-Medium for all new compounds. In order to pursue additional tests, the determination of physical properties of the new compounds, including critical micelle building concentrations, could aid the process.

4.7 Synthesis of truncated muraymycin derivatives

4.7.1 Synthesis of target compounds TT1: Cbz-*allo*-Thr($COC_{12}H_{25}$)-NuAA and TT2: H-*allo*-Thr($COC_{12}H_{25}$)-NuAA

The designed truncated compounds were supposed to give further insights into the role and importance of lipophilic side chain when the urea dipeptide moiety is removed from the muraymycin scaffold.

Muraymycin derivative **TT1** was obtained from the mixed fraction of compound **51**. As shown in **Fig. 79**, the *tert*-butyl ester and the TBDMS groups of **51mix** were cleaved under the well-known conditions.[135,140] The TFA-salt **TT1** was isolated by HPLC purification with 5.4% yield over two steps. The low yield certainly results from the usage of a mixed fraction containing unknown impurities (cf. section 4.4.2). Yet, sufficient quantities could be isolated for biological testing.

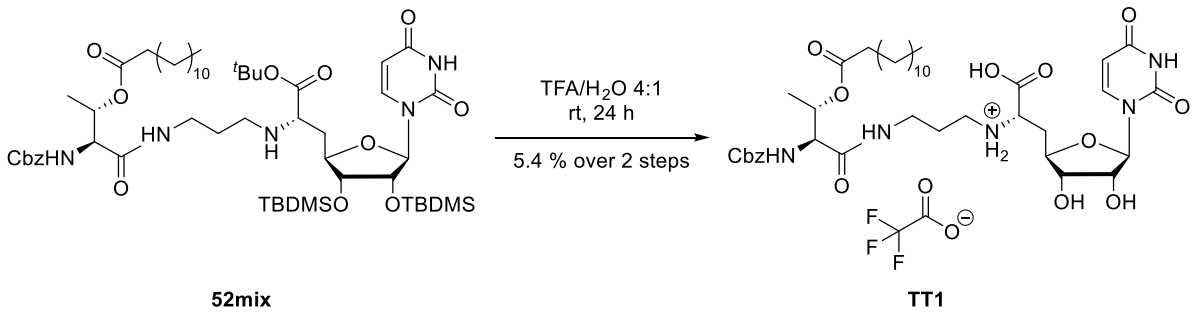

Fig. 79: Global deprotection of **52mix** to gain truncated muraymycin derivative **TT1**.

In contrast to the previous substances, **TT1** was insoluble in MeOH-d_4, so DMSO-d_6 had to be used to record the NMR spectra. The poor solubility also impaired the biological tests. Precipitation of the substance in water or medium was regularly observed during testing leading to inconclusive results (cf. section 4.8).

Although the rearrangement of the lipophilic side chain was not expected, the desired connectivity of the lipophilic side chain was nevertheless proven by the HMBC NMR-spectrum. Here, the cross peaks between 3'''-H or 2^{vi}-H with the carbonyl carbon atom C-1^{vi} confirm the desired structure (cf. **Fig. 80**).

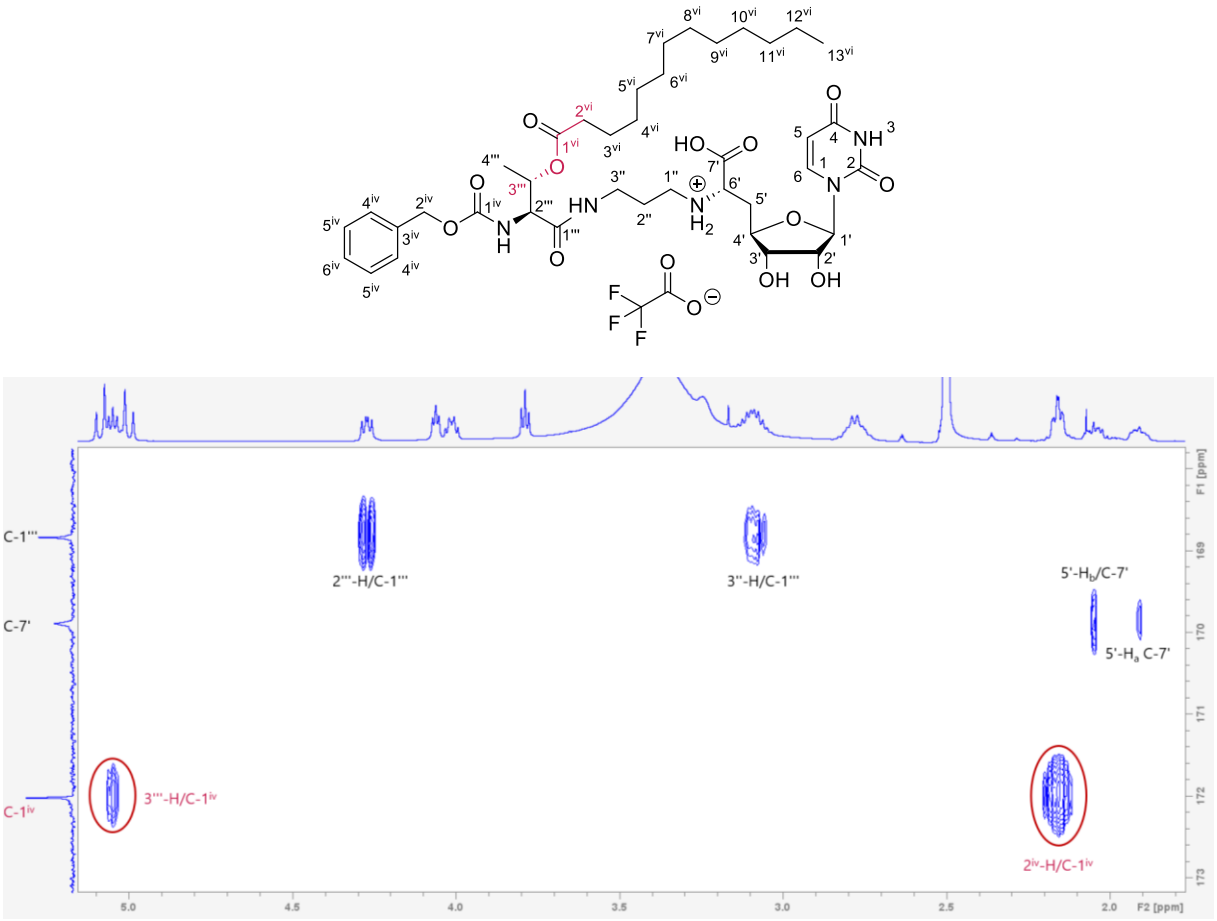

Fig. 80: Excerpt of the HMBC spectrum, proving the connectivity of the lipophilic side chain to the backbone of the truncated muraymycin derivative **TT1**.

The poor solubility of compound **TT1** is likely due to its amphiphilic character, which could facilitate micelle formation. This would make the solubility in different solvents highly dependent on concentration. The nucleosyl amino acid is hydrophilic while the lipophilic side chain and the Cbz-protection group show lipophilic characteristics. To confirm the presence of micelles, further investigation is required, such as determining the critical micelle formation concentration.

The second truncated muraymycin **TT2** has a free amine at the *allo*-Thr moiety, thus making the structure more hydrophilic. However, the new compound still has an amphiphilic character. For the synthesis, a small amount of bis-TFA salt **78** was stirred in aqueous trifluoroacetic acid (80%) for 24 hours at room temperature. Then, the solvent was removed in high vacuum and the residue was lyophilized. Compound **TT2** was isolated after purification by HPLC with a yield of 39% (cf. **Fig. 81**).

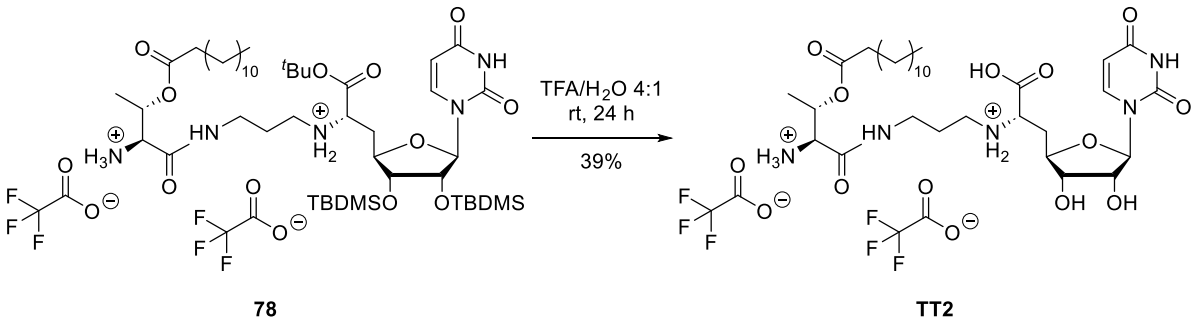

Fig. 81: Global deprotection of **78** to obtain muraymycin derivative **TT2**.

The intramolecular rearrangement of the lipophilic side chain was not expected, as the amine is inactive in its TFA salt form and the connectivity of reactant **78** had already been proven. The HMBC NMR-spectrum of **TT2** was nevertheless analyzed to confirm the desired structure. As illustrated in **Fig. 82**, the connectivity was proven by the cross peaks between the protons 3'''-H or 2^{vi}-H and the carbonylic carbon atom C-1^{vi}.

The new derivative showed improved solubility in MeOH-d_4 compared to **TT1**. The increased solubility is likely caused by the increased hydrophilicity due to the introduction of the positively charged free primary amine.

Where applicable, both compounds were tested against MraY and different *E. coli* strains. These results can be found in section 4.8.

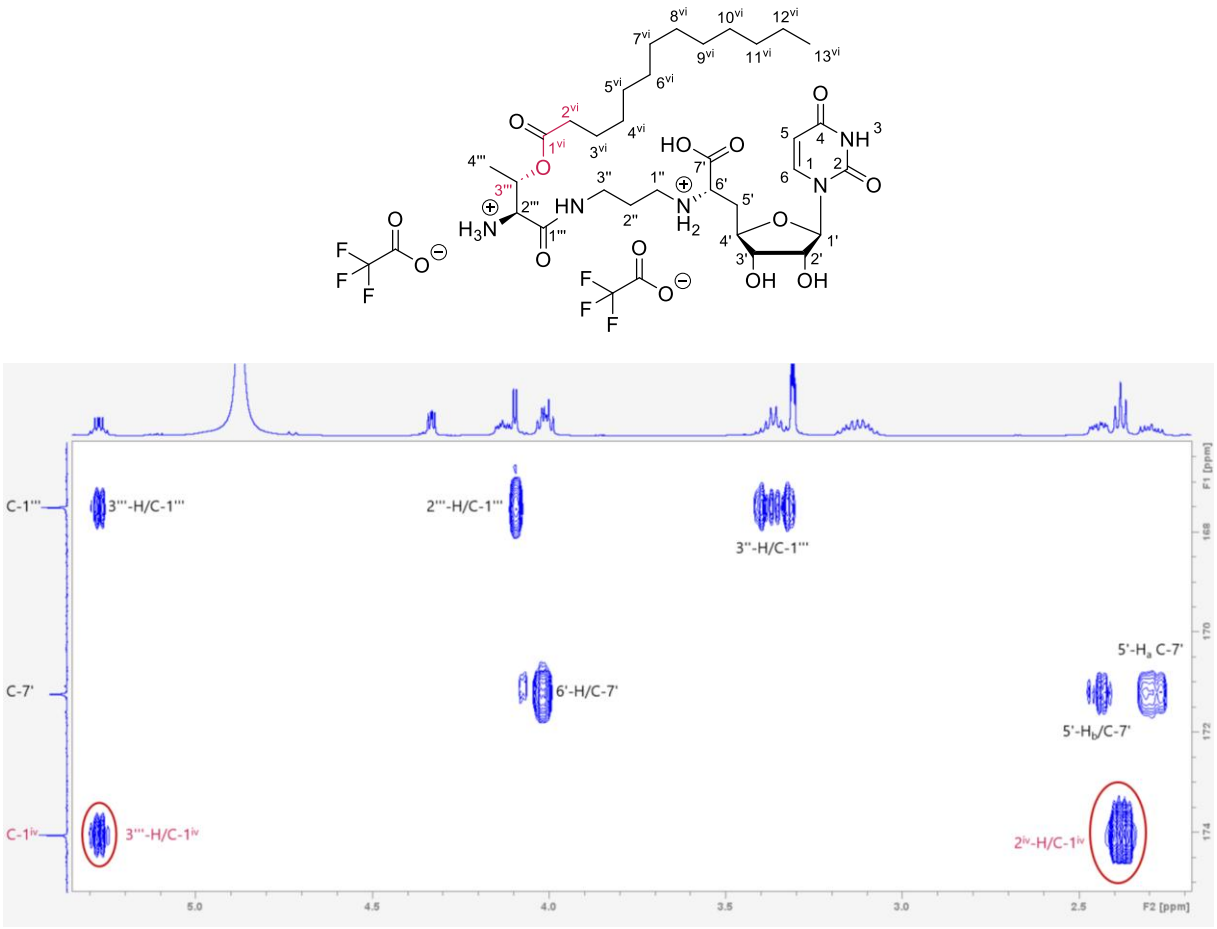

Fig. 82: Excerpt of the HMBC spectrum, proving the connectivity of the lipophilic side chain to the backbone of the truncated muraymycin derivative **TT2**.

4.7.2 Synthesis target compounds TT3: Ac-*allo*-Thr($COC_{12}H_{25}$)-NuAA and TT4: Ac-*allo*-Thr($COCH_3$)-NuAA

It was expected that the 2'''-NH moiety in **TT1** (Cbz-protected amine/carbamate) and **TT2** (amine) would interact differently with the target enzyme. In order to minimize the influence of this particular position in the scaffold, another truncated compound was required. Here, the amine was replaced by an amide, thus mimicking the corresponding amide in the muraymycin scaffold (cf. **Fig. 83**, compound **TT3**). So, the interaction at the target is likely comparable to the full-length muraymycin. For this purpose, the smallest possible amide (acetyl amide) was chosen to minimize additional interactions with the target enzyme. Due to the nucleophilic character of the secondary amine at the 6'-position, which could lead to side reactions under standard acetylation conditions (e.g. pyridine and acetic anhydride,[158] cf. section 4.5.2.), the acetyl group was introduced via peptide coupling with acetic acid. This strategy was already established by K. Leyerer and could be applied on the executed synthesis.[146] Compared to the published protocol, the coupling reagents were replaced (PyBOP/

HOBt to HATU), because of the already discussed challenges which were observed by the usage of PyBOP and HOBt (cf. section 4.2.2). First, glacial acetic acid and one equivalent of DIPEA were dissolved in dry dichloromethane at room temperature. The clear mixture was stirred for 10 minutes in order to ensure complete deprotonation of the acid. Then, HATU was added, and the mixture was stirred for 30 minutes to form the active ester. The reaction mixture was cooled to 0 °C and the remaining equivalents of the base were added before bis-TFA salt **78** in dry dichloromethane was added dropwise. The reaction mixture was stirred for 18 hours, during which it gradually warmed up to room temperature. Based on LC-MS and TLC-monitoring, the reaction was ended by dilution with ethyl acetate. The organic layer was washed with water. After removal of the solvent, the desired product was verified by LC-MS (m/z = 982.88 $[M+H]^+$).

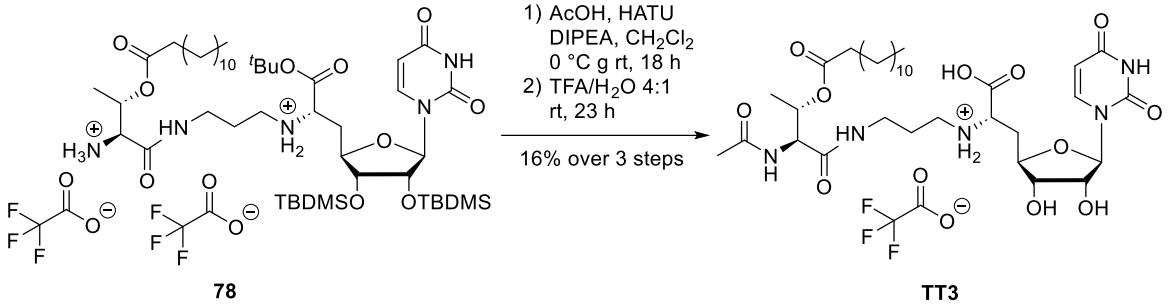

Fig. 83: Synthesis of derivative **TT3** via peptide coupling and global deprotection.

The residue was dissolved in aqueous trifluoroacetic acid (80%). The reaction was monitored by LC-MS and thus ended after 23 hours. The solvent was removed under reduced pressure. The acetylated compound **TT3** was isolated after HPLC purification as a colorless solid in 16% yield over three steps. The connectivity of the lipophilic side chain was confirmed by the HMBC spectrum. Here, a cross peak showed the interaction between 2'''-H and C-1^{iv}, which proved the connection of the acetyl moiety (cf. **Fig. 84**). Unfortunately the cross peak between 3'''-H and C-1^{v}, which proved the location of the lipophilic side chain, was not detected. But as the acetyl group was located at the wanted position, no migration of the lipophilic side chain could have taken place. Furthermore, the significant chemical shifts of the involved protons and carbon atoms (positions: 6', 3''' and 2^{v}) were compared to the corresponding atoms in other verified structures. Overall, the NMR analyses confirmed the desired connectivity and thus the structure of compound **TT3**.

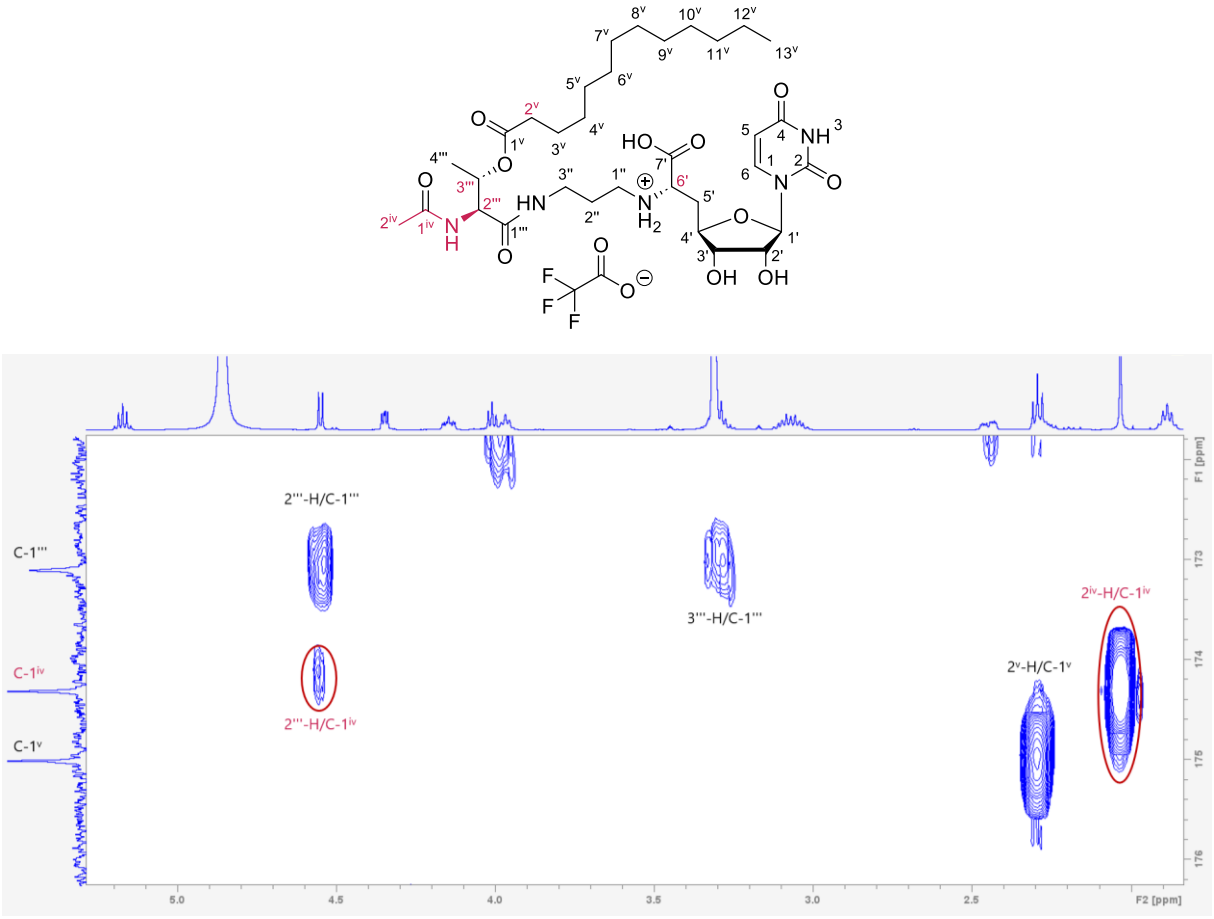

Fig. 84: Excerpt of the HMBC spectrum, proving the connectivity of the acetyl amide moiety at the 2'''-position to the backbone of the truncated muraymycin derivative **TT3**.

In addition, truncated compound **TT4** (cf. **Fig. 85**) was synthesized as a reference. It's design featured an acetyl group at the 2'''-NH moiety and an acetyl side chain. This design ensured that the interaction of the amide and the ester moiety would remain, while no strong interaction with the target, based on the lipophilic side chain, would influence the obtained IC_{50} values. The acetylation of bis-TFA salt **90** was carried out as described for compound **TT3**. Here, **90** was taken from a batch, which contained the rearranged side product **90SP** (cf. section 4.5.2, **Fig. 68**). It was hypothesized that the secondary alcohol in side product **90SP** might also act as a nucleophile in this synthesis. However, this was not observed. Analysis with LC-MS during and after the reaction showed the molecular mass of the reactant. As described above, it is not possible to distinguish between the required reactant and its rearranged side product **90SP**. Therefore, it was assumed that the detected compound was **90SP**. It should be noted that the intramolecular rearrangement could additionally occur during the peptide coupling with amine **90** (cf. section 4.5.2). So, the amount of rearranged side product **90SP** might even increase during the peptide coupling.

After work-up, the residue was dissolved in aqueous trifluoroacetic acid (80%). The reaction was stirred for 22 hours at room temperature. The solvent was removed under reduced pressure and the crude product was purified by HPLC, yielding mono-TFA salt **TT4** in 6.5% over two steps (calcd. from the amount of used acetic acid). The yield loss is most likely due to the intramolecular shift of the acetyl group in **90**, as the rearranged product does not undergo acetylation under the applied conditions.

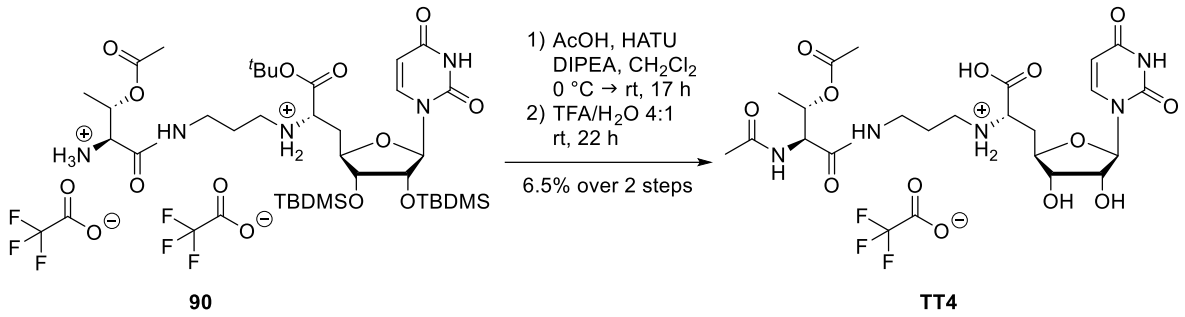

Fig. 85: Synthesis of derivative **TT4** via peptide coupling and global deprotection.

The amide structure at the 2'''-position was confirmed using the HMBC NMR spectrum (cf. **Fig. 86**). The comparison of the NMR data of **TT4** with those of **TT3** and pure compound **90** also confirmed the presence amide moiety at the 2'''-position, and moreover the intact secondary amine at the 6'-position. In addition, the cross peaks between 3'''-H or 2^{v}-H with carbonyl carbon atom C-1^{v} could be detected, thus confirming the acetyl ester moiety.

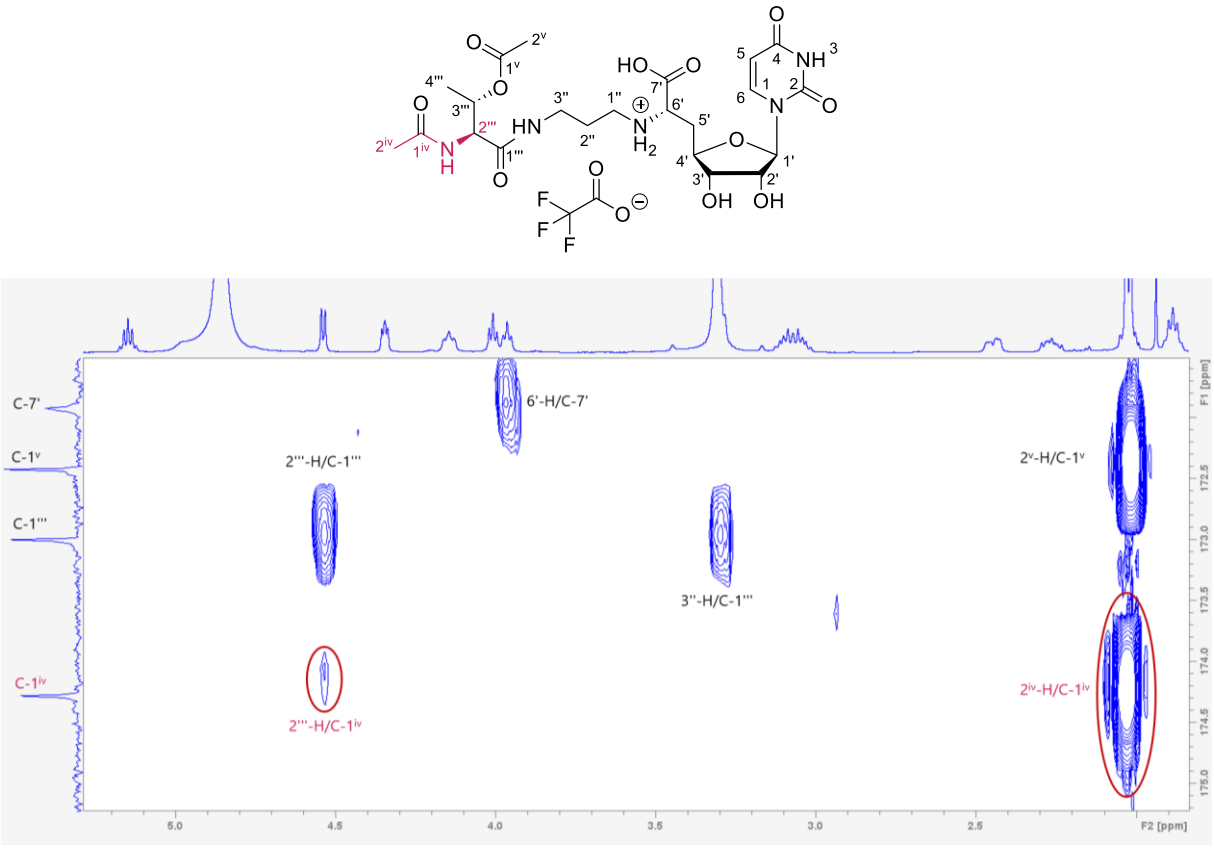

Fig. 86: Excerpt of the HMBC spectrum, proving the connectivity of the acetyl amide moiety at the 2'''-position to the backbone of the truncated muraymycin derivative **TT4**.

4.8 Biological evaluation of the truncated muraymycin derivatives

To provide more insight into the effect of the lipophilic side chain, which might be overlain by the effect of the urea dipeptide moiety, truncated derivatives were also tested in the biological assays (cf. **Table 3**). Here, the interaction with MraY was evaluated and the activity of the new derivatives against the two already mentioned *E. coli* strains was attempted. [96,120,121,135,144,172–174]

Even though the inhibitory activity against MraY is lowered, the compounds which contain a $COC_{12}H_{25}$ alkyl side chain (**TT1**, **TT2** and **TT3**), still show affinity towards the target enzyme in the low to moderate micromolar range. With the biological data received for derivative **TT4** (**R³** = Ac) it is demonstrated that the absence of a longer lipophilic side chain leads to complete affinity loss towards the target enzyme, if it cannot be compensated by another strong interaction. This result is consistent with the data of the reference compound **93** (Ac-Leu-NuAA),[146,147] which contains only Leu as the central amino acid. Here, the lipophilic side chain and the hydroxy moiety in position 3 are missing, thus confirming that the presence of a lipophilic side chain significantly affects the target affinity.

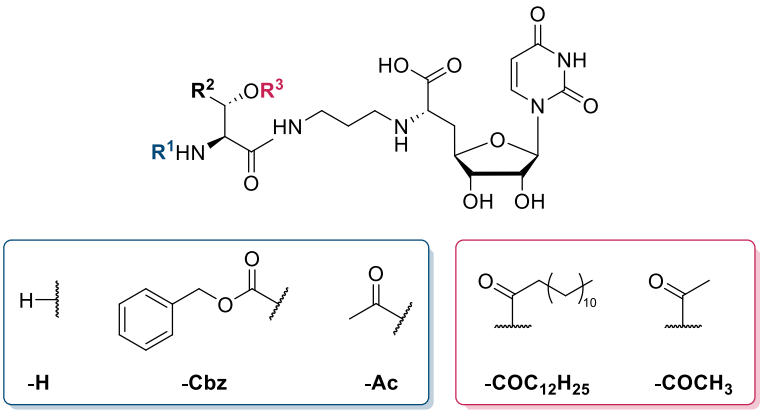

Table 3: Biological data of the truncated *allo*-Thr muraymycin derivatives. (references: **93** and **94**).[146,147]

compound	MraY IC_{50} [µM]
TT1: Cbz-*allo*-Thr($COC_{12}H_{25}$)-NuAA	97 ± 19
TT2: H-*allo*-Thr($COC_{12}H_{25}$)-NuAA	1.0 ± 0.2
TT3: Ac-*allo*-Thr($COC_{12}H_{25}$)-NuAA	5.0 ± 0.7
TT4: Ac-*allo*-Thr($COCH_3$)-NuAA	>100
references	
93: Ac-Leu-NuAA[b]	>100
94: Val-Lys-Leu-NuAA	2.5 ± 0.6

[a] crude membrane preparation; [b] 1:1-ratio of L- and R-Leu; n.d. not determined yet

Comparison of the MraY inhibition data of the truncated compounds **TT1**, **TT2** and **TT3**, suggests that the chemical character (hydrogen bond donor: amine or hydrogen bond donor & acceptor: carbamate or amide) of the α-amino group in the central amino acid does not significantly affect the binding affinity towards MraY. However, the introduction of a Cbz-group (**TT1**) results in a significant (~100-fold) decrease in MraY affinity. The introduction of this bulkier group, featuring an aromatic system, is not well tolerated by the enzyme binding pocket. It can be speculated that this is due to steric reasons or a suboptimal binding conformation/affinity.

Furthermore, truncated derivatives **TT2** and **TT3** show the same target affinity as the full-length simplified muraymycin Val-Lys-Leu-NuAA **94** (cf. **Table 3**).[146,147] The data suggest that the presence of the *n*-alkyl side chain compensates for the loss of the urea dipeptide structure. Thus, it can be assumed that each moiety contributes equally to the target affinity. Overall, this confirms that a full-length muraymycin backbone, in

combination with a lipophilic side chain at the central amino acid, is the most favorable scaffold regarding target interaction.

The evaluation of inhibitory activity against the two *E. coli* strains was performed multiple times for the truncated muraymycins but lead to inconclusive results (cf. chapter 9). Based on their structure, it could be assumed that the compounds are able to form micelles. This could lead to dilution problems during the assay and therefore inconsistent results. Before proceeding with further tests, it is necessary to address this issue. As mentioned above, the investigation of the physical properties, such as critical micelle formation concentration, should precede further experiments.

Overall, the four truncated derivatives demonstrated that the lipophilic side chain plays an essential role in the target interaction and affinity. Their simplified structure can be used in future projects to further investigate the properties of the lipophilic side chain with regard to length, head groups, branched chains or rigidization (cf. chapter 6). In addition, the truncated structures can also be used to investigate the influence of other residues at the α-amino group of the central acid (cf. chapter 6).

4.9 Biological evaluation: stability of new muraymycin derivatives in human plasma

The attempts to evaluate the stability of different muraymycin derivatives in *E. coli* Δ*tolC* lysate and/or LB-medium turned out to be very challenging. However, to obtain an initial indication of the potential *in vivo* stability of the new compounds, four candidates were chosen to evaluate their stability in human blood plasma: Ser-containing simplified muraymycins **T1** and **T3** and *allo*-Thr-containing muraymycin derivatives **T4** and **T5** (cf. **Fig. 87**). The compounds **T1** and **T4** as well as **T3** and **T5** can be directly compared with each other, as they only differ is the central amino acid.

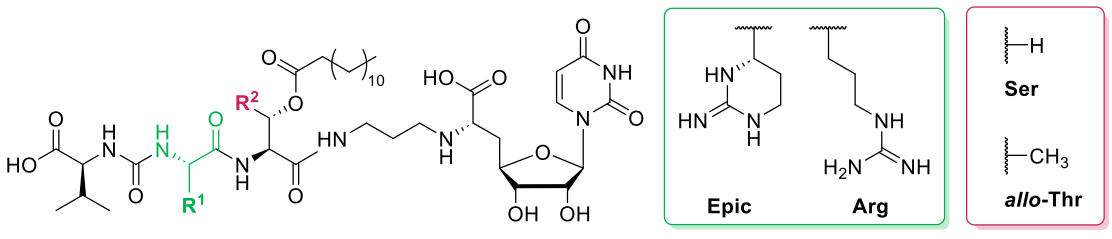

T1: Val-Epic-Ser($COC_{12}H_{25}$)-NuAA | **T4**: Val-Epic-*allo*-Thr($COC_{12}H_{25}$)-NuAA

T3: Val-Arg-Ser($COC_{12}H_{25}$)-NuAA | **T5**: Val-Arg-*allo*-Thr($COC_{12}H_{25}$)-NuAA

Fig. 87: Structures of the selected muraymycin candidates for stability evaluation in human plasma.

The main focus was to determine the stability of the ester bond, which is a potential labile segment in the muraymycin backbone. As the lipophilic side chain has been shown to play an essential role in target interaction, bacterial activity, and facilitating cell wall penetration (cf. sections 4.3, 4.6 and 4.8), it is necessary that the ester bond remains intact.

Since human plasma contains a variety of different enzymes, like esterases, glycosidases or lipases, it offers an ideal testing environment to get a first impression of the stability of the muraymycin derivatives *in vivo*.

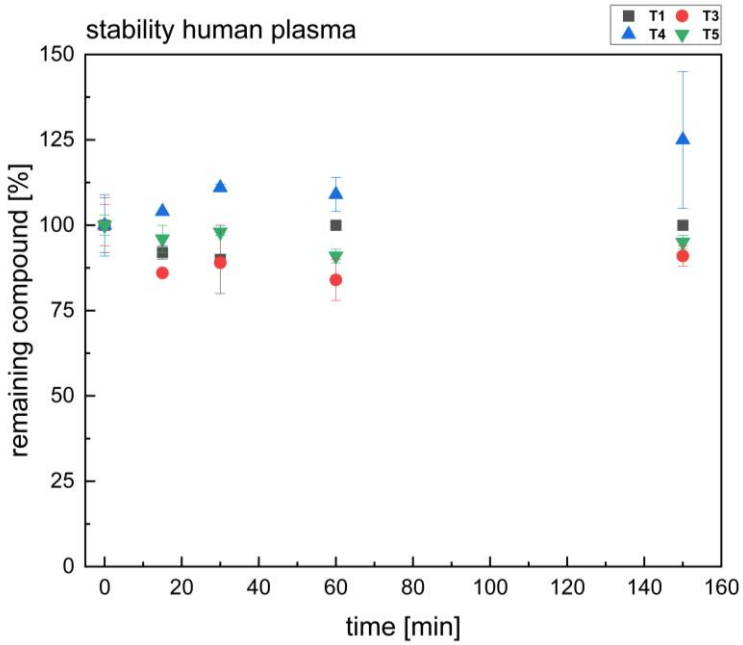

Fig. 88: Evaluation of the stability in human plasma of the selected muraymycin derivatives **T1**, **T3**, **T4** and **T5**.

Based on the results illustrated in **Fig. 88**, it can be assumed that the four selected compounds are stable in human plasma for at least 150 min (scope of measurement). Initially, it seems that the lack of an additional steric hindrance (Ser vs. *allo*-Thr) is irrelevant to the compound's stability in human plasma.

5 Summary

5.1 Synthesis of full-length and truncated muraymycin derivatives

The main aim of this thesis was the synthesis of simplified muraymycin derivatives that retain high target affinity and strong antibacterial activity. In particular, the structure of the central amino acid in the muraymycin backbone, in combination with the lipophilic side chain, was of primary interest. The role and effect of the lipophilic side chain on the potency of new muraymycin compounds were investigated in a structure-activity relationship (SAR) study. Therefore, the connectivity of the lipophilic side chain to the backbone remained an ester bond, similar to the natural compounds and the lead structure **32**. Overall, three different sets of compounds were designed and synthesized. These compounds not only featured different side chains, but the simplification of the urea dipeptide structure was also gradually pursued.

Each new derivative contained the nucleosyl amino acid **35** in the backbone. The synthesis was achieved according to the well-established protocol.[137,140,146,148] Uridine was converted into aldehyde **19** over two steps with an overall yield of 61%. In contrast to the general assumption, aldehyde **19** could be purified by silica gel column chromatography with non-nucleophilic and aprotic solvents. This finding supplements the established synthetic route and provides the opportunity for a purification step before the subsequent *Horner-Wadsworth-Emmons* reaction, if necessary. In summary, nucleosyl amino acid **35** was synthesized in eight steps with an overall yield of 32% (cf. **Fig. 89**).

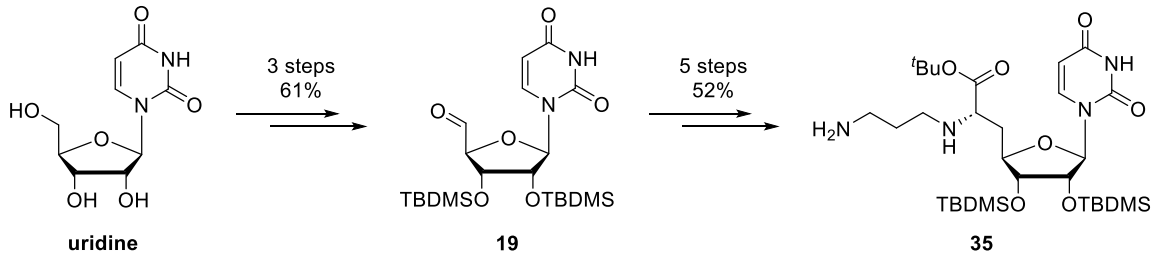

Fig. 89: Synthesis of nucleosyl amino acid **35**.

The syntheses of the central amino acids with different alkyl side chains were carried out using established synthetic routes.[153,158] For the introduction of fatty acid chains the *N*-Cbz-protected L-amino acid was converted into a *tert*-butyl ester using different esterification reagents, depending on the amino acid. Then, the desired lipophilic side

chain was introduced by *Steglich* esterification and the syntheses were completed by cleavage of the *tert*-butyl ester. For all these derivatives, the introduction of the *tert*-butyl ester was the yield-limiting step. Ether formation at the 3-OH group was observed as a side reaction during the protection. Different configurations at the 3-position (Thr) or the bulky side chain $CO^{iso}C_{15}H_{31}$ lowered the yields during the *Steglich* esterification. The synthesis of compound **51** was the only exception, as the acetylation of *allo*-Thr was accomplished in only one step with acetic anhydride in pyridine (cf. **Fig. 90**).

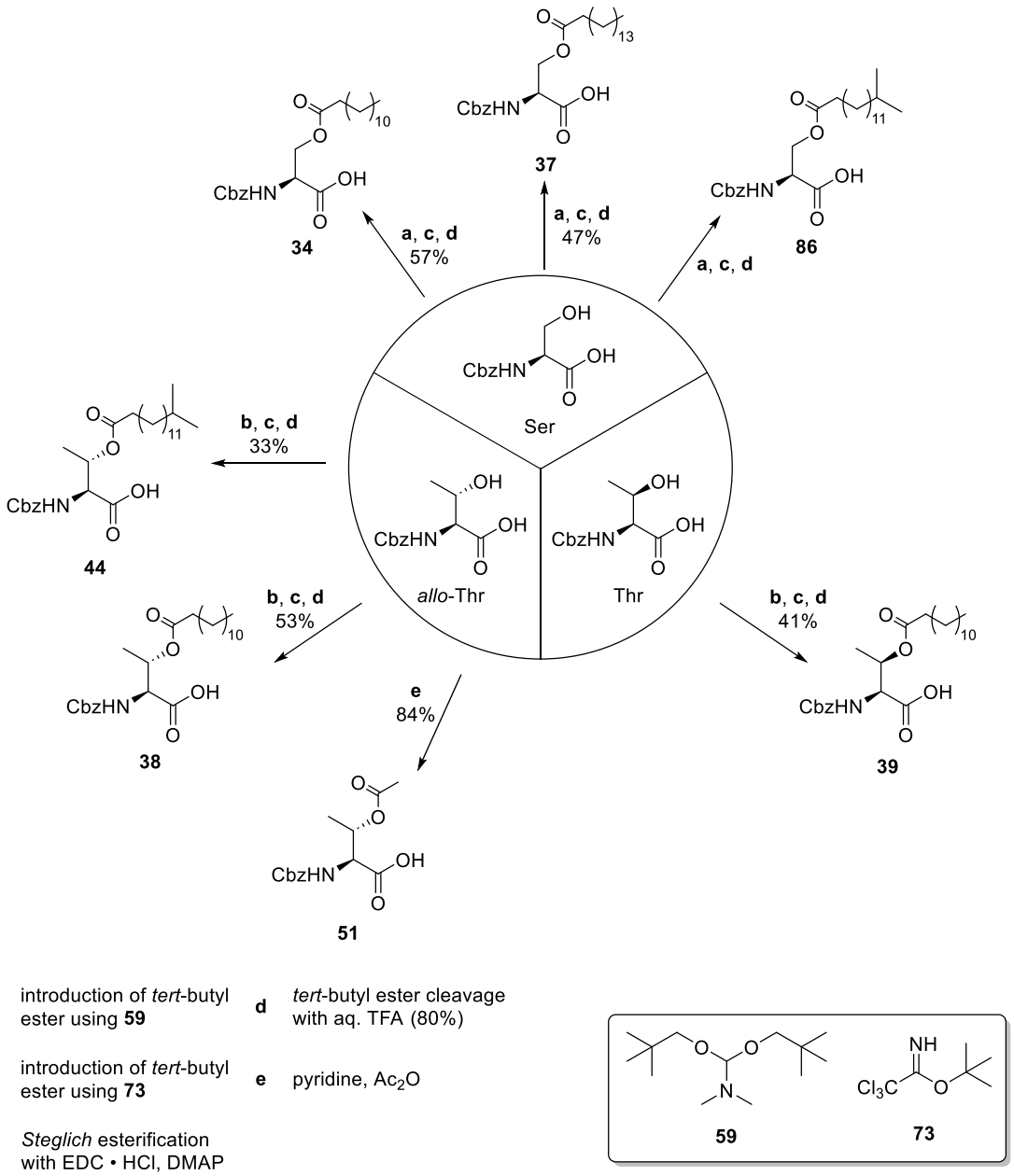

Fig. 90: Overview of the syntheses of required central building blocks.

Two special side chains had to be synthesized: the branched derivative **45**, which was introduced into **44** and **86**, and the unsaturated fatty acid **47**. For the preparation of

the lipophilic side chain corresponding to natural product muraymycin **B8**, the applied synthesis of Richardson and Williams had to be improved,[156] since the published oxidative cleavage resulted in a mixture of compounds with different chain lengths (cf. **Fig. 91**). Although the alternative route required two additional synthetic steps, no purification by silica gel column chromatography was required for the intermediates. Furthermore, the reactions can be performed without inert conditions in high yields. Pure compound **45** was obtained in 90% yield over three steps from alkene **46**. The high yields, the moderate synthetic effort and the pure isolated lipophilic side chain make the proposed synthesis a reasonable alternative to the published route.

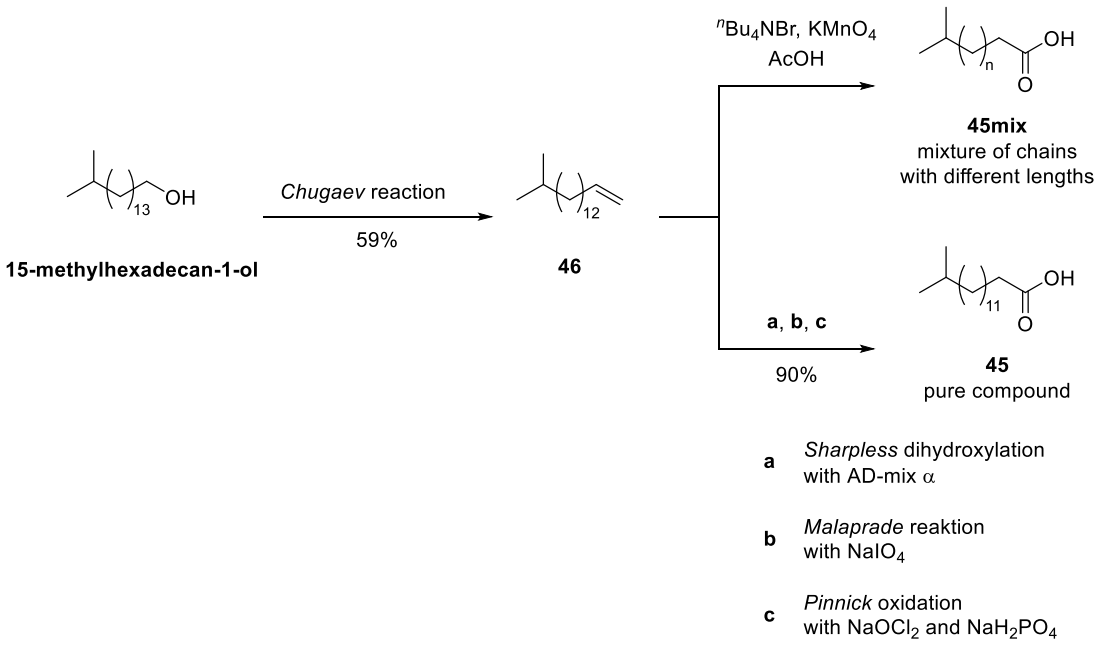

Fig. 91: Improved synthesis of branched fatty acid chain **45**.

The second special side chain was the *Z*-configurated lipophilic side chain **47**. This compound was synthesized over two steps according to the improved protocol of Wube *et al.*[157] The main difference between the published synthesis and the approach performed was the adjustment of the temperature during the *Wittig* reaction. The reaction was previously carried out at room temperature but resulted in the formation of **47** with a *Z*/*E* ratio of 85:15. After changing the conditions (starting the reaction at -82 °C and warming up to room temperature during the reaction process), the desired product was achieved with a *Z*/*E* ratio of 94:6 (cf. **Fig. 92**).

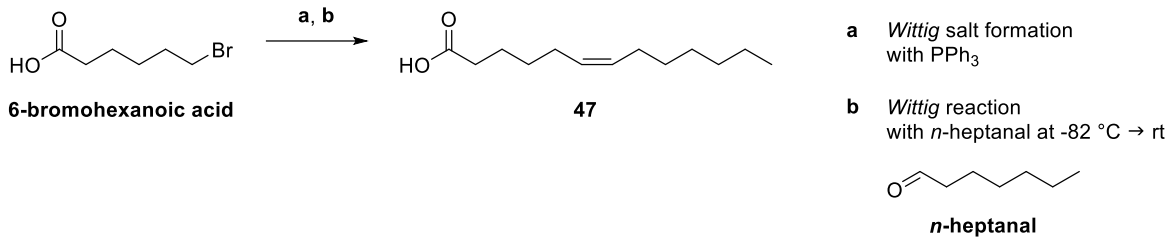

Fig. 92: Synthesis of unsaturated lipophilic side chain **47** in two steps.

Some of the new derivatives featured the simplified urea dipeptide **36**, which contains Arg instead of Epic. A two-step reaction sequence was used for the preparation,[154] in which Val *tert*-butyl ester hydrochloride was converted into the corresponding isocyanide and subsequently transformed into urea dipeptide **36**. The two-step reaction sequence provided **36** in an overall yield of 71% (cf. **Fig. 93**).

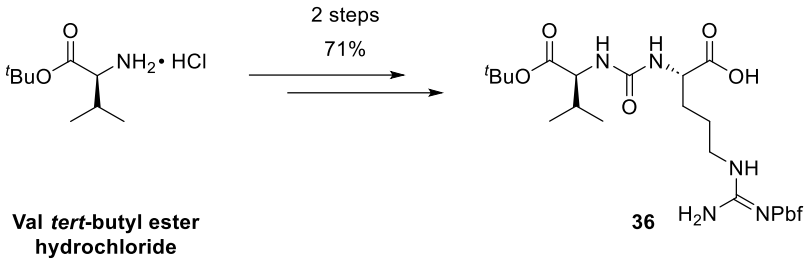

Fig. 93: Synthesis of urea dipeptide **36** in two steps.

The various building blocks were connected to each other by peptide couplings. The established conditions utilizing HOBt and PyBOP had to be modified,[146] as the formation of PyBOP by-product **64** significantly impeded the purification process by HPLC. The main problem was that the by-product **64** could not be effectively separated through washing steps during work-up. Even silica gel column chromatography proved to be ineffective for the separation of phosphine oxide **64**. In this context, it can be assumed that the lipophilic side chain of the product likely 'dragged along' the by-product. So, the primary criterion for the introduction of a new reagent was the ability to efficiently separate both the reagent and its by-products during the work-up process, preferably during the extraction process. Additionally, the peptide coupling required isomerically pure products. Consequently, alternative coupling agents were evaluated and established afterwards. Three alternatives - T_3P, HATU and EDC • HCl/HOBt - were tested. T_3P turned out to be ineligible for the first peptide coupling between nucleosyl amino acid **35** and any central building block as it led to a mixture of different components, which worsened the purification process even more than using PyBOP. HATU and EDC • HCl/HOBt, however, were both suitable for the first

peptide coupling, and were therefore equally used. In the second peptide coupling, in which the urea dipeptide was introduced into the scaffold, T_3P proved to be highly functional and was employed several times. Nevertheless, HATU became the main reagent for the second peptide coupling, as T_3P revealed reduced stability upon storage. Since both HATU and T_3P led to the same results, HATU was ultimately chosen as the main reagent.

Since the set of the Ser muraymycin derivatives was mostly synthesized using PyBOP and HOBt in the peptide couplings, multiple HPLC purification steps were required. Although this was a successful method, it was very time-consuming and not future-oriented for upcoming projects. Altogether, the Ser-containing derivatives **T1**, **T2** and **T3** were synthesized and biologically evaluated (cf. **Fig. 94**). Unfortunately, it was not possible to isolate compound **T7** as the acetyl group was cleaved during the global deprotection and/or the lyophilization. The presence of the substance was only indicated by LC-MS data. The comparable *allo*-Thr derivative with an acetyl ester (***a*T-T7**) was successfully synthesized and biologically evaluated (cf. **Fig. 95**). The peptide couplings, regardless of the coupling reagents, were usually the yield-limiting steps. The main reason may be due to the significantly increasing steric hindrance when the corresponding bulky amino acid building blocks were activated. This, combined with the steric complexity introduced by the nucleophiles (nucleosyl amino acid **35** or bis-TFA salts of coupling products between **35** and any central building block), might have kinetically hampered the coupling process. Overall, the Ser-containing muraymycin derivatives, except for **T1** (small traces of PyBOP by-product **64**) and **T7**, were isolated in pure form after HPLC purification. The connectivity of each corresponding lipophilic side chain was confirmed by HMBC NMR spectra (cf. section 4.2).

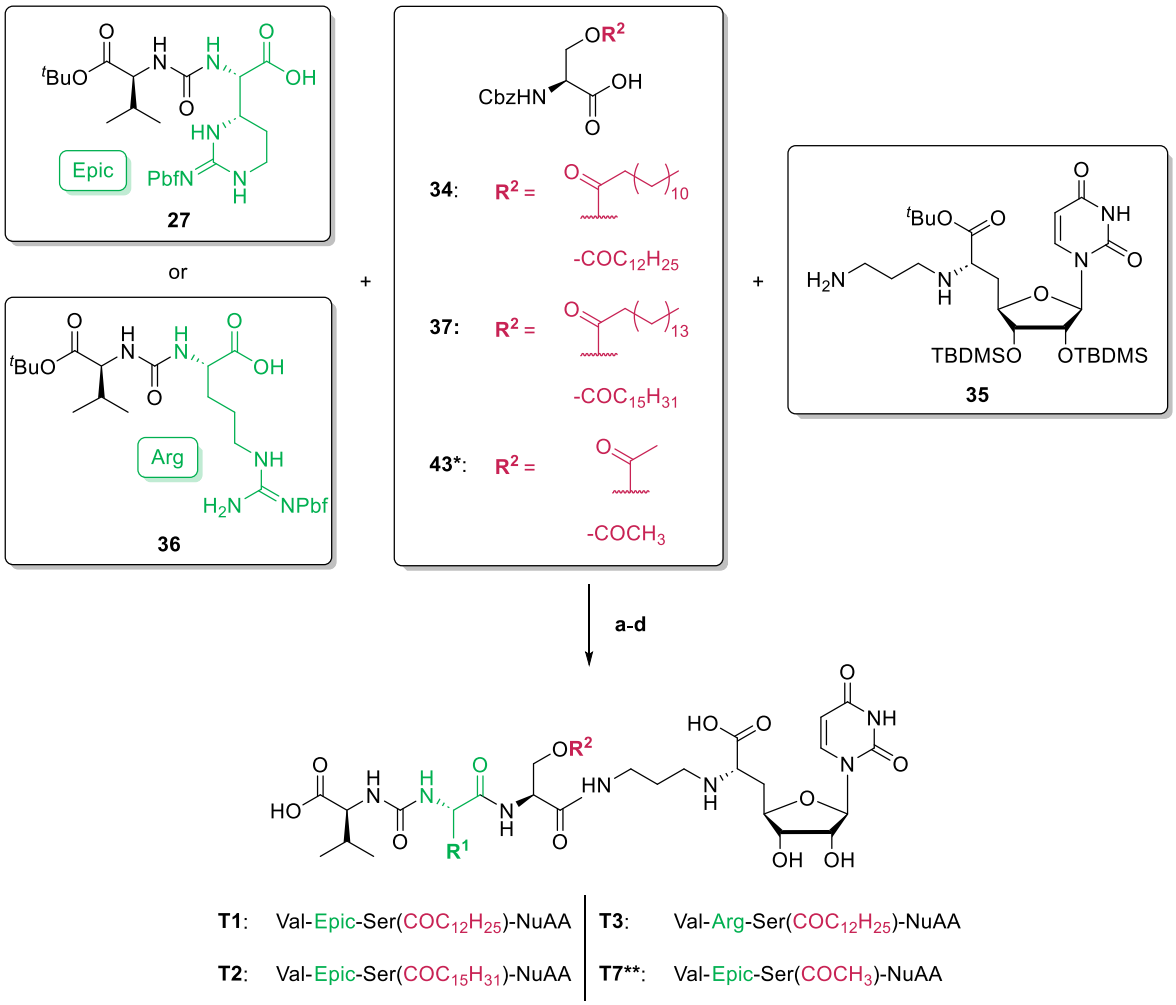

Fig. 94: Overview of the syntheses of the Ser set of muraymycin derivatives via the established tripartite approach (note: all derivatives were isolated as bis-TFA salts).

The second set of new derivatives included **T4**, **T5**, ***a*T-T7** and **T8**, all containing L-*allo*-threonine as central amino acid (cf. **Fig. 95**). So, the stereocenter at the 3-positon of this particular amino acid resembles the position in the natural products (cf. section 2.2.1, **Fig. 8**) and reference compound **32** (cf. section 2.2.3, **Fig. 12**). In addition, target compound **T6** featured L-threonine to examine the importance of the stereochemistry of the position (cf. **Fig. 95**). Overall, five new full-length muraymycin derivatives were successfully synthesized via the tripartite approach. For this set, EDC • HCl/HOBt (only for the first peptide coupling), T_3P (only for the second peptide coupling), or HATU (for both peptide couplings), were used instead of PyBOP/HOBt, thus facilitating the final

purification step. Different side chains were introduced in this set of derivatives, from the smallest possible side chain ($COCH_3$) to the branched alkyl side chain ($CO^{iso}C_{15}H_{31}$) corresponding to muraymycin **B8**. In addition, the urea dipeptide was also varied for SAR purposes.

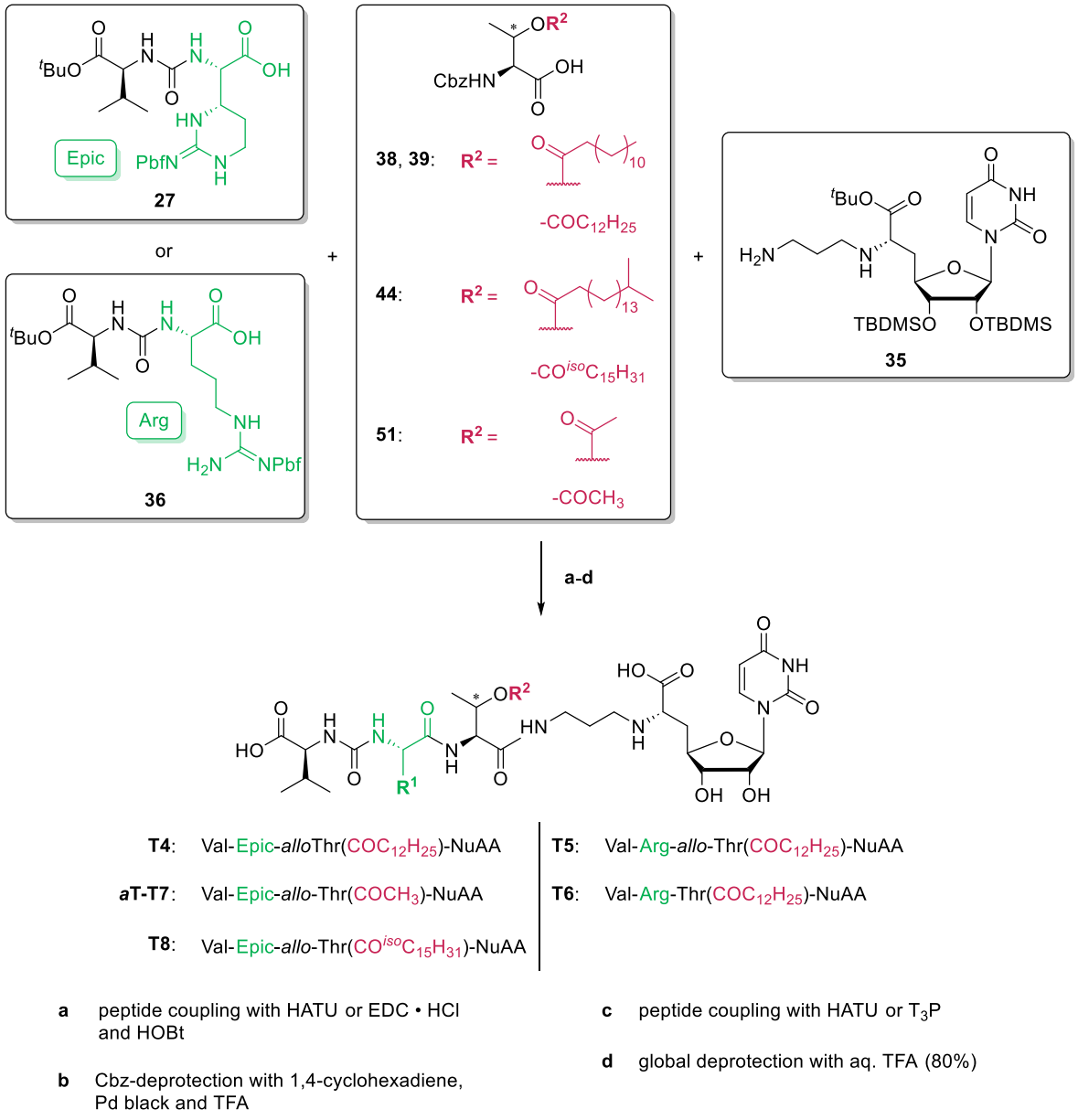

Fig. 95: Overview of the syntheses of the *allo*-Thr- or Thr-containing set of muraymycin derivatives via the established tripartite approach (note: all derivatives were isolated as bis-TFA salts).

In addition to the set of compounds illustrated in **Fig. 95**, another *allo*-Thr containing derivative was synthesized: **T9**. Here, the 'classic' tripartite approach was not utilized since the desired lipophilic side chain, containing a *Z*-double bond, was not compatible with the conditions of the Cbz-deprotection procedure using 1,4-cyclohexadiene and palladium black. Hence, the side chain had to be introduced in a later synthetic step.

Therefore, globally protected muraymycin derivative **50** was synthesized via the tripartite approach. The incorporation of the acetyl group was particularly useful for one reason: it prevented the formation of the regioisomeric side product, which was observed by M. Wirth during the second peptide coupling with the simplified lysine-containing urea dipeptide.[145]

The mild deprotection of the acetyl group, introduced in oligonucleotide synthesis by *Glen Research*,[159] led to the formation of the free alcohol **49** in high yields. Subsequent *Steglich* esterification with unsaturated lipophilic side chain **47** and global deprotection resulted in muraymycin derivative **T9** (cf. **Fig. 96**).

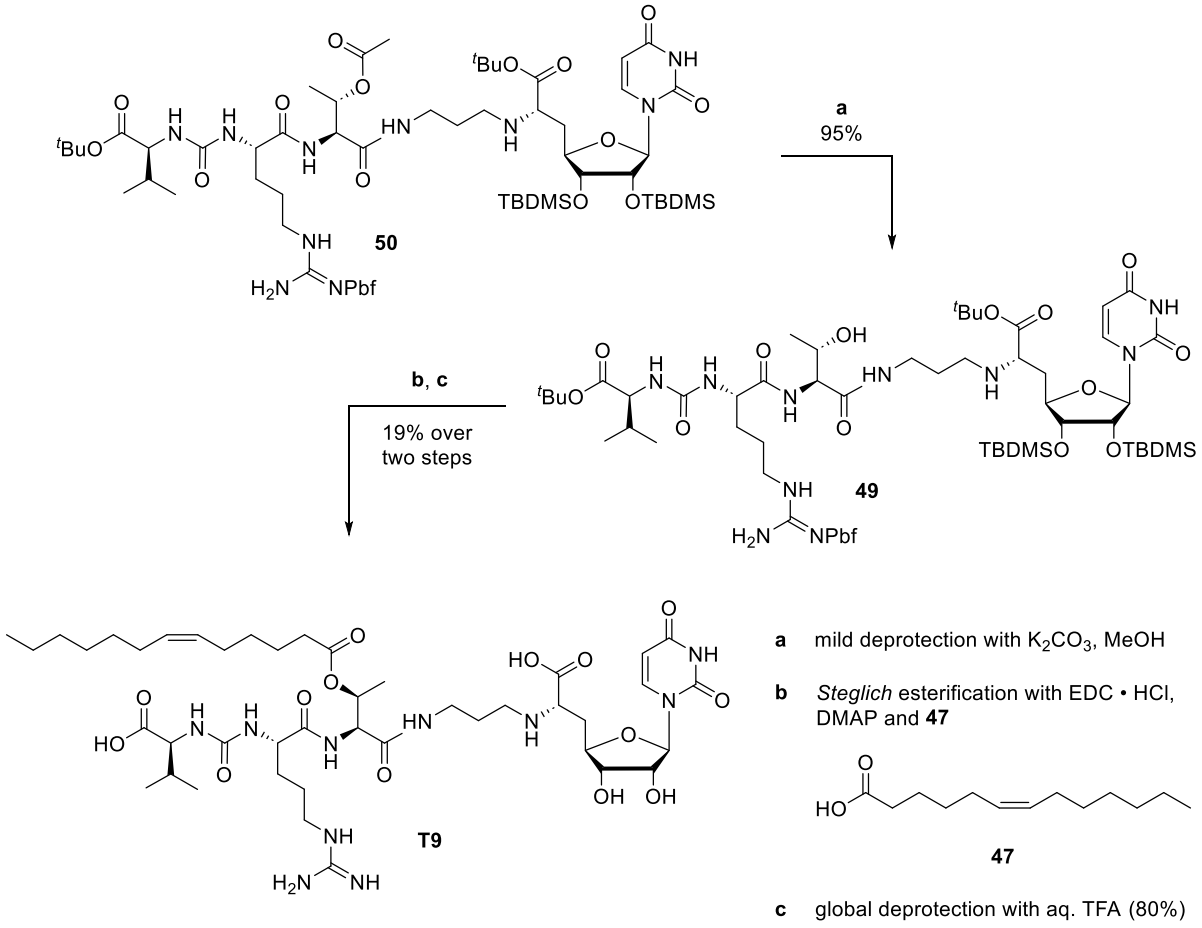

Fig. 96: Synthesis of muraymycin derivative **T9** via an alternative approach (note: **T9** was isolated as bis-TFA salt).

The alternative approach for **T9** holds great potential for future projects. Following the selective cleavage of the acetyl group, any lipophilic side chain can be introduced into the scaffold via *Steglich* esterification. The protection of the secondary alcohol as an acetyl ester prevents the formation of regioisomeric side products, thus improving the approach previously performed by M. Wirth.[145]

Overall, three Ser- and six *allo*-Thr- or Thr-containing muraymycin derivatives were synthesized. Here, three moieties were varied separately: the urea dipeptide, the central amino acid and the lipophilic side chain.

In addition to the full-length muraymycin derivatives, four truncated compounds were synthesized and biologically evaluated (cf. **Fig. 97**).

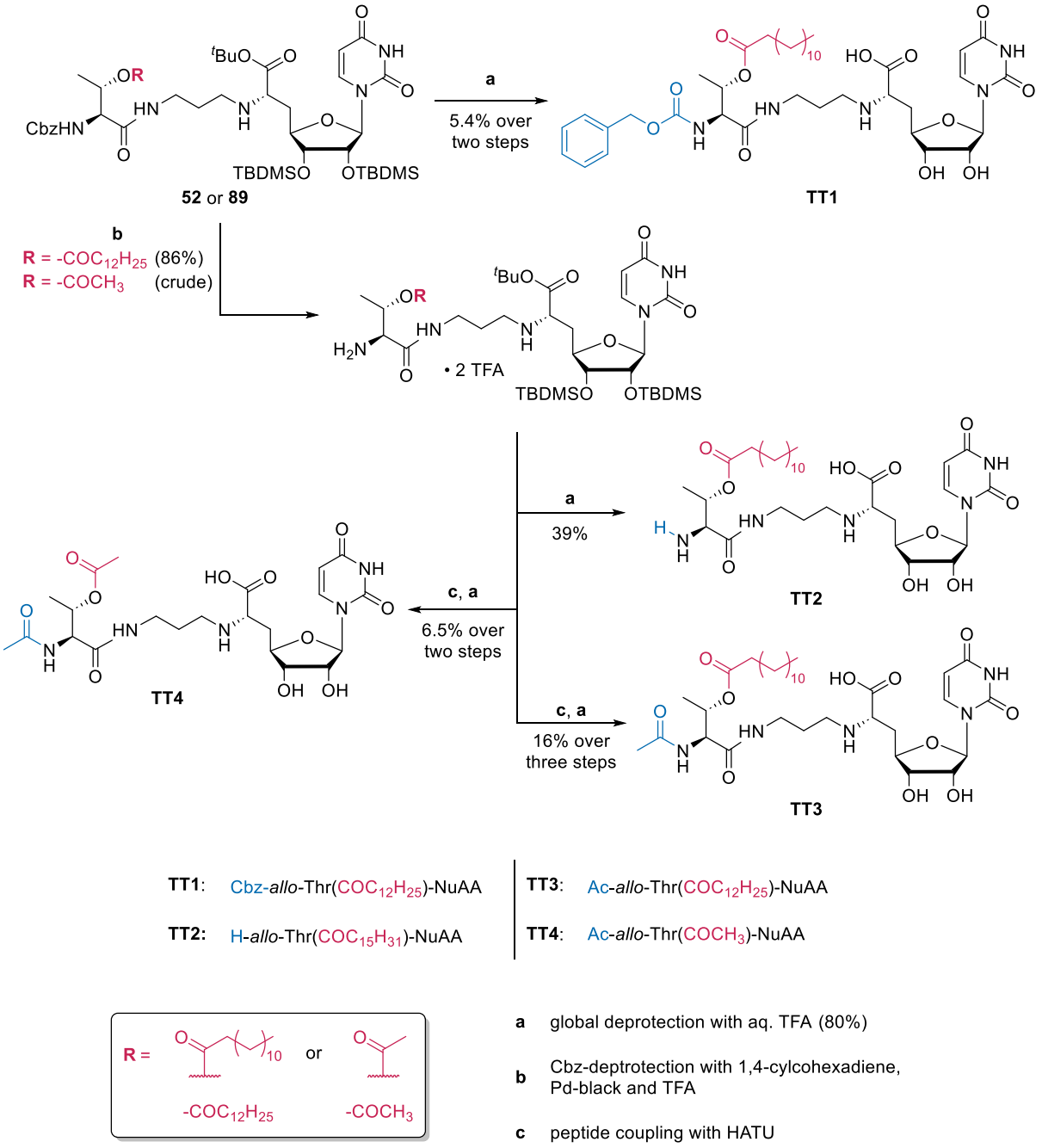

Fig. 97: Overview of the syntheses of the truncated muraymycin derivatives **TT1**-**4** (note: **TT1**, **TT3** and **TT4** were isolated as mono-TFA salts; **TT2** was isolated as bis-TFA salt).

Compound **TT1** was isolated after the global deprotection of precursor **52**, achieved during the synthesis of full-length analogs **T4** and **T5**. Compound **TT2** was isolated, after Cbz- and global deprotection from the same precursor (cf. section 4.7.1). The precursor for **TT4** was obtained after Cbz-deprotection of intermediate **89**, occurring during the synthesis of ***a*T**-**T7** and **50** resp. **T9**. The introduction of the acetyl group in **TT3** and **TT4** was achieved via peptide coupling. Standard acetylation would likely have led to the formation of side products, acetylated in the 6'-amino position in proximity to the nucleosyl amino acid. After global deprotection, truncated derivatives **TT3** and **TT4** were isolated (cf. section 4.7.2). Compound **TT4** was synthesized as a reference to compare the rest of the set of derivatives with compound **93**, which was synthesized by K. Leyerer.[146]

5.2 SAR study of the new muraymycin derivatives

The biological evaluation data of the nine new full-length muraymycin derivatives are presented in **Table 4**.

Table 4: Biological data of the new full-length muraymycin derivatives. (references: **B8**, **28** and **32**).[120,121,145]

compound	MraY IC_{50} [nM][a]	bacterial growth			
		IC_{50} [µg/mL]		MIC [µg/mL]	
		E. coli Δ*tolC*	*E. coli* DH5α	*S. aureus* Newman	*C. difficile*
L-serine					
T1: Val-Epic-Ser($COC_{12}H_{25}$)-NuAA	3.4 ± 0.2[b]	1.6	>100	>32	>32
T2: Val-Epic-Ser($COC_{15}H_{31}$)-NuAA	3.1 ± 0.3	5.5	>100	>32	8-16
T3: Val-Arg-Ser($COC_{12}H_{25}$)-NuAA	5.2 ± 0.4	6.6	>100	>32	>32
L-*allo*-threonine					
T4: Val-Epic-*allo*-Thr($COC_{12}H_{25}$)-NuAA	1.1 ± 0.1	<0.5	2.5-5	>32	2-4
T5: Val-Arg-*allo*-Thr($COC_{12}H_{25}$)-NuAA	2.2 ± 0.5	<1.3	2.5-5	>32	16-32
***a*T-T7**: Val-Epic-*allo*-Thr($COCH_3$)-NuAA	455 ± 79	>20[b]	>20[b]	>32	>32
T8: Val-Epic-*allo*-Thr($CO^{iso}C_{15}H_{31}$)-NuAA	1.8 ± 0.3	<0.1	>100	8-16	1-2
T9: Val-Arg-*allo*-Thr($COC_{12}H_{23}$)-NuAA	132 ± 43[b]	<0.3[b]	0.6-13	>32	>32
L-threonine					
T6: Val-Arg-Thr($COC_{12}H_{25}$)-NuAA	1.9 ± 0.9	<0.1	>100	>32	>32
references: 3-hydroxy-L-leucine					
B8: Val-Arg-3-hydroxy-Leu($CO^{iso}C_{15}H_{31}$)-NuAA+Arib	4.0 ± 0.7 pM	n.d.	n.d.	4-8	4-8
28: Val-Epic-3-hydroxy-Leu-NuAA	95 ± 19	50	15	>50	n.d.
32: Val-Epic-3-hydroxy-Leu($COC_{12}H_{25}$)-NuAA	5.8 ± 0.5	0.5	>100	10	2.5

[a] crude membrane preparation; [b] preliminary value; n.d. not determined yet

Overall, it was confirmed that the simplification of the urea dipeptide by replacing Epic with Arg as well as the change of the central amino acid to Ser, *allo*-Thr and Thr does not affect the target interaction with MraY. Furthermore, it was confirmed that the lipophilic side chain is beneficial for target interaction and does not only enhance the cell penetration, as previously assumed.[121] By comparison, acetylated compound ***a*T-**

T7 shows the weakest interaction with MraY, hence supporting the statement. In addition, the presence of an *iso*-propyl head group in the side chain (**T8**) did not have a positive or negative effect on the target interaction. However, rigidization of the lipophilic side chain (**T9**) reduced MraY affinity.

The inhibition of bacterial growth towards Gram-positive and Gram-negative strains varied for each compound. All derivatives, containing a long lipophilic side chain (all compounds except ***a*T-T7**) showed strong inhibition of efflux-deficient strain *E. coli* Δ*tolC*. The set containing *allo*-Thr or Thr showed overall an efficiency comparable to reference compound **32**. The data for the inhibition of *E. coli* DH5α uncovered two very potent inhibitors, compounds **T4** and **T5**. Although **T9** showed 100-fold less affinity towards the target, it still showed very promising activity against *E. coli* DH5α.

Furthermore, the activity of derivative **T8** against *S. aureus* Newman is comparable to reference compound **32** and it is only 2-fold less active than best-in class compound muraymycin **B8**. Compared to **T4**, **T8** only differs in the lipophilic side chain. Therefore, it can be proposed that the branched lipophilic side chain is beneficial for the inhibition of *S. aureus* since this compound is the only new derivative showing activity towards these bacteria. Muraymycin **B8** and **T8** share the same branched lipophilic side chain. Since the simplified compound lacks some features of muraymycin **B8**, which are important for target interaction, it can be hypothesized that this special side chain has a decisive impact on the inhibition of the bacterial growth. This would also contribute to the understanding why the natural compounds of the **B**-series contain branched lipophilic side chains.

Three of the already mentioned derivatives also demonstrated good inhibition of *C. difficile*. The best results were achieved with compound **T8**, indicating that the branched lipophilic side chain might be favorable for activity, especially against Gram-positive bacteria. Furthermore, compound **T4**, having the same scaffold as **T8** featuring only a simple *n*-alkyl chain, showed reduced activity by a factor of two. The additional replacement of Epic in the urea dipeptide moiety with Arg (**T5**) reduces the activity again by a factor of eight. Ser-containing compound **T2** also showed activity against *C. difficile*, in a range between **T4**, **T5** and reference compound **32**. This derivative contains a longer lipophilic side chain, which might be the reason behind its activity. Since the target affinity is similar for these compounds, it can be assumed that higher lipophilicity supports the antibacterial activity. This might be due to better cell

penetration or reduced efflux from the bacterial cell. The identification of the cause behind these results requires further investigation.

In addition, the data for the truncated derivatives (cf. **Table 5**) support the previous results on the role of the lipophilic side chain for target inhibition and the inhibitory activity on bacterial growth. The truncated compounds **TT2** and **TT3** showed similar affinities towards MraY as full-length derivative Val-Lys-Leu-NuAA **94**. The loss of the urea dipeptide structure was apparently compensated by the introduction of a lipophilic side chain. Furthermore, compound **TT3** showed good affinity towards MraY while the acetylated compound **TT4** or reference compound **93** (without 3-substitution at the central amino acid) does not.

Table 5: Biological data of the new truncated muraymycin derivatives (references: **93** and **94**).[146,147]

compound	MraY IC_{50} [µM]
TT1: Cbz-*allo*-Thr($COC_{12}H_{25}$)-NuAA	97 ± 19
TT2: H-*allo*-Thr($COC_{12}H_{25}$)-NuAA	1.0 ± 0.2
TT3: Ac-*allo*-Thr($COC_{12}H_{25}$)-NuAA	5.0 ± 0.7
TT4: Ac-*allo*-Thr($COCH_3$)-NuAA	>100
references	
93: Ac-Leu-NuAA[b]	>100
94: Val-Lys-Leu-NuAA	2.5 ± 0.6

[a] crude membrane preparation; [b] 1:1-ratio of L- and R-Leu; n.d. not determined yet

It was further revealed that the interaction with MraY was not significantly changed when the α-amine in the central amino acid was conserved or turned into an acetyl amide (**TT2** and **TT3**). However, the introduction of the Cbz-moiety in **TT1** reduced the target interaction. In this particular case, it is apparent that the aromatic system of the Cbz group interacts differently with the binding pocket than the actual substituent (urea dipeptide) in the full-length muraymycins. Hence, it can be assumed that the decreased affinity can be ascribed primarily to the chemical structure of the substituent and not its size. Yet, the compensating effect of the lipophilic side chain in **TT1** is likely the reason for the moderate target interaction of the compound.

Overall, these simplified structures harbor great potential to investigate the structural options in the lipophilic side chain with less synthetic effort in the future.

Although many stability tests in different biological media were performed (cf. sections 4.3, 4.6 and 4.8), a final statement cannot be given within the scope of this work. This is primarily because of the non-reproducible data. It can only be speculated that this could be due to micelle formation, resulting in solubility issues upon dilution. However, biological data of the muraymycin analogs **T1**, **T3**, **T4** and **T5** in human plasma suggest their stability for at least 150 min in this particular medium (cf. section 4.9).

The following SAR-map combines the new findings for all new muraymycins derivatives and the results from former studies. Overall, the biological data discussed above (cf. section 4.3, 4.6 and 4.8) confirm that the complete muraymycin structure contributes to the target affinity as well as bacterial inhibition ability. The replacement of Epic with Arg in the urea dipeptide has been demonstrated to be feasible. Also, the central amino acid can be replaced, whereby *allo*-Thr seems to be the best choice so far. Finally, it was shown that the introduction of a long lipophilic side chain is essential for antibacterial activity. Different lengths and structures of this particular moiety seem to influence the potency against different type of bacteria. The data also reconfirm that the impact of the lipophilic side chain predominates the effect of the amino ribose unit at the 5'-position of the nucleosyl amino acid building block (**R^3**).

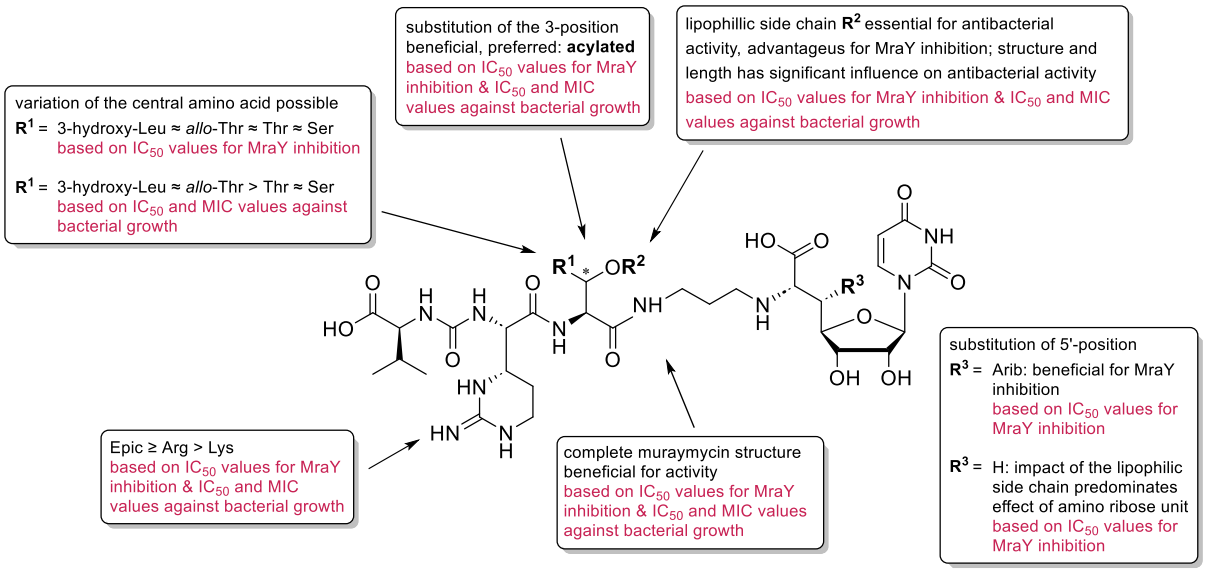

Fig. 98: Summary of the SAR study of all the new muraymycin derivatives combined with data from former studies.[121,126,132,133,144–147,149,151,152]

In conclusion, three of the new derivatives are potential new lead compounds (cf. **Fig. 99**). On the one hand **T4** and **T5**, which both are potent inhibitors of *E. coli* DH5α and show more or less inhibition of *C. difficile*. Target compound **T5** even contains the simplified urea dipeptide moiety, making this compound an even better candidate for

future projects. On the other hand, compound **T8** can also act as a compelling starting compound due to its ability to inhibit the bacterial growth of *S. aureus* and *C. difficile*.

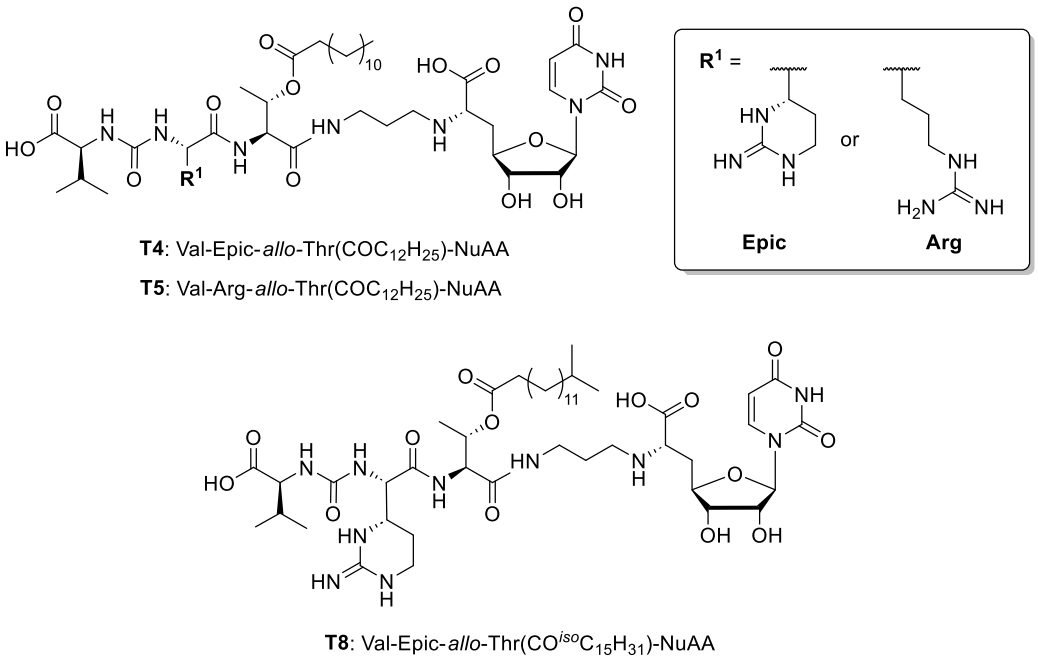

Fig. 99: Potential new lead compounds: **T4**, **T5** and **T8**.

6 Outlook

In the scope of this thesis nine full-length and four truncated muraymycin derivatives were synthesized. Most of them showed very strong inhibitory activity against the target enzyme MraY. Among these compounds, several highly potent candidates were identified, which showed strong growth inhibition not only of efflux-deficient strain *E. coli* Δ*tolC* but also of *E. coli* DH5α. Furthermore, some of the compounds were active against *C. difficile* and one of those even against of *S. aureus* (cf. section 5.2). In order to provide an overview of the factors influencing bacterial activity, the missing stability data in bacterial lysate need to be repeated for all new muraymycin derivatives. For the potent compounds, additional stability tests in human plasma need to be conducted, to gain first insights in their potential stability *in vivo*. Moreover, more *in vitro* experiments regarding cytotoxicity against human cells and uptake into different bacterial cells should also be performed in the future, envisioning the prospective applications as antibiotic. The compounds exhibiting strong inhibition of *E. coli* DH5α (**T4** and **T5**) should also be tested against the Gram-negative *Pseudomonas aeruginosa*, a highly dangerous strain of the so-called 'ESKAPE' pathogens.

It is likely that the biological assays used will need revision and optimization to be applicable to the already obtained or future compounds. Additionally, evaluating the physical properties of the known derivatives, especially their ability to form micelles, could prove to be very promising. This understanding might help in the design of new derivatives.

Regarding the synthesis of new compounds, the biological evaluation revealed that different features of the muraymycin scaffold seem to be beneficial for the activity against selected bacteria (cf. section 5.2, **Fig. 98**). It thus seems reasonable to pursue multiple approaches, rather than attempting to develop a high potent derivative addressing all the different bacteria at once.

First, it would be of interest if the biological activity of muraymycin derivative **T8** (with branched side chain $CO^{iso}C_{15}H_{31}$) could be maintained if Epic would be replaced by Arg in the urea dipeptide (cf. **Fig. 100**). If this replacement proves to be successful, the designed compound could serve as a new lead compound for future derivatives against the Gram-positive bacteria *S. aureus* and *C. difficile*. Otherwise, compound **T8** would remain the lead compound.

Second, since it was already demonstrated that the simplification of the urea dipeptide structure does not reduce the inhibition of *E. coli* DH5α, it would be reasonable to select the backbone of **T5** (Val-Arg-*allo*-Thr(CO**R**)-NuAA) as lead design for developing new derivatives targeting this bacterial strain, and potentially other Gram-negative bacteria.

The importance of the lipophilic side chain was demonstrated repeatedly within the scope of this thesis. It is therefore desirable to introduce other lipophilic side chains into the muraymycin scaffold of future derivatives to further investigate the impact of various side chain structures on biological activity. Potential candidates could be branched lipophilic side chains, similar to the moieties in muraymycin **B1** or **B3** (cf. section 2.2.1, **Fig. 8**) or based on the structures of G. Niro.[111,120,188] Furthermore, polyunsaturated chains containing multiple double bonds (e.g. omega-3 fatty acids) or those with longer or shorter *n*-alkyl chains. The latter could determine the minimum and maximum length required for bacterial activity (cf. **Fig. 100**) or whether the introduction of longer lipophilic side chains (>C_{16}) would lead to even more potent derivatives. In this context, it could also be interesting to evaluate if a maximum side chain length exists. It may also be promising to introduce rigid side chains, as in compound **T9** (cf. section 4.5.3), while shifting the position of the *Z*-double bond or alternatively, by introducing an *E*-double bond.

The refined tripartite approach, including the mild late stage deprotection of the acetyl group and the introduction of the lipophilic side chain (cf. section 4.5.3), would be very useful in this regard. Its advantages are the improved yields in the peptide couplings (cf. sections 4.5.2, 4.5.3), the non-occurrence of the regioisomer (alcohol underwent nucleophilic attack instead of amine in the central amino acid) during the second peptide coupling as observed by M. Wirth,[145] and the possibility to synthesize a large number of derivatives in a shorter time. The only difficulty is the potential intramolecular shift of the acyl moiety during the second Cbz-deprotection or second peptide coupling (cf. section 4.5.2, **Fig. 68**). However, the unreactive side product can be easily separated by silica gel column chromatography, thus making this route highly efficient.

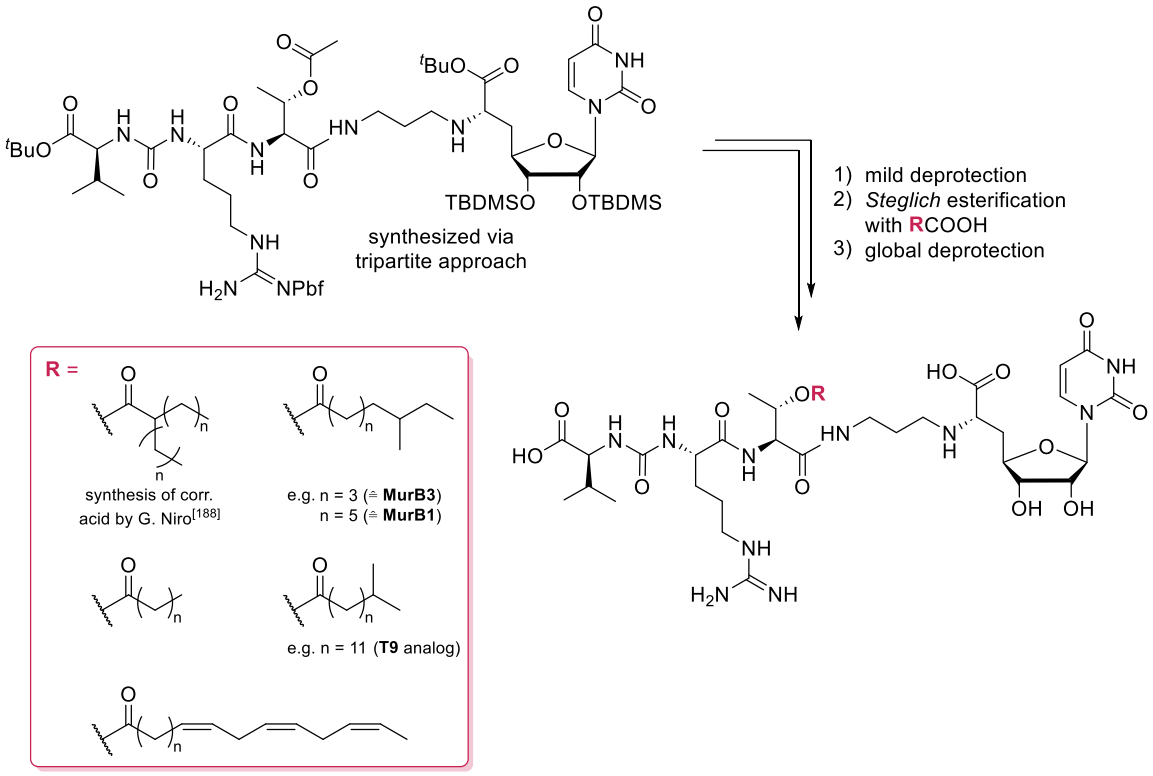

Fig. 100: Synthesis of possible future muraymycin derivatives with various lipophilic side chains via the improved tripartite approach.

Another variation could be a full-length muraymycin derivative containing cysteine as central amino acid, which would further support the SAR study. The variation – ester, thioester, and amide[149] - might contribute to a deeper understanding of the binding pocket structure.

Finally, the set of truncated muraymycins could be extended by another series. In order to counteract the observed solubility problems during testing, which presumably lead to inconsistent data regarding bacterial growth, it might be reasonable to introduce another residue into the scaffold connected to the α-amino group of the central amino acid. Based on the assumption that the main reason for the reduced solubility of the compounds upon dilution is their ability to form micelles, it might be beneficial to choose a moiety containing a terminal polar or charged head group. Here, it might be appropriate to change the length of this moiety gradually until the simplified structure features the same backbone length as in full-length muraymycins (cf. **Fig. 101**). For comparability purposes, it is reasonable that the lipophilic side chain at the central amino acid should remain the *n*-alkyl side chain $COC_{12}H_{25}$ for the set of truncated muraymycins in the first instance. This new modification might also give further insights into the target binding of the muraymycins.

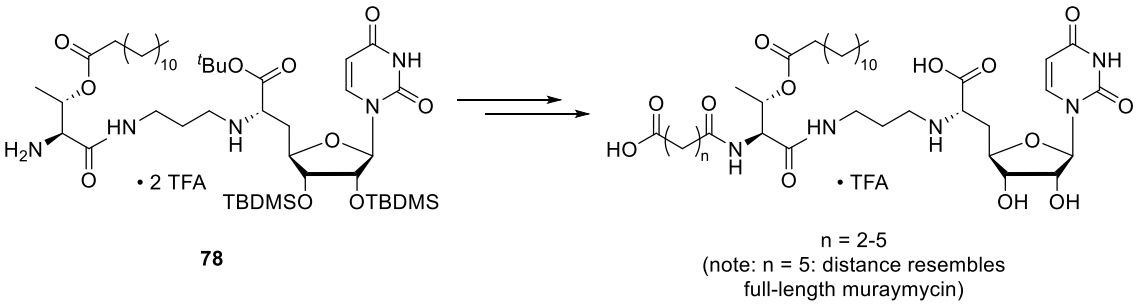

Fig. 101: Synthesis of new truncated muraymycin derivatives with various residues at the α-amine of the central amino acid.

An additional approach could be the omission of the Val moiety in the urea dipeptide moiety (cf. **Fig. 102**). This would reduce the synthetic effort while maintaining enough target binding affinity to allow investigation of the influence of different side chains structure, which can then be used in the design of potential new lead structures. Synthetically the most promising approach would be the refined tripartite approach including the mild cleavage of the acetyl ester.[159] In order to perform the described deprotection and subsequent *Steglich* esterification (cf. section 4.5.3), it is reasonable to protect the α-amino group of the introduced Arg moiety to avoid side reactions. For this purpose, the Boc-protected derivative Boc-Arg(Pbf)-OH could be a promising choice. Due to its acidic instability it is very likely that the Boc group will be cleaved along the other protecting groups during the global deprotection. The synthetic route described in **Fig. 102** will be another promising application of the refined tripartite approach.

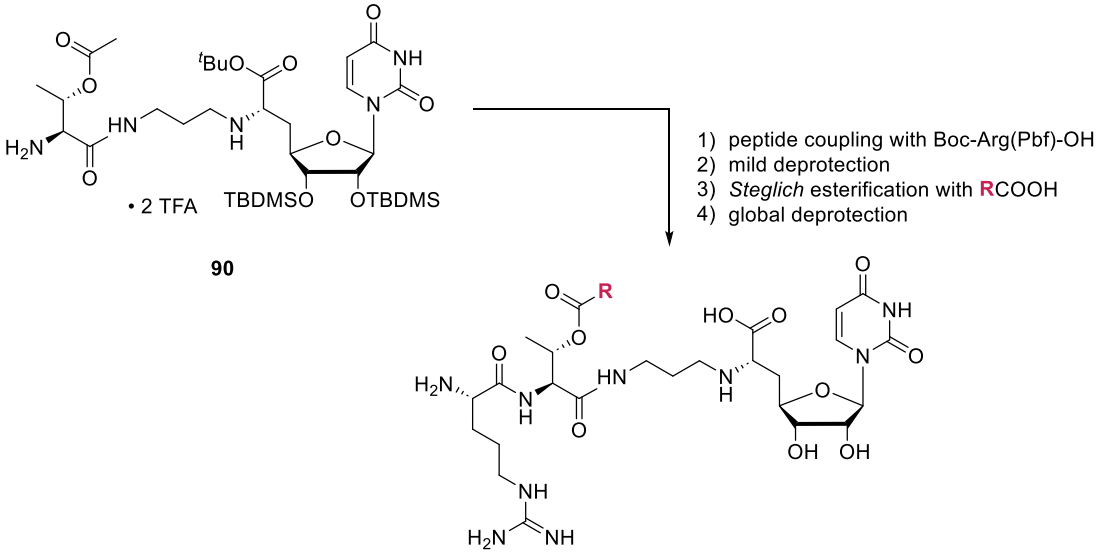

Fig. 102: Synthesis of new truncated muraymycin derivatives without terminal Val moiety.

7 Experimental

7.1 General methods

7.1.1 Working techniques

All reactions were carried out under inert gas atmosphere unless indicated otherwise. The nitrogen used was dried over phosphorous pentoxide and orange gel. The argon used had a purity level of 5.0 (99.999 Vol%). Hydrogen with a purity level of 6.0 (99.9999 Vol%) was used for reactions carried out under hydrogen atmosphere. The Schlenk technique was used for reactions sensitive to air- and/or water. For reactions requiring low temperatures, suitable freezing mixtures (water/ice (approximately 0 °C), nitrogen/acetone (down to -90° C) were used.

7.1.2 Starting materials and reagents

The reactants and reagents used were purchased in synthesis quality from *ABCR*, *Alfa Aesar*, *Sigma Aldrich*, *Merck* and *VWR* and obtained from the Central Chemical Stock of Saarland University. They were used in the respective synthesis without additional purification, unless indicated otherwise. Urea dipeptide **27** and methyl-2-methoxy-*N*-benzyloxycarbonylglycinate **54** were previously synthesized in the Ducho working group and provided for this work.

7.1.3 Solvents

The solvents used for chromatography and extraction (dichloromethane (CH_2Cl_2), ethyl acetate (EtOAc) and petroleum ether (PE)) were purchased in technical grade and purified by distillation.

For the reactions or extractions that were not carried out under inert conditions, the solvents were purchased in analytical grade and used without further purification, unless indicated otherwise.

7.1.4 Anhydrous solvents

The following anhydrous solvents were used for reactions performed under an inert gas atmosphere. The molecular sieves were stored in the drying oven and activated by heating *in vacuo* prior to use.

Acetonitrile (MeCN):	dried with the *M. Braun* solvent purification system MB-SPS-800; stored over molecular sieve (3 Å)
Dichloromethane (CH_2Cl_2):	dried with the *M. Braun* solvent purification system MB-SPS-800; stored over molecular sieve (3 Å)
Diethyl ether (Et_2O):	dried with the *M. Braun* solvent purification system MB-SPS-800; stored over molecular sieve (3 Å)
iso-Propanol (^{i}PrOH):	purchased from *Sigma Aldrich* (99.5%, extra dry); stored over molecular sieve (3 Å)
Methanol (MeOH):	p. a. quality, degassed and stored over molecular sieves (3 Å).
Pyridine (Py):	purchased from *Sigma Aldrich* (99.5%, extra dry); stored over molecular sieve (4 Å)
tert-Butanol (^{t}BuOH):	p. a. quality, degassed and stored over molecular sieves (4 Å)
Tetrahydrofuran (THF):	dried with the *M. Braun* solvent purification system MB-SPS-800; stored over molecular sieve (3 Å)
Toluene:	HPLC grade, degassed and stored over molecular sieves (4 Å)
Triethylamine:	degassed and stored over molecular sieves (4 Å)

7.1.5 Chromatography

7.1.5.1 Thin-layer chromatography (TLC)

Silica gel coated aluminum plates with fluorescent indicator (silica gel 60 F_{254}) were used for reaction controls and detection of substances. The visualizing of the substances was performed with UV light (λ = 254 nm) and/or treatment with suitable staining reagents under heating.

- *Vanillin/sulfuric acid solution (VSS)*:
  vanillin (5 g), H_2SO_4 (conc., 25 mL), CH_3COOH (conc., 80 mL), dissolved in MeOH (680 mL)
- *Ninhydrin solution*:
  ninhydrin (300 mg), CH_3COOH (conc., 3 mL), dissolved in 1-butanol (100 mL)

- *$KMnO_4$ solution*:
  $KMnO_4$ (1 g), K_2CO_3 (6 g), NaOH (5% aq. (w/v), 1.5 mL), dissolved in H_2O (100 mL)
- *Bromocresol green staining solution:*
  bromocresol green (100 mg), EtOH (500 mL), NaOH (0.1 M, 5 mL)

7.1.5.2 Column chromatography

The silica gel used for normal phase column chromatography was purchased from *VWR* (silica gel Si60, grain size 40-63 µm).

7.1.5.3 High-performance liquid chromatography (HPLC)

A *Hitachi LaChrom Elite* HPLC system was used for semi-preparative HPLC separation. An Agilent 1100/1200 quaternary pump, a LiChroCart® Purospher® RP-18e column (5 µm, 10x250 mm), a Nucleodur® Phenyl/Hexyl column (5 µm, 10x250 mm) and a DAD detector were used. Mixtures of double-distilled water or methanol (HPLC grade) and acetonitrile (HPLC grade) served as the running medium. If necessary, trifluoroacetic acid (HPLC grade) was added to the solvent.

Method A: SR054
Flow rate: 3.0 mL/min, column: LiChroCart® Purospher® RP-18e column
Eluents: A - water (0.1% TFA); B - MeCN (0.1% TFA)

t [min]	0	30	40	44.5
A [%]	70	1	1	80
B [%]	30	99	99	20

Method B1: SR064_MeOH_H_2O
Flow rate: 2.5 mL/min, column: LiChroCart® Purospher® RP-18e column
Eluents: A - water; B - MeOH

t [min]	0	12	27	32	35	42
A [%]	65	20	0	0	65	65
B [%]	35	80	100	100	35	35

Method B2: SR064_MeOH_H_2O

Flow rate: 2.5 mL/min, column: Nucleodur® Phenyl/Hexyl column

Eluents: A - water; B - MeOH

t [min]	0	12	27	32	35	42
A [%]	65	20	0	0	65	65
B [%]	35	80	100	100	35	35

Method C: SR078_ACN_H_2OmitSaeure

Flow rate: 2.5 mL/min, column: Nucleodur® Phenyl/Hexyl column

Eluents: A - water (0.1% TFA); B - MeCN (0.1% TFA)

t [min]	0	14	22	24	32
A [%]	65	0	0	65	65
B [%]	35	100	100	35	35

Method D: SR095_C18ausSR054

Flow rate: 3.0 mL/min, column: LiChroCart® Purospher® RP-18e column

Eluents: A - water (0.1% TFA); B - MeCN (0.1% TFA)

t [min]	0	20	22	28	32	33
A [%]	70	24	1	1	70	70
B [%]	30	76	99	99	30	30

Method E: SR131

Flow rate: 3.0 mL/min, column: LiChroCart® Purospher® RP-18e column

Eluents: A - water (0.1% TFA); B - MeCN (0.1% TFA)

t [min]	0	18	23	26	35
A [%]	90	0	0	90	90
B [%]	10	100	100	10	10

Method F: SR189IsokratischeTreppenVersuch2

Flow rate: 3.0 mL/min, column: LiChroCart® Purospher® RP-18e column

Eluents: A - water (0.1% TFA); B - MeCN (0.1% TFA)

t [min]	0	5	8	13	18	25	28	35	35.2	40
A [%]	20	10	8	8	5	5	0	0	20	20
B [%]	80	90	92	92	95	95	100	100	80	80

Method G: SR190

Flow rate: 3.0 mL/min, column: LiChroCart® Purospher® RP-18e column

Eluents: A - water (0.1% TFA); B - MeCN (0.1% TFA)

t [min]	0	18	25	28	35
A [%]	90	0	0	90	90
B [%]	10	100	100	10	10

Method H: SR197

Flow rate: 3.0 mL/min, column: LiChroCart® Purospher® RP-18e column

Eluents: A - water (0.1% TFA); B - MeCN (0.1% TFA)

t [min]	0	30	32	35	35,5	44
A [%]	93	65	0	0	93	93
B [%]	7	35	100	100	7	7

Method I: SR204isokFinal

Flow rate: 3.0 mL/min, column: LiChroCart® Purospher® RP-18e column

Eluents: A - water (0.1% TFA); B - MeCN (0.1% TFA)

t [min]	0	3	20	22	27	27,1	32
A [%]	65	50	50	1	1	65	65
B [%]	35	50	50	99	99	35	35

7.1.6 Instrumental analytics

7.1.6.1 Nuclear magnetic resonance spectroscopy (NMR)

NMR spectra were recorded using a Bruker Fourier 300 spectrometer (^{1}H NMR: 300 MHz, ^{13}C NMR: 76 MHz), an UltraShield™-500 spectrometer (^{1}H NMR: 500 MHz, ^{13}C NMR: 126 MHz), a Bruker UltraShield™-400 Plus spectrometer (^{31}P NMR: 162 MHz) or an Ascend 500 spectrometer (^{1}H NMR: 500 MHz, ^{13}C NMR: 126 MHz, ^{19}F NMR: 471 MHz) at room temperature. The latter was also used for spectra at 100 °C. In addition, correlation spectra (^{1}H,^{1}H-COSY, ^{1}H,^{13}C-HSQC, ^{1}H,^{13}C-HMBC, ^{1}H,^{1}H-NOESY) were recorded for analysis.

All chemical shifts in ppm were reported relative to the corresponding solvent. All coupling constants are given in Hertz (Hz). The indication of the multiplicity and shape of the signals in the spectra is as follows: s = singlet, d = doublet, t = triplet, q = quartet, m = multiplet, bs = broad signal or combinations (e.g., dt = doublet of triplets). All ^{13}C NMR spectra were recorded using drive band proton decoupling. Diastereotopic protons were distinguished by the label H_a and H_b, where H_a signifies the high-field shifted signal.

7.1.6.2 Mass spectrometry (LC-MS)

Low-resolution mass spectra were recorded using a Finnigan Surveyor® MSQ Plus instrument with liquid chromatography coupling.

The Surveyor®-LC-system consisted of a pump, an AS3000-autosampler, and a UV2000 detector. A Nucleodur® 100-5 C_{18}-column (5 µm, 3x125 mm) or a RP C_6-Phenyle Nucleodur® 100-3 (3x125 mm) column (Macherey-Nagel GmbH, Duehren, Germany) was used for liquid chromatography (LC) as stationary phase. All solvents were HPLC grade. The system was operated by the standard software Xcalibur®.

Mass spectrometry was performed on a MSQ® electro spray mass spectrometer (Thermo Fisher, Dreieich, Germany). Ionization was performed by electrospray ionization (ESI) in positive and negative mode.

The injection volume was 10-20 µL and flow rate was set to 600 µL/min MS analysis was carried out at a spray voltage of 3800 V, a capillary temperature of 350 °C and a source CID of 10 V. Spectra were acquired from 100 to 2000 m/z and at 256 nm for the UV trace.

7.1.6.3 High-resolution mass spectra (HRMS)

High-resolution mass spectra were recorded using a Thermo Scientific Q Exactive Focus with upstream *Dionex* Ultimate 3000 UHPLC$^+$. A column of the type of EC 150/2 Nucleodur C_{18} Pyramid (3 µm) was used. Ionization was performed by electrospray ionization (ESI) in positive and negative mode, with detection using an Orbitrap mass spectrometer.

7.1.6.4 IR Spectroscopy

The infrared spectra were recorded on a Bruker Alpha Platinum ATR spectrometer. All wavenumbers $\tilde{\nu}$ are given in cm^{-1}.

7.1.6.5 UV/Vis Spectroscopy

UV/Vis spectra were performed on a Varian Cary 100 UV-VIS spectrometer by *Agilent Technologies*. The UV spectra were measured in a wavelength range of 800-200 nm. The respective wavelengths of the absorption maxima max are given in nm.

7.1.6.6 Polarimetry

The rotational values $[\alpha]_{20}^{D}$ of pure optically active substances were performed on the *Perkin Elmer* 341 polarimeter and are given in $[° \cdot mL/g \cdot dm]$. The quartz cuvette used had a length of 1 dm, and a sodium vapor lamp (λ = 589 nm) was used. All concentrations given are in [g/L]. MeOH was used as the solvent.

7.1.6.7 Lyophilization

The Alpha 2-4 LD Plus freeze-drying system from *Christ* was used for lyophilization of aqueous or water-containing solutions.

7.2 Synthesis of standard building blocks

7.2.1 Synthesis of reagents and precursors

7.2.1.1 Iodoxybenzoic acid (IBX)[189]

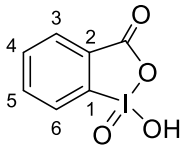

The reaction was not carried out under an inert gas atmosphere. Oxone (2 $KHSO_5$-$KHSO_4$-K_2SO_4; 59.5 g, 96.7 mmol, 3.7 eq.) was dissolved in water (240 mL). 2-Iodobenzoic acid (6.52 g, 26.3 mmol, 1.0 eq.) was added and the reaction mixture was stirred for 3 h at 70 °C. The suspension was cooled to 0 °C and filtered. The residue was washed with cooled water (8x 50 mL) and acetone (3x 50 mL). The residue was stirred in water and cooled to 2 °C for 4 d. Then, the white solid was filtered and washed with cold water. The crude product was dried under vacuum for 3 d. The resulting solid was used without further purification.

Yield (**IBX**): 3.99 g (14.2 mmol, 54%) as a white solid.

^{1}H NMR (500 MHz, DMSO-d_6): δ [ppm] = 7.82-7.87 (m, 1 H, 3-H), 7.98-8.05 (m, 2 H, 4-H, 6-H), 8.13-8.16 (m, 1 H, 5-H).

^{13}C NMR (126 MHz, DMSO-d_6): δ [ppm] = 124.99 (C-3), 130.08 (C-6), 131.45 (C-1), 132.94 (C-5), 133.37 (C-4), 146.55 (C-2), 167.47 (C=O).

$C_7H_5O_4I$ (280.02)

7.2.1.2 *N*-Cbz-3,3-diethoxypropylamine 57[137,140]

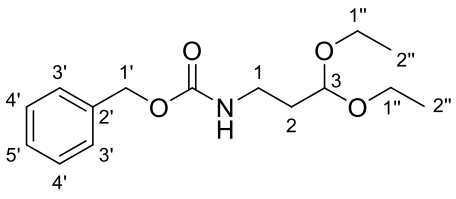

Dry triethylamine (3.5 mL, 25 mmol, 2.1 eq.) was added to a solution of 1-amino-3,3-diethoxypropane (2.0 mL, 12 mmol, 1.0 eq.) in dry dichloromethane (35 mL). The solution was cooled to 0 °C. At this temperature, benzyl chloroformate (2.1 mL, 15 mmol, 1.3 eq.) was added over 10 min and the resulting solution was stirred for 18 h. During this time, the reaction mixture warmed up to room temperature. The organic

layer was washed with saturated ammonium chloride solution (2x 30 mL), saturated sodium bicarbonate solution (30 mL) and brine (30 mL) and dried over sodium sulfate. The solvent was removed under reduced pressure. The title compound was obtained after purification by silica gel column chromatography (80 g, 5x11 cm, PE:EtOAc 8:2).

Yield (**57**): 2.99 g (10.6 mmol, 88%) as a yellowish oil.

TLC: R_f = 0.28 (PE:EtOAc 7:3).

^{1}H NMR (500 MHz, $CHCl_3$-d_1): δ [ppm] = 1.20 (t, $^3J_{2''\text{-H}/1''\text{-H}}$ = 7.1 Hz, 6 H, 2''-H), 1.83 (dt, $^3J_{2\text{-H}/1\text{-H}}$ = 6.2 Hz, $^3J_{2\text{-H}/3\text{-H}}$ = 5.7 Hz, 2 H, 2-H), 3.30 (dt, $^3J_{1\text{-H}/2\text{-H}}$ = 6.2 Hz, $^3J_{1\text{-H}/\text{NH}}$ = 6.1 Hz, 2 H, 1-H), 3.49 (dq, $^2J_{1''\text{-H}a/1''\text{-H}b}$ = 9.2 Hz, $^3J_{1''\text{-H}a/2''\text{-H}}$ = 7.1 Hz, 2 H, 1''-H_a), 3.68 (dq, $^2J_{1''\text{-H}b/1''\text{-H}a}$ = 9.2 Hz, $^3J_{1''\text{-H}b/2''\text{-H}}$ = 7.1 Hz, 2 H, 1''-H_b), 4.55 (t, $^3J_{3\text{-H}/2\text{-H}}$ = 5.7 Hz, 1 H, 3-H), 5.09 (s, 2 H, 1'-H), 5.21 (bs, 1 H, NH), 7.28-7.33 (m, 1 H, 5'-H), 7.33-7.37 (m, 4 H, 3'-H, 4'-H).

^{13}C NMR (126 MHz, $CHCl_3$-d_1): δ [ppm] = 15.25 (C-2''), 33.33 (C-2), 37.12 (C-1), 61.72 (C-1''), 66.47 (C-1'), 101.96 (C-3), 127.96, 128.42 (C-3', C-4', C-5'), 136.70 (C-2'), 156.30 (NC(=O)O).

LC-MS (ESI^+): m/z = 282.45 $[M+H]^+$.

$C_{15}H_{23}NO_4$ (281.35)

7.2.1.3 *N*-Cbz-3-aminopropanal 41[135,140]

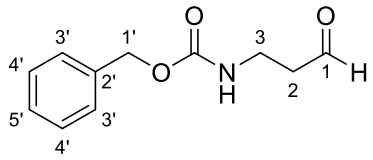

This reaction was not carried out under an inert gas atmosphere. Hydrochloric acid (0.5 M, 21.2 mL, 10.6 mmol, 1.0 eq.) was added to a solution of *N*-Cbz-3,3-diethoxy-propylamine **57** (2.97 g, 10.6 mmol, 1.0 eq.) in tetrahydrofuran (30 mL). The solution was stirred for 105 min at room temperature. Then saturated sodium bicarbonate solution (400 mL) was added, and the aqueous layer was extracted with ethyl acetate (3x 250 mL). The combined organic layers were dried over sodium sulfate. The solvent was removed under reduced pressure. The title compound was obtained after purification by silica gel column chromatography (80 g, 5x11 cm, PE:EtOAc 8:2).

Yield (**41**): 1.94 g (9.38 mmol, 88%) as a white solid.

TLC: R_f = 0.31 (PE:EtOAc 1:1).

^{1}H NMR (500 MHz, $CHCl_3$-d_1): δ [ppm] = 2.74 (t, $^3J_{2\text{-H}/3\text{-H}}$ = 5.9 Hz, 2 H, 2-H), 3.49 (dt, $^3J_{3\text{-H}/2\text{-H}}$ = 5.9 Hz, $^3J_{3\text{-H}/\text{NH}}$ = 6.0 Hz, 2 H, 3-H), 5.08 (s, 2 H, 1'-H), 5.15 (bs, 1 H, NH), 7.29-7.38 (m, 5 H, 3'-H, 4'-H, 5'-H), 9.80 (s, 1 H, 1-H).

^{13}C NMR (126 MHz, $CHCl_3$-d_1): δ [ppm] = 34.44 (C-2), 44.06 (C-3), 66.73 (C-1'), 128.06, 128.13, 128.50 (C-3', C-4', C-5'), 136.34 (C-2'), 156.26 (NC(=O)O), 201.13 (C-1).

LC-MS (ESI^+): m/z = 230.29 $[M+Na]^+$.

$C_{11}H_{13}NO_3$ (207.23)

7.2.1.4 Methyl ester phosphonate 55[137,140,163,164]

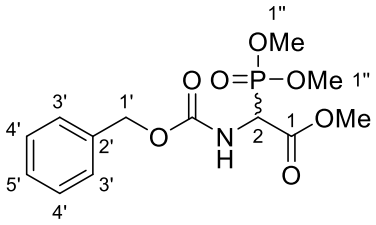

Phosphorous trichloride (3.8 mL, 44 mmol, 1.1 eq.) was added dropwise to a solution of methyl-2-methoxy-*N*-benzyloxycarbonylglycinate **54** (10.0 g, 39.5 mmol, 1.0 eq.) in dry toluene (50 mL) at 110 °C. The resulting solution was stirred for 4 h at 110 °C. Then, trimethyl phosphite (5.2 mL, 44 mmol, 1.1 eq.) was added and the resulting solution was stirred for further 2 h at 110 °C. The reaction mixture was cooled to room temperature and the solvent was removed under reduced pressure. Then, the crude product was dissolved in ethyl acetate (300 mL) and washed with saturated sodium bicarbonate solution (3x 150 mL), water (150 mL) and brine (150 mL) and was dried over sodium sulfate. The solvent was removed under reduced pressure. The crude product was suspended in *n*-hexane for 30 min. The precipitated title compound was dried under vacuum for 4 d. The precipitation was repeated, resulting in another batch of the title compound.

Yield (**55**): 10.5 g (31.6 mmol, 80%) as a white solid.

^{1}H NMR (500 MHz, DMSO-d_6): δ [ppm] = 3.69 (d, $^3J_{1''\text{-H}/\text{P}}$ = 11.0 Hz, 3 H, 1''-H), 3.70 (d, $^3J_{1''\text{-H}/\text{P}}$ = 11.0 Hz, 3 H, 1''-H), 3.71 (s, 3 H, $COOCH_3$), 4.83 (dd, $^2J_{2\text{-H}/\text{P}}$ = 23.9 Hz, $^3J_{2\text{-H}/\text{NH}}$ = 9.3 Hz, 1 H, 2-H), 5.04-5.12 (m, 2 H, 1'-H), 7.30-7.34 (m, 1 H, 5'-H), 7.36-7.39 (m, 4 H, 3'-H, 4'-H), 8.37 (dd, $^3J_{\text{NH}/2\text{-H}}$ = 9.3 Hz, $^4J_{\text{NH}/\text{P}}$ = 2.5 Hz, 1 H, NH).

^{13}C NMR (126 MHz, DMSO-d_6): δ [ppm] = 2.05 (d, $^{1}J_{C\text{-}2/P}$ = 148.8 Hz, C-2), 52.81 (COO<u>C</u>H$_3$), 53.72 (d, $^{2}J_{C\text{-}1''/P}$ = 6.7 Hz, C-1''), 53.73 (d, $^{2}J_{C\text{-}1''/P}$ = 6.4 Hz, C-1''), 66.10 (C-1'), 127.76, 127.94, 128.39 (C-3', C-4', C-5'), 136.68 (C-2'), 156.17 (d, $^{3}J_{NC(=O)O/P}$ = 8.9 Hz, NC(=O)O), 167.24 (d, $^{2}J_{C\text{-}1/P}$ = 3.8 Hz, C-1).

^{31}P NMR (162 MHz, DMSO-d_6): δ [ppm] = 18.82.

LC-MS (ESI$^+$): m/z = 354.25 $[M+Na]^+$.

$C_{13}H_{18}NO_7P$ (331.26)

7.2.1.5 Free acid phosphonate 56[137,140,163,164]

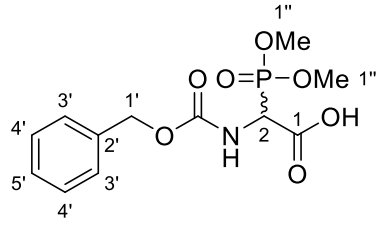

The reaction was not carried out under an inert gas atmosphere. Aqueous sodium hydroxide solution (2 M, 7.55 mL, 15.1 mmol, 1.0 eq.) was added to a solution of methyl ester phosphonate **55** (5.00 g, 15.1 mmol, 1.0 eq.) in 1,4-dioxane (4.5 mL) at 12 °C. The resulting solution was stirred for 80 min at 12 °C. Then, the pH was adjusted to pH = 1 by adding hydrochloric acid (5 M). The solution was diluted with water (20 mL) and ethyl acetate (40 mL). After phase separation, the aqueous layer was extracted with ethyl acetate (4x 20 mL). The combined organic layer was dried over sodium sulfate and the solvent was removed under reduced pressure. The colorless crude product was dried under vacuum and used without further purification.

Yield (**56**): 4.72 g (14.9 mmol, 99%) as a colorless oil.

^{1}H NMR (500 MHz, DMSO-d_6): δ [ppm] = 3.68 (d, $^{3}J_{1''\text{-}H/P}$ = 10.9 Hz, 3 H, 1''-H), 3.70 (d, $^{3}J_{1''\text{-}H/P}$ = 11.7 Hz, 3 H, 1''-H), 4.71 (dd, $^{2}J_{2\text{-}H/P}$ = 24.1 Hz, $^{3}J_{2\text{-}H/NH}$ = 9.5 Hz, 1 H, 2-H), 5.04-5.12 (m, 2 H, 1'-H), 7.30-7.35 (m, 1 H, 5'-H), 7.35-7.39 (m, 4 H, 3'-H, 4'-H), 8.14 (dd, $^{3}J_{NH/2\text{-}H}$ = 9.5 Hz, $^{4}J_{NH/P}$ = 1.7 Hz, 1 H, NH), 13.34 (bs, 1 H, COOH).

^{13}C NMR (126 MHz, DMSO-d_6): δ [ppm] = 52.54 (d, $^{1}J_{C\text{-}2/P}$ = 147.9 Hz, C-2), 54.02 (d, $^{2}J_{C\text{-}1''/P}$ = 6.5 Hz, C-1''), 66.83 (C-1'), 128.17, 128.34, 128.82 (C-3', C-4', C-5'), 137.23 (C-2'), 156.64 (d, $^{3}J_{NC(=O)O/P}$ = 8.6 Hz, NC(=O)O), 168.34 (d, $^{2}J_{C\text{-}1/P}$ = 4.0 Hz, C-1).

^{31}P NMR (162 MHz, DMSO-d_6): δ [ppm] = 19.78.

LC-MS (ESI^+): m/z = 340.25 $[M+Na]^+$.

$C_{12}H_{16}NO_7P$ (317.26)

7.2.1.6 *Tert*-butyl ester phosphonate 20[137,140,163,164]

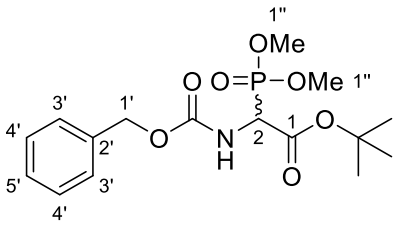

A solution of free acid phosphonate **56** (4.72 g, 14.9 mmol, 1.0 eq.) in dry dichloromethane (50 mL) was added to *tert*-butanol (200 mL) over molecular sieve (3/4 Å). The solution was stirred for 4 h at room temperature. Then *N*-ethoxycarbonyl-2-ethoxy-1,2-dihydroquinoline (4.43 g, 17.9 mmol, 1.2 eq.) was added and the resulting mixture was stirred for further 17 h at room temperature. The molecular sieves were filtered off through celite® and washed with ethyl acetate (4x 100 mL). The solvent was removed under reduced pressure. The residue was dissolved in ethyl acetate (250 mL) and cooled to 0 °C. The organic layer was washed with cooled hydrochloric acid (0.5 M, 3x 50 mL) and saturated sodium bicarbonate solution (2x 50 mL) and was dried over sodium sulfate. The solvent was removed under reduced pressure. The title compound was obtained after purification by silica gel column chromatography (100 g, 6x9 cm, PE:EtOAc 1:1 → 4:6).

Yield (**20**): 4.11 g (11.0 mmol, 74%) as a white solid.

TLC: R_f = 0.17 (CH_2Cl_2:MeOH 9:1).

^{1}H NMR (500 MHz, DMSO-d_6): δ [ppm] = 1.42 (s, 9 H, $OC(CH_3)_3$), 3.69 (d, $^3J_{1''\text{-H/P}}$ = 10.9 Hz, 3 H, 1''-H), 3.70 (d, $^3J_{1''\text{-H/P}}$ = 11.1 Hz, 3 H, 1''-H), 4.68 (dd, $^2J_{2\text{-H/P}}$ = 23.7 Hz, $^3J_{2\text{-H/NH}}$ = 9.4 Hz, 1 H, 2-H), 5.05-5.11 (m, 2 H, 1'-H), 7.30-7.35 (m, 1 H, 5'-H), 7.35-7.39 (m, 4 H, 3'-H, 4'-H), 8.20 (dd, $^3J_{\text{NH/2-H}}$ = 9.4 Hz, $^4J_{\text{NH/P}}$ = 2.1 Hz, 1 H, NH).

^{13}C NMR (126 MHz, DMSO-d_6): δ [ppm] = 27.47 ($OC(\underline{C}H_3)_3$, 52.68 (d, $^1J_{\text{C-2/P}}$ = 146.8 Hz, C-2), 53.57 (d, $^2J_{\text{C-1''/P}}$ = 6.4 Hz, C-1''), 65.99 (C-1'), 82.29 ($O\underline{C}(CH_3)_3$), 127.70, 127.87, 128.33 (C-3', C-4', C-5'), 136.71 (C-2'), 156.15 (d, $^3J_{CP}$ = 8.9 Hz, NC(=O)O), 165.53 (d, $^2J_{CP}$ = 3.4 Hz, C-1).

^{31}P NMR (162 MHz, DMSO-d_6): δ [ppm] = 19.46.

LC-MS (ESI^+): m/z = 374.25 $[M+H]^+$.

$C_{14}H_{24}NO_7P$ (373.34)

7.2.1.7 *S*-methyl *O*-(15-methylhexadecyl) carbonodithioate 81[156]

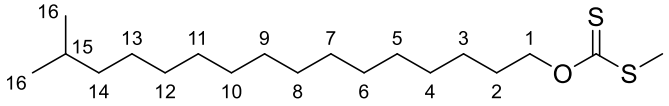

Sodium hydride (60% in mineral oil, 395 mg, 9.88 mmol, 2.5 eq.) was added to a solution of 15-methylhexadecan-1-ol (1.00 g, 3.90 mmol, 1.0 eq.) in dry tetrahydrofuran (12 mL) at 0 °C. The mixture was stirred for 1 h at room temperature. Carbon disulfide (360 µL, 5.96 mmol, 1.5 eq.) in dry tetrahydrofuran (600 µL) was added to the suspension at 0 °C and stirred for 1 h at room temperature. Iodomethane (370 µL, 5.94 mmol, 1.5 eq.) in dry tetrahydrofuran (600 µL) was added to the suspension at 0 °C and the reaction mixture was stirred for 5 h at room temperature. The reaction mixture was diluted with saturated ammonium chloride solution (25 mL) and extracted with ethyl acetate (3x 20 mL). The combined organic layers were dried over sodium sulfate. The solvent was removed under reduced pressure. The title compound was obtained after purification by silica gel column chromatography (42 g, 3.5x11 cm, PE:EtOAc 100:0 → 98.2 → 95:5).

Yield (**81**): 1.10 g (3.17 mmol, 81%) as a yellow oil.

TLC: R_f = 0.65 (PE:EtOAc 95:5).

^{1}H NMR (500 MHz, MeOH-d_4): δ [ppm] = 0.88 (d, $^3J_{16\text{-H}/15\text{-H}}$ = 6.7 Hz, 6 H, 16-H), 1.15-1.21 (m, 2 H, 14-H), 1.25-1.38 (m, 20 H, 4-13-H), 1.38-1.46 (m, 2 H, 3-H), 1.53 (tsep, $^3J_{15\text{-H}/16\text{-H}}$ = 6.7 Hz, $^3J_{15\text{-H}/14\text{-H}}$ = 6.6 Hz, 1 H, 15-H), 1.81 (tt, $^3J_{2\text{-H}/3\text{-H}}$ = 7.4 Hz, $^3J_{2\text{-H}/1\text{-H}}$ = 6.6 Hz, 2 H, 2-H), 2.55 (s, 3 H, SCH_3), 4.61 (t, $^3J_{1\text{-H}/2\text{-H}}$ = 6.6 Hz, 2 H, 1-H).

^{13}C NMR (126 MHz, MeOH-d_4): δ [ppm] = 19.53 (SCH_3), 23.57 (C-16), 27.50 (C-3), 29.06 (C-3-14), 29.67 (C-2), 29.82 (C-15), 30.80, 31.10, 31.15, 31.23, 31.27, 31.29, 31.33, 31.56 (C-3-14), 40.77 (C-14), 75.63 (C-1), 218.01 (OC(=S)S).

$C_{19}H_{38}OS_2$ (346.63)

7.2.1.8 15-Methylhexadec-1-ene 46[156]

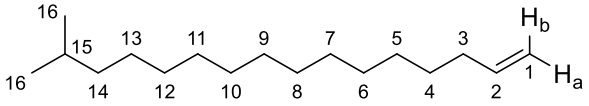

A 250 mL three-neck round bottom flask was equipped with a reflux condenser and a bleach trap (with aqueous sodium hypochlorite solution). Methyl xanthate **81** (1.10 g, 3.17 mmol, 1.0 eq.) was heated slowly over a *Bunsen* burner flame for 5 min under constant nitrogen flow. After cooling, the reflux condenser was rinsed with petroleum ether and aqueous hypochlorous acid solution (3.7%, 30 mL). The layers were separated, and the aqueous layer was extracted with petroleum ether (3x 25 mL). The title compound was obtained after purification by silica gel column chromatography (40 g, 3.5x10.5 cm, PE 100%) to give a colorless, odorless liquid.

Yield (**46**): 551 mg (2.31 mmol, 73%) as a colorless, odorless liquid.

TLC: R_f = 0.73 (PE 100%).

^{1}H NMR (500 MHz, $CHCl_3$-d_1): δ [ppm] = 0.86 (d, $^3J_{16\text{-}H/15\text{-}H}$ = 6.6 Hz, 6 H, 16-H), 1.12-1.18 (m, 2 H, 14-H), 1.24-1.29 (m, 18 H, 5-13-H), 1.34-1.41 (m, 2 H, 4-H), 1.52 (tsep, $^3J_{15\text{-}H/16\text{-}H}$ = 6.6 Hz, $^3J_{15\text{-}H/14\text{-}H}$ = 6.6 Hz, 1 H, 15-H), 2.01-2.07 (m, 2 H, 3-H), 4.93 (ddt, $^3J_{1\text{-}Ha/2\text{-}H}$ = 10.3 Hz, $^2J_{1\text{-}Ha/1\text{-}Hb}$ = 2.2 Hz, $^4J_{1\text{-}Ha/3\text{-}H}$ = 1.1 Hz, 1 H, 1-H_a), 4.99 (ddt, $^3J_{1\text{-}Hb/2\text{-}H}$ = 17.1 Hz, $^2J_{1\text{-}Hb/1\text{-}Ha}$ = 2.2 Hz, $^4J_{1\text{-}Hb/3\text{-}H}$ = 1.6 Hz, 1 H, 1-H_b), 5.82 (ddt, $^3J_{2\text{-}H/1\text{-}Hb}$ = 17.1 Hz, $^3J_{2\text{-}H/1\text{-}Ha}$ = 10.3 Hz, $^3J_{2\text{-}H/3\text{-}H}$ = 6.7 Hz, 1 H, 2-H).

^{13}C NMR (126 MHz, $CHCl_3$-d_1): δ [ppm] = 22.81 (C-16), 27.58 (C-15), 28.13 (C-5-13), 29.11 (C-4), 29.32, 29.67, 29.78, 29.82, 29.84, 29.88, 30.10 (C-5-13), 33.98 (C-3), 39.22 (C-14), 114.21 (C-1), 139.43 (C-2).

$C_{17}H_{34}$ (238.46)

7.2.1.9 15-Methylhexadec-1,2-diole 83[178,179]

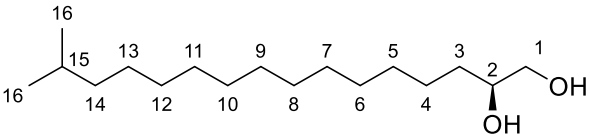

This reaction was not carried out under an inert gas atmosphere. 15-Methylhexadec-1-ene **46** (200 mg, 839 µmol, 1.0 eq.) was dissolved in a mixture of *tert*-butanol and water (1:1, 8 mL). AD-mix α (2.17 g, 1.34 mmol, 1.6 eq.) was added, and the reaction

mixture was stirred for 48 h at room temperature in darkness. The *tert*-butanol was removed under reduced pressure. The residue was extracted with ethyl acetate (3x 15 mL). The combined organic layers were washed with brine (40 mL) and dried over sodium sulfate. The title compound was obtained after removal of the solvent and was used without further purification.

Yield (**83**): 219 mg (804 µmol, 96%) as white solid.

TLC: R_f = 0.29 (CH_2Cl_2:MeOH 9:1).

^{1}H NMR (500 MHz, $CHCl_3$-d_1): δ [ppm] = 0.86 (d, $^3J_{16\text{-H}/15\text{-H}}$ = 6.6 Hz, 6 H, 16-H), 1.15 (dt, $^3J_{14\text{-H}/15\text{-H}}$ = 6.8 Hz, $^3J_{14\text{-H}/13\text{-H}}$ = 6.8 Hz, 2 H, 14-H), 1.23-1.34 (m, 19 H, 4-H_a, 5-13-H), 1.41-1.46 (m, 3 H, 3-H, 4-H_b), 1.51 (tsep, $^3J_{15\text{-H}/14\text{-H}}$ = 6.8 Hz, $^3J_{15\text{-H}/16\text{-H}}$ = 6.6 Hz, 1 H, 15-H), 3.44 (dd, $^2J_{1\text{-H}a/1\text{-H}b}$ = 11.0 Hz, $^3J_{1\text{-H}a/2\text{-H}}$ = 7.7 Hz, 1 H, 1-H_a), 3.66 (dd, $^2J_{1\text{-H}b/1\text{-H}a}$ = 11.0 Hz, $^3J_{1\text{-H}b/2\text{-H}}$ = 3.1 Hz, 1 H, 1-H_b), 3.68-3.74 (m, 1 H, 2-H).

^{13}C NMR (126 MHz, $CHCl_3$-d_1): δ [ppm] = 22.81 (C-16), 25.68 (C-4), 27.56 (C-5-13), 28.11 (C-15), 29.69, 29.73, 29.79, 29.82, 29.83, 29.87, 30.09 (C-5-13), 33.36 (C-3), 39.21 (C-14), 67.01 (C-1), 72.47 (C-2).

IR (ATR) υ [cm^{-1}]: 3744, 3323, 2951, 2914, 2848, 1470, 1086, 1066, 718, 578.

HRMS (ESI^-): calcd. for $C_{17}H_{35}O_2^-$: 271.2642, found: 271.2622 $[M\text{-}H]^-$.

$C_{17}H_{36}O_2$ (272.27)

7.2.1.10 14-Methylhexadecanal 84

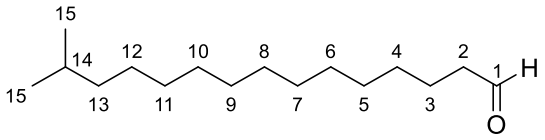

The reaction was not carried out under an inert gas atmosphere. 15-methylhexadecane-1,2-diol **83** (48.5 mg, 178 µmol, 1.0 eq.) was dissolved in *tert*-butanol (2.5 mL). A solution of sodium periodate (76.1 mg, 356 µmol, 2.0 eq.) in water (2.5 mL) was added, and the reaction mixture was stirred for 2 h at room temperature in darkness. The *tert*-butanol was removed under reduced pressure. The residue was extracted with diethyl ether (3x 2 mL). The title compound was obtained after removal of the solvent and was used without further purification.

Yield (**84**): 42.3 mg (176 µmol, 99%) as a colorless oil.

^{1}H NMR (500 MHz, $CHCl_3$-d_1): δ [ppm] = 0.86 (d, $^{3}J_{16\text{-}H/15\text{-}H}$ = 6.6 Hz, 6 H, 16-H), 1.09-1.18 (m, 2 H, 13-H), 1.22-1.35 (m, 18 H, 4-12-H), 1.44-1.56 (m, 1 H, 14-H), 1.56-1.69 (m, 2 H, 3-H), 2.41 (dt, $^{3}J_{2\text{-}H/3\text{-}H}$ = 7.4 Hz, $^{3}J_{2\text{-}H/1\text{-}H}$ = 1.9 Hz, 2 H, 2-H), 9.76 (t, $^{3}J_{1\text{-}H/2\text{-}H}$ = 1.9 Hz, 1 H, 1-H).

^{13}C NMR (126 MHz, $CHCl_3$-d_1): δ [ppm] = 22.22 (C-3), 22.80 (C-15), 27.55 (C-4-12), 28.10 (C-14), 29.30, 29.49, 29.56, 29.71, 29.77, 29.80, 29.84, 30.07 (C-4-12), 39.19 (C-13), 44.06 (C-2), 203.18 (C-1).

LC-MS (ESI^+): m/z = 282.40 $[M+MeCN+H]^+$.

$C_{16}H_{32}O$ (240.25)

7.2.1.11 14-Methylpentadecanoic acid 45

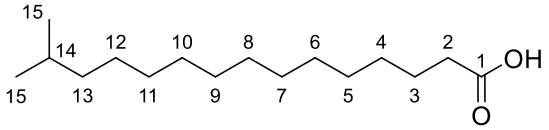

The reaction was not carried out under an inert gas atmosphere. 14-methylpentadecanal **84** (32.3 mg, 134 µmol, 1.0 eq.) was dissolved in *tert*-butanol (2.5 mL). Then, an aqueous hydrogen peroxide solution (33%, 400 µL, 5.66 mmol, 42 eq.) was added to the solution. A mixture of sodium chlorite (109 mg, 1.21 mmol, 9.0 eq.) and sodium dihydrogen phosphate (146 mg, 936 µmol, 7.0 eq) in water (1.0 mL) was added dropwise and the reaction mixture was stirred for 19 h at room temperature. The *tert*-butanol was removed under reduced pressure. The aqueous layer was extracted with *n*-hexane (4x 2.5 mL). The title compound was obtained after removal of the solvent and was used without further purification.

Yield (**45**): 32.8 mg (128 mmol, 95%) as a white solid.

TLC: R_f = 0.47 (PE:EtOAc:HCOOH acid 78:20:2).

^{1}H NMR (500 MHz, DMSO-d_6): δ [ppm] = 0.84 (d, $^{3}J_{15\text{-}H/14\text{-}H}$ = 6.7 Hz, 6 H, 15-H), 1.13 (dt, $^{3}J_{13\text{-}H/14\text{-}H}$ = 6.7 Hz, $^{3}J_{13\text{-}H/12\text{-}H}$ = 6.8 Hz, 2 H, 13-H), 1.19-1.29 (m, 18 H, 4-12-H), 1.43-1.54 (m, 3 H, 3-H, 14-H), 2.17 (t, $^{3}J_{2\text{-}H/3\text{-}H}$ = 7.4 Hz, 2 H, 2-H), 11.86 (bs, 1 H, COOH).

^{13}C NMR (126 MHz, DMSO-d_6): δ [ppm] = 22.52 (C-15), 24.50 (C-3), 26.78 (C-4-12), 27.38 (C-14), 28.55, 28.74, 28.90, 29.98, 29.02, 29.03, 29.06, 29.30 (C-4-12), 33.68 (C-2), 38.47 (C-13), 174.52 (C-1).

IR (ATR) υ [cm^{-1}]: 2915, 2850, 1694, 1472, 1409, 1229, 1206, 1187, 915, 717.

LC-MS (ESI^-): m/z = 255.33 $[M-H]^-$.

HRMS (ESI^-): calcd. for $C_{16}H_{31}O_2^-$: 255.2329, found: 255.2306 $[M-H]^-$.

$C_{16}H_{32}O_2$ (256.24)

7.2.1.12 (5-Carboxypentyl) triphenylphosphonium bromide 48[157]

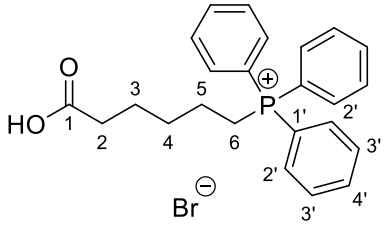

A mixture of 6-bromohexanoic acid (1.00 g, 5.13 mmol, 1.0 eq.) and triphenyl phosphine (1.35 g, 5.15 mmol, 1.0 eq.) in dry toluene (6 mL) was refluxed for 46 h. The reaction mixture was cooled to room temperature and the solvent was removed under reduced pressure. Then, the residue was redissolved in toluene (10 mL) and refluxed for 30 min. After filtration at 110 °C, the title compound was obtained and used without further purification.

Yield (**48**): 2.05 g (4.48 mmol, 87%) as a white solid.

^{1}H NMR (500 MHz, DMSO-d_6): δ [ppm] = 1.44-1.58 (m, 6 H, 3-H, 4-H, 5-H), 2.16 (t, $^3J_{2\text{-H}/3\text{-H}}$ = 6.9 Hz, 2 H, 2-H), 3.55-3.64 (m, 2 H, 6-H), 7.74-7.84 (m, 12 H, 2'-H, 3'-H), 7.87-7.93 (m, 3 H, 4'-H), 12.06 (s, 1 H, COOH).

^{13}C NMR (126 MHz, DMSO-d_6): δ [ppm] = 20.10 (d, $^1J_{\text{C-6/P}}$ = 49.9 Hz, C-6), 21.55 (d, $^3J_{\text{C-4/P}}$ = 4.4 Hz, C-4), 23.64 (C-3), 29.31 (d, $^2J_{\text{C-5/P}}$ = 17.1 Hz, C-5), 33.26 (C-2), 118.54 (d, $^1J_{\text{C-1'/P}}$ = 85.4 Hz, C-1'), 130.22 (d, $^2J_{\text{C-2'/P}}$ = 12.4 Hz, C-2'), 133.59 (d, $^3J_{\text{C-3'/P}}$ = 10.1 Hz, C-3'), 134.87 (d, $^4J_{\text{C-4'/P}}$ = 2.8 Hz, C-4'), 174.26 (C-1).

^{31}P NMR (162 MHz, DMSO-d_6): δ [ppm] = 24.04.

LC-MS (ESI^+): m/z = 377.22 $[M-Br^-]^+$.

HRMS (ESI^+): calcd. for $C_{24}H_{26}O_2P^+$: 377.1665, found: 377.1649 $[M-Br^-]^+$.

$C_{24}H_{26}O_2P^+ \cdot Br^-$ (457.35)

7.2.1.13 (*Z*)-Tridec-6-enoic acid 47[157]

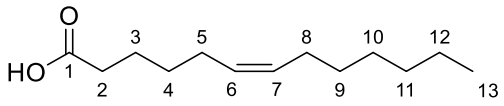

Sodium bis(trimethylsilyl)amide solution (1 M in dry tetrahydrofuran, 1.3 mL, 1.3 mmol, 2.0 eq.) was added dropwise to a suspension of phosphonium salt **48** (300 mg, 656 µmol, 1.0 eq.) in dry tetrahydrofuran (5 mL). The mixture was stirred for 2 h at room temperature. The suspension was cooled to -82 °C. Then, heptanal (91.4 µL, 656 µmol, 1.0 eq.) in dry tetrahydrofuran (0.5 mL) was added dropwise at -82 °C and the reaction mixture was stirred for further 16 h. During this time, the reaction mixture warmed up to room temperature. The reaction mixture was purred in water (10 mL) and was then extracted with diethyl ether (3x 15 mL). The aqueous layer was acidified (pH ≈ 2) with aqueous hydrogen chloride solution (10%) and extracted with diethyl ether (3x 30 mL). The solvent of the latter organic layer was removed under reduced pressure. The title compound was obtained after purification by silica gel column chromatography (50 g, 3x24 cm, PE:EtOAc:HCOOH 90:10:1).

Yield (**47**): 71.3 g (336 µmol, 51%) as a colorless yellow oil (*Z*/*E* = 94:6).

TLC: R_f = 0.30 (PE:EtOAc:HCOOH 90:10:1).

^{1}H NMR (500 MHz, DMSO-d_6, 100 °C): δ [ppm] = 0.88 (t, $^3J_{13\text{-H}/12\text{-H}}$ = 7.0 Hz, 3 H, 13-H), 1.26-1.33 (m, 8 H, 9-12-H), 1.37 (tt, $^3J_{4\text{-H}/5\text{-H}}$ = 7.4 Hz, $^3J_{4\text{-H}/3\text{-H}}$ = 7.4 Hz, 2 H, 4-H), 1.55 (tt, $^3J_{3\text{-H}/2\text{-H}}$ = 7.5 Hz, $^3J_{3\text{-H}/4\text{-H}}$ = 7.4 Hz, 2 H, 3-H), 1.99-2.06 (m, 4 H, 5-H, 8-H), 2.20 (t, $^3J_{2\text{-H}/3\text{-H}}$ = 7.5 Hz, 2 H, 2-H), 5.34 (dt, $^3J_{6\text{-H}/7\text{-H}}$ = 10.8 Hz, $^3J_{6\text{-H}/5\text{-H}}$ = 5.3 Hz, 1 H, 6-H), 5.36 (dt, $^3J_{7\text{-H}/6\text{-H}}$ = 10.8 Hz, $^3J_{7\text{-H}/8\text{-H}}$ = 5.4 Hz, 1 H, 7-H), 11.49 (s, 1 H, COOH).

^{13}C NMR (126 MHz, DMSO-d_6, 100 °C): δ [ppm] = 13.10 (C-13), 21.35 (C-9-12), 23.67 (C-3), 25.83 (C-5), 26.11 (C-8), 27.66 (C-9-12), 28.14 (C-4), 28.50, 30.51 (C-9-12), 33.14 (C-2), 128.74 (C-6), 129.35 (C-7), 173.43 (C-1).

LC-MS (ESI^-): m/z = 211.48 $[M-H]^-$.

HRMS (ESI^+): calcd. for $C_{13}H_{25}O_2^+$: 213.1850, found: 213.1850 $[M+H]^+$.

$C_{13}H_{24}O_2$ (212.33)

7.2.2 Synthesis of the nucleoside building block

7.2.2.1 2',3',5'-*O*-tris-(*tert*-butyldimethylsily)uridine 53[137,140]

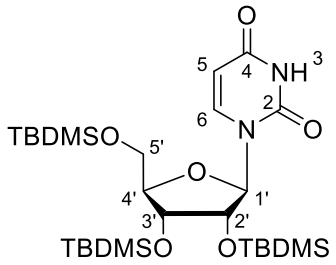

Imidazole (6.29 g, 92.4 mmol, 4.5 eq.) and *tert*-butyldimethylsilyl chloride (13.9 g, 92.2 mmol, 4.5 eq.) were added to a solution of uridine (5.00 g, 20.5 mmol, 1.0 eq.) in dry pyridine (50 mL). The reaction mixture was stirred for 3 d at room temperature. Water (10 mL) was added to the cooled (0 °C) reaction mixture. The solvent was removed under reduced pressure and the residue was dissolved in ethyl acetate (350 mL). The organic layer was washed with water (3x 175 mL), saturated sodium bicarbonate solution (175 mL) and brine (175 mL) and was dried over sodium sulfate. The solvent was removed under reduced pressure. The title compound was obtained after purification by silica gel column chromatography (300 g, 7x20 cm, PE: EtOAc 8:2).

Yield (**53**): 9.83 g (16.8 mmol, 82%) as a colorless foamy solid.

TLC: R_f = 0.71 (PE:EtOAc 1:1).

^{1}H NMR (500 MHz, DMSO-d_6): δ [ppm] = -0.03 (s, 3 H, $SiCH_3$), 0.02 (s, 3 H, $SiCH_3$), 0.08 (s, 3 H, $SiCH_3$), 0.09 (s, 3 H, $SiCH_3$), 0.10 (s, 3 H, $SiCH_3$), 0.10 (s, 3 H, $SiCH_3$), 0.83 (s, 9 H, $SiC(CH_3)_3$), 0.88 (s, 9 H, $SiC(CH_3)_3$), 0.90 (s, 9 H, $SiC(CH_3)_3$), 3.71 (dd, $^2J_{5'\text{-}Ha/5'\text{-}Hb}$ = 11.5 Hz, $^3J_{5'\text{-}Ha/4'\text{-}H}$ = 2.9 Hz, 1 H, 5'-H_a), 3.86 (dd, $^2J_{5'\text{-}Hb/5'\text{-}Ha}$ = 11.5 Hz, $^3J_{5'\text{-}Hb/4'\text{-}H}$ = 3.6 Hz, 1 H, 5'-H_b), 3.94 (ddd, $^3J_{4'\text{-}H/3'\text{-}H}$ = 3.8 Hz, $^3J_{4'\text{-}H/5'\text{-}Hb}$ = 3.6 Hz, $^3J_{4'\text{-}H/5'\text{-}Ha}$ = 2.9 Hz, 1 H, 4'-H), 4.06 (dd, $^3J_{3'\text{-}H/4'\text{-}H}$ = 3.8 Hz, $^3J_{3'\text{-}H/2'\text{-}H}$ = 3.8 Hz, 1 H, 3'-H), 4.22 (dd, $^3J_{2'\text{-}H/1'\text{-}H}$ = 5.8 Hz, $^3J_{2'\text{-}H/3'\text{-}H}$ = 3.8 Hz, 1 H, 2'-H), 5.63 (d, $^3J_{5\text{-}H/6\text{-}H}$ = 8.2 Hz, 1 H, 5-H), 5.81 (d, $^3J_{1'\text{-}H/2'\text{-}H}$ = 5.8 Hz, 1 H, 1'-H), 7.77 (d, $^3J_{6\text{-}H/5\text{-}H}$ = 8.2 Hz, 1 H, 6-H), 11.42 (s, 1 H, 3-NH).

^{13}C NMR (126 MHz, DMSO-d_6): δ [ppm] = -5.59 ($SiCH_3$), -5.54 ($SiCH_3$), -4.97 ($SiCH_3$), -4.92 ($SiCH_3$), -4.78 ($SiCH_3$), -4.59 ($SiCH_3$), 17.63 ($SiC(CH_3)_3$), 17.78 ($SiC(CH_3)_3$), 18.06 ($SiC(CH_3)_3$), 25.59 ($SiC(CH_3)_3$), 25.73 ($SiC(CH_3)_3$), 25.84 ($SiC(CH_3)_3$), 62.35 (C-5'), 71.68 (C-3'), 74.51 (C-2'), 84.79 (C-4'), 86.97 (C-1'), 101.93 (C-5), 139.92 (C-6), 150.65 (C-2), 162.93 (C-4).

LC-MS (ESI^+): m/z = 587.25 $[M+H]^+$.

$C_{27}H_{54}N_2O_6Si_3$ (586.99)

7.2.2.2 2',3'-*O*-*bis*-(*tert*-butyldimethylsily)uridine 42[137,140]

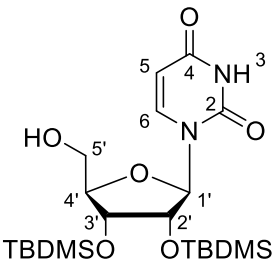

The reaction was not carried out under an inert gas atmosphere. Aqueous trifluoroacetic acid (50%, 38 mL) was added dropwise to a solution of 2',3',5'-*O*-tris-(*tert*-butyldimethylsilyl)uridine **53** (3.65 g, 6.21 mmol, 1.0 eq.) in tetrahydrofuran (70 mL) at 0 °C. The reaction was stirred for 5.5 h at 0 °C. Then, saturated sodium bicarbonate solution (200 mL) and sodium carbonate were added to the reaction until a pH ≈ 8 was reached. The aqueous layer was extracted with ethyl acetate (2x 100 mL). The combined organic layers were dried over sodium sulfate. The solvent was removed under reduced pressure. The title compound was obtained after purification by silica gel column chromatography (290 g, 6x24 cm, CH_2Cl_2:EtOAc 7:3).

Yield (**42**): 2.77 g (5.86 mmol, 94%) as a white solid.

TLC: R_f = 0.30 (CH_2Cl_2:EtOAc 7:3).

^{1}H NMR (500 MHz, DMSO-d_6): δ [ppm] = -0.03 (s, 3 H, $SiCH_3$), 0.02 (s, 3 H, $SiCH_3$), 0.08 (s, 3 H, $SiCH_3$), 0.09 (s, 3 H, $SiCH_3$), 0.83 (s, 9 H, $SiC(CH_3)_3$), 0.89 (s, 9 H, $SiC(CH_3)_3$), 3.56 (ddd, $^2J_{5'\text{-}H_a/5'\text{-}H_b}$ = 12.1 Hz, $^3J_{5'\text{-}H_a/OH}$ = 4.3 Hz, $^3J_{5'\text{-}H_a/4'\text{-}H}$ = 3.0 Hz, 1 H, 5'-H_a), 3.65 (ddd, $^2J_{5'\text{-}H_b/5'\text{-}H_a}$ = 12.1 Hz, $^3J_{5'\text{-}H_b/OH}$ = 4.9 Hz, $^3J_{5'\text{-}H_b/4'\text{-}H}$ = 3.5 Hz, 1 H, 5'-H_b), 3.88 (ddd, $^3J_{4'\text{-}H/5'\text{-}H_b}$ = 3.5 Hz, $^3J_{4'\text{-}H/5'\text{-}H_a}$ = 3.0 Hz, $^3J_{4'\text{-}H/3'\text{-}H}$ = 3.0 Hz, 1 H, 4'-H), 4.13 (dd, $^3J_{3'\text{-}H/2'\text{-}H}$ = 4.5 Hz, $^3J_{3'\text{-}H/4'\text{-}H}$ = 3.0 Hz, 1 H, 3'-H), 4.25 (dd, $^3J_{2'\text{-}H/1'\text{-}H}$ = 6.0 Hz, $^3J_{2'\text{-}H/3'\text{-}H}$ = 4.5 Hz, 1 H, 2'-H), 5.23 (dd, $^3J_{OH/5'\text{-}H_b}$ = 4.9 Hz, $^3J_{OH/5'\text{-}H_a}$ = 4.3 Hz, 1 H, OH), 5.69 (d, $^3J_{5\text{-}H/6\text{-}H}$ = 8.1 Hz, 1 H, 5-H), 5.81 (d, $^3J_{1'\text{-}H/2'\text{-}H}$ = 6.0 Hz, 1 H, 1'-H), 7.93 (d, $^3J_{6\text{-}H/5\text{-}H}$ = 8.1 Hz, 1 H, 6-H), 11.35 (s, 1 H, NH).

^{13}C NMR (126 MHz, DMSO-d_6): δ [ppm] = -5.05 ($SiCH_3$), -4.87 ($SiCH_3$), -4.76 ($SiCH_3$), -4.63 ($SiCH_3$), 17.61 ($SiC(CH_3)_3$), 17.76 ($SiC(CH_3)_3$), 25.59 ($SiC(CH_3)_3$), 25.72 ($SiC(CH_3)_3$),

60.40 (C-5'), 71.91 (C-3'), 74.53 (C-2'), 85.52 (C-4'), 86.84 (C-1'), 102.02 (C-5), 140.35 (C-6), 150.76 (C-2), 162.97 (C-4).

LC-MS (ESI^+): m/z = 473.42 $[M+H]^+$.

$C_{21}H_{40}N_2O_6Si_2$ (472.73)

7.2.2.3 2',3'-*O*-bis-(*tert*-butyldimethylsily)uridine 5'-aldehyde 19[137,140]

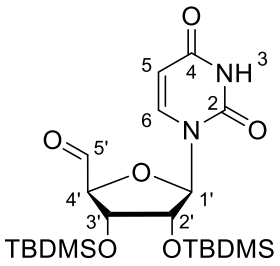

2-Iodoxybenzoic acid (stabilized with benzoic acid and isophthalic acid; 1.50 g, 5.36 mmol, 2.5 eq.) was added to a solution of 2',3'-*O*-bis-(*tert*-butyldimethylsilyl)uridine **42** (1.02 g, 2.16 mmol, 1.0 eq.) in dry acetonitrile (20 mL). The reaction mixture was stirred for 120 min at 80 °C. The suspension was cooled to 0 °C, filtered and washed with ethyl acetate (3x 20 mL). The solvent was removed under reduced pressure. The title compound was obtained after purification by silica gel column chromatography (60 g, 5x8 cm, Et_2O:CH_2Cl_2 1:1).

Yield (**19**): 803 mg (1.71 mmol, 79% calcd. from the ^1H NMR spectrum) as a colorless foamy solid with traces of stabilizer.

TLC: R_f = 0.18 (PE:EtOAc 3:7).

^1H NMR (500 MHz, $CHCl_3$-d_1): δ [ppm] = 0.01 (s, 3 H, $SiCH_3$), 0.05 (s, 3 H, $SiCH_3$), 0.12 (s, 3 H, $SiCH_3$), 0.12 (s, 3 H, $SiCH_3$), 0.87 (s, 9 H, $SiC(CH_3)_3$), 0.93 (s, 9 H, $SiC(CH_3)_3$), 4.24 (dd, $^3J_{3'\text{-H}/2'\text{-H}}$ = 4.0 Hz, $^3J_{3'\text{-H}/4'\text{-H}}$ = 3.5 Hz, 1 H, 3'-H), 4.33 (dd, $^3J_{2'\text{-H}/1'\text{-H}}$ = 5.7 Hz, $^3J_{2'\text{-H}/3'\text{-H}}$ = 4.0 Hz, 1 H, 2'-H), 4.54 (d, $^3J_{4'\text{-H}/3'\text{-H}}$ = 3.5 Hz, 1 H, 4'-H), 5.73 (d, $^3J_{1'\text{-H}/2'\text{-H}}$ = 5.7 Hz, 1 H, 1'-H), 5.80 (dd, $^3J_{5\text{-H}/6\text{-H}}$ = 8.2 Hz, $^4J_{5\text{-H}/3\text{-NH}}$ = 2.1 Hz, 1 H, 5-H), 7.68 (d, $^3J_{6\text{-H}/5\text{-H}}$ = 8.2 Hz, 1 H, 6-H), 8.62 (bs, 1 H, 3-NH), 9.82 (s, 1 H, 5'-H).

^{13}C NMR (126 MHz, $CHCl_3$-d_1): δ [ppm] = -4.84 ($SiCH_3$), -4.79 ($SiCH_3$), -4.55 ($SiCH_3$), -4.38 ($SiCH_3$), 18.05 ($SiC(CH_3)_3$), 18.19 ($SiC(CH_3)_3$), 25.79 ($SiC(CH_3)_3$), 25.85 ($SiC(CH_3)_3$), 73.19 (C-3'), 73.85 (C-2'), 88.46 (C-4'), 92.48 (C-1'), 102.81 (C-5), 141.67 (C-6), 150.03 (C-2), 162.94 (C-4), 199.60 (C-5').

LC-MS (ESI^+): m/z = 471.45 $[M+H]^+$.

$C_{21}H_{38}N_2O_6Si_2$ (470.23)

7.2.2.4 *Z*-didehydro nucleosyl amino acid 21[137,140]

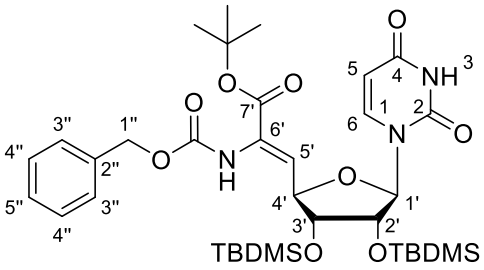

Potassium bis(trimethylsilyl)amide solution (0.5 M in dry toluene, 6.8 mL, 3.4 mmol, 0.8 eq) was dissolved with dry tetrahydrofuran (17 mL) and cooled to -82 °C. Phosphonate **20** (1.27 g, 3.04 mmol, 0.8 eq.) was dissolved in dry tetrahydrofuran (17 mL) and added to the reaction mixture at -82 °C. The reaction was stirred for 15 min at -82 °C. A solution of aldehyde **19** (1.99 g, 4.24 mmol, 1.0 eq.) in dry tetrahydrofuran (20 mL) was added dropwise over 45 min to the cooled solution. The reaction mixture was stirred for 14 h. During this time, the suspension warmed up to room temperature. The reaction mixture was stirred for 1 h at room temperature. Then, the reaction mixture was cooled to 10 °C and methanol (5 mL) was added, the mixture was diluted with ethyl acetate (150 mL). The organic layer was washed with semi-saturated brine (2x 250 mL). The aqueous layer was extracted with ethyl acetate (2x 100 mL) and the combined organic layers were dried over sodium sulfate. The solvent was removed under reduced pressure. The title compound was obtained after purification by silica gel column chromatography (200 g, 6x16 cm, PE:EtOAc 7:3).

Yield (**21**): 1.33 g (1.86 mmol, 44% over two steps) as a colorless foamy solid.

TLC: R_f = 0.46 (PE:EtOAc 1:1).

^{1}H NMR (500 MHz, $CHCl_3$-d_1): δ [ppm] = 0.07 (s, 3 H, $SiCH_3$), 0.08 (s, 3 H, $SiCH_3$), 0.09 (s, 3 H, $SiCH_3$), 0.11 (s, 3 H, $SiCH_3$), 0.89 (s, 9 H, $SiC(CH_3)_3$), 0.90 (s, 9 H, $SiC(CH_3)_3$), 1.47 (s, 9 H, $OC(CH_3)_3$), 3.95 (dd, $^3J_{3'\text{-H}/4'\text{-H}}$ = 6.3 Hz, $^3J_{3'\text{-H}/2'\text{-H}}$ = 3.9 Hz, 1 H, 3'-H), 4.34 (dd, $^3J_{2'\text{-H}/3'\text{-H}}$ = 3.9 Hz, $^3J_{2'\text{-H}/1'\text{-H}}$ = 3.4 Hz, 1 H, 2'-H), 4.87 (dd, $^3J_{4'\text{-H}/5'\text{-H}}$ = 7.8 Hz, $^3J_{4'\text{-H}/3'\text{-H}}$ = 6.3 Hz, 1 H, 4'-H), 5.14 (s, 2 H, 1''-H), 5.58 (d, $^3J_{1'\text{-H}/2'\text{-H}}$ = 3.4 Hz, 1 H, 1'-H), 5.73 (dd, $^3J_{5\text{-H}/6\text{-H}}$ = 8.2 Hz, $^4J_{5\text{-H}/3\text{-NH}}$ = 2.3 Hz, 1 H, 5-H), 6.26 (d, $^3J_{4'\text{-H}/5'\text{-H}}$ = 7.8 Hz, 1 H, 5'-H), 6.75

(bs, 1 H, 6'-NH), 7.27 (d, $^{3}J_{6\text{-H}/5\text{-H}}$ = 8.2 Hz, 1 H, 6-H), 7.30 - 7.34 (m, 5 H, 3''-H, 4''-H, 5''-H), 8.50 (bs, 1 H, 3-NH).

^{13}C NMR (126 MHz, $CHCl_3$-d_1): δ [ppm] = -4.71 ($SiCH_3$), -4.66 ($SiCH_3$), -4.35 ($SiCH_3$), -4.27 ($SiCH_3$), 18.16 (Si<u>C</u>$(CH_3)_3$), 18.25 (Si<u>C</u>$(CH_3)_3$), 25.92 (SiC(<u>C</u>$H_3)_3$), 25.98 (SiC(<u>C</u>$H_3)_3$), 28.00 (OC(<u>C</u>$H_3)_3$), 67.66 (C-1''), 74.81 (C-2'), 76.21 (C-3'), 79.35 (C-4'), 82.81 (O<u>C</u>$(CH_3)_3$), 92.99 (C-1'), 102.46 (C-5), 124.75 (C-5'), 128.31, 128.45, 128.66 (C-3'', C-4'', C-5''), 131.41 (C-6'), 135.91 (C-2''), 140.61 (C-6), 149.82 (C-2), 153.66 (NC(=O)O), 162.84 (C-4), 162.90 (C-7').

LC-MS (ESI^+): m/z = 740.27 $[M+Na]^+$.

$C_{35}H_{55}N_3O_9Si_2$ (718.00)

7.2.2.5 (6'*S*)-*N*-Cbz-protected nucleosyl amino acid 22[137,140]

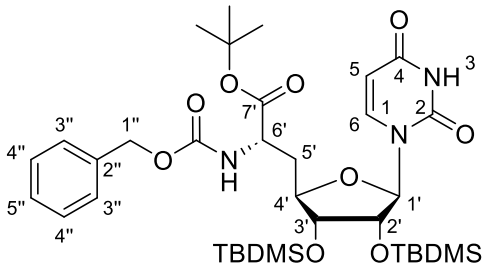

(*S,S*)-Me-DUPHOS-Rh (2 spatula tips) was added to a solution of *Z*-didehydro nucleosyl amino acid **21** (568 mg, 792 µmol, 1.0 eq.) in dry methanol (20 mL). The reaction mixture was stirred for 5 d under hydrogen atmosphere (1 bar) at room temperature. The solvent was removed under reduced pressure and the title compound was obtained after purification by silica gel column chromatography (50 g, 5x8 cm, PE:EtOAc 7:3).

Yield (**22**): 517 mg (719 µmol, 91%) as a colorless foamy solid.

TLC: R_f = 0.41 (PE:EtOAc 7:3).

^{1}H NMR (500 MHz, C_6H_6-d_6): δ [ppm] = -0.07 (s, 3 H, $SiCH_3$), 0.04 (s, 3 H, $SiCH_3$), 0.16 (s, 3 H, $SiCH_3$), 0.20 (s, 3 H, $SiCH_3$), 0.95 (s, 9 H, $SiC(CH_3)_3$), 1.00 (s, 9 H, $SiC(CH_3)_3$), 1.33 (s, 9 H, $OC(CH_3)_3$), 2.09-2.18 (m, 1 H, 5'-H_a), 2.28 (ddd, $^{2}J_{5'\text{-H}b/5'\text{-H}a}$ = 14.1 Hz, $^{3}J_{5'\text{-H}b/6'\text{-H}}$ = 7.7 Hz, $^{3}J_{5'\text{-H}b/4'\text{-H}}$ = 2.6 Hz, 1 H, 5'-H_b), 3.76 (dd, $^{3}J_{3'\text{-H}/4'\text{-H}}$ = 4.8 Hz, $^{3}J_{3'\text{-H}/2'\text{-H}}$ = 4.8 Hz, 1 H, 3'-H), 4.39-4.45 (m, 2 H, 2'-H, 4'-H), 4.59-4.64 (m, 1 H, 6'-H), 5.02 (s, 2 H, 1''-H), 5.58 (d,

$^{3}J_{5\text{-H}/6\text{-H}}$ = 8.0 Hz, 1 H, 5-H), 5.61 (d, $^{3}J_{1'\text{-H}/2'\text{-H}}$ = 2.8 Hz, 1 H, 1'-H), 5.73 (d, $^{3}J_{6'\text{-NH}/6'\text{-H}}$ = 6.4 Hz, 1 H, 6'-NH), 7.04-7.24 (m, 6 H, 6-H, 3''-H, 4''-H, 5''-H), 9.39 (bs, 1 H, 3-NH).

^{13}C NMR (126 MHz, C_6H_6-d_6): δ [ppm] = -4.76 ($SiCH_3$), -4.65 ($SiCH_3$), -4.24 ($SiCH_3$), -4.07 ($SiCH_3$), 18.25 (Si<u>C</u>$(CH_3)_3$), 18.28 (Si<u>C</u>$(CH_3)_3$), 26.05 (SiC(<u>C</u>$H_3)_3$), 26.13 (SiC(<u>C</u>$H_3)_3$), 27.87 (OC(<u>C</u>$H_3)_3$), 36.58 (C-5'), 52.80 (C-6'), 67.00 (C-1''), 75.07 (C-2'), 75.93 (C-3'), 80.99 (C-4'), 82.24 (O<u>C</u>$(CH_3)_3$), 92.86 (C-1'), 102.45 (C-5), 128.34, 128.50, 128.66 (C-3'', C-4'', C-5''), 137.08 (C-2''), 140.83 (C-6), 150.65 (C-2), 155.89 (NC(=O)O), 163.70 (C-4), 171.00 (C-7').

LC-MS (ESI^+): m/z = 742.21 $[M+Na]^+$.

$C_{35}H_{57}N_3O_9Si_2$ (720.01)

7.2.2.6 Cbz-deprotected nucleosyl amino acid derivative 23[146,148]

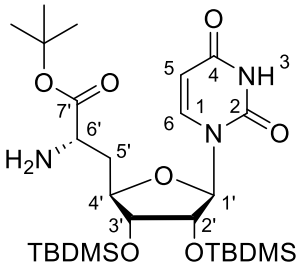

1,4-Cyclohexadiene (500 µL, 5.37 mmol, 10.2 eq.) and palladium black (5 spatula tips) were added to a solution of (6'*S*)-*N*-Cbz protected nucleosyl amino acid **22** (381 mg, 529 µmol, 1.0 eq.) in dry *iso*-propanol (20 mL). The reaction mixture was stirred for 1 h at 40 °C (water bath). The reaction mixture was filtered through a syringe filter. The filter was washed with methanol (4x 5 mL). The title compound was obtained after removal of the solvent and was used without further purification.

Yield (**23**): 305 mg (521 µmol, 98%) as colorless solid.

TLC: R_f = 0.40 (CH_2Cl_2:MeOH 9:1).

^{1}H NMR (500 MHz, MeOH-d_4): δ [ppm] = 0.10 (s, 3 H, $SiCH_3$), 0.11 (s, 3 H, $SiCH_3$), 0.12 (s, 3 H, $SiCH_3$), 0.14 (s, 3 H, $SiCH_3$), 0.91 (s, 9 H, $SiC(CH_3)_3$), 0.94 (s, 9 H, $SiC(CH_3)_3$), 1.48 (s, 9 H, $OC(CH_3)_3$), 1.85 (ddd, $^{2}J_{5'\text{-H}a/5'\text{-H}b}$ = 14.1 Hz, $^{3}J_{5'\text{-H}a/4'\text{-H}}$ = 11.3 Hz, $^{3}J_{5'\text{-H}a/6'\text{-H}}$ = 5.1 Hz, 1 H, 5'-H_a), 2.11 (ddd, $^{2}J_{5'\text{-H}b/5'\text{-H}a}$ = 14.1 Hz, $^{3}J_{5'\text{-H}b/6'\text{-H}}$ = 8.2 Hz, $^{3}J_{5'\text{-H}b/4'\text{-H}}$ = 2.6 Hz, 1 H, 5'-H_b), 3.52 (dd, $^{3}J_{6'\text{-H}/5'\text{-H}b}$ = 8.2 Hz, $^{3}J_{6'\text{-H}/5'\text{-H}a}$ = 5.1 Hz, 1 H, 6'-H), 3.89 (dd, $^{3}J_{3'\text{-H}/4'\text{-H}}$ = 5.0 Hz, $^{3}J_{3'\text{-H}/2'\text{-H}}$ = 4.6 Hz, 1 H, 3'-H), 4.13 (ddd, $^{3}J_{4'\text{-H}/5'\text{-H}a}$ = 11.3 Hz,

$^3J_{4'\text{-H}/3'\text{-H}}$ = 5.0 Hz, $^3J_{4'\text{-H}/5'\text{-H}_b}$ = 2.6 Hz, 1 H, 4'-H), 4.31 (dd, $^3J_{2'\text{-H}/3'\text{-H}}$ = 4.6 Hz, $^3J_{2'\text{-H}/1'\text{-H}}$ = 4.3 Hz, 1 H, 2'-H), 5.74 (d, $^3J_{5\text{-H}/6\text{-H}}$ = 8.1 Hz, 1 H, 5-H), 5.77 (d, $^3J_{1'\text{-H}/2'\text{-H}}$ = 4.3 Hz, 1 H, 1'-H), 7.66 (d, $^3J_{6\text{-H}/5\text{-H}}$ = 8.1 Hz, 1 H, 6-H).

^{13}C NMR (126 MHz, MeOH-d_4): δ [ppm] = -4.53 ($SiCH_3$), -4.47 ($SiCH_3$), -4.42 ($SiCH_3$), -4.01 ($SiCH_3$), 18.86 ($SiC(\underline{C}H_3)_3$), 18.92 ($SiC(\underline{C}H_3)_3$), 26.37 ($Si\underline{C}(CH_3)_3$), 26.43 ($Si\underline{C}(CH_3)_3$), 28.30 ($OC(\underline{C}H_3)_3$), 39.50 (C-5'), 53.77 (C-6'), 75.93 (C-2'), 76.59 (C-3'), 82.57 ($O\underline{C}(CH_3)_3$), 82.90 (C-4'), 91.97 (C-1'), 102.92 (C-5), 142.66 (C-6), 152.16 (C-2), 166.13 (C-4), 175.14 (C-7').

LC-MS (ESI^+): m/z = 586.47 $[M+H]^+$.

$C_{27}H_{51}N_3O_7Si_2$ (585.33)

7.2.2.7 *N*-Cbz-protected nucleosyl amino acid derivative 58[137,140]

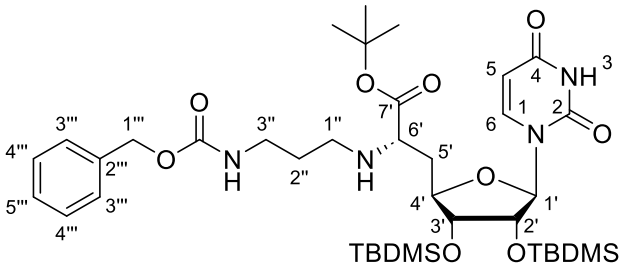

Cbz-deprotected nucleosyl amino acid **23** (225 mg, 384 µmol, 1.0 eq.) was dissolved in dry tetrahydrofuran (18 mL) over molecular sieve (4 Å). After 15 min, *N*-Cbz-3-amino-propanal **41** (80.0 mg, 386 µmol, 1.0 eq.) was added and the reaction mixture was stirred for 24 h at room temperature. Sodium triacetoxyborohydride (163 mg, 771 µmol, 2.0 eq.) and Amberlyst-15^{TM} (18.6 mg) were added to the reaction mixture. Then, the reaction mixture was stirred for 3 d at room temperature. The mixture was filtered over celite® and washed with ethyl acetate (3x 30 mL). The organic layer was washed with saturated sodium carbonate solution (150 mL). The aqueous layer was extracted with ethyl acetate (3x50 mL) and the combined organic layers were dried over sodium sulfate. The solvent was removed under reduced pressure. The title compound was obtained after purification by silica gel column chromatography (65 g, 5x8 cm, CH_2Cl_2:MeOH 98:2).

Yield (**58**): 250 mg (321 µmol, 84%) as colorless foamy solid.

TLC: R_f = 0.33 (CH_2Cl_2:MeOH 95:5).

^{1}H NMR (300 MHz, DMSO-d_6): δ [ppm] = -0.01 (s, 3 H, $SiCH_3$), 0.03 (s, 3 H, $SiCH_3$), 0.07 (s, 3 H, $SiCH_3$), 0.08 (s, 3 H, $SiCH_3$), 0.83 (s, 9 H, $SiC(CH_3)_3$), 0.87 (s, 9 H, $SiC(CH_3)_3$), 1.40 (s, 9 H, $OC(CH_3)_3$), 1.51 (ddt, $^{3}J_{2''\text{-}H/1''\text{-}H_a}$ = 7.1 Hz, $^{3}J_{2''\text{-}H/1''\text{-}H_b}$ = 6.9 Hz, $^{3}J_{2''\text{-}H/3''\text{-}H}$ = 6.7 Hz, 2 H, 2''-H), 1.82-1.92 (m, 2 H, 5'-H_a, 5'-H_b), 2.38 (dt, $^{2}J_{1''\text{-}H_a/1''\text{-}H_b}$ = 11.1 Hz, $^{3}J_{1''\text{-}H_a/2''\text{-}H}$ = 7.1 Hz, 1 H, 1''-H_a), 2.47-2.56 (m, 1 H, 1''-H_b), 3.02 (dt, $^{3}J_{3''\text{-}H/2''\text{-}H}$ = 6.7 Hz, $^{3}J_{3''\text{-}H/3''\text{-}NH}$ = 6.1 Hz, 2 H, 3''-H), 3.11 (dd, $^{3}J_{6'\text{-}H/5'\text{-}H_a}$ = 6.8 Hz, $^{3}J_{6'\text{-}H/5'\text{-}H_b}$ = 6.8 Hz, 1 H, 6'-H), 3.84-3.91 (m, 2 H, 3'-H, 4'-H), 4.33 (dd, $^{3}J_{2'\text{-}H/1'\text{-}H}$ = 5.0 Hz, $^{3}J_{2'\text{-}H/3'\text{-}H}$ = 4.6 Hz, 1 H, 2'-H), 4.99 (s, 2 H, 1'''-H), 5.67 (d, $^{3}J_{5\text{-}H/6\text{-}H}$ = 8.4 Hz, 1 H, 5-H), 5.70 (d, $^{3}J_{1'\text{-}H/2'\text{-}H}$ = 5.0 Hz, 1 H, 1'-H), 7.19 (t, $^{3}J_{3''\text{-}NH/3''\text{-}H}$ = 6.1 Hz, 1 H, 3''-NH), 7.26-7.39 (m, 5 H, 3'''-H, 4'''-H, 5'''-H), 7.61 (d, $^{3}J_{6\text{-}H/5\text{-}H}$ = 8.4 Hz, 1 H, 6-H), 11.35 (bs, 1 H, 3-NH).

^{13}C NMR (76 MHz, DMSO-d_6): δ [ppm] = -4.98 ($SiCH_3$), -4.97 ($SiCH_3$), -4.81 ($SiCH_3$), -4.49 ($SiCH_3$), 17.52 ($SiC(CH_3)_3$), 17.65 ($SiC(CH_3)_3$), 25.56 ($SiC(CH_3)_3$), 25.66 ($SiC(CH_3)_3$), 27.63 ($OC(CH_3)_3$), 29.92 (C-2''), 36.30 (C-5'), 38.45 (C-3''), 44.62 (C-1''), 59.15 (C-6'), 65.06 (C-1'''), 73.51 (C-2'), 74.54 (C-3'), 80.25 (C-4'), 80.92 ($OC(CH_3)_3$), 88.49 (C-1'), 102.05 (C-5), 127.66, 128.29 (C-3''', C-4''', C-5'''), 137.24 (C-2'''), 140.96 (C-6), 150.60 (C-2), 156.05 (NC(=O)O), 162.96 (C-4), 173.39 (C-7').

LC-MS (ESI^+): m/z = 777.33 $[M+H]^+$.

$C_{38}H_{64}N_4O_9Si_2$ (777.42)

7.2.2.8 Cbz-deprotected nucleosyl amino acid derivative 35[146,148]

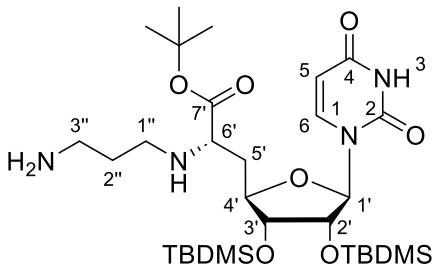

1,4-Cyclohexadiene (65.0 µL, 687 µmol, 8.8 eq.) and palladium black (2 spatula tips) were added to a solution of nucleosyl amino acid **58** (60.4 mg, 77.7 µmol, 1.0 eq.) in dry *iso*-Propanol (6 mL). The reaction was stirred for 30 min at 35° C (water bath), then 1,4-cyclohexadiene (65.0 µL, 687 µmol, 8.8 eq.) and palladium black (1 spatula tip) were added again. The reaction mixture was stirred for 1 h at 35 °C and then filtered through a syringe filter. The filter was washed with methanol (3x 4 mL). The title compound was obtained after removal of the solvent and was used without further purification.

Yield (**35**): 50.0 mg (77.7 µmol, quant.) as a colorless foamy solid.

^{1}H NMR (300 MHz, MeOH-d_4): δ [ppm] = 0.08 (s, 3 H, $SiCH_3$), 0.10 (s, 3 H, $SiCH_3$), 0.12 (s, 3 H, $SiCH_3$), 0.13 (s, 3 H, $SiCH_3$), 0.91 (s, 9 H, $SiC(CH_3)_3$), 0.94 (s, 9 H, $SiC(CH_3)_3$), 1.49 (s, 9 H, $OC(CH_3)_3$), 1.67 (ddt, $^3J_{2''\text{-H}/3''\text{-H}}$ = 7.0 Hz, $^3J_{2''\text{-H}/1''\text{-H}_a}$ = 6.9 Hz, $^3J_{2''\text{-H}/1''\text{-H}_b}$ = 6.9 Hz, 2 H, 2''-H), 1.80 (ddd, $^2J_{5'\text{-H}a/5'\text{-H}b}$ = 14.0 Hz, $^3J_{5'\text{-H}a/4'\text{-H}}$ = 10.9 Hz, $^3J_{5'\text{-H}a/6'\text{-H}}$ = 4.8 Hz, 1 H, 5'-H_a), 1.94 (ddd, $^2J_{5'\text{-H}b/5'\text{-H}a}$ = 14.0 Hz, $^3J_{5'\text{-H}b/6'\text{-H}}$ = 8.8 Hz, $^3J_{5'\text{-H}b/4'\text{-H}}$ = 3.0 Hz, 1 H, 5'-H_b), 2.52-2.68 (m, 2 H, 1''-H_a, 1''-H_b), 2.76 (t, $^3J_{3''\text{-H}/2''\text{-H}}$ = 7.0 Hz, 2 H, 3''-H), 3.22-3.27 (m, 1 H, 6'-H), 3.80 (dd, $^3J_{3'\text{-H}/4'\text{-H}}$ = 4.8 Hz, $^3J_{3'\text{-H}/2'\text{-H}}$ = 4.7 Hz, 1 H, 3'-H), 3.97 (ddd, $^3J_{4'\text{-H}/5'\text{-H}a}$ = 10.9 Hz, $^3J_{4'\text{-H}/3'\text{-H}}$ = 4.8 Hz, $^3J_{4'\text{-H}/5'\text{-H}b}$ = 3.0 Hz, 1H, 4'-H), 4.38 (dd, $^3J_{2'\text{-H}/3'\text{-H}}$ = 4.7 Hz, $^3J_{2'\text{-H}/1'\text{-H}}$ = 4.5 Hz, 1 H, 2'-H), 5.73 (d, $^3J_{5\text{-H}/6\text{-H}}$ = 8.1 Hz, 1 H, 5-H), 5.73 (d, $^3J_{1'\text{-H}/2'\text{-H}}$ = 4.5 Hz, 1 H, 1'-H), 7.62 (d, $^3J_{6\text{-H}/5\text{-H}}$ = 8.1 Hz, 1 H, 6-H).

^{13}C NMR (76 MHz, MeOH-d_4): δ [ppm] = -4.32 ($SiCH_3$), -4.27 ($SiCH_3$), -4.26 ($SiCH_3$), -3.85 ($SiCH_3$), 19.03 ($SiC(CH_3)_3$), 19.09 ($SiC(CH_3)_3$), 26.56 ($SiC(CH_3)_3$), 26.61 ($SiC(CH_3)_3$), 28.57 ($OC(CH_3)_3$), 32.64 (C-2''), 38.16 (C-5'), 40.83 (C-3''), 46.75 (C-1''), 60.97 (C-6'), 75.85 (C-2'), 76.80 (C-3'), 82.92 (C-4'), 83.03 ($OC(CH_3)_3$), 92.61 (C-1'), 103.17 (C-5), 144.03 (C-6), 152.25 (C-2), 167.53 (C-4), 175.13 (C-7').

LC-MS (ESI^+): m/z = 643.39 $[M+H]^+$.

$C_{30}H_{58}N_4O_7Si_2$ (642.38)

7.2.3 Synthesis of the central building blocks

7.2.3.1 Cbz-Ser($COC_{12}H_{25}$)-OH 34[153]

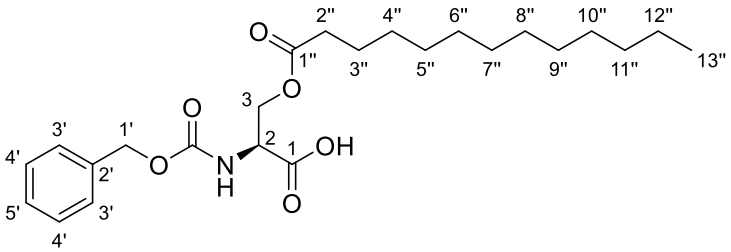

The reaction was not carried out under an inert gas atmosphere. Cbz-Ser($COC_{12}H_{25}$)-O^{t}Bu **61** (230 mg, 469 µmol, 1.0 eq.) was dissolved in aqueous trifluoroacetic acid (80%, 45 mL) and stirred for 2.5 h at room temperature. The solvent was removed under reduced pressure. The title compound was obtained after lyophilization and was used without further purification.

Yield (**34**): 200 mg (458 µmol, 98%) as a white solid.

^{1}H NMR (300 MHz, DMSO-d_6): δ [ppm] = 0.86 (t, $^3J_{13''\text{-H}/12''\text{-H}}$ = 6.7 Hz, 3 H, 13''-H), 1.20-1.27 (m, 18 H, 4''-12''-H), 1.49 (tt, $^3J_{3''\text{-H}/2''\text{-H}}$ = 7.1 Hz, $^3J_{3''\text{-H}/4''\text{-H}}$ = 6.7 Hz, 2 H, 3''-H), 2.26 (t, $^3J_{2''\text{-H}/3''\text{-H}}$ = 7.1 Hz, 2 H, 2''-H), 4.15 (dd, $^2J_{3\text{-H}a/3\text{-H}b}$ = 12.1 Hz, $^3J_{3\text{-H}a/2\text{-H}}$ = 8.4 Hz, 1 H, 3-H$_a$), 4.30-4.39 (m, 2 H, 2-H, 3-H$_b$), 5.05 (s, 2 H, 1'-H), 7.28-7.39 (m, 5 H, 3'-H, 4'-H, 5'-H), 7.70 (d, $^3J_{\text{NH}/2\text{-H}}$ = 7.9 Hz, 1 H, NH), 12.97 (bs, 1 H, COOH).

^{13}C NMR (76 MHz, DMSO-d_6): δ [ppm] = 13.92 (C-13''), 22.05 (C-4''-12''), 24.24 (C-3''), 28.36, 28.66, 28.83, 28.97, 29.00, 31.25 (C-4''-12''), 33.30 (C-2''), 52.29 (C-2), 63.27 (C-3), 65.53 (C-1'), 127.68, 127.80, 128.29 (C-3', C-4', C-5'), 136.86 (C-2'), 156.02 (NC(=O)O), 170.84 (C-1), 172.65 (C-1'').

LC-MS (ESI$^+$): m/z = 436.37 [M+H]$^+$.

$C_{17}H_{23}NO_6$ (435.56)

7.2.3.2 Cbz-Ser($COC_{15}H_{31}$)-O^{t}Bu 62[145,153]

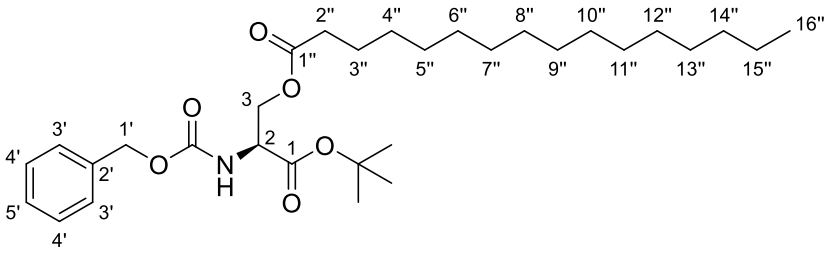

Hexadecanoic acid (271 mg, 1.05 mmol, 1.5 eq.), 4-dimethylaminopyridine (215 mg, 1.76 mmol, 2.5 eq.) and EDC • HCl (340 mg, 1.77 mmol, 2.5 eq.) were added to a solution of Cbz-Ser-O^{t}Bu **60** (208 mg, 702 µmol, 1.0 eq.) in dry tetrahydrofuran (20 mL). The reaction mixture was stirred for 6 h at room temperature. Then, hydrochloric acid (0.5 M, 110 mL) was added. After extraction with dichloromethane (3x 110 mL) and drying over sodium sulfate, the solvent was removed under reduced pressure. The title compound was obtained after purification by silica gel column chromatography (50 g, 4x13 cm, PE:EtOAc 9:1).

Yield (**62**): 350 mg (657 µmol, 94%) as a white solid.

TLC: R_f = 0.68 (PE:EtOAc 1:1).

^{1}H NMR (400 MHz, DMSO-d_6): δ [ppm] = 0.85 (t, $^3J_{16''\text{-H}/15''\text{-H}}$ = 6.9 Hz, 3 H, 16''-H), 1.20-1.26 (m, 24 H, 4''-15''-H), 1.38 (s, 9 H, OC(CH_3)$_3$), 1.49 (tt, $^3J_{3''\text{-H}/2''\text{-H}}$ = 7.3 Hz,

$^{3}J_{3''\text{-H}/4''\text{-H}}$ = 7.2 Hz, 2 H, 3''-H), 2.25 (t, $^{3}J_{2''\text{-H}/3''\text{-H}}$ = 7.3 Hz, 2 H, 2''-H), 4.13-4.20 (m, 1 H, 3-H_a), 4.23-4.31 (m, 2 H, 2-H, 3-H_b), 5.05 (s, 2 H, 1'-H), 7.29-7.38 (m, 5 H, 3'-H, 4'-H, 5'-H), 7.75 (d, $^{3}J_{2\text{-NH}/2\text{-H}}$ = 7.7 Hz 1 H, 2-NH).

^{13}C NMR (101 MHz, DMSO-d_6): δ [ppm] = 13.92 (C-16''), 22.07 (C-4''-15''), 24.24 (C-3''), 27.51 (OC($\underline{C}H_3$)$_3$), 28.36, 28.64, 28.68, 28.81, 28.93, 28.98, 28.99, 31.27 (C-4''-15''), 33.30 (C-2''), 53.56 (C-2), 62.87 (C-3), 65.55 (C-1'), 81.28 (O$\underline{C}$(CH_3)$_3$) 127.71, 127.82, 128.29 (C-3', C-4', C-5'), 136.86 (C-2'), 155.87 (NC(=O)O), 168.51 (C-1), 172.53 (C-1'').

LC-MS (ESI$^+$): m/z = 556.69 $[M+Na]^+$.

$C_{31}H_{51}NO_6$ (533.75)

7.2.3.3 Cbz-Ser($COC_{15}H_{31}$)-OH 37[153]

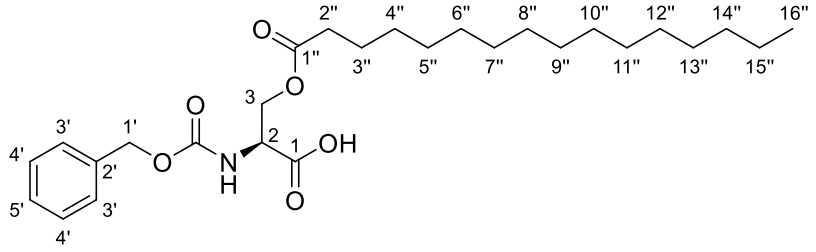

The reaction was not carried out under an inert gas atmosphere. Cbz-Ser($COC_{15}H_{31}$)-O^{t}Bu **62** (100 mg, 187 µmol, 1.0 eq.) was dissolved in aqueous trifluoroacetic acid (80%, 18 mL) and stirred for 2.5 h at room temperature. The title compound was obtained after lyophilization and was used without further purification.

Yield (**37**): 73.4 mg (154 µmol, 82%) as a white solid.

TLC: R_f = 0.32 (CH_2Cl_2:MeOH 9:1).

^{1}H NMR (500 MHz, MeOH-d_4): δ [ppm] = 0.90 (t, $^{3}J_{16''\text{-H}/15''\text{-H}}$ = 6.9 Hz, 3 H, 16''-H), 1.26-1.32 (m, 24 H, 4''-15''-H), 1.58 (tt, $^{3}J_{3''\text{-H}/2''\text{-H}}$ = 7.2 Hz, $^{3}J_{3''\text{-H}/4''\text{-H}}$ = 6.9 Hz, 1 H, 3''-H), 2.30 (t, $^{3}J_{2''\text{-H}/3''\text{-H}}$ = 7.2 Hz, 2 H, 2''-H), 4.33 (dd, $^{2}J_{3\text{-H}a/3\text{-H}b}$ = 11.2 Hz, $^{3}J_{3\text{-H}a/2\text{-H}}$ = 5.9 Hz, 1 H, 3-H_a), 4.45 (dd, $^{2}J_{3\text{-H}b/3\text{-H}a}$ = 11.2 Hz, $^{3}J_{3\text{-H}b/2\text{-H}}$ = 3.8 Hz, 1 H, 3-H_b), 4.53 (dd, $^{3}J_{2\text{-H}/3\text{-H}a}$ = 5.9 Hz, $^{3}J_{2\text{-H}/3\text{-H}b}$ = 3.8 Hz, 1 H, 2-H), 5.07-5.16 (m, 2 H, 1'-H), 7.26-7.32 (m, 1 H, 5'-H), 7.32-7.39 (m, 4 H, 3'-H, 4'-H).

^{13}C NMR (126 MHz, MeOH-d_4): δ [ppm] = 14.56 (C-16''), 23.75 (C-4''-15''), 25.90 (C-3''), 30.15, 30.41, 30.49, 30.60, 30.75, 30.78, 30.80, 33.09 (C-4''-15''), 34.77 (C-2''), 54.60

(C-2), 64.61 (C-3), 67.72 (C-1'), 128.80, 129.00, 129.46 (C-3', C-4', C-5'), 138.13 (C-2'), 158.46 (NC(=O)O), 172.52 (C-1), 175.03 (C-1'').

IR (ATR) υ [cm^{-1}]: 2918, 2850, 1720, 1652, 1464, 1355, 1171, 1089, 1037, 946.

LC-MS (ESI^+): m/z = 478.28 $[M+H]^+$.

HRMS (ESI^+): calcd. for $C_{27}H_{42}NO_6^-$: 476.3017, found: 476.3017 $[M-H]^-$.

$C_{27}H_{43}NO_6$ (477.64)

7.2.3.4 Cbz-Ser(CO*iso*$C_{15}H_{31}$)-O*t*Bu 85[145,153]

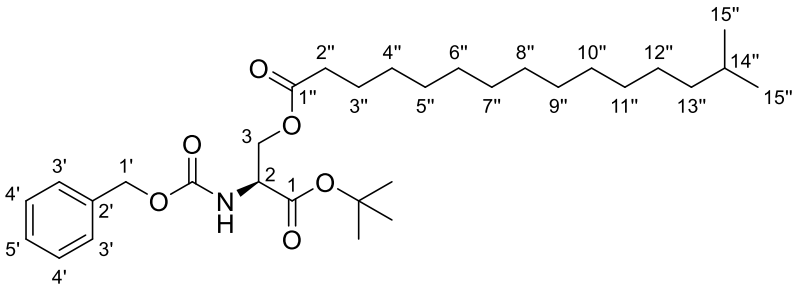

14-Methylpentadecanoic acid **45mix** (130 mg; crude: contained derivatives with different chain lengths), 4-dimethylaminopyridine (105 mg, 859 µmol, 2.5 eq.) and EDC • HCl (163 mg, 850 µmol, 2.5 eq.) were added to a solution of Cbz-Ser-O*t*Bu **60** (100 mg, 339 µmol, 1.0 eq.) in dry tetrahydrofuran (10 mL). The reaction mixture was stirred for 22.5 h at room temperature. Then, hydrochloric acid (0.5 M, 60 mL) was added. After extraction with dichloromethane (3x 60 mL) and drying over sodium sulfate, the solvent was removed under reduced pressure. The title compound was obtained after purification by silica gel column chromatography (1. 50 g, 4x12cm, PE:EtOAc 9:1 and 2. 55 g, 4x13 cm, PE:EtOAc 95:5).

Yield (**85**): 121 mg (as a mixture of the title compound and derivatives with different chain lengths) as a colorless oily fluid.

TLC: R_f = 0.73 (PE:EtOAc 1:1).

^{1}H NMR (500 MHz, DMSO-d_6): δ [ppm] = 0.84 (d, $^3J_{15''\text{-H}/14''\text{-H}}$ = 6.6 Hz, 6 H, 15''-H), 1.12 (dt, $^3J_{13''\text{-H}/12''\text{-H}}$ = 6.8 Hz, $^3J_{13''\text{-H}/14''\text{-H}}$ = 6.6 Hz, 2 H, 13''-H), 1.19-1.27 (m, 18 H, 4''-12''-H), 1.39 (s, 9 H, $OC(CH_3)_3$), 1.44-1.53 (m, 3 H, 3''-H, 14''-H), 2.25 (t, $^3J_{2''\text{-H}/3''\text{-H}}$ = 7.4 Hz, 2 H, 2''-H), 4.13-4.19 (m, 1 H, 3-H_a), 4.23-4.30 (m, 2 H, 2-H, 3-H_b), 5.04 (s, 2 H, 1'-H), 7.29-7.34 (m, 1 H, 5'-H), 7.34-7.39 (m, 4 H, 3'-H, 4'-H), 7.75 (d, $^3J_{NH/2\text{-H}}$ = 7.9 Hz, 1 H, NH).

^{13}C NMR (126 MHz, DMSO-d_6): δ [ppm] = 22.51 (C-15''), 24.25 (C-3''), 26.75 (C-4''-12''), 27.70 (C-14''), 27.53 (OC($\underline{C}H_3)_3$), 28.37, 28.64, 28.81, 28.93, 28.98, 29.03, 29.27 (C-4''-12''), 33.31 (C-2''), 38.45 (C-13''), 53.57 (C-2), 62.88 (C-3), 65.57 (C-1'), 81.30 (O$\underline{C}(CH_3)_3$), 127.73, 127.84, 128.31 (C-3', C-4', C-5'), 136.87 (C-2'), 155.98 (NC(=O)O), 168.52 (C-1), 172.56 (C-1'').

LC-MS (ESI$^+$): m/z = 556.49 $[M+Na]^+$.

$C_{31}H_{51}NO_6$ (533.75)

7.2.3.5 Cbz-Ser(CO$^{iso}C_{15}H_{31}$)-OH 86[153]

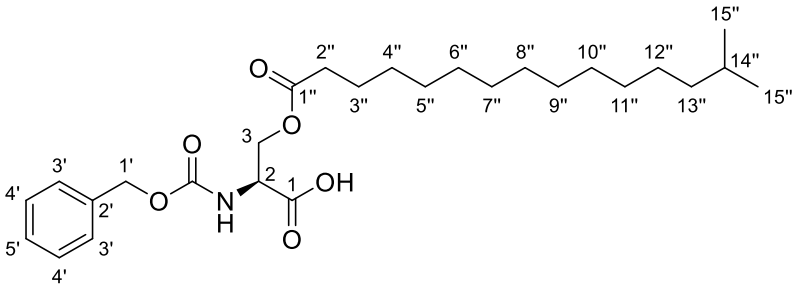

The reaction was not carried out under an inert gas atmosphere. Cbz-Ser(CO$^{iso}C_{15}H_{31}$)-O^{t}Bu **85** (92.2 mg; crude: contained derivatives with different chain lengths) was dissolved in aqueous trifluoroacetic acid (80%, 6 mL). The reaction mixture was stirred for 2.5 h at room temperature. The title compound was obtained after lyophilization and was used without further purification.

Yield (**86**): 81.4 mg (as a mixture of the title compound and derivatives with different chain lengths) as a colorless solid.

TLC: R_f = 0.28 (CH_2Cl_2:MeOH 9:1).

^{1}H NMR (500 MHz, DMSO-d_6, 100 °C): δ [ppm] = 0.85 (d, $^3J_{15''\text{-}H/14''\text{-}H}$ = 6.6 Hz, 6 H, 15''-H), 1.17 (dt, $^3J_{13''\text{-}H/12''\text{-}H}$ = 6.7 Hz, $^3J_{13''\text{-}H/14''\text{-}H}$ = 6.6 Hz, 2 H, 13''-H), 1.24-1.32 (m, 18 H, 4''-12''-H), 1.49-1.55 (m, 3 H, 3''-H, 14''-H), 2.26 (t, $^3J_{2''\text{-}H/3''\text{-}H}$ = 7.4 Hz, 2 H, 2''-H), 4.18-4.24 (m, 1 H, 3-H_a), 4.33-4.40 (m, 2 H, 2-H, 3-H_b), 5.08 (s, 2 H, 1'-H), 7.16 (bs, 1 H, NH), 7.28-7.33 (m, 1 H, 5'-H), 7.34-7.38 (m, 4 H, 3'-H, 4'-H).

^{13}C NMR (126 MHz, DMSO-d_6, 100 °C): δ [ppm] = 21.83 (C-15''), 23.77 (C-3''), 26.09 (C-4''-12''), 26.80 (C-14''), 27.87, 28.03, 28.22, 28.35, 28.38, 28.41, 28.70 (C-4''-12''), 32.97 (C-2''), 27.98 (C-13''), 52.85 (C-2), 62.44 (C-3), 65.23 (C-1'), 127.96, 127.15 127.71 (C-3', C-4', C-5'), 136.49 (C-2'), 155.29 (NC(=O)O), 169.99(C-1), 171.98(C-1'').

IR (ATR) υ [cm^{-1}]: 2919, 2851, 1745, 1719, 1464, 1354, 1227, 1202, 1168, 696.

LC-MS (ESI^+): m/z = 478.33 $[M+H]^+$.

HRMS (ESI^+): calcd. for $C_{27}H_{42}NO_6^-$: 476.3017, found: 476.3011 $[M+H]^-$.
calcd. for $C_{26}H_{40}NO_6^-$: 462.2861, found: 462.2855 $[M+H]^-$.
calcd. for $C_{25}H_{38}NO_6^-$: 448.2704, found: 448.2697 $[M+H]^-$.

$C_{27}H_{43}NO_6$ (477.64)

7.2.3.6 Cbz-*allo*-Thr-O^{t}Bu 74[175]

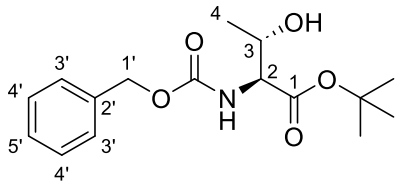

Tert-butyl 2,2,2-trichloroacetimidate **73** (172 µL, 962 µmol, 1.2 eq.) was added dropwise to a solution of the Cbz-*allo*-Thr-OH (203 mg, 802 µmol, 1.0 eq.) in dry tetrahydrofuran (3 mL). The reaction mixture was stirred for 22 h at room temperature, and 2,2,2-trichloroacetimidate (72.0 µL, 402 µmol, 0.5 eq.) was added again after 18 h. The solvent was removed under reduced pressure. The title compound was obtained after purification by silica gel column chromatography (20 g, 3x10 cm, PE:EtOAc 3:1).

Yield (**74**): 136 mg (440 µmol, 55%) as a colorless, high viscous fluid.

TLC: R_f = 0.33 (PE:EtOAc 3:2).

^{1}H NMR (500 MHz, $CHCl_3$-d_1): δ [ppm] = 1.18 (d, $^3J_{4\text{-}H/3\text{-}H}$ = 6.4 Hz, 3 H, 4-H), 1.47 (s, 9 H, $OC(CH_3)_3$), 4.14-4.20 (m, 1 H, 3-H), 4.33-4.39 (m, 1 H, 2-H), 5.12 (s, 2 H, 1'-H), 5.68 (d, $^3J_{NH/2\text{-}H}$ = 5.5 Hz, 1 H, NH), 7.30-7.34 (m, 1 H, 5'-H), 7.34-7.37 (m, 4 H, 3'-H, 4'-H).

^{13}C NMR (126 MHz, $CHCl_3$-d_1): δ [ppm] = 18.48 (C-4), 28.12 ($OC(\underline{C}H_3)_3$), 59.98 (C-2), 67.45 (C-1'), 69.35 (C-3), 83.21 ($O\underline{C}(CH_3)_3$), 128.29, 128.41, 128.69 (C-3', C-4', C-5'), 136.16 (C-2'), 157.03 (NC(=O)O), 169.22 (C-1).

LC-MS (ESI^+): m/z = 332.33 $[M+Na]^+$.

$C_{16}H_{23}NO_5$ (309.36)

7.2.3.7 Cbz-*allo*-Thr($COC_{12}H_{25}$)-O^{t}Bu 76[145,153]

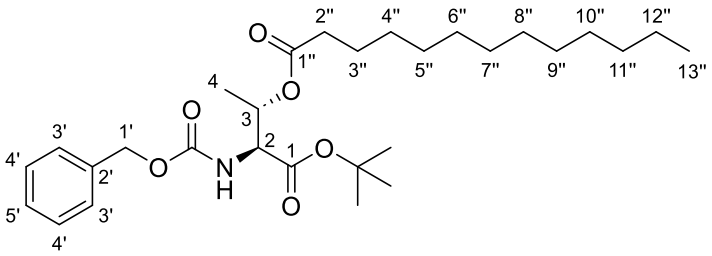

Tridecanoic acid (122 mg, 569 µmol, 1.5 eq.), 4-dimethylaminopyridine (118 mg, 966 mmol, 2.6 eq.) and EDC • HCl (182 mg, 949 µmol, 2.5 eq.) were added to a solution of Cbz-*allo*-Thr-O^{t}Bu **74** (117 mg, 379 µmol, 1.0 eq.) in dry tetrahydrofuran (10 mL). The reaction mixture was stirred for 6.5 h at room temperature. Then, hydrochloric acid (0.5 M, 40 mL) was added. After extraction with dichloromethane (3x 30 mL) and drying over sodium sulfate, the solvent was removed under reduced pressure. The title compound was obtained after purification by silica gel column chromatography (25 g, 3x11 cm, PE:EtOAc 9:1).

Yield (**76**): 188 mg (372 µmol, 98%) as a colorless fluid.

TLC: R_f = 0.33 (PE:EtOAc 9:1).

^{1}H NMR (500 MHz, DMSO-d_6): δ [ppm] = 0.85 (t, $^3J_{13''\text{-H}/12''\text{-H}}$ = 6.9 Hz, 3 H, 13''-H), 1.16 (d, $^3J_{4\text{-H}/3\text{-H}}$ = 6.5 Hz, 3 H, 4-H), 1.20-1.26 (m, 18 H, 4''-12''-H), 1.40 (s, 9 H, OC(CH_3)$_3$), 1.43-1.50 (m, 2 H, 3''-H), 2.12-2.29 (m, 2 H, 2''-H), 4.29 (dd, $^3J_{2\text{-H}/\text{NH}}$ = 9.0 Hz, $^3J_{2\text{-H}/3\text{-H}}$ = 5.7 Hz, 1 H, 2-H), 5.05-5.09 (m, 2 H, 3-H, 1'-H), 7.29-7.33 (m, 1 H, 5'-H), 7.33-7.39 (m, 4 H, 3'-H, 4'-H), 7.81 (d, $^3J_{\text{NH}/2\text{-H}}$ = 9.0 Hz, 1 H, NH).

^{13}C NMR (126 MHz, DMSO-d_6): δ [ppm] = 13.95 (C-13''), 15.73 (C-4), 22.10 (C-4''-12''), 24.21 (C-3''), 27.53 (OC($\underline{C}H_3$)$_3$), 28.34, 28.65, 28.71, 28.84, 28.96, 29.01, 29.07, 31.29 (C-4''-12''), 33.55 (C-2''), 57.39 (C-2), 65.60 (C-1'), 68.97 (C-3), 81.34 (O$\underline{C}$(CH_3)$_3$, 127.70, 127.84, 128.32 (C-3', C-4', C-5'), 136.91 (C-2'), 156.23 (NC(=O)O), 168.44(C-1), 172.01 (C-1'').

LC-MS (ESI$^+$): m/z = 528.37 $[M+Na]^+$.

$C_{29}H_{47}NO_6$ (505.70)

7.2.3.8 Cbz-*allo*-Thr($COC_{12}H_{25}$)-OH 38[153]

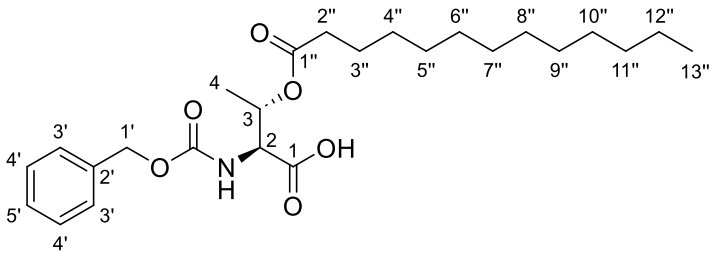

The reaction was not carried out under an inert gas atmosphere. Cbz-*allo*-Thr($COC_{12}H_{25}$)-O^{t}Bu **76** (255 mg, 504 µmol, 1.0 eq.) was dissolved in aqueous trifluoroacetic acid (80%, 10 mL). The reaction mixture was stirred for 3.5 h at room temperature. The title compound was obtained after lyophilization and was used without further purification.

Yield (**38**): 222 mg (494 µmol, 98%) as a white solid.

^{1}H NMR (500 MHz, DMSO-d_6, 100 °C): δ [ppm] = 0.88 (t, $^3J_{13''\text{-H}/12''\text{-H}}$ = 6.9 Hz, 3 H, 13''-H), 1.21 (d, $^3J_{4\text{-H}/3\text{-H}}$ = 6.5 Hz, 3 H, 4-H), 1.24-1.33 (m, 18 H, 4''-12''-H), 1.52 (tt, $^3J_{3''\text{-H}/2''\text{-H}}$ = 7.3 Hz, $^3J_{3''\text{-H}/4''\text{-H}}$ = 7.2 Hz, 2 H, 3''-H), 2.20 (t, $^3J_{2''\text{-H}/3''\text{-H}}$ = 7.3 Hz, 2 H, 2''-H), 4.38 (dd, $^3J_{2\text{-H}/\text{NH}}$ = 9.0 Hz, $^3J_{2\text{-H}/3\text{-H}}$ = 5.3 Hz, 1 H, 2-H), 5.04-5.11 (m, 2 H, 1'-H), 5.15 (dq, $^3J_{3\text{-H}/4\text{-H}}$ = 6.5 Hz, $^3J_{3\text{-H}/2\text{-H}}$ = 5.3 Hz, 1 H, 3-H), 7.16-7.23 (m, 1 H, NH), 7.29-7.34 (m, 1 H, 5'-H), 7.34-7.38 (m, 4 H, 3'-H, 4'-H), 12.51 (bs, 1 H, COOH).

^{13}C NMR (126 MHz, DMSO-d_6, 100 °C): δ [ppm] = 13.12 (C-13''), 15.13 (C-4), 21.38 (C-4''-12''), 24.71 (C-3''), 27.84, 28.01, 28.22, 28.34, 28.35, 28.36, 28.38, 30.66 (C-4''-12''), 33.26 (C-2''), 56.62 (C-2), 65.27 (C-1'), 68.66 (C-3), 126.97, 127.16, 127.71 (C-3', C-4', C-5'), 136.50 (C-2'), 155.51 (NC(=O)O), 169.91 (C-1), 171.49 (C-1'').

IR (ATR) υ [cm^{-1}]: 3302, 2914, 2848, 1695, 1540, 1381, 1230, 1201, 1046, 695.

LC-MS (ESI$^-$): m/z = 448.47 [M-H]$^-$.

HRMS (ESI$^-$): calcd. for $C_{25}H_{38}NO_6^-$: 448.2704, found: 448.2694 [M-H]$^-$.

$C_{25}H_{39}NO_6$ (449.59)

7.2.3.9 Cbz-*allo*-Thr(CO^{iso}C$_{15}$H$_{31}$)-O^{t}Bu 82[145,153]

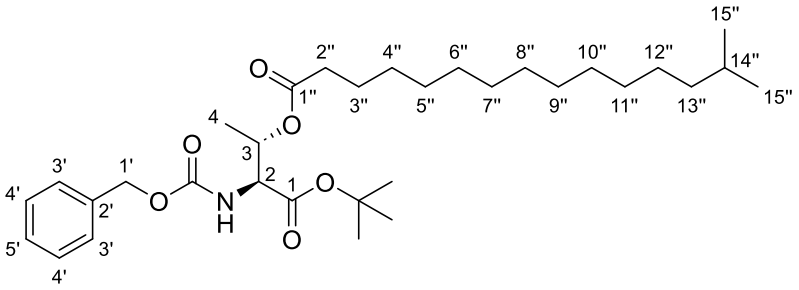

14-Methylpentadecanoic acid (25.0 mg, 97.5 µmol, 1.5 eq.), 4-dimethylaminopyridine (20.4 mg, 167 µmol, 2.6 eq.) and EDC • HCl (31.2 mg, 163 µmol, 2.5 eq.) were added to a solution of the Cbz-*allo*-Thr-O^{t}Bu **74** (20.1 mg, 65.0 µmol, 1.0 eq.) in dry tetrahydrofuran (2 mL). The reaction mixture was stirred for 22 h at room temperature. Then, hydrochloric acid (0.5 M, 8 mL) was added. After extraction with dichloromethane (4x 6 mL) and drying over sodium sulfate, the solvent was removed under reduced pressure. The title compound was obtained after purification by silica gel column chromatography (25 g, 1.5x17 cm, PE:EtOAc 95:5).

Yield (**82**): 21.6 mg (39.4 µmol, 61%) as a colorless oily fluid.

TLC: R_f = 0.30 (PE:EtOAC 9:1).

^{1}H NMR (500 MHz, DMSO-d$_6$): δ [ppm] = 0.84 (d, $^{3}J_{15''\text{-H}/14''\text{-H}}$ = 6.7 Hz, 6 H, 15''-H), 1.12 (dt, $^{3}J_{13''\text{-H}/14''\text{-H}}$ = 7.4 Hz, $^{3}J_{13''\text{-H}/12''\text{-H}}$ = 7.1 Hz, 2 H, 13''-H), 1.16 (d, $^{3}J_{4\text{-H}/3\text{-H}}$ = 6.5 Hz, 3 H, 4-H), 1.21-1.24 (m, 18 H, 4''-12''-H), 1.40 (s, 9 H, OC(CH$_3$)$_3$), 1.43-1.54 (m, 3 H, 3''-H, 14''-H), 2.12-2.25 (m, 2 H, 2''-H), 4.29 (dd, $^{3}J_{2\text{-H}/\text{NH}}$ = 9.1 Hz, $^{3}J_{2\text{-H}/3\text{-H}}$ = 6.7 Hz, 1 H, 2-H), 5.00-5.10 (m, 3 H, 3-H, 1'-H), 7.29-7.34 (m, 1 H, 5'-H), 7.34-7.37 (m, 4 H, 3'-H, 4'-H), 7.80 (d, $^{3}J_{\text{NH}/2\text{-H}}$ = 9.1 Hz 1 H, NH).

^{13}C NMR (126 MHz, DMSO-d$_6$): δ [ppm] = 15.73 (C-4), 22.51 (C-15''), 24.20 (C-3''), 26.76 (C-4''-12''), 27.37 (C-14''), 27.52 (C(<u>C</u>H$_3$)$_3$), 28.32, 28.62, 28.81, 28.92 28.98, 29.00, 29.04, 29.28 (C-4''-12''), 33.54 (C-2''), 38.46 (C-13''), 57.39 (C-2), 65.60 (C-1'), 68.96 (C-3), 81.33 (<u>C</u>(CH$_3$)$_3$), 127.69, 127.83, 128.31 (C-3', C-4', C-5'), 136.90 (C-2'), 156.22 (NC(=O)O), 168.43 (C-1), 172.00 (C-1'').

IR (ATR) υ [cm^{-1}]: 2924, 2853, 1728, 1503, 1456, 1368, 1217, 1155, 1086, 697.

LC-MS (ESI^{+}): m/z = 570.44 [M+Na]$^{+}$.

HRMS (ESI^{+}): calcd. for $C_{32}H_{53}NO_6Na^{+}$: 570.3766, found: 570.3753 [M+Na]$^{+}$.

$C_{32}H_{53}NO_6$ (547.78)

7.2.3.10 Cbz-*allo*-Thr($CO^{iso}C_{15}H_{31}$)-OH 44[145,153]

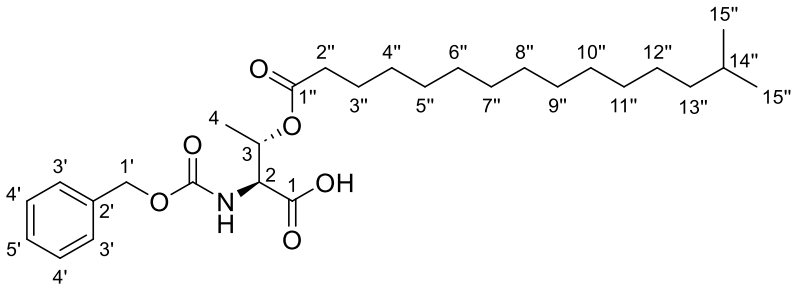

The reaction was not carried out under an inert gas atmosphere. Cbz-*allo*-Thr($CO^{iso}C_{15}H_{31}$)-O^{t}Bu **82** (15.1 mg, 27.6 µmol, 1.0 eq.) was dissolved in aqueous trifluoroacetic acid (80%, 2 mL). The reaction mixture was stirred for 3 h at room temperature. The title compound was obtained after lyophilization and was used without further purification.

Yield (**44**): 13.4 mg (27.4 µmol, 99%) as a colorless solid.

TLC: R_f = 0.44 (CH_2Cl_2:MeOH 9:1).

^{1}H NMR (500 MHz, DMSO-d_6, 100 °C): δ [ppm] = 0.87 (d, $^3J_{15''\text{-H}/14''\text{-H}}$ = 6.6 Hz, 6 H, 15''-H), 1.17 (dt, $^3J_{13''\text{-H}/12''\text{-H}}$ = 6.5 Hz, $^3J_{13''\text{-H}/14''\text{-H}}$ = 6.0 Hz, 2 H, 13''-H), 1.21 (d, $^3J_{4\text{-H}/3\text{-H}}$ = 6.6 Hz, 3 H, 4-H), 1.24-1.30 (m, 18 H, 4''-12''-H), 1.48-1.59 (m, 3 H, 3''-H, 14''-H), 2.20 (t, $^3J_{2''\text{-H}/3''\text{-H}}$ = 7.4 Hz, 2 H, 2''-H), 4.37 (dd, $^3J_{2\text{-H}/\text{NH}}$ = 9.1 Hz, $^3J_{2\text{-H}/3\text{-H}}$ = 5.3 Hz, 1 H, 2-H), 5.04-5.11 (m, 2 H, 1'-H), 5.15 (dq, $^3J_{3\text{-H}/4\text{-H}}$ = 6.6 Hz, $^3J_{3\text{-H}/2\text{-H}}$ = 5.3 Hz, 1 H, 3-H), 7.18 (d, $^3J_{\text{NH}/2\text{-H}}$ = 9.1 Hz, 1 H, NH), 7.28-7.34 (m, 1 H, 5'-H), 7.34-7.38 (m, 4 H, 3'-H, 4'-H), 12.52 (bs, 1 H, COOH).

^{13}C NMR (126 MHz, DMSO-d_6, 100 °C): δ [ppm] = 15.10 (C-4), 21.82 (C-15''), 23.70 (C-3''), 26.06 (C-4''-12''), 26.77 (C-14''), 27.83, 27.99, 28.20, 28.31, 28.35, 28.36, 28.38, 28.67 (C-4''-12''), 33.24 (C-2''), 37.95 (C-13''), 56.61 (C-2), 65.24 (C-1'), 68.66 (C-3), 126.95, 127.14, 127.69 (C-3', C-4', C-5'), 136.49 (C-2'), 155.48 (NC(=O)O), 169.88 (C-1), 171.48 (C-1'').

IR (ATR) υ [cm^{-1}]: 3333, 2919, 2849, 1734, 1651, 1551, 1316, 1253, 1199, 1050.

LC-MS (ESI$^+$): m/z = 492.45 $[M+H]^+$.

HRMS (ESI$^-$): calcd. for $C_{28}H_{44}NO_6^-$: 490.3174, found: 490.3167 $[M+H]^-$.

$C_{28}H_{45}NO_6$ (491.67)

7.2.3.11 Cbz-*allo*-Thr($COCH_3$)-OH 51[153,158]

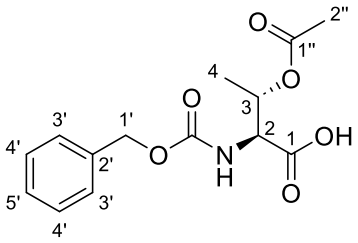

A mixture of dry pyridine (1.8 mL, 22 mmol, 34.4 eq.) and acetic anhydride (900 µL, 9.50 mmol, 15.0 eq.) was stirred for 15 min at room temperature. Then, the clear solution was cooled to 0 °C. Cbz-*allo*-Thr-OH (162 mg, 640 µmol, 1.0 eq.) was added in small portions. The reaction mixture was stirred for 1 h at 0 °C. Cooled water (0° C, 10 mL) was added to the reaction mixture. The resulting solution was extracted with ethyl acetate (3x 15 mL), the organic layer was dried over sodium sulfate. The solvent was removed under reduced pressure. The residue was co-evaporated with toluene (2x 5 mL), acetonitrile (2x 5 mL) and dichloromethane (2x 5 mL). The title compound was obtained after purification by silica gel column chromatography (35 g, 3x16 cm, PE:EtOAc:HCOOH 40:60:1).

Yield (**51**): 159 mg (538 µmol, 84%) as a colorless liquid.

TLC: R_f = 0.34 (PE:EtOAc:HCOOH 40:60:1).

^{1}H NMR (500 MHz, DMSO-d_6): δ [ppm] = 1.16 (d, $^3J_{4\text{-H}/3\text{-H}}$ = 6.4 Hz, 3 H, 4-H), 1.91 (s, 3 H, 2''-H), 4.39 (dd, $^3J_{2\text{-H}/\text{NH}}$ = 9.2 Hz, $^3J_{2\text{-H}/3\text{-H}}$ = 5.8 Hz, 1 H, 2-H), 5.02-5.07 (m, 2 H, 1'-H), 5.10 (dq, $^3J_{3\text{-H}/4\text{-H}}$ = 6.4 Hz, $^3J_{3\text{-H}/2\text{-H}}$ = 5.8 Hz, 1 H, 3-H), 7.29-7.35 (m, 1 H, 5'-H), 7.75-7.39 (m, 4 H, 3'-H, 4'-H), 7.78 (d, $^3J_{\text{NH}/2\text{-H}}$ = 9.2 Hz, 1 H, NH), 13.00 (bs, 1 H, COOH).

^{13}C NMR (126 MHz, DMSO-d_6): δ [ppm] = 15.43 (C-4), 20.86 (C-2''), 56.43 (C-2), 65.62 (C-1'), 69.14 (C-3), 127.76, 127.84, 128.34 (C-3', C-4', C-5'), 136.92 (C-2'), 156.34 (NC(=O)O), 169.66 (C-1''), 170.76 (C-1).

IR (ATR) υ [cm^{-1}]: 3324, 3034, 2986, 1711, 1587, 1227, 1601,1026, 697, 738.

LC-MS (ESI^+): m/z = 318.23 $[M+Na]^+$.

HRMS (ESI^+): calcd. for $C_{14}H_{18}NO_6^+$: 296.1129, found: 296.1123 $[M+H]^+$.

$C_{14}H_{17}NO_6$ (295.29)

7.2.3.12 Cbz-Thr-O^{t}Bu 75[175]

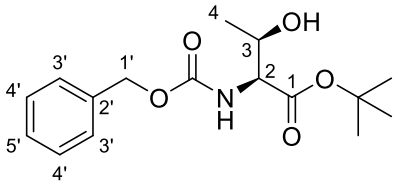

Tert-butyl 2,2,2-trichloroacetimidate **73** (170 µL, 962 µmol, 1.2 eq) was added dropwise to a solution of Cbz-Thr-OH (200 mg, 790 µmol, 1.0 eq.) in dry tetrahydrofuran (3 mL). The reaction mixture was stirred for 24 h at room temperature, and 2,2,2-trichloroacetimidate (85.0 µL, 475 µmol, 0.6 eq.) was added again after 21 h. The solvent was removed under reduced pressure. The title compound was obtained after purification by silica gel column chromatography (25 g, 3x12 cm, PE:EtOAc 4:1).

Yield (**75**): 128 mg (414 µmol, 52%) as a colorless, high viscous fluid.

TLC: R_f = 0.41 (PE:EtOAc 3:2).

^{1}H NMR (500 MHz, $CHCl_3$-d_1): δ [ppm] = 1.23 (d, $^3J_{4\text{-H}/3\text{-H}}$ = 6.7 Hz, 3 H, 4-H), 1.47 (s, 9 H, $OC(CH_3)_3$), 4.21 (dd, $^3J_{2\text{-H}/\text{NH}}$ = 8.7 Hz, $^3J_{2\text{-H}/3\text{-H}}$ = 2.1 Hz, 1 H, 2-H), 4.24-4.30 (m, 1 H, 3-H), 5.12 (s, 2 H, 1'-H), 5.55 (d, $^3J_{\text{NH}/2\text{-H}}$ = 8.7 Hz, 1 H, NH), 7.30-7.34 (m, 1 H, 5'-H), 7.34-7.38 (m, 4 H, 3'-H, 4'-H).

^{13}C NMR (126 MHz, $CHCl_3$-d_1): δ [ppm] = 20.04 (C-4), 28.09 ($OC(\underline{C}H_3)_3$), 59.62 (C-2), 67.31 (C-1'), 68.45 (C-3), 82.77 ($O\underline{C}(CH_3)_3$), 128.17, 128.29, 128.63 (C-3', C-4', C-5'), 136.30 (C-2'), 156.80 (NC(=O)O), 170.29 (C-1).

LC-MS (ESI^+): m/z = 332.34 $[M+Na]^+$.

HRMS (ESI^+): calcd. for $C_{16}H_{24}NO_5^+$: 310.1649, found: 310.1631 $[M+H]^+$.

$C_{16}H_{23}NO_5$ (309.36)

7.2.3.13 Cbz-Thr($COC_{12}H_{25}$)-O^{t}Bu 77[145,153]

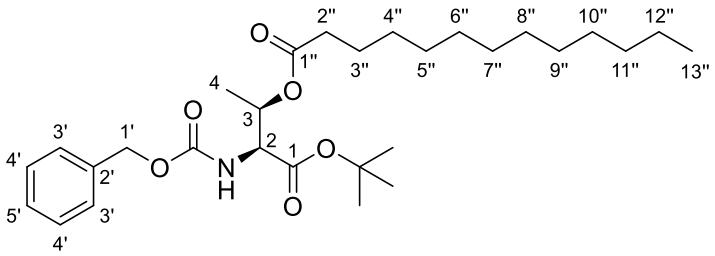

Tridecanoic acid (131 mg, 611 µmol, 1.5 eq.), 4-dimethylaminopyridine (123 mg, 1.01 mmol, 2.5 eq.) and EDC • HCl (194 mg, 1.01 mmol, 2.5 eq.) were added to a solution of Cbz-Thr-O^{t}Bu **75** (125 mg, 405 µmol, 1.0 eq.) in dry tetrahydrofuran (10 mL). The reaction mixture was stirred for 6.5 h at room temperature. Then, hydrochloric acid (0.5 M, 40 mL) was added. After extraction with ethyl acetate (3x 30 mL) and drying over sodium sulfate, the solvent was removed under reduced pressure. The title compound was obtained after purification by silica gel column chromatography (25 g, 3x12 cm, PE:EtOAc 95:5).

Yield (**77**): 160 mg (316 µmol, 78%) as a colorless liquid.

TLC: R_f = 0.28 (PE:EtOAc 95:5).

^{1}H NMR (500 MHz, DMSO-d_6): δ [ppm] = 0.85 (t, $^3J_{13''\text{-H}/12''\text{-H}}$ = 6.7 Hz, 3 H, 13''-H), 1.15 (d, $^3J_{4\text{-H}/3\text{-H}}$ = 6.6 Hz, 3 H, 4-H), 1.20-1.25 (m, 18 H, 4''-12''-H), 1.37 (s, 9 H, OC(CH_3)$_3$), 1.44-1.53 (m, 2 H, 3''-H), 2.15-2.27 (m, 2 H, 2''-H), 4.22 (dd, $^3J_{2\text{-H}/\text{NH}}$ = 9.0 Hz, $^3J_{2\text{-H}/3\text{-H}}$ = 3.8 Hz, 1 H, 2-H), 5.04-5.10 (m, 2 H, 1'-H), 5.20 (dq, $^3J_{3\text{-H}/4\text{-H}}$ = 6.6 Hz, $^3J_{3\text{-H}/2\text{-H}}$ = 3.8 Hz, 1 H, 3-H), 7.29-7.34 (m, 1 H, 5'-H), 7.35-7.40 (m, 4 H, 3'-H, 4'-H), 7.66 (d, $^3J_{\text{NH}/2\text{-H}}$ = 9.0 Hz, 1 H, NH).

^{13}C NMR (126 MHz, DMSO-d_6): δ [ppm] = 13.94 (C-13''), 16.50 (C-4), 22.08 (C-4''-12''), 24.28 (C-3''), 27.49 (OC($\underline{C}H_3$)$_3$), 28.39, 28.61, 28.68, 28.81, 28.92, 28.97, 28.99, 31.28 (C-4''-12''), 33.51 (C-2''), 58.06 (C-2), 65.65 (C-1'), 69.16 (C-3), 81.17 (O$\underline{C}$(CH_3)$_3$), 127.70, 127.83, 128.32 (C-3', C-4', C-5'), 136.90 (C-2'), 156.57 (NC(=O)O), 168.54 (C-1), 171.93 (C-1'').

LC-MS (ESI$^+$): m/z = 506.69 $[M+H]^+$.

HRMS (ESI$^+$): calcd. for $C_{29}H_{48}NO_6^+$: 506.3477, found: 506.3465 $[M+H]^+$.

$C_{29}H_{47}NO_6$ (505.70)

7.2.3.14 Cbz-Thr($COC_{12}H_{25}$)-OH 39[153]

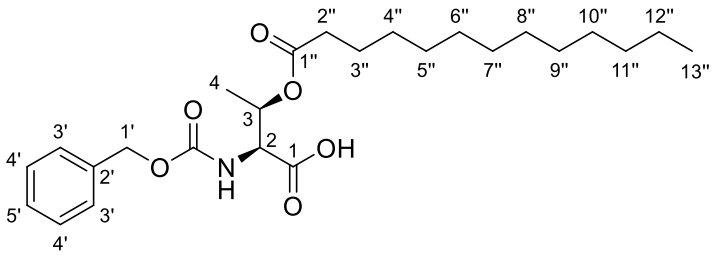

The reaction was not carried out under an inert gas atmosphere. Cbz-Thr($COC_{12}H_{25}$)-O^{t}Bu **77** (142 mg, 281 µmol, 1.0 eq.) was dissolved in aqueous trifluoroacetic acid (80%, 5 mL). The reaction mixture was stirred for 3.5 h at room temperature. The title compound was obtained after lyophilization and was used without further purification.

Yield (**39**): 125 mg (278 µmol, 99%) as a white solid.

^{1}H NMR (500 MHz, DMSO-d_6): δ [ppm] = 0.85 (t, $^3J_{13''\text{-H}/12''\text{-H}}$ = 6.9 Hz, 3 H, 13''-H), 1.16 (d, $^3J_{4\text{-H}/3\text{-H}}$ = 6.5 Hz, 3 H, 4-H), 1.20-1.29 (m, 18 H, 4''-12''-H), 1.43-1.52 (m, 2 H, 3''-H), 2.20 (t, $^3J_{2''\text{-H}/3''\text{-H}}$ = 7.4 Hz, 2 H, 2''-H), 4.25 (dd, $^3J_{2\text{-H}/\text{NH}}$ = 9.1 Hz, $^3J_{2\text{-H}/3\text{-H}}$ = 4.0 Hz, 1 H, 2-H), 5.06 (s, 2 H, 1'-H), 5.19 (dq, $^3J_{3\text{-H}/4\text{-H}}$ = 6.5 Hz, $^3J_{3\text{-H}/2\text{-H}}$ = 4.0 Hz, 1 H, 3-H), 7.29-7.34 (m, 1 H, 5'-H), 7.34-7.40 (m, 4 H, 3'-H, 4'-H), 7.61 (d, $^3J_{\text{NH}/2\text{-H}}$ = 9.1 Hz, 1 H, NH), 12.88 (bs, 1 H, COOH).

^{13}C NMR (126 MHz, DMSO-d_6): δ [ppm] = 13.96 (C-13''), 16.68 (C-4), 22.09 (C-4''-12''), 24.38 (C-3''), 28.39, 28.66, 28.71, 28.87, 29.00, 29.01, 29.03, 31.29 (C-4''-12''), 33.62 (C-2''), 57.47 (C-2), 65.64 (C-1'), 69.23 (C-3), 127.70, 127.83, 128.34 (C-3', C-4', C-5'), 136.91 (C-2'), 156.59 (NC(=O)O), 171.06 (C-1), 172.06 (C-1'').

IR (ATR) υ [cm^{-1}]: 3402, 2918, 2848, 1738, 1666, 1556, 1262, 1157, 1090, 695.

LC-MS (ESI$^+$): m/z = 450.40 [M-H]$^+$.

HRMS (ESI$^+$): calcd. for $C_{25}H_{39}NO_6Na^+$: 472.2670, found: 472.2657 [M+Na]$^+$.

$C_{25}H_{39}NO_6$ (449.59)

7.2.4 Synthesis of the urea dipeptide

7.2.4.1 Val *tert*-butyl ester isocyanate 40[154]

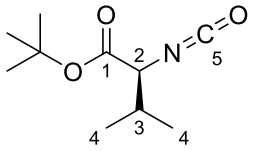

A 25 mL three-neck round bottom flask was equipped with a neutralizing gas trap containing a sodium bicarbonate solution. Valine *tert*-butyl ester hydrochloride (200 mg, 954 µmol, 1.0 eq.) was dissolved in a mixture of saturated sodium bicarbonate solution and dichloromethane (1:1, 8 mL). The reaction mixture was cooled to 0 °C. Then, triphosgene (92.4 mg, 311 µmol, 0.33 eq.) was added under vigorous stirring and the reaction mixture was stirred for 25 min at 0 °C. The layers were separated, and the aqueous layer was extracted with dichloromethane (4x 10 mL). The combined organic layers were dried over sodium sulfate. The title compound was obtained after removal of the solvent and was used without further purification.

Yield (**40**): 183 mg (846 µmol, 96%) as a colorless liquid.

^{1}H NMR (500 MHz, $CHCl_3$-d_1): δ [ppm] = 0.89 (d, $^{3}J_{4\text{-H}/3\text{-H}}$ = 6.8 Hz, 3 H, 4-H), 1.01 (d, $^{3}J_{4\text{-H}/3\text{-H}}$ = 6.8 Hz, 3 H, 4-H), 1.50 (s, 9 H, $OC(CH_3)_3$), 2.21 (dsept, $^{3}J_{3\text{-H}/4\text{-H}}$ = 6.8 Hz, $^{3}J_{3\text{-H}/2\text{-H}}$ = 3.7 Hz, 1 H, 3-H), 3.80 (d, $^{3}J_{2\text{-H}/3\text{-H}}$ = 3.7 Hz, 1 H, 2-H).

^{13}C NMR (126 MHz, $CHCl_3$-d_1): δ [ppm] = 16.43 (C-4), 19.99 (C-4), 28.08 ($OC(\underline{C}H_3)_3$), 31.91 (C-3), 64.08 (C-2), 83.25 ($O\underline{C}(CH_3)_3$) 127.62 (C-5), 170.13 (C-2).

$C_{10}H_{17}NO_3$ (199.25)

7.2.4.2 ^{t}BuO-Val-Arg(Pbf)-OH 36[154]

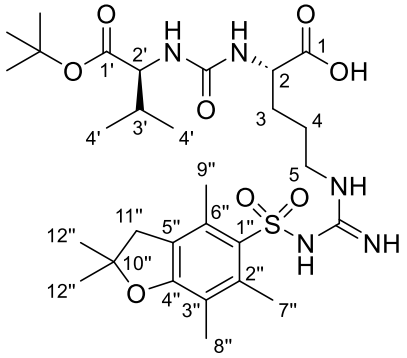

A solution of H-Arg(Pbf)-OH (118 mg, 753 µmol, 1.0 eq.) in dry dimethylformamide (8 mL) was added to a solution of valine *tert*-butyl ester isocyanate **40** (149 mg, 748 µmol, 1.0 eq.) in dry tetrahydrofuran (5 mL). The reaction mixture was stirred for 19 h at room temperature. Ethyl acetate (15 mL) was added, and the organic layer was washed with hydrochloric acid (1 M, 3x 10 mL). Then, the aqueous layer was extracted with ethyl acetate (40 mL). The combined organic layers were dried over sodium sulfate. The solvent was removed under reduced pressure. The title compound was obtained after purification by silica gel column chromatography (60 g, 5x9 cm, EtOAc:CH_2Cl_2:HCOOH 60:40:1) and lyophilization.

Yield (**36**): 348 mg (556 µmol,74%) as a white solid.

TLC: R_f = 0.10 (EtOAc:CH_2Cl_2:HCOOH 60:40:1).

^{1}H NMR (500 MHz, MeOH-d_4): δ [ppm] = 0.92 (d, $^{3}J_{4'\text{-H}/3'\text{-H}}$ = 6.9 Hz, 3 H, 4'-H), 0.96 (d, $^{3}J_{4'\text{-H}/3'\text{-H}}$ = 6.9 Hz, 3 H, 4'-H), 1.45 (s, 6 H, 12''-H), 1.46 (s, 9 H, OC(CH_3)$_3$), 1.55-1.67 (m, 3 H, 3-H_a, 4-H), 1.78-1.86 (m, 1 H, 3-H_b), 2.06-2.13 (m, 1 H, 3'-H), 2.08 (s, 3 H, 9''-H), 2.51 (s, 3 H, 7''-H), 2.57 (s, 3 H, 8''-H), 2.99-3.01 (m, 2 H, 11''-H), 3.14-3.24 (m, 2 H, 5-H), 4.07 (d, $^{3}J_{2'\text{-H}/3'\text{-H}}$ = 5.0 Hz, 1 H, 2'-H), 4.22-4.27 (m, 1 H, 2-H).

^{13}C NMR (126 MHz, MeOH-d_4): δ [ppm] = 12.49 (C-9''), 17.95 (C-4'), 18.35 (C-8''), 19.56 (C-7''), 26.74 (C-4), 28.34 (C-12''), 28.70 (OC($\underline{C}H_3$)$_3$), 30.94 (C-3), 32.16 (C-3'), 41.60 (C-5), 43.95 (C-11''), 53.79 (C-2), 60.04 (C-2'), 82.53 (O$\underline{C}$(CH_3)$_3$), 87.64 (C-10''), 118.43 (C-6''), 126.01 (C-2''), 133.50 (C-5''), 134.32 (C-3''), 139.38 (C-1''), 158.11 (NC(=NH)N), 159.85 (C-4''), 160.30 (NC(=O)N), 173.43 (C-1'), 176.17 (C-1).

LC-MS (ESI$^+$): m/z = 626.07 $[M+H]^+$.

$C_{29}H_{47}N_5O_8S$ (625.78)

7.3 Synthesis of muraymycin derivatives with L-serine

7.3.1 Cbz-Ser($COC_{12}H_{25}$)-NuAA 63[146,153]

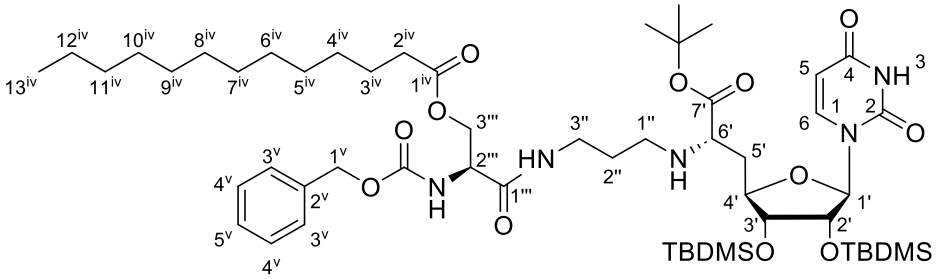

HOBt (32.2 mg, 238 µmol, 1.0 eq.), PyBOP (125 mg, 240 µmol, 1.0 eq.) and dry *N*,*N*-diisopropylethylamine (81.0 µL, 476 µmol, 2.0 eq.) were added to a solution of Cbz-Ser($COC_{12}H_{25}$)-OH **34** (104 mg, 239 µmol, 1.0 eq.) in dry tetrahydrofuran (13 mL). The solution was stirred for 30 min at room temperature. Then, it was then cooled to 0 °C and nucleosyl amino acid **35** (153 mg, 238 µmol, 1.0 eq.) in dry tetrahydrofuran (17 mL) was added dropwise. The reaction mixture was stirred for 1 h at 0 °C followed by 24 h at room temperature. The solvent was removed under reduced pressure. The title compound was obtained after purification by silica gel column chromatography (80 g, 4x15 cm, CH_2Cl_2:MeOH 98:2).

Yield (**63**): 139 mg (131 µmol, 55%, calcd. from the ^{1}H NMR spectrum) as a yellow oil with rests of tri(pyrrolidine-1-yl) phosphine oxide **64**.

TLC: R_f = 0.42 (CH_2Cl_2:MeOH 9:1).

^{1}H NMR (500 MHz, MeOH-d_4): δ [ppm] = 0.08 (s, 3 H, $SiCH_3$), 0.10 (s, 3 H, $SiCH_3$), 0.12 (s, 3 H, $SiCH_3$), 0.13 (s, 3 H, $SiCH_3$), 0.89 (t, $^3J_{13iv\text{-}H/12iv\text{-}H}$ = 6.9 Hz, 3 H, 13^{iv}-H), 0.91 (s, 9 H, $SiC(CH_3)_3$), 0.93 (s, 9 H, $SiC(CH_3)_3$), 1.27-1.30 (m, 18 H, 4^{iv}-12^{iv}-H), 1.48 (s, 9 H, $OC(CH_3)_3$), 1.54-1.60 (m, 2 H, 3^{iv}-H), 1.64-1.72 (m, 2 H, 2''-H), 1.93 (ddd, $^2J_{5'\text{-}Ha/5'\text{-}Hb}$ = 13.9 Hz, $^3J_{5'\text{-}Ha/6'\text{-}H}$ = 11.0 Hz, $^3J_{5'\text{-}Ha/4'\text{-}H}$ = 4.7 Hz, 1 H, 5'-H_a), 2.00-2.07 (m, 1 H, 5'-H_b), 2.29 (t, $^3J_{2iv\text{-}H/3iv\text{-}H}$ = 7.3 Hz, 2 H, 2^{iv}-H), 2.51-2.59 (m, 1 H, 1''-H_a), 2.61-2.68 (m, 1 H, 1''-H_b), 2.86-2.87 (m, 1 H, 2'''-H), 3.23-3.30 (m, 2 H, 3''-H), 3.32-3.37 (m, 1 H, 6'-H), 3.90 (dd, $^3J_{3'\text{-}H/2'\text{-}H}$ = 5.6 Hz, $^3J_{3'\text{-}H/4'\text{-}H}$ = 4.7 Hz, 1 H, 3'-H), 4.04-4.09 (m, 1 H, 4'-H), 4.24-4.29 (m, 1 H, 3'''-H_a), 4.31-4.33 (m, 1 H, 3'''-H_b), 4.39 (dd, $^3J_{2'\text{-}H/3'\text{-}H}$ = 5.6 Hz, $^3J_{2'\text{-}H/1'\text{-}H}$ = 4.8 Hz, 1 H, 2'-H), 5.06-5.13 (m, 2 H, 1^v-H), 5.74 (d, $^3J_{5\text{-}H/6\text{-}H}$ = 8.0 Hz, 1 H, 5-H), 5.76 (d, $^3J_{1'\text{-}H/2'\text{-}H}$ = 4.8 Hz, 1 H, 1'-H), 7.28-7.32 (m, 1 H, 5^v-H), 7.32-7.39 (m, 4 H, 3^v-H, 4^v-H), 7.65 (d, $^3J_{6\text{-}H/5\text{-}H}$ = 8.0 Hz, 1 H, 6-H).

^{13}C NMR (126 MHz, MeOH-d_4): δ [ppm] = -4.27 ($SiCH_3$), -4.24 ($SiCH_3$), -3.83 ($SiCH_3$), 14.06 (C-13^{iv}), 19.03 ($SiC(CH_3)_3$), 19.09 ($SiC(CH_3)_3$), 23.88 (C-4^{iv}-12^{iv}), 26.07 (C-3^{iv}), 26.56 ($SiC(CH_3)_3$), 26.62 ($SiC(CH_3)_3$), 28.60 ($OC(CH_3)_3$), 30.33 (C-2''), 30.59, 30.63, 30.76, 30.91, 30.94, 33.22 (C-4^{iv}-12^{iv}), 34.98 (C-2^{iv}), 37.97 (C-3''), 37.74 (C-5'), 45.71 (C-1'') 54.94 (C-2'''), 60.83 (C-6'), 64.89 (C-3'''), 68.07 (C-1^{v}), 75.94 (C-2'), 76.74 (C-3'), 82.76 (C-4'), 83.16 ($OC(CH_3)_3$), 92.25 (C-1'), 103.20 (C-5), 129.10, 129.26, 129.66 (C-3^{v}, C-4^{v}, C-5^{v}), 138.18 (C-2^{v}), 143.00 (C-6), 152.27 (C-2), 158.45 (NC(=O)O), 166.16 (C-4), 171.59, 171.70 (C-7', C-1'''), 175.09 (C-1^{iv}).

LC-MS (ESI^+): m/z = 1061.02 $[M+H]^+$.

$C_{54}H_{93}N_5O_{21}Si_2$ (1060.53)

7.3.2 Target compound T1: Val-Epic-Ser($COC_{12}H_{25}$)-NuAA[145,146,148,153]

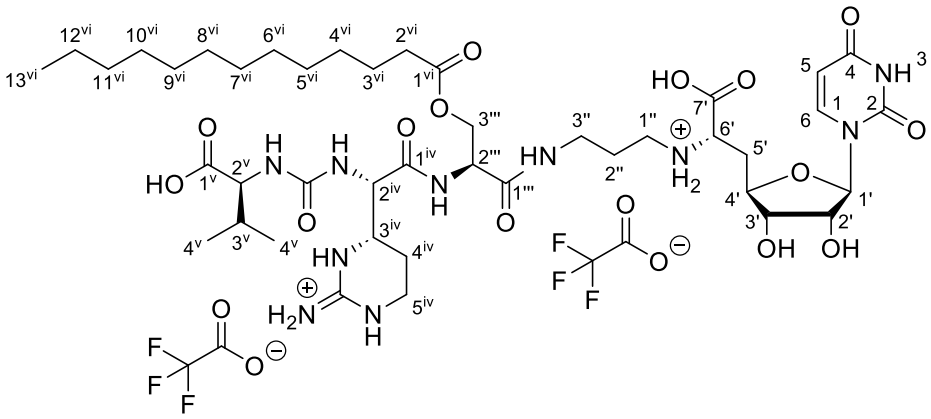

1,4-Cyclohexadiene (110 µL, 1.17 mmol, 10.0 eq.), palladium black (3 spatula tips), and trifluoroacetic acid (1.80 µL, 234 µmol, 2.0 eq., added as a 10% solution in dry *iso*-propanol) were added to a solution of Cbz-Ser($COC_{12}H_{25}$)-NuAA **63** (124 mg, 117 µmol, 1.0 eq.) in dry *iso*-propanol (4.4 mL). After 2 h, 1,4-cyclohexadiene (100 µL, 1.06 mmol, 9.1 eq.) and palladium black (4 spatula tips) were added again. The reaction was stirred for 1 h and then filtered through a syringe filter. The filter was washed with methanol (5x 5 mL). The solvent was removed under reduced pressure to give bis-TFA salt **65**. It was identified by LC-MS and was used without further purification (LC-MS (ESI^+): m/z = 926.55 $[M+H]^+$).

HOBt (10.1 mg, 74.7 µmol, 1.0 eq.), PyBOP (40.2 mg, 77.2 µmol, 1.0 eq.) and dry *N*,*N*-diisopropylethylamine (38.0 µL, 223 µmol, 3.0 eq.) were added to a mixture of ^{t}BuO-Val-Epic(Pbf)-OH **27** (47.0 mg, 75.3 µmol, 1.0 eq.) in dry tetrahydrofuran (12.5 mL). The reaction mixture was stirred for 30 min at room temperature. The solution was cooled

to 0 °C and bis-TFA salt **65** (109 mg) in dry tetrahydrofuran (10 mL) was added dropwise over 20 min. The solution was stirred for 1 h at 0 °C and then for 5.5 h at room temperature. The solvent was removed in high vacuum. The coupling product was identified by LC-MS (LC-MS (ESI$^+$): m/z = 766.40 $[M+2H]^{2+}$).

The residue was dissolved in aqueous trifluoroacetic acid (80%, 12.5 mL) and stirred for 25 h at room temperature. The solution was diluted with water (10 mL) and the solvent was removed in high vacuum. The residue was dissolved in a mixture of MeCN:H_2O:TFA (70:30:0.1) and the solvent was removed by lyophilization. The title compound was isolated after purification by HPLC.

Yield (**T1**): 3.47 mg (2.97 µmol, 2.5% over three steps) as a white solid.

HPLC (semi-preparative): 1. t_R = 15.2 min (method **A**, conc. of injection: ~46 mg/mL in H_2O:MeCN:TFA 65:35:0.1).

2. t_R = 14.6 min (method **A**, conc. of injection: ~11 mg/mL in H_2O:MeCN:TFA 65:35:0.1).

3. t_R = 20.5 min (methods **B1**/**B2**, conc. of injection: ~1.2-7.4 mg/mL in MeOH).

^{1}H NMR (500 MHz, MeOH-d_4): δ [ppm] = 0.90 (t, $^3J_{13^{vi}\text{-H}/12^{vi}\text{-H}}$ = 7.2 Hz, 3 H, 13^{vi}-H), 0.95 (d, $^3J_{4^{v}\text{-H}/3^{v}\text{-H}}$ = 6.8 Hz, 3 H, 4^{v}-H), 0.99 (d, $^3J_{4^{v}\text{-H}/3^{v}\text{-H}}$ = 6.8 Hz, 3 H, 4^{v}-H), 1.27-1.32 (m, 18 H, 4^{vi}-12^{vi}-H), 1.55-1.63 (m, 2 H, 3^{vi}-H), 1.88-1.93 (m, 2 H, 2''-H), 1.93-1.99 (m, 2 H, 4^{iv}-H), 2.14-2.22 (m, 1 H, 3^{v}-H), 2.25-2.33 (m, 1 H, 5'-H$_a$), 2.33 (t, $^3J_{2^{vi}\text{-H}/3^{vi}\text{-H}}$ = 7.6 Hz, 2 H, 2^{vi}-H), 2.40-2.49 (m, 1 H, 5'-H$_b$), 3.07-3.18 (m, 2 H, 1''-H), 3.31-3.40 (m, 3 H, 3''-H, 5^{iv}-H$_a$), 3.40-3.48 (m, 1 H, 5^{iv}-H$_b$), 3.72-3.80 (m, 1 H, 3^{iv}-H), 3.94 (dd, $^3J_{6'\text{-H}/5'\text{-H}_a}$ = 6.2 Hz, $^3J_{6'\text{-H}/5'\text{-H}_b}$ = 6.2 Hz, 1 H, 6'-H), 4.02 (dd, $^3J_{3'\text{-H}/4'\text{-H}}$ = 5.7 Hz, $^3J_{3'\text{-H}/2'\text{-H}}$ = 5.5 Hz, 1 H, 3'-H), 4.13-4.16 (m, 1 H, 4'-H), 4.17 (d, $^3J_{2^{v}\text{-H}/3^{v}\text{-H}}$ = 4.7 Hz, 1 H, 2^{v}-H), 4.34-4.41 (m, 3 H, 2'-H, 3'''-H), 4.43 (d, $^3J_{2^{iv}\text{-H}/3^{iv}\text{-H}}$ = 8.0 Hz, 1 H, 2^{iv}-H), 4.55 (dd, $^3J_{2'''\text{-H}/3'''\text{-H}_a}$ = 5.5 Hz, $^3J_{2'''\text{-H}/3'''\text{-H}_b}$ = 5.5 Hz, 1 H, 2'''-H), 5.68 (d, $^3J_{1'\text{-H}/2'\text{-H}}$ = 3.7 Hz, 1 H, 1'-H), 5.73 (d, $^3J_{5\text{-H}/6\text{-H}}$ = 7.9 Hz, 1 H, 5-H), 7.61 (d, $^3J_{6\text{-H}/5\text{-H}}$ = 7.9 Hz, 1 H, 6-H).

^{13}C NMR (126 MHz, MeOH-d_4): δ [ppm] = 14.43 (C-13^{vi}), 17.93 (C-4^{v}), 19.76 (C-4^{v}), 22.28 (C-4^{iv}), 23.73 (C-4^{vi}-12^{vi}), 25.88 (C-3^{vi}), 27.44 (C-2''), 30.21, 30.44, 30.47, 30.62, 30.73, 30.75, 30.78 (C-4^{vi}-12^{vi}), 31.70 (C-3^{v}), 33.07 (C-4^{vi}-12^{vi}), 34.18 (C-5'), 34.75 (C-2^{vi}), 37.15, 37.45 (C-3'', C-5^{iv}), 45.31 (C-1''), 52.14 (C-3^{iv}), 54.79 (C-2'''), 56.65 (C-2^{iv}), 59.65

(C-2^{v}), 60.36 (C-6'), 64.08 (C-3'''), 73.91 (C-2'), 74.80 (C-3'), 81.49 (C-4'), 94.45 (C-1'), 103.10 (C-5), 144.08 (C-6), 152.18 (C-2), 155.58 (NC(=NH)N), 160.31 (NC(=O)N), 166.05 (C-4), 171.71 (C-7'), 172.07 (C-1'''), 172.39 (C-1^{iv}), 175.00 (C-1^{vi}), 175.77 (C-1^{v}).

^{19}F NMR (282 MHz, MeOH-d_4): δ [ppm] = -76.87.

IR (ATR) υ [cm^{-1}]: 3307, 2925, 2854, 1661, 1559, 1183, 1134, 838, 800, 722.

UV (HPLC) λ [nm]: 260, 210.

$[\boldsymbol{\alpha}]_{\boldsymbol{D}}^{\boldsymbol{20}}$ = +16.0 (c = 1.25 · 10^{-3} g/mL, MeOH).

LC-MS (ESI$^+$): m/z = 939.54 $[M+H]^+$.

HRMS (ESI$^+$): calcd. for $C_{42}H_{71}N_{10}O_{14}^+$: 939.5146, found: 939.5132 $[M+H]^+$.

$C_{42}H_{70}N_{10}O_{14}$ (939.08)

$C_{42}H_{72}N_{10}O_{14}^{2+}$ • 2 $C_2F_3O_2^-$ (1167.12)

7.3.3 Cbz-Ser($COC_{15}H_{31}$)-NuAA 66[146,153]

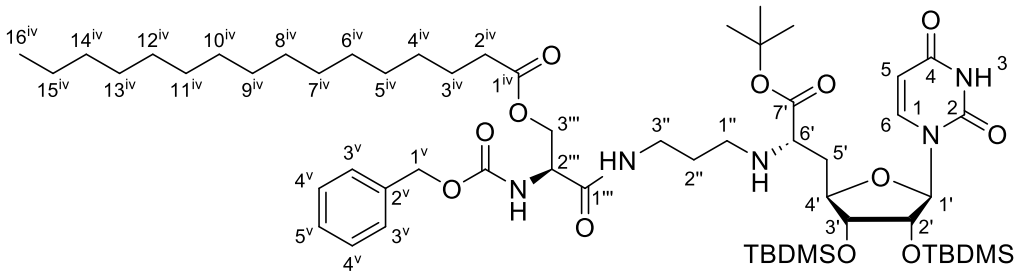

HOBt (12.6 mg, 93.3 µmol, 1.0 eq.), PyBOP (48.4 mg, 93.0 µmol, 1.0 eq.) and dry *N*,*N*-diisopropylethylamine (35.0 µL, 206 µmol, 2.2 eq.) were added to a solution of Cbz-Ser($COC_{15}H_{31}$)-OH **37** (45.1 mg, 94.4 µmol, 1.0 eq.) in dry tetrahydrofuran (5 mL). The solution was stirred for 30 min at room temperature. Then, it was cooled to 0 °C and nucleosyl amino acid **35** (59.8 mg, 93.0 µmol, 1.0 eq.) in dry tetrahydrofuran (6.5 mL) was added dropwise. The reaction mixture was stirred for 1 h at 0 °C and then for 24 h at room temperature. The solvent was removed under reduced pressure. The title compound was obtained after purification by silica gel column chromatography (80 g, 4x15 cm, CH_2Cl_2:MeOH 98:2).

Yield (**66**): 61.0 mg (55.3 µmol, 59%) as a colorless foamy solid.

TLC: R_f = 0.49 (CH_2Cl_2:MeOH 9:1).

^{1}H NMR (300 MHz, MeOH-d_4): δ [ppm] = 0.08 (s, 3 H, $SiCH_3$), 0.10 (s, 3 H, $SiCH_3$), 0.12 (s, 3 H, $SiCH_3$), 0.13 (s, 3 H, $SiCH_3$), 0.87-0.91 (m, 12 H, $SiC(CH_3)_3$, 16^{iv}-H), 0.93 (s, 9 H, $SiC(CH_3)_3$), 1.25-1.32 (m, 24 H, 4^{iv}-15^{iv}-H), 1.48 (s, 9 H, $OC(CH_3)_3$), 1.53-1.61 (m, 2 H, 3^{iv}-H), 1.65-1.72 (m, 2 H, 2''-H), 1.86-1.97 (m, 1 H, 5'-H_a), 1.98-2.08 (m, 1 H, 5'-H_b), 2.30 (t, $^{3}J_{2iv\text{-}H/3iv\text{-}H}$ = 7.7 Hz, 2 H, 2^{iv}-H), 2.50-2.70 (m, 2 H, 1''-H), 3.21-3.29 (m, 1 H, 3''-H_a), 3.33-3.38 (m, 1 H, 3''-H_b), 3.42-3.57 (m, 1 H, 6'-H), 3.88-3.93 (m, 1 H, 3'-H), 4.02-4.11 (m, 1 H, 4'-H), 4.20-4.28 (m, 1 H, 3'''-H_a), 4.28-4.43 (m, 4 H, 2'-H, 2'''-H, 3'''-H_b), 5.08-5.14 (m, 2 H, 1^{v}-H), 5.74 (d, $^{3}J_{5\text{-}H/6\text{-}H}$ = 7.9 Hz, 1 H, 5-H), 5.76 (d, $^{3}J_{1'\text{-}H/2'\text{-}H}$ = 4.0 Hz, 1 H, 1'-H), 7.27-7.33 (m, 1 H, 5^{v}-H), 7.33-7.38 (m, 4 H, 3^{v}-H, 4^{v}-H), 7.64 (d, $^{3}J_{6\text{-}H/5\text{-}H}$ = 7.9 Hz, 1 H, 6-H).

^{13}C NMR (76 MHz, MeOH-d_4): δ [ppm] = -4.41 ($SiCH_3$), -4.39 ($SiCH_3$), -3.99 ($SiCH_3$), -3.97 ($SiCH_3$), 14.45 (C-16^{iv}), 18.87 ($SiC(CH_3)_3$), 18.94 ($SiC(CH_3)_3$), 23.73 (C-4^{iv}-15^{iv}), 25.92 (C-3^{iv}), 26.41 ($SiC(CH_3)_3$), 26.47 ($SiC(CH_3)_3$), 28.47 ($OC(CH_3)_3$), 30.18, 30.44, 30.47, 30.61, 30.79, 33.07 (C-4^{iv}-15^{iv}), 34.83 (C-2^{iv}), 38.00 (C-5'), 38.42 (C-3''), 45.52 (C-1''), 54.99 (C-2'''), 60.73 (C-6'), 65.23 (C-3'''), 67.93 (C-1^{v}), 75.91 (C-2'), 76.60 (C-3'), 82.66 (C-4'), 82.96 ($OC(CH_3)_3$), 92.57 (C-1'), 103.08 (C-5), 128.95, 129.51 (C-3^{v}, C-4^{v}, C-5^{v}), 138.07 (C-2^{v}), 142.65 (C-6), 152.14 (C-2), 157.14 (NC(=O)O), 166.06 (C-4), 171.52 (C-1'''), 174.95 (C-1^{iv}).

LC-MS (ESI^+): m/z = 1102.78 $[M+H]^+$.

$C_{54}H_{93}N_5O_{21}Si_2$ (1102.61)

7.3.4 Target compound T2: Val-Epic-Ser($COC_{15}H_{31}$)-NuAA[145,146,148,153]

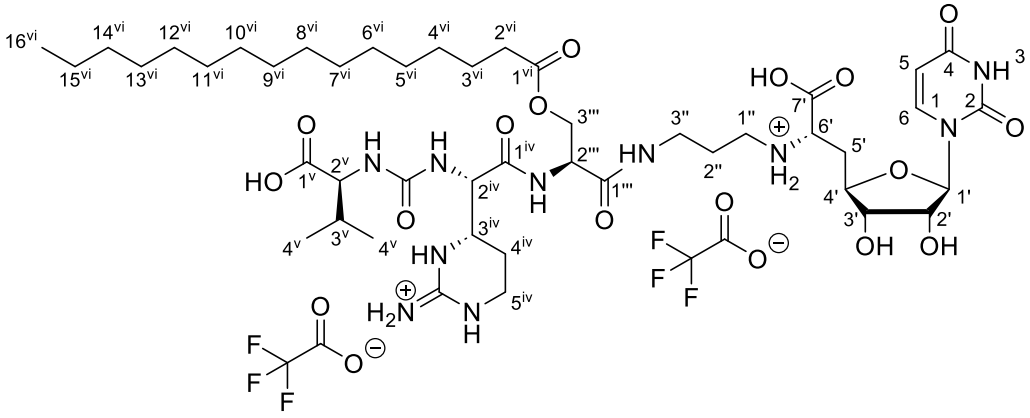

1,4-Cyclohexadiene (52.0 µL, 55.3 µmol, 10.0 eq.), palladium black (1 spatula tip) and trifluoroacetic acid (11.0 µL, 111 µmol, 2.0 eq., added as a 10% solution in dry *iso*-propanol) were added to a solution of Cbz-Ser(*C*$OC_{15}H_{31}$)-NuAA **66** (61.0 mg,

55.3 µmol, 1.0 eq.) in dry *iso*-propanol (3.8 mL). The reaction was stirred for 3.5 h at room temperature. Then, the reaction mixture was filtered through a syringe filter. The filter was washed with methanol (4x 5 mL). The solvent was removed under reduced pressure to give the bis-TFA salt **67**. It was identified by LC-MS and was used without further purification (LC-MS (ESI^+): m/z = 968.56 $[M+H]^+$).

HOBt (6.50 mg, 48.1 µmol, 1.0 eq.), PyBOP (25.8 mg, 49.3 µmol, 1.0 eq.) and dry *N*,*N*-diisopropylethylamine (24.5 µL, 144 µmol, 3.0 eq.) were added to a mixture of ^{t}BuO-Val-Epic(Pbf)-OH **27**(31.8 mg, 51.0 µmol, 1.1 eq.) in dry tetrahydrofuran (8 mL). The reaction mixture was stirred for 30 min at room temperature. Then, it was cooled to 0 °C and bis-TFA salt **67** (57.6 mg, 48.1 µmol, 1.0 eq.) in dry tetrahydrofuran (6.4 mL) was added dropwise over 10 min. The solution was stirred for 1 h at 0 °C and then for 28 h at room temperature. The solvent was removed under reduced pressure and the residue was purified by HPLC. The product was identified by LC-MS (LC-MS (ESI^+): m/z = 787.71 $[M+2H]^{2+}$).

The residue was dissolved in aqueous trifluoroacetic acid (80%, 30 mL) and stirred for 28 h at room temperature. The solution was diluted with water (50 mL) and the solvent was removed by lyophilization. The title compound was isolated after purification by HPLC.

Yield (**T2**): 3.92 mg (3.24 µmol, 5.9% over three steps) as a white solid.

HPLC (semi-preparative): before global deprotection: t_R = 20 min (method: **B1**, conc. of injection: 13.2 mg/mL in MeOH).

after global deprotection: t_R = 16-19 min (method: **A**, conc. of injection: 6.2 mg/mL in MeCN:H_2O:TFA 65:35:0.1).

^{1}H NMR (500 MHz, MeOH-d_4): δ [ppm] = 0.90 (t, $^3J_{16^{vi}\text{-H}/15^{vi}\text{-H}}$ = 7.0 Hz, 3 H, 16^{vi}-H), 0.95 (d, $^3J_{4^{v}\text{-H}/3^{v}\text{-H}}$ = 6.7 Hz, 3 H, 4^{v}-H), 0.99 (d, $^3J_{4^{v}\text{-H}/3^{v}\text{-H}}$ = 6.9 Hz, 3 H, 4^{v}-H), 1.27-1.31 (m, 24 H, 4^{vi}-15^{vi}-H), 1.55-1.63 (m, 24 H, 3^{vi}-H), 1.88-1.98 (m, 4 H, 2''-H, 4^{iv}-H), 2.15-2.22 (m, 1 H, 3^{v}-H), 2.24-2.31 (m, 1 H, 5'-H_a), 2.34 (t, $^3J_{2^{vi}\text{-H}/3^{vi}\text{-H}}$ = 7.5 Hz, 2 H, 2^{vi}-H), 2.40-2.49 (m, 1 H, 5'-H_b), 3.09-3.16 (m, 2 H, 1''-H), 3.32-3.47 (m, 4 H, 3''-H, 5^{iv}-H), 3.76 (ddd, $^3J_{3^{iv}\text{-H}/2^{iv}\text{-H}}$ = 7.2 Hz, $^3J_{3^{iv}\text{-H}/4^{iv}\text{-H}_a}$ = 6.2 Hz, $^3J_{3^{iv}\text{-H}/4^{iv}\text{-H}_b}$ = 6.2 Hz, 1 H, 3^{iv}-H), 3.93-3.99 (m, 1 H, 6'-H), 4.02 (dd, $^3J_{3'\text{-H}/4'\text{-H}}$ = 5.8 Hz, $^3J_{3'\text{-H}/2'\text{-H}}$ = 5.8 Hz, 1 H, 3'-H), 4.13-4.16 (m, 1 H, 4'-H), 4.17 (d, $^3J_{2^{v}\text{-H}/3^{v}\text{-H}}$ = 4.7 Hz, 1 H, 2^{v}-H), 4.35-4.40 (m, 3 H, 2'-H, 3'''-H), 4.43 (d,

$^{3}J_{3iv\text{-}H/2iv\text{-}H}$ = 7.2 Hz, 1 H, 2^{iv}-H), 4.55 (dd, $^{3}J_{2'''\text{-}H/3'''\text{-}Ha}$ = 5.4 Hz, $^{3}J_{2'''\text{-}H/3'''\text{-}Hb}$ = 5.4 Hz, 2'''-H), 5.68 (d, $^{3}J_{1'\text{-}H/2'\text{-}H}$ = 3.7 Hz, 1 H, 1'-H), 5.73 (d, $^{3}J_{5\text{-}H/6\text{-}H}$ = 8.0 Hz, 1 H, 5-H), 7.61 (d, $^{3}J_{6\text{-}H/5\text{-}H}$ = 8.0 Hz, 1 H, 6-H).

^{13}C NMR (126 MHz, MeOH-d_4): δ [ppm] = 14.42 (C-16^{vi}), 17.92 (C-4^{v}), 19.75 (C-4^{v}), 22.26 (C-4^{iv}), 23.71 (C-4^{vi}-15^{vi}), 25.87 (C-3^{vi}), 27.43 (C-2''), 30.20, 30.30, 30.43, 30.61, 30.72, 30.73, 30.77 (C-4^{vi}-15^{vi}), 31.69 (C-3^{v}), 33.05 (C-4^{vi}-15^{vi}), 34.14 (C-5'), 34.73 (C-2^{vi}), 37.14, 37.44 (C-3'', C-5^{iv}), 45.30 (C-1''), 52.14 (C-3^{iv}), 54.77 (C-2'''), 56.74 (C-2^{iv}), 59.63 (C-2^{v}), 64.06 (C-3'''), 73.89 (C-2'), 74.79 (C-3'), 81.46 (C-4'), 94.46 (C-1'), 103.08 (C-5), 144.06 (C-6), 152.16 (C-2), 155.56 (NC(=NH)N), 160.29 (NC(=O)N), 166.03 (C-4), 172.05 (C-1'''), 172.36 (C-1^{iv}), 174.98 (C-1^{vi}), 175.75 (C-1^{v}).

^{19}F NMR (471 MHz, MeOH-d_4): δ [ppm] = -76.97.

IR (ATR) υ [cm^{-1}]: 3307, 2923, 2854, 1686, 1557, 1183, 1134, 836, 800, 720.

UV (HPLC) λ [nm]: 260, 212.

$[\boldsymbol{\alpha}]_{\boldsymbol{D}}^{\boldsymbol{20}}$ = +13.0 (c = 2.3 • 10^{-3} g/mL, MeOH).

LC-MS (ESI^{+}): m/z = 981.59 $[M+H]^{+}$.

HRMS (ESI^{+}): calcd. for $C_{45}H_{78}N_{10}O_{14}^{2+}$: 981.5616, found: 981.5608 $[M+H]^{+}$.

$C_{45}H_{76}N_{10}O_{14}$ (981.17)

$C_{45}H_{78}N_{10}O_{14}^{2+}$ • 2 $C_2F_3O_2^{-}$ (1209.21)

7.3.5 Target compound T3: Val-Arg-Ser($COC_{12}H_{25}$)-NuAA[145,153,170]

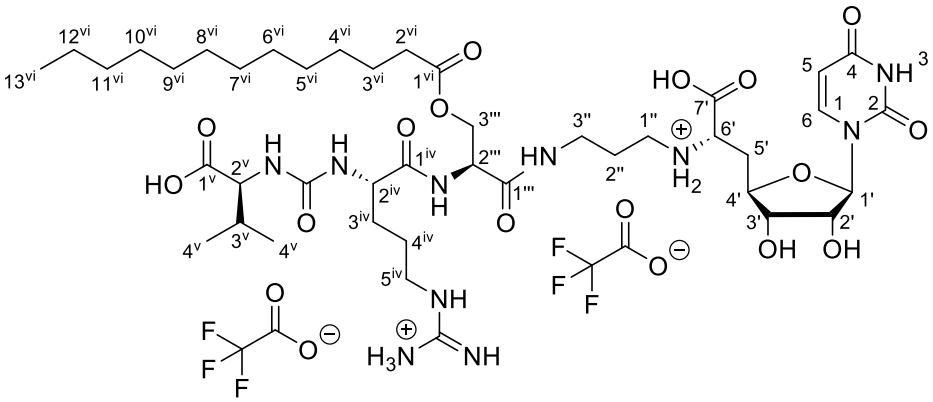

^{t}BuO-Val-Arg(Pbf)-OH **36** (32.6 mg, 52.1 µmol, 1.0 eq.), H-Ser($COC_{12}H_{25}$)-NuAA bis-TFA salt **65** (59.8 mg, 51.5 µmol, 1.0 eq.) and dry *N*,*N*-diisopropylethylamine (31.0 µL, 182 µmol, 3.5 eq.) were diluted in dry ethyl acetate (1.5 mL). The reaction mixture was

cooled to 0 °C and stirred for 15 min at this temperature. T_3P (50% in dry ethyl acetate, 77.2 µL, 129 µmol, 2.5 eq.) was added to the reaction mixture. After 30 min at 0 °C, ethyl acetate (15 mL) was added, and the organic layer was washed with water (2x 5 mL) and brine (5 mL). The organic layer was dried over sodium sulfate and the solvent was removed under reduced pressure. The residue was purified by HPLC. The product was identified by LC-MS (LC-MS (ESI^+): m/z = 1534.39 $[M+H]^+$).

The residue was dissolved in aqueous trifluoroacetic acid (80%, 10 mL) and the solution was stirred for 24 h at room temperature. The solution was diluted with water (50 mL) and the solvent was removed by lyophilization. The title compound was isolated after purification by HPLC.

Yield (**T3**): 2.30 mg (1.99 µmol, 3.8% over two steps) as a colorless solid.

HPLC (semi-preparative): before global deprotection: t_R = ~19 min (method: **C**, conc. of injection: 12.3 mg/mL in MeOH).

after global deprotection: t_R = ~14-16 min (method: **D**, conc. of injection: ~8 mg/mL in H_2O:MeCN:TFA 70:30:0.1).

^{1}H NMR (500 MHz, MeOH-d_4): δ [ppm] = 0.90 (t, $^3J_{13vi\text{-}H/12vi\text{-}H}$ = 7.0 Hz, 3 H, 13^{vi}-H), 0.95 (d, $^3J_{4v\text{-}H/3v\text{-}H}$ = 6.9 Hz, 3 H, 4^{v}-H), 1.00 (d, $^3J_{4v\text{-}H/3v\text{-}H}$ = 6.9 Hz, 3 H, 4^{v}-H), 1.27-1.33 (m, 18 H, 4^{vi}-12^{vi}-H), 1.55-1.62 (m, 2 H, 3^{vi}-H), 1.65-1.73 (m, 3 H, 3^{iv}-H_a, 4^{iv}-H), 1.81-1.87 (m, 1 H, 3^{iv}-H_b), 1.87-1.95 (m, 2 H, 2''-H), 2.14-2.21 (m, 1 H, 3^{v}-H), 2.24-2.30 (m, 1 H, 5'-H_a), 2.32 (t, $^3J_{2vi\text{-}H/3vi\text{-}H}$ = 7.5 Hz, 2 H, 2^{vi}-H), 2.43 (ddd, $^2J_{5'\text{-}Hb/5'\text{-}Ha}$ = 14.7 Hz, $^3J_{5'\text{-}Hb/6'\text{-}H}$ = 6.4 Hz, $^3J_{5'\text{-}Hb/4'\text{-}H}$ = 3.1 Hz, 1 H, 5'-H_b), 3.10 (t, $^3J_{1''\text{-}H/2''\text{-}H}$ = 7.0 Hz, 2 H, 1''-H), 3.23 (t, $^3J_{5iv\text{-}H/4iv\text{-}H}$ = 6.7 Hz, 2 H, 5^{iv}-H), 3.25-3.29 (m, 1 H, 3''-H_a), 3.33-3.40 (m, 1 H, 3''-H_b), 3.95 (dd, $^3J_{6'\text{-}H/5'\text{-}Hb}$ = 6.4 Hz, $^3J_{6'\text{-}H/5'\text{-}Ha}$ = 6.2 Hz, 2 H, 6'-H), 4.01 (dd, $^3J_{3'\text{-}H/4'\text{-}H}$ = 6.0 Hz, $^3J_{3'\text{-}H/2'\text{-}H}$ = 6.0 Hz, 1 H, 3'-H), 4.14-4.21 (m, 3 H, 4'-H, 2^{iv}-H, 2^{v}-H), 4.33-4.41 (m, 3 H, 2'-H, 3'''-H), 4.51 (dd, $^3J_{2'''\text{-}H/3'''\text{-}Ha}$ = 5.9 Hz, $^3J_{2'''\text{-}H/3'''\text{-}Hb}$ = 4.9 Hz, 1 H, 2'''-H), 5.68 (d, $^3J_{1'\text{-}H/2'\text{-}H}$ = 3.8 Hz, 1 H, 1'-H), 5.73 (d, $^3J_{5\text{-}H/6\text{-}H}$ = 8.1 Hz, 1 H, 5-H), 7.61 (d, $^3J_{6\text{-}H/5\text{-}H}$ = 8.1 Hz, 1 H, 6-H).

^{13}C NMR (126 MHz, MeOH-d_4): δ [ppm] = 14.43 (C-13^{vi}), 17.99 (C-4^{v}), 19.83 (C-4^{v}), 23.73 (C-4^{vi}-12^{vi}), 25.91 (C-3^{vi}), 26.09, 30.21 (C-3^{iv}, C-4^{iv}), 27.43 (C-2''), 30.44, 30.47, 30.57, 30.62, 30.74, 30.75, 30.78 (C-4^{vi}-12^{vi}), 31.86 (C-3^{v}), 33.07 (C-4^{vi}-12^{vi}), 34.20 (C-5'), 34.79 (C-2^{vi}), 36.95 (C-3''), 41.91 (C-5^{iv}), 45.19 (C-1''), 54.58 (C-2'''), 55.11, 59.54 (C-2^{iv}, C-2^{v}), 60.14 (C-6'), 64.17 (C-3'''), 73.96 (C-2'), 74.81 (C-3'), 81.56 (C-4'), 94.41 (C-1'),

103.04 (C-5), 144.06 (C-6), 152.16 (C-2), 158.66 (NC(=NH)N), 160.65 (NC(=O)N), 166.09 (C-4), 171.75 (C-7'), 172.12 (C-1'''), 175.08 (C-1^{vi}), 175.47 (C-1^{iv}), 175.84 (C-1^{v}).

^{19}F NMR (471 MHz, MeOH-d_4): δ [ppm] = -76.95.

IR (ATR) υ [cm^{-1}]: 3346, 2925, 2854, 1660, 1554, 1465, 1185, 1136, 800, 720, 533.

UV (HPLC) λ [nm]: 260, 210.

LC-MS (ESI^+): m/z = 941.44 $[M+H]^+$.

HRMS (ESI^+): calcd. for $C_{42}H_{74}N_{10}O_{14}^{2+}$: 471.2688, found: 471.2678 $[M+2H]^{2+}$.

$C_{42}H_{72}N_{10}O_{14}$ (941.09)

$C_{42}H_{74}N_{10}O_{14}^{2+}$ • 2 $C_2F_3O_2^-$ (1169.14)

7.4 Synthesis of muraymycin derivatives with L-*allo*-threonine

7.4.1 Cbz-*allo*-Thr($COC_{12}H_{25}$)-NuAA 52

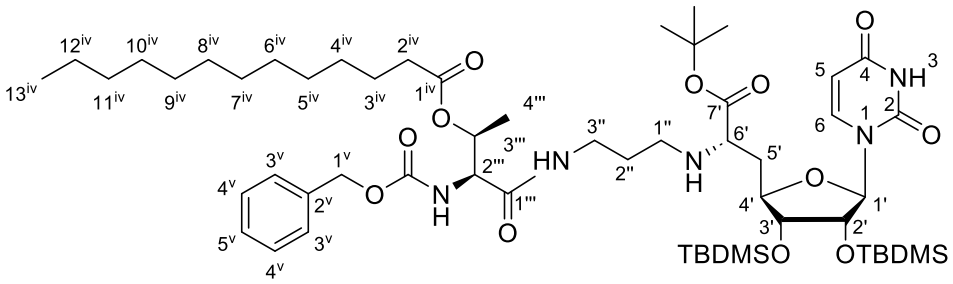

Alternative 1:

Dry *N*,*N*-diisopropylethylamine (11.3 µL, 66.3 µmol, 1.0 eq.) was added to a solution of Cbz-*allo*-Thr($COC_{12}H_{25}$)-OH **38** (29.8 mg, 66.3 µmol, 1.0 eq.) in dry dichloromethane (1 mL). After 30 min, HATU (38.8 mg, 102 µmol, 1.5 eq.) was added and the reaction mixture was stirred for 30 min at room temperature. The mixture was cooled to 0 °C and dry *N*,*N*-diisopropylethylamine (11.3 µL, 66.3 µmol, 1.0 eq.) was added. Nucleosyl amino acid **35** (42.6 mg, 66.3 µmol, 1.0 eq.) in dry dichloromethane (1.5 mL) was added dropwise at this temperature. The reaction was stirred for 23 h. During this time, the reaction mixture was allowed to warm up to room temperature. Then, an aqueous ammonium chloride solution (1 M, 10 mL) was added. The aqueous layer was extracted with ethyl acetate (3x 10 mL). The combined organic layer was washed with saturated sodium bicarbonate solution (20 mL) and brine (20 mL) and dried over sodium sulfate. The solvent was removed under reduced pressure. The title compound was obtained

after purification by silica gel column chromatography (15 g, 2x9 cm, CH_2Cl_2:MeOH 100:0 → 98:2).

Yield (**52**): 32.3 mg (30.1 µmol, 45%) as a colorless foamy solid.

TLC: R_f = 0.38 (CH_2Cl_2:MeOH 9:1).

^{1}H NMR (500 MHz, DMSO-d_6): δ [ppm] = 0.00 (s, 3 H, $SiCH_3$), 0.03 (s, 3 H, $SiCH_3$), 0.07 (s, 3 H, $SiCH_3$), 0.08 (s, 3 H, $SiCH_3$), 0.83 (s, 9 H, $SiC(CH_3)_3$), 0.84-0.86 (m, 3 H, 13^{iv}-H), 0.87 (s, 9 H, $SiC(CH_3)_3$), 1.11 (d, $^3J_{4'''\text{-H}/3'''\text{-H}}$ = 6.4 Hz, 3 H, 4'''-H), 1.18-1.23 (m, 18 H, 4^{iv}-12^{iv}-H), 1.40 (s, 9 H, $OC(CH_3)_3$), 1.42-1.54 (m, 4 H, 2''-H, 3^{iv}-H), 1.84-1.91 (m, 2 H, 5'-H_a, 5'-H_b), 1.93-2.04 (m, 1 H, 6'-NH), 2.12-2.21 (m, 2 H, 2^{iv}-H), 2.34-2.41 (m, 1 H, 1''-H_a), 2.45-2.52 (m, 1 H, 1''-H_b), 3.03-3.17 (m, 3 H, 6'-H, 3''-H), 3.84-3.92 (m, 2 H, 3'-H, 4'-H), 4.23 (dd, $^3J_{2'''\text{-H}/2'''\text{-NH}}$ = 9.0 Hz, $^3J_{2'''\text{-H}/3'''\text{-H}}$ = 6.9 Hz, 1 H, 2'''-H), 4.32 (dd, $^3J_{2'\text{-H}/1'\text{-H}}$ = 4.3 Hz, $^3J_{2'\text{-H}/3'\text{-H}}$ = 4.3 Hz, 1 H, 2'-H), 4.98-5.09 (m, 3 H, 3'''-H, 1^v-H), 5.65-5.71 (m, 2 H, 5-H, 1'-H), 7.28-7.33 (m, 1 H, 5^v-H), 7.33-7.38 (m, 4 H, 3^v-H, 4^v-H), 7.53 (d, $^3J_{2'''\text{-NH}/2'''\text{H}}$ = 9.0 Hz, 1 H, 2'''-NH), 7.60 (d, $^3J_{6\text{-H}/5\text{-H}}$ = 8.0 Hz, 1 H, 6-H), 7.99 (bs, 1 H, 3''-NH), 11.36 (s, 1 H, 3-H).

^{13}C NMR (126 MHz, DMSO-d_6): δ [ppm] = -4.97 ($SiCH_3$), -4.95 ($SiCH_3$), -4.82 ($SiCH_3$), -4.47 ($SiCH_3$), 15.82 (C-4'''), 17.74 (Si<u>C</u>$(CH_3)_3$), 17.65 (Si<u>C</u>$(CH_3)_3$), 22.08 (C-4^{iv}-12^{iv}), 24.28 (C-3^{iv}), 25.58 (SiC(<u>C</u>$H_3)_3$), 26.68 (SiC(<u>C</u>$H_3)_3$), 27.63 (OC(<u>C</u>$H_3)_3$), 28.38, 28.69, 28.86, 28.98, 29.00, 29.03 (C-4^{iv}-12^{iv}), 29.50 (C-2''), 31.28 (C-4^{iv}-12^{iv}), 33.63 (C-2^{iv}), 36.37 (C-5'), 36.88 (C-3''), 44.73 (C-1''), 57.53 (C-2'''), 59.17 (C-6'), 65.56 (C-3'''), 69.29 (C-1^v), 73.61 (C-2'), 74.54 (C-3'), 80.76 (C-4'), 80.26 (O<u>C</u>$(CH_3)_3$), 88.62 (C-1'), 102.09 (C-5), 127.64, 127.78, 128.30 (C-3^v, C-4^v, C-5^v), 136.91 (C-2^v), 140.92 (C-6), 150.58 (C-2), 156.01 (NC(=O)O), 162.99 (C-4), 168.47 (C-1'''), 171.88 (C-1^{iv}), 173.43 (C-7').

LC-MS (ESI$^+$): m/z = 1074.45 $[M+H]^+$.

Alternative 2:[146]

Dry *N*,*N*-diisopropylethylamine (21.8 µL, 128 µmol, 1.0 eq.), HOBt (17.4 mg, 129 µmol, 1.0 eq.) and EDC • HCl (24.6 mg, 128 µmol, 1.0 eq.) were added to a solution of Cbz-*allo*-Thr($COC_{12}H_{25}$)-OH **38** (57.6 mg, 128 µmol, 1.0 eq.) in dry tetrahydrofuran (3 mL). After 1 h, nucleosyl amino acid **35** (42.6 mg, 66.3 µmol, 1.0 eq.) in dry tetrahydrofuran (5 mL) was added dropwise at this temperature. The reaction was stirred for 23 h. During this time, the reaction mixture was allowed to warm up to room temperature.

Ethyl acetate (30 mL) was added, and the organic layer was washed with saturated sodium carbonate solution (15 mL). The aqueous layer was extracted with ethyl acetate (30 mL). The combined organic layer was dried over sodium sulfate. The solvent was then removed under reduced pressure. The title compound was obtained after purification by silica gel column chromatography (30 g, 3x14 cm, CH_2Cl_2:MeOH 100:0 → 98:2 → 95:5).

Yield (**52**): 60.2 mg (56.0 µmol, 44%) as a colorless foamy solid.

^{1}H NMR (500 MHz, MeOH-d_4): δ [ppm] = 0.09 (s, 3 H, $SiCH_3$), 0.10 (s, 3 H, $SiCH_3$), 0.12 (s, 3 H, $SiCH_3$), 0.13 (s, 3 H, $SiCH_3$), 0.90 (t, $^3J_{13iv\text{-}H/12iv\text{-}H}$ = 7.1 Hz, 3 H, 13^{iv}-H), 0.91 (s, 9 H, $SiC(CH_3)_3$), 0.93 (s, 9 H, $SiC(CH_3)_3$), 1.22 (d, $^3J_{4'''\text{-}H/3'''\text{-}H}$ = 6.5 Hz, 3 H, 4'''-H), 1.26-1.30 (m, 18 H, 4^{iv}-12^{iv}-H), 1.48 (s, 9 H, $OC(CH_3)_3$), 1.52-1.59 (m, 2 H, 3^{iv}-H), 1.64-1.73 (m, 2 H, 2''-H), 1.91 (ddd, $^2J_{5'\text{-}H_a/5'\text{-}H_b}$ = 14.0 Hz, $^3J_{5'\text{-}H_a/4'\text{-}H}$ = 11.1 Hz, $^3J_{5'\text{-}H_a/6'\text{-}H}$ = 4.6 Hz, 1 H, 5'-H_a), 2.00-2.08 (m, 1 H, 5'-H_b), 2.23 (t, $^3J_{2iv\text{-}H/3iv\text{-}H}$ = 7.4 Hz, 2 H, 2^{iv}-H), 2.53 (dt, $^2J_{1''\text{-}H_a/1''\text{-}H_b}$ = 11.7 Hz, $^3J_{1''\text{-}H_a/2''\text{-}H}$ = 6.8 Hz, 1 H, 1''-H_a), 2.62 (dt, $^2J_{1''\text{-}H_b/1''\text{-}H_a}$ = 11.7 Hz, $^3J_{1''\text{-}H_b/2''\text{-}H}$ = 6.9 Hz, 1 H, 1''-H_b), 3.26 (t, $^3J_{3''\text{-}H/2''\text{-}H}$ = 6.6 Hz, 2 H, 3''-H), 3.32-3.35 (m, 1 H, 6'-H), 3.90 (dd, $^3J_{3'\text{-}H/2'\text{-}H}$ = 4.9 Hz, $^3J_{3'\text{-}H/4'\text{-}H}$ = 4.7 Hz, 1 H, 3'-H), 4.06 (ddd, $^3J_{4'\text{-}H/5'\text{-}H_a}$ = 11.1 Hz, $^3J_{4'H/3'\text{-}H}$ = 4.7 Hz, $^3J_{4'\text{-}H/5'\text{-}H_b}$ = 2.8 Hz, 1 H, 4'-H), 4.33 (dd, $^3J_{2'\text{-}H/3'\text{-}H}$ = 4.9 Hz, $^3J_{2'\text{-}H/1'\text{-}H}$ = 4.4 Hz, 1 H, 2'-H), 4.40 (d, $^3J_{2'''\text{-}H/3'''\text{-}H}$ = 6.2 Hz, 1 H, 2'''-H), 5.01-5.16 (m, 3 H, 3'''-H, 1^v-H), 5.75 (d, $^3J_{5\text{-}H/6\text{-}H}$ = 8.1 Hz, 1 H, 5-H), 5.77 (d, $^3J_{1'\text{-}H/2'\text{-}H}$ = 4.4 Hz, 1 H, 1'-H), 7.27-7.32 (m, 1 H, 5^v-H), 7.32-7.38 (m, 4 H, 3^v-H, 4^v-H), 7.65 (d, $^3J_{6\text{-}H/5\text{-}H}$ = 8.1 Hz, 1 H, 6-H).

^{13}C NMR (126 MHz, MeOH-d_4): δ [ppm] = -4.44 ($SiCH_3$), -4.42 ($SiCH_3$), -4.40 ($SiCH_3$), -3.99 ($SiCH_3$), 14.45 (C-13^{iv}), 16.04 (C-4'''), 18.87 ($SiC(CH_3)_3$), 18.94 ($SiC(CH_3)_3$), 23.74 (C-4^{iv}-12^{iv}), 25.91 (C-3^{iv}), 26.40 ($SiC(CH_3)_3$), 26.46 ($SiC(CH_3)_3$), 28.45 ($OC(CH_3)_3$), 30.17 (C-2''), 30.30, 30.43, 30.48, 30.62, 30.75, 30.77, 30.79 (C-4^{iv}-12^{iv}), 33.08 (C-2^{iv}), 35.20 (C-5'), 38.48 (C-3''), 46.14 (C-1''), 59.19 (C-2'''), 60.75 (C-6'), 67.86 (C-3'''), 71.11 (C-1^v), 75.91 (C-2'), 76.56 (C-3'), 82.60 (C-4'), 82.87 ($OC(CH_3)_3$), 91.87 (C-1'), 103.04 (C-5), 128.90, 129.49, 129.49 (C-3^v-5^v), 138.13 (C-2^v), 142.69 (C-6), 152.12 (C-2), 158.38 (NC(=O)O), 166.06 (C-4), 171.37 (C-1'''), 174.45 (C-1^{iv}), 174.79 (C-7').

LC-MS (ESI^+): m/z = 1074.95 $[M+H]^+$.

$C_{55}H_{95}N_5O_{12}Si_2$ (1074.56)

7.4.2 H-*allo*-Thr($COC_{12}H_{25}$)-NuAA bis-TFA salt 78[148,153]

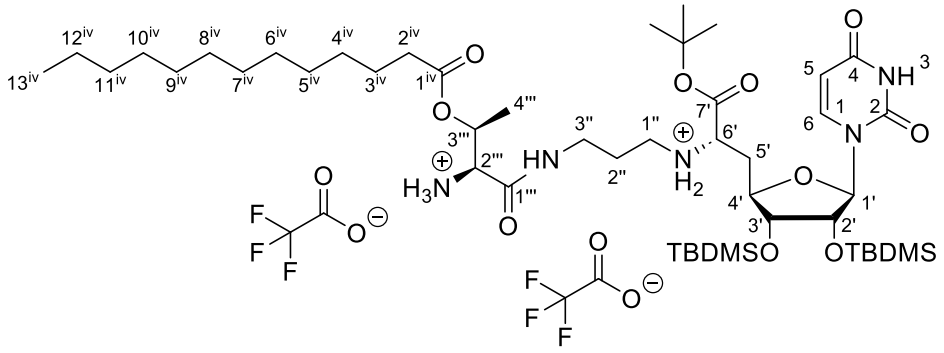

1,4-Cyclohexadiene (71.0 µL, 753 µmol, 25.0 eq.), palladium black (3 spatula tips) and trifluoracetic acid (4.70 µL, 60.2 µmol, 2.0 eq., added as a 10% solution in dry *iso*-propanol) were added to a solution of Cbz-*allo*-Thr($COC_{12}H_{25}$)-NuAA **52** (32.3 mg, 30.1 µmol, 1.0 eq.) in dry *iso*-propanol (1.2 mL). The reaction was stirred for 3 h at 40 °C (water bath). The residue was filtered through a syringe filter. The filter was washed with methanol (4x 5 mL). The title compound was obtained after removal of the solvent and was used without further purification.

Yield (**78**): 30.4 mg (26.0 µmol, 86%) as a colorless foamy solid.

^{1}H NMR (500 MHz, MeOH-d_4): δ [ppm] = 0.07 (s, 3 H, $SiCH_3$), 0.12 (s, 3 H, $SiCH_3$), 0.15 (s, 3 H, $SiCH_3$), 0.16 (s, 3 H, $SiCH_3$), 0.90 (t, $^3J_{13iv\text{-}H/12iv\text{-}H}$ = 6.4 Hz, 3 H, 13^{iv}-H), 0.92 (s, 9 H, $SiC(CH_3)_3$), 0.95 (s, 9 H, $SiC(CH_3)_3$), 1.28-1.31 (m, 21 H, 4'''-H, 4^{iv}-12^{iv}-H), 1.54 (s, 9 H, $OC(CH_3)_3$), 1.58-1.66 (m, 2 H, 3^{iv}-H), 1.91-1.98 (m, 2 H, 2''-H), 2.17-2.28 (m, 1 H, 5'-H_a), 2.28-2.36 (m, 1 H, 5'-H_b), 2.38 (t, $^3J_{2iv\text{-}H/3iv\text{-}H}$ = 7.4 Hz, 2 H, 2^{iv}-H), 3.08-3.19 (m, 2 H, 1''-H), 3.32-3.35 (m, 1 H, 3''-H_a), 3.38-3.43 (m, 1 H, 3''-H_b), 4.05-4.09 (m, 3 H, 3'-H, 6'-H, 2'''-H), 4.20 (ddd, $^3J_{4'\text{-}H/5'\text{-}H_a}$ = 11.7 Hz, $^3J_{4'\text{-}H/3'\text{-}H}$ = 4.4 Hz, $^3J_{4'\text{-}H/5'\text{-}H_b}$ = 2.5 Hz, 1 H, 4'-H), 4.67 (dd, $^3J_{2'\text{-}H/1'\text{-}H}$ = 4.7 Hz, $^3J_{2'\text{-}H/3'\text{-}H}$ = 4.7 Hz, 1 H, 2'-H), 5.27 (dq, $^3J_{3'''\text{-}H/4'''\text{-}H}$ = 6.6 Hz, $^3J_{3'''\text{-}H/2'''\text{-}H}$ = 4.2 Hz, 1 H, 3'''-H), 5.60 (d, $^3J_{1'\text{-}H/2'\text{-}H}$ = 4.7 Hz, 1 H, 1'-H), 5.75 (d, $^3J_{5\text{-}H/6\text{-}H}$ = 8.1 Hz, 1 H, 5-H), 7.65 (d, $^3J_{6\text{-}H/5\text{-}H}$ = 8.1 Hz, 1 H, 6-H).

^{13}C NMR (126 MHz, MeOH-d_4): δ [ppm] = -4.55 ($SiCH_3$), -4.52 ($SiCH_3$), -4.36 ($SiCH_3$), -4.06 ($SiCH_3$), 14.43 (C-13^{iv}), 15.30 (C-4'''), 18.84 ($SiC(CH_3)_3$), 18.93 ($SiC(CH_3)_3$), 23.73 C-4^{iv}-12^{iv}), 25.76 (C-3^{iv}), 26.36 ($SiC(CH_3)_3$), 26.40 ($SiC(CH_3)_3$), 27.49 (C-2''), 28.23 ($OC(CH_3)_3$), 30.17, 30.31, 30.43, 30.47, 30.61, 30.72, 30.75, 30.78 (C-4^{iv}-12^{iv}), 34.34 (C-5'), 34.79 (C-2^{iv}), 37.83 (C-3''), 45.47 (C-1''), 57.47 (C-2'''), 59.08 (C-6'), 69.11 (C-3'''), 74.24 (C-2'), 76.35 (C-3'), 81.92 (C-4'), 86.35 ($OC(CH_3)_3$), 95.41 (C-1'), 103.21 (C-5), 144.87 (C-6), 152.17 (C-2), 165.91 (C-4), 167.24 (C-1'''), 168.79 (C-7'), 174.01 (C-1^{iv}).

^{19}F NMR (471 MHz, MeOH-d_4): δ [ppm] = -77.06.

LC-MS (ESI$^+$): m/z = 940.44 $[M+H]^+$.

$C_{47}H_{89}N_5O_{10}Si_2$ (940.42)

$C_{47}H_{91}N_5O_{10}Si_2^{2+} \cdot 2\ C_2F_3O_2^-$ (1168.46)

7.4.3 Target compound T4: Val-Epic-*allo*-Thr($COC_{12}H_{25}$)-NuAA[145,153,170]

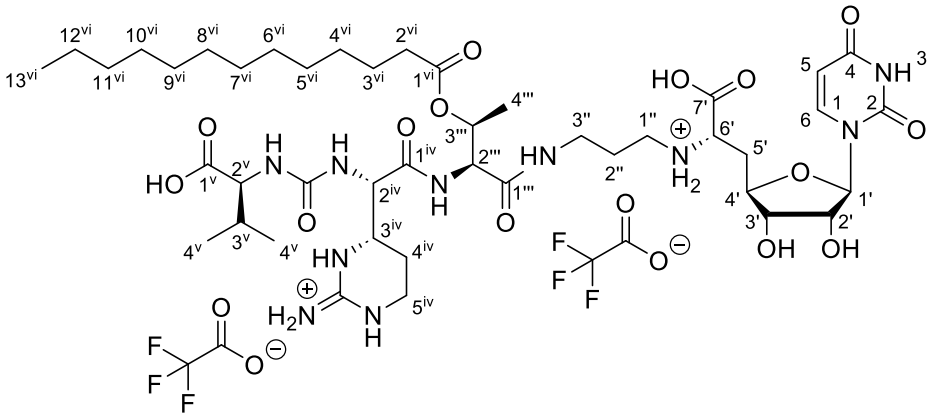

^{t}BuO-Val-Epic(Pbf)-OH **27**(16.5 mg, 26.5 µmol, 1.0 eq.), H-*allo*-Thr($COC_{12}H_{31}$)-NuAA bis-TFA salt **78** (30.8 mg, 26.4 µmol, 1.0 eq.) and *N*,*N*-diisopropylethylamine (15.7 µL, 93.3 µmol, 3.5 eq.) were dissolved in dry ethyl acetate (1.0 mL). The reaction mixture was cooled to 0 °C and stirred for 15 min at this temperature. T_3P (50% in dry ethyl acetate, 39.3 µL, 66.1 µmol, 2.5 eq.) was added to the reaction mixture. The reaction was stirred for 1 h at 0 °C and then for 15 min at room temperature. Then, ethyl acetate (15 mL) was added, and the organic layer was washed with water (2x 5 mL) and brine (5 mL). The organic layer was dried over sodium sulfate, and the solvent was removed under reduced pressure. The coupling product was identified by LC-MS (LC-MS (ESI$^+$): m/z = 1548.80 $[M+H]^+$).

The residue was dissolved in aqueous trifluoroacetic acid (80%, 5 mL) and stirred for 24 h at room temperature. The solvent was removed under reduced pressure, the residue was dissolved in water and was lyophilized. The title compound was isolated after purification by HPLC.

Yield (**T4**): 2.99 mg (2.53 µmol, 10% over two steps) as a white solid.

HPLC (semi-preparative): t_R = 15.6 min (method: **A**, conc. of injection: 12.5 mg/mL in MeOH).

^{1}H NMR (500 MHz, MeOH-d_4): δ [ppm] = 0.90 (t, $^{3}J_{13^{vi}\text{-H}/12^{vi}\text{-H}}$ = 7.0 Hz, 3 H, 13^{vi}-H), 0.94 (d, $^{3}J_{4^{v}\text{-H}/3^{v}\text{-H}}$ = 6.9 Hz, 3 H, 4^{v}-H), 0.99 (d, $^{3}J_{4^{v}\text{-H}/3^{v}\text{-H}}$ = 6.9 Hz, 3 H, 4^{v}-H), 1.27-1.34 (m, 21 H, 4'''-H, 4^{vi}-12^{vi}-H), 1.55-1.64 (m, 2 H, 3^{vi}-H), 1.84-1.93 (m, 2 H, 2''-H), 1.93-1.97 (m, 2 H, 4^{iv}-H), 2.15-2.22 (m, 1 H, 3^{v}-H), 2.22-2.28 (m, 1 H, 5'-H$_a$), 2.30 (t, $^{3}J_{2^{vi}\text{-H}/3^{vi}\text{-H}}$ = 7.4 Hz, 2 H, 2^{vi}-H), 2.44 (ddd, $^{2}J_{5'\text{-H}b/5'\text{-H}a}$ = 14.7 Hz, $^{3}J_{5'\text{-H}b/6'\text{-H}}$ = 6.4 Hz, $^{3}J_{5'\text{-H}b/4'\text{-H}}$ = 3.2 Hz, 1 H, 5'-H$_b$), 3.03-3.18 (m, 2 H, 1''-H), 3.23 (dt, $^{2}J_{3''\text{-H}a/3''\text{-H}b}$ = 13.9 Hz, $^{3}J_{3''\text{-H}a/2''\text{-H}}$ = 6.2 Hz, 1 H, 3''-H$_a$), 3.32-3.35 (m, 1 H, 5^{iv}-H$_a$), 3.38-3.47 (m, 2 H, 3''-H$_b$, 5^{iv}-H$_b$), 3.75 (ddd, $^{3}J_{3^{iv}\text{-H}/2^{iv}\text{-H}}$ = 8.2 Hz, $^{3}J_{3^{iv}\text{-H}/4^{iv}\text{-H}a}$ = 5.5 Hz, $^{3}J_{3^{iv}\text{-H}/4^{iv}\text{-H}b}$ = 5.5 Hz, 1 H, 3^{iv}-H), 3.90 (dd, $^{3}J_{6'\text{-H}/5'\text{-H}b}$ = 6.4 Hz, $^{3}J_{6'\text{-H}/5'\text{-H}a}$ = 6.3 Hz, 1 H, 6'-H), 4.01 (dd, $^{3}J_{3'\text{-H}/4'\text{-H}}$ = 6.4 Hz, $^{3}J_{3'\text{-H}/2'\text{-H}}$ = 5.9 Hz, 1 H, 3'-H), 4.16 (ddd, $^{3}J_{4'\text{-H}/5'\text{-H}a}$ = 10.0 Hz, $^{3}J_{4'\text{-H}/3'\text{-H}}$ = 6.4 Hz, $^{3}J_{4'\text{-H}/5'\text{-H}b}$ = 3.2 Hz, 1 H, 4'-H), 4.18 (d, $^{3}J_{2^{v}\text{-H}/3^{v}\text{-H}}$ = 4.8 Hz, 1 H, 2^{v}-H), 4.36 (dd, $^{3}J_{2'\text{-H}/3'\text{-H}}$ = 5.9 Hz, $^{3}J_{2'\text{-H}/1'\text{-H}}$ = 3.8 Hz, 1 H, 2'-H), 4.48 (d, $^{3}J_{2^{iv}\text{-H}/3^{iv}\text{-H}}$ = 8.2 Hz, 1 H, 2^{iv}-H), 4.51 (d, $^{3}J_{2'''\text{-H}/3'''\text{-H}}$ = 6.3 Hz, 1 H, 2'''-H), 5.15 (dq, $^{3}J_{3'''\text{-H}/4'''\text{-H}}$ = 6.4 Hz, $^{3}J_{3'''\text{-H}/2'''\text{-H}}$ = 6.3 Hz,1 H, 3'''-H), 5.68 (d, $^{3}J_{1'\text{-H}/2'\text{-H}}$ = 3.8 Hz, 1 H, 1'-H), 5.73 (d, $^{3}J_{5\text{-H}/6\text{-H}}$ = 8.1 Hz, 1 H, 5-H), 7.60 (d, $^{3}J_{6\text{-H}/5\text{-H}}$ = 8.1 Hz, 1 H, 6-H).

^{13}C NMR (126 MHz, MeOH-d_4): δ [ppm] = 14.43 (C-13^{vi}), 17.92 (C-4^{v}), 19.76 (C-4^{v}), 22.14 (C-4^{iv}), 23.73 (C-4^{iv}-12^{iv}), 25.92 (C-3^{vi}), 27.53 (C-2''), 30.18, 30.42, 30.47, 30.61, 30.72, 30.75, 30.77 (C-4^{vi}-12^{vi}), 31.74 (C-3^{v}), 33.07 (C-4^{vi}-12^{vi}), 34.37 (C-5'), 35.12 (C-2^{vi}), 37.15 (C-3''), 37.32 (C-5^{iv}), 45.46 (C-1''), 52.08 (C-3^{iv}), 56.47 (C-2^{iv}), 58.46 (C-2'''), 59.59 (C-2^{v}), 70.47 (C-3'''), 73.93 (C-2'), 74.77 (C-3'), 81.63 (C-4'), 94.40 (C-1'), 103.10 (C-5), 144.02 (C-6), 152.21 (C-2), 155.54 (NC(=NH)N), 160.19 (NC(=O)N), 166.03 (C-4), 171.78 (C-7'), 171.99 (C-1'''), 172.32 (C-1^{iv}), 174.54 (C-1^{vi}), 175.76 (C-1^{v}).

^{19}F NMR (471 MHz, MeOH-d_4): δ [ppm] = -76.99.

IR (ATR) υ [cm^{-1}]: 3290, 2924, 2853, 1662, 1651, 1633, 1547, 1201, 1179, 1133.

UV (HPLC) λ [nm]: 260, 205.

LC-MS (ESI^{+}): m/z = 953.73 [M+H]$^{+}$.

HRMS (ESI^{+}): calcd. for $C_{43}H_{74}N_{10}O_{14}^{2+}$: 477.2688, found: 477.2677 [M+2H]$^{+}$.

$C_{43}H_{72}N_{10}O_{14}$ (953.10)

$C_{43}H_{74}N_{10}O_{14}^{2+}$ • 2 $C_2F_3O_2^{-}$ (1181.14)

7.4.4 Target compound T5: Val-Arg-*allo*-Thr($COC_{12}H_{25}$)-NuAA[145,153,170]

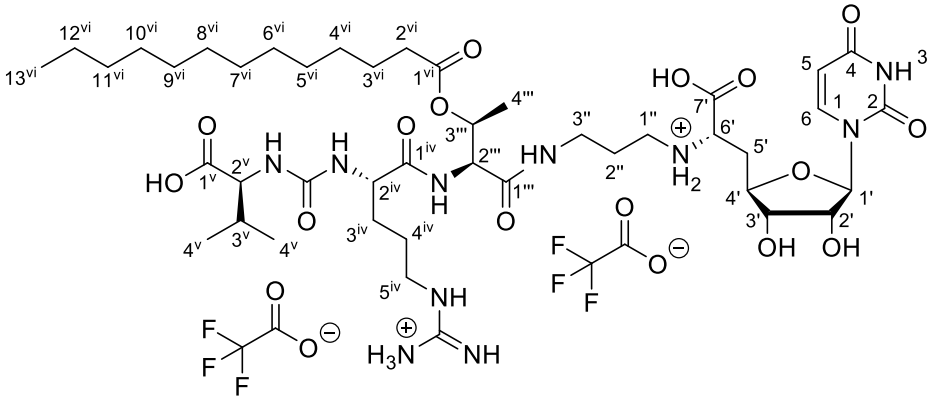

^{t}BuO-Val-Arg(Pbf)-OH **36** (14.1 mg, 22.5 µmol, 1.0 eq.), H-*allo*-Thr($COC_{12}H_{25}$)-NuAA bis-TFA salt **78** (25.5 mg, 21.8 µmol, 1.0 eq.) and dry *N*,*N*-diisopropylethylamine (13.0 µL, 76.4 µmol, 3.5 eq.) were diluted in dry ethyl acetate (0.9 mL). The reaction mixture was cooled to 0 °C and stirred for 15 min at this temperature. T_3P (50% in dry ethyl acetate, 32.4 µL, 54.5 µmol, 2.5 eq.) was added to the reaction mixture. The reaction was stirred for 45 min at 0 °C. Then, ethyl acetate (15 mL) was added, and the organic phase was washed with water (2x 5 mL) and brine (5 mL). The organic layer was dried over sodium sulfate, and the solvent was removed under reduced pressure. The coupling product was identified by LC-MS (LC-MS (ESI$^+$): m/z = 1548.80 $[M+H]^+$).

The residue was dissolved in aqueous trifluoroacetic acid (80%, 5 mL) and stirred for 24 h at room temperature. The solvent was removed under reduced pressure, the residue was dissolved in water and was lyophilized. The title compound was isolated after purification by HPLC.

Yield (**T5**): 5.68 mg (4.80 µmol, 22% over two steps) as a white solid.

HPLC (semi-preparative): t_R = 15.3 min (method: **D**, conc. of injection: 13.9 mg/mL in MeOH).

^{1}H NMR (500 MHz, MeOH-d_4): δ [ppm] = 0.90 (t, $^3J_{13^{vi}\text{-H}/12^{vi}\text{-H}}$ = 6.9 Hz, 3 H, 13^{vi}-H), 0.95 (d, $^3J_{4^{v}\text{-H}/3^{v}\text{-H}}$ = 6.9 Hz, 3 H, 4^{v}-H), 1.00 (d, $^3J_{4^{v}\text{-H}/3^{v}\text{-H}}$ = 6.9 Hz, 3 H, 4^{v}-H), 1.26-1.34 (m, 21 H, 4'''-H, 4^{vi}-12^{vi}-H), 1.54-1.63 (m, 2 H, 3^{vi}-H), 1.63-1.72 (m, 3 H, 3^{iv}-H_a, 4^{iv}-H), 1.80-1.86 (m, 1 H, 3^{iv}-H_b), 1.87-1.95 (m, 2 H, 2''-H), 2.17 (dsept, $^3J_{3^{v}\text{-H}/4^{v}\text{-H}}$ = 6.9 Hz, $^3J_{3^{v}\text{-H}/2^{v}\text{-H}}$ = 6.7 Hz, 1 H, 3^{v}-H), 2.29 (t, $^3J_{2^{vi}\text{-H}/3^{vi}\text{-H}}$ = 7.5 Hz, 2 H, 2^{vi}-H), 2.30-2.35 (m, 1 H, 5'-H_a), 2.44 (ddd, $^2J_{5'\text{-H}b/5'\text{-H}a}$ = 14.7 Hz, $^3J_{5'\text{-H}b/6'\text{-H}}$ = 6.6 Hz, $^3J_{5'\text{-H}b/4'\text{-H}}$ = 2.9 Hz, 1 H, 5'-H_b), 3.03-3.14 (m, 2 H, 1''-H), 3.18-3.26 (m, 2 H, 5^{iv}-H), 3.28-3.30 (m, 2 H, 3''-H), 4.00

(dd, $^{3}J_{6'\text{-H}/5'\text{-H}_b}$ = 6.6 Hz, $^{3}J_{6'\text{-H}/5'\text{-H}_a}$ = 6.3 Hz, 1 H, 6'-H), 4.01 (dd, $^{3}J_{3'\text{-H}/4'\text{-H}}$ = 6.1 Hz, $^{3}J_{3'\text{-H}/2'\text{-H}}$ = 5.9 Hz, 1 H, 3'-H), 4.14-4.17 (m, 1 H, 4'-H), 4.18 (d, $^{3}J_{2^{v}\text{-H}/3^{v}\text{-H}}$ = 6.7 Hz, 1 H, 2^{v}-H), 4.22 (dd, $^{3}J_{2^{iv}\text{-H}/3^{iv}\text{-H}_a}$ = 7.7 Hz, $^{3}J_{2^{iv}\text{-H}/3^{iv}\text{-H}_b}$ = 5.2 Hz, 1 H, 2^{iv}-H), 4.36 (dd, $^{3}J_{2'\text{-H}/3'\text{-H}}$ = 5.9 Hz, $^{3}J_{2'\text{-H}/1'\text{-H}}$ = 3.9 Hz, 1 H, 2'-H), 4.50 (d, $^{3}J_{2'''\text{-H}/3'''\text{-H}}$ = 6.2 Hz, 1 H, 2'''-H), 5.15 (dq, $^{3}J_{3'''\text{-H}/4'''\text{-H}}$ = 6.4 Hz, $^{3}J_{3'''\text{-H}/2'''\text{-H}}$ = 6.2 Hz, 1 H, 3'''-H), 5.70 (d, $^{3}J_{1'\text{-H}/2'\text{-H}}$ = 3.9 Hz, 1 H, 1'-H), 5.73 (d, $^{3}J_{5\text{-H}/6\text{-H}}$ = 8.1 Hz, 1 H, 5-H), 7.61 (d, $^{3}J_{6\text{-H}/5\text{-H}}$ = 8.1 Hz, 1 H, 6-H).

^{13}C NMR (126 MHz, MeOH-d_4): δ [ppm] = 14.44 (C-13^{vi}), 16.93 (C-4'''), 18.01 (C-4^{v}), 19.79 (C-4^{v}), 23.73 (C-4^{iv}-12^{iv}), 25.95 (C-3^{vi}), 26.14 (C-4^{iv}), 27.52 (C-2''), 30.20 (C-3^{iv}), 30.43, 30.47, 30.62, 30.73, 30.75, 30.78, 30.64 (C-4^{vi}-12^{vi}), 31.84 (C-3^{v}), 33.07 (C-4^{vi}-12^{vi}), 34.15 (C-5'), 35.19 (C-2^{vi}), 37.00 (C-3''), 41.92 (C-5^{iv}), 45.21 (C-1''), 54.83 (C-2^{iv}), 58.11 (C-2'''), 59.53 (C-2^{v}), 59.89 (C-6'), 70.94 (C-3'''), 74.00 (C-2'), 74.80 (C-3'), 81.29 (C-4'), 94.25 (C-1'), 103.08 (C-5), 143.95 (C-6), 153.16 (C-2), 158.65 (NC(=NH)N), 160.57 (NC(=O)N), 166.08 (C-4), 171.70 (C-7'), 171.98 (C-1'''), 174.71 (C-1^{vi}), 175.24 (C-1^{iv}), 175.89 (C-1^{v}).

^{19}F NMR (471 MHz, MeOH-d_4): δ [ppm] = -76.97.

IR (ATR) υ [cm^{-1}]: 3308, 2926, 2854, 1667, 1645, 1552, 1466, 1200, 1135, 721.

UV (HPLC) λ [nm]: 257, 210.

LC-MS (ESI^+): m/z = 956.72 $[M+H]^+$.

HRMS (ESI^+): calcd. for $C_{43}H_{76}N_{10}O_{14}^{2+}$: 478.2766, found: 478.2752 $[M+2H]^{2+}$.

$C_{43}H_{74}N_{10}O_{14}$ (955.12)

$C_{43}H_{76}N_{10}O_{14}^{2+}$ • 2 $C_2F_3O_2^-$ (1183.17)

7.4.5 Cbz-*allo*-Thr(CO^{iso}C$_{15}$H$_{31}$)-NuAA mono-TFA salt 87[146]

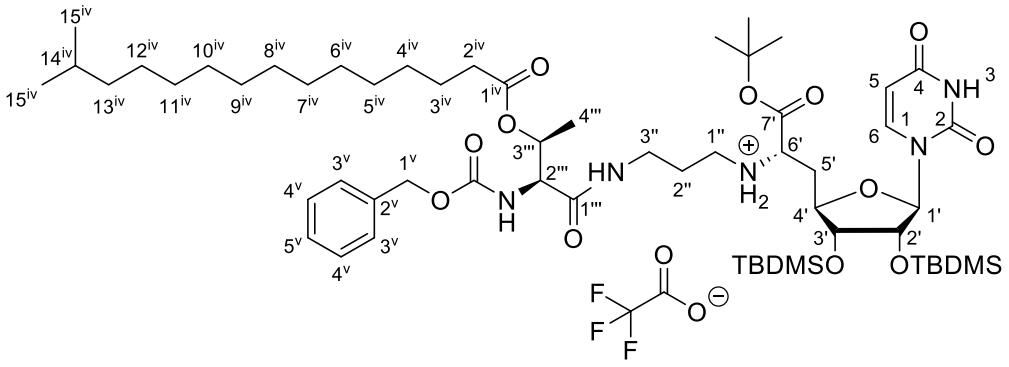

Dry *N*,*N*-diisopropylethylamine (13.1 µL, 77.0 µmol, 1.0 eq.) was added to a solution of Cbz-*allo*-Thr(CO^{iso}C$_{15}$H$_{31}$)-OH **44mix** (37.8 mg, crude: derivatives with different chain lengths) in dry tetrahydrofuran (2 mL). The resulting reaction mixture was stirred for 30 min at 0 °C. Then, HOBt (10.5 mg, 77.7 µmol, 1.0 eq.) and EDC • HCl (14.8 mg, 125 µmol, 1.0 eq.) were added at 0° C. After 1 h, nucleosyl amino acid **35** (49.6 mg, 77.1 µmol, 1.0 eq.) in dry tetrahydrofuran (3 mL) was added dropwise at this temperature. The reaction was stirred for 14.5 h. During this time, the reaction mixture was allowed to warm up to room temperature. Ethyl acetate (30 mL) was added, and the organic layer was washed with saturated sodium carbonate solution (30 mL). The aqueous layer was extracted with ethyl acetate (15 mL). The combined organic layers were dried over sodium sulfate. The solvent was removed under reduced pressure. The title compound was obtained after purification by silica gel column chromatography (15 g, 1.5x21 cm, PE:EtOAc 2:8) and HPLC.

Yield (**87**): 25.4 mg (20.6 µmol, 27%) as a colorless foamy solid.

HPLC (semi-preparative): t_R = ~25 min (method: **F**, conc. of injection: 12 mg/mL in DMSO).

^{1}H NMR (500 MHz, MeOH-d$_4$): δ [ppm] = 0.07 (s, 3 H, SiCH$_3$), 0.11 (s, 3 H, SiCH$_3$), 0.15 (s, 3 H, SiCH$_3$), 0.16 (s, 3 H, SiCH$_3$), 0.88 (d, $^3J_{15iv\text{-}H/14iv\text{-}H}$ = 6.6 Hz, 6 H, 15^{iv}-H), 0.91 (s, 9 H, SiC(CH$_3$)$_3$), 0.95 (s, 9 H, SiC(CH$_3$)$_3$), 1.14-1.20 (m, 2 H, 13^{iv}-H), 1.24 (d, $^3J_{4'''\text{-}H/3'''\text{-}H}$ = 6.3 Hz, 3 H, 4'''-H), 1.26-1.31 (m, 18 H, 4^{iv}-12^{iv}-H), 1.48-1.52 (m, 1 H, 14^{iv}-H), 1.53 (s, 9 H, OC(CH$_3$)$_3$), 1.54-1.59 (m, 2 H, 3^{iv}-H), 1.86-1.93 (m, 2 H, 2''-H), 2.18-2.27 (m, 3 H, 2^{iv}-H, 5'-H$_a$), 2.33 (ddd, $^2J_{5'\text{-}H_b/5'\text{-}H_a}$ = 14.1 Hz, $^3J_{5'\text{-}H_b/4'\text{-}H}$ = 11.8 Hz, $^3J_{5'\text{-}H_b/6'\text{-}H}$ = 4.6 Hz, 1 H, 5'-H$_b$), 3.02-3.14 (m, 2 H, 1''-H), 3.32-3.36 (m, 2 H, 3''-H), 4.03 (dd, $^3J_{6'\text{-}H/5'\text{-}H_a}$ = 9.1 Hz, $^3J_{6'\text{-}H/5'\text{-}H_b}$ = 4.6 Hz, 1 H, 6'-H), 4.06 (dd, $^3J_{3'\text{-}H/4'\text{-}H}$ = 4.6 Hz, $^3J_{3'\text{-}H/2'\text{-}H}$ = 4.6 Hz, 1 H, 3'-H),

4.21 (ddd, $^{3}J_{4'\text{-H}/5'\text{-H}_b}$ = 11.8 Hz, $^{3}J_{4'\text{-H}/3'\text{-H}}$ = 4.6 Hz, $^{3}J_{4'\text{-H}/5'\text{-H}_a}$ = 2.3 Hz, 1 H, 4'-H), 4.38 (d, $^{3}J_{2'''\text{-H}/3'''\text{-H}}$ = 5.9 Hz, 1 H, 2'''-H), 4.66 (dd, $^{3}J_{2'\text{-H}/3'\text{-H}}$ = 4.6 Hz, $^{3}J_{2'\text{-H}/1'\text{-H}}$ = 4.5 Hz, 1 H, 2'-H), 5.03-5.17 (m, 2 H, 1^{v}-H), 5.18 (dq, $^{3}J_{3'''\text{-H}/4'''\text{-H}}$ = 6.3 Hz, $^{3}J_{3'''\text{-H}/2'''\text{-H}}$ = 5.9 Hz, 1 H, 3'''-H), 5.59 (d, $^{3}J_{1'\text{-H}/2'\text{-H}}$ = 4.5 Hz, 1 H, 1'-H), 5.71 (d, $^{3}J_{5\text{-H}/6\text{-H}}$ = 8.1 Hz, 1 H, 5-H), 7.28-7.32 (m, 1 H, 5^{v}-H), 7.32-7.38 (m, 4 H, 3^{v}-H, 4^{v}-H), 7.60 (d, $^{3}J_{6\text{-H}/5\text{-H}}$ = 8.1 Hz, 1 H, 6-H).

^{13}C NMR (126 MHz, MeOH-d_4): δ [ppm] = -4.35 (2x $SiCH_3$), -4.49 ($SiCH_3$), -4.02 ($SiCH_3$), 16.12 (C-4'''), 18.25 ($SiC(CH_3)_3$), 18.94 ($SiC(CH_3)_3$), 23.05 (C-15^{iv}), 25.90 (C-3^{iv}), 26.39 ($SiC(CH_3)_3$), 26.42 ($SiC(CH_3)_3$), 27.63 (C-2''), 28.23 ($OC(CH_3)_3$), 28.54, 29.15, 30.16, 30.42, 30.60, 30.74, 30.78, 30.81, 31.09, 31.04 (C-4^{iv}-12^{iv}, C-14^{iv}), 34.28 (C-5'), 35.15 (C-2^{iv}), 36.71 (C-3''), 40.24 (C-13^{iv}), 44.98 (C-1''), 59.26 (C-6'), 59.55 (C-2'''), 67.98 (C-1^{v}), 70.66 (C-3'''), 74.37 (C-2'), 76.35 (C-3'), 81.80 (C-4'), 86.27 ($OC(CH_3)_3$), 95.30 (C-1'), 103.10 (C-5), 128.90, 129.14, 129.52 (C-3^{v}-5^{v}), 138.01 (C-2^{v}), 144.66 (C-6), 152.78 (C-4), 158.62 (NC(=O)O), 165.89 (C-2), 168.73 (C-7'), 173.10 (C-1'''), 174.46 (C-1^{iv}).

^{19}F NMR (471 MHz, MeOH-d_4): δ [ppm] = -77.13.

UV (HPLC) λ [nm]: 259, 216.

LC-MS (ESI^+): m/z = 1116.95 $[M+H]^+$.

HRMS (ESI^+): calcd. for $C_{58}H_{102}N_5O_{12}Si_2^+$: 1116.7059, found: 1116.6989 $[M+H]^+$.

$C_{58}H_{101}N_5O_{12}Si_2$ (1116.64)

$C_{58}H_{102}N_5O_{12}Si_2^+ \cdot C_2F_3O_2^-$ (1230.66)

7.4.6 Target compound T8: Val-Epic-*allo*-Thr(CO^{iso}C$_{15}$H$_{31}$)-NuAA[145,148,153]

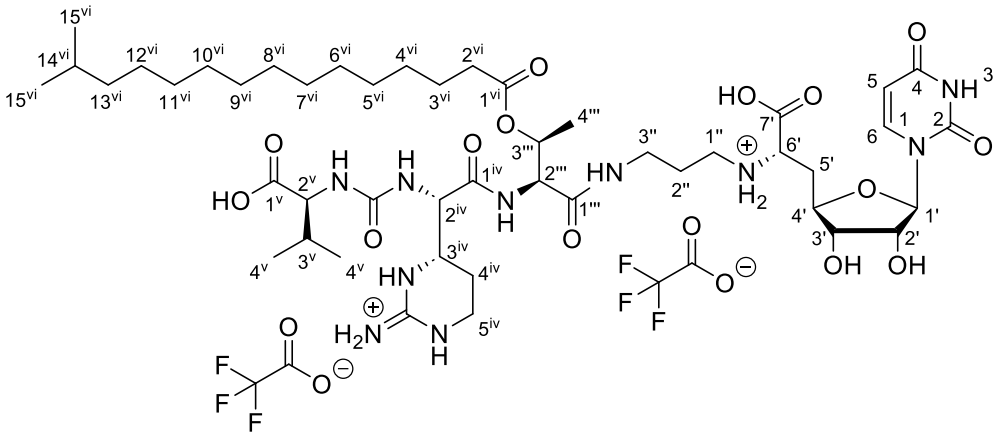

1,4-Cyclohexadiene (13.8 µL, 146 µmol, 11.1 eq.), palladium black (1.5 spatula tips) and trifluoroacetic acid (2.25 µL, 29.2 µmol, 2.2 eq., added as a 10% solution in dry *iso*-propanol) were added to a solution of Cbz-*allo*-Thr(CO^{iso}C$_{15}$H$_{31}$)-NuAA mono-TFA salt **87** (16.3 mg, 13.2 µmol, 1.0 eq.) in dry *iso*-propanol (1.5 mL). The reaction mixture was stirred for 3 h at room temperature. The reaction mixture was filtered through a syringe filter and the filter was washed with methanol (5x 6 mL). The solvent was removed under reduced pressure to give the bis-TFA salt **88**. The title compound was identified by LC-MS and was used without further purification (LC-MS (ESI$^+$): m/z = 982.91 [M+H]$^+$).

Dry *N*,*N*-diisopropylethylamine (1.72 µL, 10.1 µmol, 1.0 eq.) was added to a solution of ^{t}BuO-Val-Epic(Pbf)-OH **27** (6.37 mg, 10.2 µmol, 1.0 eq.) in dry dichloromethane (0.5 mL). After 10 min, HATU (5.92 mg, 15.6 µmol, 1.5 eq.) was added. After 30 min, the reaction mixture was cooled to 0 °C and dry *N*,*N*-diisopropylethylamine (4.29 µL, 25.2 µmol, 2.5 eq.) was added. Then, bis-TFA salt **88** (12.2 mg, 10.1 µmol, 1.0 eq.) in dry dichloromethane (0.9 mL) was added dropwise at this temperature. The reaction was stirred for 18 h. During this time, the reaction mixture was allowed to warm up to room temperature. Then, HATU (4.07 mg, 10.7 µmol, 1.1 eq.) and dry dichloromethane (0.5 mL) were added again. The reaction mixture was stirred for further 24 h at room temperature. The solvent was removed under reduced pressure. The residue was dissolved in ethyl acetate (3 mL). The organic layer was washed with water (1 mL). The layers were separated, and the aqueous layer was extracted with ethyl acetate (2x 2 mL). The solvent was removed under reduced pressure. The coupling product was identified by LC-MS (LC-MS (ESI$^+$): m/z = 1589.88 [M+H]$^+$).

The residue was dissolved in aqueous trifluoroacetic acid (80%, 2 mL) and was stirred for 24 h at room temperature. The solvent was removed under reduced pressure, the residue was dissolved in water and lyophilized. The title compound was isolated after purification by HPLC.

Yield (**T8**): 1.58 mg (1.29 µmol, 9.8% over three steps) as a white solid.

HPLC (semi-preparative): t_R = 19.6 min (method: **D**, conc. of injection: ~13.0 mg/mL in MeOH).

^{1}H NMR (500 MHz, MeOH-d_4): δ [ppm] = 0.89 (d, $^3J_{15^{vi}\text{-H}/14^{vi}\text{-H}}$ = 6.6 Hz, 3 H, 15^{vi}-H), 0.95 (d, $^3J_{4^{v}\text{-H}/3^{v}\text{-H}}$ = 6.9 Hz, 3 H, 4^{v}-H), 1.00 (d, $^3J_{4^{v}\text{-H}/3^{v}\text{-H}}$ = 6.9 Hz, 3 H, 4^{v}-H), 1.16-1.21 (m, 2 H, 13^{vi}-H), 1.27-1.35 (m, 21 H, 4'''-H, 4^{vi}-12^{vi}-H), 1.53 (dsept, $^3J_{14^{vi}\text{-H}/15^{vi}\text{-H}}$ = 6.6 Hz, $^3J_{14^{vi}\text{-H}/13^{vi}\text{-H}}$ = 6.6 Hz, 2 H, 14^{vi}-H), 1.57-1.64 (m, 2 H, 3^{vi}-H), 1.86-1.93 (m, 2 H, 2''-H), 1.93-1.98 (m, 1 H, 4^{iv}-H) 2.15-2.22 (m, 1 H, 3^{v}-H), 2.26 (ddd, $^2J_{5'\text{-H}a/5'\text{-H}b}$ = 14.8 Hz, $^3J_{5'\text{-H}a/4'\text{-H}}$ = 10.1 Hz, $^3J_{5'\text{-H}a/6'\text{-H}}$ = 6.3 Hz, 1 H, 5'-H_a), 2.31 (t, $^3J_{2^{vi}\text{-H}/3^{vi}\text{-H}}$ = 7.4 Hz, 2 H, 2^{vi}-H), 2.44 (ddd, $^2J_{5'\text{-H}b/5'\text{-H}a}$ = 14.8 Hz, $^3J_{5'\text{-H}b/6\text{-H}}$ = 6.3 Hz, $^3J_{5'\text{-H}b/4'\text{-H}}$ = 3.3 Hz, 1 H, 5'-H_b), 3.04-3.17 (m, 2 H, 1''-H), 3.24 (dt, $^2J_{3''\text{-H}a/3''\text{-H}b}$ = 13.9 Hz, $^3J_{3''\text{-H}a/2''\text{-H}}$ = 6.1 Hz, 1 H, 3''-H_a), 3.32-3.36 (m, 1 H, 5^{iv}-H_a), 3.40-3.48 (m, 2 H, 3''-H_b, 5^{iv}-H_b), 3.75 (ddd, $^3J_{3^{iv}\text{-H}/2^{iv}\text{-H}}$ = 8.3 Hz, $^3J_{3^{iv}\text{-H}/4^{iv}\text{-H}a}$ = 5.5 Hz, $^3J_{3^{iv}\text{-H}/4^{iv}\text{-H}b}$ = 5.5 Hz, 1 H, 3^{iv}-H), 3.90 (dd, $^3J_{6'\text{-H}/5'\text{-H}a}$ = 6.3 Hz, $^3J_{6'\text{-H}/5'\text{-H}b}$ = 6.3 Hz, 1 H, 6'-H), 4.02 (dd, $^3J_{3'\text{-H}/4'\text{-H}}$ = 6.4 Hz, $^3J_{3'\text{-H}/2'\text{-H}}$ = 5.9 Hz, 1 H, 3'-H), 4.17 (ddd, $^3J_{4'\text{-H}/5'\text{-H}a}$ = 10.1 Hz, $^3J_{4'\text{-H}/3'\text{-H}}$ = 6.4 Hz, $^3J_{4'\text{-H}/5'\text{-H}b}$ = 3.3 Hz, 1 H, 4'-H), 4.19 (d, $^3J_{2^{v}\text{-H}/3^{v}\text{-H}}$ = 4.8 Hz, 1 H, 2^{v}-H), 4.37 (dd, $^3J_{2'\text{-H}/3'\text{-H}}$ = 5.9 Hz, $^3J_{2'\text{-H}/1'\text{-H}}$ = 3.8 Hz, 1 H, 2'-H), 4.49 (d, $^3J_{2^{iv}\text{-H}/3^{iv}\text{-H}}$ = 8.3 Hz, 1 H, 2^{iv}-H), 4.52 (d, $^3J_{2'''\text{-H}/3'''\text{-H}}$ = 6.4 Hz, 1 H, 2'''-H), 5.16 (dq, $^3J_{3'''\text{-H}/4'''\text{-H}}$ = 6.4 Hz, $^3J_{3'''\text{-H}/2'''\text{-H}}$ = 6.4 Hz, 1 H, 3'''-H), 5.69 (d, $^3J_{1'\text{-H}/2'\text{-H}}$ = 3.8 Hz, 1 H, 1'-H), 5.74 (d, $^3J_{5\text{-H}/6\text{-H}}$ = 8.1 Hz, 1 H, 5-H), 7.61 (d, $^3J_{6\text{-H}/5\text{-H}}$ = 8.1 Hz, 1 H, 6-H).

^{13}C NMR (126 MHz, MeOH-d_4): δ [ppm] = 16.73 (C-4'''), 17.93 (C-4^{v}), 19.76 (C-4^{v}), 22.14 (C-4^{iv}), 23.04 (C-15^{iv}), 25.92 (C-3^{vi}), 27.54 (C-2''), 28.54 (C-4^{vi}-12^{vi}), 29.16 (C-14^{vi}) , 30.19, 30.43, 30.62, 30.73, 30.78, 30.81, 31.04 (C-4^{vi}-12^{vi}), 31.74 (C-3^{v}), 34.41 (C-5'), 35.13 (C-2^{vi}), 37.15 (C-3''), 37.31 (C-5^{iv}), 40.25 (C-13^{vi}), 45.46 (C-1''), 52.07 (C-3^{iv}), 56.46 (C-2^{iv}), 58.47 (C-2'''), 59.60 (C-2^{v}), 60.75 (C-6'), 70.47 (C-3'''), 73.94 (C-2'), 74.77 (C-3'), 81.67 (C-4'), 94.38 (C-1'), 103.10 (C-5), 144.02 (C-6), 152.22 (C-2), 155.54 (NC(=NH)N), 160.19 (NC(=O)N), 166.03 (C-4), 171.85 (C-7'), 171.99 (C-1'''), 172.33 (C-1^{iv}), 174.55 (C-1^{vi}), 175.76 (C-1^{v}).

^{19}F NMR (471 MHz, MeOH-d_4): δ [ppm] = -76.99.

IR (ATR) υ [cm^{-1}]: 3293, 2924, 2853, 1668, 1633, 1550, 1200, 1182, 1134, 721.

UV (HPLC) λ [nm]: 260, 205.

LC-MS (ESI^+): m/z = 955.87 $[M+H]^+$.

HRMS (ESI^+): calcd. for $C_{46}H_{80}N_{10}O_{14}^{2+}$: 955.5772, found: 955.5755 $[M+H]^+$.

$C_{46}H_{78}N_{10}O_{14}$ (995.19)

$C_{46}H_{80}N_{10}O_{14}^{2+}$ • 2 $C_2F_3O_2^-$ (1223.23)

7.4.7 Cbz-*allo*-Thr($COCH_3$)-NuAA 89

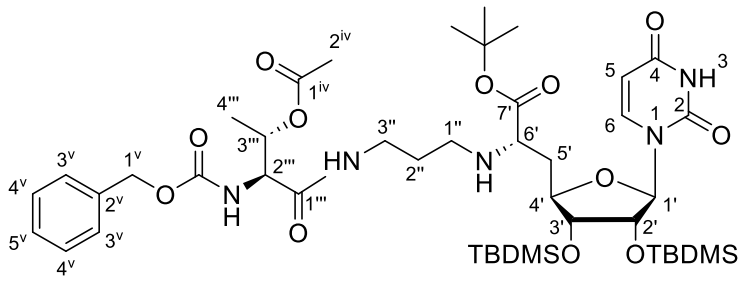

Dry *N*,*N*-diisopropylethylamine (20.4 µL, 120 µmol, 1.0 eq.) was added to a solution of Cbz-*allo*-Thr($COCH_3$)-OH **51** (37.4 mg, 127 µmol, 1.1 eq.) in dry dichloromethane (1.8 mL). After 10 min, HATU (68.7 mg, 181 µmol, 1.5 eq.) was added. Then, the reaction mixture was cooled to 0 °C and dry *N*,*N*-diisopropylethylamine (20.4 µL, 120 µmol, 1.0 eq.) was added. Then, nucleosyl amino acid **35** (76.1 mg, 118 µmol, 1.0 eq.) in dry dichloromethane. (2.7 mL) was added dropwise at this temperature. The reaction was stirred for 14 h. During this time, the reaction mixture was allowed to warm up to room temperature. Water (10 mL) was added to the reaction mixture. The layers were separated, and the aqueous layer was extracted with dichloromethane (3x 10 mL). The combined organic layer was dried over sodium sulfate. The solvent was removed under reduced pressure. The title compound was obtained after purification by silica gel column chromatography (8 g, 1.5x12 cm, CH_2Cl_2:MeOH 100:0 → 98.5:1.5 → 95:5).

Yield (**89**): 71.6 mg (77.8 µmol, 66%) as a colorless foamy solid.

TLC: R_f = 0.43 (CH_2Cl_2:MeOH 9:1).

^{1}H NMR (500 MHz, MeOH-d_4): δ [ppm] = 0.08 (s, 3 H, $SiCH_3$), 0.10 (s, 3 H, $SiCH_3$), 0.12 (s, 3 H, $SiCH_3$), 0.13 (s, 3 H, $SiCH_3$), 0.91 (s, 9 H, $SiC(CH_3)_3$), 0.93 (s, 9 H, $SiC(CH_3)_3$), 1.22

(d, $^{3}J_{4'''\text{-}H/3'''\text{-}H}$ = 6.5 Hz, 3 H, 4'''-H), 1.48 (s, 9 H, OC(CH_3)$_3$), 1.69 (ddt, $^{3}J_{2''\text{-}H/1''\text{-}H_a}$ = 6.6 Hz, $^{3}J_{2''\text{-}H/1''\text{-}H_b}$ = 6.6 Hz, $^{3}J_{2''\text{-}H/3''\text{-}H}$ = 6.5 Hz, 2 H, 2''-H), 1.90-1.94 (m, 1 H, 5'-H_a), 1.96 (s, 3 H, 2^{iv}-H), 2.00-2.09 (m, 1 H, 5'-H_b), 2.57 (dt, $^{2}J_{1''\text{-}H_a/1''\text{-}H_b}$ = 12.1 Hz, $^{3}J_{1''\text{-}H_a/2''\text{-}H}$ = 6.6 Hz, 1 H, 1''-H_a), 2.66 (dt, $^{2}J_{1''\text{-}H_b/1''\text{-}H_a}$ = 12.1 Hz, $^{3}J_{1''\text{-}H_b/2''\text{-}H}$ = 6.6 Hz, 1 H, 1''-H_b), 3.24-3.29 (m, 2 H, 3''-H), 3.38 (dd, $^{3}J_{6'\text{-}H/5'\text{-}H_a}$ = 9.0 Hz, $^{3}J_{6'\text{-}H/5'\text{-}H_b}$ = 4.3 Hz, 1 H, 6'-H), 3.92 (dd, $^{3}J_{3'\text{-}H/4'\text{-}H}$ = 4.6 Hz, $^{3}J_{3'\text{-}H/2'\text{-}H}$ = 4.5 Hz, 1 H, 3'-H), 4.07 (ddd, $^{3}J_{4'\text{-}H/5'\text{-}H_a}$ = 11.1 Hz, $^{3}J_{4'H/3'\text{-}H}$ = 4.6 Hz, $^{3}J_{4'\text{-}H/5'\text{-}H_b}$ = 2.8 Hz, 1 H, 4'-H), 4.36 (dd, $^{3}J_{2'\text{-}H/3'\text{-}H}$ = 4.5 Hz, $^{3}J_{2'\text{-}H/1'\text{-}H}$ = 4.3 Hz, 1 H, 2'-H), 4.40 (d, $^{3}J_{2'''\text{-}H/3'''\text{-}H}$ = 6.0 Hz, 1 H, 2'''-H), 5.05-5.16 (m, 3 H, 3'''-H, 1^{v}-H), 5.75 (d, $^{3}J_{5\text{-}H/6\text{-}H}$ = 8.0 Hz, 1 H, 5-H), 5.76 (d, $^{3}J_{1'\text{-}H/2'\text{-}H}$ = 4.3 Hz, 1 H, 1'-H), 7.27-7.32 (m, 1 H, 5^{v}-H), 7.32-7.38 (m, 4 H, 3^{v}-H, 4^{v}-H), 7.64 (d, $^{3}J_{6\text{-}H/5\text{-}H}$ = 8.0 Hz, 1 H, 6-H).

^{13}C NMR (126 MHz, MeOH-d_4): δ [ppm] = -4.47 ($SiCH_3$), -4.42 (2x $SiCH_3$), -4.01 ($SiCH_3$), 15.96 (C-4'''), 18.86 (Si<u>C</u>(CH_3)$_3$), 18.92 (Si<u>C</u>(CH_3)$_3$), 26.38 (SiC(<u>C</u>H_3)$_3$), 26.44 (SiC(<u>C</u>H_3)$_3$), 28.41 (OC(<u>C</u>H_3)$_3$), 30.10 (C-2''), 21.07 (C-2^{iv}), 37.72 (C-5'), 38.28 (C-3''), 46.01 (C-1''), 59.11 (C-2'''), 60.62 (C-6'), 67.88 (C-1^{v}), 71.30 (C-3'''), 75.73 (C-2'), 76.53 (C-3'), 82.55 (C-4'), 83.13 (O<u>C</u>(CH_3)$_3$), 92.11 (C-1'), 103.04 (C-5), 128.92, 129.07, 129.48 (C-3^{v}, C-4^{v}, C-5^{v}), 138.09 (C-2^{v}), 142.88 (C-6), 152.12 (C-2), 158.41 (NC(=O)O), 166.03 (C-4), 171.43 (C-1'''), 171.88 (C-1^{iv}), 174.30 (C-7').

LC-MS (ESI^+): m/z = 920.74 $[M+H]^+$.

HRMS (ESI^+): calcd. for $C_{44}H_{74}N_5O_{12}Si_2^+$: 920.4868, found: 920.4798 $[M+H]^+$.

$C_{44}H_{73}N_5O_{12}Si_2$ (920.26)

7.4.8 H-*allo*-Thr($COCH_3$)-NuAA bis-TFA salt 90[145,148,153]

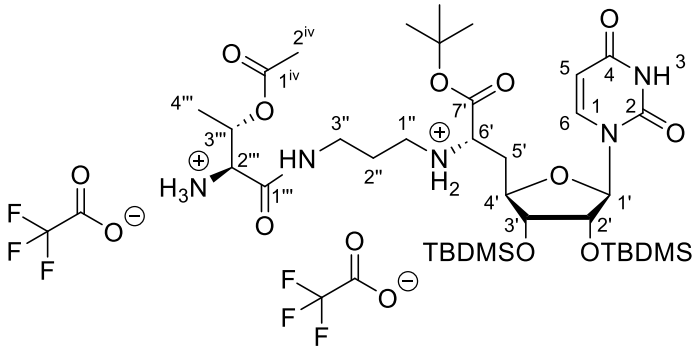

1,4-Cyclohexadiene (120 µL, 1.27 mmol, 11.9 eq.), palladium black (3 spatula tips), trifluoroacetic acid (19.0 µL, 247 µL, 2.3 eq., added as a 10% solution in dry *iso*-propanol) were added to a solution of Cbz-*allo*-Thr($COCH_3$)-NuAA **89** (98.1 mg, 122 µmol,

1.0 eq.) in dry *iso*-propanol (5.0 mL). The reaction was stirred for 2 h at room temperature. The residue was filtered through a syringe filter and the filter was washed with methanol (6x 4 mL). The title compound was obtained after removal of the solvent and was used without further purification.

Yield (**90**): 113 mg (100%: 108 mg) as a colorless foamy solid.

^{1}H NMR (500 MHz, MeOH-d_4): δ [ppm] = 0.07 (s, 3 H, $SiCH_3$), 0.11 (s, 3 H, $SiCH_3$), 0.15 (s, 3 H, $SiCH_3$), 0.15 (s, 3 H, $SiCH_3$), 0.91 (s, 9 H, $SiC(CH_3)_3$), 0.95 (s, 9 H, $SiC(CH_3)_3$), 1.30 (d, $^{3}J_{4'''\text{-H}/3'''\text{-H}}$ = 6.7 Hz, 3 H, 4'''-H), 1.54 (s, 9 H, $OC(CH_3)_3$), 1.95 (ddt, $^{3}J_{2''\text{-H}/3''\text{-H}}$ = 7.6 Hz, $^{3}J_{2''\text{-H}/1''\text{-H}_a}$ = 7.5 Hz, $^{3}J_{2''\text{-H}/1''\text{-H}_b}$ = 7.3 Hz, 2 H, 2''-H), 2.10 (s, 3 H, 2^{iv}-H), 2.24 (ddd, $^{2}J_{5'\text{-H}_a/5'\text{-H}_b}$ = 14.1 Hz, $^{3}J_{5'\text{-H}_a/6'\text{-H}}$ = 9.4 Hz, $^{3}J_{5'\text{-H}_a/4'\text{-H}}$= 2.4 Hz, 1 H, 5'-$H_a$), 2.34 (ddd, $^{2}J_{5'\text{-H}_b/5'\text{-H}_a}$ = 14.1 Hz, $^{3}J_{5'\text{-H}_b/4'\text{-H}}$ = 11.8 Hz, $^{3}J_{5'\text{-H}_b/6'\text{-H}}$ = 4.3 Hz, 1 H, 5'-H_b), 3.07-3.19 (m, 2 H, 3''-H), 3.32-3.36 (m, 1 H, 1''-H_a), 3.39 (dt, $^{2}J_{1''\text{-H}_b/1''\text{-H}_a}$ = 14.0 Hz, $^{3}J_{1''\text{-H}_b/2''\text{-H}}$ = 7.3 Hz, 1 H, 1''-H_b), 4.03-4.07 (m, 2 H, 3'-H, 6'-H), 4.09 (d, $^{3}J_{2'''\text{-H}/3'''\text{-H}}$ = 4.3 Hz, 1 H, 2'''-H), 4.20 (ddd, $^{3}J_{4'\text{-H}/5'\text{-H}_b}$ = 11.8 Hz, $^{3}J_{4'\text{-H}/3'\text{-H}}$ = 4.3 Hz, $^{3}J_{4'\text{-H}/5'\text{-H}_a}$ = 2.4 Hz, 1 H, 4'-H), 4.62 (dd, $^{3}J_{2'\text{-H}/1'\text{-H}}$ = 4.7 Hz, $^{3}J_{2'\text{-H}/3'\text{-H}}$ = 4.7 Hz, 1 H, 2'-H), 5.26 (dq, $^{3}J_{3'''\text{-H}/4'''\text{-H}}$ = 6.7 Hz, $^{3}J_{3'''\text{-H}/2'''\text{-H}}$ = 4.3 Hz, 1 H, 3'''-H), 5.63 (d, $^{3}J_{1'\text{-H}/2'\text{-H}}$ = 4.7 Hz, 1 H, 1'-H), 5.75 (d, $^{3}J_{5\text{-H}/6\text{-H}}$ = 8.1 Hz, 1 H, 5-H), 7.66 (d, $^{3}J_{6\text{-H}/5\text{-H}}$ = 8.1 Hz, 1 H, 6-H).

^{13}C NMR (126 MHz, MeOH-d_4): δ [ppm] = -4.57 ($SiCH_3$), -4.57 ($SiCH_3$), -4.39 ($SiCH_3$), -4.08 ($SiCH_3$), 15.26 (C-4'''), 18.83 ($SiC(CH_3)_3$), 18.91 ($SiC(CH_3)_3$), 20.83 (C-2^{iv}), 26.35 ($SiC(CH_3)_3$), 26.38 ($SiC(CH_3)_3$), 27.44 (C-2''), 28.20 ($OC(CH_3)_3$), 34.33 (C-5'), 37.77 (C-1''), 45.43 (C-3''), 57.40 (C-2'''), 59.03 (C-6'), 69.23 (C-3'''), 74.42 (C-2'), 76.30 (C-3'), 81.80 (C-4'), 86.27 ($OC(CH_3)_3$), 94.81 (C-1'), 103.19 (C-5), 144.57 (C-6), 152.16 (C-2), 165.92 (C-4), 167.21 (C-1'''), 168.74 (C-7'), 171.30 (C-1^{iv}).

^{19}F NMR (471 MHz, MeOH-d_4): δ [ppm] = -77.00.

LC-MS (ESI$^+$): m/z = 786.73 $[M+H]^+$.

$C_{36}H_{67}N_5O_{10}Si_2$ (786.13)

$C_{36}H_{69}N_5O_{10}Si_2^{2+}$ • 2 $C_2F_3O_2^-$ (1014.17)

7.4.9 Target compound *a*T-T7: Val-Epic-*allo*-Thr($COCH_3$)-NuAA[153]

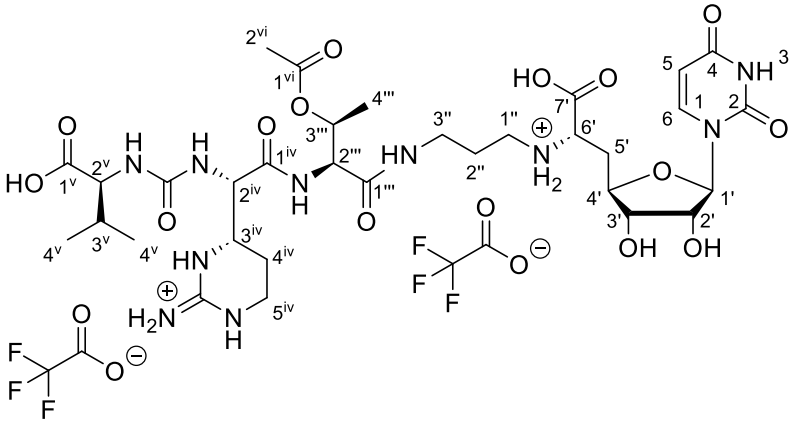

Dry *N*,*N*-diisopropylethylamine (11.0 µL, 120 µmol, 1.0 eq.) was added to a solution of ^{t}BuO-Val-Epic(Pbf)-OH **27** (40.1 mg, 64.3 µmol, 1.0 eq.) in dry dichloromethane (0.5 mL). After 10 min, HATU (36.8 mg, 96.8 µmol, 1.5 eq.) was added. After 30 min, the reaction mixture was cooled to 0 °C and dry *N*,*N*-diisopropylethylamine (27.3 µL, 161 µmol, 2.5 eq.) was added. Then, H-*allo*-Thr($COCH_3$)-NuAA bis-TFA salt **90** (65.2 mg, 64.3 µmol, 1.0 eq.) in dry dichloromethane (2.0 mL) was added dropwise at this temperature. The reaction was stirred for 17 h. During this time, the reaction mixture was allowed to warm up to room temperature. Water (5 mL) was added to the reaction mixture at 0 °C. The layers were separated, and the aqueous layer was extracted with dichloromethane (3x 8 mL). The solvent was removed under reduced pressure. The coupling product was identified by LC-MS (LC-MS (ESI$^+$): m/z = 1392.16 $[M+H]^+$).

The residue was dissolved in aqueous trifluoroacetic acid (80%, 7 mL) and the reaction mixture was stirred for 22 h at room temperature. The solvent was removed under reduced pressure, the residue was dissolved in water at 0 °C and lyophilized. The title compound was isolated after purification by HPLC.

Yield (***a*T-T7**): 15.0 mg (14.6 µmol, 22% over two steps) as a white solid.

HPLC (semi-preparative): t_R = 18.7 min (method: **H**, conc. of injection: ~34.5 mg/mL in H_2O).

^{1}H NMR (500 MHz, MeOH-d_4): δ [ppm] = 0.94 (d, $^3J_{4^v\text{-H}/3^v\text{-H}}$ = 6.9 Hz, 3 H, 4^v-H), 0.99 (d, $^3J_{4^v\text{-H}/3^v\text{-H}}$ = 6.8 Hz, 3 H, 4^v-H), 1.29 (d, $^3J_{4'''\text{-H}/3'''\text{-H}}$ = 6.4 Hz, 3 H, 4'''-H), 1.89-1.97 (m, 4 H, 2''-H, 4^{iv}-H), 2.03 (s, 3 H, 2^{vi}-H), 2.18 (dqq, $^3J_{3^v\text{-H}/4^v\text{-H}}$ = 6.9 Hz, $^3J_{3^v\text{-H}/4^v\text{-H}}$ = 6.8 Hz, $^3J_{3^v\text{-H}/2^v\text{-H}}$ = 5.1 Hz, 1 H, 3^v-H), 2.32 (ddd, $^2J_{5'\text{-H}a/5'\text{-H}b}$ = 14.8 Hz, $^3J_{5'\text{-H}a/4'\text{-H}}$ = 10.3 Hz, $^3J_{5'\text{-H}a/6'\text{-H}}$ = 6.1 Hz, 1 H, 5'-H_a), 2.45 (ddd, $^2J_{5'\text{-H}b/5'\text{-H}a}$ = 14.8 Hz, $^3J_{5'\text{-H}b/6'\text{-H}}$ = 6.7 Hz,

$^{3}J_{5'\text{-}H_b/4'\text{-}H}$ = 2.8 Hz, 1 H, 5'-H_b), 3.10 (dt, $^{2}J_{1''\text{-}H_a/1''\text{-}H_b}$ = 12.9 Hz, $^{3}J_{1''\text{-}H_a/2''\text{-}H}$ = 7.2 Hz, 1 H, 1''-H_a), 3.14 (dt, $^{2}J_{1''\text{-}H_b/1''\text{-}H_a}$ = 12.9 Hz, $^{3}J_{1''\text{-}H_b/2''\text{-}H}$ = 7.2 Hz, 1 H, 1''-H_b), 3.28-3.38 (m, 3 H, 3''-H, 5^{iv}-H_a), 3.44 (dt, $^{2}J_{5iv\text{-}H_b/5iv\text{-}H_a}$ = 12.3 Hz, $^{3}J_{5iv\text{-}H_b/4iv\text{-}H}$ = 6.1 Hz, 1 H, 5^{iv}-H_b), 3.76 (ddd, $^{3}J_{3iv\text{-}H/2iv\text{-}H}$ = 7.9 Hz, $^{3}J_{3iv\text{-}H/4iv\text{-}H_a}$ = 5.7 Hz, $^{3}J_{3iv\text{-}H/4iv\text{-}H_b}$ = 5.7 Hz, 1 H, 3^{iv}-H), 4.02 (dd, $^{3}J_{3'\text{-}H/4'\text{-}H}$ = 6.0 Hz, $^{3}J_{3'\text{-}H/2'\text{-}H}$ = 5.9 Hz, 1 H, 3'-H), 4.05 (dd, $^{3}J_{6'\text{-}H/5'\text{-}H_b}$ = 6.7 Hz, $^{3}J_{6'\text{-}H/5'\text{-}H_a}$ = 6.1 Hz, 1 H, 6'-H), 4.14-4.17 (m, 1 H, 4'-H), 4.18 (d, $^{3}J_{2v\text{-}H/3v\text{-}H}$ = 5.1 Hz, 1 H, 2^{v}-H), 4.36 (dd, $^{3}J_{2'\text{-}H/3'\text{-}H}$ = 5.9 Hz, $^{3}J_{2'\text{-}H/1'\text{-}H}$ = 3.9 Hz, 1 H, 2'-H), 4.49 (d, $^{3}J_{2iv\text{-}H/3iv\text{-}H}$ = 7.9 Hz, 1 H, 2^{iv}-H), 4.54 (d, $^{3}J_{2'''\text{-}H/3'''\text{-}H}$ = 6.2 Hz, 1 H, 2'''-H), 5.14 (dq, $^{3}J_{3'''\text{-}H/4'''\text{-}H}$ = 6.4 Hz, $^{3}J_{3'''\text{-}H/2'''\text{-}H}$ = 6.2 Hz,1 H, 3'''-H), 5.71 (d, $^{3}J_{1'\text{-}H/2'\text{-}H}$ = 3.9 Hz, 1 H, 1'-H), 5.73 (d, $^{3}J_{5\text{-}H/6\text{-}H}$ = 8.1 Hz, 1 H, 5-H), 7.61 (d, $^{3}J_{6\text{-}H/5\text{-}H}$ = 8.1 Hz, 1 H, 6-H).

^{13}C NMR (126 MHz, MeOH-d_4): δ [ppm] = 16.64 (C-4'''), 17.87 (C-4^{v}), 19.71 (C-4^{v}), 21.08 (C-2^{vi}), 22.15 (C-4^{iv}), 27.50 (C-2''), 31.72 (C-3^{v}), 34.10 (C-5'), 37.24 (C-3''), 37.32 (C-5^{iv}), 45.42 (C-1''), 52.05 (C-3^{iv}), 56.60 (C-2^{iv}), 58.23 (C-2'''), 59.60 (C-2^{v}), 59.69 (C-6'), 70.74 (C-3'''), 74.00 (C-2'), 74.76 (C-3'), 81.20 (C-4'), 94.04 (C-1'), 103.12 (C-5), 143.87 (C-6), 152.18 (C-2), 155.55 (NC(=NH)N), 160.23 (NC(=O)N), 166.04 (C-4), 171.29 (C-7'), 171.88 (C-1'''), 172.00 (C-1^{vi}), 172.30 (C-1^{iv}), 175.78 (C-1^{v}).

^{19}F NMR (471 MHz, MeOH-d_4): δ [ppm] = -76.92.

LC-MS (ESI$^+$): m/z = 799.55 $[M+H]^+$.

IR (ATR) υ [cm^{-1}]: 3295, 3080, 2965, 1652, 1555, 1240, 1198, 1132, 1098, 720.

HRMS (ESI$^+$): calcd. for $C_{32}H_{52}N_{10}O_{14}^{2+}$: 400.1827, found: 400.1800 $[M+2H]^{2+}$.

UV (HPLC) λ [nm]: 262, 208.

$C_{32}H_{50}N_{10}O_{14}$ (798.81)

$C_{32}H_{52}N_{10}O_{14}^{2+}$ • 2 $C_2F_3O_2^-$ (1026.85)

7.4.10 ^{t}BuO-Val-Arg(Pbf)-*allo*-Thr($COCH_3$)-NuAA 50

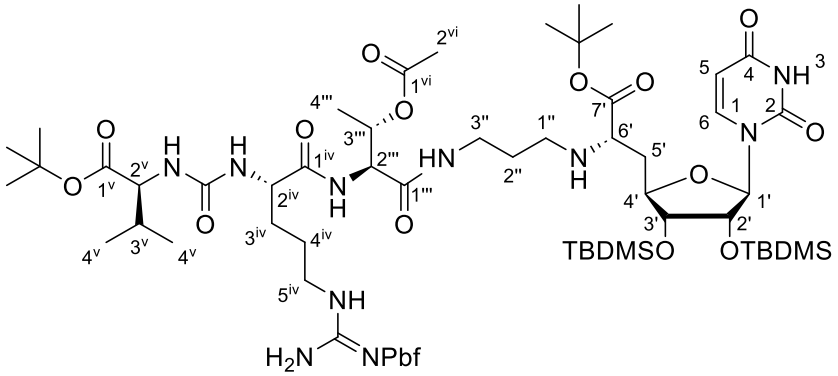

Dry *N*,*N*-diisopropylethylamine (19.0 µL, 112 µmol, 1.0 eq.) was added to a solution of ^{t}BuOH-Val-Arg(Pbf)-OH **36** (70.0 mg, 112 µmol, 1.0 eq.) in dry dichloromethane (0.8 mL). After 15 min, HATU (63.7 mg, 168 µmol, 1.5 eq.) was added. After 30 min, the reaction mixture was cooled to 0 °C and dry *N*,*N*-diisopropylethylamine (47.7 µL, 280 µmol, 2.5 eq.) was added. Then, H-*allo*-Thr($COCH_3$)-NuAA bis-TFA salt **90** (114 mg, 112 µmol, 1.0 eq.) in dry dichloromethane (3.5 mL) was added dropwise at this temperature. The reaction was stirred for 16 h. During this time, the reaction mixture was allowed to warm up to room temperature. Water (5 mL) was added to the reaction mixture at 0 °C. The layers were separated, and the aqueous layer was extracted with dichloromethane (6x 5 mL). The combined organic layer was washed with brine (15 mL) and dried over sodium sulfate. The solvent was removed under reduced pressure. The title compound was obtained after purification by silica gel column chromatography (38 g, 3x17 cm, CH_2Cl_2:MeOH (100:0 → 98.5:1.5 → 80:20). The purity of the product was estimated by LC-MS due to the complexity of the NMR data (LC-MS (ESI^+): m/z = 1394.43 $[M+H]^+$, 697.59 $[M+2H]^{2+}$).

Yield (**50**): 106 mg (~76.1 µmol, ~65%) as a white solid.

TLC: R_f = 0.37 (CH_2Cl_2:MeOH 9:1).

LC-MS (ESI^+): m/z = 1394.43 $[M+H]^+$, 697.59 $[M+2H]^+$.

$C_{65}H_{112}N_{10}O_{17}SSi_2$ (1393.89)

7.4.11 ^{t}BuO-Val-Arg(Pbf)-*allo*-Thr-NuAA 49[159]

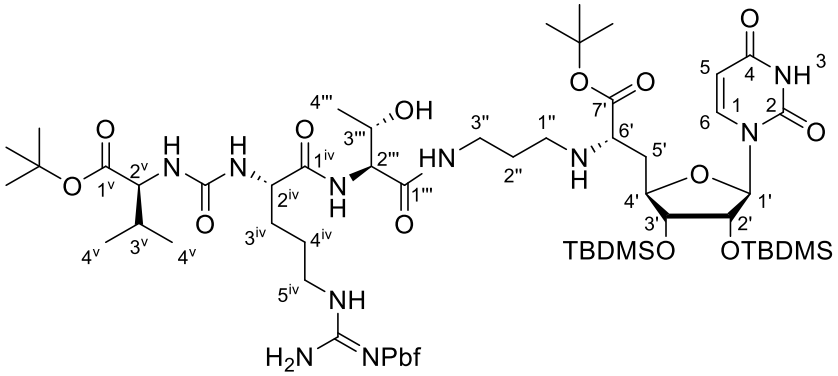

Anhydrous potassium carbonate (3.38 mg, 24.5 µmol, 0.5 eq.) was added to a solution of muraymycin derivative **50** (67.2 mg, 48.2 µmol, 1.0 eq.) in dry methanol (0.9 mL). Potassium carbonate was added again after 30 min (1.20 mg, 8.68 µmol, 0.2 eq.), after 100 min (1.50 mg, 10.9 µmol, 0.2 eq.) and after 180 min (1.20 mg, 8.68 µmol, 0.2 eq.). The suspension was stirred vigorously for a total of 5.5 h. The solvent was removed under reduced pressure. Then, the residue was dissolved in water (2 mL) and was extracted with diethyl ether (5x 2 mL). The solvent was removed under reduced pressure. The title compound was identified by LC-MS (LC-MS (ESI$^+$): m/z = 1352.37 $[M+H]^+$, 676.80 $[M+2H]^{2+}$) and HRMS (m/z = 1351.7412 $[M+H]^+$, 676.3743 $[M+2H]^{2+}$) and was used without further purification.

Yield (**49**): 62.1 mg (~45.9 µmol, ~95%) as a colorless solid.

LC-MS (ESI$^+$): m/z = 1352.37 $[M+H]^+$, 676.80 $[M+2H]^{2+}$.

HRMS (ESI$^+$): calcd. for $C_{63}H_{112}N_{10}O_{16}SSi_2^{2+}$: 676.3753, found: 676.3743 $[M+2H]^{2+}$.
calcd. for $C_{63}H_{111}N_{10}O_{16}SSi_2^{+}$: 1351.7434, found: 1351.7412 $[M+H]^+$.

$C_{63}H_{110}N_{10}O_{16}SSi_2$ (1351.86)

7.4.12 Target compound T9: Val-Arg-*allo*-Thr($COC_{12}H_{23}$)-NuAA[145,146,153]

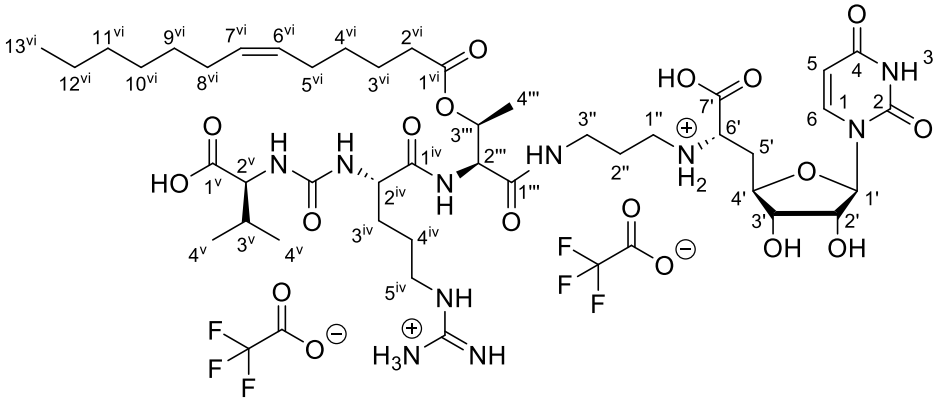

EDC • HCl (7.21 mg, 37.6 mmol, 2.6 eq.) was added to a solution of muraymycin derivative **49** (19.8 mg, 14.7 µmol, 1.0 eq.), (*Z*)-tridec-6-enoic acid **47** (4.92 mg, 23.2 µmol, 1.6 eq.) and 4-dimethylaminopyridine (4.20 mg, 34.4 mmol, 2.3 eq.) in dry tetrahydrofuran (0.6 mL). The reaction mixture was stirred for 5.5 h at room temperature. Then, hydrochloric acid (0.5 M, 2 mL) was added. After extraction with ethyl acetate (4x 2 mL), the solvent was removed under reduced pressure. The coupling product was identified by LC-MS (LC-MS (ESI$^+$): m/z = 1546.75 $[M+H]^+$).

The residue was dissolved in aqueous trifluoroacetic acid (80%, 3 mL) and stirred for 23 h at room temperature. The solvent was removed under reduced pressure, the residue was dissolved in water and lyophilized. The title compound was isolated after purification by HPLC.

Yield (**T9**): 3.29 mg (2.79 µmol, 19% over two steps) as a white solid.

HPLC (semi-preparative): t_R = 15.7 min (method: **D**, conc. of injection: 11.1 mg/mL in DMSO).

^{1}H NMR (500 MHz, MeOH-d_4): δ [ppm] = 0.90 (t, $^3J_{13vi\text{-}H/12vi\text{-}H}$ = 7.0 Hz, 3 H, 13^{vi}-H), 0.94 (d, $^3J_{4v\text{-}H/3v\text{-}H}$ = 6.9 Hz, 3 H, 4^{v}-H), 0.99 (d, $^3J_{4v\text{-}H/3v\text{-}H}$ = 6.9 Hz, 3 H, 4^{v}-H), 1.29 (d, $^3J_{4'''\text{-}H/3'''\text{-}H}$ = 6.5 Hz, 3 H, 4'''-H), 1.30-1.40 (m, 10 H, 4^{vi}-H, 9^{vi}-12^{vi}-H), 1.60 (tt, $^3J_{3vi\text{-}H/4vi\text{-}H}$ = 7.6 Hz, $^3J_{3vi\text{-}H/2vi\text{-}H}$ = 7.5 Hz, 2 H, 3^{vi}-H), 1.62-1.70 (m, 3 H, 3^{iv}-H_a, 4^{iv}-H), 1.79-1.85 (m, 1 H, 3^{iv}-H_b), 1.85-1.95 (m, 2 H, 2''-H), 2.00-2.08 (m, 4 H, 5^{vi}-H, 8^{vi}-H), 2.12-2.19 (m, 1 H, 3^{v}-H), 2.21 (ddd, $^2J_{5'\text{-}Ha/5'\text{-}Hb}$ = 14.8 Hz, $^3J_{5'\text{-}Ha/4'\text{-}H}$ = 9.8 Hz, $^3J_{5'\text{-}Ha/6'\text{-}H}$ = 6.5 Hz, 1 H, 5'-H_a), 2.30 (t, $^3J_{2vi\text{-}H/3vi\text{-}H}$ = 7.5 Hz, 2 H, 2^{vi}-H), 2.40 (ddd, $^2J_{5'\text{-}Hb/5'\text{-}Ha}$ = 14.8 Hz, $^3J_{5'\text{-}Hb/6'\text{-}H}$ = 6.4 Hz, $^3J_{5'\text{-}Hb/4'\text{-}H}$ = 3.3 Hz, 1 H, 5'-H_b), 3.02 (dt, $^2J_{1''\text{-}Ha/1''\text{-}Hb}$ = 12.8 Hz, $^3J_{1''\text{-}Ha/2''\text{-}H}$ = 7.2 Hz, 1 H, 1''-H_a), 3.08 (dt, $^2J_{1''\text{-}Hb/1''\text{-}Ha}$ = 12.8 Hz, $^3J_{1''\text{-}Hb/2''\text{-}H}$ = 7.5 Hz, 1 H,

1''-H_b), 3.19-3.25 (m, 3 H, 3''-H_a, 5^{iv}-H), 3.36-3.43 (m, 1 H, 3''-H_b), 3.72 (dd, $^3J_{6'\text{-H}/5'\text{-H}_a}$ = 6.5 Hz, $^3J_{6'\text{-H}/5'\text{-H}_b}$ = 6.4 Hz, 1 H, 6'-H), 3.99 (dd, $^3J_{3'\text{-H}/4'\text{-H}}$ = 6.0 Hz, $^3J_{3'\text{-H}/2'\text{-H}}$ = 5.9 Hz, 1 H, 3'-H), 4.15-4.20 (m, 1 H, 4'-H), 4.18 (d, $^3J_{2^v\text{-H}/3^v\text{-H}}$ = 4.9 Hz, 1 H, 2^v-H), 4.26 (dd, $^3J_{2^{iv}\text{-H}/3^{iv}\text{-H}_a}$ = 8.0 Hz, $^3J_{2^{iv}\text{-H}/3^{iv}\text{-H}_b}$ = 5.5 Hz, 1 H, 2^{iv}-H), 4.35 (dd, $^3J_{2'\text{-H}/3'\text{-H}}$ = 5.9 Hz, $^3J_{2'\text{-H}/1'\text{-H}}$ = 3.8 Hz, 1 H, 2'-H), 4.44 (d, $^3J_{2'''\text{-H}/3'''\text{-H}}$ = 6.6 Hz, 1 H, 1 H, 2'''-H), 5.13 (dq, $^3J_{3'''\text{-H}/2'''\text{-H}}$ = 6.6 Hz, $^3J_{3'''\text{-H}/4'''\text{-H}}$ = 6.5 Hz, 1 H, 3'''-H), 5.33 (dt, $^3J_{6^{vi}\text{-H}/7^{vi}\text{-H}}$ = 11.4 Hz, $^3J_{6^{vi}\text{-H}/5^{vi}\text{-H}}$ = 6.2 Hz, 1 H, 6^{vi}-H), 5.38 (dt, $^3J_{7^{vi}\text{-H}/6^{vi}\text{-H}}$ = 11.4 Hz, $^3J_{7^{vi}\text{-H}/8^{vi}\text{-H}}$ = 6.1 Hz, 1 H, 7^{vi}-H), 5.69 (d, $^3J_{1'\text{-H}/2'\text{-H}}$ = 3.8 Hz, 1 H, 1'-H), 5.73 (d, $^3J_{5\text{-H}/6\text{-H}}$ = 8.1 Hz, 1 H, 5-H), 7.61 (d, $^3J_{6\text{-H}/5\text{-H}}$ = 8.1 Hz, 1 H, 6-H).

^{13}C NMR (126 MHz, MeOH-d_4): δ [ppm] = 14.43 (C-13^{vi}), 17.01 (C-4'''), 17.96 (C-4^v), 19.75 (C-4^v), 23.70 (C-4^{vi}, C-9^{vi}-12^{vi}), 25.55 (C-3^{vi}), 26.03 (C-4^{iv}), 27.65 (C-2''), 27.82, 28.19 (C-5^{vi}, C-8^{vi}), 30.05 30.24, 30.80 (C-4^{vi}, C-9^{vi}-12^{vi}), 30.97 (C-3^{iv}), 31.87 (C-3^v), 32.92 (C-4^{vi}, C-9^{vi}-12^{vi}), 34.69 (C-5'), 35.05 (C-2^{vi}), 36.96 (C-3''), 41.84 (C-5^{iv}), 45.42 (C-1''), 54.41 (C-2^{iv}), 58.31 (C-2'''), 59.45 (C-2^v), 61.62 (C-6'), 70.72 (C-3'''), 73.99 (C-2'), 74.80 (C-3'), 81.95 (C-4'), 94.19 (C-1'), 103.04 (C-5), 143.95 (C-6), 152.18 (C-2), 158.67 (NC(=NH)N), 160.39 (NC(=O)N), 166.06 (C-4), 172.16 (C-1'''), 172.66 (C-7'), 174.41 (C-1^{vi}), 175.13 (C-1^{iv}), 175.94 (C-1^v).

^{19}F NMR (471 MHz, MeOH-d_4): δ [ppm] = -76.94.

IR (ATR) υ [cm^{-1}]: 3349, 3200, 2928, 2858, 1652, 1556, 1463, 1386, 1184, 1134.

UV (HPLC) λ [nm]: 257, 213.

LC-MS (ESI^+): m/z = 953.80 $[M+H]^+$, 477.60 $[M+2H]^{2+}$.

HRMS (ESI^+): calcd. for $C_{43}H_{74}N_{10}O_{14}^{2+}$: 477.2688, found: 477.2675 $[H+2H]^{2+}$.

$C_{43}H_{72}N_{10}O_{14}$ (953.11)

$C_{43}H_{74}N_{10}O_{14}^{2+}$ • 2 $C_2F_3O_2^-$ (1181.15)

7.5 Synthesis of muraymycin derivatives with L-threonine

7.5.1 Cbz-Thr($COC_{12}H_{25}$)-NuAA mono-TFA salt 79[146]

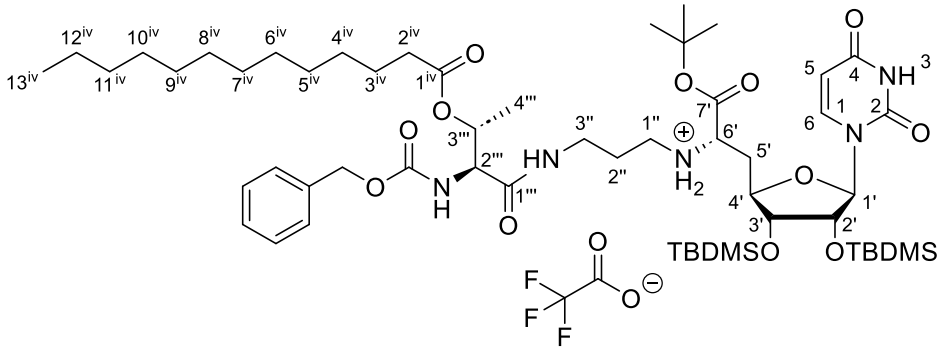

Dry *N*,*N*-diisopropylethylamine (12.4 µL, 72.9 µmol, 1.0 eq.) was added to a solution of Cbz-Thr($COC_{12}H_{25}$)-OH **39** (32.5 mg, 72.3 µmol, 1.0 eq.) in dry tetrahydrofuran (2 mL). The resulting reaction mixture was stirred for 30 min at 0 °C. Then, HOBt (9.89 mg, 73.2 µmol, 1.0 eq.) and EDC • HCl (14.0 mg, 73.0 µmol, 1.0 eq.) were added at 0° C. After 1 h, nucleosyl amino acid **35** (46.7 mg, 72.6 µmol, 1.0 eq.) in dry tetrahydrofuran (3 mL) was added dropwise at this temperature. The reaction was stirred for 14.5 h. During this time, the reaction mixture was allowed to warm up to room temperature. Ethyl acetate (30 mL) was added, and the organic layer was washed with saturated sodium carbonate solution (30 mL). Then, the solvent was removed under reduced pressure. The title compound was obtained after purification by silica gel column chromatography (15 g, 1.5x25 cm, PE:EtOAc 2:8) and HPLC.

Yield (**79**): 33.8 mg (28.4 µmol, 39%) as a colorless foamy solid.

HPLC (semi-preparative): t_R = ~23.5 min (method: **G**, conc. of injection: 11 mg/mL in DMSO).

^{1}H NMR (500 MHz, MeOH-d_4): δ [ppm] = 0.07 (s, 3 H, $SiCH_3$), 0.11 (s, 3 H, $SiCH_3$), 0.15 (s, 3 H, $SiCH_3$), 0.16 (s, 3 H, $SiCH_3$), 0.90 (t, $^3J_{13iv\text{-}H/12iv\text{-}H}$ = 7.8 Hz, 3 H, 13^{iv}-H), 0.91 (s, 9 H, $SiC(CH_3)_3$), 0.95 (s, 9 H, $SiC(CH_3)_3$), 1.26 (d, $^3J_{4'''\text{-}H/3'''\text{-}H}$ = 6.5 Hz, 3 H, 4'''-H), 1.27-1.30 (m, 18 H, 4^{iv}-12^{iv}-H), 1.53 (s, 9 H, $OC(CH_3)_3$), 1.54-1.60 (m, 2 H, 3^{iv}-H), 1.85-1.92 (m, 2 H, 2''-H), 2.18-2.36 (m, 4 H, 5'-H, 2^{iv}-H), 3.03 (dt, $^2J_{1''\text{-}H_a/1''\text{-}H_b}$ = 13.0 Hz, $^3J_{1''\text{-}H_a/2''\text{-}H}$ = 6.7 Hz, 1 H, 1''-H_a), 3.11 (dt, $^2J_{1''\text{-}H_b/1''\text{-}H_a}$ = 13.0 Hz, $^3J_{1''\text{-}H_b/2''\text{-}H}$ = 7.2 Hz, 1 H, 1''-H_b), 3.25 (dt, $^2J_{3''\text{-}H_a/3''\text{-}H_b}$ = 13.4 Hz, $^3J_{3''\text{-}H_a/2''\text{-}H}$ = 6.6 Hz, 1 H, 3''-H_a), 3.36 (dt, $^2J_{3''\text{-}H_b/3''\text{-}H_a}$ = 13.4 Hz, $^3J_{3''\text{-}H_b/2''\text{-}H}$ = 6.7 Hz, 1 H, 3''-H_b), 4.03 (dd, $^3J_{6'\text{-}H/5'\text{-}H_a}$ = 9.0 Hz, $^3J_{6'\text{-}H/5'\text{-}H_b}$ = 4.5 Hz, 1 H, 6'-H), 4.07 (dd, $^3J_{3'\text{-}H/2'\text{-}H}$ = 4.6 Hz, $^3J_{3'\text{-}H/4'\text{-}H}$ = 4.6 Hz, 1 H, 3'-H), 4.18-4.22 (m, 1 H, 4'-H),

4.23 (d, $^{3}J_{2'''\text{-H}/3'''\text{-H}}$ = 3.8 Hz, 1 H, 2'''-H), 4.69 (dd, $^{3}J_{2'\text{-H}/1'\text{-H}}$ = 4.7 Hz, $^{3}J_{2'\text{-H}/3'\text{-H}}$ = 4.6 Hz, 1 H, 2'-H), 5.06-5.18 (m, 2 H, 1^{v}-H), 5.31-5.38 (m, 1 H, 3'''-H), 5.58 (d, $^{3}J_{1'\text{-H}/2'\text{-H}}$ = 4.7 Hz, 1 H, 1'-H), 5.72 (d, $^{3}J_{5\text{-H}/6\text{-H}}$ = 8.1 Hz, 1 H, 5-H), 7.28-7.34 (m, 1 H, 5^{v}-H), 7.34-7.40 (m, 4 H, 3^{v}-H, 4^{v}-H), 7.62 (d, $^{3}J_{6\text{-H}/5\text{-H}}$ = 8.1 Hz, 1 H, 6-H).

^{13}C NMR (126 MHz, MeOH-d_4): δ [ppm] = -4.49 ($SiCH_3$), -4.34 (2x $SiCH_3$), -4.02 ($SiCH_3$), 14.45 (C-13^{iv}), 17.50 (C-4'''), 18.85 ($SiC(CH_3)_3$), 18.95 ($SiC(CH_3)_3$), 23.73 (C-4^{iv}-12^{iv}), 26.39 ($SiC(CH_3)_3$), 26.42 ($SiC(CH_3)_3$), 27.62 (C-3^{iv}), 28.23 ($OC(CH_3)_3$), 27.61 (C-2''), 30.17, 30.43, 30.47, 30.62, 30.76, 33.07 (C-4^{iv}-12^{iv}), 34.29 (C-5'), 35.01 (C-2^{iv}), 36.81 (C-3''), 45.04 (C-1''), 59.11 (C-6'), 60.49 (C-2'''), 68.11 (C-1^{v}), 70.81 (C-3'''), 74.23 (C-2'), 76.36 (C-3'), 81.90 (C-4'), 86.23 ($OC(CH_3)_3$), 95.45 (C-1'), 103.12 (C-5), 128.99, 129.18, 129.52 (C-3^{v}-5^{v}), 137.93 (C-2^{v}), 144.85 (C-6), 152.07 (C-2), 158.78 (NC(=O)O), 165.87 (C-4), 168.87 (C-7'), 173.52 (C-1'''), 174.47 (C-1^{iv}).

^{19}F NMR (471 MHz, MeOH-d_4): δ [ppm] = -77.21.

LC-MS (ESI^+): m/z = 1074.82 $[M+H]^+$.

HRMS (ESI^+): calcd. for $C_{55}H_{96}N_5O_{12}Si_2^+$: 1074.6589, found: 1074.6519 $[M+H]^+$.

UV (HPLC) λ [nm]: 259, 209.

$C_{55}H_{95}N_5O_{12}Si_2$ (1074.56)

$C_{55}H_{96}N_5O_{12}Si_2^+ \cdot C_2F_3O_2^-$ (1188.58)

7.5.2 Target compound T6: Val-Arg-Thr($COC_{12}H_{25}$)-NuAA[145,148,153]

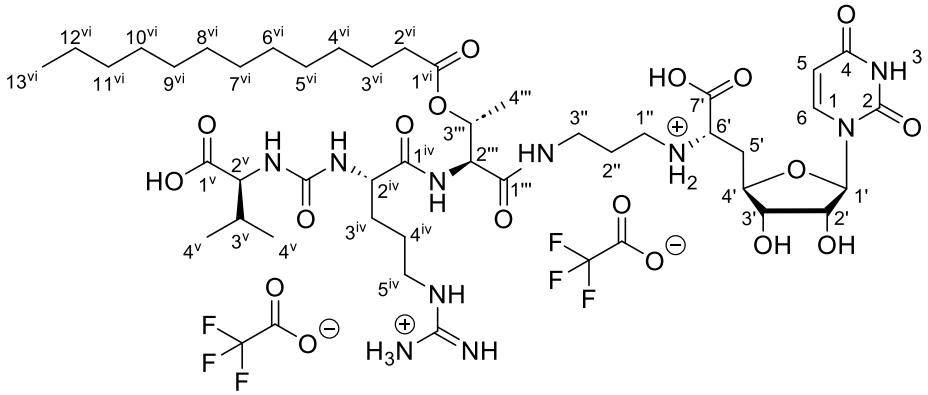

1,4-Cyclohexadiene (26.9 µL, 285 µmol, 11.0 eq.), palladium black (2 spatula tips) and trifluoroacetic acid (4.39 µL, 57.0 µmol, 2.2 eq., added as a 10% solution in dry *iso*-propanol) were added to a solution of Cbz-Thr($COC_{12}H_{25}$)-NuAA **79** (30.6 mg, 25.8 µmol, 1.0 eq.) in dry *iso*-propanol (2 mL). The reaction mixture was stirred for 4 h

at room temperature. The reaction mixture was filtered through a syringe filter and the filter was washed with methanol (7x 3 mL). The solvent was removed under reduced pressure to give the bis-TFA salt **80**. It was identified by LC-MS and was used without further purification (LC-MS (ESI$^+$): m/z = 940.86 [M+H]$^+$).

Dry *N*,*N*-diisopropylethylamine (3.80 µL, 22.4 µmol, 1.0 eq.) was added to a solution of ^{t}BuO-Val-Arg(Pbf)-OH **36** (14.0 mg, 22.4 µmol, 1.0 eq.) in dry dichloromethane (0.5 mL). After 10 min, HATU (12.6 mg, 33.1 µmol, 1.5 eq.) was added. After 30 min, the reaction mixture was cooled to 0 °C and dry *N*,*N*-diisopropylethylamine (9.50 µL, 56.0 µmol, 2.5 eq.) was added. Then, bis-TFA salt **80** (26.1 mg, 22.3 µmol, 1.0 eq.) in dry dichloromethane (0.7 mL) was added dropwise at this temperature. The reaction was stirred for 18 h. During this time, the reaction mixture was allowed to warm up to room temperature. Then, HATU (8.39 mg, 22.1 µmol, 1.0 eq.) and dry dichloromethane (0.5 mL) were added again. The reaction mixture was stirred for further 24 h at room temperature. The solvent was removed under reduced pressure. The residue was dissolved in ethyl acetate (3 mL). The organic layer was washed with water (1 mL) The layers were separated, and the aqueous layer was extracted with ethyl acetate (3x 2 mL). The solvent was removed under reduced pressure. The coupling product was identified by LC-MS (LC-MS (ESI$^+$): m/z = 1549.78 [M+H]$^+$).

The residue was dissolved in aqueous trifluoroacetic acid (80%, 3 mL) and stirred for 19 h at room temperature. The solvent was removed under reduced pressure, the residue was dissolved in water and lyophilized. The title compound was isolated after purification by HPLC.

Yield (**T6**): 2.04 mg (1.54 µmol, 6.7% over three steps) as a white solid.

HPLC (semi-preparative): t_R = 11.2 min (method: **I**, conc. of injection: 12.6 mg/mL in MeOH).

^{1}H NMR (500 MHz, MeOH-d$_4$): δ [ppm] = 0.90 (t, $^3J_{13^{vi}\text{-H}/12^{vi}\text{-H}}$ = 7.0 Hz, 3 H, 13^{vi}-H), 0.94 (d, $^3J_{4^{v}\text{-H}/3^{v}\text{-H}}$ = 6.9 Hz, 3 H, 4^{v}-H), 0.99 (d, $^3J_{4^{v}\text{-H}/3^{v}\text{-H}}$ = 6.9 Hz, 3 H, 4^{v}-H), 1.25 (d, $^3J_{4'''\text{-H}/3'''\text{-H}}$ = 6.5 Hz, 3 H, 4'''-H), 1.27-1.31 (m, 18 H, 4^{vi}-12^{vi}-H), 1.54-1.62 (m, 2 H, 3^{vi}-H), 1.63-1.72 (m, 3 H, 3^{iv}-H$_a$, 4^{iv}-H), 1.82-1.93 (m, 3 H, 2''-H, 3^{iv}-H$_b$), 2.13-2.24 (m, 2 H, 5'-H$_a$, 3^{v}-H), 2.30 (t, $^3J_{2^{vi}\text{-H}/3^{vi}\text{-H}}$ = 7.5 Hz, 2 H, 2^{vi}-H), 2.40 (ddd, $^2J_{5'\text{-H}b/5'\text{-H}a}$ = 14.6 Hz, $^3J_{5'\text{-H}b/6'\text{-H}}$ = 6.1 Hz, $^3J_{5'\text{-H}b/4'\text{-H}}$ = 3.5 Hz, 1 H, 5'-H$_b$), 3.00-3.11 (m, 2 H, 1''-H), 3.19-3.26 (m, 2 H, 5^{iv}-H), 3.28-3.30 (m, 2 H, 3''-H), 3.71 (dd, $^3J_{6'\text{-H}/5'\text{-H}a}$ = 6.4 Hz, $^3J_{6'\text{-H}/5'\text{-H}b}$ = 6.1 Hz, 1 H,

6'-H), 4.00 (dd, $^{3}J_{3'\text{-H}/4'\text{-H}}$ = 6.2 Hz, $^{3}J_{3'\text{-H}/2'\text{-H}}$ = 5.9 Hz, 1 H, 3'-H), 4.17 (ddd, $^{3}J_{4'\text{-H}/5'\text{-H}_a}$ = 9.8 Hz, $^{3}J_{4'\text{-H}/3'\text{-H}}$ = 6.2 Hz, $^{3}J_{4'\text{-H}/5'\text{-H}_b}$ = 3.5 Hz, 1 H, 4'-H), 4.20 (d, $^{3}J_{2^{v}\text{-H}/3^{v}\text{-H}}$ = 4.9 Hz, 1 H, 2^{v}-H), 4.30 (dd, $^{3}J_{2^{iv}\text{-H}/3^{iv}\text{-H}_a}$ = 7.9 Hz, $^{3}J_{2^{iv}\text{-H}/3^{iv}\text{-H}_b}$ = 5.4 Hz, 1 H, 2^{iv}-H), 4.35 (dd, $^{3}J_{2'\text{-H}/3'\text{-H}}$ = 5.9 Hz, $^{3}J_{2'\text{-H}/1'\text{-H}}$ = 3.8 Hz, 1 H, 2'-H), 4.41 (d, $^{3}J_{2'''\text{-H}/3'''\text{-H}}$ = 4.3 Hz, 1 H, 2'''-H), 5.32 (dq, $^{3}J_{3'''\text{-H}/4'''\text{-H}}$ = 6.5 Hz, $^{3}J_{3'''\text{-H}/2'''\text{-H}}$ = 4.3 Hz,1 H, 3'''-H), 5.68 (d, $^{3}J_{1'\text{-H}/2'\text{-H}}$ = 3.8 Hz, 1 H, 1'-H), 5.73 (d, $^{3}J_{5\text{-H}/6\text{-H}}$ = 8.1 Hz, 1 H, 5-H), 7.61 (d, $^{3}J_{6\text{-H}/5\text{-H}}$ = 8.1 Hz, 1 H, 6-H).

^{13}C NMR (126 MHz, MeOH-d_4): δ [ppm] = 14.43 (C-13^{vi}), 17.40 (C-4^{vi}-12^{vi}), 17.94 (C-4^{v}), 19.82 (C-4^{v}), 23.73 (C-4^{vi}-12^{vi}), 25.98 (C-3^{vi}), 26.07 (C-4^{iv}), 27.51 (C-2''), 30.15, 30.21, 30.42, 30.47, 30.64, 30.76, 30.79 (C-4^{vi}-12^{vi}), 30.74 (C-3^{iv}), 31.89 (C-3^{v}), 33.07 (C-4^{vi}-12^{vi}), 34.75 (C-5'), 35.09 (C-2^{vi}), 37.00 (C-3''), 41.87 (C-5^{iv}), 45.44 (C-1''), 54.50 (C-2^{iv}), 58.57 (C-2'''), 59.47 (C-2^{v}), 61.74 (C-6'), 70.80 (C-3'''), 73.97 (C-2'), 74.79 (C-3'), 82.08 (C-4'), 94.29 (C-1'), 103.03 (C-5), 144.05 (C-6), 152.19 (C-2), 158.68 (NC(=NH)N), 160.49 (NC(=O)N), 166.08 (C-4), 172.29 (C-1'''), 172.75 (C-7'), 174.42 (C-1^{vi}), 175.48 (C-1^{iv}), 175.94 (C-1^{v}).

^{19}F NMR (471 MHz, MeOH-d_4): δ [ppm] = -76.97.

IR (ATR) υ [cm^{-1}]: 3324, 2926, 2855, 1653, 1558, 1542, 1508, 1201, 1135, 1068.

UV (HPLC) λ [nm]: 260, 207.

LC-MS (ESI^+): m/z = 955.90 $[M+H]^+$.

HRMS (ESI^+): calcd. for $C_{43}H_{75}N_{10}O_{14}^+$: 955.5459, found: 955.5439 $[M+H]^+$.

$C_{43}H_{74}N_{10}O_{14}$ (955.12)

$C_{43}H_{76}N_{10}O_{14}^{2+}$ • 2 $C_2F_3O_2^-$ (1183.17)

7.6 Synthesis of truncated muraymycin derivatives

7.6.1 Truncated target compound TT1: Cbz-*allo*-Thr($COC_{12}H_{25}$)-NuAA

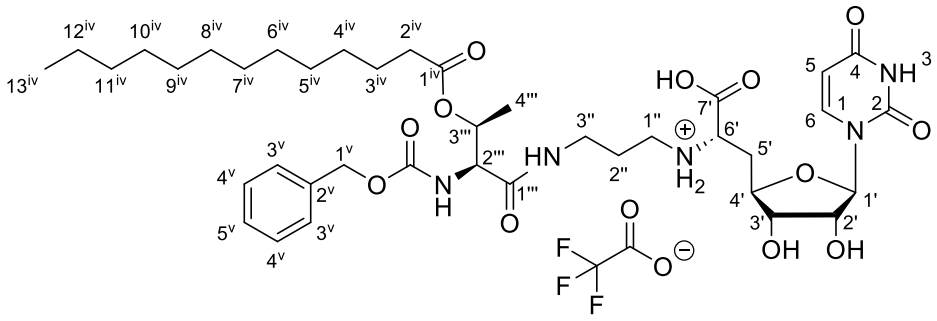

The reaction was not carried out under an inert gas atmosphere. Cbz-*allo*-Thr($COC_{12}H_{25}$)-NuAA **52** (19.5 mg, crude) was dissolved in aqueous trifluoroacetic acid (80%, 5 mL) and stirred for 24 h at room temperature. The solution was diluted with water (10 mL) and the solvent was removed by lyophilization. The title compound was isolated after purification by HPLC.

Yield (**TT1**): 3.99 mg (4.41 µmol, 5.4% over two steps from **38**) as a white solid.

HPLC (semi-preparative): t_R = 15.2 min (method: **E**, conc. of injection: 30.0 mg/mL in MeOH).

^{1}H NMR (500 MHz, DMSO-d_6): δ [ppm] = 0.85 (t, $^3J_{13iv\text{-}H/12iv\text{-}H}$ = 6.9 Hz, 3 H, 13^{iv}-H), 1.11 (d, $^3J_{4'''\text{-}H/3'''\text{-}H}$ = 6.5 Hz, 3 H, 4'''-H), 1.18-1.28 (m, 18 H, 4^{iv}-12^{iv}-H), 1.41-1.50 (m, 2 H, 3^{iv}-H), 1.64-1.72 (m, 2 H, 2''-H), 1.91 (ddd, $^2J_{5'\text{-}H_a/5'\text{-}H_b}$ = 13.5 Hz, $^3J_{5'\text{-}H_a/4'\text{-}H}$ = 8.0 Hz, $^3J_{5'\text{-}H_a/6'\text{-}H}$ = 4.9 Hz, 1 H, 5'-H$_a$), 2.00-2.09 (m, 1 H, 5'-H$_b$), 2.13-2.19 (m, 2 H, 2^{iv}-H), 2.72-2.84 (m, 2 H, 1''-H), 3.03-3.16 (m, 2 H, 3''-H), 3.20-3.27 (m, 1 H, 6'-H), 3.79 (dd, $^3J_{3'\text{-}H/4'\text{-}H}$ = 5.7 Hz, $^3J_{3'\text{-}H/2'\text{-}H}$ = 5.3 Hz, 1 H, 3'-H), 4.01 (ddd, $^3J_{4'\text{-}H/5'\text{-}H_a}$ = 8.0 Hz, $^3J_{4'\text{-}H/3'\text{-}H}$ = 5.7 Hz, $^3J_{4'\text{-}H/5'\text{-}H_b}$ = 5.6 Hz, 1 H, 4'-H), 4.06 (dd, $^3J_{2'\text{-}H/3'\text{-}H}$ = 5.3 Hz, $^3J_{2'\text{-}H/1'\text{-}H}$ = 4.5 Hz, 1 H, 2'-H), 4.27 (dd, $^3J_{2'''\text{-}H/2'''\text{-}NH}$ = 9.6 Hz, $^3J_{2'''\text{-}H/3'''\text{-}H}$ = 6.2 Hz, 1 H, 2'''-H), 4.98-5.11 (m, 3 H, 3'''-H, 1^v-H), 5.38 (bs, 1 H, 6'-NH), 5.61 (d, $^3J_{5\text{-}H/6\text{-}H}$ = 8.1 Hz, 1 H, 5-H), 5.67 (d, $^3J_{1'\text{-}H/2'\text{-}H}$ = 4.5 Hz, 1 H, 1'-H), 7.29-7.33 (m, 1 H, 5^v-H), 7.33-7.39 (m, 4 H, 3^v-H, 4^v-H), 7.60 (d, $^3J_{6\text{-}H/5\text{-}H}$ = 8.1 Hz, 1 H, 6-H), 7.63 (d, $^3J_{2'''\text{-}NH/2'''\text{-}H}$ = 9.6 Hz, 1 H, 2'''-NH), 8.14 (dd, $^3J_{3''\text{-}NH/3''\text{-}H_a}$ = 5.5 Hz, $^3J_{3''\text{-}NH/3''\text{-}H_b}$ = 5.5 Hz, 1 H, 1'''-NH), 11.34 (s, 1 H, 3-NH).

^{13}C NMR (126 MHz, DMSO-d_6): δ [ppm] = 13.96 (C-13^{iv}), 15.51 (C-4'''), 22.09 (C-4^{iv}-12^{iv}), 24.28 (C-3^{iv}), 26.56 (C-2''), 28.37, 28.70, 28.88, 28.99, 29.01, 29.03, 31.29 (C-4^{iv}-12^{iv}), 34.27 (C-5'), 33.61 (C-2^{iv}), 36.13 (C-3''), 43.65 (C-1''), 58.76 (C-6'), 57.39 (C-2'''),

65.64 (C-1^{v}), 69.25 (C-3'''), 72.95 (C-2'), 73.16 (C-3'), 80.40 (C-4'), 89.27 (C-1'), 101.90 (C-5), 127.32, 127.69, 128.81 (C-3^{v}, C-4^{v}, C-5^{v}), 136.91 (C-2^{v}), 141.30 (C-6), 150.54 (C-2), 156.17 (NC(=O)O), 163.07 (C-4), 168.82 (C-1'''), 169.87 (C-7'), 172.00 (C-1^{iv}).

^{19}F NMR (471 MHz, MeOH-d_4): δ [ppm] = -73.43.

IR (ATR) υ [cm^{-1}]: 3326, 2923, 2853, 1676, 1631, 1525, 1232, 1203, 1025, 696.

UV (HPLC) λ [nm]: 260, 208.

LC-MS (ESI$^+$): m/z = 790.74 [M+H]$^+$.

HRMS (ESI$^+$): calcd. for $C_{39}H_{60}N_5O_{12}^+$: 790.4233, found: 790.4205 [M+H]$^+$.

$C_{39}H_{59}N_5O_{12}$ (789.42)

$C_{39}H_{60}N_5O_{12}^+ \bullet C_2F_3O_2^-$ (903.95)

7.6.2 Truncated target compound TT2: H-*allo*-Thr($COC_{12}H_{25}$)-NuAA

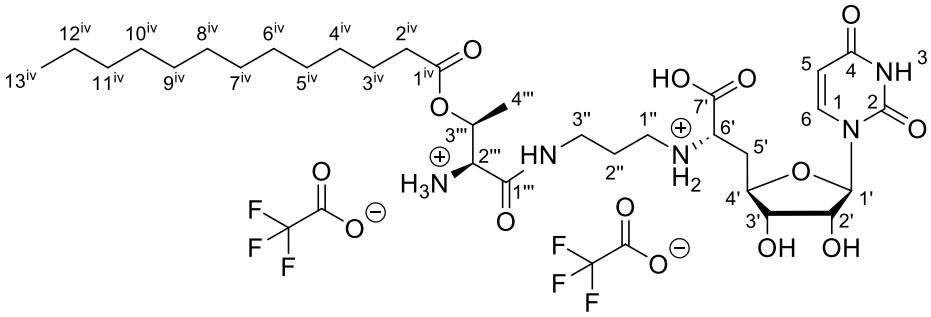

The reaction was not carried out under an inert gas atmosphere. H-*allo*-Thr($COC_{12}H_{25}$)-NuAA bis-TFA salt **78** (21.0 mg, 18.0 µmol, 1.0 eq.) was dissolved in aqueous trifluoroacetic acid (80%, 5 mL) and stirred for 24 h at room temperature. The solvent was removed under reduced pressure, the residue was dissolved in water and lyophilized. The title compound was isolated after purification by HPLC.

Yield (**TT2**): 6.19 mg (7.00 µmol, 39%) as a white solid.

HPLC (semi-preparative): t_R = 14.1 min (method: **E**, conc. of injection: 16.1 mg/mL in MeOH).

^{1}H NMR (500 MHz, MeOH-d_4): δ [ppm] = 0.90 (t, $^3J_{13^{iv}\text{-H}/12^{iv}\text{-H}}$ = 7.0 Hz, 3 H, 13^{iv}-H), 1.27-1.36 (m, 18 H, 4^{iv}-12^{iv}-H), 1.31 (d, $^3J_{4'''\text{-H}/3'''\text{-H}}$ = 6.7 Hz, 3 H, 4'''-H), 1.58-1.66 (m, 2 H, 3^{iv}-H), 1.91-1.99 (m, 2 H, 2''-H), 2.29 (ddd, $^2J_{5'\text{-H}a/5'\text{-H}b}$ = 14.8 Hz, $^3J_{5'\text{-H}a/4'\text{-H}}$ = 10.3 Hz, $^3J_{5'\text{-H}a/6'\text{-H}}$ = 6.0 Hz, 1 H, 5'-H$_a$), 2.38 (t, $^3J_{2^{iv}\text{-H}/3^{iv}\text{-H}}$ = 7.5 Hz, 2 H, 2^{iv}-H), 2.44 (ddd,

$^{2}J_{5'\text{-}H_b/5'\text{-}H_a}$ = 14.8 Hz, $^{3}J_{5'\text{-}H_b/6'\text{-}H}$ = 6.5 Hz, $^{3}J_{5'\text{-}H_b/4'\text{-}H}$ = 3.0 Hz, 1 H, 5'-H_b), 3.06-3.20 (m, 2 H, 1''-H), 3.32-3.42 (m, 2 H, 3''-H), 4.00 (dd, $^{3}J_{3'\text{-}H/4'\text{-}H}$ = 6.4 Hz, $^{3}J_{3'\text{-}H/2'\text{-}H}$ = 6.0 Hz, 1 H, 3'-H), 4.02 (dd, $^{3}J_{6'\text{-}H/5'\text{-}H_b}$ = 6.5 Hz, $^{3}J_{6'\text{-}H/5'\text{-}H_a}$ = 6.0 Hz, 1 H, 6'-H), 4.10 (d, $^{3}J_{2'''\text{-}H/3'''\text{-}H}$ = 4.2 Hz, 1 H, 2'''-H), 4.13 (ddd, $^{3}J_{4'\text{-}H/5'\text{-}H_a}$ = 10.3 Hz, $^{3}J_{4'\text{-}H/3'\text{-}H}$ = 6.4 Hz, $^{3}J_{4'\text{-}H/5'\text{-}H_b}$ = 3.0 Hz, 1 H, 4'-H), 4.33 (dd, $^{3}J_{2'\text{-}H/3'\text{-}H}$ = 6.0 Hz, $^{3}J_{2'\text{-}H/1'\text{-}H}$ = 3.8 Hz, 1 H, 2'-H), 5.27 (dq, $^{3}J_{3'''\text{-}H/4'''\text{-}H}$ = 6.7 Hz, $^{3}J_{3'''\text{-}H/2'''\text{-}H}$ = 4.2 Hz, 1 H, 3'''-H), 5.70 (d, $^{3}J_{1'\text{-}H/2'\text{-}H}$ = 3.8 Hz, 1 H, 1'-H), 5.72 (d, $^{3}J_{5\text{-}H/6\text{-}H}$ = 8.1 Hz, 1 H, 5-H), 7.60 (d, $^{3}J_{6\text{-}H/5\text{-}H}$ = 8.1 Hz, 1 H, 6-H).

^{13}C NMR (126 MHz, MeOH-d_4): δ [ppm] = 14.42 (C-13^{iv}), 15.38 (C-4'''), 23.72 (C-4^{iv}-12^{iv}), 25.75 (C-3^{iv}), 27.43 (C-2''), 30.15, 30.42, 30.46, 30.60, 30.71, 30.74, 30.76, 33.06 (C-4^{iv}-12^{iv}), 34.27 (C-5'), 34.27 (C-2^{iv}), 37.55 (C-3''), 45.55 (C-1''), 57.49 (C-2'''), 59.92 (C-6'), 69.13 (C-3'''), 74.03 (C-2'), 74.73 (C-3'), 81.21 (C-4'), 94.13 (C-1'), 103.11 (C-5), 143.80 (C-6), 152.18 (C-2), 166.03 (C-4), 167.49 (C-1'''), 171.22 (C-7'), 174.04 (C-1^{iv}).

^{19}F NMR (471 MHz, MeOH-d_4): δ [ppm] = -76.92.

IR (ATR) υ [cm^{-1}]: 2925, 2853, 1672, 1465, 1419, 1384, 1265, 1201, 1182, 1133.

UV (HPLC) λ [nm]: 260, 201.

LC-MS (ESI^+): m/z = 656.59 $[M+H]^+$.

HRMS (ESI^+): calcd. for $C_{31}H_{54}N_5O_{10}^+$: 656.3866, found: 656.3844 $[M+H]^+$.

$C_{31}H_{53}N_5O_{10}$ (655.79)

$C_{31}H_{55}N_5O_{10}^{2+}$ • 2 $C_2F_3O_2^-$ (883.84)

7.6.3 Truncated target compound TT3: *N*-Ac-*allo*-Thr($COC_{12}H_{25}$)-NuAA[146,148,153]

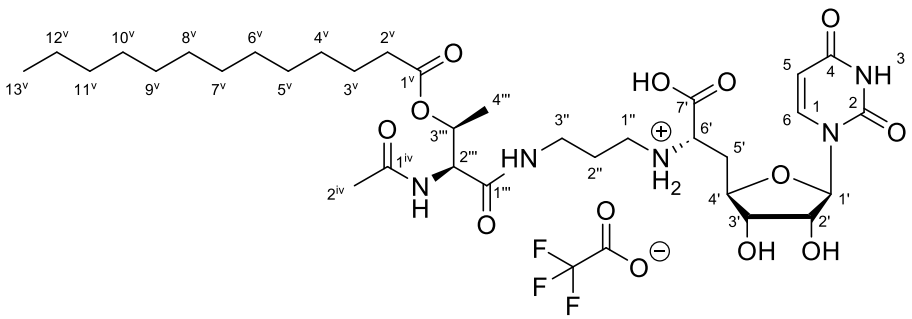

1,4-Cyclohexadiene (12.9 µL, 137 µmol, 10.0 eq.), palladium black (2 spatula tips) and trifluoroacetic acid (2.10 µL, 27.4 µmol, 2.0 eq., added as a 10% solution in dry *iso*-propanol) were added to a solution of Cbz-*allo*-Thr($COC_{12}H_{25}$)-NuAA **52** (14.7 mg,

13.7 µmol, 1.0 eq.) in dry *iso*-propanol (1.5 mL). The reaction was stirred for 1.5 h at room temperature. The residue was filtered using a syringe filter. The filter was washed with methanol (6x 4 mL). The solvent was removed under reduced pressure to give the bis-TFA salt **78**. It was identified by LC-MS (LC-MS (ESI^+): m/z = 940.90 $[M+H]^+$) and was used without further purification.

Dry *N*,*N*-diisopropylethylamine (1.90 µL, 11.2 µmol, 1.0 eq.) was added to a solution of glacial acetic acid (0.64 µL, 11.2 µmol, 1.0 eq.) in dry dichloromethane (0.1 mL). After 10 min, HATU (6.50 mg, 17.1 µmol, 1.5 eq.) was added. After 30 min, the reaction mixture was cooled to 0 °C and *N*,*N*-diisopropylethylamine (4.72 µL, 25.2 µmol, 2.5 eq.) was added. Muraymycin analog **78** (13.0 mg, 11.1 µmol, 1.0 eq.) in dry dichloro-methane (0.8 mL) was added dropwise at this temperature. The reaction was stirred for 18 h. During this time, the reaction mixture was allowed to warm up to room temperature. The solvent was removed under reduced pressure. The residue was dissolved in ethyl acetate (2.5 mL). The organic layer was washed with water (1 mL). The layers were separated, and the aqueous layer was extracted with ethyl acetate (2x 2.5 mL). The solvent was removed under reduced pressure. The coupling product was identified by LC-MS (LC-MS (ESI^+): m/z = 982.88 $[M+H]^+$) and was used without further purification.

The residue was dissolved in aqueous trifluoroacetic acid (80%, 2 mL) and was stirred for 23 h at room temperature. The solvent was removed under reduced pressure. The title compound was isolated after purification by HPLC.

Yield (**TT3**): 1.81 mg (2.23 µmol, 16% over three steps) as a white solid.

HPLC (semi-preparative): t_R = 16.5 min (method: **E**, conc. of injection: ~17.0 mg/mL in MeOH).

^{1}H NMR (500 MHz, MeOH-d_4): δ [ppm] = 0.90 (t, $^3J_{13^v\text{-H}/12^v\text{-H}}$ = 7.0 Hz, 3 H, 13^v-H), 1.27 (d, $^3J_{4'''\text{-H}/3'''\text{-H}}$ = 6.5 Hz, 3 H, 4'''-H), 1.23-1.34 (m, 18 H, 4^v-12^v-H), 1.59 (tt, $^3J_{3^v\text{-H}/2^v\text{-H}}$ = 7.2 Hz, $^3J_{3^v\text{-H}/4^v\text{-H}}$ = 6.9 Hz, 2 H, 3^v-H), 1.88 (ddt, $^3J_{2''\text{-H}/1''\text{-H}_a}$ = 6.9 Hz, $^3J_{2''\text{-H}/1''\text{-H}_b}$ = 6.7 Hz, $^3J_{2''\text{-H}/3''\text{-H}}$ = 6.7 Hz, 2 H, 2''-H), 2.03 (s, 3 H, 2^{iv}-H), 2.22-2.27 (m, 1 H, 5'-H_a), 2.29 (t, $^3J_{2^v\text{-H}/3^v\text{-H}}$ = 7.2 Hz, 2 H, 2^v-H), 2.45 (ddd, $^2J_{5'\text{-H}_b/5'\text{-H}_a}$ = 14.8 Hz, $^3J_{5'\text{-H}_b/6'\text{-H}}$ = 6.3 Hz, $^3J_{5'\text{-H}_b/4'\text{-H}}$ = 3.1 Hz, 2 H, 5'-H_b), 3.04 (dt, $^2J_{1''\text{-H}_a/1''\text{-H}_b}$ = 12.8 Hz, $^3J_{1''\text{-H}_a/2''\text{-H}}$ = 6.9 Hz, 1 H, 1''-H_a), 3.10 (dt, $^2J_{1''\text{-H}_b/1''\text{-H}_a}$ = 12.8 Hz, $^3J_{1''\text{-H}_b/2''\text{-H}}$ = 6.7 Hz, 1 H, 1''-H_b), 3.24-3.29 (m, 2 H, 3''-H), 3.97 (dd, $^3J_{6'\text{-H}/5'\text{-H}_b}$ = 6.3 Hz, $^3J_{6'\text{-H}/5'\text{-H}_a}$ = 6.2 Hz, 1 H, 6'-H), 4.01 (dd, $^3J_{3'\text{-H}/4'\text{-H}}$ =

6.5 Hz, $^{3}J_{3'\text{-H}/2'\text{-H}}$ = 6.0 Hz, 1 H, 3'-H), 4.14 (ddd, $^{3}J_{4'\text{-H}/5'\text{-H}_a}$ = 10.1 Hz, $^{3}J_{4'\text{-H}/3'\text{-H}}$ = 6.5 Hz, $^{3}J_{4'\text{-H}/5'\text{-H}_b}$ = 3.1 Hz, 1 H, 4'-H), 4.35 (dd, $^{3}J_{2'\text{-H}/3'\text{-H}}$ = 6.0 Hz, $^{3}J_{2'\text{-H}/1'\text{-H}}$ = 4.7 Hz, 1 H, 2'-H), 4.55 (d, $^{3}J_{2'''\text{-H}/3'''\text{-H}}$ = 6.3 Hz, 1 H, 2'''-H), 5.17 (dq, $^{3}J_{3'''\text{-H}/4'''\text{-H}}$ = 6.5 Hz, $^{3}J_{3'''\text{-H}/2'''\text{-H}}$ = 6.3 Hz, 2 H, 3'''-H), 5.68 (d, $^{3}J_{1'\text{-H}/2'\text{-H}}$ = 4.7 Hz, 1 H, 1'-H), 5.72 (d, $^{3}J_{5\text{-H}/6\text{-H}}$ = 8.1 Hz, 1 H, 5-H), 7.60 (d, $^{3}J_{6\text{-H}/5\text{-H}}$ = 8.1 Hz, 1 H, 6-H).

^{13}C NMR (126 MHz, MeOH-d_4): δ [ppm] = 14.96 (C-13^{v}), 16.89 (C-4'''), 23.04 (C-2^{iv}), 24.26 (C-4^{v}-12^{v}), 26.45 (C-3^{v}), 28.11 (C-2''), 30.69, 30.95, 30.99, 31.13, 31.25, 31.28, 31.30, 33.60 (C-4^{v}-12^{v}), 34.63 (C-5'), 35.70 (C-2^{v}), 37.38 (C-3''), 45.73 (C-1''), 58.54 (C-2'''), 60.23 (C-6'), 71.17 (C-3'''), 74.51 (C-2'), 75.30 (C-3'), 81.74 (C-4'), 95.01 (C-1'), 103.55 (C-5), 144.53 (C-6), 152.64 (C-2), 166.58 (C-4), 171.64 (C-7'), 173.10 (C-1'''), 174.30 (C-1^{iv}), 175.00 (C-1^{v}).

^{19}F NMR (471 MHz, MeOH-d_4): δ [ppm] = -76.97.

IR (ATR) υ [cm^{-1}]: 3325, 2923, 2851, 1681, 1650, 1201, 1168, 1134, 839, 721.

UV (HPLC) λ [nm]: 260, 202.

LC-MS (ESI^{+}): m/z = 698.51 $[M+H]^{+}$.

HRMS (ESI^{+}): calcd. for $C_{33}H_{56}N_5O_{11}^{+}$: 698.3971, found: 698.3956 $[M+H]^{+}$.

$C_{33}H_{55}N_5O_{11}$ (697.83)

$C_{33}H_{56}N_5O_{11}^{+} \bullet C_2F_3O_2^{-}$ (811.85)

7.6.4 Truncated target compound TT4: *N*-Ac-*allo*-Thr(COCH$_3$)-NuAA[146]

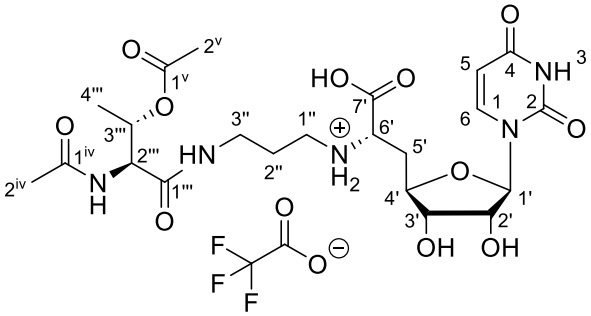

Dry *N*,*N*-diisopropylethylamine (6.10 µL, 35.9 µmol, 1.0 eq.) was added to a solution of acetic acid (2.10 µL, 37.7 µmol, 1.0 eq.) in dry dichloromethane (0.2 mL). After 10 min, HATU (20.5 mg, 53.9 µmol, 1.5 eq.) was added. After 30 min, the reaction mixture was cooled to 0 °C and dry *N*,*N*-diisopropylethylamine (15.3 µL, 90.0 µmol, 2.5 eq.) was added. H-*allo*-Thr(COCH$_3$)-NuAA bis-TFA salt **90** (36.4 mg, 35.9 µmol, 1.0 eq.) in dry

dichloromethane (1.5 mL) was added dropwise at this temperature. The reaction was stirred for 30 min at 0 °C, then for 5 h at room temperature. Then, water (2 mL) was added to the reaction mixture. The layers were separated, and the aqueous layer was extracted with dichloromethane (4x 2 mL). The solvent was removed under reduced pressure. The product was identified by LC-MS (LC-MS (ESI$^+$): m/z = 828.16 $[M+H]^+$) and was used without further purification.

The residue was dissolved in aqueous trifluoroacetic acid (80%, 2 mL) and stirred for 24 h at room temperature. The solvent was removed under reduced pressure. The title compound was isolated after purification by HPLC.

Yield (**TT4**): 1.56 mg (2.37 µmol, 6.5% over two steps, calcd. from AcOH) as a colorless solid.

HPLC (semi-preparative): t_R = 11.2 min (method: **I**, conc. of injection: ~15 mg/mL in MeOH).

^{1}H NMR (500 MHz, MeOH-d_4): δ [ppm] = 1.27 (d, $^3J_{4'''\text{-H}/3'''\text{-H}}$ = 6.5 Hz, 3 H, 4'''-H), 1.88 (dt, $^3J_{2''\text{-H}/3''\text{-H}}$ = 6.7 Hz, $^3J_{2''\text{-H}/1''\text{-H}_a}$ = 6.6 Hz, $^3J_{2''\text{-H}/1''\text{-H}_b}$ = 6.6 Hz, 1 H, 2''-H), 2.02 (s, 3 H, 2^{v}-H), 2.03 (s, 3 H, 2^{iv}-H), 2.26 (ddd, $^2J_{5'\text{-H}_a/5'\text{-H}_b}$ = 14.8 Hz, $^3J_{5'\text{-H}_a/4'\text{-H}}$ = 10.0 Hz, $^3J_{5'\text{-H}_a/6'\text{-H}}$ = 6.3 Hz, 1 H, 5'-H_a), 2.45 (ddd, $^2J_{5'\text{-H}_b/5'\text{-H}_a}$ = 14.8 Hz, $^3J_{5'\text{-H}_b/6\text{-H}}$ = 6.3 Hz, $^3J_{5'\text{-H}_b/4'\text{-H}}$ = 3.0 Hz, 1 H, 5'-H_b), 3.04 (dt, $^2J_{1''\text{-H}_a/1''\text{-H}_b}$ = 14.6 Hz, $^3J_{1''\text{-H}_a/2''\text{-H}}$ = 6.6 Hz, 1 H, 1''-H_a), 3.10 (dt, $^2J_{1''\text{-H}_b/1''\text{-H}_a}$ = 14.6 Hz, $^3J_{1''\text{-H}_b/2''\text{-H}}$ = 6.6 Hz, 1 H, 1''-H_b), 3.27-3.30 (m, 2 H, 3''-H), 3.96 (dd, $^3J_{6'\text{-H}/5'\text{-H}_a}$ = 6.3 Hz, $^3J_{6'\text{-H}/5'\text{-H}_b}$ = 6.3 Hz, 1 H, 6'-H), 4.01 (dd, $^3J_{3'\text{-H}/4'\text{-H}}$ = 6.4 Hz, $^3J_{3'\text{-H}/2'\text{-H}}$ = 5.9 Hz, 1 H, 3'-H), 4.14 (ddd, $^3J_{4'\text{-H}/5'\text{-H}_a}$ = 10.0 Hz, $^3J_{4'\text{-H}/3'\text{-H}}$ = 6.4 Hz, $^3J_{4'\text{-H}/5'\text{-H}_b}$ = 3.0 Hz, 1 H, 4'-H), 4.35 (dd, $^3J_{2'\text{-H}/3'\text{-H}}$ = 5.9 Hz, $^3J_{2'\text{-H}/1'\text{-H}}$ = 3.6 Hz, 1 H, 2'-H), 4.54 (d, $^3J_{2'''\text{-H}/3'''\text{-H}}$ = 6.3 Hz, 1 H, 2'''-H), 5.15 (dq, $^3J_{3'''\text{-H}/4'''\text{-H}}$ = 6.5 Hz, $^3J_{3'''\text{-H}/2'''\text{-H}}$ = 6.3 Hz,1 H, 3'''-H), 5.68 (d, $^3J_{1'\text{-H}/2'\text{-H}}$ = 3.6 Hz, 1 H, 1'-H), 5.72 (d, $^3J_{5\text{-H}/6\text{-H}}$ = 8.1 Hz, 1 H, 5-H), 7.60 (d, $^3J_{6\text{-H}/5\text{-H}}$ = 8.1 Hz, 1 H, 6-H).

^{13}C NMR (126 MHz, MeOH-d_4): δ [ppm] = 16.90 (C-4'''), 21.58 (C-2^{v}), 23.01 (C-2^{iv}), 28.11 (C-2''), 34.77 (C-5'), 37.38 (C-3''), 45.76 (C-1''), 58.45 (C-2'''), 60.65 (C-6'), 71.46 (C-3'''), 74.50 (C-2'), 75.28 (C-3'), 81.95 (C-4'), 94.93 (C-1'), 103.54 (C-5), 144.54 (C-6), 152.65 (C-2), 166.59 (C-4), 171.29 (C-7'), 172.41 (C-1^{v}), 172.99 (C-1'''), 174.27 (C-1^{iv}).

^{19}F NMR (471 MHz, MeOH-d_4): δ [ppm] = -76.98.

IR (ATR) υ [cm^{-1}]: 3293, 1667, 1539, 1429, 1377, 1258, 1182, 1131, 800, 721.

UV (HPLC) λ [nm]: 260, 204.

LC-MS (ESI^+): m/z = 544.42 $[M+H]^+$.

HRMS (ESI^+): calcd. for $C_{22}H_{34}N_5O_{11}^+$: 544.2250, found: 544.2241 $[M+H]^+$.

$C_{22}H_{33}N_5O_{11}$ (543.53)

$C_{22}H_{34}N_5O_{11}^+ \bullet C_2F_3O_2^-$ (657.55)

7.7 Biological evaluation

7.7.1 Fluorescence based *in vitro* activity assay

The assay was performed by N. Kagerah and M. Lutz according to previously described the method.[96,121,172–174] To determine the inhibitory activity towards MraY (IC_{50}), the increase in fluorescence intensity was determined at the wavelengths λ_{ex} = 355 nm and λ_{em} = 520 nm (BMG Labtech POLARstar Omega, 384-well plate format) over time. Each well contained 20 µL of the following composition: buffer (100 mM Tris-HCl buffer pH 7.5, 200 mM potassium chloride, 10 mM magnesium chloride, 0.1% Triton X-100, 5% DMSO), dansylated Parks nucleotide[174] (synthetic, 7.5 µM), undecaprenyl phosphate (50 µM) and a solution of the compound (in DMSO) in varying concentrations. The membrane preparation containing MraY[174] was added to the mixture and the measurement was started simultaneously. The measurement was performed in triplicate. MraY activity was now determined by a linear fit of the fluorescence intensity curve (period: 0-2 min). By plotting the enzymatic activity against the logarithmic inhibitor concentrations, the IC_{50} value could be determined by a sigmoidal fit.

7.7.2 Determination of antibacterial activity

Antibacterial activities were determined by M. Jankowski and N. Kagerah using a previously described method.[135] Here, the first row of a 96-well plate under sterile conditions was filled with 4 µL of a suitable concentrated solution of the test compound (DMSO) and 194 µL LB medium. After mixing, 100 µL of the solution were transferred to the next row, which was prepared with 100 µL LB medium. This procedure is repeated until a range of different concentrations of the compound is achieved. A culture of the corresponding strain (*S. aureus* Newman, *E. coli* Δ*tolC* and *E. coli* DH5α) was shaken in LB medium (10 mL) for 16 h at 37 °C and 180 rpm. It was then diluted by adding 100 µL of the overnight culture in 10 mL LB medium. This mixture was incubated until the value of optical density OD_{600} = 0.6 was reached. 100 µL of the resulting bacterial suspension was added to each well hole. The plate was incubated for 16 h at 37 °C and 180 rpm. The optical density was determined both before and after the incubation period.

The determination of the antibacterial *C. difficile* activity was performed at Prof. Dr. Sören Beckers laboratory at Saarland University, Institute for Medical Microbiology and Hygiene in Homburg.

7.7.3 Determination of stability

The stability assays were performed by M. Jankowski. The calibration was performed using a dilution series of the respective chemical compound (conc.: 5 µM, 2.5 µM, 1 µM, 0.5 µM, 0.25 µM and 0.1 µM) in MiiliQ-water.

7.7.3.1 Bacterial Cell Lysate *E. coli* Δ*tolC*

The bacterial cell lysate was obtained from *E. coli* Δ*tolC*. Therefore, the cells grew in LB medium at 37 °C until an optical density of OD_{600} = 0.6 was reached. The cells were separated from the medium by centrifugation (3060 • g, 4 °C), and the resulting pellet was resuspended in sodium phosphate buffer with protease inhibitor. Then, the cells were lysed using ultrasound (10 cycles at 80% power, 15 s pulse, with a 45 s pause). After centrifugation, the lysate was separated from the pellet and used for stability measurements.

For the stability assay, 27 µL of the lysate was mixed with 3 µL of a 100 µM solution of the respective compound (1 µL from the 20 mM stock solution in 199 µL buffer). Diphenhydramine solution (1.5 µM) was used as stop-solution. 60 µL of this solution were added to the respective sample at the time-depending moment. After mixing, the mixture was cooled on ice. The measurements were taken at 0 (two measure points: 1. stop-solution was added to the lysate before the compound; 2. compound was added to the lysate before the stop-solution), 15, 30, 60, and 150 min in duplicate after another centrifugation. Detection of the compounds in the supernatant was performed by HPLC-coupled HRMS.

7.7.3.2 Luria-Bertani Medium

The used LB medium consisted of 5 g yeast extract, 10 g peptone, 5 g sodium chloride and 1 L of water.

For the stability assay, 27 µL of the LB medium was mixed with 3 µL of a 100 µM solution of the respective compound (1 µL from the 20 mM stock solution in 199 µL buffer). Diphenhydramine solution (1.5 µM) was used as stop-solution. 60 µL of this

solution were added to the respective sample at the time-depending moment. After mixing, the mixture was cooled on ice. The measurements were taken at 0 (two measure points: 1. stop-solution was added to the LB-medium before the compound; 2. compound was added to the LB-medium before the stop-solution), 15, 30, 60, and 150 min in duplicate after another centrifugation. Detection of the compounds in the supernatant was performed by HPLC-coupled HRMS.

7.7.3.3 Human Plasma

First, the used plasma was diluted 1:10 with MilliQ water.

For the stability assay, 27 µL of the diluted plasma was mixed with 3 µL of a 100 µM solution of the respective compound (1 µL from the 20 mM stock solution in 199 µL buffer). Diphenhydramine solution (1.5 µM) was used as stop-solution. 60 µL of this solution were added to the respective sample at the time-depending moment. After mixing, the mixture was cooled on ice. The measurements were taken at 0 (two measure points: 1) stop-solution was added to the LB-medium before the compound; 2) compound was added to the LB-medium before the stop-solution), 15, 30, 60, and 150 min in duplicate after another centrifugation. Detection of the compounds in the supernatant was performed by HPLC-coupled HRMS.

8 Literature

[1] E. Oldfield, X. Feng. Resistance-resistant antibiotics. *Trends in Pharmacol. Sci.* **2014**, *35*, 664-674.

[2] M. P. Ferraz. Antimicrobial Resistance: The Impact from and on Society According to One Health Approach. *Societies* **2024**, *14*, 187.

[3] M. I. Hutchings, A. W. Truman, B. Wilkinson. Antibiotics: past, present and future. *Curr. Opin. Microbiol.* **2019**, *51*, 72-80.

[4] S. A. Waksman. What is an antibiotic or antibiotic substance? *Mycologia* **1947**, *39*, 565-569.

[5] S. A. Waksman. History of the Word 'Antibiotic'. *J. Hist. Med. Allied Sci.* **1973**, *28*, 284-286.

[6] E. P. Abraham, E. Chain. An Enzyme from Bacteria able to Destroy Penicillin. *Nature* **1940**, *3713*, 837.

[7] A. Fleming. On the Antibacterial Action of Cultures of a Penicillium, with Special reference to their Use in the Isolation of *B. Influenzae*. *Br. J. Exp. Pathol.* **1929**, *10*, 226-236.

[8] E. Chain, H. W. Florey, A. D. Gardner, N. G. Heatley, M. A. Jennings, J. Orr-Ewing, A. G. Sanders. Penicillin as a Chemotherapeutic Agent. *The Lancet* **1940**, *236*, 226-228

[9] L. Colebrook, M. Kenny. Treatment of Human Puerperal Infections, and of Experimental Infections in Mice, with Prontosil. *The Lancet* **1936**, 1279-1281.

[10] M. Wainwright, J. E. Kristiansen. On the 75th anniversary of Prontosil. *Dyes Pigments* **2011**, *88*, 231-234.

[11] I. Chopra, M. Roberts. Tetracycline Antibiotics: Mode of Action, Applications, Molecular Biology, and Epidemiology of Bacterial Resistance. *Microbiol. Mol. Biol. Rev.* **2001**, *65*, 232-260.

[12] A. Schatz, E. Bugle, S. A. Waksman. Streptomycin, a Substance Exhibiting Antibiotic Activity against Gram-Positive and Gram-Negative Bacteria. *Exp. Biol. Med.* **1944**, *55*, 66-69.

[13] S. A. Waksman. Streptomycin: Background, Isolation, Properties, and Utilization. *Science* **1953**, *118*, 259-266.

[14] F. R. Bruniera, F. M. Ferreira, L. R. M. Saviolli, M. R. Bacci, D. Feder, L. A. Azzalis, V. B. C. Junqueira, F. L. A. Fonseca. The use of vancomycin with its therapeutic and adverse effects: a review. *Eur. Rev. Med. Pharmacol. Sci.* **2015**, *19*, 694-700.

[15] E. Rubinstein, Y. Keynan. Vancomycin revisited - 60 years later. *Front. Public Health* **2014**, 2:217.

[16] B. Ribeiro da Cunha, L. P. Fonseca, C. R. C. Calado. Antibiotic Discovery: Where Have We Come from, Where Do We Go?. *Antibiotics* **2019**, *8*, 45.

[17] C. Walsh. Where will new antibiotics come from? *Nat. Rev. Microbiol.* **2003**, *1*, 65-70.

[18] K. Lewis. Platforms for antibiotic discovery. *Nat. Rev. Drug Discov.* **2013**, *12*, 371-387.

[19] A. Ishak, N. Mazonakis, N. Spernovasilis, K. Akinosoglou, C. Tsioutis. Bactericidal versus bacteriostatic antibacterials: clinical significance, differences and synergistic potential in clinical practice. *J. Antimicrob. Chemother.* **2024**, *80*, 1-17.

[20] H. L. Stennett, C. R. Back, P. R. Race. Derivation of a Precise and Consistent Timeline for Antibiotic Development. *Antibiotics* **2022**, *11*, 1237.

[21] F. Von Nussbaum, M. Brands, B. Hinzen, S. Weigand, D. Häbich. Antibakterielle Naturstoffe in der medizinischen Chemie - Exodus oder Renaissance? *Angew. Chem.* **2006**, *118*, 5194-5254.

[22] F. Von Nussbaum, M. Brands, B. Hinzen, S. Weigand, D. Häbich. Antibacterial Natural Products in Medicinal Chemistry - Exodus or Revival? *Angew. Chem. Int. Ed.* **2006**, *45*, 5072-5129.

[23] J. Davies. Where have all the antibiotics gone? *Can. J. Infect. Dis. Med. Microbiol.* **2006**, *17*, 287-290.

[24] A. Baran, A. Kwiatkowska, L. Potocki. Antibiotics and Bacterial Resistance - A Short Story of an Endless Arms Race. *Int. J. Mol. Sci.* **2023**, *24*, 5777.

[25] G. Taubes. The Bacteria Fight Back. *Science* **2008**, *231*, 356-361.

[26] C. Walsh. Molecular mechanisms that confer antibacterial drug resistance. *Nature* **2000**, *406*, 775-781.

[27] K. C. Nicolaou, S. Rigol. A brief history of antibiotics and select advances in their synthesis. *J. Antibiot.* (*Tokyo*) **2018**, *71*, 153-184.

[28] S. R. Palumbi. Humans as the World's Greatest Evolutionary Force. *Science* **2001**, *293*, 1785-1790.

[29] R. Sauermann, M. Rothenburger, W. Graninger, C. Joukhadar. Daptomycin: A Review 4 Years after First Approval. *Pharmacology* **2008**, *81*, 79-91.

[30] R. Mahajan. Bedaquiline: First FDA-approved tuberculosis drug in 40 years. *Int. J. Appl. Basic Med. Res.* **2013**, *3*, 1-2.

[31] S. Harbarth. Antibiotikatherapie - Einfluss des Antibiotikaverbrauchs auf Resistenzbildung und -selektion. *Anästhesiol. Intensivmed. Notfallmedizin Schmerzther.* **2007**, *2*, 130-135.

[32] S. B. Levy, B. Marshall. Antibacterial resistance worldwide: causes, challenges and responses. *Nat. Med.* **2004**, *10*, S122-S129

[33] D. G. J. Larsson, C.-F. Flach. Antibiotic resistance in the environment. *Nat. Rev. Microbiol.* **2022**, *20*, 257-269.

[34] K. Lewis. The Science of Antibiotic Discovery. *Cell* **2020**, *181*, 29-45.

[35] P. Spigaglia. Recent advances in the understanding of antibiotic resistance in *Clostridium difficile* infection. *Ther. Adv. Infect. Dis.* **2016**, *3*, 23-42.

[36] B. K. Sandhu, S. M. McBride. *Clostridioides difficile*. *Trends Microbiol.* **2018**, *26*, 1049-1050.

[37] V. N. Abdullatif, A. Noymer. *Clostridium difficile* Infection: An Emerging Cause of Death in the Twenty-First Century. *Biodemography Soc. Biol.* **2016**, *62*, 198-207.

[38] *CDC. Antibiotic Resistance Threats in the United States, 2019. Atlanta, GA: U.S. Department of Health and Human Services, CDC*, **2019**.

[39] C. E. Flynn, J. Guarner. Emerging Antimicrobial Resistance. *Mod. Pathol.* **2023**, *36*, 100249.

[40] D. M. P. De Oliveira, B. M. Forde, T. J. Kidd, P. N. A. Harris, M. A. Schembri, S. A. Beatson, D. L. Paterson, M. J. Walker. Antimicrobial Resistance in ESKAPE Pathogens. *Clin. Microbiol. Rev.* **2020**, *33*, e00181-19.

[41] *WHO Bacterial Priority Pathogens List 2024: Bacterial Pathogens of Public Health Importance, to Guide Research, Development, and Strategies to Prevent and Control Antimicrobial Resistance*, World Health Organization, Geneva, **2024**.

[42] *Antimicrobial Resistance in the EU/EEA (EARS-Net) - Annual Epidemiological Report 2023*, European Centre For Disease Prevention And Control, Stockholm, **2024**.

[43] I. M. Gould. Treatment of bacteraemia: meticillin-resistant *Staphylococcus aureus* (MRSA) to vancomycin-resistant *S. aureus* (VRSA). *Int. J. Antimicrob. Agents* **2013**, *42*, S17-S21.

[44] M. Otto. Community-associated MRSA: What makes them special? *Int. J. Med. Microbiol.* **2013**, *303*, 324-330.

[45] G. Regea. Review on Antibiotics Resistance and its Economic Impacts. *J. of Pharmacol. & Clin. Res.* **2018**, *5*, 1-11.

[46] E. M. Darby, E. Trampari, P. Siasat, M. S. Gaya, I. Alav, M. A. Webber, J. M. A. Blair. Molecular mechanisms of antibiotic resistance revisited. *Nat. Rev. Microbiol.* **2023**, *21*, 280-295.

[47] M. F. Chellat, L. Raguž, R. Riedl. Antibiotikaresistenzen gezielt überwinden. *Angew. Chem.* **2016**, *128*, 6710-6738.

[48] M. N. Alekshun, S. B. Levy. Molecular Mechanisms of Antibacterial Multidrug Resistance. *Cell* **2007**, *128*, 1037-1050.

[49] M. Jukič, S. Gobec, M. Sova. Reaching toward underexplored targets in antibacterial drug design. *Drug Dev. Res.* **2019**, *80*, 6-10.

[50] M. Tyers, G. D. Wright. Drug combinations: a strategy to extend the life of antibiotics in the 21st century. *Nat. Rev. Microbiol.* **2019**, *17*, 141-155.

[51] J. V. Heijenoort. Formation of the glycan chains in the synthesis of bacterial peptidoglycan. *Glycobiology* **2001**, *11*, 25R-36R.

[52] P. A. Lambert. Cellular impermeability and uptake of biocides and antibiotics in Gram-positive bacteria and mycobacteria. *J. Appl. Microbiol.* **2002**, *92*, 46S-54S.

[53] W. Vollmer, D. Blanot, M. A. de Pedro. Peptidoglycan structure and architecture. *FEMS Microbiol. Rev.* **2008**, *32*, 149-167.

[54] Y. Liu, E. Breukink. The Membrane Steps of Bacterial Cell Wall Synthesis as Antibiotic Targets. *Antibiotics* **2016**, *5*, 28; doi:10.3390/antibiotics5030028.

[55] T. D. H. Bugg, D. Braddick, C. G. Dowson, D. I. Roper. Bacterial cell wall assembly: still an attractive antibacterial target. *Trends Biotechnol.* **2011**, *29*, 167-173.

[56] A. M. Glauert, M. J. Thornley. The Topography of the Bacterial Cell Wall. *Annu. Rev. Microbiol.* **1969**, *23*, 159-198.

[57] T. J. Silhavy, D. Kahne, S. Walker. The Bacterial Cell Envelope. *Cold Spring Harb. Perspect. Biol.* **2010**, *2*, a000414.

[58] T. Beveridge. Mechanism of Gram Variability in Select Bacteria. *J. Bacteriol.* **1990**, *172*, 1609-1620.

[59] T. Beveridge. Use of the Gram stain in microbiology. *Biotech. Histochem.* **2001**, *76,* 3, 111-118.

[60] A. J. F. Egan, W. Vollmer. The physiology of bacterial cell division. *Ann. N. Y. Acad. Sci.* **2013**, *1277*, 8-28.

[61] A. Tamura, N. Ohashi, H. Urakami, S. Miyamura. Classification of *Rickettsia tsutsugamushi* in a New Genus, *Orientia* gen. nov., as *Orientia tsutsugamushi* comb. nov. *Int. J. Syst. Bacteriol.* **1995**, *45*, 589-591.

[62] W. Tantibhedhyangkul, A. Ben Amara, J. Textoris, L. Gorvel, E. Ghigo, C. Capo, J.-L. Mege. *Orientia tsutsugamushi*, the causative agent of scrub typhus, induces an inflammatory program in human macrophages. *Microb. Pathog.* **2013**, *55*, 55-63.

[63] C. Otten, M. Brilli, W. Vollmer, P. H. Viollier, J. Salje. Peptidoglycan in obligate intracellular bacteria. *Mol. Microbiol.* **2018**, *107*, 142-163.

[64] J. van Heijenoort. Recent advances in the formation of the bacterial peptidoglycan monomer unit. *Nat. Prod. Rep.* **2001**, *18*, 503-519.

[65] S. Garde, P. K. Chodisetti, M. Reddy. Peptidoglycan: Structure, Synthesis, and Regulation. *EcoSal Plus* **2021**; doi: 10.1128/ecosalplus.ESP-0010-2020.

[66] T. Touzé, D. Mengin-Lecreulx. Undecaprenyl Phosphate Synthesis. *EcoSal Plus* **2008**; doi: 10.1128/ecosalplus.4.7.1.7.

[67] H. Barreteau, A. Kovač, A. Boniface, M. Sova, S. Gobec, D. Blanot. Cytoplasmic steps of peptidoglycan biosynthesis. *FEMS Microbiol. Rev.* **2008**, *32*, 168-207.

[68] D. Wiegmann, S. Koppermann, M. Wirth, G. Niro, K. Leyerer, C. Ducho. Muraymycin nucleoside-peptide antibiotics: uridine-derived natural products as lead structures for the development of novel antibacterial agents. *Beilstein J. Org. Chem.* **2016**, *12*, 769-795.

[69] L. Jolly, P. Ferrari, D. Blanot, J. van Heijenoort, F. Fassy, D. Mengin-Lecreulx. Reaction mechanism of phosphoglucosamine mutase from *Escherichia coli*. *Eur. J. Biochem.* **1999**, *262*, 202-210.

[70] D. Mengin-Lecreulx, J. Van Heijenoort. Copurification of glucosamine-1-phosphate acetyltransferase and *N*-acetylglucosamine-1-phosphate uridyltransferase activities of *Escherichia coli*: characterization of the *glmU* gene product as a bifunctional enzyme catalyzing two subsequent steps in the pathway for UDP-*N*-acetylglucosamine synthesis. *J. Bacteriol.* **1994**, *176*, 5788-5795.

[71] A. M. Gehring, W. J. Lees, D. J. Mindiola, C. T. Walsh, E. D. Brown. Acetyltransfer Precedes Uridylyltransfer in the Formation of UDP-*N*-acetylglucosamine in Separable Active Sites of the Bifunctional GlmU Protein of *Escherichia coli*. *Biochemistry* **1996**, *35*, 579-585.

[72] L.-T. Sham, E. K. Butler, M. D. Lebar, D. Kahne, T. G. Bernhardt, N. Ruiz. MurJ is the flippase of lipid-linked precursors for peptidoglycan biogenesis. *Science* **2014**, *345*, 220–222.

[73] M. S. Butler, A. D. Buss. Natural products - The future scaffolds for novel antibiotics? *Biochem. Pharmacol.* **2006**, *71*, 919-929.

[74] B. C. Chung, J. Zhao, R. A. Gillespie, D.-Y. Kwon, Z. Guan, J. Hong, P. Zhou, S.-Y. Lee. Crystal Structure of MraY, an Essential Membrane Enzyme for Bacterial Cell Wall Synthesis. *Science* **2013**, *341*, 1012-1016.

[75] B. Al-Dabbagh, S. Olatunji, M. Crouvoisier, M. El Ghachi, D. Blanot, D. Mengin-Lecreulx, A. Bouhss. Catalytic mechanism of MraY and WecA, two paralogues of the polyprenyl-phosphate *N*-acetylhexosamine 1-phosphate transferase superfamily. *Biochimie* **2016**, *127*, 249-257.

[76] B. Al-Dabbagh, X. Henry, M. E. Ghachi, G. Auger, D. Blanot, C. Parquet, D. Mengin-Lecreulx, A. Bouhss. Active Site Mapping of MraY, a Member of the Polyprenyl-phosphate *N*-Acetylhexosamine 1-Phosphate Transferase Superfamily, Catalyzing the First Membrane Step of Peptidoglycan Biosynthesis. *Biochemistry* **2008**, *47*, 8919-8928.

[77] W. G. Struve, R. K. Sinha, F. C. Neuhaus, M. S. Prime. On the Initial Stage in Peptidoglycan Synthesis. Phospho-*N*-acetylmuramyl-pentapeptide Translocase (Uridine Monophosphate) *Biochemistry* **1966**, *5*, 82-93.

[78] W. G. Struve, F. C. Neuhaus. Evidence for an Initial Acceptor of UDP-*N*Ac-Muramyl-Pentapeptide in the Synthesis of Bacterial Mucopeptide. *Biochem. Biophys. Res. Commun.* **1965**, *18*, 6-12.

[79] J. S. Anderson, M. Matsuhashi, M. A. Haskin, J. L. Strominger. Lipid-Phosphoacetylmuraymyl-Pentapeptide and Lipid-Phosphodisaccharide-Pentapeptide: Presumed Membrane Transport Intermediates in Cell Wall Synthesis. *Biochemistry* **1965**, *53*, 881-889.

[80] M. Ikeda, M. Wachi, H. K. Jung, F. Ishino, M. Matsuhashi. The *Escherichia coli mraY* Gene Encoding UDP-*N*-Acetylmuramoyl-Pentapeptide: Undecaprenyl-Phosphate Phospho-*N*-Acetylmuramoyl-Pentapeptide Transferase. *J. Bacteriol.* **1991**, *173*, 1021-1026.

[81] D. S. Boyle, W. D. Donachie. *mraY* Is an Essential Gene for Cell Growth in *Escherichia coli*. *J. Bacteriol.* **1998**, *180*, 6429-6432.

[82] A. Bouhss, D. Mengin-Lecreulx, D. Le Beller, J. Van Heijenoort. Topological analysis of the MraY protein catalysing the first membrane step of peptidoglycan synthesis. *Mol. Microbiol.* **1999**, *34*, 576-585.

[83] A. Bouhss, M. Crouvoisier, D. Blanot, D. Mengin-Lecreulx. Purification and Characterization of the Bacterial MraY Translocase Catalyzing the First Membrane Step of Peptidoglycan Biosynthesis. *J. Biol. Chem.* **2004**, *279*, 29974-29980.

[84] Y. Ma, D. Münch, T. Schneider, H.-G. Sahl, A. Bouhss, U. Ghoshdastider, J. Wang, V. Dötsch, X. Wang, F. Bernhard. Preparative Scale Cell-free Production and Quality Optimization of MraY Homologues in Different Expression Modes. *J. Biol. Chem.* **2011**, *286*, 38844-38853.

[85] A. J. Lloyd, P. E. Brandish, A. M. Gilbey, T. D. H. Bugg. Phospho-*N*-Acetyl-Muramyl-Pentapeptide Translocase from *Escherichia coli*: Catalytic Role of Conserved Aspartic Acid Residues. *J. Bacteriol.* **2004**, *186*, 1747-1757.

[86] M. G. Heydanek, W. G. Struve, F. C. Neuhaus. On the Initial Stage in Peptidoglycan Synthesis III. Kinetics and Upcoupling of Phospho-*N*-acetylmuramyl-pentapeptide Translocase (Uridine 5'-Phosphate). *Biochemistry* **1969**, *8*, 1214-1221.

[87] T. G. Bernhardt, W. D. Roof, R. Young. Genetic evidence that the bacteriophage ϕX174 lysis protein inhibits cell wall synthesis. *Proc. Natl. Acad. Sci. U.S.A.* **2000**, *97*, 4297-4302.

[88] C. Dini. MraY Inhibitors as Novel Antibacterial Agents. *Curr. Top. Med. Chem.* **2005**, *5*, 1221-1236.

[89] T. D. H. Bugg, M. T. Rodolis, A. Mihalyi, S. Jamshidi. Inhibition of phospho-Mur*N*Ac-pentapeptide translocase (MraY) by nucleoside natural product antibiotics, bacteriophage ϕX174 lysis protein E, and cationic antibacterial peptides. *Bioorg. Med. Chem.* **2016**, *24*, 6340-6347.

[90] L. Thilmont, S. Rosinus, M. Lutz, C. Rohrbacher, C. Ducho. Chapter Two - Nucleoside-derived inhibitors of MraY: Medicinal chemistry with natural products. *Annu. Rep. Med. Chem.* **2023**, *60*, 29-85.

[91] T. D. H. Bugg, R. V. Kerr. Mechanism of action of nucleoside antibacterial natural product antibiotics. *J. Antibiot. (Tokyo)* **2019**, *72*, 865-876.

[92] A. Takatsuki, K. Arima, G. Tamura. Tunicamycin, a New Antibiotic I. Isolation and Characterization of Tunicamycin. *J. Antibiot. (Tokyo)* **1971**, *24*, 215-223.

[93] A. Takatsuki, G. Tamura. Tunicamycin, a New Antibiotic. II. Some biological Prperties of the Antiviral activity of Tunicamycin. *J. Antibiot. (Tokyo)* **1971**, *24*, 224-231.

[94] A. Takatsuki, G. Tamura. Tunicamycin, a New Antibiotic. III: Reversal of the Antiviral Activity of Tunicamycin by Aminosugars and their Derivatives. *J. Antibiot. (Tokyo)* **1971**, *24*, 232-238.

[95] A. Takatsuki, K. Kawamura, M. Okina, Y. Kodama, T. Ito, G. Tamura. The Structure of Tunicamycin. *Agric. Biol. Chem.* **1977**, *41*, 2307-2309.

[96] P. E. Brandish, K.-I. Kimura, M. Inukai, R. Southgate, J. T. Lonsdale, T. D. H. Bugg. Modes of Action of Tunicamycin, Liposidomycin B, and Mureidomycin A: Inhibition of Phospho-*N*-Acetylmuramyl-Pentapeptide Translocase from *Escherichia coli*. *Antimicrob. Agents Chemother.* **1996**, *40*, 1640-1644.

[97] M. Inukai, F. Isono, S. Takahashi, R. Enokita, Y. Sakaida, T. Haneishi. Mureidomycins A-D, Novel Peptidylnucleoside Antibiotics with Spheroplast Forming Activity. I. Taxonomy, Fermentation, Isolation and Physico-chemical Properties. *J. Antibiot. (Tokyo)* **1989**, *42*, 662-666.

[98] F. Isono, M. Inukai, S. Takahashi, T. Haneishi, T. Kinoshita, H. Kuwano. Mureidomycins A-D, Novel Peptidylnucleoside Antibiotics with Spheroplast Forming Activity. II. Structural Elucidation. *J. Antibiot. (Tokyo)* **1989**, *42*, 667-673.

[99] F. Isono, T. Katayama, M. Inukai, T. Haneishi. Mureidomycins A-D, Novel Peptidylnucleoside Antibiotics with Spheroplast Forming Activity. III. Biological Properties. *J. Antibiot. (Tokyo)* **1989**, *42*, 674-679.

[100] F. Isono, M. Inukai. Mureidomycin A, a New Inhibitor of Bacterial Peptidoglycan Synthesis. *Antimicrob. Agents Chemother.* **1991**, *35*, 234-236.

[101] K. Isono, M. Uramoto, H. Kusakabe, K.-I. Kimura, K. Izaki, C. C. Nelson, J. A. McCloskey. Liposidomycins: Novel Nucleoside Antibiotics which inhibit Bacterial Peptidoglycan Synthesis. *J. Antibiot. (Tokyo)* **1985**, *38*, 1617-1621.

[102] M. Ubukata, K. Kimura, K. Isono, C. C. Nelson, J. M. Gregson, J. A. McCloskey. Structure Elucidation of Liposidomycins, a Class of Complex Lipid Nucleoside Antibiotics. *J. Org. Chem.* **1992**, *57*, 6392-6403.

[103] S. Kagami, K. Kimura, Y. Ikeda, H. Takahashi, H. Kusakabe, H. Osada, K. Isono, M. Yoshihama. New Types of Liposidomycins Which Inhibit Bacterial Peptidoglycan Synthesis Produced by Streptomyces. *Actinomycetologica* **1998**, *12*, 110-119.

[104] F. Sarabia, L. Martín-Ortiz, F. J. López-Herrera. A Convergent Synthetic Approach to the Nucleoside-Type Liposidomycin Antibiotics. *Org. Lett.* **2003**, *5*, 3927-3930.

[105] H. Yamaguchi, S. Sato, S. Yoshida, K. Takada, M. Itoh. Capuramycin, a New Nucleoside Antibiotic: Taxonomy, Fermentation, Isolation and Characterization. *J. Antibiot. (Tokyo)* **1986**, *34*, 1047–1053.

[106] V. M. Reddy, L. Einck, C. A. Nacy. In Vitro Antimycobacterial Activities of Capuramycin Analogues. *Antimicrob. Agents Chemother.* **2008**, *52*, 719–721.

[107] M. Igarashi, N. Nakagawa, N. Doi, S. Hattori, H. Naganawa, M. Hamada. Caprazamycin B, a Novel Anti-tuberculosis Antibiotic, from Streptomyces sp. *J. Antibiot. (Tokyo)* **2003**, *56*, 580–583.

[108] M. Igarashi, Y. Takahashi, T. Shitara, H. Nakamura, H. Naganawa, T. Miyake, Y. Akamatsu. Caprazamycins, Novel Lipo-nucleoside Antibiotics, from Streptomyces sp. *J. Antibiot. (Tokyo)* **2005**, *58*, 327-337.

[109] B. Patel, P. Ryan, V. Makwana, M. Zunk, S. Rudrawar, G. Grant. Caprazamycins: Promising lead structures acting on a novel antibacterial target MraY. *Eur. J. Med. Chem.* **2019**, *171*, 462-474.

[110] Y.-I. Lin, Z. Li, G. D. Francisco, L. A. McDonald, R. A. Davis, G. Singh, Y. Yang, T. S. Mansour. Muraymycins, Novel Peptidoglycan Biosynthesis inhibitors: Semisynthesis and SAR of Their Derivatives. *Bioorg. Med. Chem. Lett.* **2002**, *12*, 2341-2344.

[111] L. A. McDonald, L. R. Barbieri, G. T. Carter, E. Lenoy, J. Lotvin, P. J. Petersen, M. M. Siegel, G. Singh, R. T. Williamson. Structures of the Muraymycins, Novel Peptidoglycan Biosynthesis Inhibitors. *J. Am. Chem. Soc.* **2002**, *124*, 10260-10261.

[112] K. Yamamoto, T. Sato, Y. Hikiji, A. Katsuyama, T. Matsumaru, F. Yakushiji, S.-I. Yokota, S. Ichikawa. Synthesis and biological evaluation of a MraY selective

analogue of tunicamycins. *Nucleosides Nucleotides Nucleic Acids* **2020**, *39*, 349-364.

[113] N. I. Howard, T. D. H. Bugg. Synthesis and activity of 5'-Uridinyl dipeptide analogues mimicking the amino terminal peptide chain of nucleoside antibiotic mureidomycin A. *Bioorg. Med. Chem.* **2003**, *11*, 3083-3099.

[114] E. Bogatcheva, T. Dubuisson, M. Protopopova, L. Einck, C. A. Nacy, V. M. Reddy. Chemical modification of capuramycins to enhance antibacterial activity. *J. Antimicrob. Chemother.* **2011**, *66*, 578-587.

[115] A. L. Biecker, X. Liu, J. S. Thorson, Z. Yang, S. G. Van Lanen. Biosynthetic and Synthetic Strategies for Assembling Capuramycin-Type Antituberculosis Antibiotics. *Molecules* **2019**, *24*, 433.

[116] S. Ichikawa, M. Yamaguchi, L. S. Hsuan, Y. Kato, A. Matsuda. Carbacaprazamycins: Chemically Stable Analogues of the Caprazamycin Nucleoside Antibiotics. *ACS Infect. Dis.* **2015**, *1*, 151-156.

[117] B. C. Chung, E. H. Mashalidis, T. Tanino, M. Kim, A. Matsuda, J. Hong, S. Ichikawa, S.-Y. Lee. Structural insights into inhibition of lipid I production in bacterial cell wall synthesis. *Nature* **2016**, *533*, 557-560.

[118] J. K. Hakulinen, J. Hering, G. Brändén, H. Chen, A. Snijder, M. Ek, P. Johansson. MraY-antibiotic complex reveals details of tunicamycin mode of action. *Nat. Chem. Biol.* **2017**, *13*, 265-267.

[119] E. H. Mashalidis, B. Kaeser, Y. Terasawa, A. Katsuyama, D.-Y. Kwon, K. Lee, J. Hong, S. Ichikawa, S.-Y. Lee. Chemical logic of MraY inhibition by antibacterial nucleoside natural products. *Nat. Commun.* **2019**, *10*, 2917.

[120] Z. Cui, X. Wang, S. Koppermann, J. S. Thorson, C. Ducho, S. G. Van Lanen. Antibacterial Muraymycins from Mutant Strains of Streptomyces sp. NRRL 30471. *J. Nat. Prod.* **2018**, *81*, 942-948.

[121] S. Koppermann, Z. Cui, P. D. Fischer, X. Wang, J. Ludwig, J. S. Thorson, S. G. Van Lanen, C. Ducho. Insights into the Target Interaction of Naturally Occurring Muraymycin Nucleoside Antibiotics. *ChemMedChem* **2018**, *13*, 779-784.

[122] O. Ries, C. Carnarius, C. Steinem, C. Ducho. Membrane-interacting properties of the functionalised fatty acid moiety of muraymycin antibiotics. *Med. Chem. Commun.* **2015**, *6*, 879-886.

[123] J. Hering, E. Dunevall, M. Ek, G. Brändén. Structural basis for selective inhibition of antibacterial target MraY, a membrane-bound enzyme involved in peptidoglycan synthesis. *Drug Discov. Today* **2018**, *23*, 1426-1435.

[124] E. H. Mashalidis, S.-Y. Lee. Structures of Bacterial MraY and Human GPT Provide Insights into Rational Antibiotic Design. *J. Mol. Biol.* **2020**, *432*, 4946-4963.

[125] A. Yamashita, E. Norton, P. J. Petersen, B. A. Rasmussen, G. Singh, Y. Yang, T. S. Mansour, D. M. Ho. Muraymycins, novel peptidoglycan biosynthesis inhibitors: synthesis and SAR of their analogues. *Bioorg. Med. Chem. Lett.* **2003**, *13*, 3345-3350.

[126] A. Katsuyama, S. Ichikawa. Synthesis and Medicinal Chemistry of Muraymycins, Nucleoside Antibiotics. *Chem. Pharm. Bull. (Tokyo)* **2018**, *66*, 123-131.

[127] T. Tanino, S. Ichikawa, M. Shiro, A. Matsuda. Total Synthesis of (−)-Muraymycin D2 and Its Epimer. *J. Org. Chem.* **2010**, *75*, 1366-1377.

[128] S. Hirano, S. Ichikawa, A. Matsuda. Total Synthesis of Caprazol, a Core Structure of the Caprazamycin Antituberculosis Antibiotics. *Angew. Chem. Int. Ed.* **2005**, *44*, 1854-1856.

[129] S. Hirano, S. Ichikawa, A. Matsuda. Development of a Highly β-Selective Ribosylation Reaction without Using Neighboring Group Participation: Total Synthesis of (+)-Caprazol, a Core Structure of Caprazamycins. *J. Org. Chem.* **2007**, *72*, 9936-9946.

[130] S. Hirano, S. Ichikawa, A. Matsuda. Synthesis of Caprazamycin Analogues and Their Structure-Activity Relationship for Antibacterial Activity. *J. Org. Chem.* **2008**, *73*, 569-577.

[131] T. Tanino, S. Ichikawa, B. Al-Dabbagh, A. Bouhss, H. Oyama, A. Matsuda. Synthesis and Biological Evaluation of Muraymycin Analogues Active against Anti-Drug-Resistant Bacteria. *ACS Med. Chem. Lett.* **2010**, *1*, 258-262.

[132] T. Tanino, B. Al-Dabbagh, D. Mengin-Lecreulx, A. Bouhss, H. Oyama, S. Ichikawa, A. Matsuda. Mechanistic Analysis of Muraymycin Analogues: A Guide to the Design of MraY Inhibitors. *J. Med. Chem.* **2011**, *54*, 8421-8439.

[133] Y. Takeoka, T. Tanino, M. Sekiguchi, S. Yonezawa, M. Sakagami, F. Takahashi, H. Togame, Y. Tanaka, H. Takemoto, S. Ichikawa, A. Matsuda. Expansion of Antibacterial Spectrum of Muraymycins toward Pseudomonas aeruginosa. *ACS Med. Chem. Lett.* **2014**, *5*, 556-560.

[134] K. Mitachi, B. A. Aleiwi, C. M. Schneider, S. Siricilla, M. Kurosu. Stereocontrolled Total Synthesis of Muraymycin D1 Having a Dual Mode of Action against Mycobacterium tuberculosis. *J. Am. Chem. Soc.* **2016**, *138*, 12975-12980.

[135] A. P. Spork, M. Büschleb, O. Ries, D. Wiegmann, S. Boettcher, A. Mihalyi, T. D. H. Bugg, C. Ducho. Lead Structures for New Antibacterials: Stereocontrolled Synthesis of a Bioactive Muraymycin Analogue. *Chem. - Eur. J.* **2014**, *20*, 15292-15297.

[136] A. P. Spork, C. Ducho. Novel 5'-deoxy nucleosyl amino acid scaffolds for the synthesis of muraymycin analogues. *Org. Biomol. Chem.* **2010**, *8*, 2323-2326.

[137] A. P. Spork, D. Wiegmann, M. Granitzka, D. Stalke, C. Ducho. Stereoselective Synthesis of Uridine-Derived Nucleosyl Amino Acids. *J. Org. Chem.* **2011**, *76*, 10083-10098.

[138] M. Büschleb, Synthese von Capreomycidin- und Epicapreomycidin-haltigen Naturstoff-Bausteinen, Dissertation, Georg-August-University Göttingen, Göttingen, **2012**.

[139] O. Ries, Synthese und Eigenschaften der Lipid-Einheit von Muraymycin-Antibiotika, Georg-August-University Göttingen, **2012**.

[140] A. P. Spork, Synthetische Untersuchungen zur Nucleosid-Einheit von Muraymycin-Antibiotika, Dissertation, Georg-August-University Göttingen, Göttingen, **2012**.

[141] X.-F. Zhu, H. J. Williams, A. I. Scott. Facile and highly selective 5'-desilylation of multisilylated nucleosides. *Perkin Trans.* **2000**, 2305-2306.

[142] O. Ries, M. Büschleb, M. Granitzka, D. Stalke, C. Ducho. Amino acid motifs in natural products: synthesis of *O*-acylated derivatives of (2*S*,3*S*)-3-hydroxyleucine. *Beilstein J. Org. Chem.* **2014**, *10*, 1135-1142.

[143] T. Laïb, J. Chastanet, J. Zhu. Diastereoselective Synthesis of γ-Hydroxy-β-amino Alcohols and (2*S*,3*S*)-β-Hydroxyleucine from Chiral D-(*N*,*N*-Dibenzylamino) serine (TBDMS) Aldehyde. *J. Org. Chem.* **1998**, *63*, 1709-1713.

[144] A. P. Spork, S. Koppermann, S. Schier (Née Wohnig), R. Linder, C. Ducho. Analogues of Muraymycin Nucleoside Antibiotics with Epimeric Uridine-Derived Core Structures. *Molecules* **2018**, *23*, 2868.

[145] M. Wirth, Untersuchungen zur Membreanpermeabilität von *O*-acylierten Muraymycinen, Dissertation, Universität des Saarlandes, Saarbrücken, **2019**.

[146] K. Leyerer, Muraymycin Nucleoside Antibiotics: Novel SAR Insights and Synthetic Approaches, Universität des Saarlandes, Saarbrücken **2018**.

[147] K. Leyerer, S. Koppermann, C. Ducho. Solid Phase-Supported Synthesis of Muraymycin Analogues. *Eur. J. Org. Chem.* **2019**, *2019*, 7420–7431.

[148] D. Wiegmann, Neue Strategien zur Entwicklung von Derivaten der Muraymycin-Antibiotika mit verbesserter biologischer Aktivität, Dissertation, Universität des Saarlandes, Saarbrücken, **2016**.

[149] C. Rohrbacher, Synthese neuartiger Muraymycin-Konjugate zur Verbesserung der bakteriellen Zellaufnahme, Dissertation, Universität des Saarlandes, Saarbrücken, **2023**.

[150] C. Rohrbacher, R. Zscherp, S. C. Weck, P. Klahn, C. Ducho. Synthesis of an Antimicrobial Enterobactin-Muraymycin Conjugate for Improved Activity Against Gram-Negative Bacteria. *Chem. – Eur. J.* **2023**, *29*, e202202408.

[151] A. Heib, G. Niro, S. C. Weck, S. Koppermann, C. Ducho. Muraymycin Nucleoside Antibiotics: Structure-Activity Relationship for Variations in the Nucleoside Unit. *Molecules* **2019**, *25*, 22.

[152] D. Wiegmann, S. Koppermann, C. Ducho. Aminoribosylated Analogues of Muraymycin Nucleoside Antibiotics. *Molecules* **2018**, *23*, 3085; doi: 10.3390/ molecules23123085

[153] S. Rosinus, Synthese von Muraymycin-Analoga mit Variationen in der Peptidkette, Masterarbeit, Universität des Saarlandes, Saarbrücken **2020**.

[154] C. M. Schütz, Inhibitoren der bakteriellen Translocase und Collagenase als potentielle Antibiotika, Masterarbeit, Universität des Saarlandes, Saarbrücken **2016**.

[155] A. P. Spork, S. Koppermann, B. Dittrich, R. Herbst-Irmer, C. Ducho. Efficient synthesis of the core structure of muraymycin and caprazamycin nucleoside antibiotics based on a stereochemically revised sulfur ylide reaction. *Tetrahedron Asymmetry* **2010**, *21*, 763-766.

[156] M. B. Richardson, S. J. Williams. A practical synthesis of long-chain iso-fatty acids (iso-C_{12}–C_{19}) and related natural products. *Beilstein J. Org. Chem.* **2013**, *9*, 1807-1812.

[157] A. A. Wube, A. Hüfner, C. Thomaschitz, M. Blunder, M. Kollroser, R. Bauer, F. Bucar. Design, synthesis and antimycobacterial activities of 1-methyl-2-alkenyl-4(1*H*)-quinolones. *Bioorg. Med. Chem.* **2011**, *19*, 567-579.

[158] A. Previero, L.-G. Barry, M.-A. Coletti-Previero. *O*-Acylation of Hydroxylamino Acids in Presence of Free Amino Groups. *Biochim. Biophys. Acta BBA - Protein Struct.* **1972**, *263*, 7-13.

[159] *Deprotection Guide*, Glen Research, **2020**.

[160] L. Kürti, B. Czakó, *Strategic Applications of Named Reactions in Organic Synthesis*, Elsevier, Academic Press, Amsterdam; Boston; Heidelberg, **2005**.

[161] L. Horner, H. Hoffmann, H. G. Wippel. Phosphororganische Verbindungen, XII. Phosphinoxyde als Olefinierungsreagenzien. *Chem. Ber.* **1958**, *91*, 61-63.

[162] W. S. Wadsworth, W. D. Emmons. The Utility of Phosphonate Carbanions in Olefin Synthesis. *J. Am. Chem. Soc.* **1961**, *83*, 1733-1738.

[163] U. Zoller, D. Ben-Ishai. Amidoalkylation of mercaptans with glyoxylic acid derivatives. *Tetrahedron* **1975**, *31*, 863-866.

[164] R. G. Vaswani, A. R. Chamberlin. Stereocontrolled Total Synthesis of (-)-Kaitocephalin. *J. Org. Chem.* **2008**, *73*, 1661-1681.

[165] J. D. More, N. S. Finney. A Simple and Advantageous Protocol for the Oxidation of Alcohols with *o*-Iodoxybenzoic Acid (IBX). *Org. Lett.* **2002**, *4*, 3001-3003.

[166] R. Mazurkiewicz, A. Kuźnik, M. Grymel, N. Kuźnik. ^{1}H NMR spectroscopic criteria for the configuration of *N*-acyl-α,β-dehydro-α-amino acid esters. *Magn. Reson. Chem.* **2005**, *43*, 36-40.

[167] M. J. Burk. C_2-Symmetric Bis(phospholanes) and Their Use in Highly Enantioselective Hydrogenation Reactions. *J. Am. Chem. Soc.* **1991**, *113*, 8518-8519.

[168] T. Masquelin, E. Broger, K. Müller, R. Schmid, D. Obrecht. Synthesis of Enantiomerically Pure D- and L-(Heteroaryl)alanines by asymmetric hydrogenation of (*Z*)-α-amino-α,β-didehydro esters. *Helv. Chim. Acta* **1994**, *77*, 1395-1411.

[169] J. Halpern. Mechanism and Stereoselectivity of Asymmetric Hydrogenation. *Science* **1982**, *217*, 401-407.

[170] R. Y. Nimje, D. Vytla, P. Kuppusamy, R. Velayuthaperumal, L. B. Jarugu, C. A. Reddy, N. K. Chikkananjaiah, R. A. Rampulla, C. L. Cavallaro, J. Li, A. Mathur, A. Gupta, A. Roy. Synthesis of Differentially Protected Azatryptophan Analogs via $Pd_2(dba)_3$/XPhos Catalyzed Negishi Coupling of *N*-Ts Azaindole Halides with Zinc Derivative from Fmoc-Protected *tert*-Butyl (*R*)-2-Amino-3-iodopropanoate. *J. Org. Chem.* **2020**, *85*, 11519-11530.

[171] J. R. Dunetz, J. Magano, G. A. Weisenburger. Large-Scale Applications of Amide Coupling Reagents for the Synthesis of Pharmaceuticals. *Org. Process Res. Dev.* **2016**, *20*, 140-177.

[172] P. E. Brandish, M. K. Burnham, J. T. Lonsdale, R. Southgate, M. Inukai, T. D. H. Bugg. Slow Binding Inhibition of Phospho-*N*-acetylmuramyl-pentapeptide-translocase (*Escherichia coli*) by Mureidomycin A. *J. Biol. Chem.* **1996**, *271*, 7609-7614.

[173] T. Stachyra, C. Dini, P. Ferrari, A. Bouhss, J. Van Heijenoort, D. Mengin-Lecreulx, D. Blanot, J. Biton, D. Le Beller. Fluorescence Detection-Based Functional Assay for High-Throughput Screening for MraY. *Antimicrob. Agents Chemother.* **2004**, *48*, 897-902.

[174] S. Wohnig, A. P. Spork, S. Koppermann, G. Mieskes, N. Gisch, R. Jahn, C. Ducho. Total Synthesis of Dansylated Park's Nucleotide for High-Throughput MraY Assays. *Chem. - Eur. J.* **2016**, *22*, 17813-17819.

[175] S. Shabani, C. A. Hutton. Total Synthesis of Seongsanamide B. *Org. Lett.* **2020**, *22*, 4557-4561.

[176] A. P. Krapcho, J. R. Larson, J. M. Eldridge. Potassium permanganate oxidations of terminal olefins and acetylenes to carboxylic acids of one less carbon. *J. Org. Chem.* **1977**, *42*, 3749-3753.

[177] A. J. Fatiadi. The Classical Permanganate Ion: Still a Novel Oxidant in Organic Chemistry. *Synthesis* **1987**, *2*, 85-127.

[178] J. Weihrather, Totalsynthese von Anti-HV-aktiven Mniopetalen und strukturellen Analoga, Dissertation, Universität des Saarlandes, Saarbrücken **2013**.

[179] J. Weihrather, J. Jauch. Total Synthesis of Mniopetals A, B, C and D. *Synlett* **2013**, *24*, 1410-1414.

[180] M. M. Zhao, J. Li, E. Mano, Z. J. Song, D. M. Tschaen, E. J. J. Grabowski, P. J. Reider. Oxidation of Primary Alcohols to Carboxylic Acids with Sodium Chlorite Catalyzed by TEMPO and Bleach. *J. Org. Chem.* **1999**, *64*, 2564-2566.

[181] M. M. Zhao, J. Li, E. Mano, Z. J. Song, D. M. Tschaen, A. Ghosh, J. Sieser, W. Cai, S. E. Kelly. Oxidation of Primary Alcohols to Carboxylic Acids with Sodium Chlorite Catalyzed by TEMPO and Bleach: 4-Methoxyphenylacetic Acid. *Org. Synth.* **2005**, *81*, 195-203.

[182] A. R. Fersht, W. P. Jencks. Acetylpyridinium ion intermediate in pyridine-catalyzed hydrolysis and acyl transfer reactions of acetic anhydride. Observation, kinetics, structure-reactivity correlations, and effects of concentrated salt solutions. *J. Am. Chem. Soc.* **1970**, *92*, 5432-5442.

[183] P. A. Byrne, D. G. Gilheany. The modern interpretation of the Wittig reaction mechanism. *Chem. Soc. Rev.* **2013**, *42*, 6670-6696.

[184] R. Robiette, J. Richardson, V. K. Aggarwal, J. N. Harvey. Reactivity and Selectivity in the Wittig Reaction: A Computational Study. *J. Am. Chem. Soc.* **2006**, *128*, 2394-2409.

[185] M. Karplus. Contact Electron-Spin Coupling of Nuclear Magnetic Moments. *J. Chem. Phys.* **1959**, *30*, 11-15.

[186] M. Karplus. Vicinal Proton Coupling in Nuclear Magnetic Resonance. *J. Am. Chem. Soc.* **1963**, *85*, 2870-2871.

[187] S. Bienz, L. Bigler, T. Fox, H. Meier, *Spektroskopische Methoden in der organischen Chemie - Hesse-Meier-Zeeh*, 9te überarbeitete Auflage, Georg Thieme Verlag KG, Stuttgart, **2016**.

[188] G. Niro, Studies on the Selectivity of Nucleoside Antibiotics, Dissertation, Universität des Saarlandes, Saarbrücken, **2019**.

[189] M. Frigerio, M. Santagostino, S. Sputore. A User-Friendly Entry to 2-Iodoxybenzoic Acid (IBX). *J. Org. Chem.* **1999**, *64*, 4537-4538.

[190] V. Böttner, Untersuchungen zu Synthese und Eigenschaften von Oligonucleotid-Prodrugs, Dissertation, Universität des Saarlandes, Saarbrücken, **2019**.

9 Appendix

Stabilities of different target compounds in different media

Used compounds:

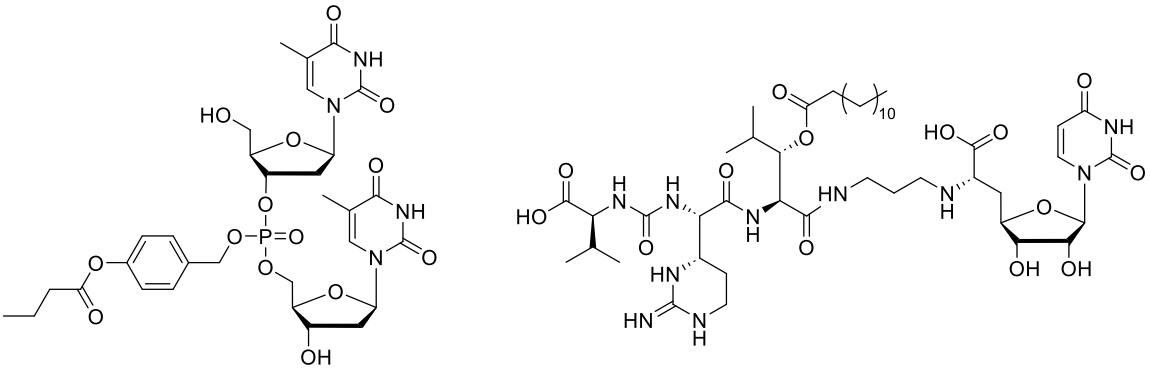

95

half live in BakLys(*E. coli* Δ*tolC*): $t_{1/2} \approx 9$ min

32

Fig. 103: Tested compounds: compound **32**, synthesized by M. Wirth and reference compound **95**, with known half-life, synthesized by V. Böttner.[145,190]

Target compound **T1**

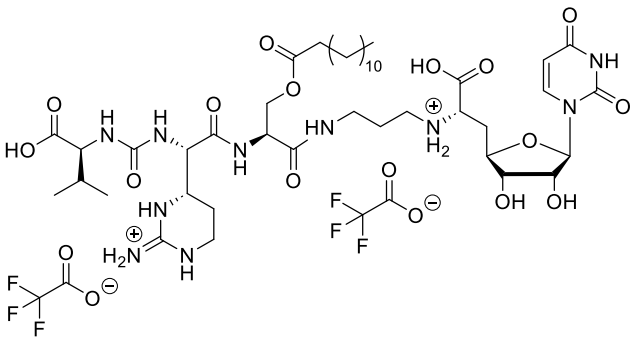

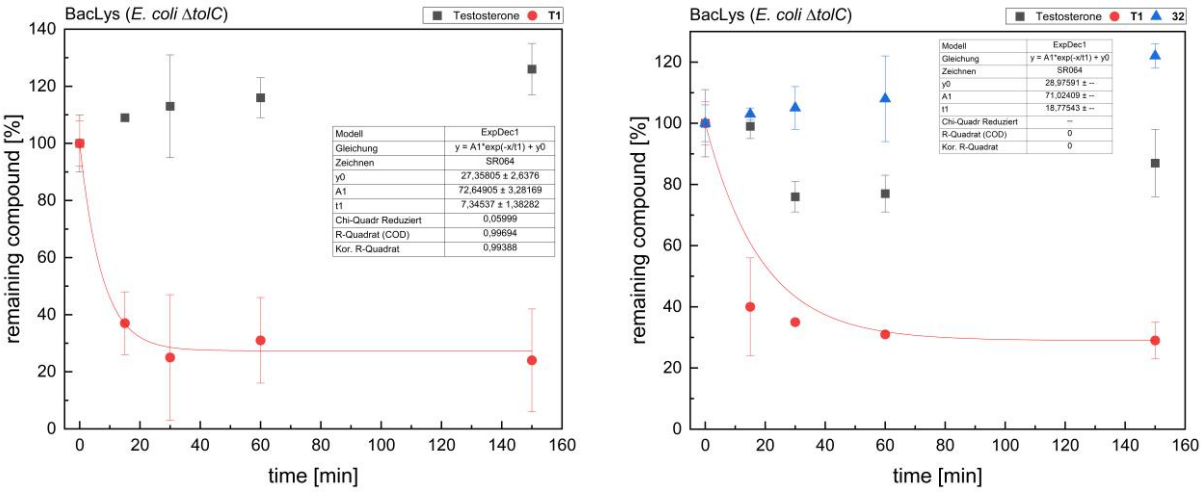

Fig. 104: Evaluation of the stability of **T1** (reference: testosterone and **32**) in *E. coli* Δ*tolC* lysate with visible plateau formation after ~25% (left) or ~33% (right) of the initial concentration.

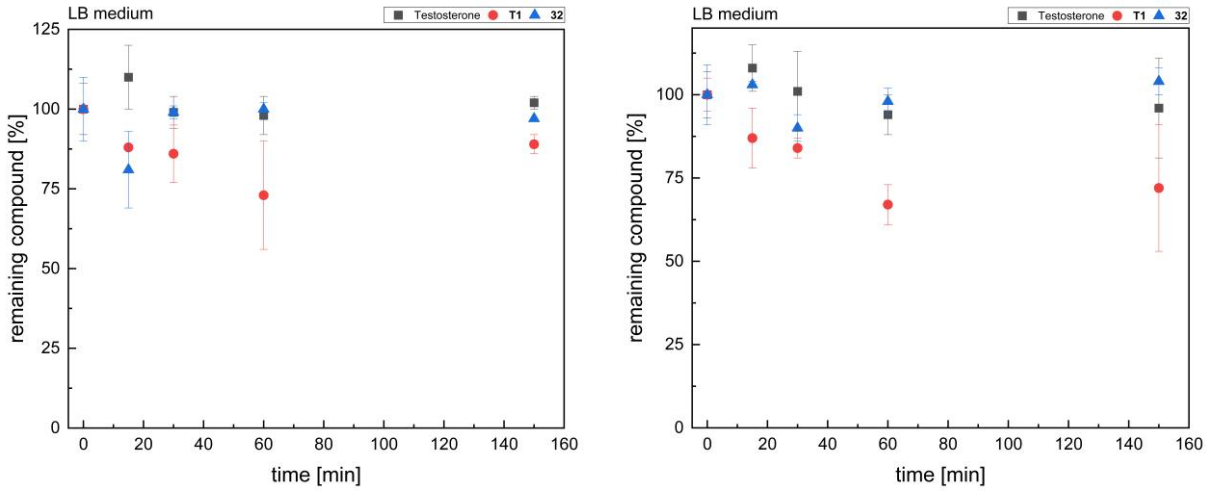

Fig. 105: Evaluation of the stability of **T1** (reference: testosterone and **32**) in LB medium.

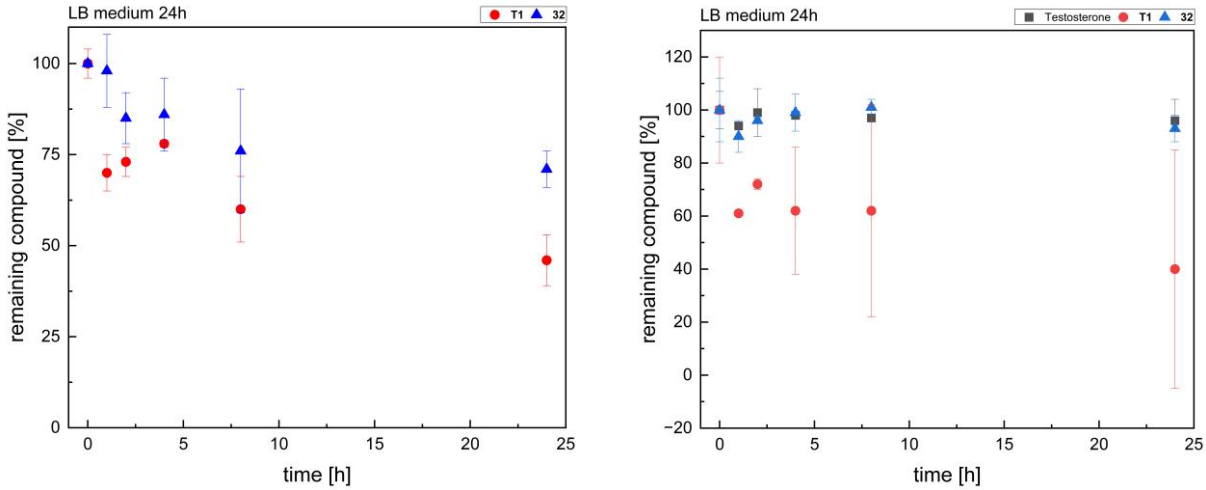

Fig. 106: Evaluation of the stability of **T1** (reference: testosterone and/or **32**) in LB medium over 24 h.

Target compound **T2**

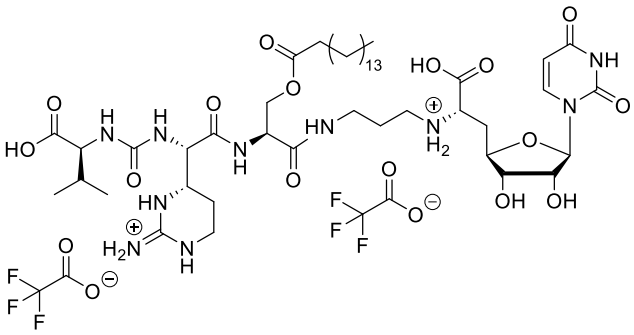

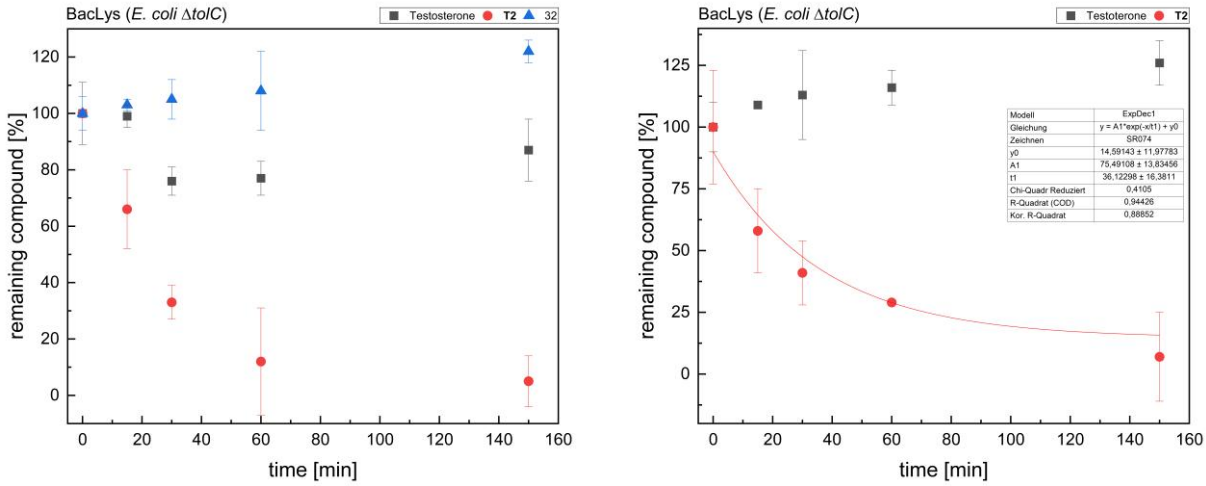

Fig. 107: Evaluation of the stability of **T2** (reference: testosterone and **32**) in *E. coli* Δ*tolC* lysate.

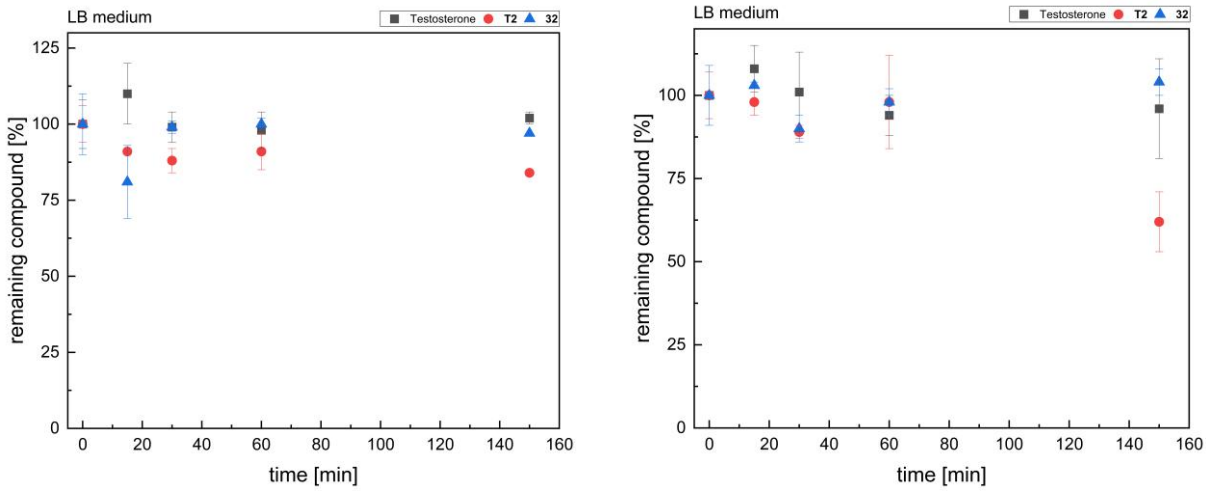

Fig. 108: Evaluation of the stability of **T2** (reference: testosterone and **32**) in LB medium.

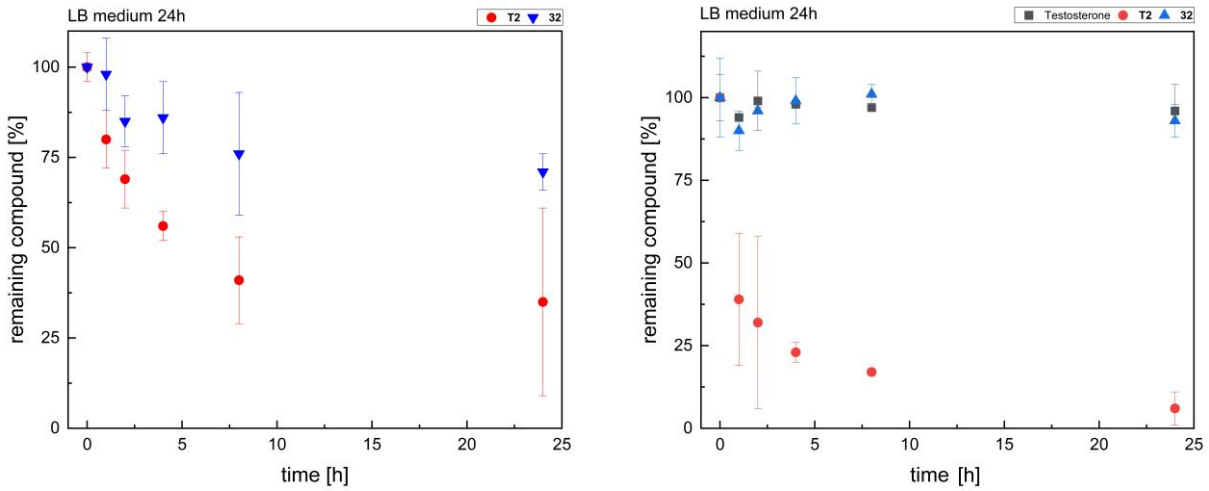

Fig. 109: Evaluation of the stability of **T2** (reference: testosterone and **32**) in LB medium over 24 h.

Target compound **T3**

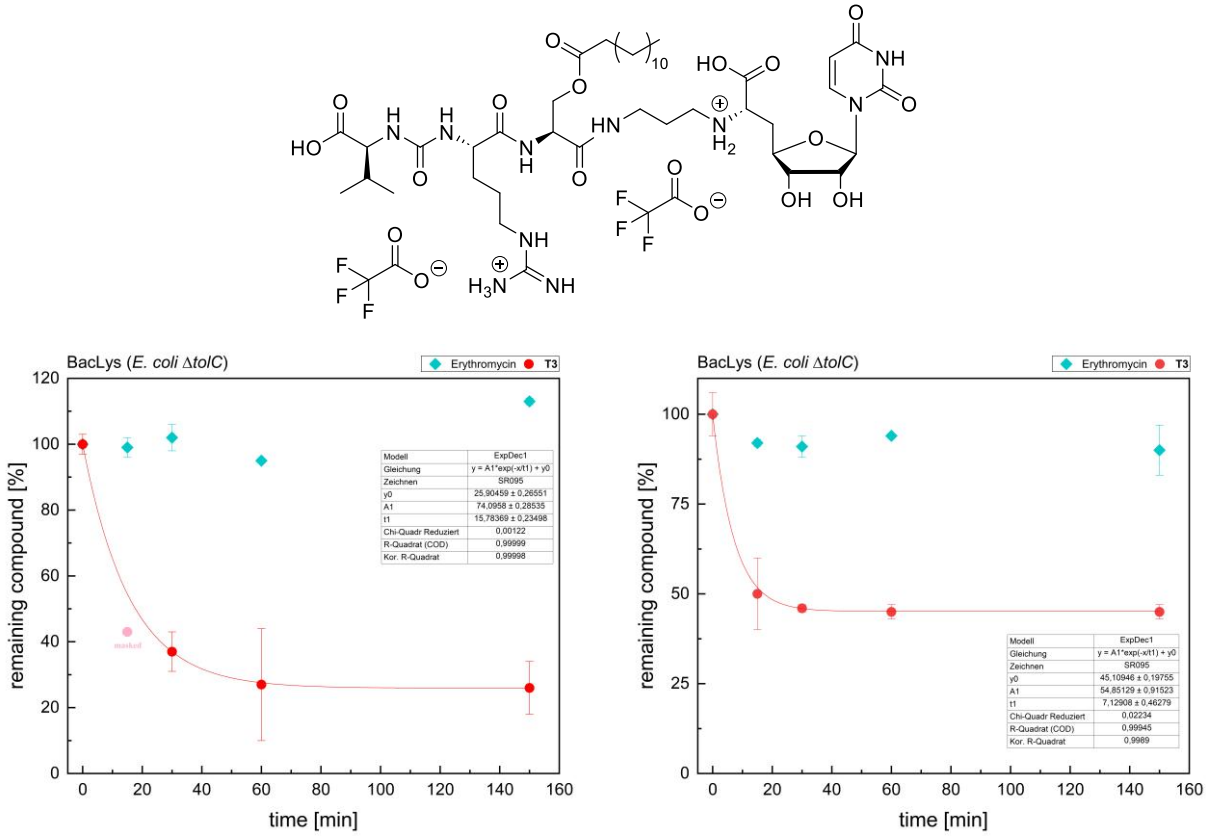

Fig. 110: Evaluation of the stability of **T3** (reference: erythromycin) in *E. coli* Δ*tolC* lysate with visible plateau formation after ~30% (left) or ~45% (right) of the initial concentration (note: masked value at 15 min (left)).

Target compound **T4**

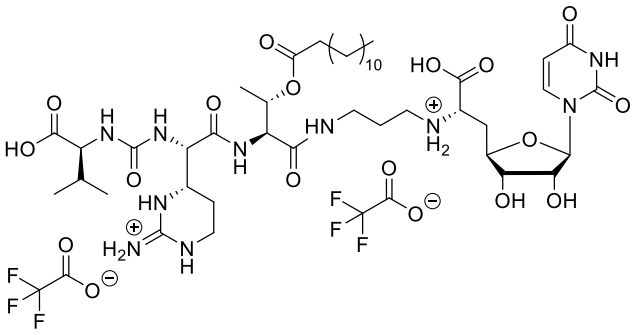

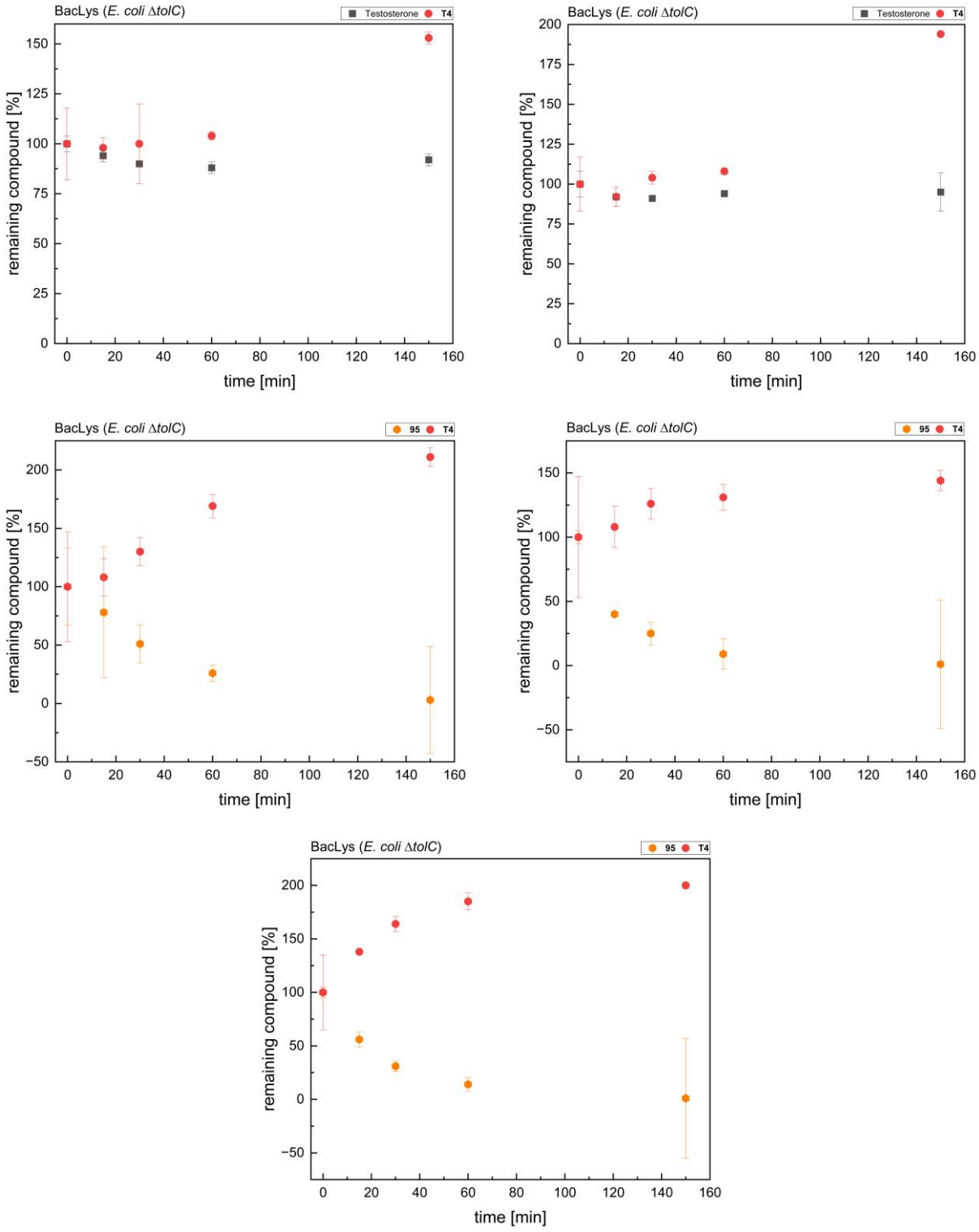

Fig. 111: Different attempts to define the stability of **T4** in *E. coli* Δ*tolC* lysate (reference: testosterone and **95**[190]).

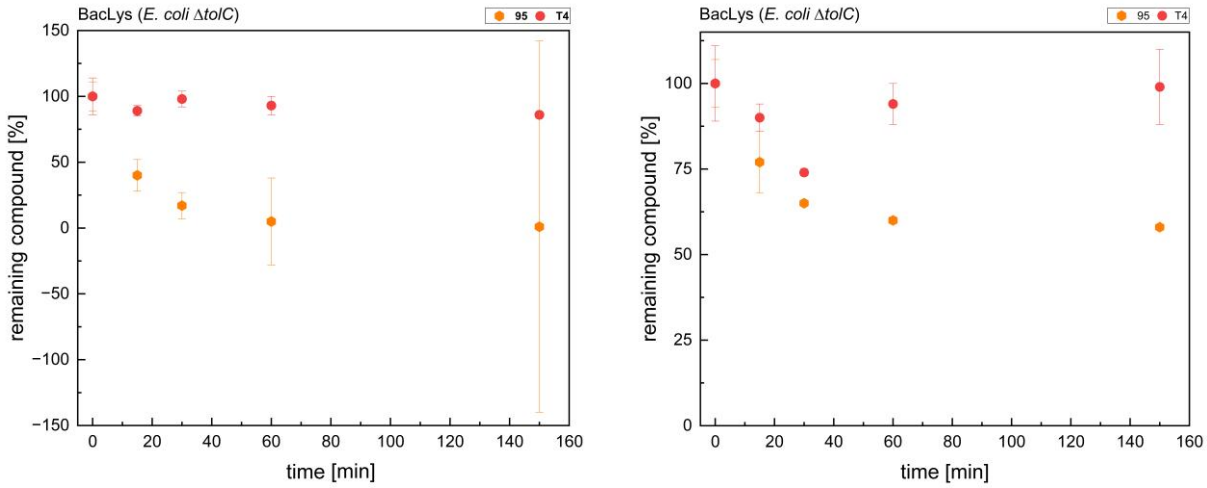

Fig. 112: Two attempts to define the stability of **T4** in *E. coli* Δ*tolC* lysate without internal standard (reference: **95**[190]).

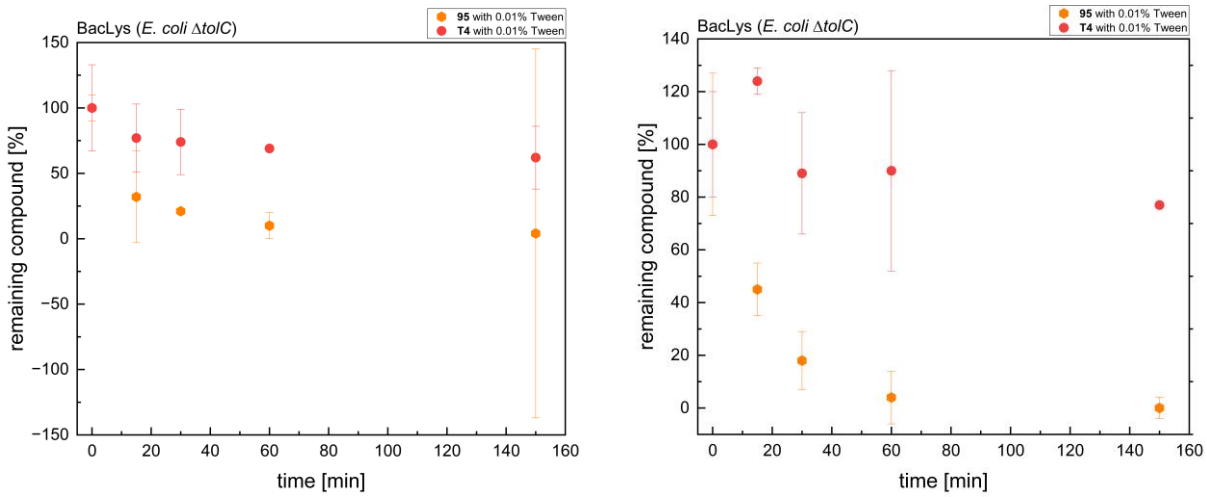

Fig. 113: Two attempts to define the stability of **T4** in *E. coli* Δ*tolC* lysate without internal standard and with Tween (reference: **95**[190]).

Target compound **T5**

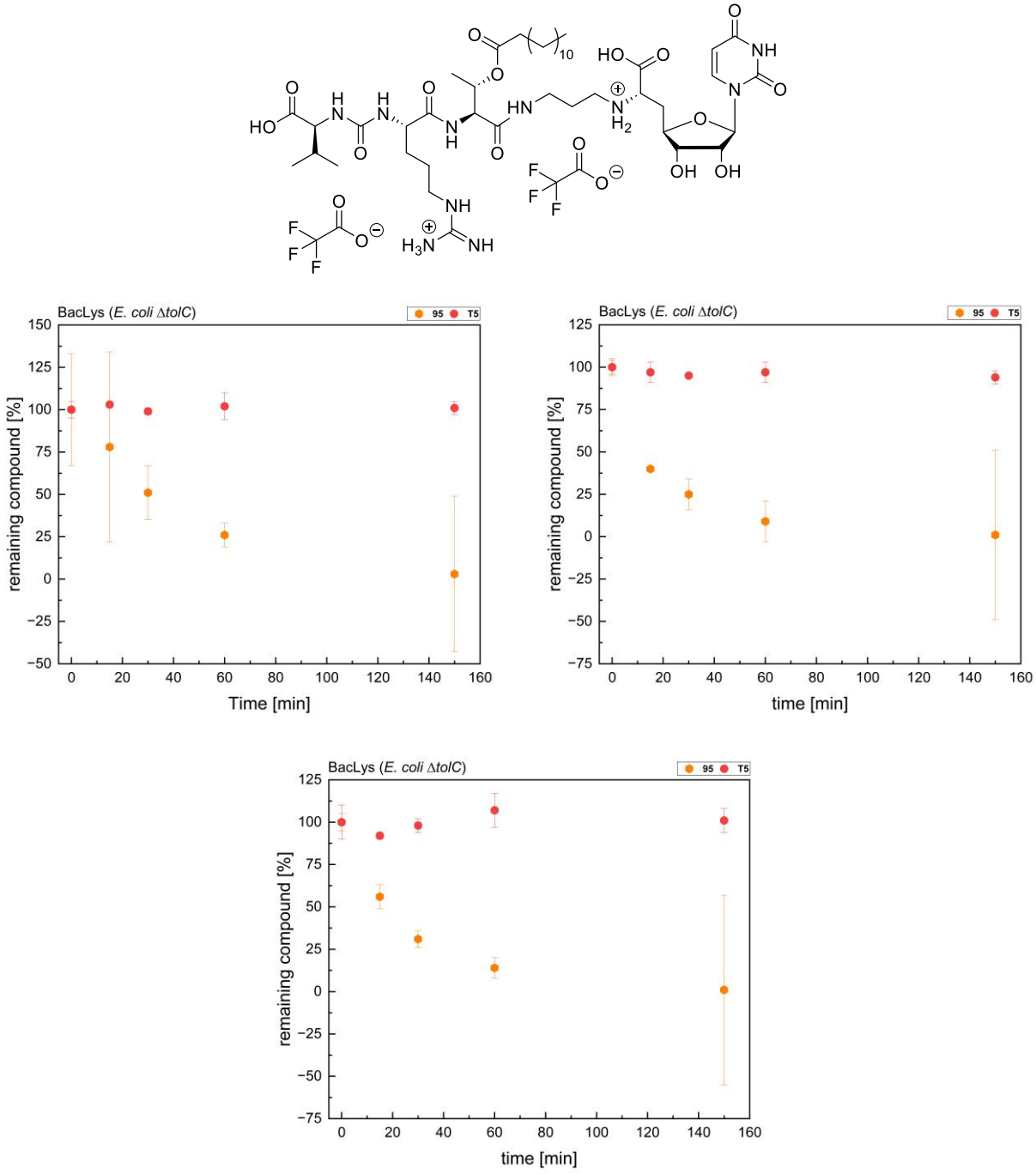

Fig. 114: Evaluation of the stability of **T5** in *E. coli* Δ*tolC* lysate (reference: **95**[190] as compound with known half-life of ~35min).

Bacterial growth inhibition of the truncated derivatives

Truncated target compound **TT1**

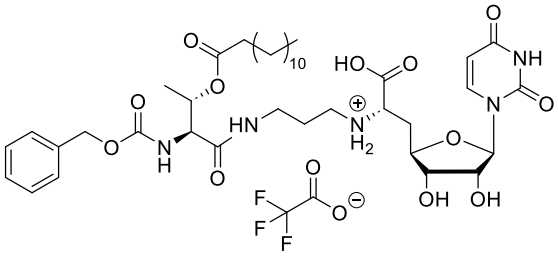

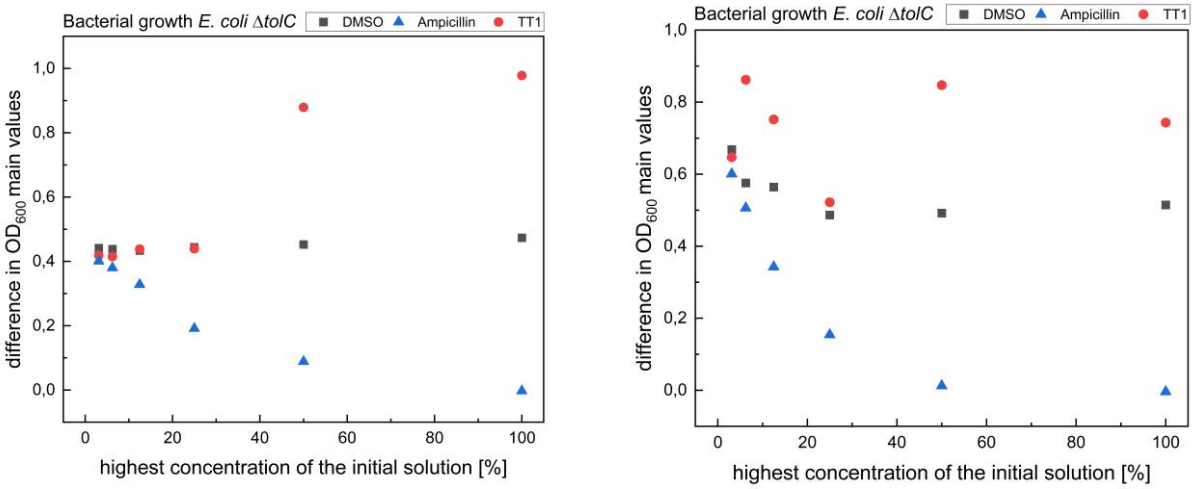

Fig. 115: Activity against the bacterial growth of *E. coli* Δ*tolC* of **T1** (reference DMSO (blank) and ampicillin (highest conc. 5 µg/mL)).

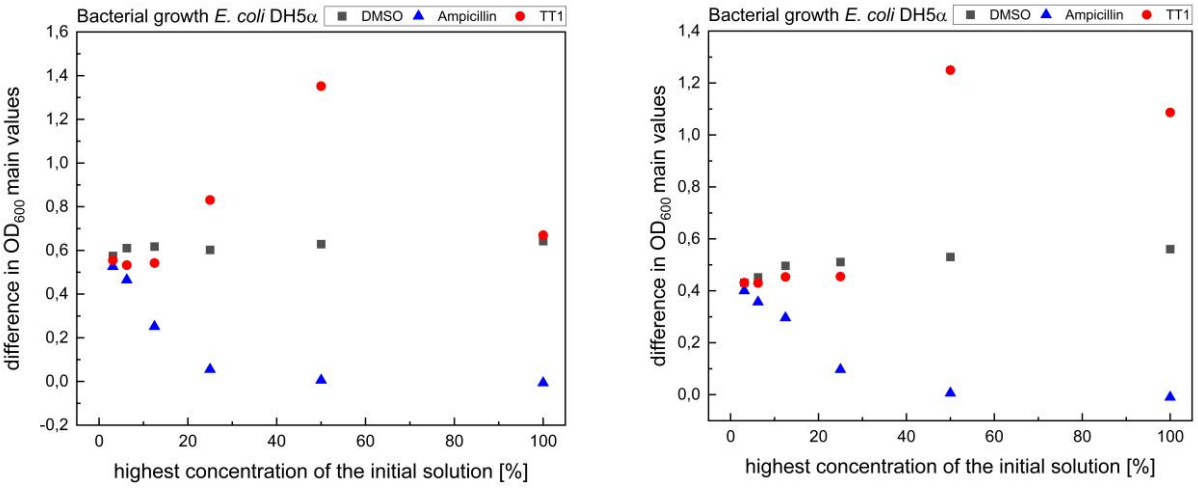

Fig. 116: Activity against the bacterial growth of *E. coli* DH5α of **T1** (reference DMSO (blank) and ampicillin).

Truncated target compound **TT2**

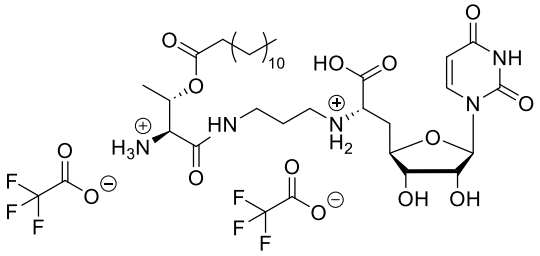

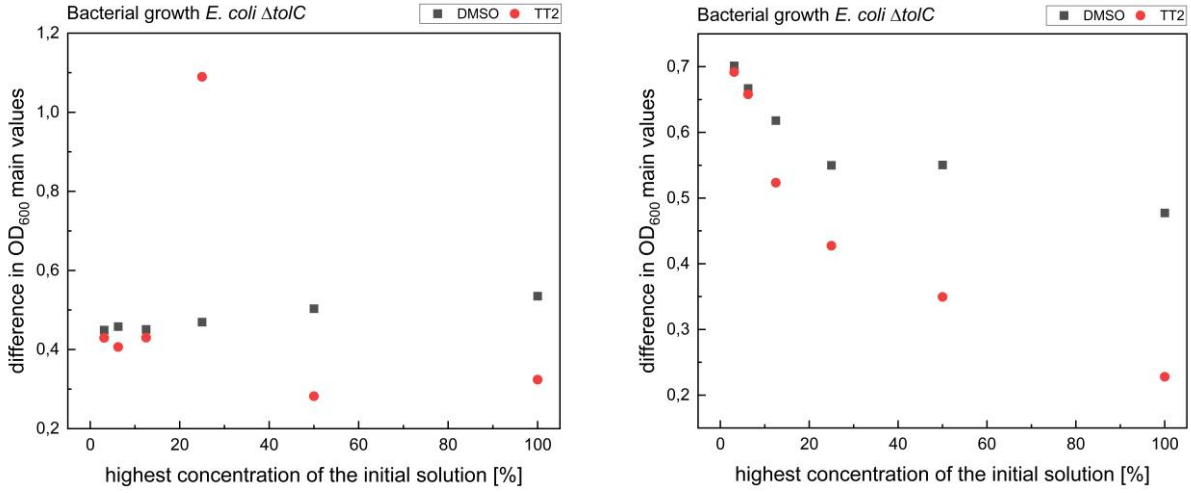

Fig. 117: Activity against the bacterial growth of *E. coli* Δ*tolC* of **T2** (reference DMSO (blank) and ampicillin (highest conc. 5 µg/mL)).

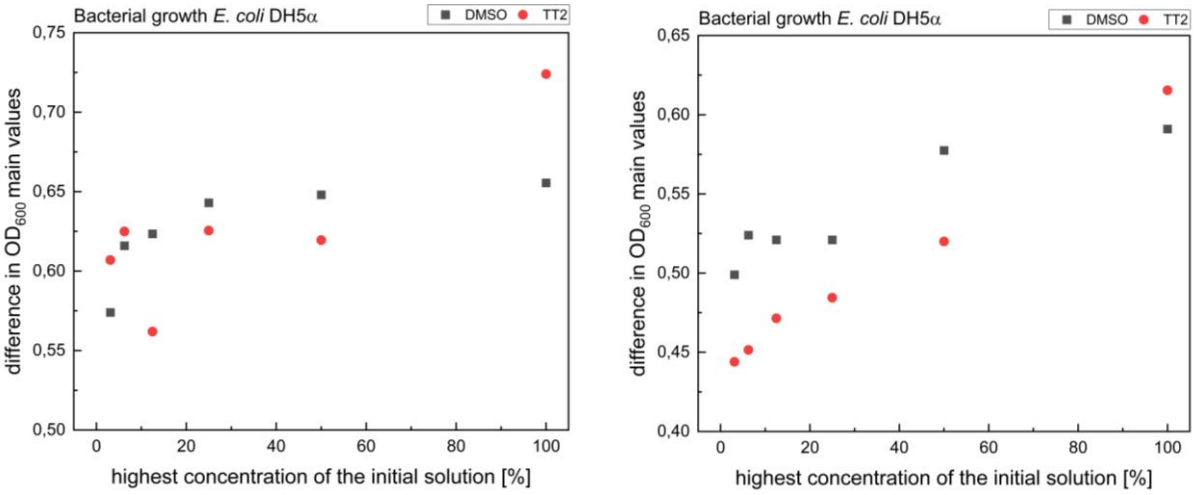

Fig. 118: Activity against the bacterial growth of *E. coli* DH5α of **T2** (reference DMSO (blank)).

Truncated target compound **TT3**

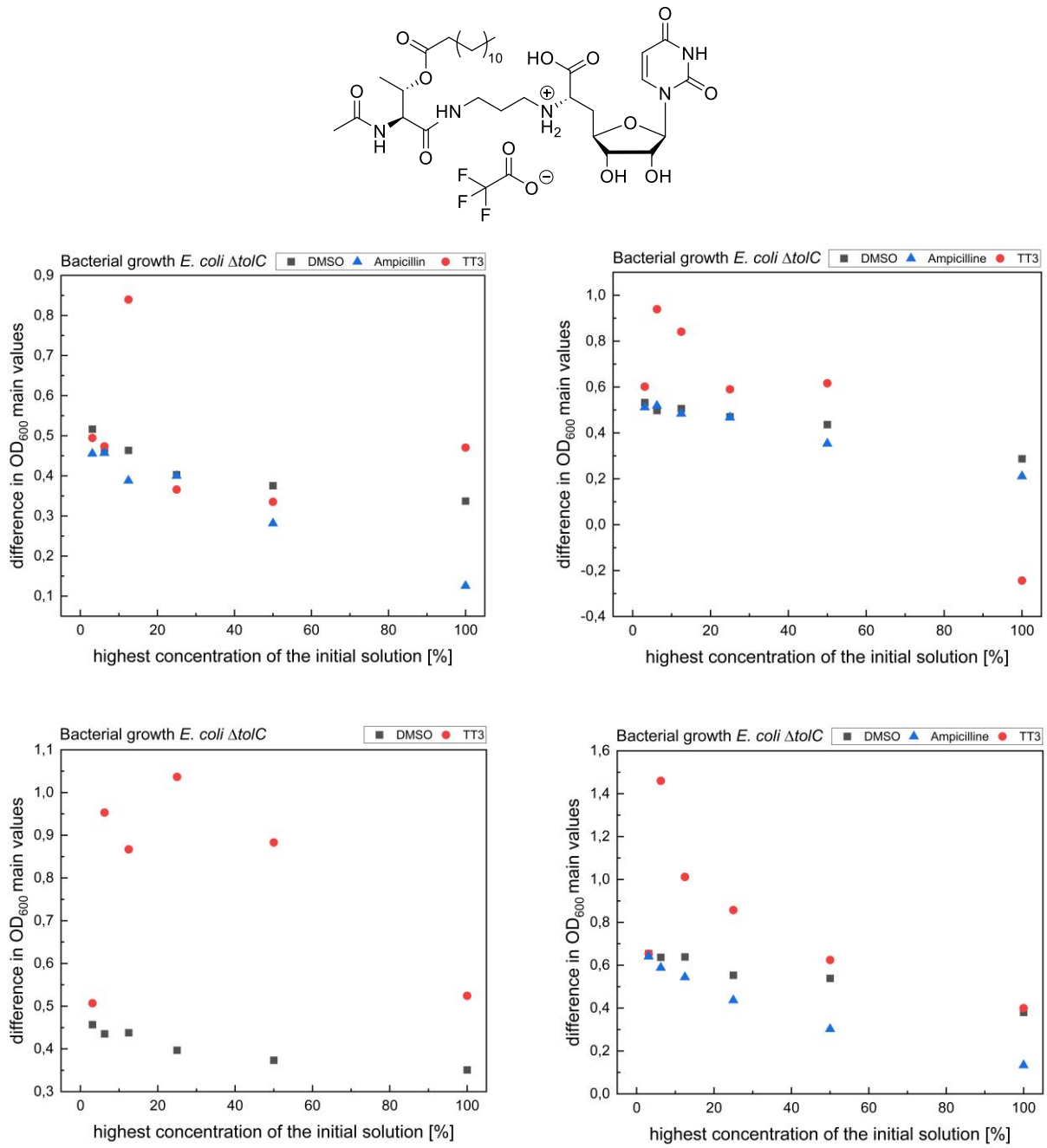

Fig. 119: Activity against the bacterial growth of *E. coli* Δ*tolC* of **T3** (reference DMSO (blank) and ampicillin (highest conc. 5 µg/mL)).

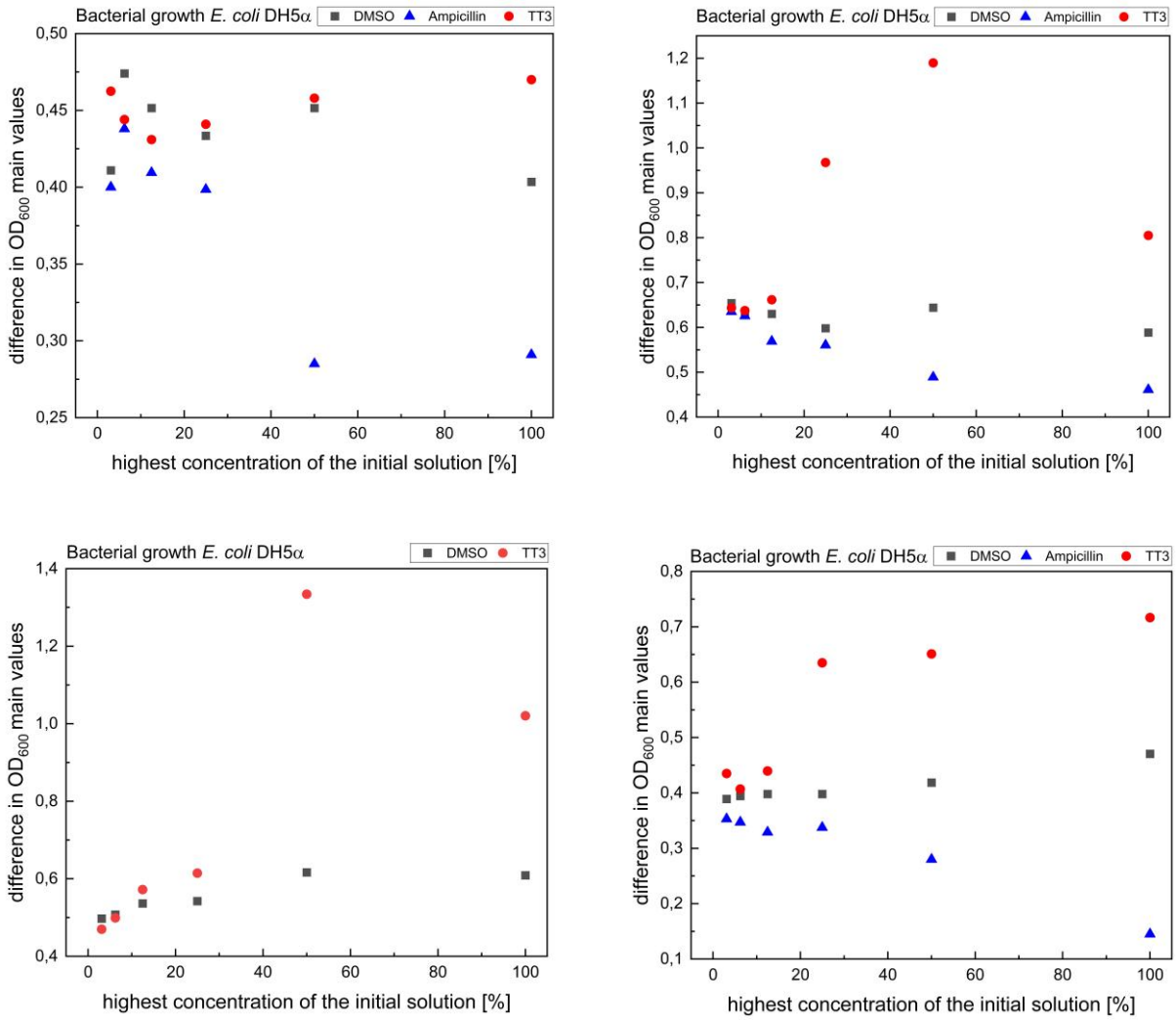

Fig. 120: Activity against the bacterial growth of *E. coli* DH5α of **T3** (reference DMSO (blank) and ampicillin (highest conc. 5 µg/mL)).

Truncated target compound **TT4**

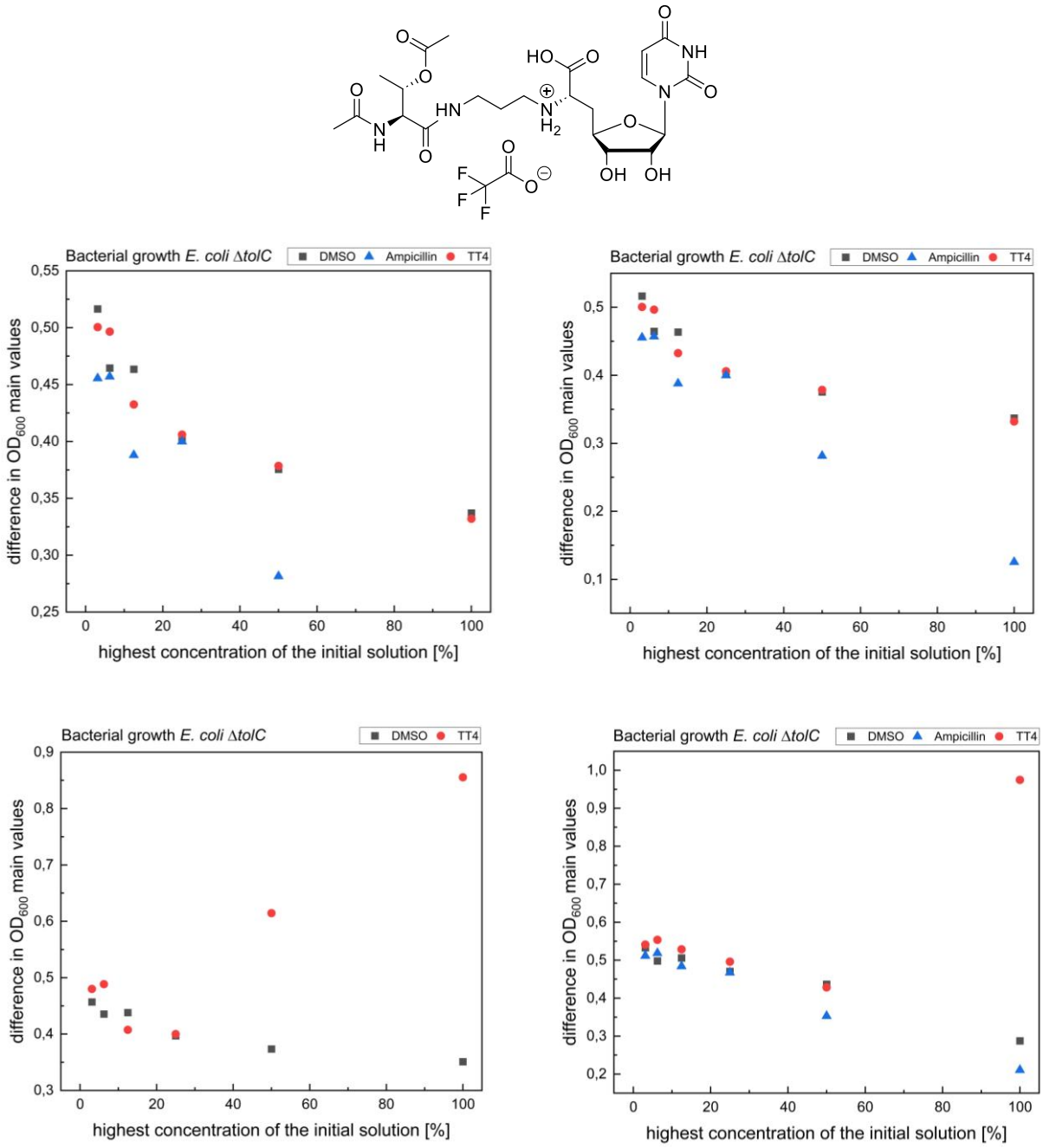

Fig. 121: Activity against the bacterial growth of *E. coli* Δ*tolC* of **T4** (reference DMSO (blank) and ampicillin (highest conc. 5 µg/mL)).

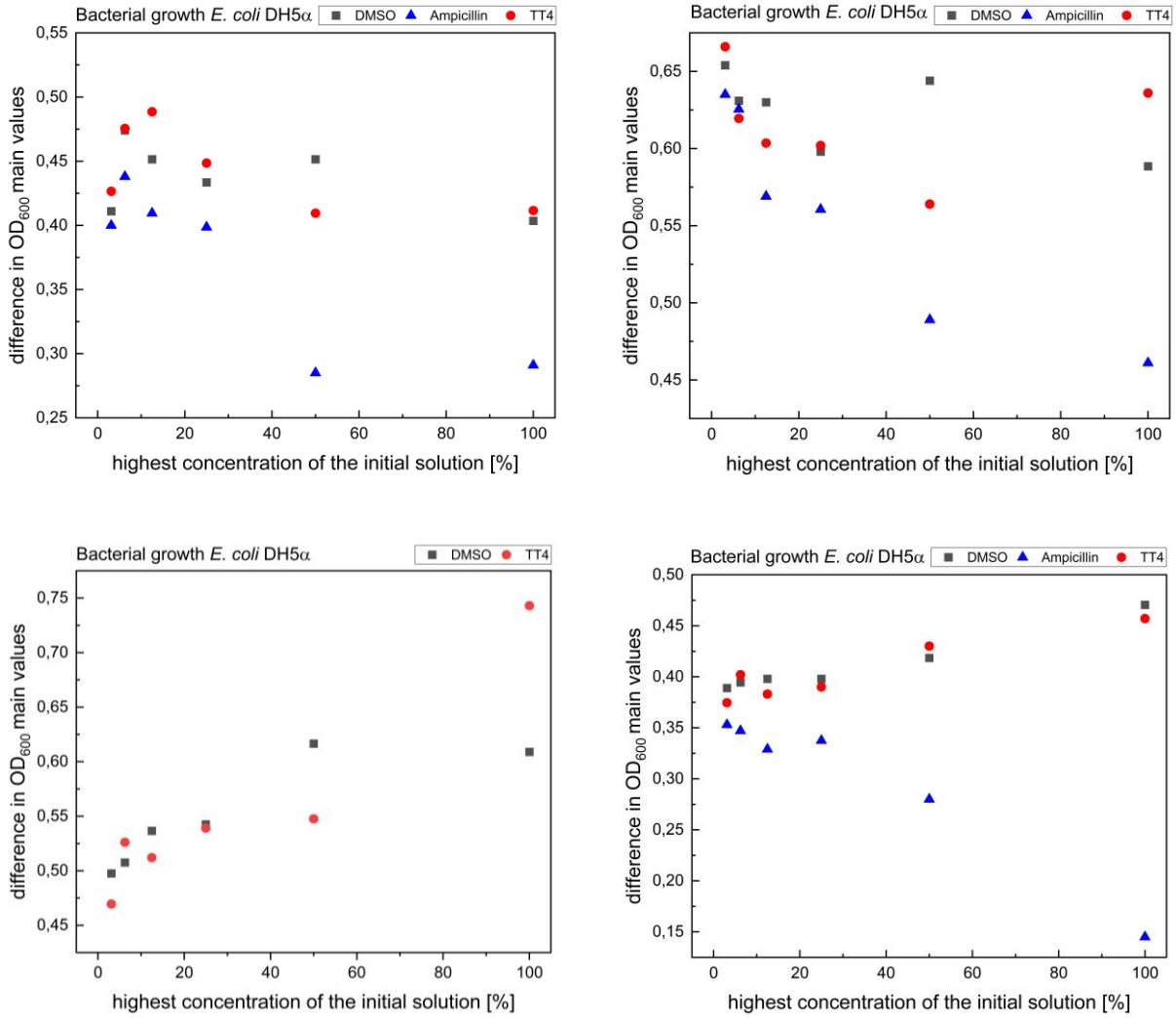

Fig. 122: Activity against the bacterial growth of *E. coli* DH5α of **T4** (reference DMSO (blank) and ampicillin (highest conc. 5 µg/mL)).

Danksagung

Ich möchte mich zuerst bei Herrn Prof. Dr. Cristian Ducho neben dem interessanten Promotionsthema und seiner steten Diskussionsbereitschaft für die Möglichkeit bedanken, meine Forschung auf vielen internationalen Konferenzen vorstellen zu können.

Herrn Prof. Dr. Johann Jauch danke ich für die Übernahme des Zweitgutachtens. Darüber hinaus möchte ich mich auch rückblickend für die Zeit bei Ihnen im Arbeitskreis bedanken, die für meine wissenschaftliche Tätigkeit eine große Bereicherung war.

Herrn Dr. Josef Zapp danke ich für die Übernahme des Gutachtens als akademischer Mitarbeiter. Darüber hinaus möchte ich mich für die stete Hilfe bei der Aufnahme und Diskussion von NMR-Spektren bedanken.

Den Mitarbeitern des Arbeitskreises danke ich für die gemeinsame Zeit. Ich möchte mich vor allem bei Marina Jankowski, Nathalie Kagerah und Marcel Lutz für die Durchführung und Evaluierung der biologischen Daten danken.

Sven Lauterbach, Laura Thilmont, Dr. Stefan Boettcher und Priv.-Doz. Dr. Martin Frotscher danke ich für die gemeinsame Zusammenarbeit im Intstru-Praktikum.

Mein besonderer Dank gilt Anna Heib, Marcel und Priv.-Doz. Dr. Matthias Engel, die mir häufig zur Seite standen – besonders auch während meiner „Endphase“. Vielen Dank für eure Korrekturen – besonders dir, Anna!

Meinen beiden Wahlpflicht-Studenten Ronja Priester und Nico Bachmann danke ich für ihr Engagement und ihren Beitrag zu dieser Arbeit.

Ein sehr großer Danke geht an Vici Shi und Lucas Neuschwander, die mir seit sehr langer Zeit immer zur Seite stehen. Ohne euch wäre die Schulzeit, das Studium und die Promotion nicht dieselbe gewesen. Egal wie weit wir voneinander weg sind, unser Zusammenhalt wird davon nicht beeinflusst. Ich danke euch!

Einen weiterer, sehr großer Danke geht an meine Musiker-Crew: Matthias Schirg, Julia Meßmer, Angela & Johannes Berg, Johanne Mayer, Anne Altmeyer, Kai Vogelgesang, Max Leffer und Lars Lehmann. Ohne euch hätte ich weder mein Studium noch meine Promotion überstanden. Ich danke euch für die vielen gemeinsamen Proben, Abende und die gemeinsame Zeit. Danke Julia und Lars, dass ihr mich in meiner Endphase unterstützt habt.

Bei Sven möchte ich mich für die gemeinsame schöne Zeit bedanken. Vielen Dank, dass du mich stets unterstützt hast und mir in den letzten Jahren zur Seite gestanden hast. Danke für die gemeinsamen Unternehmungen und die vielen schönen Stunden.

Bei meiner Familie möchte ich mich für den jahrelangen Rückhalt in allen Lebenslagen bedanken.

Danke Oma - danke für die immer offene Tür, deine leckeren Koch- und Backkünste und deine nie endende Geduld und Freude mir seit Kindesbeinen an, die Welt zu erklären. Ich bin sehr froh, dass du in den letzten Jahren immer wieder gezeigt hast, dass du eine Kämpferin bist.

Der größte Dank gebührt meinen Eltern, besonders meiner Mama – danke, dass du immer für mich da bist, mich stets ermutigt hast und immer an mich geglaubt hast.

Zu guter Letzt möchte ich mich bei meinem Opa bedanken, dem ich diese Arbeit widme. Danke, dass du, solange du konntest, immer für mich da warst und mein moralischer Norden warst und immer noch bist. Ich habe deine Stärke immer bewundert. Ich vermisse dich.